AGARD-CP-237
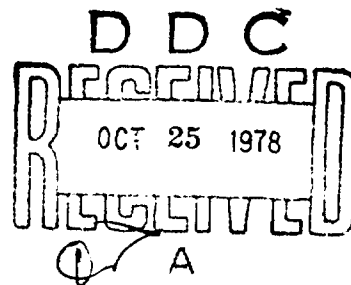
AGARD

ADVISORY GROUP FOR AEROSPACE RESEARCH & DEVELOPMENT

7 RUE ANCELLE 92200 NEUILLY SUR SEINE FRANCE

AGARD CONFERENCE PROCEEDINGS No. 237
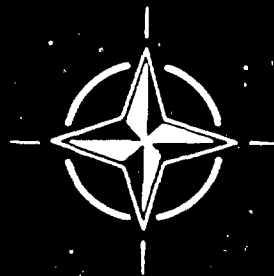
Seal Technology in Gas Turbine Engines

D D C

NORTH ATLANTIC TREATY ORGANIZATION

78 10 24

AGARD-CP-237

NORTH ATLANTIC TREATY ORGANIZATION

ADVISORY GROUP FOR AEROSPACE RESEARCH AND DEVELOPMENT

(ORGANISATION DU TRAITE DE L'ATLANTIQUE NORD)
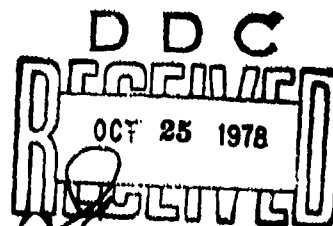
AGARD Conference Proceedings No.237

SEAL TECHNOLOGY IN GAS TURBINE ENGINES.

Aug 78

278 p.

D D C

OCT 25 1978

A

78 10 24 030

THE MISSION OF AGARD

The mission of AGARD is to bring together the leading personalities of the NATO nations in the fields of science and technology relating to aerospace for the following purposes:

— Exchanging of scientific and technical information;

— Continuously stimulating advances in the aerospace sciences relevant to strengthening the common defence posture;

— Improving the co-operation among member nations in aerospace research and development;

— Providing scientific and technical advice and assistance to the North Atlantic Military Committee in the field of aerospace research and development;

— Rendering scientific and technical assistance, as requested, to other NATO bodies and to member nations in connection with research and development problems in the aerospace field;

— Providing assistance to member nations for the purpose of increasing their scientific and technical potential;

— Recommending effective ways for the member nations to use their research and development capabilities for the common benefit of the NATO community.

The highest authority within AGARD is the National Delegates Board consisting of officially appointed senior representatives from each member nation. The mission of AGARD is carried out through the Panels which are composed of experts appointed by the National Delegates, the Consultant and Exchange Program and the Aerospace Applications Studies Program. The results of AGARD work are reported to the member nations and the NATO Authorities through the AGARD series of publications of which this is one.

Participation in AGARD activities is by invitation only and is normally limited to citizens of the NATO nations.

iii

PREFACE

This meeting was one of a series in the gas turbine engine field sponsored and arranged by the Propulsion and Energetics Panel of AGARD to stimulate discussion and information transfer between specialists.

The purpose of the meeting was to provide a forum to discuss technology of gas turbine engine seals. The discussion was limited to cases where relative motion exists between parts of the seals. Both gas path and oil path seals were covered.

The initial presentation was a comprehensive survey showing the effect of engine operation on seal performance and the effect of seal performance on engine performance. This survey was followed by presentations on new developments in material technology that influences seal design and operation. The user's view of seals focussed on operational performance, its impact on airline operations, maintainability of seals including repair techniques, and maintenance costs.

Engine producers contributed discussions based on their experience in the development of seals for large and small engines.

The program included presentations upon laboratory measurements and other investigations of seal behaviour as well as the development of suitable test facilities.

Methods of design and performance computations were presented and applied to some particular seal configurations.

Cette réunion faisait partie d'une série consacrée au domaine des turbines à gaz et était organisée sous l'égide du Panel Energétique et Propulsion de l'AGARD, dans le but d'encourager les discussions et les échanges d'informations entre spécialistes de cette discipline.

Elle avait pour objet de constituer un forum ou fut étudiée la technologie des joints de turbines à gaz. L'étude fut limitée aux cas où intervient un mouvement relatif entre les diverses partie des joints, et couvrit à la fois les circuits de gaz et les circuits d'huile.

Au cours du premier exposé, il fut procédé à un tour d'horizon exhaustif des effets du fonctionnement du moteur sur les performances des joints, et réciproquement. Les communications suivantes furent consacrées aux développements récents en matière de technologie des matériaux et à leur impact sur la conception et le fonctionnement des joints. Le point de vue de l'usager fut essentiellement centré sur les performances opérationnelles, leur influence sur l'exploitation des lignes aériennes, la maintenabilité des joints, y compris les techniques de réparation, et les coûts de maintenance.

Les motoristes rendirent compte de leur expérience dans le domaine du développement des joints pour moteurs de petites et de grandes dimensions.

Le programme comprit également des exposés sur les mesures en laboratoire et autres recherches sur le comportement des joints, ainsi que sur le développement d'installations d'essais adéquates. Les méthodes de conception et de calcul des performances furent également présentées, et appliquées à certaines configurations particulières de joints.

CONTENTS

by

B. Wrigley

CONCLUSIONS

- In-service performance deterioration is a serious problem for Commercial Operators and Air Forces, particularly in view of the developing fuel situation.

- Seal wear is a major factor in performance deterioration and there is therefore a significant financial incentive to improve sealing technology.

- Useful research is in progress particularly for advanced seal design, but in the field of rubbing and erosion research has been insufficiently systematic and has generally had to wait for the initiative given by service problems.

- Useful measurement techniques already exist.

- The conference was clearly necessary, in fact over-due. The quality of papers and participation was of a high standard. The general awareness of the problems and the relevance of the papers is in itself remarkable.

RECOMMENDATIONS

- Blade tip and labyrinth seal rubbing phenomena need further study.

- Engine demonstration of advanced sealing concepts should be encouraged.

- Relevant heat transfer phenomena should be incorporated in future discussion.

- Measurement techniques need to be improved, further.

- Resources should be provided to deal with the above recommendations.

It should be noted that in this field the resources that need to be committed are much smaller than in, for example, the primary turbomachinery fields.

- Sealing design must be integrated into the engine mechanical design and component aerodynamic design processes.

- A follow-on activity of PEP Working Group 08 which had dealt with engine deterioration in Air Force Service, is deemed necessary. It should be invited to provide data on the influence of sealing as experienced by military users.

- Solutions must be developed for existing engines and their derivatives, as these engines will consume most of the fuel up to the end of the century.

TECHNICAL EVALUATION REPORT

by

B. Wrigley

1. INTRODUCTION

The 51st meeting of the Propulsion and Energetics Panel on Seal Technology in Gas Turbine Engines was held at Church House, Westminister, England on 6th and 7th April 1978. The meeting was arranged under five main headings:

- material technology, particularly as applied to main flow path blade tip seals.

- user's view of seal technology.

- measurements of seal behaviour.

- laboratory experiments.

- design aids.

The meeting was held in four sessions, the last one incorporating a round table discussion.

The presentations were relevant, timely and well received, covering both aircraft and industrial gas turbines.

Wide ranging comment indicated the value of the meeting and suggested the need for a continuing commitment in this field.

2. SUMMARY

There are two major issues forcing the pace of sealing technology:

- the quest for improved engine efficiency, in a period of rising fuel prices.

- poor in-service reliability of seals and engine performance deterioration in the most recent generation of subsonic jet engines.

The meeting also identified the following issues:-

- A significant factor in performance deterioration is the increased clearance and aerofoil distortion caused by abrasion and erosion.

- The influence of thermal and mechanical forces on seal clearances.

These forces are usually of a transient nature.

Suitable techniques for measuring these effects were described.

- Current high bypass ratio engine designs have included features detrimental to achieving low seal leakage.

- A wide range of experiments has shown the potential of advanced sealing techniques for leakage reduction but this work has not yet been taken through to engine demonstration to any substantial extent, nor has the wear characteristic of such seals been adequately established.

3. RECOMMENDATIONS

- Further study is required on blade tip and labyrinth seal rubbing phenomena and should include fully representative experimental work and the development of theoretical understanding. Consideration should be given to establishing more formal relationships with machining research.

- Seal design should be thoroughly integrated into the engine design process. The mechanical designer must ensure from the preliminary design phase onwards that the engine is structurally and thermally beneficial to good seal design. The aerodynamicist must integrate sealing quality into his judgements concerning direction of research and engine design.

- Opportunity should be provided for the demonstration of advanced seals in representative engines; sufficient confidence will only be established in such seals if reliability and integrity can be demonstrated.

- User experience represented in the conference was mainly that of a major US trunk operator. Further information is required, reflecting other geographical locations, smaller operators, industrial users and particularly from military services. Referring to the successful work of PEP Working Group 08 which dealt with Aero Engine Deterioration in Air Force Service, a follow-on activity should be invited to report on experience with seals by military users.

- Compressor and turbine aerodynamicists should work towards a better understanding of clearance sensitivity.

    he commercial field present engines and derivatives of these engines will account for nearly ch ntal fuel consumption up to 2000 AD (Ref.B.). Research should be directed therefore to improving the present engines and not just the so-called E^3 engines,* which may not enter service until after 1990.

- Further discussion on associated heat transfer phenomena should be organised. Future engine improvements will depend greatly on tuning the heat transfer process to reduce clearance.

4. DISCUSSION

The papers have been slightly regrouped, to allow development of the different subjects starting from the views expressed by users.

4.1 USERS VIEW OF SEAL TECHNOLOGY

Paper No.1 by L.P. Ludwig identified the effect of rising fuel price on the significance of the fuel term in DOC. Recent development to high overall pressure ratios was cited as the significant factor in causing gas turbines to be more sensitive to sealing standard. Large values for in-service performance deterioration were described, references being given for commercial and military operation.

Paper No.5 by C.R. Smith enlarged on these themes, particularly emphasising the engine suppliers' responsibility to ensure the operator gets a good return on investment. Fuel consumption was the largest factor in DOC and deterioration of specific fuel consumption therefore particularly critical, both for its direct effect and the consequences on shop loading and overhaul costs of trying to maintain the fleet at the best average level of performance. Primary gas flow path sealing was the major source of performance deterioration, although secondary flow system sealing could not be ignored. Primary flow path deteriorations were caused by tip abrasion (unshrouded HP turbine blades) and excessive erosion of static shrouds. Wear of bearing chamber carbon face seals were associated with high temperatures and long time between overhauls. The need for closer control of oil cooling of the rubbing elements was identified to prevent the coking which often occurs at long lives. The financial incentive for improvement of sealing technology was stated to be the current cost to the operator arising from sealing problems e.g. for a large US operator: $14m annually. The 'Sealing' cost might eventually reach 70% of the engine maintenance bill. An appropriate economic climate therefore exists in which to promote the necessary research, design and development effort.

4.2 SEAL MANUFACTURE, RUBBING AND EROSION

The significant causes of performance deterioration identified in 4.1 are categorised in paper No.1 by L.P. Ludwig, which surveyed the available seal lining materials and their limitations particularly with respect to environmental temperature and rub energy. Blade tips and labyrinth seal knives have required abradable static liners. Choice of liner has usually been an uncertain process not helped by ignorance of penetration rate. The balance between good abradability and erosion of the liner has been difficult to achieve. A cine-film illustrated short and repeated hot rubs, a similar phenomenon being described in ref.A with low rub penetration rates. Greater certainty was indicated for the coating of a drum rotor, usually a hard oxide abrasive. The potential benefits of ceramic or ceramic/metal shrouds for HP turbine blade tips was indicated, further research being required owing to the very high local heat transfer coefficients present.

Paper No.2 by J.G. Ferguson described testing techniques of differing sophistication for abradable linings. The debris removal mechanism was cited as a possible cause of discrepancy between rubbing tests, highlighting the requirement for truly representative testing including airflow. Method of application as well as the composition of the abradable lining have been significant factors in determining quality. Experimental techniques for testing abradables have not allowed confident selection of material for engine seals. A.R. Stetson in Paper No.3 dealt specifically with compressor vane tip abrasion. The value of an extremely sharp abrasive in minimising vane metal loss, tip distortion and temperature was clearly established. By implication increase of clearance above the pre-determined penetration was also minimised. Plasma spraying was shown to reduce the abrasiveness seriously and it was necessary to use a low temperature bond to avoid this. The coating could be easily sprayed to size and required curing. It was cleared for use at up to 700°K.

Another manufacturing technique, for an abradable felt, was described in Paper No.4 by A. Hivert. As with the abrasive material of the previous paper low thermal conductivity was a characteristic. The manufacturing process for the fibres and the moulding technique for the felt were described. A soluble bond for easier repair was available for temperatures up to 611°K. Brazing was necessary at higher temperatures.

The lack of consistency between rig and engine tests of abradable tip seals noted by J.G. Ferguson is also brought out in Paper No.14 by C.W. Elrod. In order to tackle this deficiency an engine representative rig has been designed and is currently being commissioned. A specific feature of testing will cover titanium ignition phenomena. Complementary testing with laser ignition of representative titanium alloy samples was described. The effect of air velocity, pressure and temperature on burning rate and propagation to other 'aerofoils' was examined. Fires could be extinguished by a high concentration of Argon.

* E^3 = energy efficient engine

4.3 ADVANCED SEALS AND LABORATORY EXPERIMENTS

The introductory survey by L.P. Ludwig described the use of sliding face seals for bearing chamber sealing in a high pressure environment. An example showing substantial SFC improvement compared with labyrinth seals was given.

Paper No.11 presented by E. Rollins described a range of tests undertaken on small, low rubbing speed, hydraulic face seals. Data were presented which showed the effect of rotational speed on pumping between the sliding contact faces. (The cooling flow rates appear to be generous for the size of seal and similar values for oil as the cooling medium could present difficulties with oil feed and scavenge in small gas turbines). An approach to the design of such a seal is provided by Dr B.S. Nau in Paper No.19. The interface loading in the gap between the sliding surfaces is considered and a computational model presented which allows for cavitation in the interface. When program testing is complete correlation with the results of Paper No.11 should be considered.

L.P. Ludwig's second paper (No.16) showed that some important aspects of gas turbine secondary flow system leakage can be tackled with a fair chance of success. The examination provided for pneumatic self-acting seals, showed that high enough values of pressure, rubbing speed, face run-out and temperature have already been demonstrated to allow consideration for arduous gas turbine application. Furthermore heat generation was much less than conventional carbon contact seals. Methods for dealing with steady and dynamic (seal face runout) situations were described and performance and wear characteristics in tests up to 500 hours duration were discussed. With further effort to prove reliability and in particular low wear rates over a long period, it should be possible to provide a feasible alternative to the present methods of sealing bearing chambers in high pressure environments.

Paper No.17 by Professor D. Dini again identified the advantages of the self-acting pneumatic seal as one of a range of advanced seal types proposed for modern high performance gas turbines. Inexpensive laboratory testing but at engine representative conditions has shown the low leakage potential but with some variations, which may be due to unanticipated local distortions. The paper showed the need to understand accurately the force mechanisms in such seals, if consistency and long life are to be achieved. An oil slinger seal was mentioned, which was also covered by D.C. Whitlock in Paper No.7. This type of seal is quite positive and has no rubbing parts.

Paper No.13 by H.L. Stocker considered performance development of labyrinth seals. Results were presented which showed gains from refinement of seal knife configuration and the effect of the material and construction of the static member. At 0.51 mm clearance and seal pressure ratio of 2.0 (conditions for which stepped seals are generally considered), a leakage flow range of greater than 2:1 was indicated for the full range of seals tested.

At the larger clearances the value of a honeycomb lining on a straight-through seal, and knife inclination for a stepped seal was highlighted. The data are particularly important for demonstrating the effect of rotation. It is clear that the engine designer has been provided with good labyrinth seal performance data, from which seal configurations can be selected, providing of course consideration for the mechanical and rubbing behaviour is given.

Integrity rather than engine performance was the motivation of the remaining two papers in this section. T. Boyman in paper No.8 presented data relevant to bearing chambers sealed by low pressure drop labyrinths. More accurate prediction of the failure point, defined by oil leaking from the bearing chamber through the labyrinth, should be possible from the relationship established between oil outward diffusion rate and inward airflow. H. Benckert in Paper No.9 described the theoretical and experimental examination of the pneumatic forces present with swirling flow through a labyrinth. For machines operating with high density flow the forces can be significant. Further work is in progress covering changes to the labyrinth proportions.

4.4 SYSTEM DESIGN AND MEASUREMENT TECHNIQUES

Integration of bearing chamber seals into the design of the oil system, with particular reference to venting and scavenging arrangements, was described in paper No.7 by D.C. Whitlock. Seal performance was described and assessed against the background of system integrity. Designs ranged from labyrinth sealed chambers of varying degrees of sophistication, to carbon face seals and positive hydraulic seals using the strong centrifugal fields present. Principles and criteria for chamber design, of value to the engine designer, were established.

D.A. Campbell in Paper No.18 presented an approach to the design of disc sealing and cooling systems, an important topic owing to the large disc entrained air flows on present and future high rim speed discs. Minimising the cooling air supplied to disc cavities is dependent on associated seal performance. It is important in the design of these systems that secondary flows are not reduced at the expense of disc integrity. A benefit of 0.5% SFC was quoted for halving disc sealing flows on a large transport engine.

P.E.A. Stewart and K.A. Brasnett in Paper No.10 on X-ray measurement techniques described a powerful diagnostic tool, which does not require special engine preparation other than installation in a medically safe test bed. Transient surveys have generally been made to define the timing for instantaneous X-ray photographs, of high accuracy for a wide range of metal thicknesses. Complementary methods, which can provide continuous output of clearance but which require an engine to be specially instrumented, were described in Paper No.12 by C.R. Amsbury and J.W.H. Chivers. The value of the existing techniques in understanding seal clearance behaviour was stressed. Even so the need for further development of measurement techniques was indicated.

5. ROUND TABLE DISCUSSION

    Members: Mr A.J.B. Jackson (Moderator), UK
              Ing Gen A. Journeau, France
              Mr L.P. Ludwig, U.S.A.
              Prof F. Wazelt, Germany
              Mr B. Wrigley, UK

    Each of the members gave their comments after which there was general discussion.

    Several speakers emphasised the need to increase research and development activity.   In no way was
    the effort thought to be equivalent to that in the primary turbo machinery areas, particularly when allow-
    ance was made for the possible return on investment.   F. Mahler drew attention to the increased depend-
    ence on good sealing of the future energy efficient engines and suggested that component aerodynamic
    design could be dictated by sealing technology.

    Attention was also drawn to the necessity for engine designs which maintain roundness and concent-
    ricity.   It was suggested that positive evidence was available from the most recent large subsonic trans-
    port engines, that attention, particularly in the conceptual phase of design, to rotor and casing rigidity,
    will substantially reduce in-service deterioration rate.

    The importance of good measurement techniques was again emphasised.   Although the terms of reference
    of the conference were limited to seals with relative movement, some speakers used this discussion to
    identify leakage potential between adjacent stationary parts.   The value of the conference was stressed
    as was the need for further meetings.

    In his resume Mr Jackson again emphasised the powerful incentive for advancing sealing technology.
    He thought that the technology was considerably behind turbomachinery and posed a question for operators.
    Taking the analogy of hot end life extension by adopting 'flexible' thrust ratings, were there operating
    techniques which would extend seal lives?

6. CONCLUSIONS

    ● In-service performance deterioration is serious in its direct financial impact and also due to
       its effect on the maintenance and repair burden.

    ● Seal deterioration, particularly in the primary flowpath, contributes substantially to the
       performance deterioration.   Although the majority of fresh evidence was from commercial operation,
       it is well known that the Air Forces suffer similar problems.

    ● Although much research in this field is in hand, the commitment of resources and money is not
       commensurate with either the need to fix current engines or the potential return in future energy
       efficient engines.   It appears from an assessment of the papers, against the background of service
       problems, that the majority of the current research work is of a 'fire-fighting' nature.   This
       seems to apply particularly in the fields of rubbing and erosion, where only slowly is a systematic
       campaign, aimed at providing a sound base for future designs, being mounted.

    ● An abrasive coating should be fiercely abrasive to minimise wear beyond the penetration depth and
       to minimise heat generation.   Such coatings are feasible.   Plasma spraying seriously reduces
       abrasiveness.

    ● The relationship between labyrinth seal flow resistance and clearance and lining material, has been
       established for a range of labyrinth configurations.   However there is scope for further correlation
       of existing test data.

    ● Sealing problems generally require an understanding of clearance variation and measurement techniques
       are vital.   Useful techniques, including X-ray measurements, have been described but the need for
       much more compact probes, which can provide a continuous signal, was identified.

    ● It appears that there is considerable variation of opinion regarding the sensitivity of compressor
       efficiency to tip clearance.

    ● Different engine companies adopt a traditional, perhaps even reactionary approach to bearing chamber
       sealing.   This caution is a consequence of the necessity for extremely high standards of integrity
       in this context and the failure to provide engine demonstration of alternative approaches.   The
       NASA work on pneumatic self-acting seals is encouraging, particularly for high pressure environments,
       and has the potential for overcoming some of the draw-backs of current low leakage seals.

    ● Heat transfer phenomena associated with clearance control was not covered adequately.   The following
       areas are clearly important:-

       ● thermal response of rotating discs

       ● casing thermal response, particularly the heat transfer mechanism over blade tips

       ● heat distribution during a rub

       ● local effects in labyrinth seals

    ● Future energy efficient engines are likely to prove more demanding with respect to the standard
       of sealing required.

REFERENCES

1. Ludwig, L.P.   Gas Path Sealing In Turbine Engines.

2. Ferguson, J.G.   Use of Coatings in Turbomachinery Gas Path Seals.

3. Stetson, A.R.   Abrasive Coatings as Self-Clearing Gas Turbine Compressor
    Vogan, J.W.   Vane Tip Seals.
    Compton, W.A.

4. Genley , E.   Application des Feutres Métalliques OHP aux Joints
    Rivert, A.   d'Etanchéité de Turbomachines

5. Smith, C.R.   American Airlines' Operational and Maintenance Experience with
                       Aerodynamic Seals and Oil Seals in Turbofan Engines.

7. Whitlock, D.C.   Oil Sealing of Aero Engine Bearing Compartments.

8. Boyman, T.   Transport Phenomena in Labyrinth-Seals of Turbomachines.
    Suter, P.

9. Benckert, H.   Studies on Vibrations Stimulated by Lateral Forces in Sealing
    Wachter, J.   Gaps.

10. Stewart, P.A.E.   The Contribution of Dynamic X-Ray to Gas Turbine Air Sealing
    Brasnett, K.A.   Technology.

11. Bollina, E.   Experimental Results on High Speed Double Mechanical Seals.
    Casci, C.
    Macchi, E.

12. Amsbury, C.R.   Systems for the Measurement of Rotor Tip Clearance and Displacement
    Chivers, J.W.H.   in a Gas Turbine

13. Stocker, H.L.   Determining and Improving Labyrinth Seal Performance in Current
                       and Advanced High Performance Gas Turbines.

14. Elrod, C.W.   Factors Associated with Rub Tolerance of Compressor Tip Seals.

16. Ludwig, L.P.   Self-Acting Shaft Seals.

17. Dini, D.   Self-Active Lift   Seal Application for High Pressure Engines

18. Campbell, D.A.   Gas Turbine Disc Sealing System Design.

19. Nau, B.S.   A Computational Tool for Mechanical Seal Design.
    Rowles, R.T.

NOTE: Papers 6 and 15 were cancelled.

A   NASA Tech Paper 1128 - 'Friction and wear of several Compressor Gas Path Materials'.
    R.C. Bill and D.W. Wisander.

B   ASME Paper 78-GT-192 - 'Advanced Turbofan Engines for Low Fuel Consumption'.
    W. Sens

GAS PATH SEALING IN TURBINE ENGINES

by
Lawrence P. Ludwig
National Aeronautics and Space Administration
Lewis Research Center
Cleveland, Ohio 44135

SUMMARY

A survey of gas path seals is presented with particular attention given to sealing clearance effects on engine component efficiency. The effects on compressor pressure ratio and stall margin are pointed out. Various case-rotor relative displacements, which affect gas path seal clearances, are identified. Forces produced by nonuniform sealing clearances and their effect on rotor stability are discussed qualitatively, and recent work on turbine-blade-tip sealing for high temperatures is described. The need for active clearance control and for engine structural analysis is discussed. The functions of the internal-flow system and its seals are reviewed.

1. INTRODUCTION

Aircraft gas turbine engines have many sealing locations: along the shaft, over rotor blade tips, and between stages. A large engine may have over 50 (Fig. 1), and the cumulative effect of leakage on engine power, thrust, and aircraft range can be significant. Reference 1 characterizes gas path sealing as a fundamental and continuing problem, which worsens as gas turbine engines advance to higher cycle pressures and temperatures. Of particular interest is the effect of sealing on engine efficiency, which has taken on added interest because of the pending petroleum scarcity and attendant higher prices.

The airline industry in the United States consumes only 10% of the total petroleum demand in the United States. By 1985 consumption may reach 15% (Fig. 2 from Ref. 2), but fuel cost may markedly impact the aircraft industry.

Reference 3 emphasizes the need for low fuel consumption now and in the near future because of fuel prices, with fuel reaching 53.5% of the direct operating cost (DOC) when the price is 50 cents per gallon (see Table I). In the long term, when demand for oil exceeds productive capacity (Ref. 4), a sharp price increase is anticipated by some (see Fig. 3). In general, anticipated fuel scarcity and prices mean that new engines, in addition to the four basic requirements of reliability, durability, low maintenance, and increased power, must also be fuel efficient.

Reference 5 gives additional information on the relative impact of various parameters on DOC and this is shown in Fig. 4, which reveals that DOC is much more sensitive to changes in specific fuel consumption (SFC) than engine weight. Increased fuel scarcity and prices also focus attention on engine performance deterioration, which for high pressure ratio engines is due mainly to the opening up of sealing clearances by erosion and wear.

Engines of the 1950 design era operate at relatively low pressure ratios, and clearances over the blade tips were large enough to avoid rubbing. Modern engines have pressure ratios in the range of 25:1, and to preserve efficiency the sealing clearances were reduced. These smaller clearances made rubbing contact at sealing locations inevitable and brought about the introduction of "abradable" materials, which are designed to wear sacrificially.

Abradable materials, which can solve only part of the sealing clearance problem, have not been fully successful because of the erosion and wear of blades. Evidence of this is in airline reports, which note on engine overhaul, that these modern engines deteriorate faster than earlier ones. Typically, high bypass ratio engines have a specific fuel consumption (SFC) increase of 1 to 1½ % per year (Ref. 6); periodic overhauls do not fully recover this efficiency loss (Fig. 5). The final result is an engine with a fuel consumption which is 3 to 10% higher than that of a new engine; Ref. 2 places the average fuel consumption increase at 7%. For a military turbofan Ref. 7 places the SFC increase at near 2½% in 250 hours and indicates that much of this is due to increases in seal leakage. In addition to the effect on efficiency, the sealing clearances also have a significant effect on the compressor stall margin and are directly responsible for "thrust droop" which can be as high as 12% (Ref. 7).

The objective of this study was to survey the present state-of-the-art of turbine engine sealing with attention given to (1) the sensitivity of component efficiency to sealing; (2) the mechanical and thermal effects which control the sealing clearances; and (3) technology needs.

2. SEALING LOCATIONS AND SEAL TYPES

Primary Gas Path, Compressor and Turbine

In general, primary gas path seals perform two functions:

(1) To minimize gas recirculation

(2) To minimize gas leakage out of the primary gas path.

Sealing to minimize gas recirculation is found at the following compressor (Fig. 6) and turbine (Fig. 7) locations:

(1) Rotor stages

(a) For unshrouded rotors between blade tips and the case inner wall (Figs. 6(a) and 7(a)) and for shrouded rotors between blade shroud and the case (Figs. 6(b) and 7(b))

(b) Blade roots and platforms.

(2) Stator stages - For cantilevered vanes between compressor vane tips and rotor (Fig. 6(b)), and for shrouded vanes between the inner shroud and the rotor labyrinth teeth (Figs. 6(a) and 7(b)).

(3) Cavities - Rim sealing (Fig. 7(b)) to prevent hot gas ingestion into the turbine cavities.

Sealing to limit gas loss from the primary gas path occurs at the following locations:

(1) Flanges

(2) Vane pivots (Fig. 6(c)) - Compressor leakage at the vane pivots can be as high as 0.3% of engine airflow per stage (Ref. 8).

(3) Compressor and seal (Fig. 6(d) from Ref. 9) - Controls cooling and purging flows and rotor thrust balance. Leakage is in the range of 0.6% of engine airflow in some engines (Ref. 8). Usually most of this leakage is returned to the primary flow in a lower pressure region.

Internal-Flow System

Pressurized air, which is bled off the primary flow, enters the internal-flow system and is used to purge cavities (prevent hot gas ingestion), pressurize bearing compartments, act as a sweep gas to prevent lubricant leakage, cool parts, and balance the rotor thrust. The internal-flow is largely controlled by labyrinth seals; although rubbing carbon seals are sometimes used at the mainshaft sealing locations. Problems arise because wear to these internal-flow system seals changes the amount of air delivered.

Reference 10 points out that increases in pressure ratios, bypass ratios, and turbine temperatures tend to increase the thermodynamic loss chargeable to the internal-flow system; this trend is indicated in Fig. 8, in which the SFC penalty for an increase internal-flow is plotted as a function of bypass ratio. According to those data the SFC penalty increases when either bypass ratio or pressure ratio is increased. In addition, with the continuing trend to high temperatures there is an associated requirement for more cooling and purging flow.

The marked effect of internal-flow system is also indicated by the study of Ref. 11 on the leakage effects in a small engine having a compressor flow of 2.3 kg/sec (5 lbm/sec). The performance of this engine was calculated for zero clearance and for typical seal clearances assigned to each position. The results (Fig. 9) show that the most significant losses are in the labyrinth seals for which the calculated penalty is a 17% loss in power and a 7½% increase in SFC.

As mentioned previously, the internal flows are largely controlled by labyrinth seals at various locations such as at the compressor discharge (Fig. 6(d)), high pressure turbine (Fig. 10), and bearing sumps. Labyrinth seals are attractive because of their mechanical simplicity, reliability, and freedom from limitations on axial displacements. Common configurations are the straight and stepped designs (Fig. 11). Both are reasonably effective when clearances are small. But both lose performance fast with wear. When large clearances are dictated by transient thermal conditions, the performance tends to be poor. But the stepped seals are less sensitive to clearance changes, and, in general, have significantly less leakage than the straight design.

To obtain close clearances, the labyrinth seals must be designed to tolerate rubs, and the general practice in aircraft gas turbines is to place labyrinth teeth on the rotor and ideally have all of the wear, due to interference, take place on the stator rub surface. The reasons for attempting to have all of the wear occur in the stator rub surface are:

(1) In locations in which the rubs tend to be local (accommodation of eccentricity, out-of-roundness, etc.), wear to the stator is a lesser increase in leakage area than the 360° of area increase which occurs with rotor wear.

(2) In some locations the realtive displacement of the stator and rotor includes axial and radial components that have a correspondence with an engine operating condition. As illustrated in Fig. 12(a), it is possible to accommodate interferences produced by these displacements and yet maintain an acceptable sealing clearance. On the other hand, if the rotor labyrinth teeth wear instead of the stator, the final leakage clearance is increased by the interference depth of the rub.

(3) Stator wear introduces the possibility of designing to obtain stator/rotor interlocking operation in some applications (Fig. 12(b)).

Labyrinth teeth are generally thin in order to (a) promote sharp edge orifice flow characteristics, (b) limit the amount of heat generated, and (c) restrict the amount of heat conducted into the rotor. Limiting the heat conduction into the rotor precludes a rotor thermal response, which could aggravate the rubbing and lead to a catastrophic failure.

An important part of the internal-flow system is the engine mainshaft seals, which protect the bearing sumps as illustrated in Fig. 13. Figure 14 shows several shaft seal schematics for the turbine bearing sump location. Here the basic problem is the protection of the bearing sump from the turbine cooling gas. In early engines the cooling gas pressure and temperature was relatively low and a single labyrinth seal, which restricted turbine cooling gas leakage into the sump, was adequate. Single labyrinth seals have been used to pressure differentials of 34 N/cm^2 (50 psi). At these pressures the efficiency loss due to seal leakage was generally insignificant. However, a disadvantage of the labyrinth seal, as compared with the close-clearance seals (circumferential and face), is easier passage of airborne water and dirt into the sump. In addition, for labyrinth seals, reverse pressure drops must be avoided to preclude high oil loss. In fact, a slight positive pressure differential should be maintained to prevent oil leakage.

When high-pressure air is required for turbine cooling, the multiple-labyrinth system (Fig. 14(b)) is often used (in large engines). In this system low-pressure compressor bleed surrounds the sump, and hence, provides thermal protection; leakage into the sump provides the required sump pressurization. The multiple-labyrinth seal system has higher operating temperature and speed capability than rubbing contact seals and has been used to 280 N/cm^2 (400 psi) and 922 K (1200° F). However, as engine size decreases, the multiple labyrinths becomes difficult to apply because of space restrictions (vents, bleeds, lines, etc.). Small engines therefore, require other solutions.

Conventional face seal technology (Fig. 14(c)) can be used to replace the multiple labyrinths up to pressures of 90 N/cm^2 (130 psi) and to sliding speeds of 122 m/sec (400 ft/sec). In another arrangement, which is used in some modern large engines, the labyrinth seal next to the bearing is replaced by a face seal (see Figs. 10 and 14(d)); this buffered face seal system has the advantage of relatively low leakage into the bearing sump. Also, bearing sum reverse pressure differentials are more readily tolerated. Further, according to the analysis of Ref. 12, the buffered face seal can significantly lower the efficiency penalty below that of the multilabyrinth seal system. This analysis, which was made for a large transport engine with a 25:1 pressure ratio, showed a leakage loss of 0.88% of engine airflow for the multilabyrinth seal system. In contrast, the buffered-face seal system bleeds less air from the compressor, and the seal system pressures permit recovery of the bleed loss in the low-pressure turbine. The net result of the analysis was a predicted 0.6% SFC gain.

In addition to face and labyrinth seals, ring seals are also used for mainshaft sealing. The simplest is the "floating" ring (Fig. 15(a)) which is so named because it is not restrained from moving in a radial direction and, therefore, can operate with less leakage gap clearance than the conventional labyrinth seals (Ref. 13).

Rubbing, circumferential seals operate with very low gas leakages and are therefore attractive, but the pressure differential capability is generally low because of the rubbing contact. The simplest circumferential rubbing seal is composed of a segmented carbon ring (three 120° segments) held together by a garter spring on the outside diameter (Fig. 15(b)). The gaps between the adjacent ends of the segments are a source of air leakage into the bearing cavity.

Other circumferential seal designs incorporate multiple rings with overlapping joints to eliminate the leakage at the gaps between the segments. Pressure balancing of the segments maximizes the pressure and speed capability (Fig. 15(c)). Reference 14 reports successful operation of a pressure balanced circumferential seal to 58 N/cm^2 (85 psi) and 73 m/sec (240 ft/sec).

In partial summary of this section, mainshaft sealing at the turbine bearing locations is accomplished by several different designs: (a) multilabyrinth seals, (b) rubbing contact seals, or (c) a combined system of a rubbing contact and labyrinth seals. Labyrinth seals have high leakage, which can be a performance penalty, and in small engines with restricted space the high leakage rates are difficult to accommodate. On the other hand, contact seals

have low leakage but have limited pressure and speed capabilities. A need, therefore, exists for mainshaft seals which have low leakage yet are able to function at the pressures and speeds expected in advanced engines (pressure ratios in the range of 45:1 (Ref. 15) and seal sliding speed could reach 183 to 244 m/sec (600 to 800 ft/sec)).

3. LEAKAGE FLOWS

Blade and Vane Tips Leakage Flows

Leakage flow between the blade (or vane) tip and the adjacent wall is due to

(1) The pressure difference between the suction and pressure side of the blade

(2) The relative wall movement.

The velocity gradient of the flow relative to the blade is represented by the classical Couette flow profile indicated in Fig. 16. And the velocity profile produced by the pressure difference is probably similar to that of a slit type of orifice; that is, the classical fully developed profile is not obtained because the ratio of blade thickness to clearance is small.

In the case of a compressor blade or vane tip, the pressure difference and the relative wall movement both act to cause leakage in the same direction; in a turbine these two effects oppose each other. In general, the leakage over the tips flows in a direction tending toward a normal to the main flow, and the resulting interaction of these two flows is described by some (Refs. 16 and 17) as a tip vortex such as that depicted in Fig. 17. Reference 17 gives a detailed description of the tip leakage interaction with the boundary layer. Figure 18 shows that tip leakage flow of relatively high energy tends to turn back the lower energy secondary-flow and form a core of low energy fluid; this core is pushed further toward the blade pressure side as the tip leakage increases. Observations made by the author of Ref. 18 using a multistage axial flow hydraulic pump confirm that this slot discharge rolls up into a vortex. Losses are considered to arise because the velocity component normal to the chord is not recovered.

Reference 19 presents a method for predicting tip clearance effects in turbomachinery, and a semiempirical expression is formulated using a model in which the lift is uniform along the span and only a part of the bound vortex is she' along the tip. Boundary conditions are satisfied through use of image vortices, and the associated flow is used to predict i ced drag. The semiempirical expression for efficiency drop $\Delta\eta$ from the analysis by Ref. 19 is

$$\Delta\eta = \frac{0.7 \, \lambda\psi}{\cos \beta_m} \left(1 + 10 \sqrt{\frac{\varphi\lambda A}{\psi \cos \beta_m}} \right) \tag{1}$$

in which

$$\lambda = c/s, \text{ tip clearance/blade height ratio}$$

$$\psi = \text{blade loading} = \frac{2c_p \, \Delta T_o}{\rho U^2} = \frac{2(\Delta P_o)_{isen}}{\rho U^2}$$

$$\beta_m = \text{mean air angle}$$

$$A = \text{aspect ratio of blade}$$

$$\varphi = \text{flow coefficient} = \frac{V_2}{U} = \frac{\text{fluid exit velocity}}{\text{blade speed}}$$

The preceding formula is for a cascade and does not include rotation effects. Also, the formula's applicability needs to be established over a wide range of design parameters. This suggests a need for a better mathematical model which would accurately reflect the effects of the various parameters. The complexity of the flow and the interaction of the many parameters (such as chord length, blade loading, aspect ratio, Mach number, rotational speed, etc.) suggests that the expression will continue to be semiempirical.

Labyrinth Seal Flows

Two basic approaches are used to predict labyrinth seal leakages: one is based on a pipe friction model, and the other, which seems to have wider acceptance, is based on a series of throttlings. The physics of the flow is illustrated in Figs. 19 and 20. Ideally, the kinetic energy increase across each annular orifice (stations 1 to 2 in Fig. 19) is completely dissipated in the cavity (stations 2 to 3). In actuality, the kinetic energy dissipation is not

complete, and Egli (Ref. 20) introduced the concept of "carry-over" (see fluid dynamic model in Fig. 20) in order to account for the incomplete dissipation of kinetic energy in straight labyrinth seals. Reference 21 gives the following convenient form of an Egli equation for calculating leakage, W:

$$W = A\varphi \, \alpha \, \gamma \sqrt{g\rho_u P_u} \tag{2}$$

where A is the leakage area; φ is the flow function and a function of N, P_d/P_u; α is the discharge coefficient and a function of t, c/t; γ is the carry-over factor and a function of N, c/s; P_u is the upstream pressure; ρ_u is the upstream density; N is the number of labyrinth teeth; c is the clearance; t is the tooth thickness; s is the tooth spacing; and P_d is the downstream pressure. The values of φ, α, and γ are obtained from the graphs in Fig. 21 from Ref. 22.

From the flow function curve (Fig. 21) it is seen that increasing the number of throttlings decreases flow but that the gain beyond six teeth is small. This is one reason why labyrinth seals in aircraft engines generally have six or fewer teeth.

The discharge coefficient α is affected by tooth shape, tip thickness to clearance ratio, pressure ratio across the tooth, and eccentricity. Extensive experiments (Ref. 1) have shown more complexity than indicated in Fig. 21(b). For example, the effects of tooth shape on discharge coefficient is given in Fig. 22; these data show a significant sensitivity to tooth shape. Sharp corners provide the lowest discharge coefficient; however, from a practical viewpoint, labyrinth seals generally rub, and rounded corners are common, particularly if the stator rub material is not easily abraded. Thus the discharge coefficient may approach that of a nozzle. (Please read Ref. 1 for a more complete coverage of discharge coefficient.)

Experimental data are often expressed in terms of an overall flow parameter ψ, which includes the flow function φ, discharge coefficient α, and the carry-over factor γ. Therefore, equation (2) can be expressed as

$$W = \psi A \frac{P_u}{\sqrt{T_u}} \tag{3}$$

An example of experimental data for a labyrinth seal with four teeth is shown in Fig. 23, in which the flow parameter ψ is plotted as a function of pressure ratio. These data indicate choking above a pressure ratio of about 2.5. Most engine manufacturers have considerable labyrinth seal experimental data, and their semiempirical analytical techniques based on these data (e.g., Figs. 22 and 23) permit accurate prediction of the leakage. The major error probably comes in clearance estimation.

The potential payoff of reduced leakage validates the continuing search for improved labyrinth seals. Potential reductions may result from the following:

(1) Stator rub materials that increase dissipation (data in Ref. 23 show that a honeycomb stator rub surface is most promising)

(2) Tooth edges that retain corner sharpness under rubbing and erosion conditions

(3) Geometries that reduce carry-over effects

(4) Theoretical studies for added insight with less dependence on empirical data (provide optimum designs)

(5) Closer running clearances.

4. SEALING CLEARANCE SENSITIVITY

Compressor System Sealing

Many parameters are associated with blade tip clearance leakage, some are blade loading, tip thickness, aspect ratio, wall relative speed, and Mach number. But the one favored as the most significant by many investigators is the ratio of clearance c to blade height s. References 1, 24, and 25 contain experimental data on relatively large diameter fan and compressor efficiency as a function of either clearance or c/s ratio. The data of Ref. 1 are in terms of a penalty on a baseline efficiency at near zero clearance (Fig. 24); the absolute levels of efficiency are not given. On the other hand, data in Refs. 24 and 25 are in terms of efficiency levels, and the penalty on an efficiency level at near zero clearance can be obtained through extrapolation. This, however, requires some knowledge of the behavior of the efficiency curve at small c/s ratios.

Inspection of the relationship between efficiency penalty and c/s ratio in Fig. 24 reveals these general features:

(1) The initial slope of the curve at very low c/s ratios (≈0.0005) has about a 10% efficiency penalty for each 0.01-increment in c/s ratio.

(2) The final slope of the curve is constant beyond a c/s ratio of about 0.008 and has a magnitude of about 2% efficiency penalty for each 0.01-increment in c/s ratio.

(3) There is no indication of an optimum finite clearance from an efficiency standpoint (although Ref. 19 presents a heuristic argument for the existance of an optimum clearance).

Reference 25 shows experimental multistage compressor efficiency as a function of five different clearances (see Fig. 25). The closest clearance provided a c/s ratio of 0.011. This compressor, referred to in Ref. 25 as "Alice," had eight stages and ran at a mean blade speed of 93.9 m/sec (308 ft/sec). With reference to Fig. 25 the slope of the curve is constant over a wide range of c/s and has a magnitude of 1.95. This is added evidence that the final slope of the sensitivity curve shown in Fig. 24 may have general applicability.

Data on clearance effects of single-stage fans (Ref. 24) ranges between a c/s of 0.0014 to 0.0118. Thus the data, which are shown in Fig. 26, span a region in which the slope of the sensitivity curve is rapidly changing, whereas the data for the "Alice" compressor is entirely within the final constant slope region. When drawing the curve in Fig. 26, it was assumed that the initial and final slopes would be the same as those in Fig. 24. These assumptions seemed to agree with the general trends of the curve and permitted a short extrapolation to obtain a baseline efficiency at a c/s of 0.0005. This extrapolation permits the data to be expressed in terms of efficiency penalty from a baseline. A comparison with that from Ref. 1 is given in Fig. 27. Data from Ref. 24 indicate a greater penalty, and the variances suggest additional studies are needed. In particular, data are needed at small c/s ratios.

Generally, the effect of leakage is more significant in the small engines because, the leakage flow area is relatively larger. However, a significant problem in large engines is blade tip rubbing from case bending (Ref. 26) and out-of-roundness. (This is discussed in a later section.) Even though small engines tend to be stiff and hold roundness, small engine compressor efficiency tends to be about 5% less than that for large engines (Ref. 27). This fact places increased emphasis on reducing penalties caused by clearance effects.

For a small axial compressor with a diameter of 11.770 cm (4.634 in.), Ref. 28 shows a maximum stage efficiency at design speed of 83.3%; the running tip clearance was 0.78% of the rotor blade mean span. And when the rotor diameter was machined down to increase the clearance to 2.14% of blade span, the efficiency decreased by 5.5 points. Additional data on small axial compressors are found in Ref. 27, which contains a compilation of various sources. There are variances between the sets of data, but all data indicate a serious degradation of efficiency due to clearances. A typical rate is a 1.5-percentage-point loss in efficiency for each increase of 0.01 in clearance to span ratio.

Clearance effect data for centrifugal compressors are given by Refs. 27, 29, and 30; typical data are shown in Fig. 28. For axial clearance changes at the tip, data from Ref. 27 show a 1.00-percentage-point loss for each 0.01 increase in c/s ratio (s is the axial depth of the blade at the tip). In contrast, Refs. 29 and 30 indicate a 0.37 to 0.49 percentage point loss.

As with the larger diameter compressors, the data for small-diameter compressors (axial and radial) show considerable effect on efficiency however the variances suggest that additional studies are needed. Since data for the small compressors are for c/s ratios above 0.02, there remains the question of how efficiency changes with clearance below a c/s ratio of 0.02.

In some engine designs the compressor stator vanes are cantilevered (see Fig. 6(b)), and the clearance effects are somewhat similar to those of the blade tips. Reference 1 gives data on efficiency penalty as functions of clearance to blade height ratio, and these data are shown in Fig. 29. In comparison with the blade tip data of Fig. 27, the penalties are not nearly as severe.

The other type of construction used in stator vane sealing is the inner diameter shroud depicted in Fig. 6(a). Compared with the cantilevered constructions, the inner shroud and associated labyrinth seal form annular passages underneath the primary flow path, and these passages allow circumferential flow; the net result is detrimental effect on stall margin.

Figure 30 (from Ref. 1) shows efficiency penalty for clearances in the stator vane/inner shroud type of construction. The data in Fig. 30 are for labyrinth seals having two knife edges with no carry-over blockage (no steps). A comparison of the penalties in Fig. 30 with those for cantilevered stator vanes shows that the inner shroud construction has less effect on compressor efficiency.

In regard to the preferred type of vane sealing, the inner shroud construction produces undesirable annular passages which allow circumferential flow; on the other hand, inner shroud construction provides greater structural integrity. This is important from an F.O.D. and aeroelastic stability standpoint. Further, in cantilevered construction, the clearance between the vane tips and rotor must be selected to avoid hard rubs, and therefore is generally larger than for the inner shroud construction. Vane tip rubbing has, in some cases, triggered a rotor thermal response feedback which increased the rubbing severity until catastrophic failure. However, an additional factor which favors the cantilevered construction is the significantly lower boundary-layer temperature (at the inner gas path) than with the shrouded stator vanes (Ref. 10).

In addition to the effect on efficiency, blade tip clearances also affect the stall margin and the pressure ratio. Reference 24 supplies valuable data in this regard, and some are shown in Fig. 31. The steep slope of both curves, as clearances are decreased, suggests a large potential improvement if close running clearances could be obtained. Reference 28 also provides data on stall margin as affected by clearance for a single stage fan with a relatively low tip speed of 68.1 m/sec (223.4 ft/sec). Tip clearances of 0.3, 0.6, and 1.2 mm (0.012, 0.024, and 0.047 in.) were used, and these gave c/s values of 0.0033, 0.0067, and 0.0133. Using the largest clearance as a basis, the stall margin improved by 4.7% when the clearance was reduced to 0.6 mm (0.024 in.) and improved 7.1% for the 0.3 mm (0.012 in.) clearance.

Turbine System Sealing

The decrease in turbine efficiency associated with an increase in clearance is due, in part, to unloading of the blade by leakage over the tip, and to the increase in flow area over the blade tips. In addition, when the increase in clearance occurs because of blade wear, an added loss is associated with the decrease in active blade area. In this regard, it is preferable to have the case wear instead of the blade. This is also true of compressors. These two idealized extremes, wear to the blade with none to the case, and vice versa, are illustrated in Fig. 32. Interference between the blades and case, which leads to wear, is usually caused by transient thermal differences between the rotor and the case. This is discussed in a later section.

Data from Ref. 31, which is repeated in Fig. 33, reveals that changes in clearances are accompanied by significant changes in both exit flow angle and local efficiencies over the entire blade height. These data are for different clearances (up to 8% of flow passage height), which were obtained by machining down the blade tips. Near the tip the exit flow angles showed a large change, nearly 40°. In addition, the average flow angle across the flow passage changes. This indicates that underturning accompanies increases in leakage through the clearances. Also, Fig. 33(b) reveals a large variation in local efficiency across the entire blade height with the greatest change occurring between the mean radius and the tip. Thus, clearance can affect the flow across the entire blade span.

References 32 to 34 contain experimental data on the effect of tip clearances on turbine efficiency, and Ref. 34 contains a comparison of these data, which is shown in Fig. 34. These comparisons, which are expressed as fractions of zero-tip-clearance efficiency, were obtained by linear extrapolation to zero clearance. Inspection of Fig. 34 reveals, in general, a significant impact of tip clearance on turbine efficiency, and the data show that a greater loss is associated with reaction turbines, than with impulse types, apparently because of the higher pressure difference across the blade. In this regard, the reaction turbine used in studies of Ref. 34 had an efficiency loss of 2.0% for a clearance change of 1% of blade height when the clearance change was produced by machining down the blade tips. But when the clearance was obtained by machining out the case, and with the blade tip diameter equal to the casing inside diameter (see Fig. 35(a)), the efficiency slope for a reaction turbine was 1.5% for a clearance change of 1% of blade height.

For these machined case configurations the optimum efficiency occurred when the blade tip diameter was equal to the case inside diameter (Fig. 35(a)); when the blade tip was below the case inside diameter or when the blade protruded into the machined recess (Fig. 35(b)), the losses were greater. For example, the data of Ref. 34 show that for a clearance of 2% of the blade height, the efficiency drops from 97% for zero blade extension into the recess (Fig. 35(a)) to 96% for a blade extension into the recess of 3.5% of blade height (Fig. 35(b)).

Radial-inflow turbine clearance data are reported in Ref. 35. Studies included the effect of axial clearances at the entrance and exit and the effect of radial clearances. The data reveal sensitivity to radial clearance comparable with that for the axial flow turbines.

Influence Coefficients

The real measure of the effect of seal leakages is in its effect on specific fuel consumption (SFC) which is inversely proportional to the product of cycle and propulsive efficiencies (Ref. 15). The cycle efficiency is limited mainly by gas generator component efficiency and by airbleed requirements for hot-section cooling. For a high bypass engine the propulsive efficiency depends, to a great extent, on the efficiencies of the components acting on the

bypass stream, thus the fan and low-pressure turbine efficiencies are a major influence.

Reference 15 provides data on the influence of various high bypass engine component efficiencies on the specific fuel consumption and these data are repeated in Fig. 36. It is noteworthy that for a high bypass engine a low-pressure turbine (LPT) efficiency change causes the greatest change in SFC; a 0.86% improvement in SFC for each percentage point increase in turbine efficiency. The high pressure compressor (HPC) and turbine (HPT) each provide about 0.5% SFC change for each 1% change in component efficiency.

Reference 6 provides influence coefficient type data, in terms of fuel consumption sensitivity to component deterioration, for the JT3D-3B and JT8D-9 engines. These data were determined by mathematical models of engine performance and show, for example, the following fuel flow increases for a 1% deterioration in each of the following component efficiencies:

Component	Fuel flow increase, %
Fan	0.29
HPC	.51
HPT	.58
LPT	.69

Interestingly, a 1% increase in HPT flange leakage resulted in a predicted increase in fuel flow of 1.22%. This points up not only the significance of flange sealing but also the large influence of any high pressure air loss from the cycle. In this regard, vane pivot leakage and HPC flange leakage have a similar influence. Also, it suggests that variable vanes for HPT of advanced engines be given close design study in regard to sealing effectiveness.

5. SEALING CLEARANCES

In previous sections the need for close clearances in modern gas turbine engines was stressed. A basic problem is that the radial displacements of the case and rotor are, in general, much greater than the desired operating clearances. An approximate ordering of the more significant transient and nontransient displacements which affect clearance are

(1) Thermal response of the case and rotor

(2) Centrifugal and gyroscopic loads

(3) Surge/stall displacements

(4) Thrust, aerodynamic, maneuver, gust, and landing loads

(5) Ovalization and out-of-roundness due to nonaxisymmetric structures, loads, and temperatures

(6) Case/rotor vibration and shaft thermal bow

(7) Assembly eccentricities

(8) Machining tolerance variations.

Abradable materials in labyrinth seals and over compressor blade tips can make accommodations (or allow corrections) for assembly eccentricities, machining tolerance variation between assemblies, and out-of-roundness. However, the other effects listed must be controlled through the integrated mechanical design of the whole rotor-case.

The transient thermal response of the case and the rotor is of major concern, and this response, along with the centrifugal loading, is one of the most important factors in setting the final cruise clearance. In general, the thermal response of the case and rotor are not the same because of differences in mass, cooling-air circulation, heat transfer, and material. Figure 37 illustrates the general problem of relative case/rotor displacements as it is affected by thermal response and centrifugal loading. The case tends to have a much faster thermal response to the gas path stream temperature than the rotor. The rotor growth is initially due to centrifugal force during acceleration, and if assembly clearances are too small, a rub will occur in the early part of the acceleration. On deceleration, the case's relatively fast thermal response will cause rubs if full power is demanded after a period of low power (such as in an aborted landing). This is also illustrated in Fig. 37 in which the relatively fast case response has reduced the clearance to a magnitude less than the rotor displacement due to centrifugal force. The problem can be mitigated by closer thermal matching of the case and rotor, but not completely solved. If very close cruise clearances are going to be obtained then some type of active clearance control is needed to eliminate the rub potential. In this regard, Ref. 36 describes a case cooling system, now being used in current commercial engines, which reduces the cruise clearances in the high pressure turbine. This cooling system is automatically shut off to

increase the clearance during potential rub situations.

As mentioned previously, a problem in some engines is a loss in thrust on engine acceleration. This is thought to be due to the opening up of certain critical sealing clearances and has been attributed to the fast sealing case thermal response. Magnitudes of thrust loss in the range of 12% have been reported (Ref. 7) for conditions in which throttle advance is made on a "cold" engine; for example, when the engine is started, taxied to the end of the runway, and then accelerated for takeoff.

Typical transient clearances for a high bypass engine are given in Ref. 37 for a first-stage high-pressure turbine; these data (shown in Fig. 38) show blade tip clearance changes of about 0.76 mm (0.030 in.) over a period of 400 seconds.

As mentioned previously, large engines have relatively flexible cases and rotors; these are inherent in large-diameter, flight weight structures. As a result, various thrust, aerodynamic, and gyroscopic loads cause appreciable relative displacements at certain sealing locations. An example pointed out in Ref. 26 is the engine case bending (large high bypass engine) resulting from aerodynamic loads on the inlet cowl (see illustration in Fig. 39) and from the thrust loading. These inlet lift and thrust loads, which are large during climb-out after takeoff, cause rubbing at the 12 o'clock position in the high-pressure compressor and at the 6 o'clock position in the fan.

Reference 26 also points out that vibration characteristics (response to gust, takeoff, turbulence and maneuver loads) are of fundamental importance in propulsion system design and that a piecemeal, component-by-component analysis is not sufficient because of coupling effects. The analytical method described in Ref. 26 covers the engine and airframe related components and has these two main procedural steps:

(1) The use of static models of installed propulsion system and steady-state loads to calculate preliminary magnitudes of stresses and deflections

(2) The refinement of the analysis through the use of a dynamic model of an installed propulsion system with transient flight loads, gyroscopic forces, and rotor unbalance to calculate stresses, deflections, and frequencies.

The analytical model (Ref. 38) includes the probability of exceeding a flight load, which will cause a blade tip rub; this is expressed in terms of "exceedances" (rubs) per 1000 flights. The data in Ref. 38 show that exceedances are a function of engine position, and show most of the change in clearance due to rubs occurring during the first 10 flights. This agrees with a conclusion from the study in Ref. 6 that the deterioration consisted of two portions, an initial rapid rate (wear in), which opens up the clearances, and then a slower rate, which is dependent on erosion rate and the number of adverse events (compressor stalls, hard landings, severe gusts, etc.).

In small and large engines a major consideration is the roundness of the case. For example, there could be transient effects such as the response of a horizontally split compressor case to a thermal change. In general, horizontal flanges at the split line have a different thermal response from the rest of the case, and the flange also causes the case stiffness to be nonaxisymmetric. In the hot section out-of-roundness is caused by (1) nonuniform temperatures, (2) nonaxisymmetric structures, (3) localized flange leakage, (4) nonuniform distribution of cooling air, and (5) localized flow path gaps (hot-gas recirculation). Engine operation data indicate that hot section out-of-roundness may be in the range of 0.001 cm (0.0004 in.) per centimeter of diameter. Thus, the out-of-roundness may be greater than the desired operating tip gap. And as turbine temperatures and pressures increase, both the out-of-roundness tendency and performance penalty will increase. A partial solution to out-of-roundness, of course, is in obtaining more axisymmetric temperature distribution. Also, it should be noted that out-of-roundness can be caused by strains in adjacent cases; that is, a maldistribution of temperature in one case section can influence the roundness of adjacent case sections.

Clearances can be affected by rotor and stator vibrations. Shaft dynamics motions due to rigid rotor and flexible rotor unbalance (see Table II) have received considerable attention and are amenable to analysis (Refs. 39 and 40). Modern analytical methods and shaft balancing techniques generally insure a trouble free design from a rigid rotor critical speed standpoint. Large engines generally operate above the rigid rotor critical and below the flexible rotor mode, and typical radial displacements at operating speed due to rotor unbalance are reported to be in the range of 0.010 cm (0.004 in.) in large engines. Thus in a well designed system, radial displacement due to critical speed is usually not a major factor in sealing clearances. Some small engines run above a flexible rotor mode, and recent advances in multiplane balancing techniques (Ref. 41) promise small operational displacements. However, there remain questions on response of flexible rotor under adverse conditions such as surge/stall or blade out operation.

There is concern that nonsynchronous whirl (see Table II) could be the source of clearance changes, especially in high-pressure systems. Figure 40 illustrates the general principle for a labyrinth seal. The pressure field within the labyrinth seal will, in general, not be symmetric about a plane (section A-A in Fig. 40) passing through the direction of eccentricity because of preswirl and the nonuniform clearances. (A complicating factor in labyrinth

seal is axial clearance variation due to convergence, divergence, or axial misalignment.) Since the pressure field is not symmetric about section A-A (Fig. 40), a force component will exist which is transverse to the eccentricity direction, which will tend to produce a self-excited whirl.

A similar principle applies to the case of blade whirl forces; because of nonuniform clearances and associated leakages, blade loading is not uniform (lower loading where the tip gap is larger) and the net result is an aerodynamic force transverse to the eccentricity direction.

An additional potential source of vibration is rubbing friction induced whirl. This is a complex case/rotor interaction which has not been well investigated.

The necessary use of thin sections and light-weight construction has introduced potential vibratory motions of the labyrinth seal structure, especially in larger sizes. Although fatigue cracking of the labyrinth structure is usually the final result, clearance changes with associated wear can also be produced. Instabilities are reported to have occurred when the wave speed of vibration of the rotating labyrinth component was in resonance with the flexural wave speed of the stator shroud. To preclude failure due to resonance with a flexural mode in the stator, Ref. 9 recommends stators that have a minimum angular velocity for all flexural modes at least 25% higher than the rotor speed at 100% operation. This may require experimental verification of the predicted frequencies since some stator structures are quite complex.

In addition Ref. 9 makes the interesting observation that labyrinth stator and rotor components do not have fatigue failures when supported on the discharge end. (See Fig. 41.)

Clearance management in the various seals presents a difficult engineering problem, which involves the entire rotor/case assembly, airframe integration, and operational flight loads. In modern engines knowledge of the operating clearances is inferred from rub wear patterns and engine operating history. Direct clearance measurement comes from various types of probes (capacitance, mechanical touch, laser) and from high energy X-radiography, which is capable of measuring sealing clearances within an accuracy of ±0.07 mm (±0.003 in.) (Ref. 42). In this regard Ref. 42 claims both steady-state and transient clearance can be measured and useful data obtained on

(1) Axial and radial clearances of labyrinth seals

(2) Radial blade tip clearances

(3) Rotor/stator axial clearances

(4) Component deflections.

Reference 43 describes a unique laser optical probe, which is capable of measuring blade tip clearances in compressors and turbines. (For turbine applications a small cooling flow of nitrogen gas is used to keep probe internal parts cool.) The principal of operation is based on reflected light triangulation as indicated in Fig. 42 from Ref. 43. Light from a point source is reflected from each blade tip as it passes by the probe, and the clearance reading is an average of all the blades (current research looks at individual blade clearances). A change in clearance causes a shift of the reflected light such that it falls on a different section of the output fiber optic bundle. Accuracies of ±0.025 mm (0.001 in.) are claimed, and a probe temperature environment of 1311 K (1900° F) can be tolerated. A significant feature is that the high response of the system (0.4×10^{-6} sec) permits transient clearance measurements.

6. GAS PATH SEALING MATERIALS

If gas path sealing clearances are going to be reduced to a practical minimum, some rubbing contact must be tolerated in order to compensate for eccentricities, machining tolerances, out-of-roundness, vibrations, etc. Ideally these rubbing contacts may be classified into the following two types:

(1) Low energy rub – Low-energy rubs obtained several ways. One is through the use of abradable materials, which are designed to wear instead of producing wear in the blade or labyrinth tooth (these approaches are discussed later).

(2) Abrasive – Drum rotors generally have bonded abrasive coatings which protect the rotor from wear and promote vane tip wear in case of interference. These coatings, which are usually hard oxides, also mitigate thermally induced expansions of the rotor, which would aggravate the rub and, therefore, induce thermal feedback which could end in a catastrophic failure.

A major factor that controls rub material selection is the operating temperature. In the colder sections (fan and low pressure turbine) sprayed and molded polymer systems are suitable. But in the high-pressure compressor, the higher temperatures require metal systems such as sprayed nickel/graphite. The high-pressure turbine

requires very high temperature oxidation resistant materials which, in general, are not abradable and do not provide low energy rubs. Finally, the low-pressure turbine can use some of the materials suitable for the high pressure compressor but honeycomb shrouds are the most popular.

Rub material for over fan blade tip should be abradable or have a low-energy rub property to prevent blade wear. In addition, the fan rub material is usually configured to enhance aerodynamic stability (improve fan stall margin) and acoustical damping. One common shroud material used is aluminum honeycomb, which is readily deformed by fan blade penetration. However, wear to blade tips can be a problem; further, the honeycomb material, which is a rough surface from an aerodynamic standpoint, has an associated efficiency penalty as compared with smooth rub material. Reference 44 reports a 2.5 percentage point loss for honeycomb rub material as compared to a fan with a smooth shroud. The stall margin, however, improved 12% (see Fig. 43).

Other types of fan shroud rub material are elastomer and polymer base composites, which sometimes contain fillers of hollow glass spheres to improve abradability. These rub shrouds usually contain grooves or slots, which improve the stall margin by stabilizing the fan flow near the tip. Considerable data have been published (see Refs. 45 to 47) on the effectiveness of various geometric patterns in the fan shroud. A potential problem with use of some polymeric type materials in the low-pressure compression system is the considerable amount of rub material dust created during a very hard rub under an adverse operating condition. This dust has, on occasion, exploded in the high-pressure compressor.

In the high-pressure compressor higher temperature shroud materials (metal, graphite, etc.) are required because the discharge temperatures are near 922 K (1200° F) in some modern engines, and will be even higher in advanced engines. Currently used rub materials over blade tips (outer air sealing) are designed to mitigate blade wear by serving as low-energy rub or sacrificial material. Three different types of low-energy rub materials are used (Fig. 44). The sintered metal system (density 30 to 40%) of Fig. 44(a) is representative of an abradable type material, since blade (or labyrinth tooth) penetration breaks off sintered particles. The material effectiveness is often measured by the ratio of material wear to blade wear; a ratio of 10:1 being considered a satisfactory abradability property. Abradability can be readily achieved by lowering density, but this increases the susceptibility to erosion. Thus, a basic difficulty is obtaining acceptable abradability yet maintaining adequate erosion resistance.

The sintered metal fibers depicted in Fig. 44(b) are plastically deformable rather than abradable and are usually about 20% dense. Blade (or labyrinth tooth) penetration may densify the material (as indicated schematically) and this increases the rub intensity.

A third type used in outer air sealing is the low-shear-strength 100% dense material (Fig. 44(c)); sprayed aluminum is an example. Blade penetration readily machines away the easily sheared material without excessive wear to the blades. However, the machining debris tends to stick on downstream airfoils and cause aerodynamic losses.

Studies of Ref. 48 indicate a tendency for blade wear when the penetration rate is low (typical blade penetration rates range between 0.00025 to 0.025 cm/sec (0.0001 to 0.01 in/sec). As yet, a fully satisfactory material has not been developed for outer gas path sealing. Blade wear, erosion or aerodynamic loss remain consistent problems. None have all the desirable properties, which are:

(1) No blade wear ⎫
⎬ a general problem
(2) Low energy rub ⎭

(3) Innocuous debris (a problem in sprayed aluminum and some polymers)

(4) Erosion resistance ⎫
|
(5) Impermeability ⎬ a problem in porous materials
|
(6) Smooth surface ⎭

(7) Easy repair (a problem in brazed assemblies)

Labyrinth shrouds for compressor inner gas path sealing are depicted in Fig. 45; all are designed to produce a low energy rub as compared with a 100% dense metal shroud. In the high speed rubs, which take place between the shrouds and rotor, the rub mechanisms and associated wear are not well characterized for currently used material couples. Theoretical studies (Ref. 49) on rotor/shroud interaction predict the formation of "thermal bumps" or hot spots which apparently govern the wear process. These hot spots are the result of thermal-elastic surface instabilities produced by contact. For example, experimental data show that when a labyrinth knife edge rubs against a shroud segment, the rubbing can take place over just a small segment (~5° arc) of the 360° of tooth edge (see Fig. 46). Thus, the heat input is highly localized, and a local thermal bump is generated which expands,

rubs harder, and finally wears away. This is then followed by rubbing over a second small segment which grows and then wears, etc. Evidence of localized rubbing is indicated by the heat discoloration of the tooth edge. This type of local rub interaction has been investigated from a fundamental standpoint, and a considerable body of data exist, for example, see Refs. 50 and 51.

Thermal elastic instabilities apparently occur on the blade tips as well as on the casing rub material. The most adverse operating environment from a sealing viewpoint is in the high-pressure turbine. Here the gas temperatures in some modern engines are in the range of 1700 K (2600° F). In addition to the losses due to blade tip clearances, which were previously pointed out, there is a considerable efficiency penalty associated with cooling of the turbine case rub shroud material (outer air seal). In small engines this rub shroud is a single ring; in large engines it is constructed of segments. Typically each segment is impingement cooled and is held in place by a cooler outer case structure. Figure 7(a) shows, in cross-section, a typical segment and associated attachment structure.

Turbine rub shroud materials used are generally not abradable and turbine blade tip wear is a general problem. Transfer of the blade material to the rub shroud surface can precipitate a buildup of material which causes blade wear. This mechanism is not fully understood.

Commonly used rub materials are a cast high-temperature cobalt base alloy, and sintered NiAl and NiCrAlY powders (Ref. 1). For long-term operation these materials must be cooled, by impingement and film cooling techniques, to temperatures in the range of 1311 K (1900° F). Nevertheless, thermal stress cracking, loss of dimensional stability, and erosion remain current problems. The cooling requirement in terms of engine airflow can be as high as 1% to 2%, depending on the turbine-inlet temperature. This high cooling penalty is one reason why ceramic rub materials, which require less cooling, are being developed.

The use of ceramic material allows higher rub shroud surface temperatures. Further, ceramics require less cooling air. The potential cooling airflow reduction is indicated in Fig. 47, which shows for a 1811 K (2800° F) turbine-inlet temperature and a surface temperature of 1700 K (2600° F), that the cooling air requirement is significantly less than when the surface temperature must be held to 1366 K (2000° F); Fig. 47 indicates a reduction from 2.1% to 0.3% of engine flow (Ref. 52).

An advanced ceramic/metal shroud being developed (Ref. 53) is shown in Fig. 48. It is produced by thermal spraying ceramic/metal layers on a metal substrate of a heat resistant metal alloy. The first step in the process is to spray a 0.127-mm (0.005-in.) coating of NiCrAlY on the metal substrate. This is followed by a layer composed of 60% CoCrAlY and 40% yttria stabilized zirconia (ZrO_2). Next come successive layers of 30% CoCrAlY/70% ZrO_2, and 15% CoCrAlY/85% ZrO_2. Finally, the last layer, the one exposed directly to the turbine gas, is 100% ZrO_2.

This graded layer system provides a gradual change in thermal expansion coefficient and mitigates the large thermal expansion difference between the metal substrate and the ceramic layer next to the hot gas stream. Experimental studies (Ref. 53) show that graded layer ceramic material has adequate erosion resistance at 1588 K (2400° F) surface temperature. Encouraging thermal fatigue improvement is also reported but this remains the major problem. In this regard, an analytical study of the thermal stresses during engine acceleration (takeoff) by Ref. 54 indicates that the ceramic layer is probably subjected to excessive tensile stresses under this transient operating condition.

7. CONCLUDING REMARKS

Modern gas turbines contain a multiplicity of sealing locations; a large engine may have over 50 major dynamic sealing locations; in addition, sealing is necessary at vane pivots, flanges, duct joints, and blade roots. As pointed out in the discussion, sealing can have a marked effect on engine efficiency, performance retention, thrust, compressor pressure ratio, and compressor stall margin. Much of the performance retention problem in modern engines is caused by increases in sealing clearances, with blade tip wear in the compressor and turbine being a major contributor. Improved sealing significantly increase air superiority mission radius and maximum dash distance. Also maximum thrust can be improved significantly. The performance deterioration trends suggest a sealing problem that will worsen as engine designs advance to even higher pressures and temperatures. Small engines remain a particularly challenging problem because leakage is inherently more detrimental to efficiency.

There are three general approaches to increasing sealing effectiveness, these are:

(1) Improved clearance control (reducing clearances and minimizing the amount of rubbing)

(2) Improved "abradable" materials

(3) Increased flow energy dissipation in labyrinth seals.

Of the three approaches, clearance control holds the most potential for improvement. To achieve clearance control improvements, we must know more about the relative displacement of the case and rotor, particularly under

transient conditions, in modern engines. In advanced engines more attention must be given to engine stiffness, case roundness, case bending and to case/rotor dynamics of the total assembly. In this regard, more data are needed on various external and internal aerodynamic loads such as compressor surges. Accurate prediction of case/rotor displacements will require a large computational capability to treat the total assembly. Also, new approaches and concepts, such as active clearance control (by case cooling), will be needed to mitigate effects of case/rotor differential expansion. Improved "abradable" materials will provide some accommodation for eccentricity and out-of-roundness, but the clearance problem will probably not be solved solely with improvements in rub materials. In fact, the improved clearance control approach can be used to minimize rubbing and this, then, reduces the rub material problem.

The literature contains much data about blade clearance effects in compressors and turbines. Although there are variances between the published data, there is agreement that clearance changes cause a marked change in compressor and turbine efficiency. In particular, as fan and compressor clearances approach zero, the reported data indicate a very significant improvement in component efficiency. On the other hand, operation at very close clearances introduces a potential for high deterioration rates. Thus the solution requires maintaining close clearances for the time between normal overhauls. In the turbines the data show the clearance loss increasing with reaction rate; this trend suggests that advanced highly loaded turbines will have even greater losses than indicated in the current data. Thus advanced turbines will need to run with close clearances to avoid high losses.

Mathematical models for prediction of leakage over compressor and turbine blade tips are semiempirical expressions derived from cascade data; rotation effects are not included. There is a need for improved capability to predict clearance effects and for clearer insight regarding the significance of the many parameter which apparently affect tip leakage.

The ability of various engine companies to predict labyrinth seal leakage is very good; the methods are semiempirical and involve a correlation with a large number of experiments. However, the large number and the impact of labyrinth seals on engine performance suggest studies should be made to identify unique labyrinth geometries which would reduce leakage; the potential gain is significant even if the leakage reduction is nominal. In regard to labyrinth seal theory, the thermodynamic process is well understood, but analysis from a fluid dynamic standpoint may shed light on means to increase the kinetic energy dissipation in the labyrinth cavities.

Experience indicates the need for an improved compressor "abradable" material. The wear debris from this material should not stick on downstream air foils and should not pose a dust explosion problem in the high-pressure compressor. This "abradable" material also should produce little blade wear, be erosion resistant, and have an impermeable aerodynamically smooth surface.

Sealing over the tips of the high-pressure-turbine blade is a current problem, which will become most critical in advanced engines. Ceramic rub materials for the case are needed to reduce cooling requirements and permit higher operating temperatures. These ceramic rub materials must be abradable (because close clearances will lead to rubs) and dimensionally stable to mitigate out-of-roundness and eccentricity effects.

As with the sealing of the primary-gas flow, sealing of the internal-gas flow is becoming more critical as engine's pressures and temperatures increase. There is a need for improved technology in the internal-flow system in regard to purging, heat transfer, and cooling flow control. In addition to improved labyrinth seals in the internal-flow system, mainshaft sealing with lower leakage and high pressure and speed capability would provide efficiency improvement.

REFERENCES

1. Mahler, F. H., Advanced Seal Technology. PWA-4372, 1972 (AD-739922).

2. Dugan, J. F., McAulay, J. E., Reynolds, T. W., and Strack, W. C., Fuel-Conservative Engine Technology. NASA SP-381, Aeronautical Propulsion, pp. 157-190, 1975.

3. Stern, J. A., Aircraft Propulsion. A Key to Fuel Conservation: An Aircraft Manufacturer's View. SAE Paper 760538, May 1976.

4. Legassie, R. W. A., and Ordway, F. I., A Quick Look at the National Energy Plan. Astronautics & Aeronautics, Vol. 15, No. 11, Nov. 1977, pp. 28-35.

5. Grayson, K., Improved Maintenance Practices - The Airlines' Contribution to Lower Ownership Costs. SAE Paper 760504, May 1976.

6. Sallee, G. P., Kruckenberg, H. D., and Toomey, E. H., Analysis of Turbofan Engine Performance Deterioration and Proposed Follow-on Tests. NASA CR-134769, 1975.

7. Csavina, F. L., Performance Depreciation of Some Military Turbofan Engines. AIAA Paper 76-649, July 1976.

8. Hawkins, R. M. and McKibbin, A. H., Development of Compressor End Seals Stator Interstage Seals, and Stator Pivot Seals In Advanced Air Breathing Propulsion Systems, Part I: Screening Studies and Analysis. NASA CR-72819, 1970.

9. Alford, J. S., Labyrinth Seal Designs Have Benefitted from Development and Service Experience. SAE Paper 710435, 1971.

10. Moore, A., Gas Turbine Engine Internal Air Systems - A Review of the Requirements and the Problems. ASME Paper 75-WA/GT-1, Nov. 1975.

11. Paladini, W., Static and Rotating Air/Gas Seal Evaluation. CW-WR-70-124F, 1971 (AD-730361).

12. Povinelli, Valentine P., Jr., Current Seal Designs and Future Requirements for Turbine Engine Seals and Bearings. Journal of Aircraft, Vol. 12, no. 4, April 1975, pp. 266-273.

13. Lynwander, P., Development of Helicopter Engine Seals. LYC-73-48, Nov. 1973. NASA CR-134647, 1973.

14. Schweiger, F. A., The Performance of Jet Engine Contact Seals. Lubrication Engineering, Vol. 19, June 1963, pp. 232-238.

15. Gray, D. E., and Dugan, J. F., An Early Glimpse at Long Term Subsonic Commercial Turbofan Technology Requirements - Fuel Conservation. AIAA Paper 75-1207, Sep. 1975.

16. Lakshminarayana, B. and Horlock, J. H., Tip-Clearance Flow and Losses for an Isolated Compressor Blade. University of Liverpool, R & M No. 3316, 1963.

17. Dean, R. C., Jr., Secondary Flow in Axial Compressors. MIT Thesis, 1954. Also MIT Report 54-10-T, 1954.

18. Rains, D. A., Tip Clearance Flows in Axial Flow Compressors and Pumps. California Institute of Technology Report No. 5, 1954.

19. Lakshminarayana, B., Methods of Predicting the Tip Clearance Effects in Axial Flow Turbomachinery. ASME Paper 68-WA/FE-28, Nov. 1909.

20. Egli, A., The Leakage of Steam Through Labyrinth Seals. ASME Trans., Vol. 57, No. 3, Apr. 1935, pp. 115-122.

21. Dobek, L. J., Labyrinth Seal Testing For Lift Fan Engines. NASA CR-121131, 1973.

22. Zuk, J., Dynamic Sealing Principles. NASA TM X-71851, 1976.

23. Stocker, H. L., Cox, D. M., and Holle, G. F., Aerodynamic Performance of Conventional and Advanced Design Labyrinth Seals With Solid-Smooth, Abradable, and Honeycomb Lands, Detroit Diesel Allison, EDR 9329, NASA CR-135307, Dec. 1977. (To be published.)

24. Moore, R. D. and Osborn, W. M., Effects of Tip Clearance on Overall Performance of Transonic Fan Stage With and Without Casing Treatment. NASA TM X-3479, 1977.

25. Jefferson, J. L. and Turner, R. C., Some Shrouding and Tip Clearance Effects in Axial Flow Compressors. International Shipbuilding Progress, Vol. 5, No. 42, Feb. 1958, pp. 78-101.

26. White, J. L. and Beste, D. L., Nastran Applications to Aircraft Propulsion Systems. NASA TM X-3278, NASTRAN: USER'S EXPERIENCES, pp. 91-104, 1975.

27. Benstein, E. H., Small Flying Engines Are Different - Aircraft Gas Turbine Design. AIAA Paper 74-1185, Oct. 1974.

28. Holman, F. F., Kidwell, J. R., and Ware, T. C., Small Axial Compressor Technology Program. NASA CR-134827, Vol. 1, 1976.

29. Klassen, H. A., Wood, J. R., and Schumann, L. F., Experimental Performance of a 13.65 Centimeter-Tip-Diameter Tandem-Bladed Sweptback Centrifugal Compressor Designed for a Pressure Ratio of 6. NASA TP-1091, 1977.

30. Klassen, H. A., Wood, J. R., and Schumann, L. F., Experimental Performance of a 16.10-Centimeter-Tip-Diameter Sweptback Centrifugal Compressor Designed For a 6:1 Pressure Ratio. NASA TM X-3552, 1977.

31. Holeski, D. E. and Futral, S. M., Jr., Effect of Rotor Tip Clearance on the Performance of a 5-Inch Single-Stage Axial-Flow Turbine. NASA TM X-1757, 1969.

32. Kofskey, M. G., Experimental Investigation of Three Tip-Clearance Configurations Over a Range of Tip Clearance Using a Single-Stage Turbine of High Hub-to Tip-Radius Ratio. NASA TM X-472, 1961.

33. Szanca, E. M., Behning, F. P., and Schum, H. J., Research Turbine for High-Temperature Core Engine Application. II - Effect of Rotor Tip Clearance on Overall Performance. NASA TN D-7639, Apr. 1974.

34. Haas, J. E. and Kofskey, M. G., Cold-Air Performance of a 12.766-Centimeter-Tip-Diameter Axial-Flow Cooled Turbine. III - Effect of Rotor Tip Clearance on Overall Performance of a Solid Blade Configuration. NASA TP-1032, 1977.

35. Futral, S. M., Jr. and Holeski, D. E., Experimental Results of Varying the Blade Shroud Clearance in a 6.02-Inch Radial-Inflow Turbine. NASA TN D-5513, 1970.

36. Beyerly, W. R. and Sweeney, J. G., Life Cycle Fuel Consumption of Commercial Turbofan Engines. AIAA Paper 76-645, July 1978.

37. Adamson, G. P., Development Progress-New Transport Engines, JT9D. SAE Paper 710419, May 1971.

38. Aarnes, M. N. and White, J. L., Propulsion System and Airframe Structural Integration Analysis. AIAA Paper 75-1310, Sep. 1975.

39. Gunter, E. J., Jr., Dynamic Stability of Rotor-Bearing Systems. NASA SP-113, 1966.

40. Kirk, R. G. and Gunter, E. J., Effect of Support Flexibility and Damping on the Dynamic Response of a Single Mass Flexible Rotor in Elastic Bearings. NASA CR-2083, 1972.

41. Tessarik, J. M., Flexible Rotor Balancing by Influence Coefficient Method - Multiple Critical Speeds with Rigid or Flexible Supports. NASA CR-2553, 1975.

42. Alwang, W. G. and Kinchen, B., Internal Running Clearance Measurements in Gas Turbines Using High Energy X-Radiography. In "Advances in Test Measurement, Vol. 12; Ed. by B. Washburn, Instrument Society of America, 1975, pp. 339-348.

43. Ford, M. J., Hildebrand, J. R., and Prosser, J. C., Design, Fabrication and Demonstration of a Miniaturized Tip Clearance Measuring Device. PWA-FR-6447, 1974.

44. Osborn, W. M., Lewis, G. W., Jr., and Heidelberg, L. J., Effect of Several Porous Casing Treatments on Stall Limit and on Overall Performance of an Axial-Flow Compressor Rotor. NASA TN D-6537, 1971.

45. Bailey, E. E. and Voit, C. H., Some Observations of Effects of Porous Casings on Operating Range of a Single Axial-Flow Compressor Rotor. NASA TM X-2120, 1970.

46. Prince, D. C., Jr., Wisler, D. C., and Hilvers, D. E., Study of Casing Treatment Stall Margin Improvement Phenomena - For Compressor Rotor Blade Tips Compressor Blades Rotating Stalls. NASA CR-134552, 1974.

47. Bailey, E. E., Effects of Grooved Casing Treatment on the Flow Range Capability of Single-Stage Axial-Flow Compressor. NASA TM X-2459, 1972.

48. Bill, R. C. and Shiembob, L. T., Friction and Wear of Sintered Fiber-Metal Abradable Seal Materials. NASA TM X-73650, 1977.

49. Burton, R. A., Kilaparti, S. R., and Hechmann, S. R., Modeling of Turbine Blade Tip Contact. ASME Paper 75-WA/GT-14, Nov. 1975.

50. Barber, J. R., Thermoelastic Instabilities in the Sliding of Conforming Solids. Proceedings of the Royal Society, Series A, Vol. 312, No. 1510, Sep. 1969, pp. 381-394.

51. Burton, R. A., Nerlikar, V., and Kilaparti, S. R., Thermoelastic Instability in a Seal-Like Configuration. Wear, Vol. 24, 1973, pp. 177-188.

52. Schlike, P. W., Advanced Ceramic Seal Program (Phase I) PWA 6635, 1974 (AD 781004).

53. Shiembob, L. T., Development of a Plasma Sprayed Ceramic Gas Path Seal for High Pressure Turbine Applications. NASA CR-135183, 1977.

54. Taylor, C. M., Thermal Stress Analysis of a Graded Zirconia/Metal Gas Path Seal System for Aircraft Gas Turbine Engines. NASA TM X-73658, 1977.

TABLE I. - TYPICAL DIRECT OPERATING

COSTS (FROM REF. 3)

Item	Fuel price		
	20¢/gal	35¢/gal	50¢/gal
	Direct operating cost, %		
Fuel	31.5	44.6	53.5
Depreciation	25.5	20.6	17.3
Maintenance	19.0	15.4	12.9
Crew	18.2	14.7	12.3
Insurance	5.8	4.7	4.0
Change in DOC	----	23.6	47.2

TABLE II. - VIBRATIONS AFFECTING CLEARANCES

Type	Exciting force	Comment
1. Rigid shaft whirl	Rotor unbalance	Critical speed generally lower than engine operating speed and displacements are typically small
2. Flexible shaft	Rotor unbalance	Multiplane balancing technology is available - implementation needed
3. Labyrinth seal whirl forces (tip shrouded blades and labyrinth seals with non-uniform clearances)	Nonaxisymmetric pressure in labyrinth seal which causes a force transverse to eccentricity direction	Studies are needed
4. Blade whirl forces (shrouded and unshrouded blades with nonuniform clearances)	Nonaxisymmetric blade loading due to tip leakage causes a force transverse to eccentricity direction	Studies are needed
5. Rub induced whirl	Frictional force of labyrinth teeth or of blades rubbing against case	Studies are needed
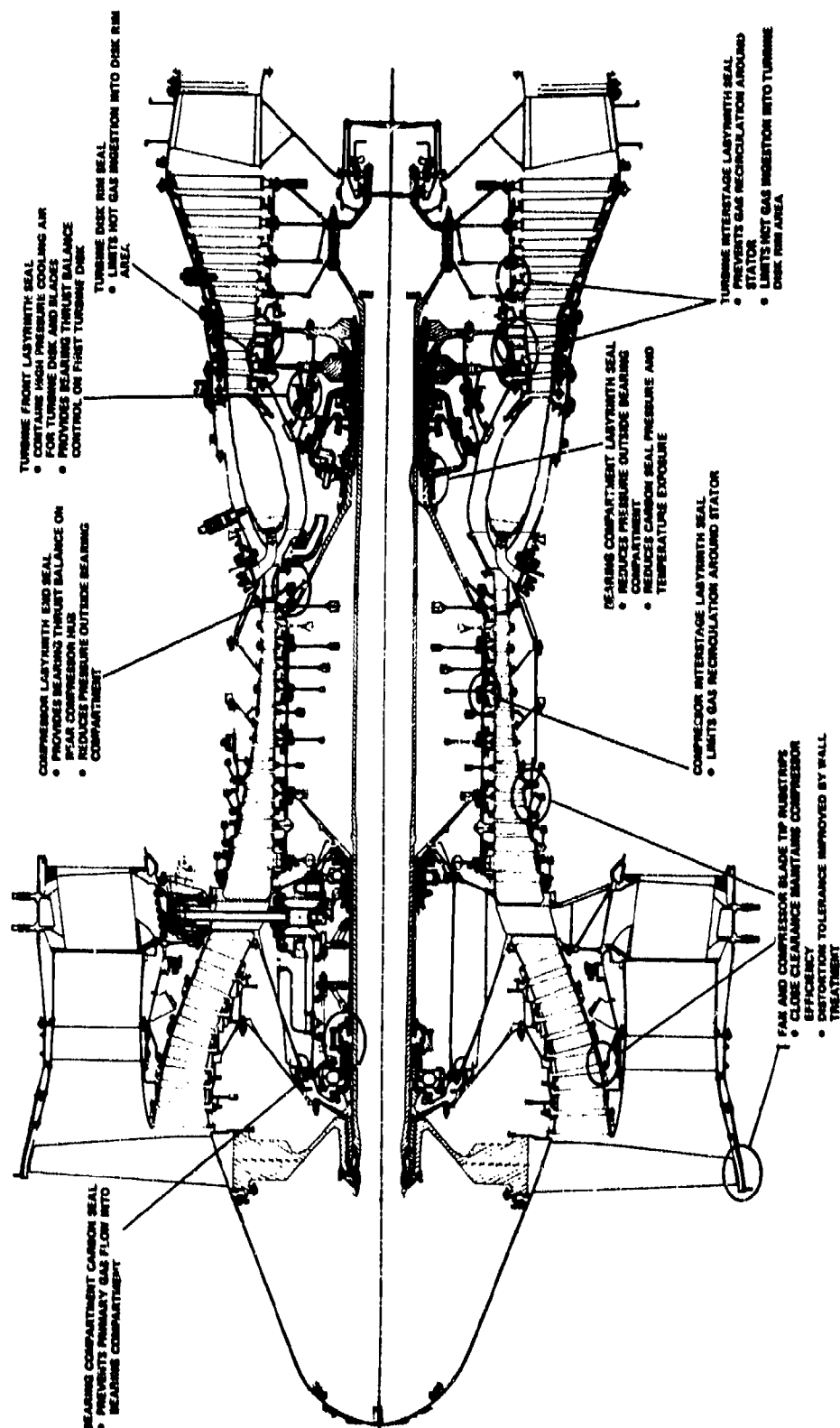
Fig.1 Modern transport engine (from Reference 1)
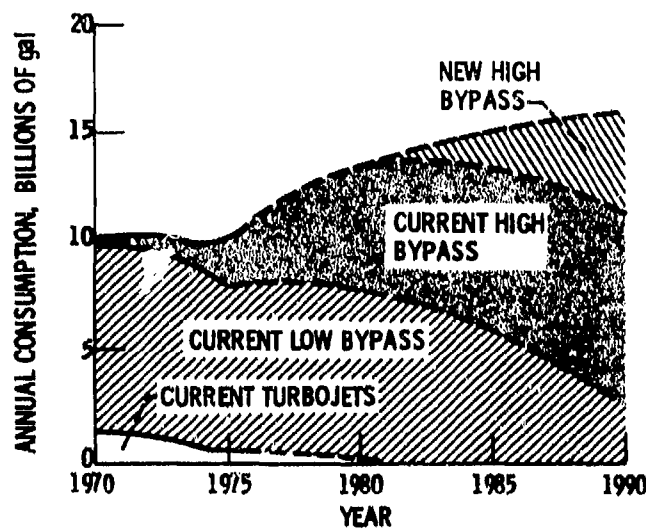
Fig.2 US airline fuel consumption by engine type (from Reference 2)
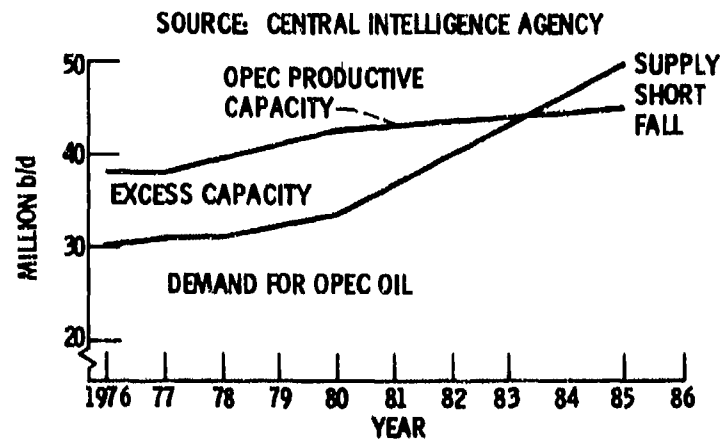
Fig.3 OPEC oil, supply/demand gap (from Reference 4)
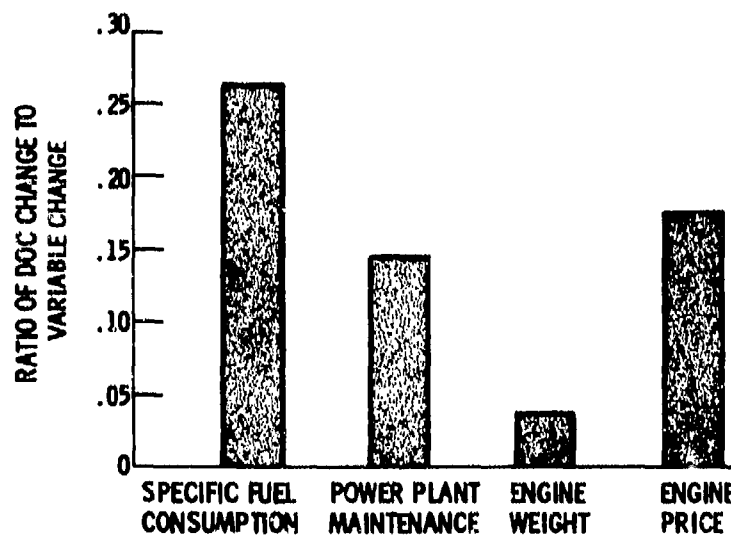
Fig.4 Direct operating cost-sensitivity to propulsion system variable (from Reference 5)
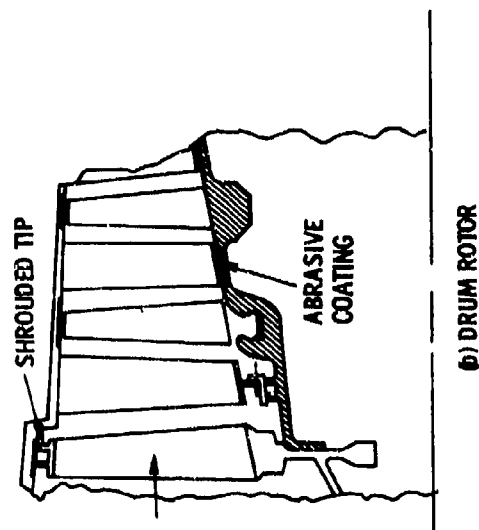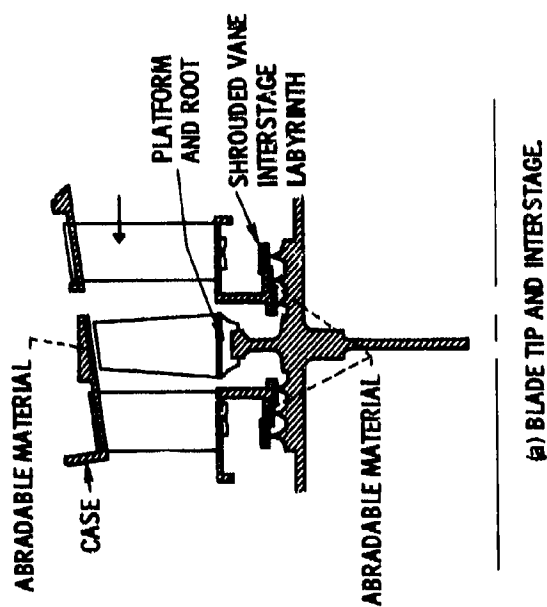
ABRADABLE MATERIAL

CASE

PLATFORM AND ROOT

SHROUDED VANE INTERSTAGE LABYRINTH

ABRADABLE MATERIAL

(a) BLADE TIP AND INTERSTAGE

SHROUDED TIP

ABRASIVE COATING

(b) DRUM ROTOR

Fig.6 Compressor sealing locations

ENGINE REPAIR

INCREASING SFC

INCREASING ENGINE TIME

Fig.5 Performance deterioration

(b) BLADE TIP.

SEGMENTED RING
OF RUB MATERIAL

LEAKAGE, FLANGE
AND BOLTS

RUB MATERIAL

STATOR

RIM
SEAL

RUB
MATERIAL

INTERSTAGE LABYRINTH

(d) SHROUDED ROTOR AND INTERSTAGE.

Fig.7   Turbine sealing locations (Ref.1)
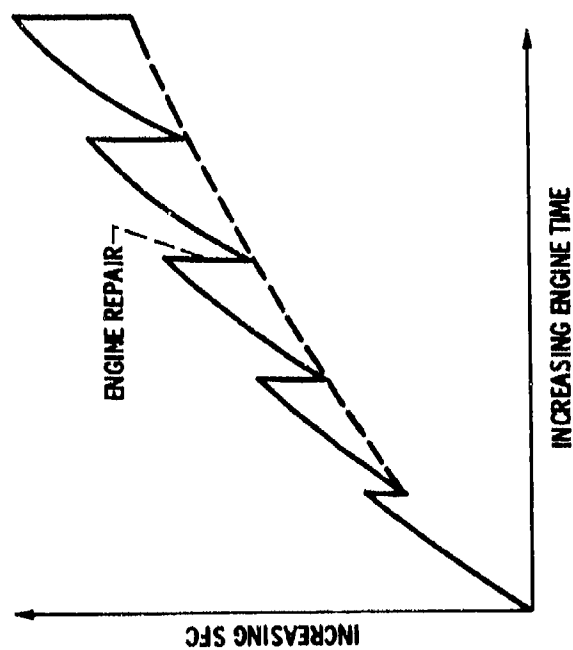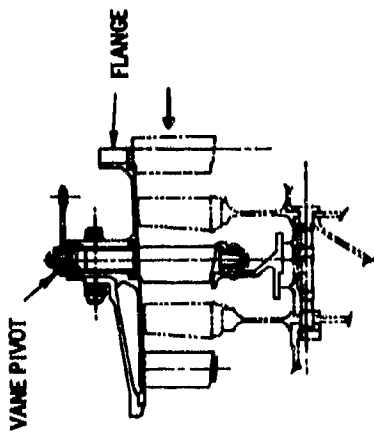
VANE PIVOT

FLANGE

(c) VANE PIVOT AND FLANGE (REF. 1).

AIRFLOW

LAST ROTOR
STAGE
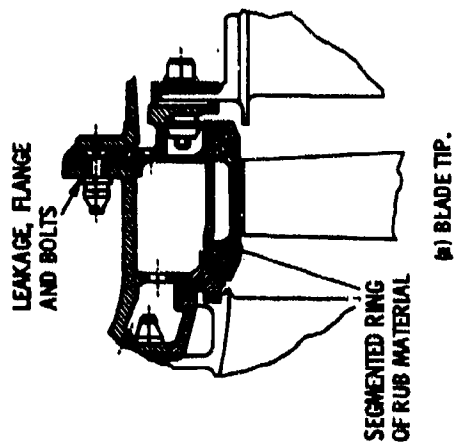
COMPRESSOR
END SEAL
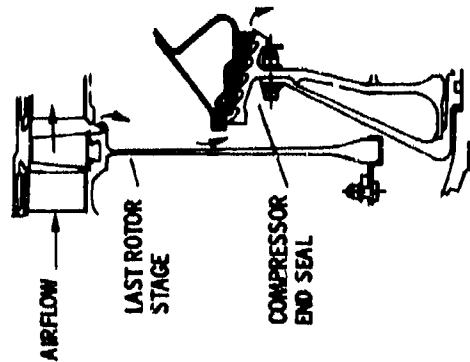
(d) COMPRESSOR DISCHARGE LABYRINTH SEAL (REF. 9).

Fig.6   Concluded
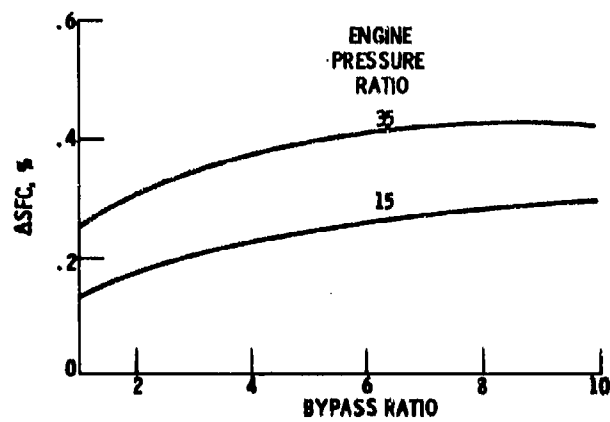
Fig.8   Effect of one percentage point increase in engine bleed on SFC
for various bypass ratios and for two pressure ratios (Ref.10)
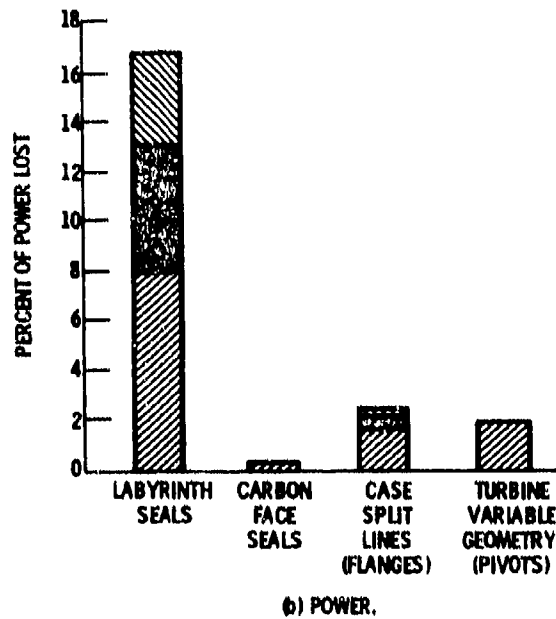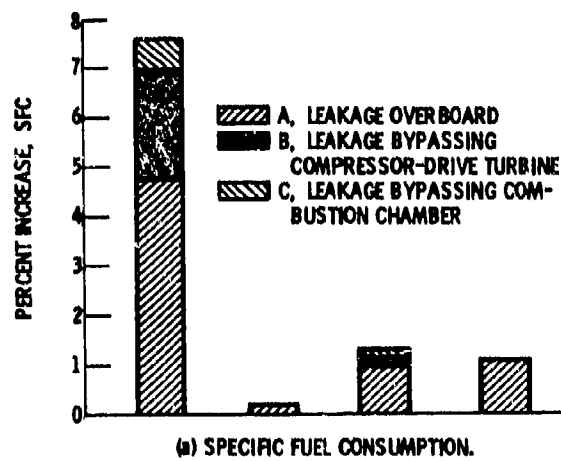

(a) SPECIFIC FUEL CONSUMPTION.

(b) POWER.

Fig.9   Calculated effects of seal leakage in a 2.3 kg per second
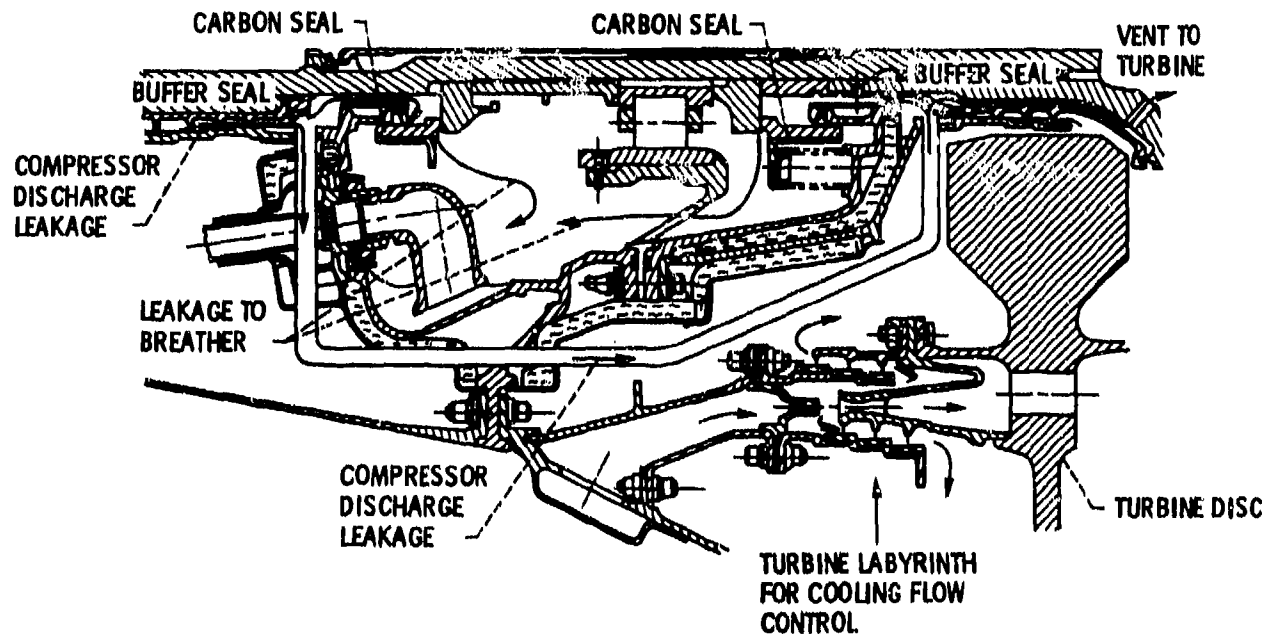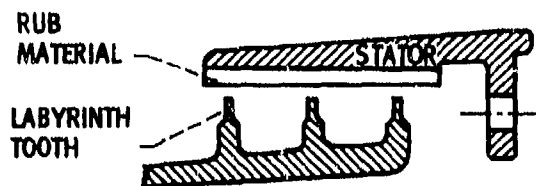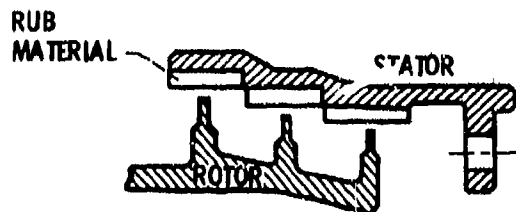(5 lbm per sec) size engine (Ref.11)

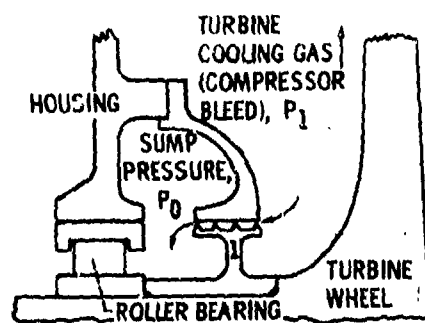Fig.10   Mainshaft and high pressure turbine labyrinth seal (from Reference 1)

(a) STRAIGHT.
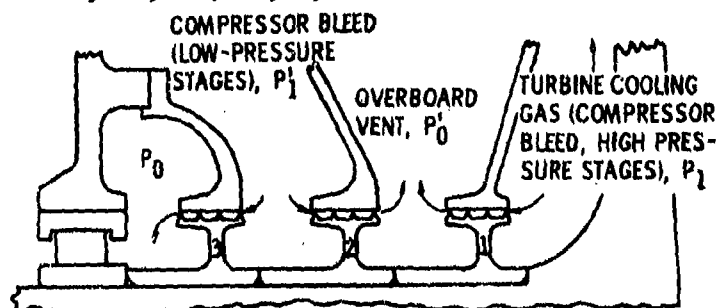

(b) STEPPED.
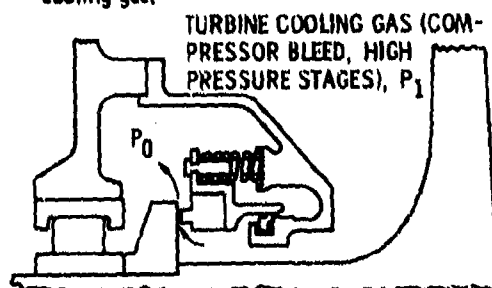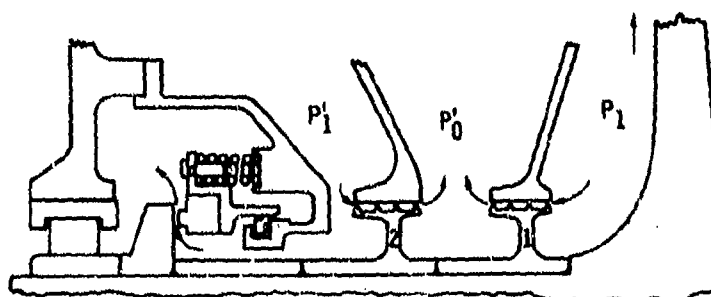
Fig.11   Labyrinth seal types

(a) RADIAL AND AXIAL MOTION.

(b) RADIAL MOTION, IDEAL INTERLOCKING.

Fig. 12   Labyrinth seal leakage areas for total interference wear to the stator

Fig. 13   Engine schematic showing main shaft seal locations

TURBINE
COOLING GAS
(COMPRESSOR
BLEED), P_1

HOUSING

SUMP
PRESSURE,
P_0

TURBINE
WHEEL

ROLLER BEARING

(a) Single labyrinth, early engines.

COMPRESSOR BLEED
(LOW-PRESSURE
STAGES), P_1'

OVERBOARD
VENT, P_0'

TURBINE COOLING
GAS (COMPRESSOR
BLEED, HIGH PRES-
SURE STAGES), P_1

P_0

(b) Multiple labyrinth for high-temperature high-pressure turbine
cooling gas.

TURBINE COOLING GAS (COM-
PRESSOR BLEED, HIGH
PRESSURE STAGES), P_1

P_0

(c) Conventional face seal.

P_1' P_0' P_1

(d) Conventional face seal with labyrinth seal for high-temperature,
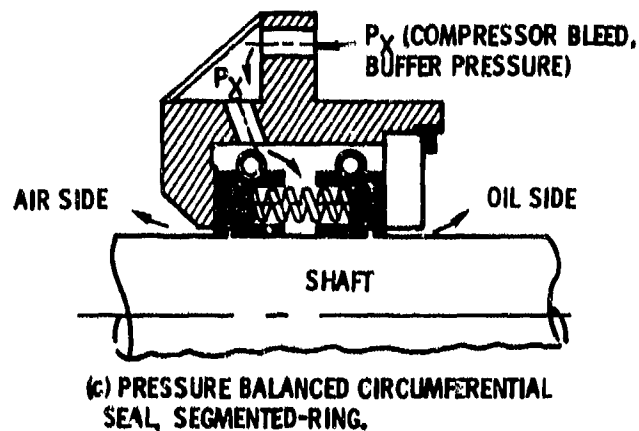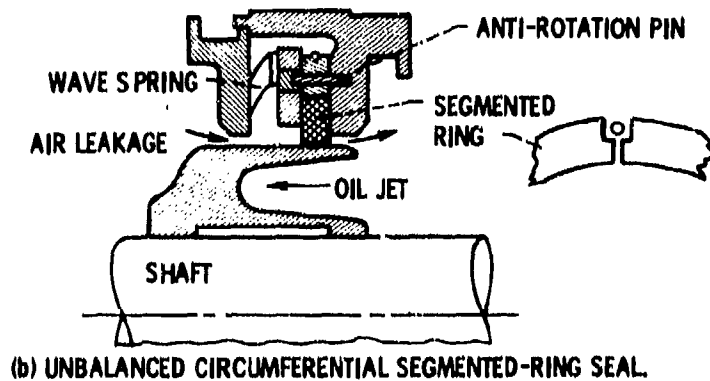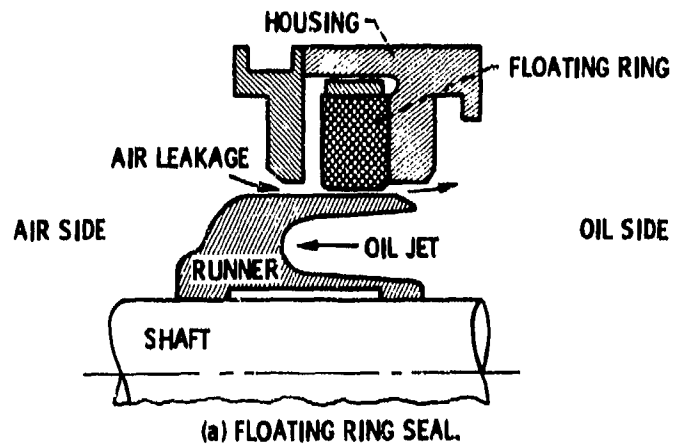high-pressure cooling gas.

Fig. 14 Seal systems

(a) FLOATING RING SEAL.

(b) UNBALANCED CIRCUMFERENTIAL SEGMENTED-RING SEAL.

(c) PRESSURE BALANCED CIRCUMFERENTIAL
SEAL, SEGMENTED-RING.

Fig. 15   Close clearance shaft seals, circumferential types

RELATIVE WALL MOTION

BLADE

BLADE

(a) COUETTE FLOW VELOCITY DISTRIBUTION DUE TO RELATIVE WALL MOTION.

(b) ORIFICE TYPE FLOW DUE TO PRESSURE DIFFERENCE.
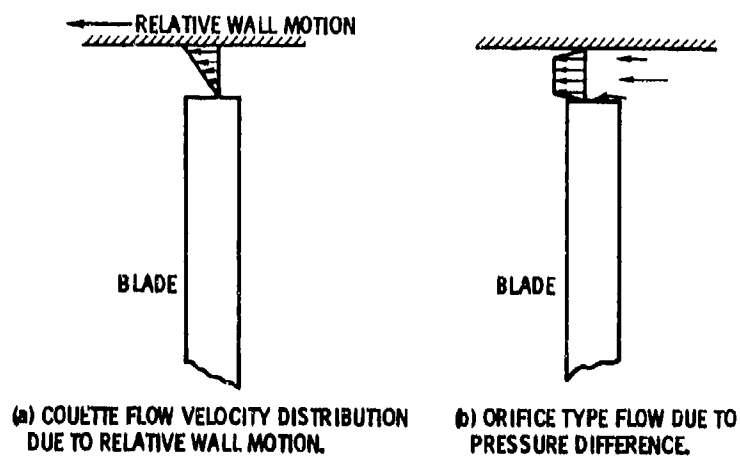
Fig.16   Flow velocity profiles

TIP LEAKAGE VORTEX

PRESSURE SIDE

ROTATION
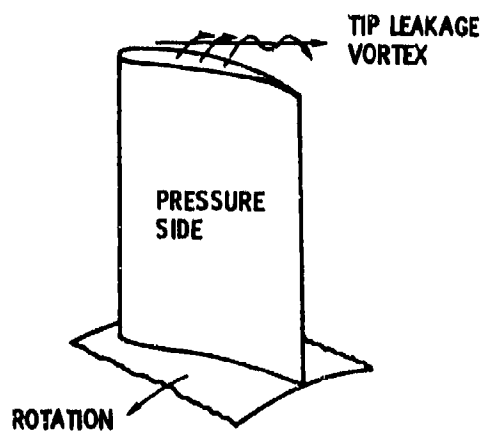
Fig.17   Vortex formed by leakage over blade tip

CASE I.D.

SECONDARY FLOW (LOW ENERGY)

HIGH ENERGY LEAKAGE FLOW

PRESSURE SIDE

SUCTION SIDE

BLADE
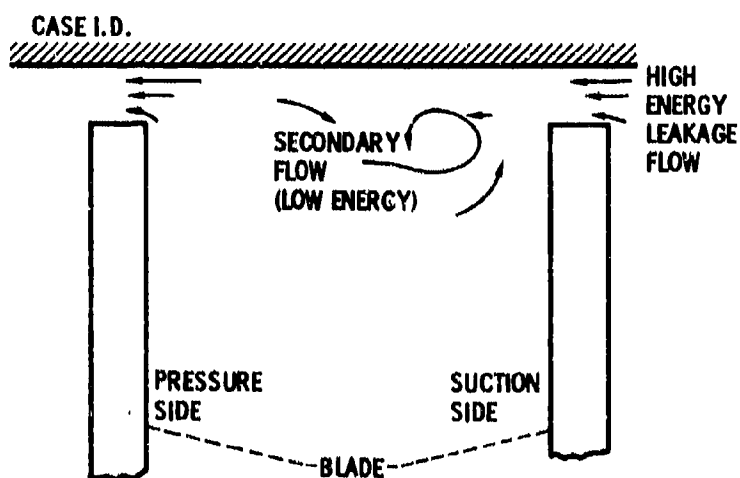
Fig.18   Interaction of leakage and secondary flow

N = NUMBER OF THROTTLINGS

N = 1

N = 2

N = 3
N = 4
N = 5

N = 6

P_d/P_u

FLOW FUNCTION, ϕ

(a) FLOW FUNCTION.

s

t

c

NOMENCLATURE

CLEARANCE, C

.020

.010

ct

DISCHARGE COEFFICIENT, a

(b) DISCHARGE COEFFICIENT

N = 8
N = 6
N = 4
N = 3
N = 2

.100

.050

c/s

CARRY OVER FACTOR, γ

(c) CARRY-OVER FACTOR.
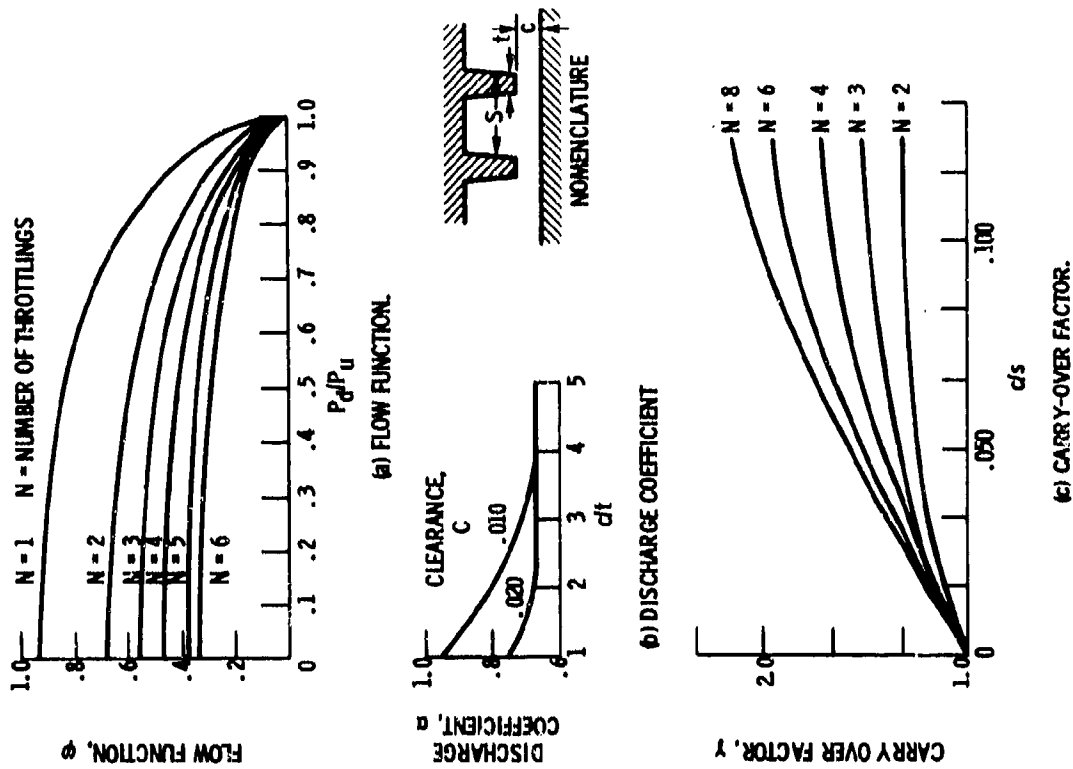
Fig.21 Plots of functions used in Egli labyrinth seal leakage equation (from Reference 22)

TOOTH

ACCELERATION, ISENTROPIC EXPANSION | KINETIC ENERGY DISSIPATION

1   2   3

TOOTH

Fig.19 Labyrinth seal, thermodynamic model

TOOTH P_2

P_1

TOOTH P_0

A_1 A_{min}

EXPANDING JET
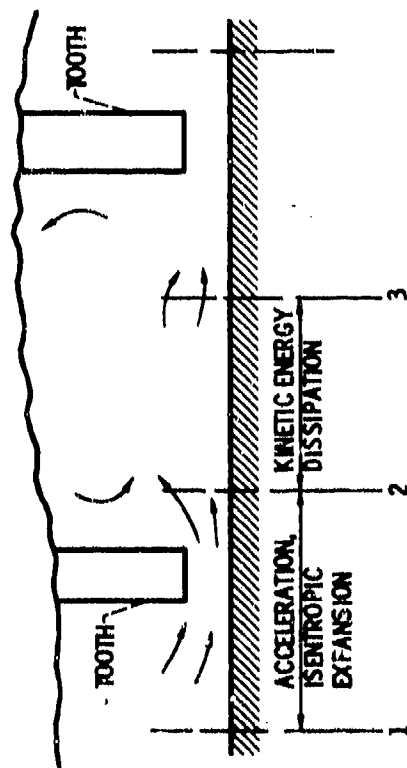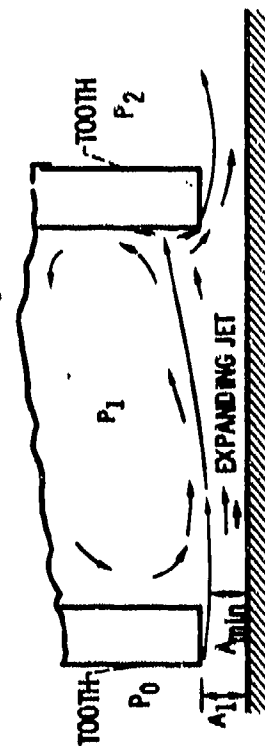
Fig.20 Labyrinth seal, fluid mechanic model illustrating the carry-over effect
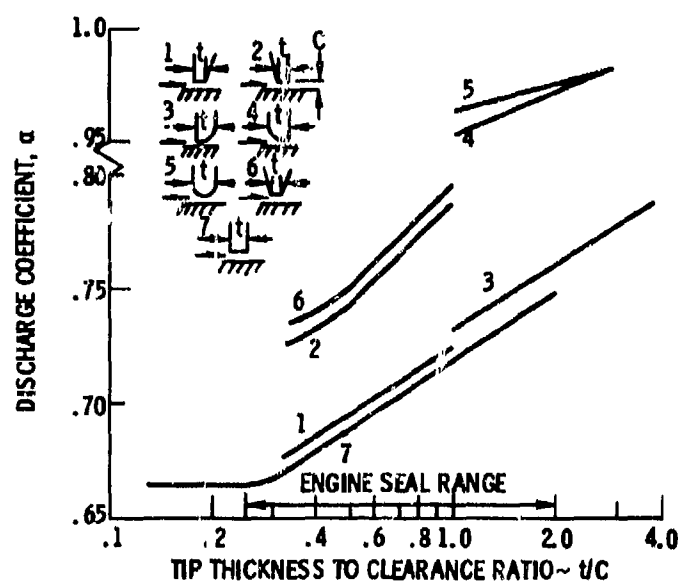
Fig.22   Effect of knife-edge tooth shape on discharge coefficient (from Reference 1)
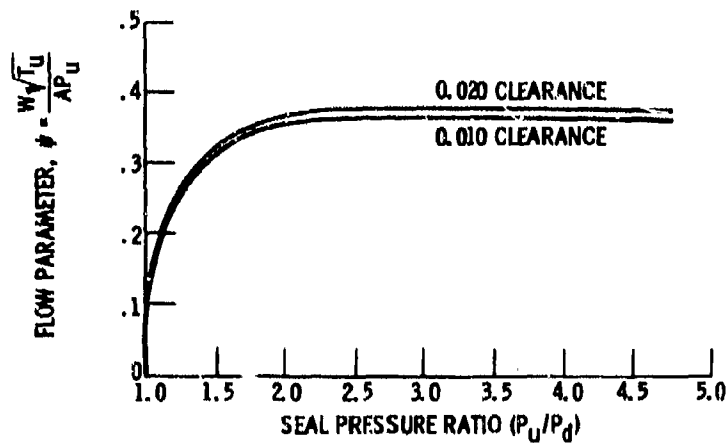
Fig.23   Flow parameter as a function of pressure ratio; 4 tooth straight seal (Ref.23)
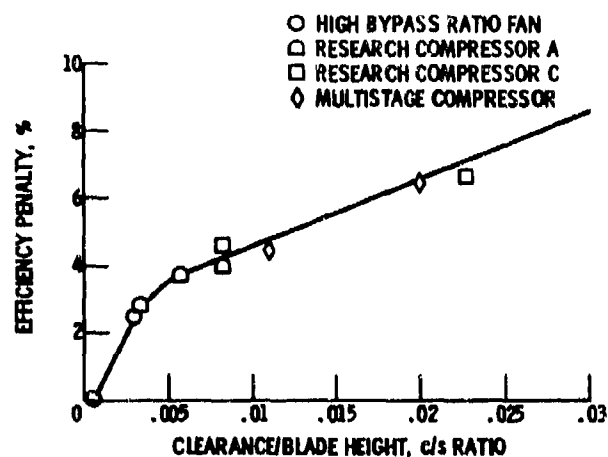
Fig.24 Axial flow compressor polytropic efficiency penalty, effect of clearance to blade height ratio (Ref.1)
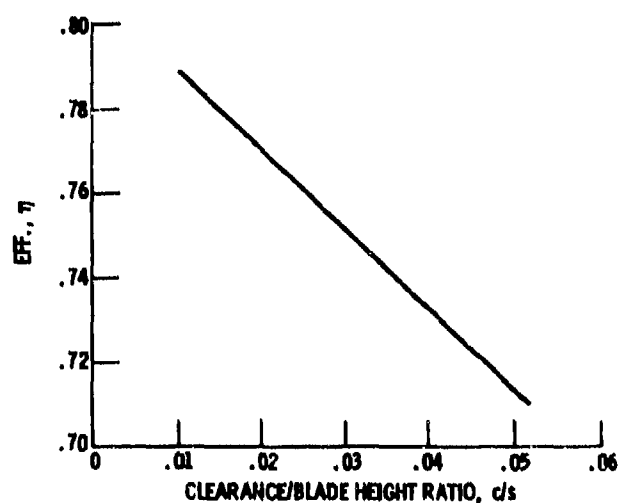
Fig.25 Compressor efficiency as a function of c/s ratio (Ref.25)
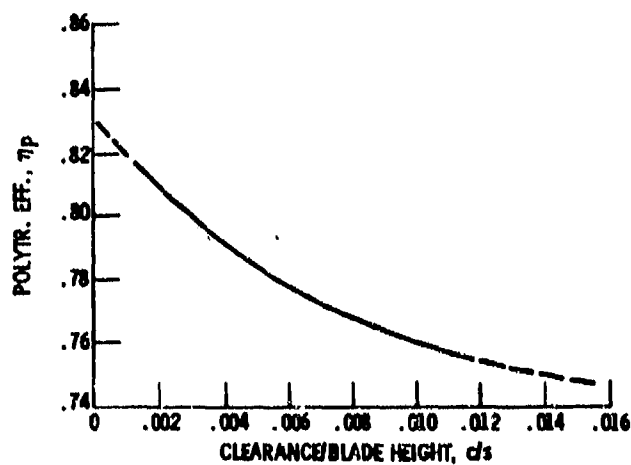
Fig.26 Single stage fan blade tip clearance sensitivity, transition region (data from Reference 24)
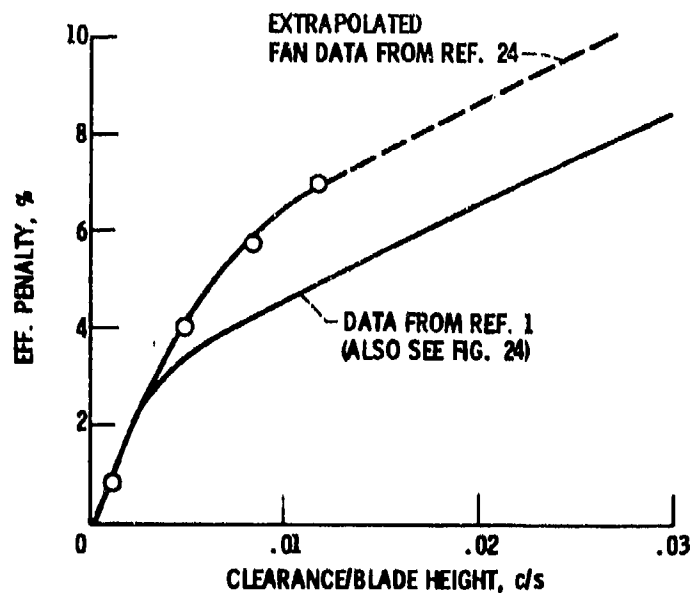
Fig.27   Fan and compressor blade tip clearance sensitivity
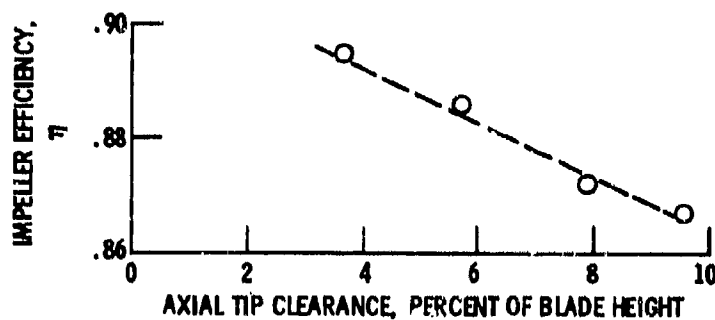
Fig.28   Variation of impeller peak efficiency with axial tip clearance for vaneless diffuser test.
Ratio of specific heat $\gamma = 1.4$ (from Reference 30)
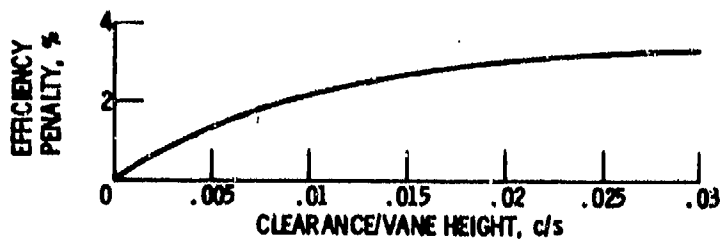
Fig.29   Efficiency penalty as a function of clearance to vane height ratio,
cantilevered vane and drum rotor (Ref.1)
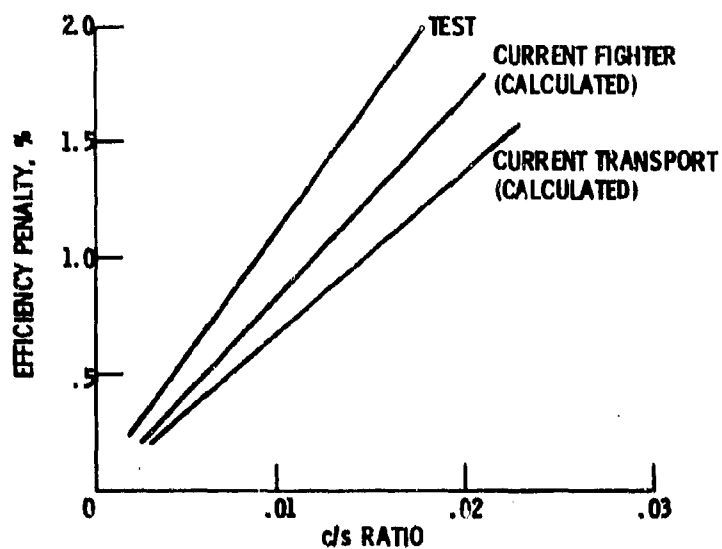
Fig.30 Compressor efficiency penalty as a function of labyrinth clearance to vane height ratio (Ref.1)
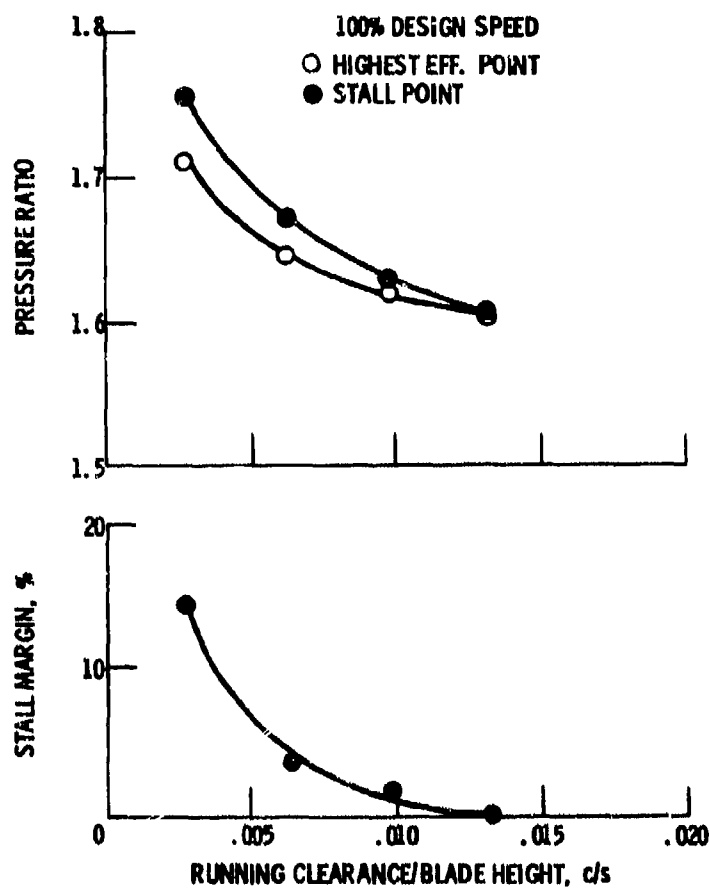
Fig.31 Single stage fan, effect of blade clearance on pressure ratio and stall margin (Ref.24)

(a) TOTAL INTERFERENCE APPEARS AS BLADE WEAR.

(b) TOTAL INTERFERENCE APPEARS AS CASE WEAR.
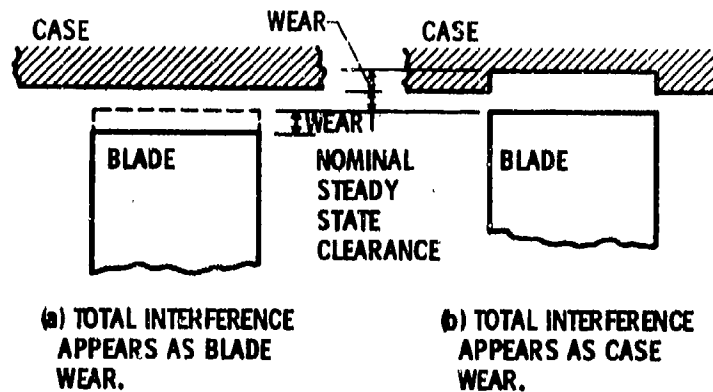
Fig.32   Illustration of two idealized extremes in wear caused by blade/case interference during transient operation

(a) VARIATION OF EXIT FLOW ANGLE WITH RADIUS RATIO.

(b) VARIATION OF TOTAL EFFICIENCY WITH RADIUS RATIO.
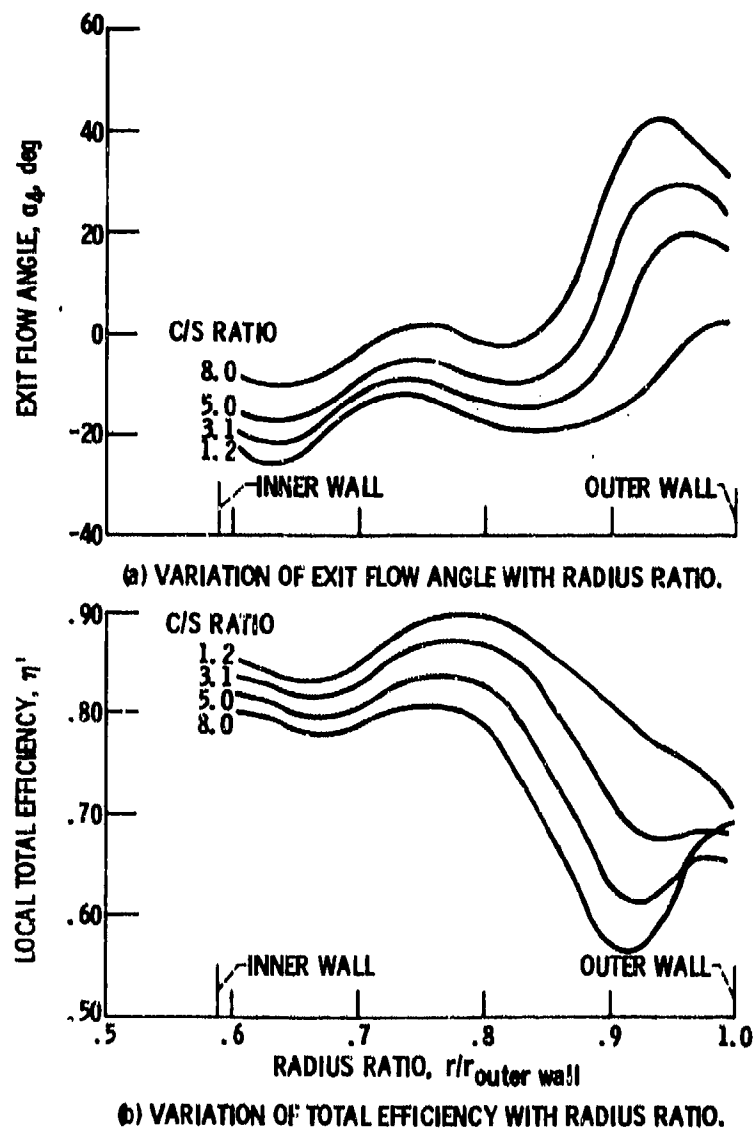
Fig.33   Survey results at rotor exit at design equivalent speed and pressure ratio. (Ref.31)

SOURCE	TURBINE	R_x	$\dfrac{[1-(\eta/\eta_0)] \times 100}{\% \text{ tip clearance}}$	
REF. 32	IMPULSE	0	0.8	CASE / BLADE
REF. 34	REACTION	.890	1.5	
REF. 32	IMPULSE	0	1.6	CASE / BLADE
REF. 33	REACTION	.805	1.8	
REF. 34	REACTION	.890	2.0	
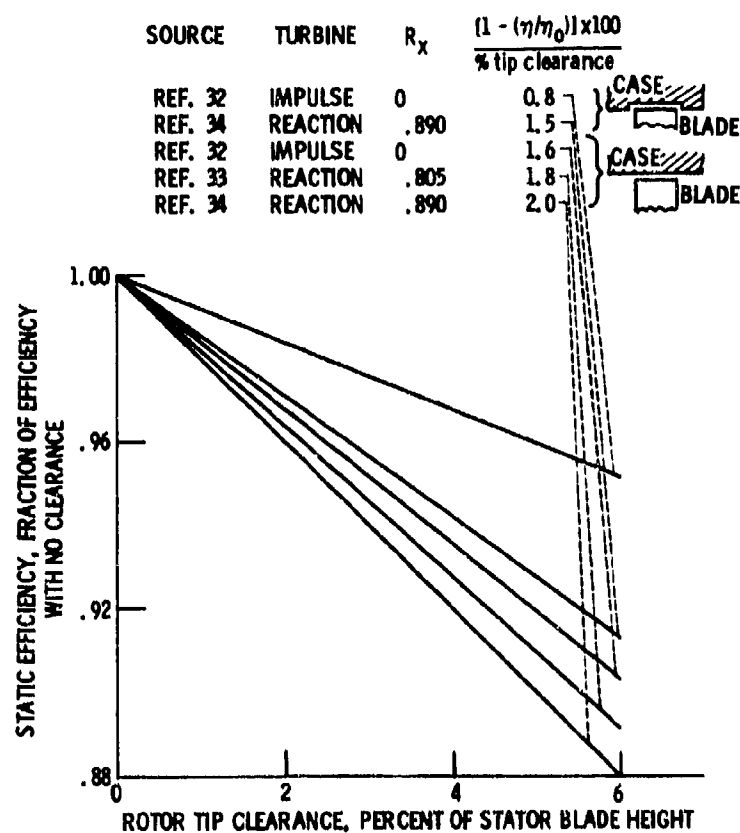
Fig.34   Effect of rotor tip clearance on performance for
various turbines (from Reference 34)

(a) BLADE TIP DIAMETER EQUAL TO
CASE INSIDE DIAMETER (OP-
TIMUM GEOMETRY).

(b) BLADE TIP DIAMETER LARGER
THAN CASE INSIDE DIAMETER.
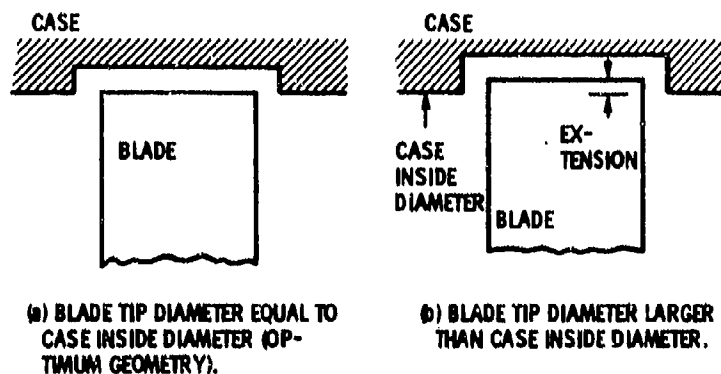
Fig.35   Recessed case configuration
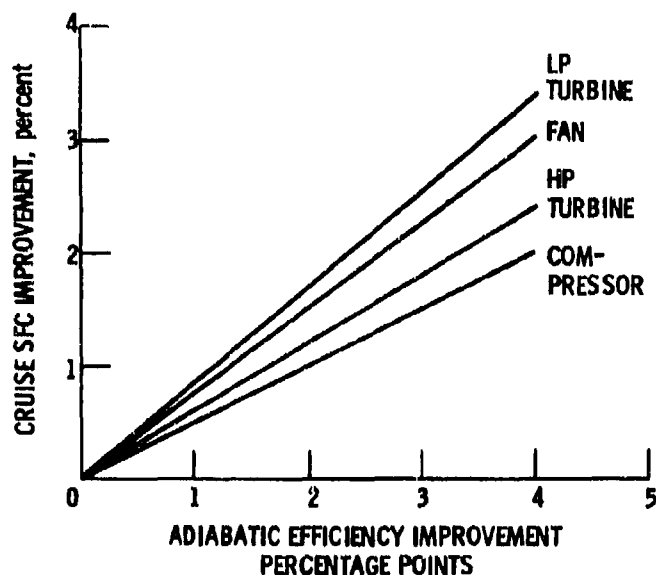
Fig.36   Relation of SFC to component efficiency (influence coefficients)
in a high bypass engine (from Reference 15)
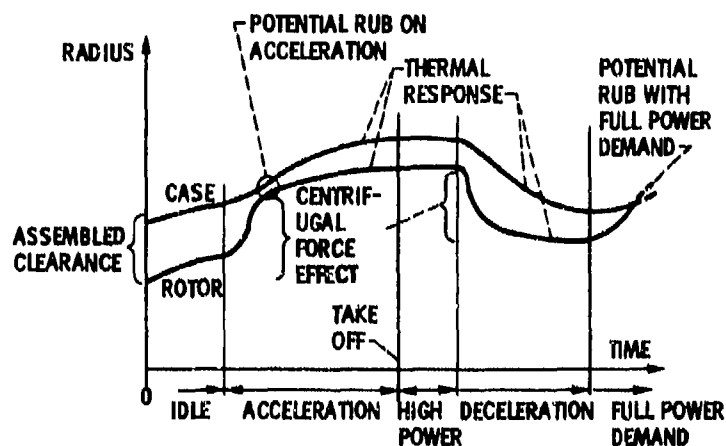
Fig.37   Illustration of variation in case to rotor clearance during engine operation
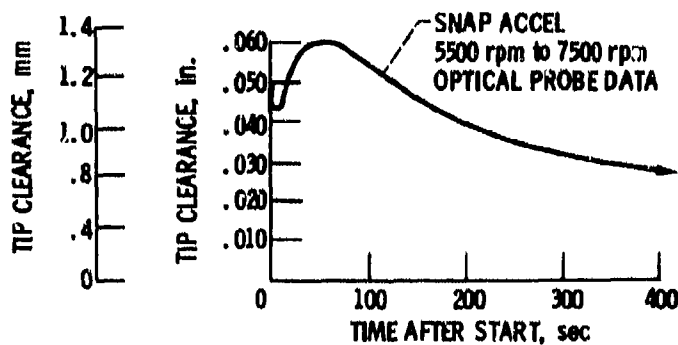
Fig.38   Turbine blade tip clearance vs time (from Reference 37)
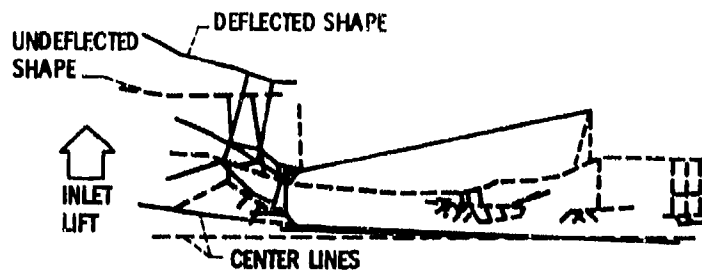
Fig.39 Propulsion system static deflection due to inlet lift (from Reference 38)

AN AERODYNAMIC FORCE TRANSVERSE
TO THE ECCENTRICITY DIRECTION TENDS
TO PRODUCE WHIRL
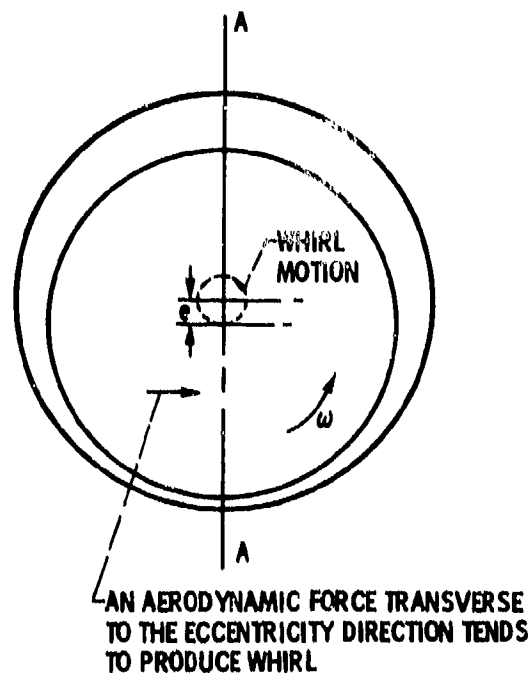
Fig.40 Eccentric labyrinth seal and blade whirl model
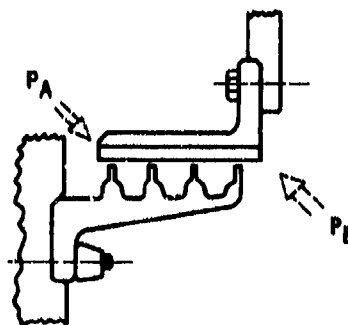
FOR $P_A > P_B$ ROTATING COMPONENTS SUPPORTED AT INLET HAVE FAILED,
STATORS SUPPORTED AT EXIT HAVE NOT FAILED

FOR $P_B > P_A$ ROTATING COMPONENTS SUPPORTED AT EXIT HAVE NOT FAILED,
STATORS SUPPORTED AT INLET HAVE FAILED

Fig.41 Effect of seal component support

POINT LIGHT
SOURCE

INPUT OUTPUT

COHERENT FIBER
OPTIC BUNDLE

B^1

A^1

INPUT LENS

OUTPUT LENS

SHROUD SURFACE

B TIP CLEARANCE

TIP CLEARANCE A
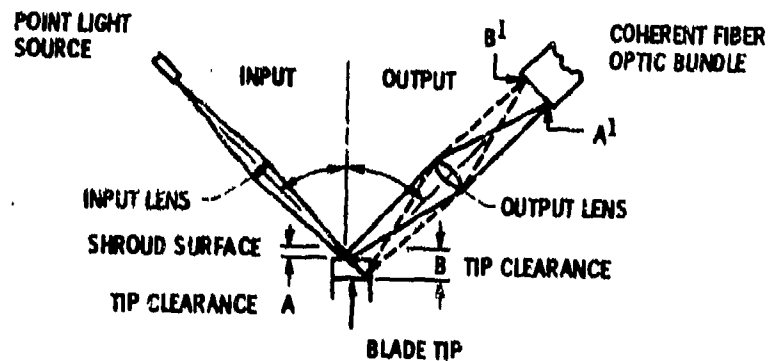
BLADE TIP

LIGHT REFLECTED FROM THE BLADE TIP IS FOCUSED THROUGH THE OUTPUT
LENS AND IS INCIDENT ON THE COHERENT FIBER OPTIC BUNDLE. AS THE
BLADE TIP CLEARANCE INCREASES, THE OUTPUT BEAM MOVES FROM
POSITION A^1 TO POSITION B^1.

Fig.42 Laser optic clearance probe (Ref.43)

EFFICIENCY, η_{ad}

PRESSURE RATIO

REFERENCE STALL
LIMIT LINE

STALL-LIMIT
LINE

REFER-
ENCE
STALL-
LIMIT
LINE

EQUIVALENT WEIGHT FLOW, $W_V\sqrt{\theta}/\delta$, lbm/sec

(a) SMOOTH CASING.

(b) HONEYCOMB CASING.
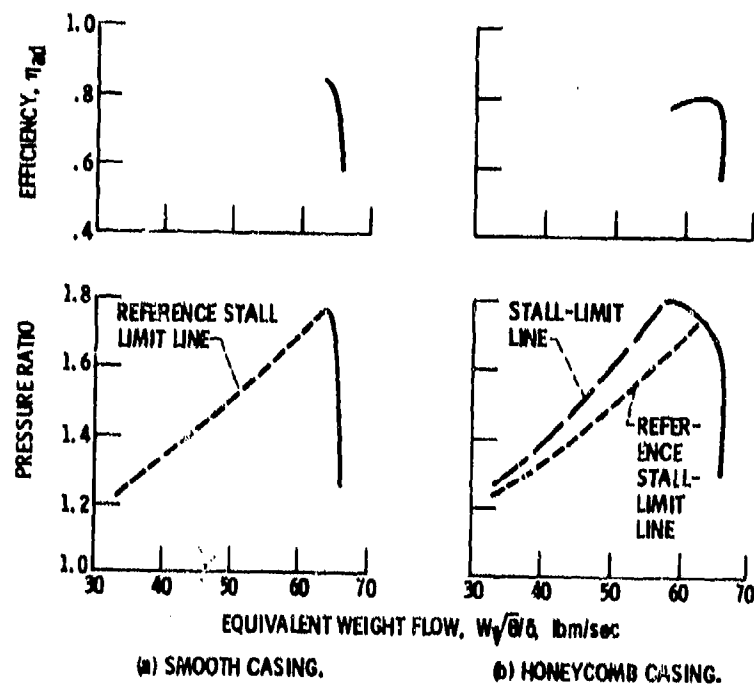
Fig.43 Fan performance as a function of casing type, 100% design speed

(a) ABRADABLE (SINTERED OR SPRAYED POROUS MATERIALS).

(b) COMPLIANT (POROUS MATERIAL)

(c) LOW SHEAR STRENGTH (SPRAYED ALUMINUM)
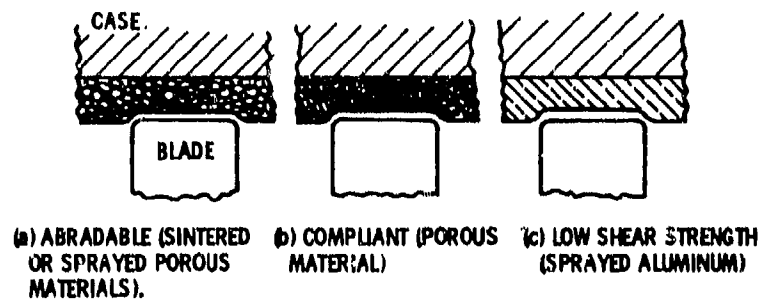
Fig.44   Illustration of types of compressor rub materials for outer air sealing

(a) STRIATED.

(b) HONEYCOMB.

(c) POROUS MATERIAL (ABRADABLE OR COMPLIANT)
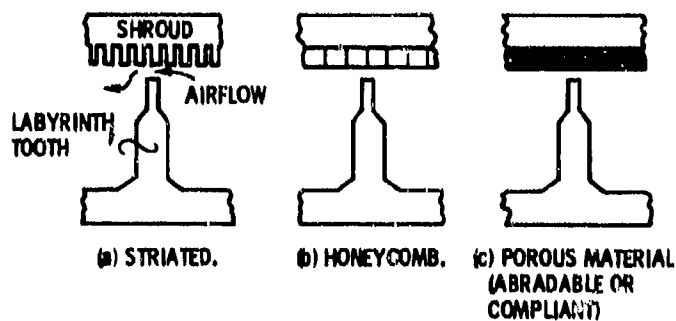
Fig.45   Inner shrouds for compressor interstage labyrinths
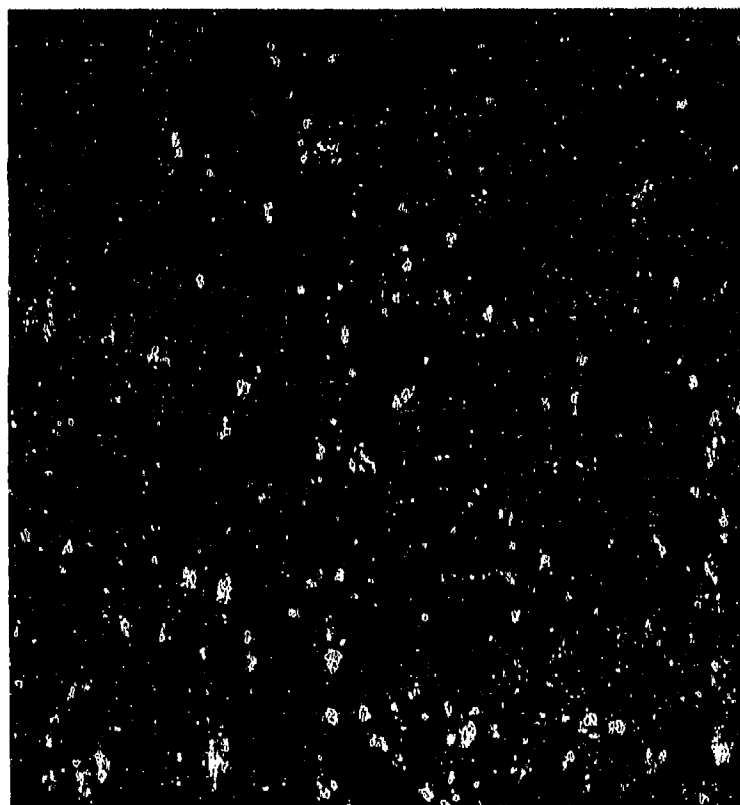
Fig.46   Labyrinth disk and knife edge showing heat discoloration due to thermal bumps generated in rubbing contact against a shroud specimen. Rubbing speed, 183 m/s (600 ft/sec)
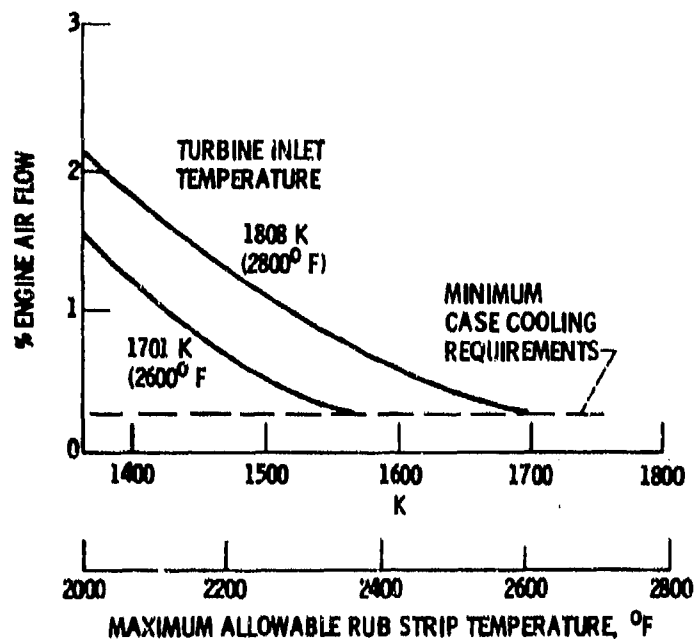
Fig.47 Cooling air flow requirement for high pressure turbine
outer air seal (data from Reference 52)

SPRAYED LAYERED
$Y_3O_2 \cdot ZrO_2/CoCrAlY$
CERAMIC COATING
PER DETAIL Ⓐ

MAR-M-509

4. 216 mm (0.166 in.)
3. 607 mm (0.142 in.)

ZrO$_2$

85/15 Z/M*

40/60 Z/M

70/30 Z/M

M-509

NiCrAlY

0. 762 mm (0.030 in.)
0. 635 mm (0.025 in.)

0. 127 mm (0.005 in.)
0. 076 mm (0.003 in.)

*Z/M = $ZrO_2/CoCrAlY$

DETAIL A

Fig.48 Typical engine seal segment (Ref.53)

DISCUSSION

A.R.Stetson, US

Dr Ludwig mentioned the ceramic seal, the one which has been developed with Pratt & Whitney under the navy sponsorship.

How has that performed, has it been actually tested in the engine?

Author's Reply

Data on the ceramic segment for high pressure turbine outer air sealing, which was developed by Pratt & Whitney, is given in Reference 52 of the paper. To my knowledge, the seal has not been developed to the point where it is a bill-of-material component for an engine. The purpose of the discussion in the paper on the ceramic segment was to point out current areas of work and to show the potential gains associated with ceramic outer air seals.

D.K.Hennecke, Germany

In one of your last slides you show a photograph (not contained in the printed paper) of liner segments which appear to be perforated in order to facilitate full coverage film cooling or effusion cooling. Are the liner segments indeed perforated by such holes and, if so, don't these holes get clogged when the rotor blades rub into the liner segments?

Author's Reply

The photograph of the turbine seal liner segments shows a sintered material with a honeycomb supporting structure. There are no cooling holes. Cooling is achieved by impingement jets against the back of the supporting structure and by film cooling which originates further upstream.

F.Willkop, Germany

In your Figure 34 one can see that you have achieved the best efficiency when the blade is running in a pocket of the casing. Now your picture shows this blade running in a very narrow pocket, but in practice we have an axial movement between case and rotor and you need an elongated pocket. We have met contrary results to this. Could you comment on your experience in the case you have axial movement of the rotor?

Author's Reply

We would agree that elongation to accommodate axial movement will act to decrease any benefit. Thus, this recessed configuration is only useful in those locations where axial motion is small. For example, turbines in certain small engines, and in the compressor.

D.A.Campbell, UK

The clearance of certain seals is much affected by shaft whirl, and the prediction of whirl amplitudes is therefore important. It is suggested that these amplitudes are significantly affected by the mechanical damping produced by features of the normal engine construction and also most particularly by special devices such as squeeze film bearings. It is therefore very desirable to include these effects in dynamic models of shaft behaviour.
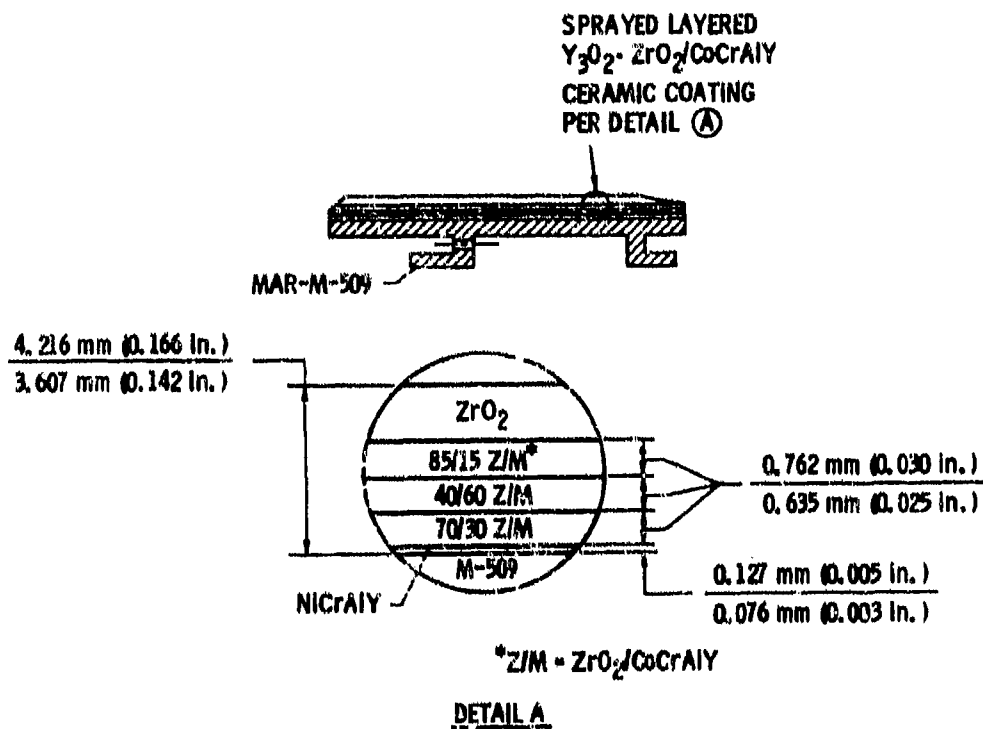
Author's Reply

We agree with your statement that squeeze film dampers are particularly useful in mitigating whirl amplitudes, but in regard to the mechanical damping produced by the normal engine construction features, it is known that spline friction (Coulomb damping) when operating above the bending critical can be detrimental. In general, nonrotating damping features, both viscous and Coulomb, are beneficial below and above the bending critical, and rotating damping features are detrimental above the bending critical but beneficial below the critical.

A.Moore, UK

Figure 45 shows various types of abradable systems. Can you please comment on the losses associated with using these types of abradables, i.e. the loss above that of a solid liner when running at the same clearance.

Author's Reply

I am familiar with the work being reported on in Paper No.13 on labyrinth seals and can say that your question is answered in detail in this paper. But, in general, two effects show up in porous abradables as compared to a *smooth* solid surface. First, the porosity allows a certain leakage in excess of that when using solid surfaces; this porosity effect being a greater percentage of the total leakage and, therefore, more pronounced at low clearances. The second effect is due to surface roughness. Porous materials may have very rough surfaces from an aerodynamic viewpoint. In labyrinth seals, this is beneficial since surface roughness promotes turbulence and increases the dissipation between labyrinth teeth. However, when abradable materials are used over compressor blade tips, the surface roughness introduces an aerodynamic penalty.

B.Wrigley, UK

Can Dr Ludwig comment on the significance of lining materials on the thermal time constant of the static member and is any particular material shown to be advantageous?

Author's Reply

I have no quantitative data on the significance of the thermal time constant of various lining materials. Since in general, the case responds faster to changes in gas stream temperature than the rotor, it is desirable to slow down the case response. Therefore, casing lining materials with low thermal conductivity should be beneficial. This suggests that from a thermal time constant standpoint, the porous materials would be preferred over, say, sprayed aluminum. So the general comment can be made that those lining materials which are made porous (sintered felt metals etc.) for rub reasons have an added advantage of low thermal conductivity which tends to slow down the stator's thermal response to the gas stream temperature. Also, it has occurred to some that an insulation coating (such as ZrO_2) applied, for example, to the inside of a titanium compressor case would slow down the thermal response and in addition would provide rub protection of the titanium case in the event of an extreme rotor imbalance. However, coating adherence needs to be demonstrated.

D.G.Ainley, UK

I agree the author's conclusion that a major problem is to achieve better control of clearance. Does the author have any news whether in relation to current engine design, the major gains to be won will arise from greater attention to reducing elastic flexibility of rotor system throughout the operating speeds or from greater attention to closer thermal matching between rotor and stator components?

Author's Reply

In regard to which approach (reduced system flexibility or better thermal match) will provide the most gains, I think that both hold much potential for improvement, especially in large engines. Of course, in the fan and low pressure compressor the system flexibility is more important than the thermal matching. But in the high compressor and in the turbine, both thermal matching and system flexibility are critical.

G.Halls, UK

I was interested to hear you talk about the situation with seals where the heat generated in the rub can cause added expansion and lead on to catastrophic failure.

I wonder if you could go into more details about the important parameters of that mechanism and in particular I am interested to know whether the size of the fin is important because it provides extra surface from which heat is lost by convection rather than conduction is effective. Do you have a prediction method for determining whether this happens or do you know that one exists?

Author's Reply

At NASA, we have made only a few analyses on failure due to the thermal effect of rubbing. In one particular case, the labyrinth teeth were carried by a rotating spacer (spacer between stages) and the relative mass of the spacer was 1/3 that of the stator mass. Therefore, the spacer mass heated up faster, and the analysis indicated that a catastrophic failure (loss of strength with increasing temperature) could be initiated by two seconds of hard rubbing.

We did not consider heat convection as related to the fin size; I do not recall anyone suggesting that it is an important factor, although it may be very significant.

It is important to note that rubbing can take place, on a labyrinth tooth, over a very short arc (see Figure 46 of Paper No.1). This is a complication from a heat transfer calculation standpoint and the practical importance of the formation of the short arc length thermal bump has not been determined.

The factors which determine whether a labyrinth seal, when experiencing a rub, will enter into a catastrophic failure are: (1) rub severity (function of tooth width, rubbing velocity, penetration rate and material properties); (2) heat conduction into the rotor (functions of tooth width, circumferential extent of the rub, thermal conductivity, thermal diffusivity, rotor mass and length of time of rubbing); (3) relative expansion of the rotor and (4) wear rates of rotor and stator.

In regard to a prediction method for assessing various designs for a rub induced catastrophic failure, I am not aware of any published methods.

P.Suter, Switzerland

I think that one major problem area concerning control of clearance between stator and moving blades is represented by the non-uniformity of the temperature profile caused by the combustion chamber performance, eventually more important than rotor dynamics or stator/rotor inertia difference effect.

Author's Reply

Dr Suter's comment is correct and I agree that the non-uniformity of the temperature profile caused by the combustor is the major factor in the clearance problem of high temperature turbines. This non-axisymmetric effect is

aggravated by non-uniform cooling and by non-axisymmetric structures. The resulting out-of-roundness in large engines is estimated to be as high as 0.05 to 0.10 cm (based on seal and blade wear data). However, there are other important clearance factors such as the transient response of the case/rotor which require that the assembled clearance be large enough to avoid rubbing on engine acceleration or deceleration (see Figure 37 in Paper No.1). Thus cruise clearance is set by transient rub considerations and not by the steady state thermal condition at cruise. To decrease this large cruise clearance, some large engines have active clearance control which shrinks the turbine case by use of cooling air once the aircraft is in a cruise condition.

I agree that thermal out-of-roundness is probably a larger factor than transient thermal response; but both are significant and each requires a different solution. Thermal out-of-roundness reduction means more attention must be given to axisymmetric structures and to temperature distribution; also abradable materials would help to solve this problem.

A.M.Campling, UK

Regarding the multilayer metallic/ceramic abradable seal element under development.

Was the coating designed to be abradable or abrasive? If abradable, what degree of erosion was experienced? If abrasive, what degree of wear was experienced? Has any difficulty been found in controlling the hardness of the final ceramic deposit?

Author's Reply

The ceramic coating is designed to be abradable. Tests have shown that the ceramic coating has a higher erosion resistance than currently used metal systems. Basically, this improved erosion resistance is due to the fact that ceramics generally have good erosion resistance when the particle impingement angle is small; and in an engine the impingement angle is about $20°$. Also, tests have shown that the blade wear is less than that for metal systems when the incursion rate is about 0.0025 cm/sec. In regard to the hardness of the final ceramic deposit, this depends on control of many parameters in the spray process and these controls need to be improved.

USE OF COATINGS IN TURBOMACHINERY GAS PATH SEALS

by

J.G. Ferguson
Manager Advanced Research Group
Mechanical Research Department
ROLLS-ROYCE LIMITED
P.O.Box 3
Filton
Bristol
BS12 7QE
England

SUMMARY

The improvements in engine performance, to be gained by maintaining close clearances in various rotating seals within a gas turbine, are essential to its economic operation. In many cases, therefore, this makes the use of coatings in these seals mandatory.

Abrasive coatings are used in some applications and in general are satisfactory. However abradable coatings are most widely used, and these are found in many seals throughout a gas turbine engine from the fan to the turbine. These coatings therefore have to cope with a temperature range from a little above ambient to 1 250°K. Test methods exist for laboratory and rig evaluation of coatings, and these are discussed, but improved methods for evaluation of erosion and abradability are required.

To overcome shortcomings in current abradable coating materials, many are at present being tailored specially to meet the conditions in particular seals within an engine. This means that there are several different coatings, within any given engine, each having a limited range of use.

New coatings are still required which can be used in a wide range of applications throughout an engine. There is, in particular, an urgent need for abradable materials which can be used in turbine seals covering a temperature range from 870°K to 1 250°K.

1.0 INTRODUCTION

The maintenance of close clearances at the various rotating seals is essential to the economic operation of a gas turbine. It is now common practice to apply coatings to one or both sealing surfaces to permit them to come into rubbing contact without incurring significant damage and with the minimum of wear. The seals can then operate safely with a minimum theoretical clearance of zero. The designers can therefore specify closer operating clearances than would otherwise be possible.

In the compressor, blade tip clearances affect both the efficiency and the handling of the engine. Excessive clearance at maximum r.p.m. results in a power loss and an increased specific fuel consumption (s.f.c.). Excessive clearance during acceleration can reduce the surge margin and limit the permissible amount of overfuelling thus reducing the acceleration rate.

Turbine tip clearances also have a significant effect on s.f.c. On some small modern high pressure turbines an increase in the clearance over the blade shrouds of .127 mm (0,005 in.) may result in an increase in s.f.c. of 0,5%.

The higher rim speeds and higher top cycle temperature needed for increased power-to-weight ratios have led to the adoption of unshrouded H.P. turbine rotor blades. This has lent new importance to turbine blade tip clearance, and highlighted the need for coatings over the blade tips.

Clearance in the main airstream labyrinth seals is equally important particularly where high pressure air is involved. On a typical medium size high pressure ratio engine for instance, an increase in the radial clearance of the compressor delivery seal of only ,076 mm (0,003 in.) can mean an increase of 1% in specific fuel consumption.

From the foregoing, it can be seen that the subject of coatings for gas path seals is taken seriously by gas turbine engine manufacturers. Despite this however there is still a long way to go before completely satisfactory coatings are found. Many coatings are currently used in service but most, if not all, have shortcomings e.g. poor erosion resistance, too little abradability, difficult to apply or repair, too expensive, etc. It becomes obvious that the requirements for suitable abradable coatings are very stringent and difficult to meet and it is hoped that this paper will serve to explain these requirements, and some of the difficulties, involved in the hope that better coatings will become available in the future.

2.0 APPLICATION OF COATINGS IN ENGINES

There are two basic seals in which coatings are used in gas turbine engines i.e. blade path seals and finned labyrinth seal bores. A general philosophy has in the past, certainly in Rolls-Royce Bristol engines, dictated the type of coating chosen for the various locations within the engine. This was determined by the need to maintain the balance of the rotating assemblies, and thus avoid unnecessary increases in clearances caused by orbitting associated with rotor unbalance. In effect, this meant that soft abradable coatings were applied to static parts, or alternatively abrasive coatings were applied to rotating parts; in either case the result was wear of the static part. In general, this means abrasive coatings applied to compressor spacer rings and abradable coatings elsewhere. This philosophy is still generally adopted, except where the coating is required to perform other duties which conflict with the rubbing requirements.

Temperature is an important parameter to consider when dealing with seal coatings. These coatings are applied throughout the engine from front to rear and therefore cover a large temperature range. The temperatures within a gas turbine can generally be split up as follows:-

Fans and L.P. Compressors	:	$280^{\circ}K$	to	$400^{\circ}K$
Front end H.P. Compressors	:	$330^{\circ}K$	to	$580^{\circ}K$
Rear end H.P. Compressors	:	$700^{\circ}K$	to	$840^{\circ}K$
H.P. Turbine Tip Seals	:	Up	to	$1\,250^{\circ}K$

The complete range of temperatures is therefore from about $280^{\circ}K$ to $1\,250^{\circ}K$. Although the ideal, which may one day be achieved, would be to have one common coating applied throughout the engine, currently a range of materials is used starting with rubbers and epoxy resins at the low temperature end, and working through to filled honeycomb at the high temperature end.

Fig.1 is a section through a typical fan engine showing some areas where coatings are applied.

3.0 BASIC REQUIREMENTS OF COATINGS

3.1 Abrasive Coatings

Abrasive coatings should ideally machine away the opposing member cleanly, without smearing, and with the minimum of heat generation.

Aluminium oxide coatings are used widely on compressor spacer rings to prevent damage to the spacer ring, which may be a structural member, in the event of a rub occurring on stator blade tips. Although soft coatings are normally used over rotor blade tips, where there is a possibility of a titanium fire, zirconia has been applied to the casing bore with the dual function of providing a protective surface to machine away the rotor blade tips cleanly and an effective barrier against penetration of the casing by burning titanium, should a severe mechanical failure occur. Aluminium oxide is also used to minimise the wear on labyrinth seal fins used in conjunction with soft coatings.

Experience with these abrasive coatings has been very good during a vast number of in-service engine hours. It is intended therefore to confine the remainder of this paper to abradable materials only.

3.2 Abradable Coatings

Abradable coatings are used in casing bores over the blade tips, and in labyrinth seal bores.

Ideally, an abradable coating is one which can be freely machined away without causing wear or significant heating of the mating part, and yet is hard enough to resist erosion. These are contradictory requirements and much of the work on soft coatings has been aimed at getting the best compromise. A really successful compromise has not yet been successfully achieved.

The labyrinth seal application is probably the most difficult to meet. When the thin fins on the labyrinth runner cut into the coating, the heat generated by friction on the thin surfaces rapidly heats the small volume of metal in the fins. This may cause softening and rapid wear of the tips. One palliative is to spray coat the fins with aluminium oxide. This gives a rougher surface which cuts more efficiently and generates less frictional heat. Even so, unless the abradable material is very easily machined, fin wear will occur.

Severe erosion of the soft coating is another feature of labyrinth seal applications. Obviously, a certain amount of erosion is caused by air-borne dust passing through the seal but the major cause is thought to be the debris generated by a seal rub.

When interference occurs between the finned rotor and the soft coating, the debris generated by the rub is effectively trapped between adjacent fins, see Fig.2. This trapped debris is then carried around at high speed and erodes more coating, generating more debris. The process continues until the fins retract due to a change in operating clearance or until there is sufficient clearance over the fin tips for the debris to escape.

The main problem in finding suitable abradable coatings is in satisfactorily equating the two conflicting requirements of erosion resistance and ease of abrasion.

Experience has shown that coatings which are relatively soft but have good cohesive strength, such as some filled resins or rubbers, can go a long way towards meeting these requirements. Unfortunately, these materials are only suitable for the lower temperatures. It is unlikely that such properties can be found in materials suitable for higher temperatures, i.e. above 600°K. For these materials, it is most probable that the solution lies in a porous or composite material having sufficient hardness to resist erosion but the required amount of cohesion to again resist erosion but allow good abradability.

4.0 TYPES OF COATING

The conflicting requirements of easy machinability and good erosion resistance have led to a number of different approaches to the abradable lining problem. These fall basically into five groups:

(i)   Filled resin mixtures, where the filler is included to give good machinability to a reasonably tough resin.

(ii) Micro-balloon filled coatings. These consist of a mass of minute hollow thin walled spheres held together by a tough organic binder.

(iii) Flame sprayed coatings, both combustion and plasma, which rely mainly on their friable structure for machinability.

(iv) Sintered metal fibres.

(v)   Thin walled honeycomb filled or unfilled.

The organic abradables used in Rolls-Royce engines include graphite-epoxy compositions, glass microsphere-epoxy compositions, and talc-epoxy compositions. Some of these materials have been, and are, proprietary materials and some have been and are being developed 'in-house' by Rolls-Royce. These materials vary in temperature capability up to approximately 500°K and are, therefore, only suitable for use in fan and compressor casings.

Early graphite-epoxy coatings were applied by a paint spray technique, using thinners. Many thin coats had to be applied, and although the coating was quite successful in engine use the length of time to apply it, and hence the relatively high cost, initiated the research for more suitable coatings. Trowellable room temperature and heat curing graphite filled epoxy compositions have been developed which have maximum service temperatures of 470°K and 500°K respectively. In some cases, surfacing of the uncured material, using a template, has eliminated the need for a post-cure machining operation.

A talc-epoxy coating has also been developed which is a one pack putty-like material stored in refrigerated containers. When required for use the material is allowed to reach room temperature after which it is formed into strips of suitable dimensions and pressed or rolled onto a suitably primed surface. This coating is suitable for use up to 470°K.

Micro balloon filled coatings used have included a proprietary room temperature curing material, 3 M's EC.3524. This coating is used for filling voids and consists of hollow glass microspheres in a two-pack epoxy resin which is applied by trowelling. Surplus material is machined off after the filler has cured. Unfortunately, this material has limited use as it is only suitable for use up to 370°K.

Coatings consisting of silica micro balloon filled 'rubbers' are also being used and developed.

The flame sprayed coatings used are all proprietary materials, but a considerable amount of 'in-house' development work is done, to optimise the material for a particular application, by variation of the spraying parameters. Some of the materials currently being used and developed are nickel/graphite produced by Sherritt Gordon, 6% silicon/aluminium + graphite, boron nitride/aluminium bronze, boron nitride/nickel chrome + aluminium, nickel/aluminium, nickel/chrome/aluminium, 6% silicon/aluminium + polyester resin, all produced by Metco.

Sintered metal fibres are being used for some applications and these include Feltmetal produced by the Brunswick Corporation and O.H.P. Felt produced by Heurchrome. These materials are available in strips and have to be bonded or brazed onto the component

requiring the abradable lining. The 'Feltmetal' is available in a number of materials including Hastelloy X, Haynes 25, Haynes 188, Driver Harris 242 and these are in fibre form typically 6-15 microns/dia.

The Heurchrome material is available in several materials including nickel/chrome and nickel/chrome/aluminium, having typical fibre diameters of 7-20 microns. Again this material has to be bonded or brazed onto the component.

Honeycomb materials have been and are being used in a variety of cell sizes and materials. These are confined mainly to use in turbines where high temperature performance is required, although some filled aluminium honeycomb has been used in a fan. In the hotter areas the honeycomb is completely or partly filled with nickel/aluminium.

5.0 METHODS OF DEVELOPING AND EVALUATING COATINGS

(a) Laboratory Development of Coatings

Before any new abradable coatings are submitted for rig or engine evaluation, certain laboratory tests are required which can be used to assess their likely performance. These should be relatively simple and quick to do to allow formulations, spray parameters, etc to be optimised.

The use of plasma or flame sprayed abradable coatings is not as straightforward as may originally have been thought. For example, two coatings which have had extensive use and development are 75%/25% and 85%/15% nickel graphite. The 'powder' used for spraying consists of very small particles of graphite with a thin nickel shell, and each particle consists of approximately 75%/25% Ni./C or 85%/15% Ni./C. See Fig.3A. However, when the material is sprayed the coating consists of a splattered nickel matrix partly filled with graphite and partly porous. The parameters used for spraying the material, and indeed the type of spray gun, can vary the proportions of nickel and graphite and the porosity of the applied coating. This can have a marked effect on the abradability and the erosion resistance of these coatings. A section through a typical applied coating is shown in Fig.3(B) at a magnification of 300 times.

The same principle applies to most other flame sprayed coatings* whether they are composites or not, and therefore a considerable amount of development work has to be done to determine the best spraying parameters for any coating. In the case of non composite materials, the spray parameters vary the porosity of the coatings.

With organic coatings variations in their properties can be achieved by varying the types and mixtures of resins and fillers.

A simple piece of apparatus to evaluate the relative abradability of a coating has been developed by Rolls-Royce Limited. It is shown in Fig.4 and consists basically of a swinging pendulum on which are mounted two cutters facing inwards. The coating is applied to two specimens and these are mounted back-to-back at the bottom of the pendulum swing. The cutter on each side is set to give 0,127 mm (0,005 in.) depth of cut and the pendulum is released from 30°. The angle of upswing is measured and from this is calculated the energy absorbed by cutting the coating. The cutter is 1,8 mm (,030 in.) wide and the energy stored is 43,44 Joules (32 ft.lb.). Coatings tested usually fall in the range of 1,4-8,1 Joules (1-6 ft.lbs.) energy loss. Results are assessed on a comparative basis relative to a coating which is known from engine running to have acceptable abradability characteristics. Using this apparatus allows the relative abradability of a coating to be assessed quickly in the laboratory in which the spraying is being done, thus helping to make the optimisation of spray parameters or formulation a more rapid process.

An equally simple piece of apparatus is used in the laboratory to initially assess the relative erosion resistance of new and development coatings prepared in the laboratory. It is shown in Fig.5 and consists of a 6,5 mm (0,026 in.) dia. sapphire nozzle placed 22 mm from the test specimen at an angle of 30° to it. Air, at 552 Kpa (80 p.s.i.), is used to blast the test specimen with 50 micron alumina grit. The test specimen is prepared by spraying a coating 2,54 mm (0,1 in.) thick onto a 50 x 50 mm x 16 SWG (2 in. x 2 in. x 16 SWG) mild steel plate. This is then placed in the erosion test apparatus and run for ½ min. or 1 min. The test specimen is turned round after each test, to allow a total of four tests to be done on each one. The average volume of material removed is determined for the four tests and this is used to make relative assessments of erosion resistance of candidate abradable coatings.

---

* A composite flame material is defined as one which has a physical mixture of one or more constituents in the powder form. The resulting applied coating then becomes a matrix of one material surrounding the others in their original or slightly modified form.

(b) Test Rig and Engine Evaluation of Coatings

Having obtained likely materials from the laboratory, or in some cases direct from outside suppliers, it is necessary to determine their suitability as an abradable coating in an engine. This can either be done by rig tests followed by final engine evaluation, or by engine tests alone.

Devising a satisfactory relatively simple rig test, for evaluating the abradability of coatings for engine use, is difficult. It is similar in many ways to the problems associated with evaluating the friction and wear characteristics of materials for use in unlubricated journal bearings, sliding joints, etc. Results of any sort of laboratory or rig test cannot be applied universally, as each particular application has differences which alter the performance, e.g. level of environmental contamination around the component, the type and speed of movement which affects the type and level of debris generation, the geometry of the component and/or the airflow around it, as these affect the way in which debris can escape. Any, or all, of these conditions can vary the order of ranking of a number of materials, which has been established by rig or even engine evaluation of a number of materials.

To partly illustrate some of these points, a series of rig tests were conducted, by Rolls-Royce Limited, on a range of flame sprayed abradable coatings. A 254 mm (10 in.) dia. wheel was used having slots machined around its circumference to simulate blade tips, which rubbed on quadrants sprayed with the test coating. From these tests, a range of coatings were ranked in order of performance. The best three coatings were then tested on a more complicated rig which utilised a stage of an engine compressor, i.e. disc, blades and casing. The coatings were applied to the casing, and this was lowered onto the blades which were rotating at a tip speed of approximately 305 m/s (1 000 ft/sec.). Results gave a reversal of ranking compared with those obtained on the small rig. It is thought that this was due to the coating, which appeared to be more abradable in the full size rig, producing a greater rate of debris generation in the small rig. This debris was unable to clear the rubbing zone quickly enough, thus causing smearing and local temperature rises resulting in 'blade tip' overheating and coating smearing. A new small scale rotating rubbing rig is at present being evaluated at Rolls-Royce which, it is hoped, will make satisfactory rankings of coatings for rotor path and finned labyrinth seal applications.

The above comments apply to coatings in the low and medium temperature ranges. Coatings for turbine use, are subjected to temperatures up to 1 250°K and this makes it even more difficult to produce a satisfactory rig. So far, Rolls-Royce have found it more realistic and expedient to test turbine coatings in the engine. Even so, this type of engine evaluation is relatively slow and time-consuming.

Evaluation of the erosion resistance of coatings is also a difficult problem. For instance, the erosion found in some rotor path seals could not be explained by basically circumferential flow as this would almost certainly not have resulted in erosion. It could, therefore, be due to some sort of 'over the tip' vortex flow, but the aerodynamisists are unable to define the type of flow over the abradable lining.

So far most cold tests have been done, using a fixed set of relatively arbitrary conditions, which have produced results of a limited value. An investigation is still required to determine the mechanism of erosion, over the blade tips and around seal fins, and so establish a more realistic erosion test method for rotor path and labyrinth seal abradable linings.

It has been established that, in general, soft materials with reasonably high levels of cohesion are very erosion-resistant. These properties vary with temperature and it is therefore necessary to do erosion tests, at a range of temperatures, in order to establish the erosion resistance of a coating for any particular operating condition. Some initial erosion tests have been done at temperatures ranging from 290°K to 550°K and these include tests on specimens that have been aged at temperatures up to 550°K for up to 1,000 hours. Results have shown that the erosion resistance of some test samples dropped, by a factor of up to six, after aging at 550°K for 1,000 hours. This illustrates the change in abradable coating erosion resistance which can occur with time at temperature. It is very important therefore to determine the erosion resistance and abradability of materials which have been aged in this way. However further investigations, at a range of temperatures, need to be incorporated in the investigation into erosion parameters mentioned above.

The current state of the art lacks the ability to confidently evaluate, by rig or bench engine testing, the suitability of an abradable coating for engines in service, and care must be taken to ensure that potentially good materials are not discarded by unrealistic rig tests. Work is proceeding to develop satisfactory evaluation methods for abradable coatings, but the necessary correlation with engine experience is a relatively time-consuming process.

(c) Methods of Quality Control

As previously explained, the properties of many of the flame sprayed coatings can vary when applied to components. It is necessary therefore to evaluate the coating as applied to each engine component. The swinging pendulum abradability rig was considered for this but it couldn't be done on the actual components and it was not possible to spray the abradability test-piece with the component. Spraying a test-piece immediately after the component is not acceptable.

There was found to be an acceptable correlation between hardness of the coating and abradability. Initially, a 'Shore' Durometer hardness tester was tried, as this is a very portable unit and can be used on almost any engine component. Unfortunately the coatings being measured were towards the top end of the 'Shore' scale, which was too insensitive. .

A Rockwell superficial hardness tester, using a 12,7 mm (0,5 in.) dia. ball and a 15 Kg load, gives acceptable readings on the Rockwell 15Y scale and values on this have been established. Larger engine components will fit around the tester such that hardness values of the coating actually on the component can be taken. For components which can't be done in this way a 16 SWG coupon at least 25 mm x 16 mm (1 in. x 0,625 in.) is placed adjacent to the land being sprayed and is thus sprayed with it. This coupon is then hardness tested as being representative of the engine coating. On each component the average of six readings taken around it is used as the hardness value for that component.

During the initial laboratory evaluation of flame sprayed coatings a hardness value for that particular coating is established and this is the value, with an established tolerance, used for subsequent quality control.

6.0 EXPERIENCE TO DATE

The following chart shows the wide range of coatings that are being used in gas turbine engines, and the areas within the engine in which they are being tried or used:-

Type of Coating	Max. Temperature Capability °K	Engine Positions in which the coatings have been used
Filled organic resins or rubbers.	500	Fan, I.P. and L.P. compressor rotor paths and seals.
Flame sprayed polyester resin + aluminium.	600	Fan, I.P., L.P. and front end H.P. compressor rotor paths and seals.
Flame sprayed nickel/graphite	725	Fan, I.P., L.P. and H.P. compressor rotor paths and seals and L.P. turbine seals.
Flame sprayed boron nitride/ aluminium bronze and boron nitride/nickel chrome in aluminium.	875	L.P. and H.P. compressor rotor paths and seals, and H.P.2 turbine seal.
Feltmetal	870	L.P., I.P. and H.P. compressor rotor paths and seals and turbine root seals.
Flame sprayed nickel/aluminium and nickel chrome/aluminium.	1 220	H.P., I.P. and L.P. turbine tip and root seals.
Honeycomb filled and unfilled (Ni.75 cells with nickel/ aluminium filler).	1 270	H.P., I.P. and L.P. turbine tip seals.

The ideal abradable coating for engine use would be one which could be applied universally in all the seals (rotor path and finned). Preferably it would be a sprayed coating, for ease of application, and would have a maximum temperature capability of say about 1 250°K.

A vast amount of engine experience has been gained in both development and service engines and this has shown that we are a long way from achieving this ideal. Problems of blade and fin wear, coating erosion and cost, are all contributing to the fact that the above range of coatings are at present required in engines.

Results from engine running have shown that fan rotor path coatings can experience more erosion than the same type of coating applied to the I.P. and H.P. compressors, and as such some of the potentially higher temperature coatings are not suitable for use in the fan casings.

As stated previously a successful abradable coating is one which will abrade cleanly, without damaging blade or fin tips, but at the same time one which will resist erosion. Some engines have produced cases where both erosion and blade tip wear have occurred together. In some of the labyrinth seals debris, produced when the fins have rubbed into the coating, has been trapped between the fins where it has eroded away the coating between the fins due to the high speed rotation of the debris.

Secondary engine problems sometimes result from the use of abradable coatings. In one case the debris from a rubber based fan blade path coating, resulted in the formulation of a degraded rubber substance in the variable inlet guide vane air control system, thus causing it to malfunction.

One of the best coatings used so far has been a flame sprayed polyester resin with an aluminium filler. It appears to have good erosion resistance and abrades away without blade tip or fin wear. The only problem is that it is limited to a maximum temperature of 600°K which only allows it to be used in the L.P., I.P. compressors and part way through most modern H.P. compressors. Apart from this coating all the others are producing some sort of problem. By careful selection of the position in the engine of each coating used, and by tailoring the spraying conditions or the resin/filler mix proportions, it is possible to limit blade tip and fin wear and coating erosion to levels which can be tolerated although in most cases they need improving upon.

So far filled honeycomb seems to be the only material suitable for use in turbine tip seals, and at present this has to be carefully tailored to each application to ensure that all possible rubs between blade tips and coating are kept to an absolute minimum. Medium to heavy rubs result in severe fin wear.

Many of the linings which are bonded or brazed to engine components give trouble with either poor bonding or areas of poor bonding, and many cases have been experienced of parts of linings breaking away during engine running. This, together with erosion problems, cost, etc., has led to a general dislike of this type of material.

7.0 CURRENT 'STATE OF THE ART'

In general, the abrasive coatings used have been developed to a satisfactory standard and are working well, having accumulated a vast number of engine running hours in service. The position regarding abradable coatings however is nowhere near as good and in many cases abradable coatings are being persisted with when they are not entirely satisfactory, because of the significant loss in engine performance which would occur if these coatings were not used. The main problem with abradable coatings, especially for temperatures above 600°K is that no material manufacturers have yet come up with a completely suitable material. It is hoped that this paper will serve to make more people aware of this fact in the hope that more suitable materials will become available.

Currently, the major part of abradable coating evaluation is being done in engines which lengthens the time for evaluation of a coating. Rolls-Royce, as engine manufacturers, are well aware of this situation and are taking steps to devise improved laboratory and rig tests. These will enable a more accurate evaluation of the abradability and erosion resistance of candidate materials to be made, so that engine tests will become final proving tests, rather than initial evaluation tests which many tend to be today.

As discussed in 5(b) above, there are difficulties in rig testing coatings for erosion resistance, and a programme of work is in hand to devise and evaluate a realistic erosion test, which will be done at the appropriate environmental temperature. However, all tests of this type are accelerated, when compared with the rate of erosion in an engine, and therefore a lengthy period of correlation work is required to fully validate these rig tests.

Abradable coatings and linings used in turbines, produce wear of the fins on the root platforms and shrouds of the turbine blades. As these fins are usually an integral part of the turbine blade, then serious wear of them would result in the blade being scrapped. To try and overcome this, various wear-resistant coatings have been applied to the fins, but so far a completely satisfactory coating has not been found, as the fins are still wearing during a rub.

3.0 CONCLUSIONS

(1) The improvements in engine performance, to be gained by maintaining close clearances at the various rotating seals within a gas turbine, are essential to its economic operation. To make the maintenance of these close clearances a practical proposition often means the use of an abradable or abrasive coating is mandatory.

(2) Abrasive coatings are much less used than abradable coatings, as most applications are not suited to the use of the abrasive ones. However, there is general satisfaction with the performance of the abrasive coatings, where they can be used.

(3) Abradable coatings are the most widely used, and are found in fan and compressor bores over the rotor blade tips, in labyrinth seal housings, in turbine liners, and in blade root seal bores.

(4) In general, the performance of abradable coatings in engines leaves much to be desired, and in many cases the situation is being coped with by coatings being carefully tailored for individual applications.

(5) Within the limited temperature capability of 600°K, an aluminium filled flame sprayed polyester coating is working satisfactorily in a wide range of engine applications.

(6) Although laboratory and rig tests exist and are being used to develop and evaluate new coatings, better methods are required. Work is being carried out within Rolls-Royce to improve a hot erosion rig test and a laboratory abradability rig, for evaluation of rotor path bore and labyrinth seal bore coatings.

(7) There is still a definite need for new abradable lining materials, preferably flame sprayed, for use in gas turbine engines. Such materials should have good erosion resistance with useful lives of 5,000 to 10,000 hours in an engine, and they should machine away cleanly without causing undue damage to blade tips or labyrinth fin tips. Coatings are especially required for the turbine areas within an engine, and these would require a temperature capability of 870°K to $1\,250^\circ$K, depending upon the particular application.

① ABRADABLE COATING OR LINING
② ABRASIVE COATING

FAN TIP SEAL ①

FINNED LABYRINTH SEALS ①

TURBINE ROOT SEALS. ①

COMPRESSOR TIP SEALS FRONT TO REAR. ①

SPACER RINGS ②

FINNED LABYRINTH SEALS ①

TURBINE TIP SEALS. ①
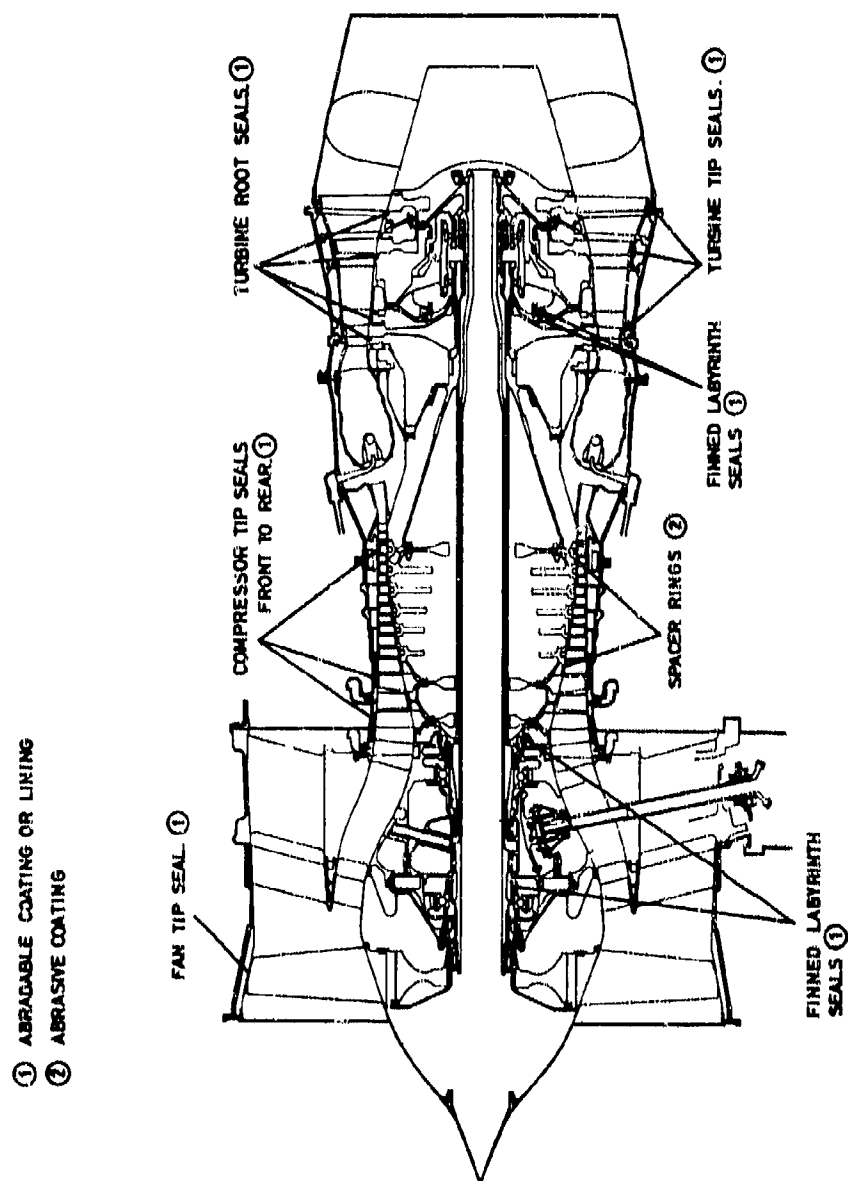
FIG. 1 TYPICAL FAN ENGINE SHOWING RANGE OF POSITIONS WITHIN THE ENGINE WHERE COATINGS ARE USED

ABRADABLE COATING

DEBRIS CARRIED AWAY BY
NORMAL LEAKAGE AIRFLOW
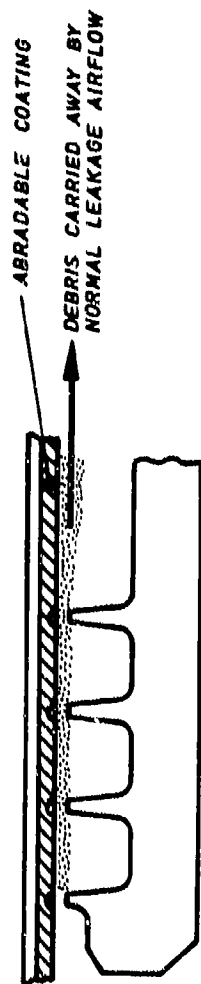
LIGHT RUBS - SHORT DURATION OR ECCENTRIC. LITTLE OR NO EROSION

ABRADABLE COATING

MUCH REDUCED AIRFLOW CARRIES
AWAY ONLY SMALL PROPORTION
OF WEAR DEBRIS

TRAPPED DEBRIS CAUSING EROSION
OF THE ABRADABLE LINING BETWEEN FINS
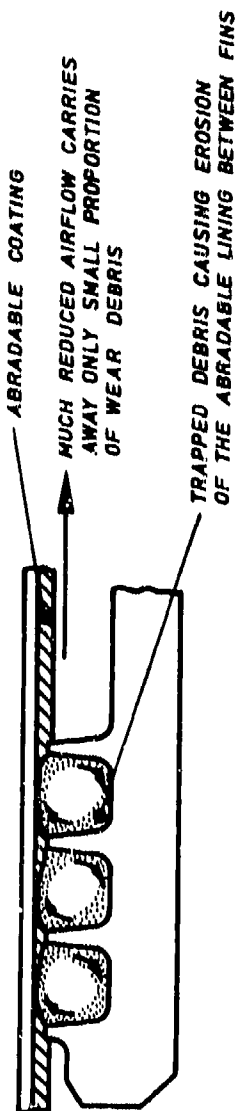
HEAVY RUBS AROUND THE PROPORTION OF THE SIGNIFICANT EROSION
CIRCUMFERENCE.

FINNED LABYRINTH SEALS

FIG. 2

NICKEL

GRAPHITE

POROSITY
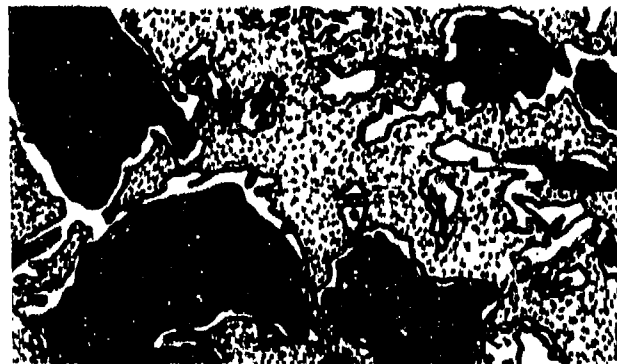
SECTION THROUGH Ni/C POWDER

FIG. 3 (A)   MAG x 600

SECTION TROUGH APPLIED COATING

FIG. 3 (B)   MAG x 300

2-12

KEY: θ1 = FREE UPSWING ANGLE
θ2 = UPSWING ANGLE AFTER CUTTING TEST COATING

ENERGY LOSS ∝ $\cos\theta_2 - \cos\theta_1$

RANGE OF ABRADABILITY OF 75/25 Ni/C OBTAINED BY USING VARYING SPRAY TECHNIQUES

COATING NOT ACCEPTABLE WHEN RUBBED BY BLADES

PASS LIMITS FOR Ni/C COATING

JOULES

FT Lbf

CUTTER

GROOVE CUT IN TEST COATING

ENERGY LOSS

Results for 75/25 % Ni/C

DIAGRAM OF LABORATORY ABRADABILITY TEST RIG

FIG. 4

BASE

TEST COATING
(SLIDES INTO
POSITION)

EROSION

TEST SPECIMEN HOLDER

SAPPHIRE
NOZZLE

SPRING LOADED
GUARD

GUARD
(RELEASE LEVER TO START TEST)

AIR/GRIT
SUPPLY PIPE

NOTE:- SPRING LOADED GUARD IS HELD IN PLACE WHILST NOZZLE AIR/GRIT CONDITIONS ARE
SET UP. GUARD SPRINGS OUT OF THE WAY WHEN EROSION TEST COMMENCES.
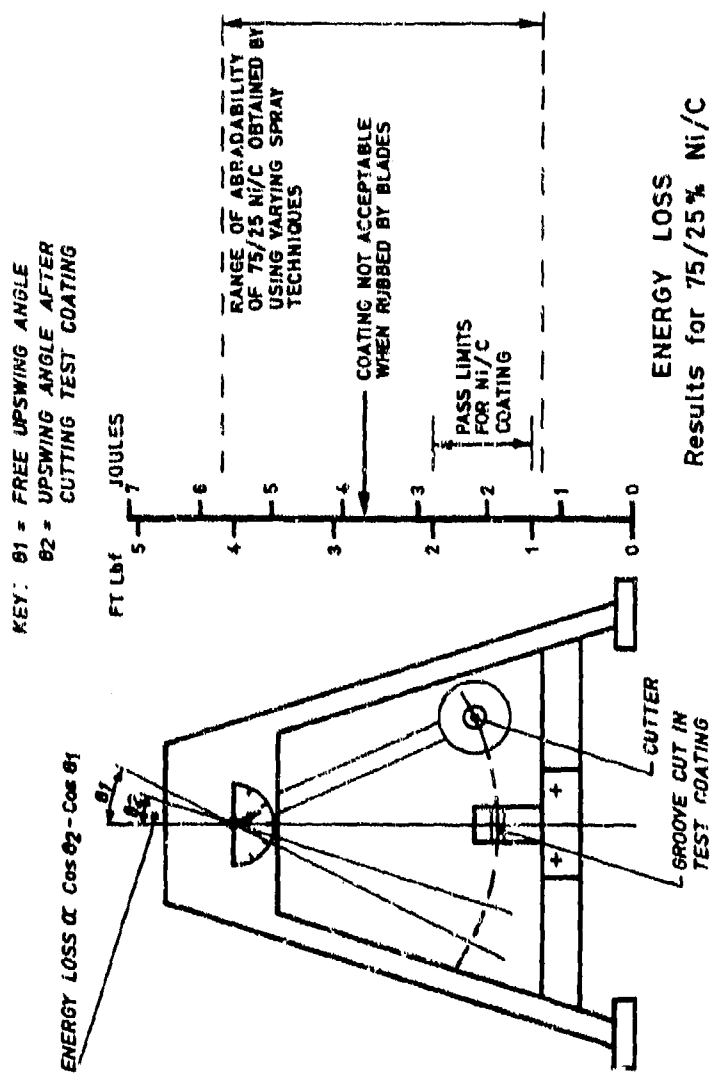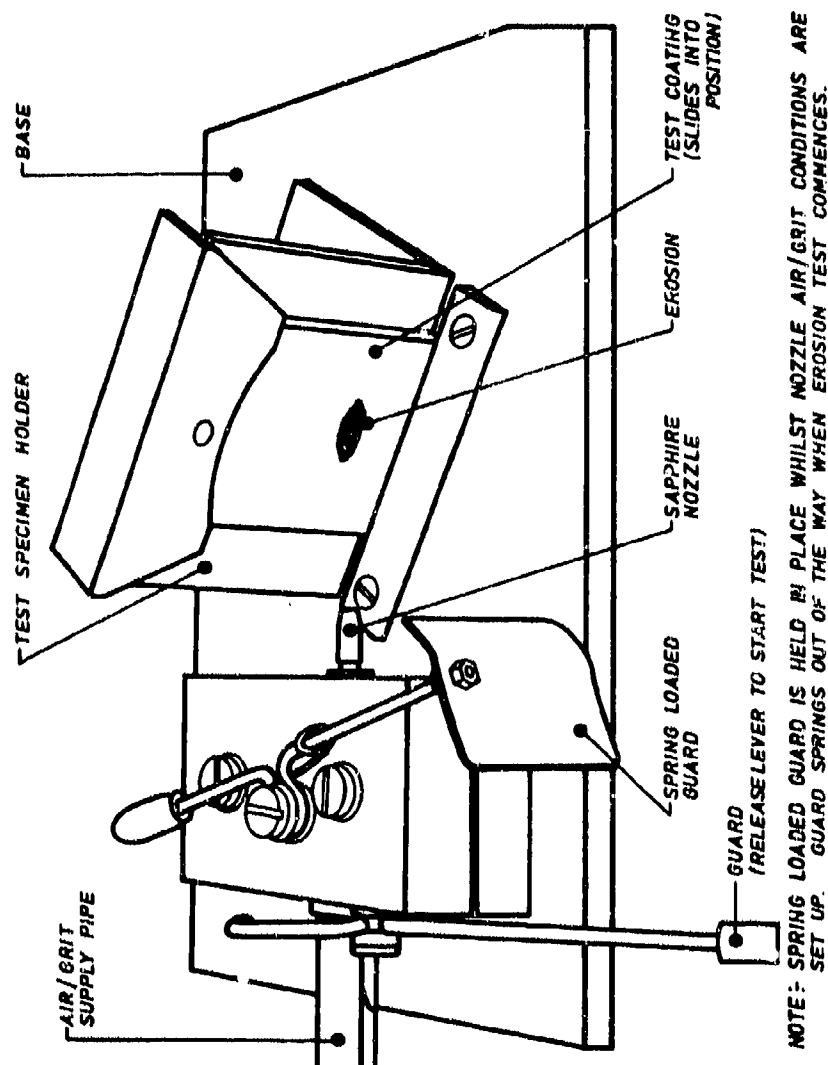
DIAGRAM OF SIMPLE LABORATORY EROSION RIG   FIG. 5

DISCUSSION

G.R.Wood, UK

Could the author comment on the compatibility of the seal material and the blade material, particularly on the turbine gas path. Is there a problem with abradable seals retaining blade material under rubbing conditions and accelerating the blade wear?

Author's Reply

There are problems with abradable lining materials retaining blade material, and these are mainly confined to the turbine gas path seals. The problems centre around finding an abradable material, capable of withstanding the temperatures in the turbine, which is sufficiently abradable.

So far experience within Rolls-Royce has been that the turbine coatings tried so far have been too hard, and as such have resulted in material being transferred from the blade tip to the coating, where it has usually become a hard oxide, which undoubtedly increases further the amount of blade tip wear.

Materials that are used at present, as turbine rotor path abradables, are better than nothing but are still too hard, and therefore all produce significant blade tip wear. We are still awaiting the availability of a truly abradable turbine liner material.

A.R.Stetson, US

You did not discuss incursion rates. It seems that on your slides you must have gone from one incursion rate to another in showing the smeared specimen to the unsmeared specimen but you did not rate it an important parameter.

Author's Reply

Throughout all the tests, compared in the slides, the incursion rate was constant at 0.25 mm 1 sec (0.010 in. 1 sec). The reason for showing these two slides was to try and emphasise the point that misleading results can be obtained by choosing the wrong design of test rig when evaluating the abradability of coatings. In the example shown, the small rig produced smearing of a coating which abraded clearly when using engine components. It is thought that this was due to the fact that debris was not able to clear the rubbing zone quickly enough.

This point is discussed in more detail in Section 5(b) of my written paper.

It was not intended to convey the impression that incursion rate is not an important parameter, as it undoubtedly is. However in the tests described, it was one of the parameters that was held constant.

J.Millward, Rolls-Royce Ltd, UK

In the two abradability tests which gave conflicting results, i.e. a smeared effect on a small lab. rig and a clean cut on an engine parts rig, was airflow used in both cases — if not this probably was the reason for the difference, i.e. different debris removal rate.

Author's Reply

The example given in the paper, i.e. that conflicting results were obtained on two different rigs which were being used to test the same coatings, was included to make the point that great care must be taken in choosing or designing a rig to test the relative abradability of coatings for use in engines.

In answer to the question; a deliberate axial flow of air was not supplied to either of the rigs. In the case of the large rig, this used engine compressor blades, and although it was a single enclosed stage and would therefore tend to "stir" the air, it would nevertheless aid the removal of debris to a much greater extent than the small dia. rig described. An axial airflow would improve the rate of debris removal and if sufficient, in the case of the small rig, would most probably give acceptable correlation with the rig utilising an engine compressor stage.

Certainly anyone wishing to conduct rotating abradability tests should consider very carefully the airflow and geometry and their likely effect upon debris removal in relation to an actual engine.

A.Mihail, France

Vous avez parlé dans votre exposé des difficultés dans l'application des matériaux abradables. Est ce qu'on peut savoir quelles sont les difficultés que vous avez rencontrées? Pouvez-vous préciser quelles sont les difficultés en question?

Faites vous des essais pour déterminer le rapport entre les conditions d'application et leurs durée dans le temps?

Author's Reply

In reply to your question I would refer you to Section 5(a) of my written paper. In it I have attempted to explain that when flame spraying composite coatings, i.e. coatings containing mixtures of materials, the final proportions

of the mixture in the applied coating can differ significantly from the mixture in the spray powder being fed to the spray gun. The final proportions, and hence properties of the coating, are affected by variations in the spraying parameters which are optimised and then rigidly controlled.

Erosion and abradability tests are done to assist in finding these optimum spray parameters which are, very often, further modified following the results of bench engine tests on these coatings.

F.Willkop, Germany

Mr Ludwig has shown in his paper that Zirkon coatings have good insulating properties. Has the author tried to examine a multilayer coating on the casing in the blade tip region, e.g. Zirkon coating with an additional cover of an abradable material?

Author's Reply

Although Zircon itself has not been tried as a part of a multilayer coating other coatings (e.g. magnesium zirconate) have been investigated. Attempts so far have been unsuccessful in producing satisfactory adhesion between an abradable lining and the ceramic insulating lining, and to date this is still a problem.

ABRASIVE COATINGS AS SELF CLEANING
GAS TURBINE COMPRESSOR VANE TIP SEALS

A. R. Stetson, Chief, Materials Engineering
J. W. Vogan, Senior Research Engineer
W. A. Compton, Director-Research

SOLAR Turbines International
An Operating Group of International Harvester
2200 Pacific Highway, P.O. Box 80966, San Diego California 92138

ABSTRACT

Efficiency of a gas turbine is reduced by vane tip losses in the compressor section. Vane tip/rotor rubs can result in catastrophic failure of a gas turbine engine. This paper describes a test rig and experimental data obtained evaluating abrasive coatings for clearance control between the vanes and the rotor in a gas turbine compressor. Plasma/flame sprayed oxides, carbides and chemically bonded abrasives were tested under conditions duplicating those encountered in the compressor section. The effectiveness of the coatings in grinding away the vane tips to provide minimum clearance without damage to the vane or rotor was determined. Coatings with rough, sharp abrasive grains were most effective. The laboratory tests were confirmed by engine development tests with a full-scale rotor.

INTRODUCTION

With rising fuel costs and increasing shortages, improved efficiency in gas turbine engines is essential. The large tip clearances currently in use in stationary turbine compressors to prevent contact due to shaft eccentricities are no longer acceptable because of loss in engine efficiency.

The problem is best illustrated by reference to a schematic in a modern industrial gas turbine compressor (Fig. 1). The vanes in the engine are static about the rotor. Spacing between the unshrouded vanes and disc spacer rings (rotor) should be minimal for greatest efficiency, i.e., clearance to permit assembly and to allow for rotor thermal and mechanical growth and thermal growth of the vane due to a ΔT between shroud and tip. Under ideal operating conditions this minimal spacing could be used. However, experience has shown that some eccentricities in the shaft can develop and clearance must be opened slightly to allow for this possibility.

Vane/rotor contact can produce bowing and imbalance by uneven heating of the rotor. Frictional heat in the vanes accentuate the initial contact by additional incursion resulting from thermal expansion. When extremely severe, vane rotor contact can produce ring spacer or vane failure and thus catastrophic engine damage. Calculations and experience have shown that the vane/rotor interference rate can be as high as 25μm/sec (0.001 in. sec) and can last for up to 30 seconds.

Increasing vane tip clearance is a very unsatisfactory approach to minimizing vane-rotor rub because it results in an overall decrease in engine performance (output power and thermal efficiency).

To effect near net clearance, a system must be developed that will permit vane/rotor tip rub without excessive heating of either component. An abrasive coating applied to the rotor was selected as one means of achieving this objective. To be effective, the coating had to meet the following requirements:

1. Remove the vane tips without generating excessive temperatures either in the rotor or the vane.

2. Be unaffected by thermal cycling between anticipated ambient temperatures and 427°C (800°F).

3. Application as a part of the normal manufacturing sequence without subsequent finishing operations.

Essentially no quantitative data was available on the performance of abrasive coatings under the anticipated operating conditions. Aluminum oxide applied by plasma or flame spraying has been used on compressor cases, with some success, to serve as an abrasive coating for removal of blade tips in the event of rub. However, no data was available on its use on the rotor. To obtain the required data on coatings, a test rig was designed and built. The rig duplicated those conditions encountered in compressor operations. Oxides and carbides were selected as the primary abrasives because of their hardness, sharp cutting edges, low cost and availability; although consideration was given to other materials during the test program.

TEST FACILITY DESIGN AND OPERATION

The test rig was designed to duplicate the conditions encountered in a Solar axial flow compressor. During operation, gas in the compressor discharge end is at a temperature of 427°C (800°F) and the surface velocity of the rotor is 305 mps (1000 fps). If a rub occurs, the vane to rotor intrusion rate may be as high as 0.025 mm per second (1 mil per second) with the maximum anticipated interference being 0.75 mm (30 mils). The test rig was designed to duplicate these conditions.

The completed rig, illustrated in Figure 2, is powered by an air driven turbine adapted for this application from one of Solar's standard production engines. Air to drive the turbine is supplied at a pressure of 0.69 MPa (100 psi) with a mass flow of 1.35 kg (3.0 lbs) per second. This value may vary from test to test depending upon the coating tested and the configuration of the test rotor.

This turbine is directly coupled to the output shaft through a flexible coupling. The relatively slow turbine speed (20,000 rpm versus 60,000 rpm plus in normal operation) reduces drive efficiency; however,

this is more than offset by the elimination of the gearbox of an electric motor driven unit. The test rig drive, as shown in Figure 2, was essentially maintenance-free after literally hundreds of test runs.

The basic test disc used in abrasive rub testing was a nominal 31 cm (12 in.) in diameter and is machined from an AISI 410 forging. Several of these were made to minimize down-time while the disc is being coated between tests. Over 50 material systems have been tested to date with this equipment.

The vane used for testing the coatings is located immediately below this disc on a platform advanced by a variable speed drive calibrated to produce an advance rate of 0.025 mm (0.001 in.) per second.

During elevated temperature operations, the disc is heated by an oxygen-acetylene torch and the vane by the hot gas generated in the cavity during the heating of the disc.

The basic instrumentation used to monitor the test consists of the following:

- Vane temperature thermocouples
- Vane stress strain gauges
- Speed sensing pickups.

These outputs were recorded by an oscillograph. Wheel temperature was monitored by a standard strip chart recorder. In addition to this basic test data, vibration levels, oil pressure, and bearing temperatures were monitored to warn of potential equipment failure.

The test procedure used with this facility is as follows. The abrasive material to be evaluated is applied to the periphery of the disc in the desired thickness. The disc is then balanced and installed on the rig. A test vane with calibrated instrumentation is installed on the drive platform and the unit is ready to run. The disc is brought up to a speed of approximately 5000 rpm and the speed held constant. The instrumentation is given a final operational check and the torch ignited. Speed is then held constant until temperature of the disc has stabilized at 427°C (800°F). Once thermal stability is achieved, the speed is increased to give test velocity of 305 mps (1000 fps) and conditions are again stabilized. The test vane is then fed into the disc periphery for 30 seconds at a rate of 0.025 mm (0.001 in.) per second. The unit is held at this speed until cool down is complete to prevent heat soak back into the bearings and turbine. After cool down, the disc and vane are removed for further examination followed by stripping and recoating of the disc for subsequent testing.

This test rig has been in operation for over three years without any significant problems. Recently, minor modifications have been made to it to incorporate a capability for the testing of bladed discs. Abradable tip seal materials have been tested at speeds of up to 430 m (1400 ft) per second and test temperatures to 1370°C (2500°F).

TESTING

SELECTION OF MATERIALS

Because of the lack of specific data on abrasive coatings for the proposed application, it was decided to test as many different material systems as were practical. Initial selection of the materials for testing was made on the following basis:

1. The material system must be potentially capable of prolonged operation at 427°C (800°F) in an oxidizing atmosphere.

2. Testing would be limited to materials that were commercially available.

3. The abrasive grain would be of a composition of demonstrable hardness with sharp, cutting edges.

4. The coating must be applied to a finish dimension without subsequent processing.

5. Application of the coating was to be compatible with our standard compressor fabrication methods.

Using these guidelines the following materials were selected for initial testing as the abrasive constituent in the coating:

- Aluminum oxide
- Chromium carbide
- Tungsten carbide
- Silicon carbide
- Chromium sesqui oxide.

Although the latter was not considered to be a true abrasive, it has shown excellent wear resistance in other applications and was included for comparison with the more abrasive materials.

Plasma spraying (P.S.) was selected as the primary method of application for these materials. The processes were well advanced at Solar and could be used to apply the coatings to the close tolerances required. Nickel aluminide was chosen as the primary bonding agent in the composite coatings since it is self-bonding to most alloys including the AISI 410 substrate. Cobalt and nickel-chromium bonding alloys were also used in a few composites as were coatings of the pure abrasive materials.

In addition to the plasma sprayed materials, a Solar developed abrasive coating (RC-1) was applied by conventional spray techniques and cured at 538°C (1000°F).

TEST PROCEDURES

The material systems evaluated were tested for the following characteristics:

- Thermal shock resistance
- Thermal stability
- Adherence
- Surface roughness
- Abrasiveness, as determined on the rub test rig.

Thermal Shock

Coatings were tested for their ability to withstand repeated thermal cycling by applying the coating to a test panel of AISI 410 steel, 77mm x 103 mm x 1.53 mm thick (3 in. x 4 in. x 0.060 in. thick). These panels were heated to 538°C (1000°F) and removed and quenched in water. This cycle was repeated ten times or until failure occurred as evidenced by spalling of the coating.

Thermal Stability

The effect of prolonged exposure to elevated temperatures was determined using panels prepared in the same manner as those used in the thermal shock tests. These panels were heated in a furnace for 500 hours at 850°F. After testing, the panels were removed and examined visually for any evidence of attack due to the prolonged exposure to the elevated temperature.

Adherence

The adherence of the coating was evaluated in two ways - band testing and tensile bond tests. For band testing, coated panels similar to those used in the previous test, differing only in size [51 mm (2 in.) square], were bent over a 12.7 mm (0.50 in.) diameter mandrel for a total bend of 180 degrees. Performance was judged on the basis of percent of material lost.

The second test for adherence, or bond strength, utilized tensile strength. The coating to be evaluated was applied to the end of a 2.54 cm (1 in.) diameter rod. A similar rod was then bonded to the coating using a high-strength epoxy adhesive. After curing the adhesive to its maximum strength, the cemented rod was placed in a tensile testing machine and the tensile force required to rupture the coating-substrate bond was measured. Bond strength was then calculated.

Surface Roughness

Surface roughness of the coating was measured using the same samples as were used in the bend test. A conventional profilometer was used to make these measurements.

Rub Testing

The periphery of the test disc was coated to a thickness of 0.25 mm (10 mils) and the disc mounted on the test rig. The test vane was instrumented with a thermocouple attached 2.5 mm (0.10 in.) from its tip and strain gauges cemented to the vanes, 32 mm (0.125 in.) from the base. The rig was brought up to an operating speed of 304 mps (1000 fps) at 427°C (800°F), and stabilized. The vane was then advanced into the coated disc at a rate of 0.025 mm (0.001 in.) per second. After the vane contacted the disc, it was allowed to advance for an additional 30 seconds at which point the feed mechanism was reversed and the vane withdrawn from contact. The unit was then shut down and the vane and disc removed for examination. Data recorded during this test were the strain on the vane, the temperature indicated by the thermocouple located 2.5 mm (0.10 in.) from the tip, and the change in wheel speed. Both the coating and the vane were examined visually for burning, metal transfer and overall appearance. Representative vanes were also sectioned for metallographic examination.

RESULTS AND DISCUSSION

Over 50 material systems were tested. Typical results are presented in Table 1 for the initial screening tests of various coatings. These results have been limited to those obtained with aluminum oxide, tungsten carbide, chromium carbide and chromium sesqui oxide abrasives. As is evident in the table, the baseline abrasive was aluminum oxide and it was tested both as a pure plasma sprayed coating and with various binders. Tungsten carbide was limited to a cobalt binder. Attempts to bond it to the substrate chemically were unsuccessful. Chromium sesqui oxide was tested only as a pure material and showed little promise. Chromium carbide was tested both with a nickel-chromium alloy binder and with nickel aluminide as the bonding agent.

The first criteria used for evaluating the coating was the ease and reliability with which it could be applied. Materials showing poor deposit efficiency were discontinued since they were not considered suitable for the end application. Chromium sesqui oxide and nickel aluminide bonded aluminum oxide were dropped at this point.

Surface roughness values ranged from 3.1 μ metre (110 microinches) for the chromium sesqui oxide to 14.1 μ metre (575 microinches) for tungsten carbide which was the coarest material tested. The majority of the abrasive materials were found to lie between 5 μ metre (200 microinches) and 11 μ metre (425 microinches). Plasma sprayed coarse aluminum oxide, which is one of the most common abrasive materials used in this and similar applications, gave a surface roughness of 5.1 μ metre (225 microinches). The RC-1

coating had a surface finish of 11 μ metre (425 microinches). Both materials appeared to be adequately rough for the proposed application.

Metallographic sections were taken of all coating types and examined visually at a magnification of 100X. The comments in the table are largely self-explanatory. Of particular note is the typical difference between plasma sprayed and chemically bonded abrasive (RC-1). This is illustrated in the scanning electron micrographs in Figures 3A and 3B. The P.S. coatings exhibited a relatively dense structure with rounded grains and thus retained little of the structure required to grind or accommodate the grinding debris. With the RC-1 abrasive coating, the structure is open and the grains retain the majority of their "as crushed" sharpness. As will be noted subsequently, sharp grains and an open structure are required in an effective self-cleaning abrasive coating. Attempts to obtain this structure by plasma or flame spraying were unsuccessful. As power was reduced to the plasma gun, for example, to decrease rounding of the edges of the abrasive grains to improve cutting efficiency, the weak, porous structure was readily wiped away during a rub. Co-spraying of a nickel aluminum bonder alloy with the abrasive grains also did not produce adequate retention of the abrasive unless plasma power was high enough to melt the abrasive grains.

The final test in this phase was for the adherence of the coatings to the substrate. Except for the chromium carbide, none of the coatings was severely damaged by the bend test. The material loss indicated in the table was largely on the edges where more severely stressed conditions exist. The nickel aluminide bonded aluminum oxide and the conventional fine grained aluminum oxide had relatively high spalling tendencies but losses were not sufficient to discontinue use of the materials on this basis. Tensile testing for bond strength showed that all of the materials were capable of meeting the low centrifugal stresses expected during operation [<680 kPa (100 psi)].

Data obtained from the bend test and bond strength test were confirmed in the thermal shock test. Thermal shock results were not tabulated. All materials passed and no significant differences were found in performance during thermal shock.

Similar tests were conducted on chemically bonded tungsten carbide abrasive grains. These data are not included. The binder under consideration did not adequately wet the tungsten carbide abrasive grains. Tensile bond strengths are not reported for the RC-1 coating since the epoxy adhesive used in these tests did not adhere consistently to it.

The rub characteristics of representative coatings tested in this series are reported in Figures 4, 5 and 6. In addition, a rub on a bare, uncoated disc is included in each to serve as a baseline. Uncoated data represents the situation in a conventional vane-rotor rub and should be used as a guideline in evaluating subsequent results.

Typical appearance of the rotor after a vane rub is shown in Figures 7, 8 and 9. Figure 7 is an uncoated disc. Chatter marks from the vane are evident. These are the result of localised metal buildup and indicate that a very high vibration level is generated in the vane during rub with the bare disc. Figure 8 is of a rotor plasma sprayed with a conventional aluminum oxide abrasive. Although chatter marks have been eliminated, the metal transfer to the disc is excessive indicating limited surface life and potential problems in rubs with multiple vanes. Figure 9 is a photograph of an RC-1 abrasive coated disc. This disc has been through the same rub test as the two previous discs but no evidence of metal transfer or coating damage can be observed. In Figure 10 the appearance of this rub is shown in actual operation. To the left of the picture is a steady stream of sparks similar to those generated by a grinding wheel. This steady grinding operation continues throughout the rub. When uncoated discs, or discs coated with plasma sprayed aluminum oxide, are tested in this manner the stream is intermittent indicating that the thermal growth occurs during rub until sufficient heating occurs to melt the tip of the vane. At this point the molten metal is thrown clear and the rub is interrupted until the vane has advanced sufficiently to resume contact. This is an undesirable situation since it tends to create a destructive rub mode and gives considerable excess vane wear, amounting to 0.25 mm (10 mils) in most cases due to thermal expansion of the vane resulting from frictional heating.

Three grades of tungsten carbide were tested and as predicted upon examination of the coating prior to test, the coarser the grain, the better the cutting action and the less metal transfer. The chromium carbide coating showed heavier transfer than any of the other materials tested and was dropped from the program.

The next criteria used in evaluating the coating's effectiveness was the temperature recorded by a Chromel Alumel thermocouple located 2.5 mm (0.10 in.) from the tip of the vane at the time of initial contact. These data are reported in Figure 4. The temperature indicated by this thermocouple lagged the contact temperature due to the mass of the vane and the distance to the rub area. Actual vane tip temperature was sufficient to generate melting in most tests. An indication of the magnitude of this delay is the discrepancy between the temperature readout of 543°C (1010°F) for the vane rub on the bare disc in comparison with the probable tip temperature in excess of 1482°C (2700°F) as indicated by the melting of the vane tip. In all cases, the application of a coating to the rotor reduced the temperatures observed on the vane. However, with the exception of the RC-1 coating, all coatings tested still created melting of the vane tip. Increasing the grain size of the tungsten carbide abrasive did not reduce the indicated vane temperature. The reverse occurred with the tungsten carbide abrasive giving an indicated vane temperature of 301°C (573°F) for the fine material and a temperature of 512°C (953°F) for the coarse material. This represents a nominal grain size variation of -325 mesh for the fine material as opposed to -150 mesh for the coarse material. The chromium carbide gave a slight temperature reduction of 21°C (60°F). These temperatures are almost identical with those obtained with the coarse tungsten carbide coating. The coarse aluminum oxide coating reduced the measured temperatures to 438°C (820°F) again indicating some improvement in performance.

Strain data, Figure 5, generally paralleled the temperature data indicating the effectiveness of the coating. The correlation was qualitative, not quantitative, as was the speed loss during rub. The data obtained from the bare disc was inconsistent with that obtained from the coated disc, with regard to

strain and speed, and this discrepancy has not been resolved. The disc coated with sharp abrasive grain (RC-1 coating), showed an increase in speed during rub caused by a slight smoothing of the disc during initial contact. The reduction in air drag was greater than the frictional drag on the disc due to rub. An overall acceleration of the disc was thus recorded for a constant driving force on the turbine.

The air drag imparted to the disc by the rough abrasive coatings is calculated from the power required by the driving turbine. The bare uncoated disc was used as a baseline and given an arbitrary value of 100. Increased mass flow required through the turbine to stabilize at operating speed was calculated and converted to relative percentage as compared with the bare uncoated disc. On this scale the increase in power amounted to between 10 and 15 percent. The data obtained are presented in Figure 6. This measurement is useful in assuring reproducible testing and comparing overall coating roughness. It is not applicable to compressor operation where the effect is not detectable based on full-scale rig test.

Appearance of the vane tips after a rub is very revealing as to the effectiveness of a coating in preventing overheating and stock removal. The appearance of a metal-metal rub, also characteristic of essentially all of the plasma sprayed coatings is shown in Figure 11. The alloy reaches a temperature near the melting point at which it is readily extruded. This extension of the material is relatively symmetric showing essentially no preference to move the material in the direction of the motion of the disc. With an efficient cutting material, e.g., the RC-1 coating, this extrusion of material does not occur as is shown in Figure 12. The vane is uniformly ground with minimum heating. Essentially no burr is formed that would interfere with blade aerodynamics.

In ranking of abrasive coatings, the two most significant test parameters appear to be temperature rise and maximum strain during a rub. These data for representative coatings are illustrated in Figures 4 and 5. The results show that many of the plasma sprayed coatings are little, if any, better than the uncoated alloy. The RC-1 coating with the retained sharp abrasive is the outstanding coating. This coating was selected for a full-size rig test.

The comparison of coated versus uncoated rotors during vane tip-rotor rub is clearly shown in Figure 13. These tests were conducted on a full-size rig to confirm the results obtained in the laboratory with full-size engine components. The vanes to the left have been rubbed against the RC-1 coated rotor. Except for a very thin wire edge, no vane deformation or burning has occurred. The vanes rubbed against the uncoated rotor are shown along side and the heavy burrs on these vanes can easily be seen. It is also evident that the vanes rubbed against the uncoated rotor have a burr both on the leading edge and the trailing edge as in the laboratory tests.

CONCLUSIONS

Properly engineered abrasive coatings applied to turbine compressor rotors are an effective means of reducing temperature increase during rub and eliminating excessive vane strain. These coatings can be applied with sufficient reliability for production usage on compressors operating up to 427°C (800°F). Some loss of efficiency might be expected due to the increased surface roughness of the rotor. However, this represents only a small percentage of the total rotor area and the effect would not be detectable in normal operation. The increase in efficiency due to operating with minimum vane clearances will far more than offset this slight increase in aerodynamic drag.

Testing of various coatings showed that conventional flame and plasma sprayed coatings lose much of their effectiveness due to a rounding or melting of the sharp edges of the abrasive grain during application. When the sharp edges of the grain were maintained by other bonding methods, cutting efficiency was greatly increased and the overheating or melting of the vane tips was eliminated. Inorganic low temperature bonds for the abrasive, e.g., the one used in RC-1, afforded the best grain sharpness retention.

Further work will be conducted with these coatings not only for use on the turbine compressor rotor but also on blade tips to overcome rub problems in the blade housing area. The use of the reduced running clearances allowed through application of abrasive coatings to parts that may come in high speed contact during operation is expected to reduce overall fuel consumption of the turbine engines significantly.

In evaluating an abrasive coating, the visual examination of the specimens after test for burrs, melting and metal transfer is one of the most reliable means of evaluating their performance. Instrumented data, such as strain gauges and thermocouples, are helpful in this evaluation but the data generated are insufficient for a final decision. The test rig built for this program because of its versatility and the speed with which it may be adapted to other configurations and the rapid test turn-around has proven invaluable for gaining practical insight into the behavior of high-speed rotating components during rub.

TABLE 1. INITIAL SCREENING TEST RESULTS FOR ROTOR ABRASIVE COATINGS APPLIED TO AN AISI 410 BASE

| Abrasive System	Ease of Application	Surface Roughness (μ metre-μ in.)	Microstructure Appearance	Adherence		Abrasive Grain Appearance
				Bend Test (% Material Lost)	Tensile Bond Strength (MPa - psi)	
Nickel Aluminide Bonded Aluminum Oxide	Difficult	4,4 – 175	Laminar with approximately 10 percent abrasive	30	29 – 4200	Rounded edges
Plasma Sprayed Aluminum Oxide (53 > 15 microns)	Moderate	5,0 – 200	Laminar with discontinuous voids	20	47 – 6800	Flat with rounded corners
Flame Sprayed Aluminum Oxide (75 > 30 microns)	Difficult to control thickness	5,7 – 225	Similar to plasma sprayed with larger voids	15	52 – 7500	Ovoid
RC-1	Easily applied to required thickness	10,6 – 425	Projecting abrasive grains bonded to substrate	5	N/A	Sharp blocky grains
Cobalt Bonded Tungsten Carbide (43 > 30 microns)	Moderate	4,5 – 180	Fine uniformly dispersed abrasive grains in metal matrix	5	52 – 7600	Metallic coating on abrasive
Cobalt Bonded Tungsten Carbide (53 > 30 microns)	Moderate	8,8 – 350	Uniform structure with evenly dispersed grains	10	45 – 6600	Rounded abrasive grains
Cobalt Bonded Tungsten Carbide (74 > 30 microns)	Easily applied to finish dimension	14,4 – 575	Open structure with approximately 20 percent voids	10	58 – 8400	Large round grains
Nickel-Chromium Bonded Chromium Carbide	Moderate	6,3 – 250	Fine fused appearance	90	64 – 9300	Fine grains dispersed in metal matrix
Nickel Aluminide Bonded Chromium Carbide	Moderate	4,4 – 175	Laminar structure with discontinuous voids	10	30 – 4300	Fine rounded grains
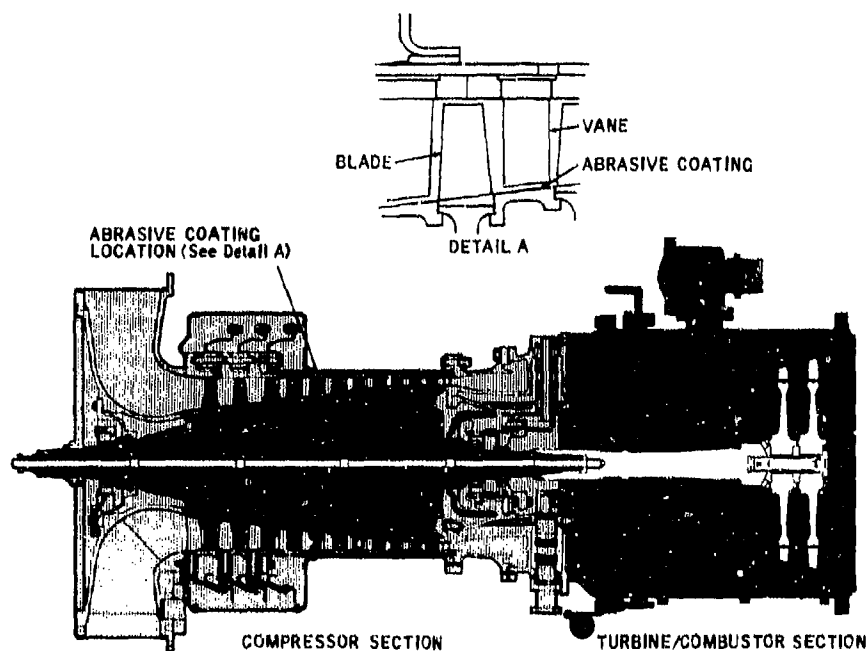
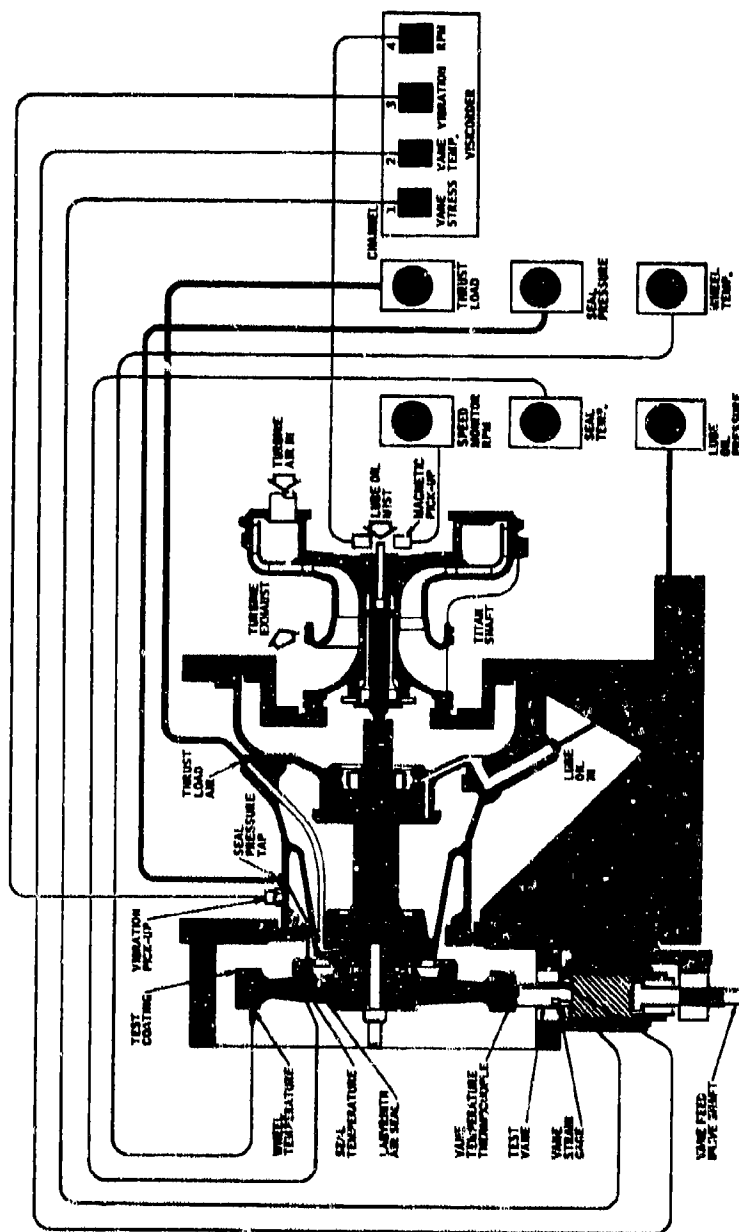
FIGURE 1. TYPICAL MODERN AXIAL FLOW COMMERCIAL GAS TURBINE

FIGURE 2. SCHEMATIC AND CROSS SECTION OF THE RUB TEST RIG FOR EVALUATION OF ABRASIVE ROTOR COATINGS
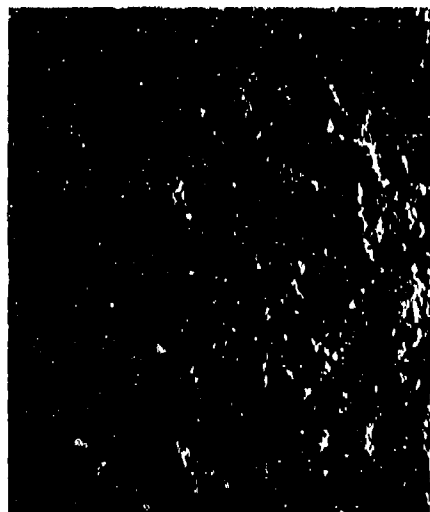
Plasma Sprayed

Gold Plated

Magnification: 50X

RC-1 Coated

Figure 3B.   Scanning Electromicrographs of the Surface of Plasma Arc Sprayed and RC-1 Chemically Bonded Abrasive Coatings
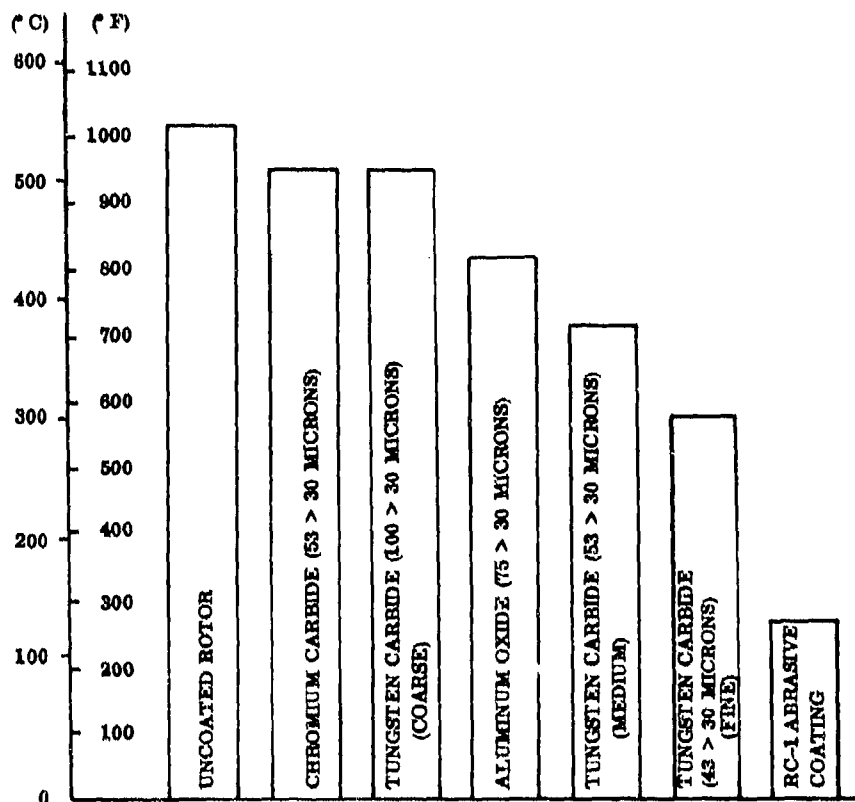
Plasma Sprayed Oxide

Bond Coat

Gold Plated

Magnification: 100X

RC-1 Coated

Figure 3A.   Scanning Electromicrographs of Cross Section of Plasma Arc Sprayed and RC-1 Chemically Bonded Abrasive Coatings

TEMPERATURE

FIGURE 4. TEMPERATURE RISE GENERATED IN THE VANE DURING RUB

(μ METRE/METRE)
(μ INCHES/IN.)
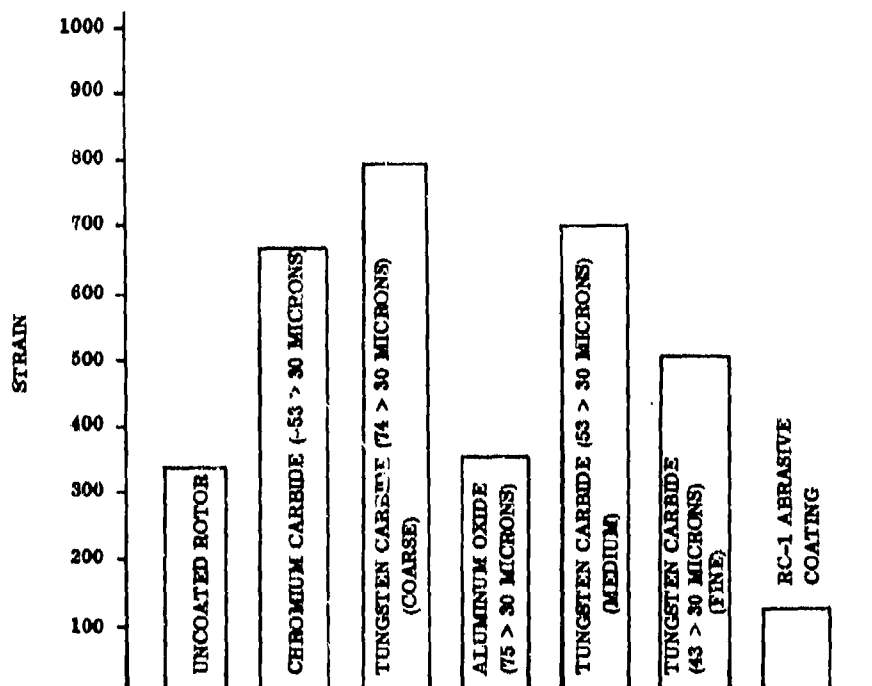
FIGURE 5. COMPARATIVE MAXIMUM VANE STRAIN VALUES GENERATED DURING ABRASIVE RUB
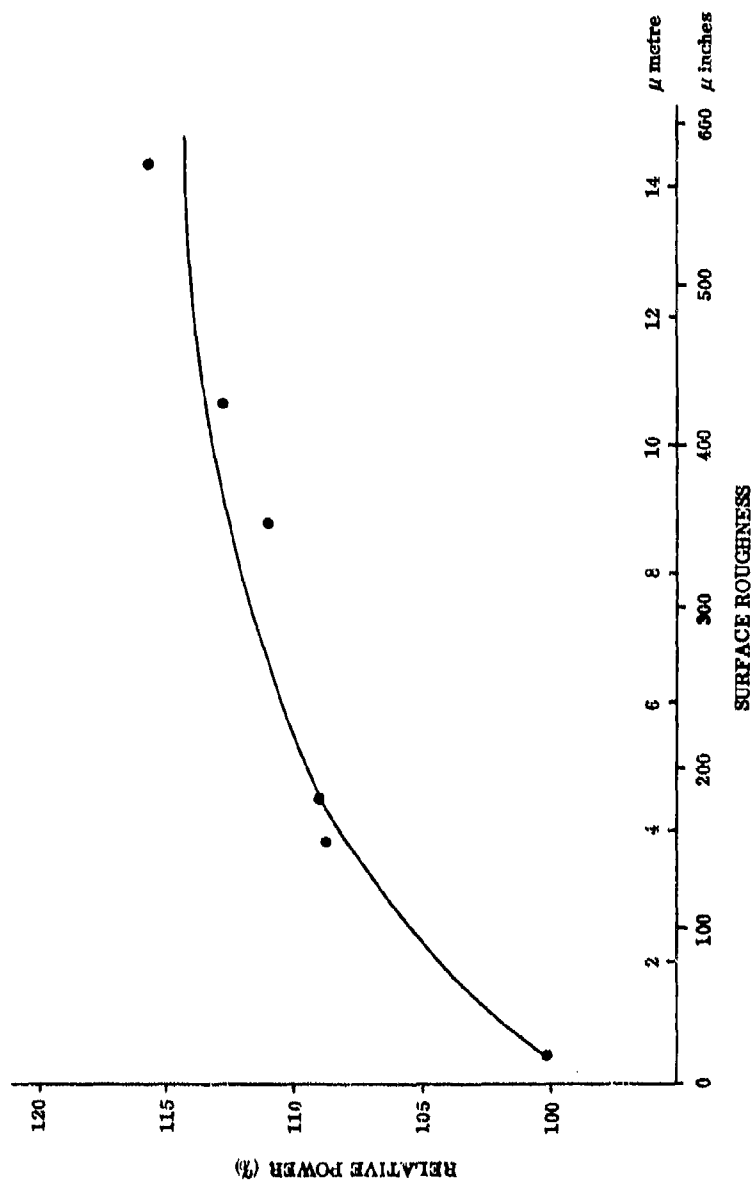
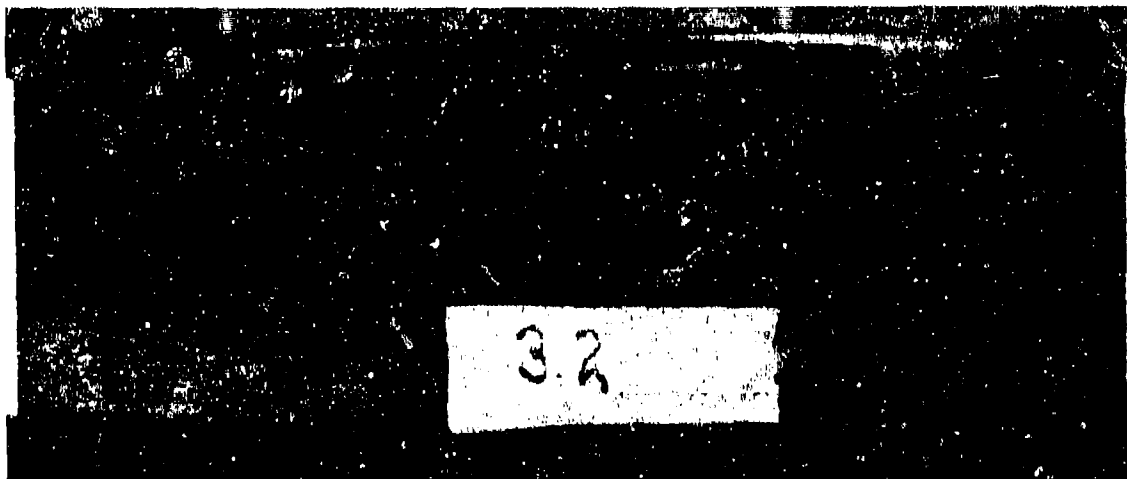FIGURE 6. RELATIVE POWER TO DRIVE COATED AND UNCOATED ROTORS AS A FUNCTION OF SURFACE FINISH

FIGURE 7. UNCOATED ROTOR AFTER 30-SECOND RUB

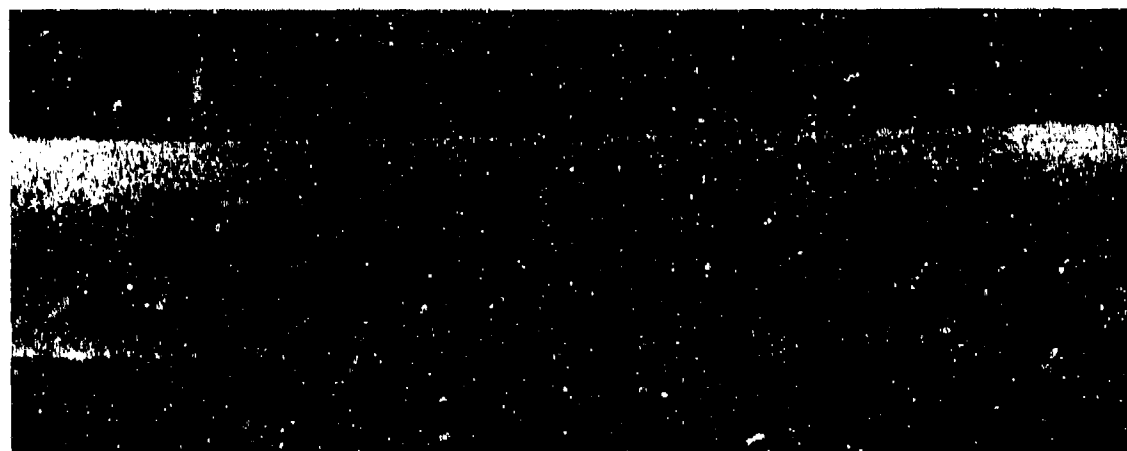FIGURE 8. APPEARANCE OF THE ALUMINUM OXIDE COATING AFTER VANE RUB

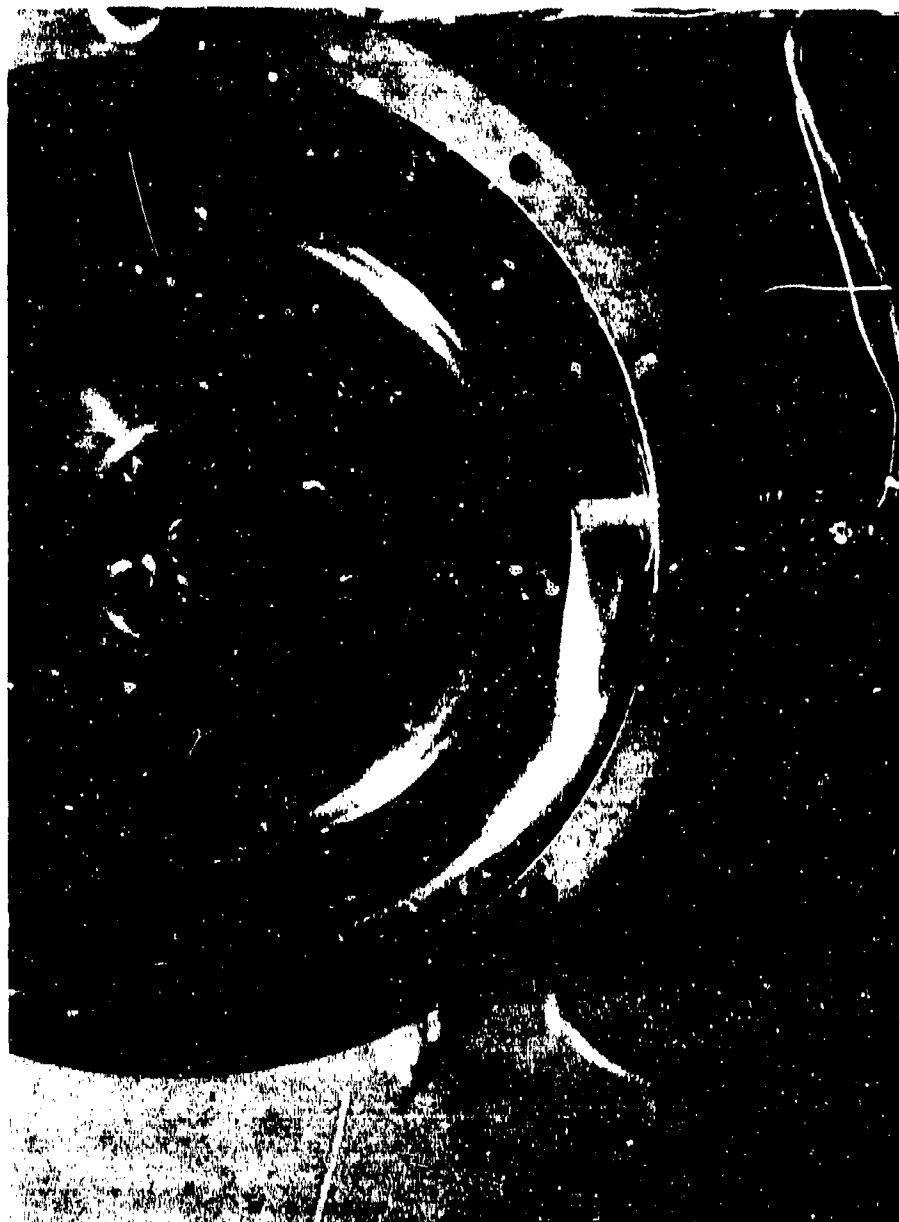FIGURE 9. ROTOR COATED WITH RC-1 AFTER RUB TEST

FIGURE 10. APPEARANCE OF RC-1 DURING RUB TEST

FIGURE 11. CROSS SECTION OF A TYPICAL VANE AFTER RUB
WITH A PLASMA SPRAY COATED ROTOR

FIGURE 12. CROSS SECTION OF A TYPICAL VANE AFTER RUB
ON RC-1 COATED ROTOR

Uncoated Rotor

RC-1 Coated Rotor

Figure 13. Vane Segments Rubbed Against a Full Scale Rotor During
Advanced Engine Development Tests

DISCUSSION

A.J.B.Jackson, UK

You mentioned that the roughness of the coating caused negligible aerodynamic loss. Have you conducted systematic tests to separate the effects on aerodynamic performance of tip clearance and coating roughness?

Author's Reply

No, I have not. Closing the tip clearance is of course the general basis of abrasive coating itself. and there is no way for us to close the tip clearance on the engine without some means of inhibiting the heating of the rotor under adverse conditions or eccentricity of operation. The only quantitative information I might say on this is that in the operation of the engine we can see a difference in its operation from the standpoint of aerodynamic efficiency changes.

J.G.Ferguson, UK

I am not sure you mentioned in your talk whether you machined the coating after you have applied it?

Author's Reply

No, it is applied to actual thickness. It is applied to within approximately $\pm 25\ \mu m$. Machining is really not feasible. You would have to diamond grind it. And we would get into an expensive operation in doing so. We think the accuracy of 1/1000 in. is satisfactory.

W.B.Litchfield, UK

What is the approximate bond strength?

Author's Reply

I did not go into these details of bond strength. It is very difficult actually to measure bond strength on a coating of this sort since it is completely open structure. But my rough guess would be that we are talking about a bond strength of about 800-1000 psi.

W.B.Litchfield

Describe process details with respect to application of RC-1.

Author's Reply

It is sprayed on like slush and fired at a thousand degrees Fahrenheit actually. The binder diffuses at that point, reacting very slightly with the aluminium and so the entire component there is fired. It is well within heat treat cycle of the rotor which is about 1125°F.

W.B.Litchfield

Can the coating be applied to vane tips?

Author's Reply

We have investigated and we are investigating tip clearance coatings of various kinds. For the low temperature application, there is no question that it could be bonded on to tip vanes or tip blades. The use temperature of this particular composition is 1000°F. There are other programs in operation with Solar, General Electric Co , and NASA in which we are looking at coatings aimed at maintaining the abrasive on to about 1000°C. It is a question of controlling that bonding mechanism. The grains are very effective at high temperature. Our experience is that flame spraying is not so effective. It is necessary to use a bonding technique around the edges of the grains, benefiting by the special structure of the grain itself.

W.B.Litchfield

Does the coating here influence in the fatigue properties of the substrate material?

Author's Reply

No, not at all.

H.L.Stocker, US

Relative to Figure 6, what was the absolute horsepower measured?

Author's Reply

The power levels used to be a requirement. Power was measured by taking the volume flow of air through the turbine that drove the rig.

H.L.Stocker

Did you account for possible turbine efficiency change in determining relative horsepower?

Author's Reply

This has been considered but it seemed to be unnecessary since experience with test rigs driven by electric motors showed that distinction was not possible whether a coating had been applied or not. There seems to be evidence in hand that the effect is small relative to others during operation.

H.L.Stocker

Did you run back-to-back tests with a smooth and rough (abrasive) surface at the same clearance in your compressor rig?

Author's Reply

Back-to-back tests were made for a vane tip clearance of approximately 30 mils. At our system the drag is primarily an aerodynamic drag of a disc freely rotating in a confined chamber and at constant clearance — no difference was noted.

H.L.Stocker

The possible effects of surface roughness on the airfoil velocity diagrams were not evaluated or determined in the way you ran your compressor rig.

Author's Reply

No.

G.Halls, UK

You talked about catastrophic failures that you occasionally experienced on the engine. Have you managed to reproduce them on this rig?

Author's Reply

Well, the catastrophic failures that had been experienced are relatively few. If you remember the design of the rig it used a solid wheel. The example that I showed happened to a ring spacer. It is only with ring spacer of course when any problem occurred in any engine facility.

Let me just add another comment: We have a program now with the Aero Propulsion Laboratory in which we plan to investigate the distribution of heat within the ring, a program in which we are going to study the heat flow under various ingression rates, the heat flow within the vane itself and within the separated rings. But within that wheel we could not. We were only looking at temperatures exclusively within the vanes. At that point, we were unable to measure the rotor temperature rise. These are vane temperature rises. Now, with the new setup with the telemetering system, we will measure the strain in the ring, the temperature distribution in the ring and also in the vane much more thoroughly than was possible in this particular program.

APPLICATION DES FEUTRES MÉTALLIQUES OHP
AUX JOINTS D'ÉTANCHÉITÉ DE TURBOMACHINES

par Emile GENIEYS

Société HEURCHROME 92700 Colombes · France

et André HIVERT

Office National d'Etudes et de Recherches Aérospatiales (ONERA) 92320 Châtillon · France

Résumé

L'ONERA a créé des feutres métalliques qui se caractérisent par une très forte porosité (jusqu'à 95 %) et une structure fine (fibres tubulaires de 10 à 30 µm). Le procédé consiste à déposer par voie électrolytique un métal comme le nickel sur des fibres de carbone provenant de la pyrolyse de la cellulose. Ces fibres en vrac sont transformées en feutres au moyen de techniques papetières de sédimentation par gravité ou centrifugation. Un frittage consolide l'édifice et élimine le carbone.

L'extrê e plasticité de ces feutres et leur aptitude à recevoir par diffusion gazeuse du chrome et de l'aluminium en for.: des matériaux particulièrement bien adaptés à la fonction de joints d'étanchéité de turbomachines. La Société Heurchrome a pris en charge leur développement (d'où leur nom OHP, pour ONERA Haute Porosité). Elle a mis a œuvre des techniques de scellement métallocéramique pour les zones à basse et moyenne température (jusqu'à 500°C), et des procédés de brasage pour les températures supérieures. Les joints ainsi réalisés sont opérationnels jusqu'à 800°C ; ils sont au stade des essais au banc pour les températures supérieures, jusqu'à 1050°C.

APPLICATION OF THE OHP METALLIC FELTS TO TURBOMACHINES SEALS

Summary

ONERA developed metallic felts characterized by a very high porosity (up to 95 %) and a fine structure (10 to 30-µm-dia-tubular fibers). The process consists in depositing by electrolytic means a metal, such as nickel, on carbon fibers made by pyrolysis of cellulose. These loose fibers are transformed into felts by means of paper works techniques of sedimentation by gravity or centrifugation. A sintering operation consolidates the material and eliminates the carbon.

The extreme plasticity of these felts and their aptitude to receive by gaseous diffusion chromium or aluminium make them particularly suitable for turbomachine seals. The Heurchrome Company took charge of their industrial development (hence their name OHP, for ONERA High Porosity). It implemented metallo-ceramic sealing techniques for the low and medium temperatures (up to 500°C) and brazing processes for higher temperatures. The seals fabricated this may are operational up to 800°C , they are at the bench testing stage for higher temperatures, up to 1050°C.

INTRODUCTION

L'accroissement du rendement thermo-dynamique des turbomachines est un souci constant des motoristes. L'augmentation des températures et des pressions qui contribue puissamment à cette évolution a conféré un rôle primordial aux joints d'étanchéité entre les divers niveaux de pression.

Les joints des turbines à gaz : joints de labyrinthes, joints de carters compresseurs, joints de carters turbines, doivent remplir à priori trois conditions essentielles :

- forte porosité globale : condition de légèreté et d'innocuité pour les pièces antagoniste.

- structure fine : condition de bonne étanchéité et d'abradabilité régulière et inoffensive.

- résistance à l'oxydation et à la corrosion pour les applications où les joints travaillent à haute ou moyenne température.

De plus, ces caractéristiques ne doivent pas être obtenues au détriment de leur résistance mécanique, en particulier, résistance à l'érosion par les gaz circulant à grande vitesse.

Les travaux que l'ONERA a conduit dans ce domaine se sont orientés, dès le départ, vers la création d'un feutre métallique qui, par sa structure enchevêtrée, présente une solidité considérablement supérieure aux matériaux de même porosité provenant du frittage de particules fines et équiaxes. (1)

La méthode de fabrication définie, parfaitement originale, a permis d'obtenir un matériau adaptable aux divers problèmes, parfois très difficiles, rencontrés dans ce domaine des joints de turbines à gaz.

Cette méthode prévoit la fabrication d'un feutre de nickel pur qui est l'élément de départ de toute une série de produits différents adaptés à chacun des problèmes spécifiques. Ce feutre de de nickel est ensuite transformé par des opérations de métallisation qui permettent d'obtenir un feutre homogène de composition : nickel-chrome, fer-nickel-chrome, nickel-aluminium, nickel-fer-chrome-aluminium, nickel-chrome-aluminium, etc.

Certaines de ces opérations de métallisation peuvent être réalisées sur le feutre lui-même avant mise en place sur son support. Certaines autres ne sont effectuées qu'après brasage des feutres sur leur support. En particulier, cette dernière méthode permet d'obtenir des feutres capables de résister à des températures largement supérieures à 1000°C.

Pour des raisons de commodité ces feutres métalliques ONERA à structure fine et haute porosité seront désignés par l'expression feutres OHP (pour "ONERA Haute Porosité"). On examinera successivement leur fabrication, leurs caractéristiques et leur application aux différents joints d'étanchéité des turbomachines.

I. FABRICATION DES FEUTRES OHP

A- Feutres de Nickel

La technique retenue pour cette fabrication est basée essentiellement sur l'utilisation de fibres métalliques obtenues par dépôt électrolytique sur des fibres de carbone. Le feutre est réalisé en cinq opérations principales successives.

a. Des fibres de cellulose sont pyrolysées en vrac à 1000°C, sous protection d'une atmosphère d'azote enrichie de xylène, pour obtenir par dépôt de carbone pyrolytique, la conductibilité nécessaire.

b. Les fibres de carbone ainsi obtenues sont revêtues de nickel par dépôt électrolytique au tonneau.

c. Les fibres nickelées sont dispersées dans l'eau puis sédimentées par gravitation ou centrifugation. On obtient ainsi un feutre brut qui, bien que peu solide, est néanmoins aisément manipulable.

d. Cette ébauche est ensuite frittée à 1050°C dans l'hydrogène humide ce qui a pour effet de consolider par diffusion les points de jonction et d'éliminer le carbone sous forme de CO et de CH_4.

e. Enfin, le matériau peut être plané et comprimé pour adapter sa structure à l'utilisation envisagée.

Cette technique de fabrication donne au maître d'œuvre, la possibilité d'intervenir sur toute une série de paramètres en cours de fabrication. Les caractéristiques du produit final sont, en conséquence, modifiées. Parmi les paramètres importants, on peut citer la nature de la cellulose (coton, viscose, etc.), l'épaisseur du dépôt électrolytique de nickel, la température de frittage, le taux de compactage.

B- Feutres d'alliage

Le feutre de Nickel est un demi produit qui pourrait déjà être utilisé pour certaines applications jusqu'à 400° environ. (premiers étages du compresseur).

En fait pour limiter le nombre de catégories, c'est un feutre nickel-chrome dont la teneur en chrome est comprise entre 25 et 30% qui est utilisé pour toutes les applications allant de la température ambiante à 750°C. Cet enrichissement en chrome du feutre de nickel est réalisé dans les conditions classiques d'une chromisation en poudre ayant comme caractéristiques essentielles :

- une forte concentration en éléments donneurs

- une bonne porosité du cément permettant un transfert aisé par diffusion gazeuse

- un dosage précis du cément pour éviter la formation de chrome alpha dans les fibres du feutre, ce qui les rendraient dures et cassantes.

D'autres opérations de ferrisation et d'alu-

minisation peuvent également être prévues. En particulier, l'opération d'aluminisation qui est, en général, réalisée après brasage du feutre aboutit à un matériau capable de résister à des températures d'utilisation supérieures à 1000°C. De plus, l'opération d'aluminisation permet en cas de fixation du feutre par brasage de transformer la nature de la brasure dans le sens très favorable d'un accroissement simultané du point de fusion et de la résistance à la corrosion.

II. CARACTERISTIQUES DES FEUTRES OHP

Les feutres OHP présentent un certain nombre de caractéristiques originales qui sont liées essentiellement à leur structure, à leur comportement, et à leur méthode de fabrication.

A- Caractéristiques liées à la forme des fibres

Les fibres métalliques qui constituent le feutre sont tout à fait différentes des fibres obtenues par voie mécanique à partir d'alliages définis. Elles sont tubulaires et peu vrillées. Cette morphologie particulière conduit à une remarquable homogénéité des feutres et à une bonne résistance en traction fig.1.

Fig. 1 — Structure d'un feutre de nickel 100C15 mettant en évidence le caractère tubulaire des fibres.

De plus, la compaction du feutre, grâce à cette caractéristique peut se faire de façon très homogène dans toute l'épaisseur, et dans de très larges limites de densité, puisqu'il est possible de passer d'une porosité de 95%, à une porosité de 40%, en conservant une excellente homogénéité.

Les fibres utilisés dans les feutres OHP ont une troisième caractéristique qui est très importante : leur finesse. Leur diamètre est compris entre 5 et 30 microns, et leur forme tubulaire ménage une porosité fermée dans le produit final.

Cette association de fibre fine et de porosité fermée confère des caractéristiques d'étanchéité aux gaz très supérieures à celles des matériaux poreux d'autre origine.

Les essais comparatifs menés dans ce domaine ont fait apparaître :

. une équivalence d'étanchéité entre un feutre OHP à 86% de porosité,

. un feutre à fibres mécaniques à 78% de porosité,

. un fritté poreux à moins de 50% de porosité.

Cette propriété des feutres OHP est extrêmement importante dans l'utilisation de ces matériaux pour la réalisation de joints de labyrinthe ou de joints de compresseur. Elle permet d'utiliser le feutre dans une très large fourchette de compactage. On mesurera plus loin l'incidence important de cette facilité sur les opérations de réalisation de joints de turbomachines.

Tableau récapitulatif

0-400°C 0-700°C 600-   700-   900-
                  800°C   1000°C 1100°C
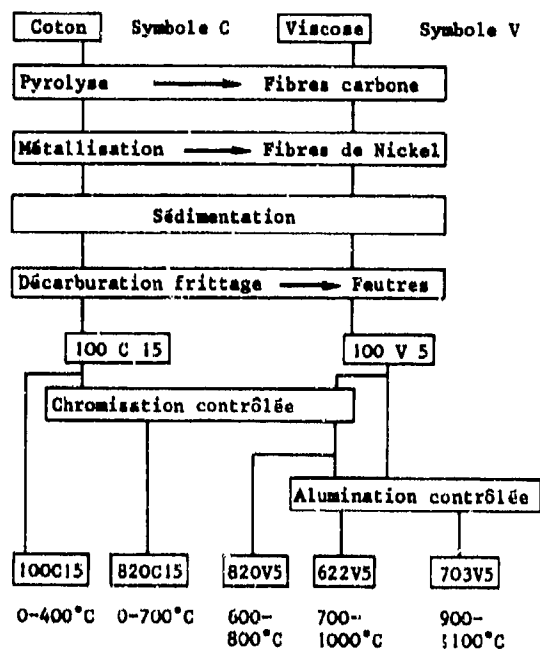
Nota : Les chiffres qui précèdent les symboles indiquent les teneurs pour 10 respectives en nickel, chrome, aluminium.
Les chiffres qui suivent les symboles sont reliés à la finesse du dépôt électrolytique (teneur en carbone des fibres en vrac).

Exemples :

	Nature de la cellulose	Diamètre des fibres tubulaires	Epaisseur au paroi	Composition Ni	Co	Al
820 C15	coton	12	3	80	20	0
622 V5	viscose	30	7	60	20	20

B - Caractéristiques liées à l'adjonction d'éléments d'apport

a) Feutres de nickel-chrome

La chromisation des feutres de nickel OHP conduit à un alliage nickel-chrome très homogène à teneur en chrome contrôlable avec précision. Il en résulte deux avantages :

. une meilleure résistance à la corrosion notamment à chaud,

. une solidité accrue par suite du renforcement et de l'élargissement des points de contact entre fibres.

b) Feutres de nickel-aluminium ou de nickel-chrome-aluminium

L'aluminisation des feutres, pour être efficace, doit correspondre à une teneur en aluminium relativement élevée qui enlève au matériaux pratiquement toute ductilité. On voit dont l'intérêt d'une aluminisation réalisée après mise en place d'un feutre chromisé ou non, par exemple, après brasage, puisque le feutre étant déjà positionné, on ne lui demande plus par la suite d'être ductile mais, par contre, on souhaite qu'il ait une résistance à l'oxydation et à la corrosion tout en conservant une bonne abradabilité.

Les feutres OHP aluminisés présentent sous cet angle des caractéristiques tout à fait exceptionnelles, puisqu'ils peuvent résister à des températures jusqu'à 1100°C, en maintenant une bonne tenue à l'érosion et des caractéristiques d'abrabilité convenables.

C - Caractéristiques liées à la méthode de fabrication

L'opération de sédimentation des feutres de nickel qui est effectuée dans un tambour tournant à grande vitesse, assure une homogénéité parfaite du feutre OHP. Les fibres mises en suspension dans un disperseur sont distribuées dans un volume d'eau relativement important à l'intérieur du dispositif centrifugeur. Cet appareil laisse une grande latitude dans le choix des épaisseurs qui peuvent aller de 0,4 à 10 mm.

Le procédé de fabrication se prête, lors de ces différentes séquences principales, à des opérateurs de contrôle qui permettent de garantir la fiabilité et la reproductibilité du produit final.

a) Contrôle des fibres en vrac

Le rapport massique carbone/nickel est mesuré systématiquement avant la vidange du tonneau d'électrolyse.

b) Contrôle du frittage et de l'élimination du carbone

Le taux d'insoluble dans l'acide chlorhydrique doit être négligeable.

c) Contrôle de l'adjonction d'éléments d'apport

Après chromisation ou aluminisation les gains de poids témoignent des concentrations atteintes.

D- Caractéristiques liées à la structure

Les feutres OHP présentent enfin une conductibilité thermique extrêmement basse. Si l'on compare à épaisseur égale la conductibilité thermique d'un feutre OHP nickel/chrome/aluminium et d'une structure nid d'abeille dans laquelle on a fait un remplissage approprié, le rapport est de 1 à 30 environ. Cette caractéristique est tout à fait essentielle puisqu'elle a pour effet de maintenir à un niveau de température beaucoup plus bas, l'anneau support des joints de turbines réalisés grâce aux feutres OHP.

Cet avantage n'est pas obtenu au détriment des propriétés mécaniques qui sont au moins équivalentes à celles des matériaux fibreux d'autres origines notamment en ce qui concerne les résistances à l'abrasion et au choc thermique.

III. APPLICATION DES FEUTRES OHP A LA REALISATION DE JOINTS D'ETANCHEITE DE TURBOMACHINES

La réalisation d'un joint de turbomachine, à partir de matériaux frittés ou projetés, se heurte à une difficulté majeure qui est celle de la fixation de ces matériaux sur la surface de l'anneau à équiper.

Les méthodes de projection doivent être mises en œuvre avec un réglage très fin de tous les paramètres, car l'adhérence sur le substrat et la qualité même dans la masse du produit projeté peuvent être modifiées de façon irréversible par un léger glissement de l'un des paramètres de l'opération. Cet inconvénient est profondément ressenti par les utilisateurs qui ne peuvent suffisamment s'assurer d'un contrôle de qualité indiscutable.

Les produits frittés posent le problème de l'adhérence sur le substrat, l'assemblage ne pouvant pratiquement se faire que par brasage. Ce brasage est une opération à température relativement élevée et, en raison de la nature du matériau que l'on doit fixer les problèmes de propreté et d'accostage sont particulièrement difficiles à résoudre.

Dans le développement des feutres OHP, ce problème a fait l'objet d'une attention particulière :

1) Ciment métallocéramique OHC 732

Dans une turbine à gaz les procédés classiques de collage sont le plus souvent disqualifiés à cause du niveau de température. Cependant, le produit OHC 732 de nature totalement inorganique permet d'atteindre des températures de service de 500°C. Il se présente sous forme d'un liquide visqueux qui après cuisson à 340°C se transforme en un ciment usinable, abradable, très adhérent. Il est insensible à l'eau, au kérosène, aux huiles minérales ou hydrauliques.

Son utilisation pour le scellement des feutres OHP évite le brasage, opération délicate et coûteuse, pour tous les joints situés dans les zones à basse ou moyenne température.

De plus, le ciment OHC 732 est soluble dans la soude caustique et, de ce fait, la réparation des pièces sur lesquelles le feutre OHP a été scellé est aisée puisque, par dissolution du ciment, il est possible sans usinage d'éliminer le feutre. Les caractéristiques générales du ciment OHC 732 sont rassemblées ci-après.

- CARACTERISTIQUES DU CIMENT OHC 732

. Caractéristiques thermiques

- stabilité thermique jusqu'à 650°C
- coefficient de dilatation : 7,2 à 10,1 x 10^{-6}
- conductibilité thermique : 1.34 x 10^{-4} Kcal/cm2/sec/°C/cm
- tenue au choc thermique : trempe à l'eau à partir de 550°C sans écaillage.

. Caractéristiques physiques

La courbe ci-après représente la force d'adhérence en fonction des températures d'utilisation. (fig.2).
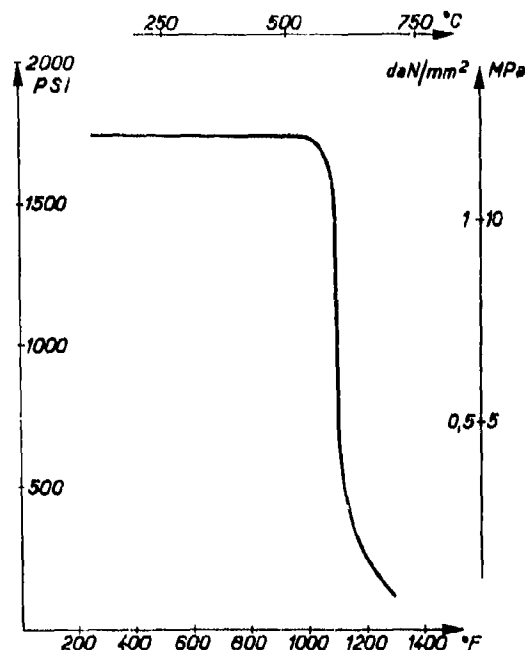

Fig. 2 -- Relation entre la température et l'adhérence sur un métal du ciment OHC 752.

. résistance chimique :

- exposition en brouillard salin à 5% 1000 heures : pas d'apparition de rouille
- acide faible : excellente tenue
- acide fort : mauvaise tenue
- soude caustique : dissolution rapide
- kérosène et huile : sans effet
- solvant organique : sans effet

2) Brasage

Pour l'utilisation des feutres à température supérieure à 500°C, il est nécessaire de réaliser une opération de brasage. Le substrat étant un superalliage réfractaire contenant du chrome et de l'aluminium, métaux très oxydables, le problème du mouillage se pose avec acuité. Pour le résoudre une atmosphère hydrogénée fluorée mise au point à l'ONERA a été retenue. Elle repose sur l'équilibre $F_2Cr + H_2 \rightleftharpoons Cr + 2FH$. Un excès de chrome maintient constante la concentration en acide fluorhydrique. Ce composé facilite la réduction d'oxydes particulièrement réfractaires notamment, le Cr2O3. L'utilisation de cette atmosphère provoque une désoxydation parfaite des feutres et du substrat sur lesquels on désire faire le brasage, et ce, dans un temps relativement court. Un deuxième problème, celui de l'accostage du feutre est également très délicat, car à la température de brasage, la plasticité du feutre est très grande et il est nécessaire de pouvoir contrôler de façon très précise la pression que l'on applique sur le feutre, si l'on veut éviter de l'écraser. Nous avons surmonté cette difficulté en utilisant une technique de dilatation différentielle, en maintenant le feutre serré sur l'anneau ou l'on veut le fixer grâce à des presses en graphite équipées d'une vis de serrage en inox dont la longueur libre détermine l'écrasement d'accostage admis pour le feutre. (fig.3). La

maîtrise de la répartition des brasures est assurée grâce à l'utilisation d'adhésifs spéciaux qui sont constitués d'un liant organique éliminable comportant une charge bien dispersée de brasure en poudre.

Fig. 3 — Dispositif d'accostage par dilatation différentielle graphite-inox d'un feutre nickel-chrome sur un anneau avant brasage.

3) Réalisation des joints - choix du feutre et de la méthode de mise en place.
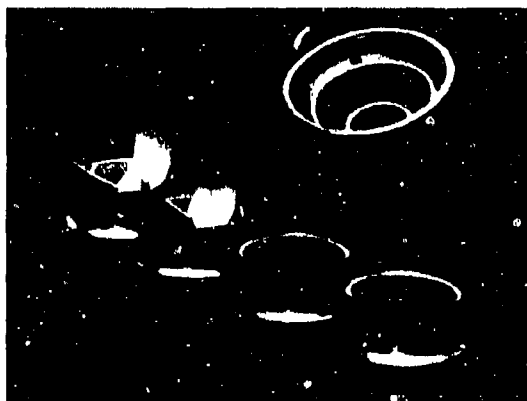

Fig. 4 — Pièces de labyrinthes d'une turbomachine de petite puissance dont l'une comporte 3 pistes, la plus petite ayant 30 mm de diamètre.

Les joints qui sont susceptibles d'être réalisés grâce à l'utilisation des feutres OHP sont les joints de labyrinthes de compresseurs, les joints de labyrinthes de turbines (fig.4), les joints de veines de compresseurs et joints de veines de turbines. La méthode d'utilisation des feutres OHP dans ces divers cas diffère de façon essentielle en fonction des niveaux de température où les joints sont situés. On peut à priori donner la règle suivante :

. de l'ambiante à 500°C : utilisation des feutres 820C15, scellés au ciment OHC 732. (2) (fig.5).

. de 500°C à 750°C : utilisation des feutres 820 C15 brasés.

. température de 750 à 850°C : utilisation des feutres 820V5 brasés (3).

. température supérieure à 800°C : utilisation d'un feutre 820C15 ou 820V5 brasé et traitement d'aluminisation de l'ensemble de la pièce après brasage. (4).

Fig. 5 — Mise en place par scellement de joints sur des carters de compresseur d'une turbine à gaz industrielle et sur des labyrinthes d'une turbomachine de petite puissance.

4) Formage et usinage

La grande compactibilité des feutres 820C15 permet de les utiliser dans un très large éventail de porosité. En conséquence, l'usinage du type classique par enlèvement de matières peut être efficacement remplacé par un simple compactage du feutre. Il peut être réalisé soit à la molette, soit avec un outil à bout rond. (fig.6). Le roulage est aisément praticable et autorise des rayons de courbure remarquablement faibles pour un matériau aussi poreux. (diamètre $\geqslant$ 10 x épaisseur).
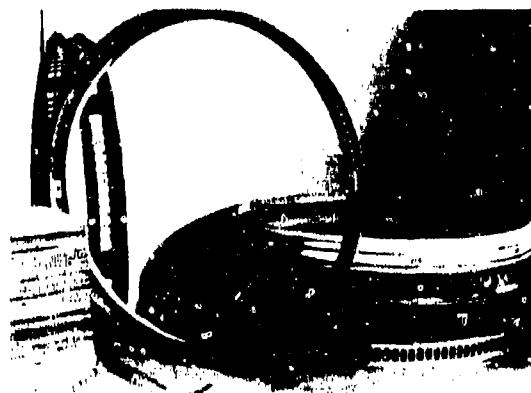

Fig. 6 — Anneaux de carters de compresseur (diamètre 800 mm) munis de leurs joints à étanchéité entièrement terminés.

En ce qui concerne les feutres aluminisés, leur usinage ne pose aucun problème particulier, mais il faut signaler que pour certains cas d'application, la mise en forme peut être réalisée par compactage au niveau du feutre avant l'opération d'aluminisation.

IV - CONCLUSION

Les feutres métalliques ONERA à structure fine et haute porosité se sont révélés particulièrement bien adaptés à la fonction de joints d'étanchéité des turbomachines.

Leur extrême plasticité initiale facilite considérablement l'acquisition de la porosité optimale, conjointement avec l'opération de mise en forme, tout en sauvegardant l'indispensable homogénéité.

Le caractère tubulaire des fibres et la forte porosité rendent les feutres en nickel remarquablement aptes à la transformation en feutre d'alliages résistant à la corrosion jusqu'à 1050°C, au moyen des procédés de transport d'éléments d'apport par l'intermédiaire d'une phase gazeuse halogénée.

Pour les joints situés dans des zones à température inférieure à 500°C la méthode de scellement par ciment métallomécanique permet des économies considérables à cause de sa simplicité opératoire et du fait qu'aucun rebut des supports n'est à prévoir puisqu'un joint défectueux peut être retiré par dissolution dans la soude. Relativement au brasage, le coût global de l'installation d'un joint d'étanchéité sur un anneau est réduit de moitié.

Au-delà de 800°C l'utilisation d'un feutre contenant une teneur important en aluminium est obligatoire. La fragilité qui en est la conséquence pose de redoutables problèmes de mise en forme. Avec le procédé qui fait l'objet de cette communication, on peut s'affranchir de cette sujétion en effectuant le formage et le brasage sur un feutre de nickel-chrome qui reste souple, puis en procédant à l'aluminisation en phase gazeusz de l'ensemble anneau-joint.

En ce qui concerne l'état de développement de ces techniques, il faut distinguer deux catégories :

- les joints à basse et moyenne température qui sont parvenus au stade opérationnel en équipant des turbomachines effectivement en service.

- les joint de turbines chaudes (850 à 1050°) qui, après avoir satisfait aux tests de simulation, sont actuellement à l'épreuve des bancs d'essais.

REFERENCES

1 - A. Hivert, P. Lepetit, A. Walder - Elaboration et application de feutres métalliques à structure fine - Congrès de Métallurgie des poudres, Grenoble, 12-16 mai 1975. Edition provisoire - TP ONERA n°1975-6.

2 - Heurchrome - Rapport au Service Technique Aéronautique n° 7394 422, juin 1976.

3 - Heurchrome - Rapport au Service Technique Aéronautique n° 7594 131, juin 1976.

4 - Heurchrome - Rapport au Service Technique Aéronautique n° 7694 231, juin 1977.

DISCUSSION

A.R.Stetson, US

You mentioned that the fine size is an advantage. What is the wall thickness of the felt you are talking about? Don't you think this could be a problem with its oxidation and high temperature resistance by decreasing the wall thickness and increasing the total surface area?

Réponse d'auteur

La structure fine des feutres nous paraît présenter un avantage sur le plan de leur ductilité et de leur efficacité en tant que joints. Les épaisseurs de paroi que nous avons retenues en fabrication sont comprises entre 2 et 8 microns en fonction de la nature des fibres de départ.

Il est évident que ceci peut présenter un inconvénient pour les problèmes de tenue à l'oxydation, mais nous avons pallié à ce problème en réalisant pour les applications à haute température par aluminisation après brasage, un alliage Nickel-Chrome-Aluminium très riche en Aluminium et en Chrome, ce qui compense très largement les problèmes créés par la faible épaisseur des parois des fibres.

Notre matériau 622 C 8 par exemple, présente des caractéristiques de tenue à l'oxydation tout à fait remarquables jusqu'à 1050°C.

P.Suter, Switzerland

You emphasized the importance of decarbonisation. Would there not be some applications where the carbon could be left within the structure?

Réponse d'auteur

La décarburation des fibres de Nickel dans l'état actuel de notre technique doit être complète si l'on veut pouvoir réaliser un frittage convenable du feutre. Les essais de décarburation partielle ont montré que le produit obtenu restait inutilisable du fait d'une trop grande friabilité.

D.C.Whitlock, UK

Would the author comment on to what thickness this felt can be produced?

Réponse d'auteur

Actuellement, nous produisons couramment des feutres dont l'épaisseur, pour une densité de l'ordre de 20%, peut varier entre 0,4 mm et 8 mm. Il n'y a pas de limitation théorique aux épaisseurs qui peuvent être réalisées. Sur un plan pratique, les équipements de fabrication ont été adaptés à cette gamme d'épaisseur.

A.M.Campling, UK

Has the seal material been proved in service and if so by whom, for how long and in what environment?

Réponse d'auteur

Les feutres OHP ont été développés récemment et équipent un certain nombre de turbines aéronautiques et industrielles depuis deux ans environ. Pour les applications labyrinthes et pour des températures allant jusqu'à 650 a 700°, notre expérience sur turbine industrielle s'appuie sur des périodes de fonctionnement sur une même machine qui dépasse à l'heure actuelle 1500 h.

Sur des turbines aéronautiques, nous avons réalisé environ 800 a 1000 joints de labyrinthes. Nous ne connaissons pas de façon précise les temps de fonctionnement unitaires, mais notre expérience globale correspond à plus de 10.000 heures de fonctionnement sur des machines différentes.

En ce qui concerne les feutres 622 Nickel -Chrome-Aluminium ils sont à l'heure actuelle en essai sur des machines de turbines aéronautiques.

AMERICAN AIRLINES' OPERATIONAL AND MAINTENANCE
EXPERIENCE WITH AERODYNAMIC SEALS AND
OIL SEALS IN TURBOFAN ENGINES

C. R. Smith
Manager Power Plant Engineering
American Airlines, Inc.
P.O. Box 51009
Tulsa, Oklahoma   74151
USA

SUMMARY

User experience with aerodynamic and oil system seal designs utilized in current
commercial turbofan engines related to operational performance, seal reliability,
seal repair techniques, and seal maintainability cost.

A general insight of gas path deterioration resulting from sealing problems and
effects of associated hardware problems upon seal performance. A broad assessment of
this deterioration is reflected in fuel consumption, maintenance requirements (engine
management), and the impact upon airline operation, including operating costs.

LIST OF SYMBOLS

AVG.	Average
E.B.	Electron Beam (welding)
ENG.	Engine(s)
FLT.	Flight
HR.	Hour
HRS.	Hours
I.D.	Inside Diameter
M	Million(s) (US Dollars)
mm	Millimeter
O.D.	Outside Diameter
US or USA	United States of America
$	US Dollars
%	Percent
¢	Cent; 1/100th of a US Dollar

INTRODUCTION

With the introduction of the first airplane, sealing of gases and liquids has
been a major problem. Sealing is classified as a problem when leakage exceeds
acceptable design limits, induces hazardous conditions, uncontrollable flow and/or
unsightly appearance. These conditions can result in excessive maintenance expense.

Advancing seal technology and ingenuity have resulted in milestone achievements
by aircraft, engine, component and systems manufacturers. However, with each suc-
ceeding generation of aircraft, increasing demands develop, and the designers
ingenuity is continually challenged.

Further advancement in seal technology is a must if the manufacturers are to
provide an end product with which the user can sell transportation at a minimum price
with a reasonable return on his investment. In the case of the airline industry,
product support investment is sizable, with fuel consumption cost being the largest
contributor to direct operating costs.

In order to meet increasing competition, in spite of lower fares, such factors
as on-time dependability, passenger comfort, etc., airline management must be inno-
vative in developing new sophisticated performance analyses and maintenance programs.
These programs must encompass such factors as efficient use of resources, improved
dependability, reduced fuel consumption, hardware repair and performance restoration,
etc., without sacrificing safety or reliability.

Design philosophies must be developed with a focus upon the end-use of the pro-
duct and the needs of the user. The ultimate success of research development and
design efforts is measured by in-service results. To the user, proper design is
reflected in seal reliability and durability over extended time periods, repairabil-
ity and low cost.

Performance of seals in turbofan engines can be categorized in terms of: a)
Reliability - the ability to maintain the sealing efficiency for which the seal was
designed under all operating conditions for extended time periods; b) Durability -
the ability of the seal to function without mechanical failure of its detailed parts
between shop visits; and c) Repairability - the ability to carry out simple and
economical repairs of those seal components which are subject to wear and tear.

Failures within these categories may be due to basic design problems, or second-ary failures resulting from associated hardware environmental conditions or, in many cases, a combination of these factors. It, therefore, becomes most important to make an accurate determination, through failure analysis, of the initial primary cause of failure. Design changes are often necessary to correct these failures which are considered seal design deficiencies; also, changes must be made to associated hard-ware if, in fact, this hardware produces the actual failure. In many cases, seal redesign can compensate for related problems and vice versa.

In summary, it is very apparent that feedback communications from the user to the designer are vital in obtaining adequate product improvement design changes. Additionally, design intelligence must be shared with the user in support of accurate seal performance deterioration and failure analysis.

All cost figures in this report are based on a 1977 US Dollar value and a fuel cost of 9.24¢ per liter (.35¢ per US Gallon).

PURPOSE

The purpose of this paper is to provide Designers and Research and Development Engineers with user experience regarding reliability, performance deterioration and its economic impact. It is this experience that vividly reveals that seals are a significant problem area in today's turbofan engines. Seals must be given the highest priority in future engine designs to reduce user maintenance cost, minimize facility capacity requirements and reduce fuel burn.

DISCUSSION
Performance Deterioration

Gas path seal deterioration, as used in this text, is a result of normal seal erosion, wear, thermal expansion and distortion, while the engine is operational and produces the specified thrust. Normal gas path seal deterioration is reflected in loss of overall efficiencies (increase in fuel flow and exhaust gas temperature) as well as gas generator mismatch. Increased fuel consumption due to loss of seal efficiencies has not been an area of great concern in the past. However, with the decrease of fossil fuel reserves and continuing fuel cost escalation, this area is now given special attention which will certainly not diminish in the foreseeable future.

Figure 1 shows that an average fuel flow deterioration of around 4% is normal for a fleet of engines after they have been through their normal refurbishment cycles. The percent of deterioration will vary with the average mean time between refurbishment which is determined by the maintenance program and its effectiveness. Obviously, the cost to maintain a low mean time between refurbishment of seals to control fuel consumption is prohibitive and will be discussed later. On a twelve aircraft high bypass engine airplane fleet, a 4% deterioration equates to an excess fuel burn costing 1.2 million US Dollars per year.

Figure 1 also gives an example of one aerodynamic seal deterioration effect. If, on all of the four engines of this aircraft fleet, the first stage turbine blade tip clearance were increased by .254 mm, the resultant excess fuel usage of .6% would cost an additional 200,000 US Dollars per year.
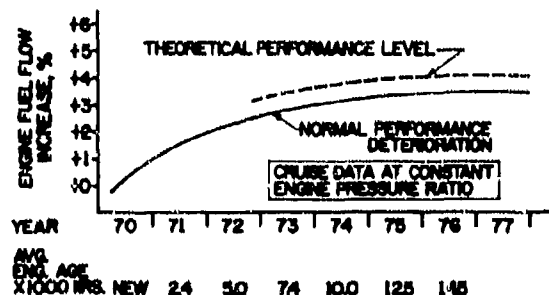

FIGURE 1: This graph depicts an example of performance deterioration after normal refurbishment efforts for a fleet of aircraft using large commercial high bypass flow engines. The dotted line shows the theoretical degradation if the first stage turbine radial tip seal were increased by .254 mm on all engines.

Mismatch of the gas generator due to gas seal deterioration is a costly maintenance, as well as fuel consumption, problem. Accumulation of operating hours and duty cycles varies between engine modules resulting in one section of an engine deteriorating more rapidly than another, causing a speed match change.

In many instances (through lack of knowledge), the maintenance program does not always provide for restoration to preclude this condition. Mismatch conditions may cause recoverable compressor stalls which usually occur during high altitude deceleration and acceleration operation. Shop Maintenance is required to correct these conditions. Figure 2 depicts this problem on a high bypass ratio engine. Also, the cost impact on a fleet basis is shown. Without preventative maintenance action, this condition can develop on a large scale as deterioration of individual seals cannot be monitored. Maintenance programs must be established based on hardware analysis at various operating times. Again, this is not an easy task due to a combination of conditions and interrelated effects. More development testing by the manufacturer and maintenance intelligence by the user is needed in order to effectively manage and improve the engine.
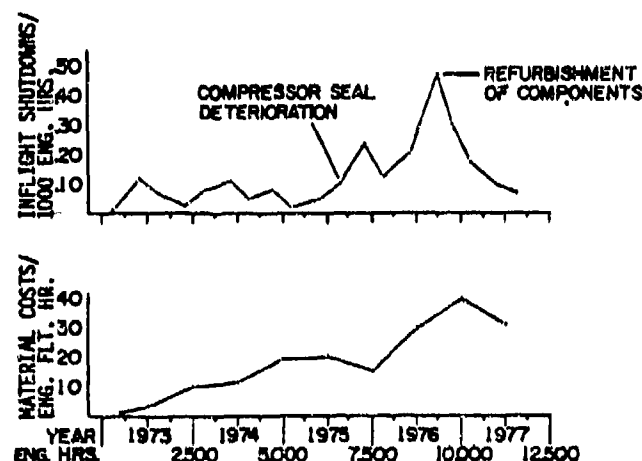
FIGURE 2: Inflight shutdown rate due to compressor stalls and material cost history of a domestic wide body aircraft fleet using high bypass ratio fan engines.

Performance retention and thrust specific fuel consumption has become major concerns with current engine operations and with new engine design. The magnitude of concern is such that currently the user is demanding from the manufacturer a performance guarantee for a specific operating period, in terms of hours or cycles, prior to a Shop Maintenance visit; also, a maximum cost guarantee in terms of labor and materials.

Deterioration of labyrinth oil seals due to clearance changes, not only produces oil consumption problems, requiring premature engine removals, but also has a secondary effect of loss in general performance and increased fuel consumption. Increase in labyrinth seal clearances occur primarily from rubbing with mating parts permitting high breather pressure within the oil scavenge system. However, most oil consumption problems due to high breather, usually are a result of a change in balance pressure across labyrinth seals due to uncontrolled air leakage at various supply sources.

Mechanical Failures

Aerodynamic and oil seal failures occur at various operating hours for a variety of reasons. Air seal failures in the hot section area occur due to thermal gradients within the part which usually results in cyclic stresses. Such an example is shown in Figure 3. This sketch shows an example where cracking in a labyrinth seal area occurs because of thermal gradient effects resulting from the seal cross-sectional thickness differences. In this case, the seal has a life limit restricting engine operating time and a redesign is pending.

One of the major air seal problems in turbofan engines is portrayed in Figure 4. This sketch depicts an abradable seal application. The cross-sectional sketch on the right shows a typical axial and radial wear or "wiping" pattern which occurs on a large turbofan engine. The wear or "wiping" action results from differential thermal expansion and contraction of various engine components whenever the engine goes through its various power excursions, such as transient operation and takeoff power application. Seal interference rubbing also occurs during high maneuver loads, coupled with rotor dynamics. This condition is aggravated by excessive rotor alignment runout and high vibration levels.
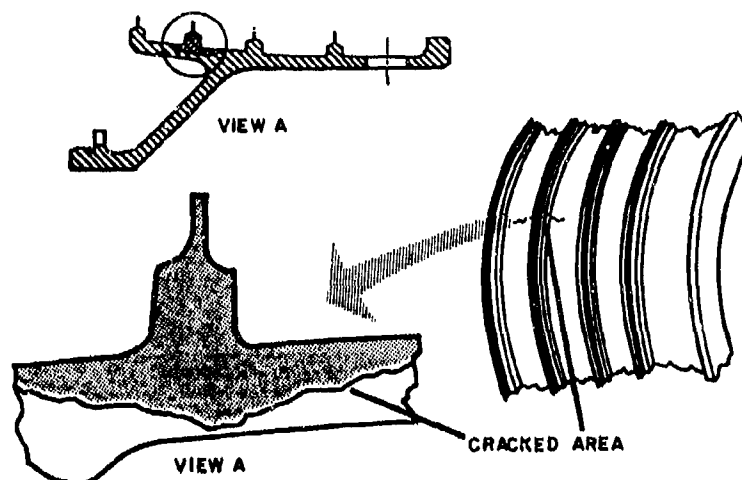
VIEW A

VIEW A

CRACKED AREA

FIGURE 3: This sketch shows cracking that occurred in a
second stage turbine rotating air seal from a large bypass
engine. The cracking was caused by cyclic thermal gradient
stresses.

In severe cases of part out-of-round conditions, or other abnormal conditions, sta-
tionary part to rotating part interference could lead to metal burning and subsequent
failure, as in the case of high pressure turbine blades.

It becomes obvious that practically all seal failures are a direct result of
either: a) thermal gradient fatigue problems with the seal and its associated
hardware, or b) axial and radial thermal expansion during maximum power excursions.

WEAR OF
HONEYCOMB

STATIONARY
ABRADABLE SEAL

BEFORE
SEAL IS RUN

AFTER
SEAL IS RUN
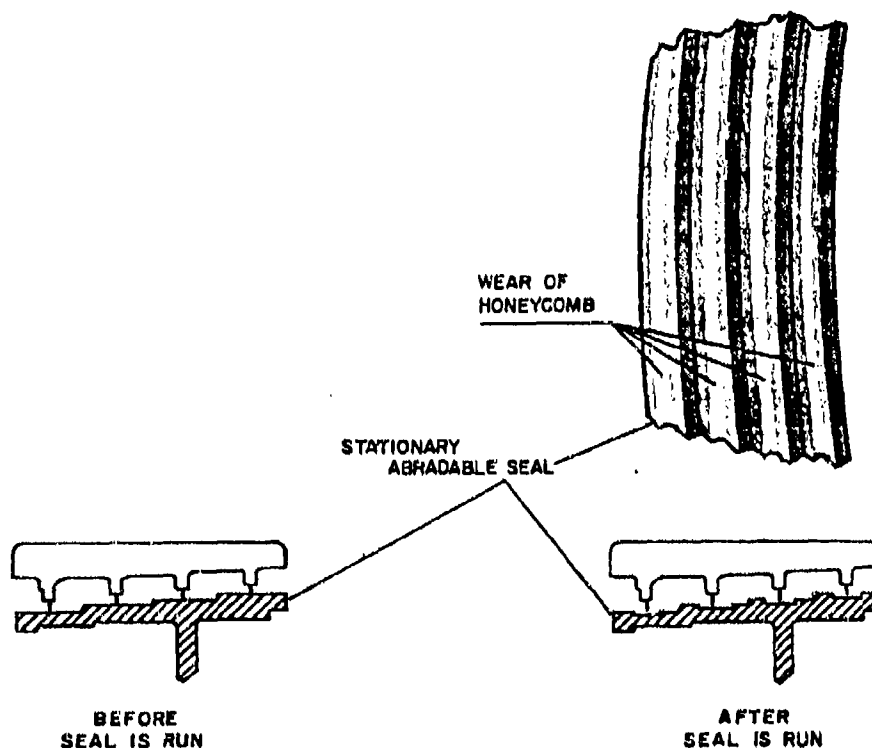
FIGURE 4: This sketch shows typical abradable seal axial and radial
wear. This is an interstage compressor seal from a large bypass engine.

Failure of carbon element oil seals develop primarily from excessive environ-
mental and frictional temperatures. Excessive seal element and face plate wear
occurs with subsequent leakage and, in some cases, element breakage. In areas having
inadequate cooling, oil coking can occur causing leakage as depicted in Figure 5.
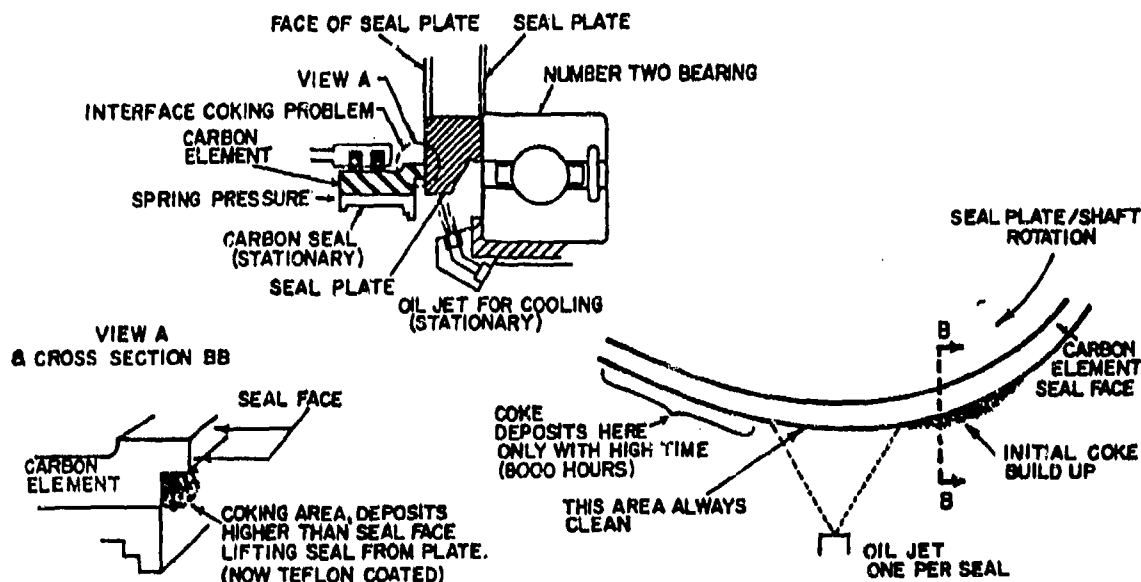
FIGURE 5: This sketch depicts a carbon coking problem in the main bearing carbon
seal of a commercial turbo fan engine.

Here again, the axial and radial growth of the engine from temperature excur-
sions produces a problem of maintaining the desired face plate to element pressure.
This accelerates wear and raises the temperature of the parts, resulting in oil vapor
phase coking. Also, with resultant seal movement, "sticking" of the seal assembly
may occur, causing a complete loss of pressure and oil leakage.

Although labyrinth seals are affected less by temperature, proper design is
influenced by pressure balances to reduce bleed air loss. Labyrinth seals can allow
the oil to become contaminated with the atmosphere (moisture, sand, etc.). Compres-
sor cleaning by motorizing the engine and injecting various nonmetallic materials
and/or liquids to restore performance is undesirable, due to exposure to oil
contamination.

Figure 6 shows that seals are a major contributor to the total reliability of
the engine. A review of the last seven years of premature removals for engines and
modules illustrates the impact of seals in general. Three classes of problems are
illustrated: a) seal failures; b) failures where seal deficiencies contributed to
the problem; and c) on-the-wing gear box removals due to seal leakage.

These problems are shown for three types of turbofan engines, namely: a) early
low bypass turbofans (1959); b) medium bypass turbofans (1965); and c) high bypass
turbofans (1970).

The early low bypass turbofan history shows that almost 32% of the unscheduled
removals are related to "seals". This number is 50% for the medium bypass turbofan
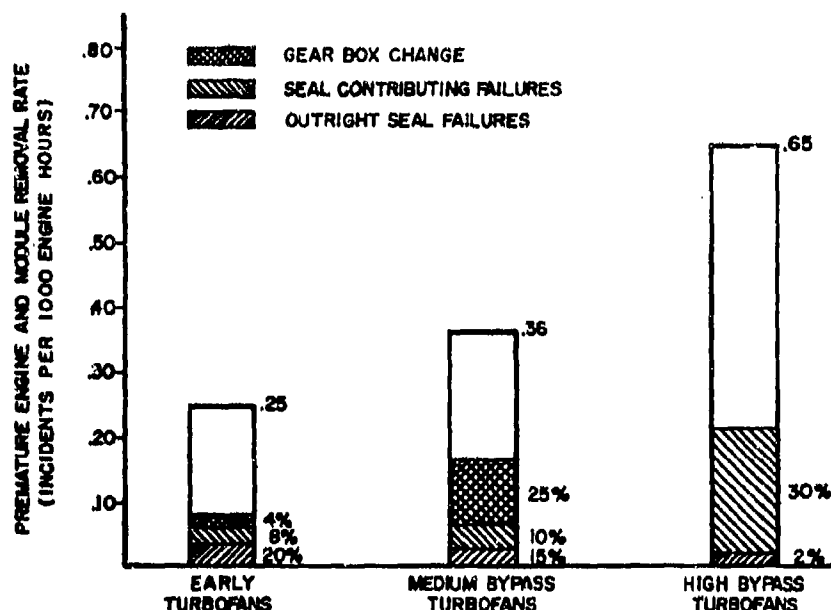and 32% of the latest, large high bypass engines.

FIGURE 6: These bar graphs depict seal problems as a percentage of the total premature engine and module/component changes over a seven year period (1970 through 1976).

This picture of seal development in high bypass engines looks good, but it is deceiving. The more frequent removals of the high bypass fan engines make it possible to manage seal performance by changing, repairing and cleaning seals with a high frequency before they deteriorate. In addition, critical seals are designed to be easily replaceable. For instance, all the carbon seals in the gear box of a late high bypass fan engine are replaceable "on-the-wing". Therefore, leakage does not seem to be a problem, but it only seems that way because the problem is managed. As the engine problems diminish, the seal problems will increase until the seal durability becomes the restrictive factor with time. Considerable work needs to be done, and is being done within the industry to understand the general engine performance deterioration phenomena.

Seal Repair

Seal repair techniques vary from the most simple, yet innovative, to the more complex. In one of American's turbofan engine models, the second stage turbine outer air seal is purchased undersize and ground as required to provide the desired clearance with the second stage turbine blades. The second stage turbine blade has a shrouded tip with two knife-edge seals. With time, the knife-edges wear or rub and erode requiring the outer air seal inside diameter to be reduced to a further undersize. This is initially accomplished by metal spraying to a maximum thickness of .500 mm. A metal spray thickness beyond this has a tendency to "flake off". The blade knife-edge can be replaced but the cost is more than the purchase price of a new outer air seal. In time, a surplus of air seals accumulates. A simple repair was developed to reduce the inside diameter while maintaining out-of-round limits. Figure 7 depicts an application of a continuous weld bead around the periphery of the seal using an automatic weld machine. This operation "shrinks" the seal, thereby enabling salvaging of would-be oversized second stage turbine air seals.

Although this is a simple repair, operational testing was conducted to establish that no adverse conditions existed. Adequate in-service testing was established to determine a 10,000 hour or 6,000 cycle life between repairs.

Turbine blade shroud knife-edge seal and non-shrouded tip wear results in scrappage of otherwise serviceable blades (up to $40,000 per engine). Replacement of the knife-edge seals by Electron Beam welding, as shown in Figure 8, has proven to be a cost saving repair. Without this repair the annual cost of the turbine blade scrappage would drastically increase. This repair technique is used in other areas, such as the turbine spacer application as shown in Figure 9.
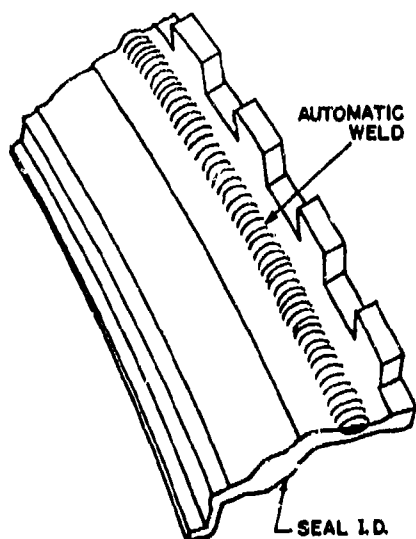
FIGURE 7: This figure depicts a method to shrink a turbine outer seal inside diameter to compensate for blade shroud seal wear.
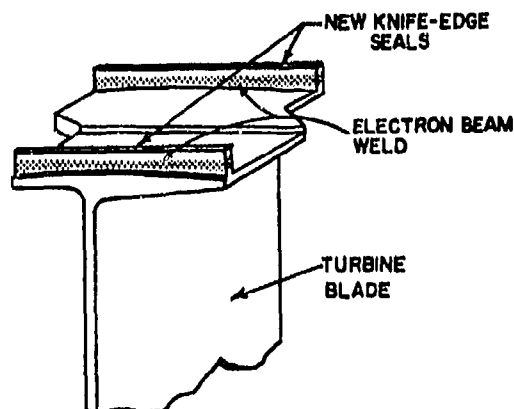
FIGURE 8: This sketch depicts replacement of turbine blade shroud knife-edge seals by Electron Beam welding.
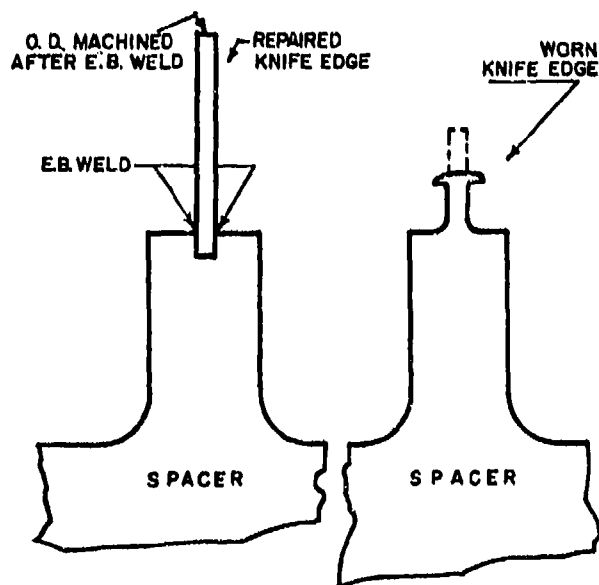

FIGURE 9: This sketch depicts a typical turbine spacer knife-edge repair by Electron Beam welding.

Figure 10 is an example of a repair to restore out-of- round of a major case. This is accomplished by removing the flange, rounding up the case, and Electron Beam welding on a replacement flange. This repair restores the case to a serviceable condition. It relieves the imposed stresses upon the seal while providing more uniform clearance between the turbine blade and outer air seal.

Main bearing carbon seal assembly refurbishment (see Figure 5) consists primarily of carbon element replacement, machining of the seal plate face to remove wear and plating to restore dimentional requirements. As a means of increasing seal life, various plating and metal spraying materials have been tried. Tungsten carbide coating on the seal plate has produced the best wear characteristics.
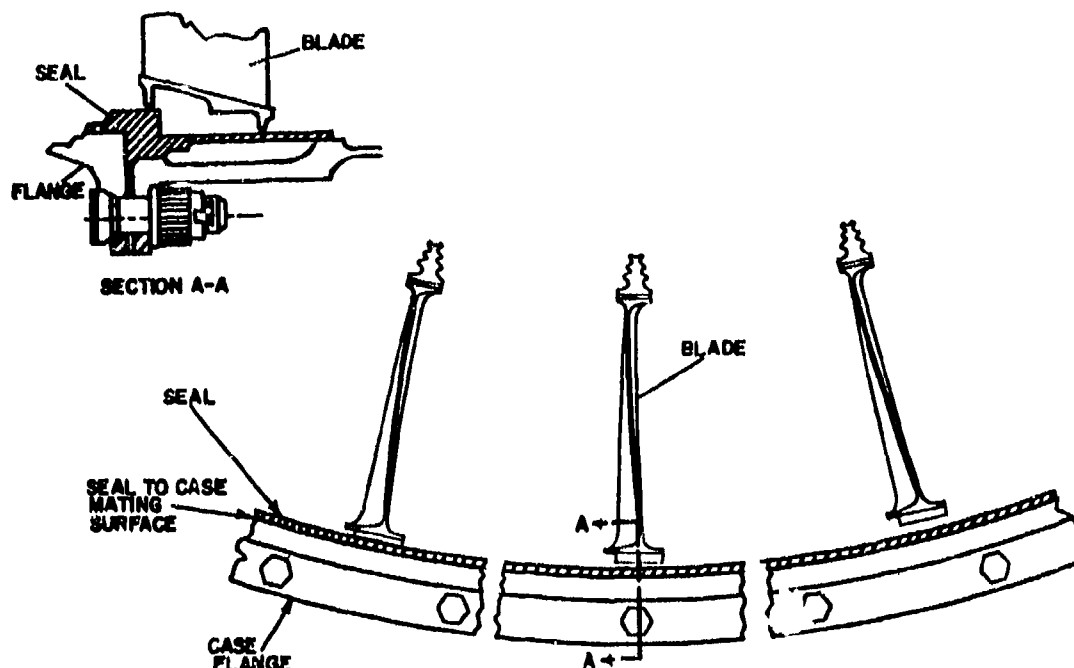
FIGURE 10: This sketch depicts result of case out-of-roundness causing turbine outer seal to conform to case, resulting in inadequate and excessive seal clearances. The left blade shows tip rub; the middle blade shows the correct clearance; the right blade shows excessive clearance.

Maintenance Operational Impact

The impact upon user operation of air and oil seal systems is reflected by product reliability and cost. As seen previously in Figure 6, seals are one of the major problem areas confronting the user. These problems produce a large volume of engines for shop maintenance, which requires an expenditure of millions of dollars each year.

As shown in Figure 11, air and oil seal parts cost are only 1.5% of the total material cost, and the seal repair labor costs are only 5% of the total engine labor cost. For a large USA airline, this cost approximates 1.5 million US Dollars per year.
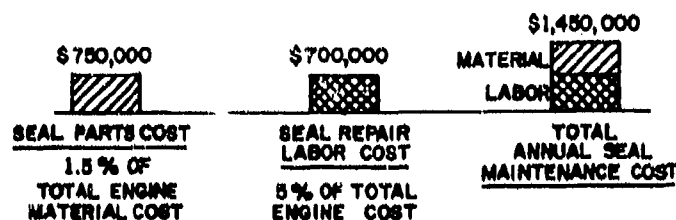
FIGURE 11: The bar graphs above show the annual engine seal maintenance cost for a large US airline engine Maintenance Base.

However, the important message of air and oil seal costs is reflected in Figure 12. It is important that air and oil seal systems be effective and reliable. Ineffective or worn air seals can contribute up to 1.5% to the engine fuel burn. On top of this, if ineffective enough, they can contribute to intolerable engine stalls and speed mis-matching. In a US airline, at 1977 fuel prices, this type of seal deterioration could amount to 5.85 million US Dollars.
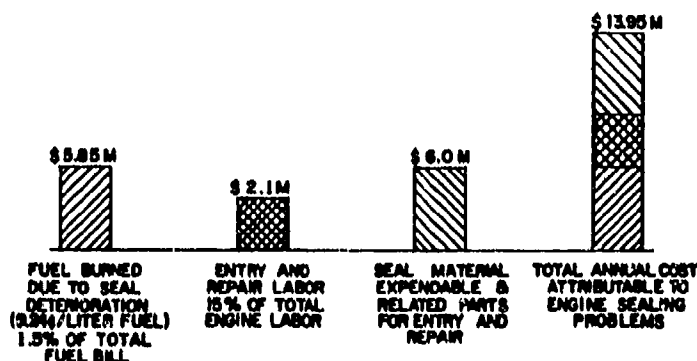
FIGURE 12: These bar graphs show the annual total cost impact resulting from "seal" problems for a large US airline.

The major cost factor is not the seal material or seal repair cost, but the entry labor, expendable and related parts costs to reach the seal inside the engine. This is graphically shown in the third column of Figure 12. This column indicates that 6 million US dollars per year is spent for this type of "entry" for seal repair or refurbishment work. This cost figure is even more dramatic when one realizes that the costs of engine handling, support facilities investment, and the inventory necessary to provide seal refurbishment to restore performance are not included.

The right-hand column of Figure 12 shows an accumulated cost figure which can be viewed as the "seal cost" total for an annual total cost burden of nearly 14 million US Dollars.

Aerodynamic seal deterioration and failure are difficult problems to manage in a commercial airline environment. No two engines deteriorate at precisely the same rate. Therefore, statistical predictions can only be used as a guideline. Effective engine management becomes almost impossible. When random and frequent "seal" problems occur, another problem arises: an unmanageable monthly engine volume fluctuation which may exceed shop capacity.

With present day instrumentation and analysis, it is extremely difficult to analyze a low performance engine and determine precisely which seal(s) (or support hardware) are causing the problem unless the seal has failed structurally or exhibits visual damage. Even with the obvious failed or damaged condition, there is the need of analysis of associated hardware and its affect upon the failure.

American Airlines operates under an engine management program which is based on the Condition Monitored Maintenance concept. Each engine is analyzed and a specific bill-of-work is developed. The concept requires collection and development of the intelligence to know what maintenance the engine needs; then doing only the necessary work to produce a product that will operate for a specified period of time within an acceptable reliability rate at a minimum cost.

Today's economics prohibit the use of an arbitrary complete overhaul concept at a specific operating time. Designers must realize that the user cannot remove engines for shop maintenance at a low operating time to refurbish multiple seal deterioration. American's shop capacity for complete overhaul of high bypass ratio engines is roughly estimated at 40 per month. Today's volume is 70 to 80 engines per month of light and heavy repairs. If engines operating in American's fleet were arbitrarily brought in for refurbishment at intervals of 2000 operating hours, the shop volume would increase to 150 to 160 engines per month. Therefore, it must be recognized that newly developed engines must operate 8000 to 10,000 hours within an acceptable failure rate and performance level.

CONCLUSIONS

With the continuing increase in fuel, material, and labor costs; the need and economic justification exists to warrant a high priority on engine design for performance efficiency with a low deterioration rate.

Two basic areas having a major effect upon the loss of seal clearances are: 1) thermal gradient fatigue problems and, 2) thermal expansion and contraction of the engine assembly with maximum thrust applications. These problems must be considered during initial design. Extensive gains must be made in these areas if the operating expense of the final product is to be maintained at a reasonable level, and provide for a reasonable return on user investment.

Further development is needed to provide a method and means of monitoring and identifying specific seal problems during operation. This will provide for more effective use of resources. Expending resources on an arbitrarily established overhaul program cannot be tolerated in the future.

DISCUSSION

R.A.Hartley, UK

Support for the speakers view on seal performance (that is that deterioration is too rapid) is that it is worse on military engines due to more thrust cycles. Abradable seals are not good enough and adjustable seals may be required to maintain the engine performance now being aimed at.

Author's Reply

Mr Hartley seems to have caught the gist of my paper in this comment. With fuel economy and reliability in mind, the aerodynamic sealing of current engines leaves much to be desired. The problem of designing and developing seals which will accommodate thermal cycle changes and, thereby, maintain high efficiency levels both during takeoff and cruise régimes, needs to be dealt with in future engine designs.

H.L.Stocker, US

How does American Airlines clean their engines an vould you attribute this process to accelerating the seal erosion problem?

Author's Reply

I interpret Mr Stocker's question regarding "cleaning of engines" to refer to "compressor wash or equivalent" of the entire engine while it is in its assembled state, and not cleaning of the individual aerodynamic and oil seal parts in their disassembled or in-repair state.

Most models of engines when compressor blades and vanes are suspected of being dirty can be cleaned to some degree by what is generally known as "water washing". The washing is generally preceded by soaking the compressor area with a kerosine and water mix. All "washings" are performed in the test cell. To be more specific, the following is a rundown on what American does on each of its four (4) engine models when a compressor cleaning is made:

P&W JT3D (Boeing 707 Aircraft Engine)

Soak the compressor section of the engine with a kerosine/water mix for 20 minutes. Rinse with water. Then run the engine at idle, ingesting 3 sacks of Carboblast (walnut shells). (This can be done since the engine has carbon rubbing oil seals in lieu of labyrinth seals.)

P&W JT8D (Boeing Aircraft Engine)

Soak the compressor section with kerosine/water mix for about 20 minutes. Then rinse with water. (This engine cannot be Carboblasted since it has labyrinth oil seals and the Carboblast material would contaminate the oil system.)

P&W JT9D (Boeing 747 Aircraft Engine)

This engine is water soaked only. Then the water is forced through the engine by belting it on the starter.

GE CF6 (McDonnell Douglas Aircraft Engine)

Water soak. Then ingest Cokeblast (carbon particles) while running the engine at idle.

We clean the compressors of the assembled engines in this manner only in the test cell, never on the airplane.

The degree of cleanliness obtained varies between engines. It is not definitely known how long the average performance increment improvement amounts to on any engine types.

The latter part of your question asks: "... and would you attribute this process to accelerating the seal erosion problem?".

As can be seen from the above descriptions, each engine has its own tailored cleaning method approved by the engine manufacturer. It is difficult to visualize seal erosion deterioration from a liquid soak and wash. On the engines where solids are ingested, the ingestants are of such a texture and composition that it is again difficult to visualize their causing a significant seal erosion. In reality, only the N1 compressor rotor seems to be cleaned. Cleaning of the N2 compressor stages seems to be minimal.

A.Moore, UK

Could you please tell me what proportion of the seal deterioration (with time) is due to erosion?

If the effect of erosion on seal performance is significant, would it not be better to use a harder coating and reduce the erosion and start with a larger clearance? This would, in theory, give a worse performance when the engine is new, but a better performance with an old engine.

Author's Reply

In view of the fact that on the newly developed engines, the state-of-art of metallurgical technology is being pushed in order to obtain high component efficiencies, saleable thrust, specific fuel consumption and exhaust gas temperature margins, the suggested approach appears to run cross-grain to the metallurgical technology push.

Typically, when the engine manufacturer first introduces an engine, he is intent on meeting his performance guarantees with seemingly little regard to putting extra "fat" into the engine to withstand large seal clearance with long life. Your point is a good one, but this has not been the practice in the past. Seemingly little thought is given to making the aerodynamic seals last a long time, especially in the hot gas scrubbed areas.

This again brings up the point that a good design approach appears to be to provide an engine design which provides a controlled clearance for the takeoff régime, then another controlled clearance for the cruise régime. Clearance control and long seal life should both be primary objectives.

R.Kervistin, France

Is there a relationship between the labyrinth seal clearance on a newly manufactured engine and one that has operated 10,000–12,000 hours?

Author's Reply

By all means, there are labyrinth seal clearance changes between a newly manufactured engine and one that has 10,000–12,000 hours, especially in those areas scrubbed by hot gases. The changes occur from erosion and in some cases rubbing, both of which result in performance losses.

American Airlines' experience shows that the seal deterioration over the long haul is lower on multi-land labyrinth seals than on rub type seals.

It is generally recognised that the rub type abradable seals are more efficient than the labyrinth type on a new engine. However, experience indicates that this efficiency advantage is usually short-lived. We have noted that a large efficiency loss occurs on a big bypass engine even after making only several power excursions in the test cell.

Again, this points to the need of the next generation of engines to have two different seal clearance levels — one for takeoff and one for cruise.

OIL SEALING OF AERO ENGINE BEARING COMPARTMENTS

D C WHITLOCK
Technical Design Group
Rolls-Royce Limited
PO Box 31
Derby DE2 8BJ, U K

SUMMARY

The basic problem of oil sealing of aero engine bearing compartments is to provide a
seal between rotating and static components, or between rotating components, accommo-
dating axial movements and possible radial excursions (such as shaft whirling). The
sealing arrangements must also conform to modular concepts of engine construction.

Such seals incur penalties on the oil system such as heat generation, air leakage and
debris generation. This paper considers means of reducing these penalties and improving
sealing integrity by developments of existing techniques.

1.0 INTRODUCTION

The purpose of oil sealing within the core engine, whilst it is necessary to main-
tain a low oil consumption, is primarily to prevent contamination of the engine with
oil. Internal oil leakage would give rise to the probabilities of a combination of
any of the following: cabin air contamination, internal fires either short term or
long term due to an accumulation of carbon, performance loss due to dirtiness of
aerodynamic parts, or engine vibration due to oil accumulation in rotating parts.

There are basically three philosophies applied to engine bearing compartment sealing
all of which involve, to varying degrees, maintaining the bearing compartment at a
lower pressure than its surroundings thus inducing an inward airflow to prevent an
outward oil leak.

(a) There is the use of 'contacting' seals (carbon face seals) which have very low
     air leakage rates for high seal pressure differences. These normally need to
     operate with high pressure differences across them in order to ensure that they
     will still function satisfactorily at low engine idle speeds. This may mean
     that the bearing compartment needs to be vented directly to the external gear-
     box which may in turn give oil scavenging problems at high altitude due to
     scavenge pump cavitation.

     Further disadvantages are their complexity and its effect upon allowing a
     simple build/strip design concept. The seals have a relatively high heat
     generation and require cooling and lubrication oil flow. Intershaft seals
     present further problems.

(b) A freely vented clearance seal system (such as labyrinth seals) can be adopted
     allowing high seal pressure drops and hence high airflows into the bearing
     compartment for effective oil sealing. The high airflows however can contri-
     bute significantly to heat to oil in high temperature regions and give oil
     separation problems when the air is eventually vented overboard.

(c) In practice very low seal pressure ratios, less than 1.01, can be effective in
     preventing oil leakage, provided careful design of the oily side of the seal
     prevents oil swamping. Thus, by ensuring that all seals at any one compart-
     ment are pressurised from the same source of cooling air and that there is
     minimal pressure variation from seal to seal, a restricted vent can be used
     controlling the bearing compartment to a pressure just below that of the
     surrounding cooling air. Such a system, by minimising the airflow into a
     bearing chamber, aids the oil separation function and reduces the heat input
     to the oil. The system is dependent upon the control of the bearings com-
     partment surround air pressure and the effects of wear on seal clearance.

In summary the first system has high sealing integrity at the expense of high
mechanical complexity. The second also has high sealing integrity but has poten-
tial oil temperature and oil separation hazards. The third system requires careful

system design to ensure adequate sealing integrity but minimises the heat to oil and oil separation problems.

It is pursuit of the third system that is considered in this paper.

2.0 RESTRICTED VENT BALANCED PRESSURE SEALING SYSTEM

Pressure Balancing

Fig. 1 represents the simplest compartment to seal, the single seal, single shaft, end compartment. It is this type of compartment that indicates that adequate sealing is obtained with low seal pressure ratio. Successful oil sealing has been achieved with a seal pressure ratio as low as 1.0005 induced by the excess capacity of the oil scavenge pump. This represents a seal air flow less than 0.001% of the core engine flow.

Fig. 2 is more typical of the factors influencing cooling air system pressures in the vicinity of a bearing compartment. Although each oil seal is pressurised from the same cooling air system, the pressure variation from front to rear of the compartment (p_a to p_c) is subject to pressure losses through the bearing support structure and to vortices induced by shaft and disc rotation. The seal pressure difference will be subject to variation in cooling airflow which may be calculable but the vortex strength is less predictable.

The vent flow must be sufficient to ensure that the compartment pressure, p_b, gives a pressure drop into the compartment across the rear seal. The pressure drop across the front seal will of course be greater than the optimum for adequate sealing.

By the simple expedient of providing an additional seal and a suitable pressure balance passage, as shown in Fig. 3, the effects of the vortex and cooling air flow variation are virtually eliminated. The balance passage flow areas are now the main influence on the pressure variation across the compartment and need only be of the order of ten times the balance seal flow area to make the pressure unbalance negligible. The effect of the balance passage will be to allow a reduction in the vent flow whilst achieving a greater tolerance to seal wear and damage.

Secondary Venting

The principle of isolating the bearing compartment from the surrounding cooling air systems can be extended from the simple balance passage, giving pressure variation independence, to multi skinning giving temperature independence and protection of the cooling air system from oil contamination in the event of a leak.

Such a system is shown in Fig. 4 applied to a two bearing, two shaft compartment which has high pressure turbine cooling air leaking into the cooling air supply for a low pressure turbine.

There are four groups of seals A, B, C and D which separate 3 passages inner, mid and outer.

Seals of group A are the bearing compartment seals. An inflow of air through those seals is achieved by venting the bearing compartment via a restrictor through the wet vent to the external gearbox. An inflow of cool air is ensured through the group B seals into the inner passage by venting the inner passage via a restrictor to some low pressure area (such as the by-pass duct). This may be referred to as the dry vent. Thus, if for any reason, a leak should occur from the bearing compartment into the inner passage, oil would not pass through the group B seals but would be carried through the dry vent thus avoiding contamination and fire hazards.

The outer passage is opened up to the lower pressure region of the LP turbine cooling air via holes Y such that there is a pressure drop across the group C seals into the outer duct. Thus the high temperature air leak from the HP turbine cooling air through the group A seals cannot find its way into the inner duct.

The balance of the LP turbine cooling air requirement would be fed via the LP turbine shaft holes at X.

The system advantages are achieved at the expense of weight and space and possibly also performance since the additional vent flow from the inner passage may be

significant. This flow must also affect the bearing compartment pressure balance unless the inner passage flow areas can be increased to compensate.

Cool Air Blanket

Fig. 5 shows a compromise solution to the bearing compartment sealing requirements accepting that weight and space are limited. The inner vented passage has been deleted with the group B seals and the cooler air is introduced to the bearing compartment seals directly via the pressure balance passage. Since the flow in this passage is reduced from that in Fig. 4 a better pressure balance can be achieved for a given passage size.

If there were no holes at Z through the HP shaft, such as in Fig. 4, the holes at Y could be suitably sized to ensure an outflow of cool air through seals C to prevent the hot HP turbine cooling air from entering the oil seal pressure balance passage. It may however be desirable to substantially dilute the hot air leak with the cooler air to reduce the heat transfer through the bearing compartment outer wall. This would be particularly important if the balance passage and the outer passage were in parallel rather than concentric as space limitations may dictate. Thus by introducing holes at Z and increasing the flow area at Y additional cool air will pass through the outer passage. Control of the overall flow of cooling air to the LP turbine can be maintained by a corresponding reduction in flow area at X.

Thus loss of the dry vent, which isolates any oil leakage, is compensated for by a higher tolerance to seal wear due to the improved pressure balance around the oil seals. The dilution of the hot air leak by the cooler air reduces the fire hazard if an oil leak should occur.

3.0 ROTATING TO STATIC SEALS

Labyrinth Seal

A bearing compartment cannot be sealed by providing an inward airflow through a fine clearance between shaft and housing as shown in Fig. 6(a). Here oil will certainly leak on shutdown as oil runs along the shaft and it may well leak during running, particularly at low pressure difference across the seal. These leaks can be avoided by a raised land as shown in Fig. 6(b) which will throw the oil clear of the shaft during running and discourage oil from running down the shaft on shutdown. However a plain bore is not as effective an air seal as a finned labyrinth seal of the same clearance occupying the same length, Fig. 6(c). Also in the event of rotating to static contact the plain bore would generate much more heat, resulting in local distortion, than would occur with the more limited contact of the finned labyrinth seal. Thus the labyrinth seal evolves as an effective oil seal.

It should be noted that the innermost (oil side) fin which acts as an oil flinger must not run inside the seal static liner to avoid oil draining out along the liner against the airflow.

If a steel or other hard lining was used the seal clearance would need to be sufficiently large to avoid metal to metal contact under any conditions. Hence it would have to take account of transient effects such as shaft whirl, differential growth rates between inner and outer seal parts and allow a small margin for ignorance of the precise transient effects. By using an abradable lining which would tolerate limited transient seal rubs, the seal clearance can be minimised thus reducing the air leakage for a given seal pressure difference. The requirements of an abradable liner for oil sealing must satisfy the following requirements :

(a) Since the debris from a seal rub will enter the bearing compartment and the oil system it must not include hard particles or be abrasive.

(b) The seal material must be compatible with the oil types to be used in the engine (this would preclude use of rubber and synthetic rubber based materials).

These are in addition to the usual requirements for mechanical integrity, erosion resistance, ease of rework etc.

Ring Seal

The ring seal, Fig. 7, has a floating ring axially located in a static housing running against a shaft mounted sleeve. The ring follows any radial excursions of

the shaft by floating in its housing, consequently the clearance between ring and sleeve can be very fine thus limiting the airflow through such a seal.

The ring seal generally requires development time to optimise ring and sleeve interface materials and finish.   It requires an oil presence to prevent wear and consequently its use is restricted to cooler environments, 250 to 300°C.   Oil gumming or carboning would cause the ring to stick in its housing and lead to severe wear between the ring and the sleeve.   Similarly high pressure difference across the seal can load it against the housing wall, inhibiting its free radial movement.

The seal will operate satisfactorily at sleeve surface speeds up to about 300 ft/sec (90 m/sec).

Within these operating limitations the ring seal can be very effective in limiting the vent air flow requirement.

4.0   INTERSHAFT SEALS

Labyrinth Seal

Intershaft labyrinth seals generally require larger clearances than rotating to static seals particularly as the seal position becomes more remote from the bearings and consequently require more air for an adequate sealing margin.

Hydraulic Seal

The hydraulic seal affords a very effective means of sealing between para-rotating shafts being able to tolerate high pressure differences with negligible airflow. The hydraulic seal, shown in Fig. 8, uses the outer shaft to support an annulus of oil between two fins, one acting as a dam and the other as a weir.

A fin on the outer diameter of the inner shaft runs immersed in the oil annulus thus providing a positive air seal.   The weir controls the oil level on one side of the fin, the level on the other side is determined by the rotational speed of the oil, the oil density and the pressure difference across the fin.

For most applications the oil speed approximates to the mean speed of the two shafts and the sealing capacity can be estimated on that basis.

i.e.   Seal pressure difference $\Delta p = \rho \omega_m (r_1^2 - r_2^2)$

ρ oil density

ω_m oil mean rotational speed

Since there are high velocity gradients in the oil, heat is generated at a hydraulic seal.   This is not generally significant relative to main shaft bearing heat generation but it must be considered with respect to local oil temperatures.   The heat generation will be minimised by avoiding excessive fin immersion.   To avoid high local oil temperatures the hydraulic seal should have a through flow of oil by feeding the oil on the opposite side of the fin to the weir.

There must be provided a suitable catchment volume to prevent the oil from the annulus spilling away from the bearing compartment on shutdown when the outer shaft rotation provides insufficient centrifugal head to maintain it.   The catchment zone should allow drainage back to the bearing compartment.   There may be a very small air leak through the drainage passages into the compartment during normal running but it would be at an insignificant flow rate.

The hydraulic seal presents difficulties with regard to assembly since the fin outside diameter must be greater than the weir and dam inside diameters.   Consequently it is often not practical to employ an assembly procedure suitable for a hydraulic seal.

However if the seal is only required to support a small pressure difference then a deformable weir could be used in conjunction with a limited interference fin, Fig. 9. Account must be taken of the compression of the weir under centrifugal load during running when assessing the seal performance.

Oil Faced Labyrinth Seal

The principle of a centrifugally supported annulus of oil can be applied to a labyrinth seal where the oil acts as a deformable self repairing seal liner, Fig. 10. The nominal seal clearance need only be that consistent with ease of assembly and strip. Thus the intershaft seal can be as efficient as a conventional rotating to static seal (may be even more so) without the assembly problems of the hydraulic seals. Since it is an airflowing seal there will still remain the need for pressure balancing. This can be adequately achieved by providing a conventional abradable linered seal of relatively large clearance as back up.

5.0 SEAL FAILURE ANALYSIS

Since the principle of the pressure balanced vented bearing compartment is to minimise the air used consistent with satisfactory oil sealing, it is necessary to do a seal failure analysis.

After assessing what increase in seal clearance above normal wear limits need to be catered for in the vicinity of the bearing compartment, the vent flow for the compartment can be calculated. It is assumed that all the seals on one shaft can fail simultaneously and that they all increase clearance by the same amount. When considering a failure on one shaft it is assumed that the seals on any other shafts are on maximum wear limits. The vent flow can then be sized such that at a failure clearance there is no reversal of airflow at any oil seal. This must be checked for each group of seals in turn. If the pressure balance around the oil seals is almost perfect it will be found that the vent flow calculated for the failure case will provide a very low pressure difference across all seals when they are all at the clearance for maximum wear allowance. In these circumstances the vent flow should be increased to bring the oil seal pressure difference up to a suitable minimum, about ¼ psi (1.7 kN/m²) at sea level static take off. Fig. 11 shows a typical plot of seal failure margin.

Thus the benefits of a well pressure balanced system are reduced vent flow with extended seal failure margins. These effects are enhanced by making use of oil faced labyrinth seals and particularly by use of hydraulic seals.

6.0 ACKNOWLEDGEMENTS

I would like to thank the Directors of Rolls-Royce Limited for permission to prepare and present this paper. My thanks also go to the Rolls-Royce Engineering Illustrations Department and PSG Limited for their invaluable assistance in executing the diagrams.

DISCUSSION

F.Willkop, Germany

I have a question concerning the hydraulic seal. Do you have experience with counter-rotating seals, their heat generation and their need of oil exchange?

Author's Reply

Tests have been carried out investigating the operation of contra-rotating hydraulic seals. These showed that such seals were not stable and would not support significant pressure difference and hence further testing was not pursued.

Fig. 1 SINGLE SEAL BEARING COMPARTMENT
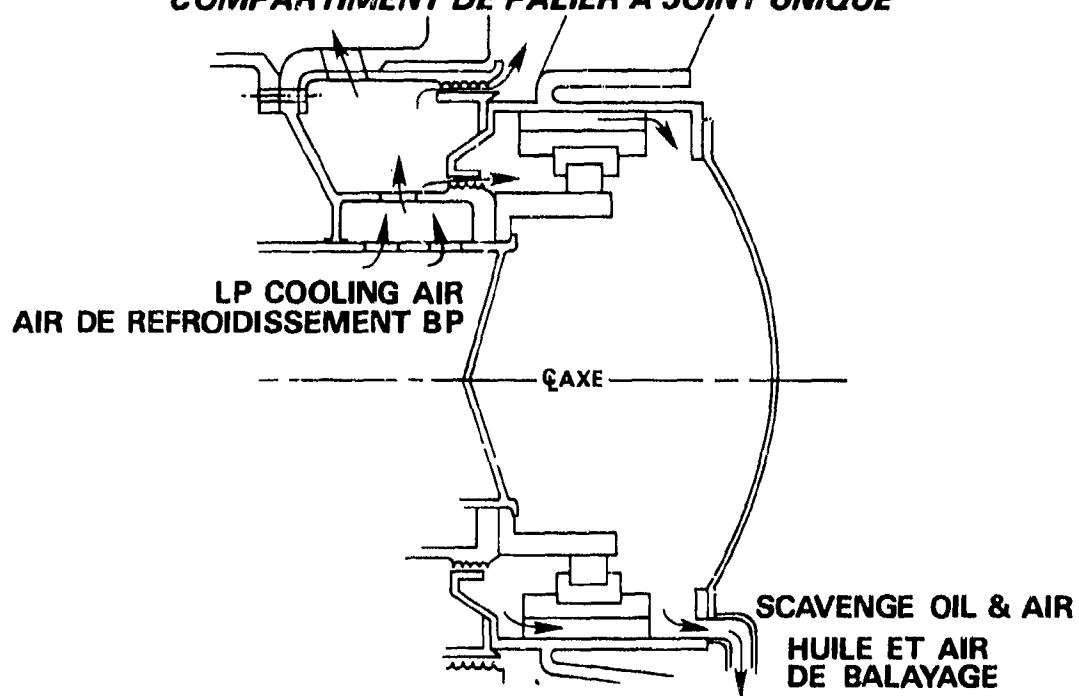## *COMPARTIMENT DE PALIER A JOINT UNIQUE*

LP COOLING AIR
AIR DE REFROIDISSEMENT BP

¢AXE

SCAVENGE OIL & AIR

HUILE ET AIR
DE BALAYAGE

Fig. 2 TYPICAL BEARING COMPARTMENT
COMPARTIMENT TYPIQUE DE PALIER

VORTEX PRESSURE GRADIENT
CHUTE DE PRESSION
TOURBILLONNAIRE

VENT RESTRICTOR
RESTRICTEUR DE VENTILATION

COOLING AIR FLOW
DEBIT D'AIR DE
REFROIDISSEMENT

Pa Pb Pc

VENT FLOW
DEBIT D'AERATION

℄ AXE

Fig. 3 PRESSURE BALANCE PASSAGE
PASSAGE D'EQUILIBRE DE PRESSION

VORTEX PRESSURE GRADIENT
CHUTE DE PRESSION
TOURBILLONNAIRE

PRESSURE BALANCE PASSAGE
PASSAGE D'EQUILIBRE
DE PRESSION

COOLING AIR FLOW
DEBIT D'AIR DE
REFROIDISSEMENT

Pa Pb Pc

VENT FLOW Pd
D'AERATION

℄ AXE

Fig. 4 SECONDARY VENTING
AERATION SECONDAIRE

DRY VENT TO BY PASS DUCT
VENTILATION SECHE A CONDUIT
DE DERIVATION

WET VENT TO EXTERNAL GEARBOX
VENTILATION HUMIDE VERS CARTER
DE TRANSMISSION EXTERIEURE

HP TURBINE COOLING AIR
AIR DE REFROIDISSEMENT DE
TURBINE A HP

HP TURBINE SHAFT
ARBRE DE TURBINE
HP

OUTER
EXTERIEUR

LP TURBINE
COOLING AIR
AIR DE REFROIDISSEMENT
DE TURBINE BP

INNER
INTERIEUR

LP TURBINE SHAFT
ARBRE DE TURBINE BP

℄ AXE

Fig. 5 COOL AIR BLANKET
ENVELOPPE D'AIR REFROIDI

WET VENT TO EXTERNAL GEARBOX
VENTILATION HUMIDE VERS CARTER DE TRANSMISSION

HP TURBINE COOLING AIR
AIR DE REFROIDISSEMENT
DE TURBINE HP

HP TURBINE SHAFT
ARBRE DE TURBINE HP

LP TURBINE COOLING AIR
AIR DE REFROIDISSEMENT
DE TURBINE BP

LP TURBINE SHAFT
ARBRE DE TURBINE BP

℄ AXE

Fig. 6 CLEARANCE TYPE OIL SEAL

JOINT D'HUILE A JEU

SEALING AIR
AIR D'ETANCHEITE

BEARING COMPARTMENT
COMPARTIMENT DE PALIER

SHAFT
ARBRE

₵ AXE

SHAFT
ARBRE

₵ AXE

SHAFT
ARBRE

₵ AXE
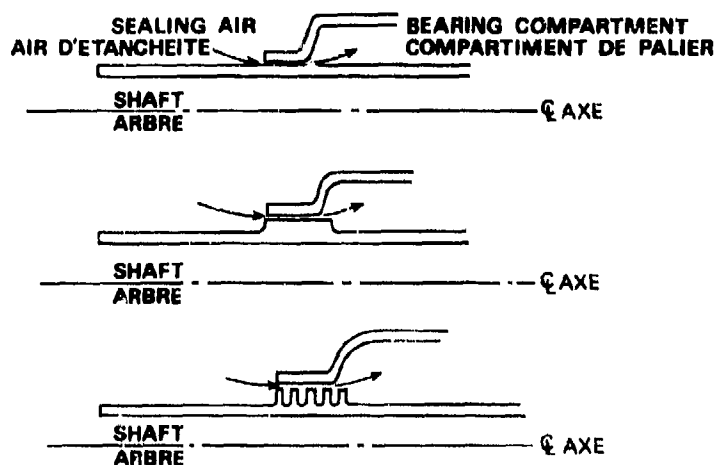
Fig. 7 RING SEAL

JOINT ANNEAU

BEARING COMPARTMENT
COMPARTIMENT DE PALIER

SEALING AIR
AIR D'ETANCHEITE

SEALING SLEEVE
MANCHON D'ETANCHEITE

SHAFT
ARBRE

₵ AXE
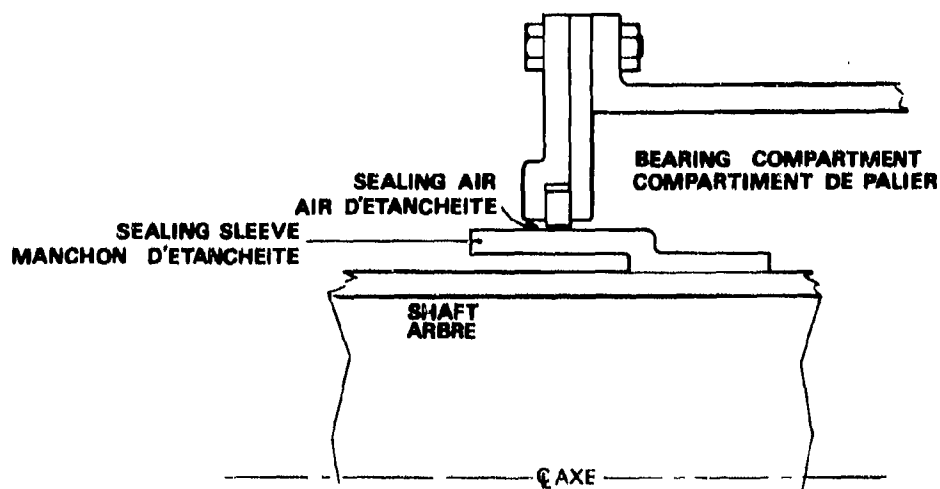
Fig. 8 HYDRAULIC SEAL
JOINT HYDRAULIQUE

(a)

Ç AXE

HP SHAFT
ARBRE HAUTE PRESSION

LP SHAFT
ARBRE BASSE PRESSION

P_2

P_1

(b) P_2 P_1

H

(c)

AXE Ç

r_2 P_2 P_1 N_H r_1

N_L
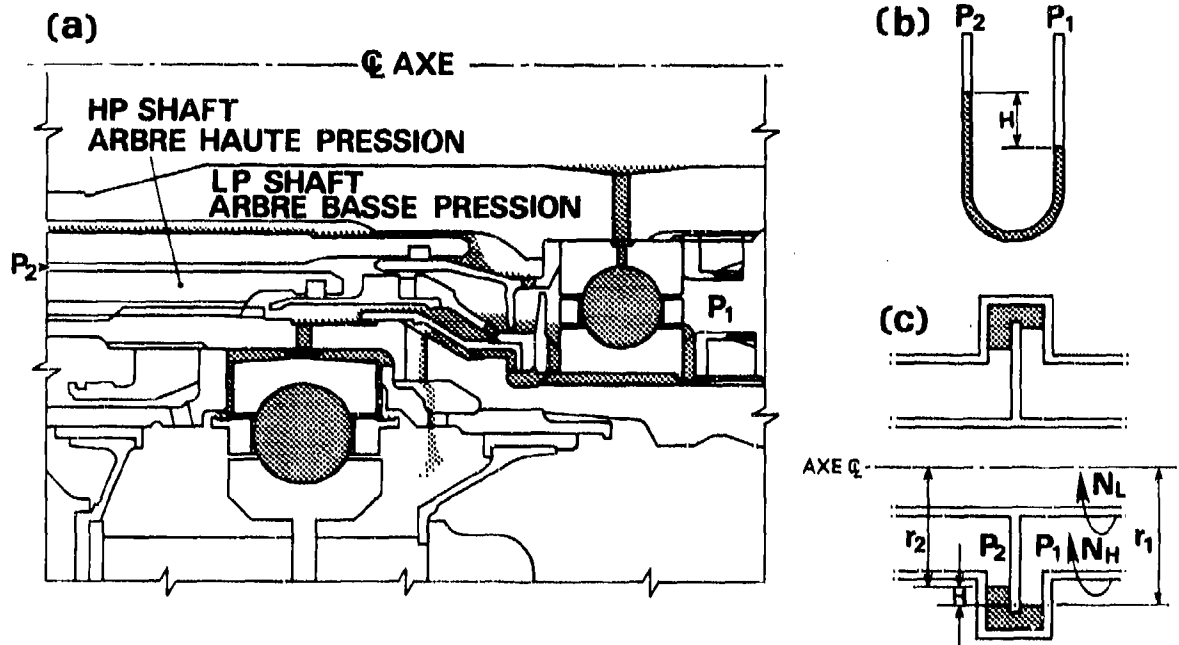
Fig. 9 HYDRAULIC SEAL WITH DEFORMABLE WEIR
JOINT HYDRAULIQUE AVEC DIGUE DEFORMABLE

HP SHAFT
ARBRE HP

DAM
BARRAGE

FIN
AILETTE

LP SHAFT
ARBRE BP

DEFORMABLE WEIR
DIGUE DEFORMABLE

OIL FEED
ALIMENTATION D'HUILE

DIFFERENCE IN OIL LEVEL
ACROSS SEAL
DIFFERENCE DE NIVEAU D'HUILE
DE L'AUTRE COTE DU JOINT

Ç AXE
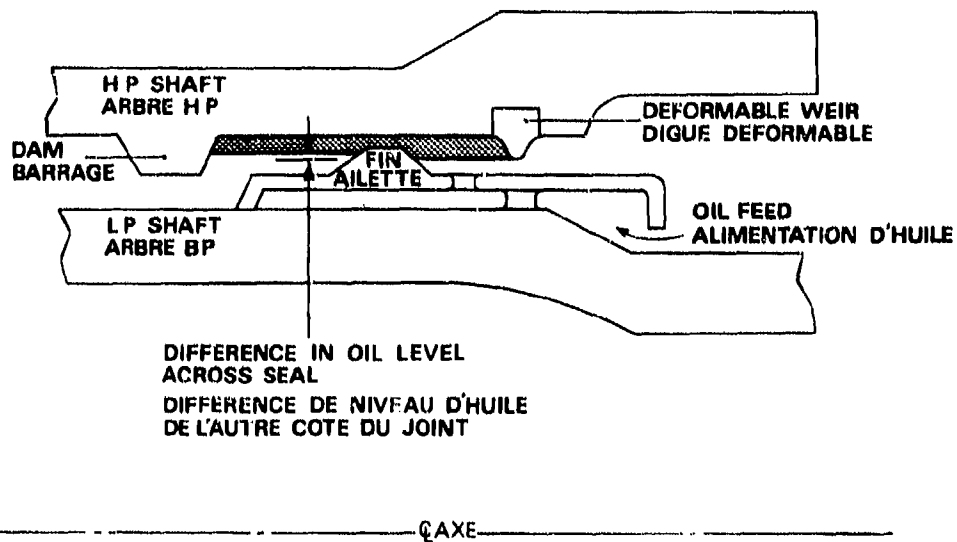
Fig. 10   OIL FACED LABYRINTH
LABYRINTHE A FACE D'HUILE

BEARING LUBRICATION
GRAISSAGE DE PALIER   HP SHAFT
ARBRE HP

OIL FEED
ALIMENTATION D'HUILE

SEALING AIR
AIR D'ETANCHEITE

LP SHAFT
ARBRE BP

℄ AXE
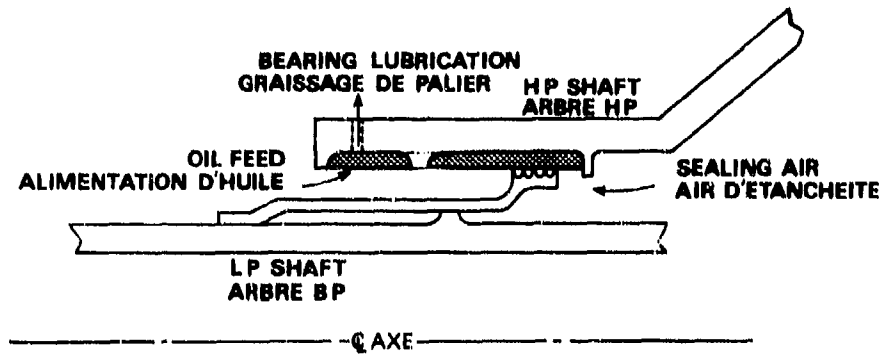
FIG.11   ESTIMATION OF SEALING SYSTEM INTEGRITY
EVALUATION DE L'INTEGRITE DU CIRCUIT D'ENTANCHEITE

Seal pressure difference

Pression différentielle du joint

Poor pressure balance
Equilibrage d'air mauvais

Effect of increased venting
Effet de ventilation augmentée

Minimum normal seal pressure difference

Pression différentielle normale minimum du joint

Good pressure balance
Equilibrage d'air bon

Nominal seal clearance
Jeu nominal du joint

Normal wear allowance
Tolerance d'usure normale

Seal failure margin
Marge de securité

Seal clearance
Jeu du joint

TRANSPORT PHENOMENA IN LABYRINTH-SEALS OF TURBOMACHINES

Tahsin BOYMAN   Peter SUTER
Assistant, Dipl.Ing.   Professeur Dr.Ing.
Ecole Polytechnique Fédérale de Lausanne
Institut de Thermique Appliquée
CH-1015 LAUSANNE (SWITZERLAND)

SUMMARY

In turbomachines it has been observed that the oil-fog and the oil-vapour produced in the region of bearings may be transported through the labyrinth-glands in the direction opposite to the buffering-fluid-flow.

Two mechanisms are found to be at the origin of this undesired transport:

- the diffusion of the oil-vapour due to the concentration gradient,
- the transport of small oil-droplets due to the complex flow created in the labyrinth-seals.

The intensity and limits of these two phenomena are studied theoretically and experimentally; experiments have been performed in a real-size-model and in a second large-scale-model, both of the "straight-through-type" with moving fins and a stationary outer cylinder.

NOMENCLATURE

Symbols

A	(m^2)	: area
B	(m, mm_N)	: breadth of one labyrinth-chamber
b	(m, mm_N)	: thickness of a fin
C	(ms^{-1})	: velocity
D	(m, mm_N)	: diameter
f	(mm_N)	: focal length in LDV
i	$(-)$	: number of labyrinth-chamber
k_M	(ms^{-1})	: mass transfer coefficient
L	(mm_N)	: distance of the laser-beams in LDV
n	(min^{-1})	: speed of rotation
Q	$(m^3 s^{-1})$	: flow rate
r, a, θ		: coordinates
β	$(°)$	: angle between the plane of laser-beams and the plane of labyrinth-fins
γ	(ppm)	: concentration of propane
μ	$(kgm^{-1}s^{-1})$	: dynamic viscosity
ρ	$(kg.m^{-3})$	: specific mass
ω	(s^{-1})	: angular frequency

$(N$: on the drawings$)$

Indices

1	: related to the inner cylinder
2	: related to the tip of the fins
3	: related to the outer cylinder
$\oslash$	: related to the real-size-model
$\oslash$	: related to the large-scale-model
a	: axial component
r	: radial component
t	: tangential component
f	: of the fluid
p	: of the particle
i	: in the i-th chamber
m	: average in the gap

Definitions

$C_{a,m}$: average axial velocity of the buffering-fluid in the gap

$$C_{a,m} = \frac{Q_f}{\frac{\pi}{4}(D_3^2 - D_2^2)}$$

Re : Reynolds number $Re = DC\rho\mu^{-1}$

Abbreviation

ppm : parts per million

1. INTRODUCTION

The labyrinth-glands are contactless leakage reducing elements for turbomachines working at high rotational speeds; according to the direction of the pressure drop a certain amount of fluid flows through the glands. When this exchange between the fluids inside and outside of the machine has to be absolutely stopped we make use of a buffering-fluid. The buffering-fluid is injected into the labyrinth-glands in order to assure two flows in opposite directions: the first one directed to the atmosphere and the second to the inner side of the machine.

In practice it has been observed that oil is transported from the region of bearings to the inner side of the turbomachine through the labyrinth-glands, in the direction opposite to the buffering-fluid-flow.

The problem may be summarized as follows (see figure 1) :

The spaces E and S are separated by a rotor equiped with fins, the outer cylinder is at rest. The fluid in S contains oil in gaseous form and oil-droplets. The pressure in E is higher than in S and due to this pressure difference we have a flow from E to S through the glands. In spite of this flow we observe oil in zone E.
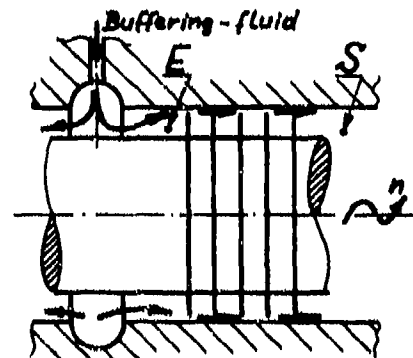
Figure 1. Schematic view of the problem

The purpose of this paper is to study the mechanisms causing this undesired transport phenomenon.

2. CLASSIFICATION OF TRANSPORT MECHANISMS

In turbomachines the lubricating oil is partially vaporized due to the heating in the bearings. Another part of this oil is atomized by centrifugation and constitutes a suspension of oil-droplets in the air, called the "oil-fog". The oil in gaseous form will be referred to as the "oil-vapour".

The following transport phenomena can be observed:

- the oil-vapour has a certain concentration in the region of bearings and can be transported by diffusion to those regions where the concentration is lower,
- large droplets end their trajectory on a stationary surface in the zone S before entering in the labyrinth-glands; smaller droplets follow the flow more or less accurately and we shall show that there is some probability that droplets can be transported by this procedure from space S to space E through the glands.

Experiments have been done in order to study seperately the two mechanisms:

- the diffusion,
- the transport of small droplets.

The determination of the rates of diffusion has been performed on a real-size-model and as to the complex flow-field in labyrinth-glands, measurements and visualization have been done on a large-scale-model. The transport of the oil-droplets of different sizes, observed in the real-size-model, can be explained by the information on the velocity-field.

3. DIFFUSION-EXPERIMENTS

3.1 Configuration of labyrinth-glands

The experimental models investigated are both of the "straight-through-type", with moving fins and a stationary outer cylinder.

The variables are the rotational speed of rotor and the average axial velocity of buffering-fluid through the gap between the fins and the outer cylinder.
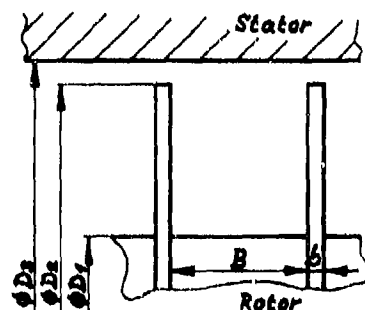
Figure 2. The chosen configuration of labyrinths
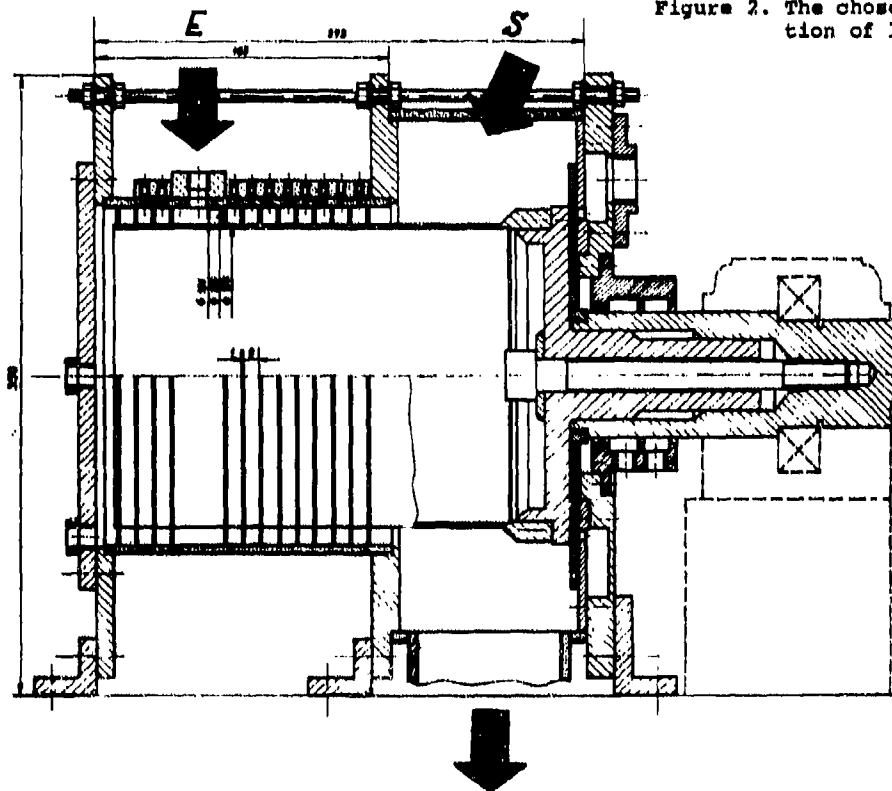
Figure 3. The real-size-model

3.2 The real-size-model

The principal dimensions of the real-size-model are given on figure 3. The annular chamber in the middle of this model simulates the zone S close to a bearing of a turbo-machine where the oil-fog and the oil-vapour are produced. The buffering-air is fed radially at station E and we have nine identical fins between the intake (E) of the buffering-air and the exit-chamber (S). The outer cylinder is made of plexiglass and equiped with 49 holes of 1 mm diameter for sampling.

A direct-current drive motor allows rotational speeds from $n_\oplus = 100$ to 9100 min^{-1}. Average axial velocities of the buffering-air in the gap are assured up to $C_{a,m\oplus} = 3\ ms^{-1}$.

3.3 Experimental equipment

The figure 4 shows the arrangement for the diffusion-experiments. Instead of oil-vapour we injected propane gas in the exit-chamber (S) and measured the propane-concentration in the samples taken through different holes on the plexiglass-cylinder.

A flame-ionisation-detector was used for the determination of propane-concentrations. The propane-concentration was maintained about 9000 ppm in the exit-chamber (S) during the measurements.
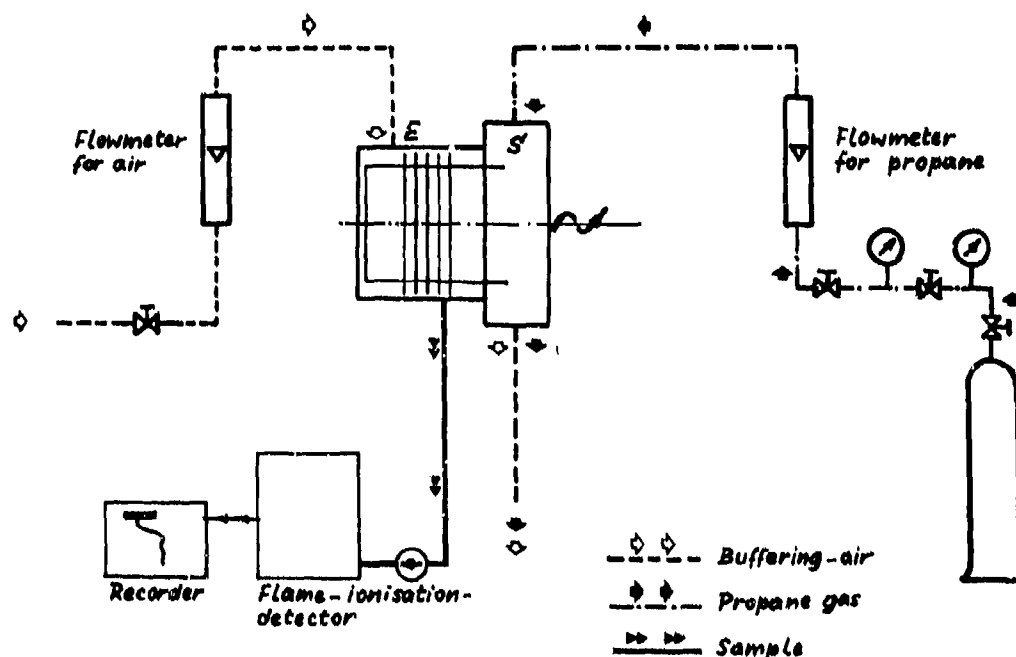
Figure 4. The arrangement for the diffusion-experiments

3.4 Results and discussion of the diffusion-experiments

The results are shown on figures 5 and 6. The figure 5 gives the variation of the propane-concentration through the glands for $n_\oplus = 9000\ min^{-1}$ and $C_{a,m\oplus} = 0,25; 0,50; 0,75; 1,00\ ms^{-1}$. The figure 6 shows that only the ratio $C_{i,s}/C_{a,m}$ is determinant and the Reynolds number (obtained with $C_{i,s}$ or $C_{a,m}$) has no influence in the investigated domain.

During the experiments the test-room concentration-level was about 25 ppm and we found the same concentration-level at station E_0 which is situated at some distance from the labyrinth-glands, on the buffering-air admission-pipe.

In our case we have not any net propane transport from S to E through the glands. Therefore, the concentration in the i-th labyrinth-chamber is the result of:

- a global transport due to the buffering-air-flow: $\dot{Q}_f\ \tau_i$ and
- a turbulent mass transfer: $k_{M,i}\ A\ (\tau_{i-1} - \tau_i)$.

Thus:

$$\dot{Q}_f \tau_i - k_{M,i}\ A\ (\tau_{i-1} - \tau_i) = 0 \qquad (1)$$

For a large number of labyrinths with an average mass transfer coefficient $k_{M,m}$, we obtain the propane-concentration in the i-th chamber (see ref. 1) :

$$\tau_i = \tau_0 \cdot exp\left(-\frac{\dot{Q}_f \cdot i}{k_{M,m} A}\right) \qquad (2)$$

Figure 5.
Results of the diffusion-
experiments for:

$n_0 = 9000 \text{ min}^{-1}$

C_{am} (ms⁻¹)	
●	1,00
×	0,75
▼	0,50
◆	0,25

Concentration of propane
in t' ambiant air

Concentration of propane (ppm)

Labyrinth-chambers

Direction of the
buffering-air-flow

Figure 6.
Results of the diffusion-
experiments for:

	n (min⁻¹)	C_{am} (ms⁻¹)
●	9000	0,500
×	7500	0,417
▼	4500	0,250
◆	3000	0,187

Concentration of propane
in the ambiant air

Concentration of propane (ppm)

Labyrinth-chambers

With $C_{e,m} = \frac{\dot{Q}_f}{A}$, equation (2) reduces to:

$$\gamma_i = \gamma_0 \cdot exp\left(-\frac{C_{e,m}}{k_{M,m}} \cdot i\right) \qquad (3)$$

Above the difference of concentration of 100 ppm between two neighbouring chambers, the four distributions given on figure 5 satisfy the equation (3). Thus, we obtain the mass transfer coefficients given on table 1. The value of $k_{M,m}$ shows a slight decrease with increasing $C_{t,a}/C_{e,m}$ ratio.

$\dfrac{C_{t,a}}{C_{e,m}}$	90	120	180	360
$k_{M,m}$	0,68	0,64	0,59	0,56

Table 1.

Below the concentration-difference of 100 ppm between two neighbouring chambers, the intensity of diffusion is reduced and an effective sealing against diffusion is obtained two or three chambers upstreams, after that the difference becomes lower than 100 ppm.

The difference of the concentrations at stations S and O is due to a protection-ring situated between the labyrinth-glands-zone and the space S.

During the diffusion-experiments it was also observed that:

- there was no perceptible variation of concentration in any-one of the labyrinth-chambers during one hour runs,
- the propane-concentration in the chambers varied proportionally to the concentration in the space S when this was varied,
- the peripherical variation of concentration in every chamber did not exceed ± 10% of the average value.

As a partial conclusion, we can say that care must be taken against the transport by diffusion when we have reduced velocities of buffering-fluid and also if only a few labyrinth-chambers are disponible.

4. DETERMINATION OF THE FLOW-FIELD IN A LABYRINTH-CHAMBER

4.1 The large-scale-model

In order to examine the details of the flow, a large-scale-model (five times greater than the real-size-model with geometrical similarity) was conceived. Figure 7 gives the principal dimensions of this model.

In this model we used water instead of air. Therefore, the hydrodynamical similarity requires the reduction of all velocities in a ratio of 85 in the water; the rotational speed is reduced 420 times. The buffering-water flows from the bottom to the top. On the outer cylinder we have two plexiglass windows for visualization and velocity measurements.
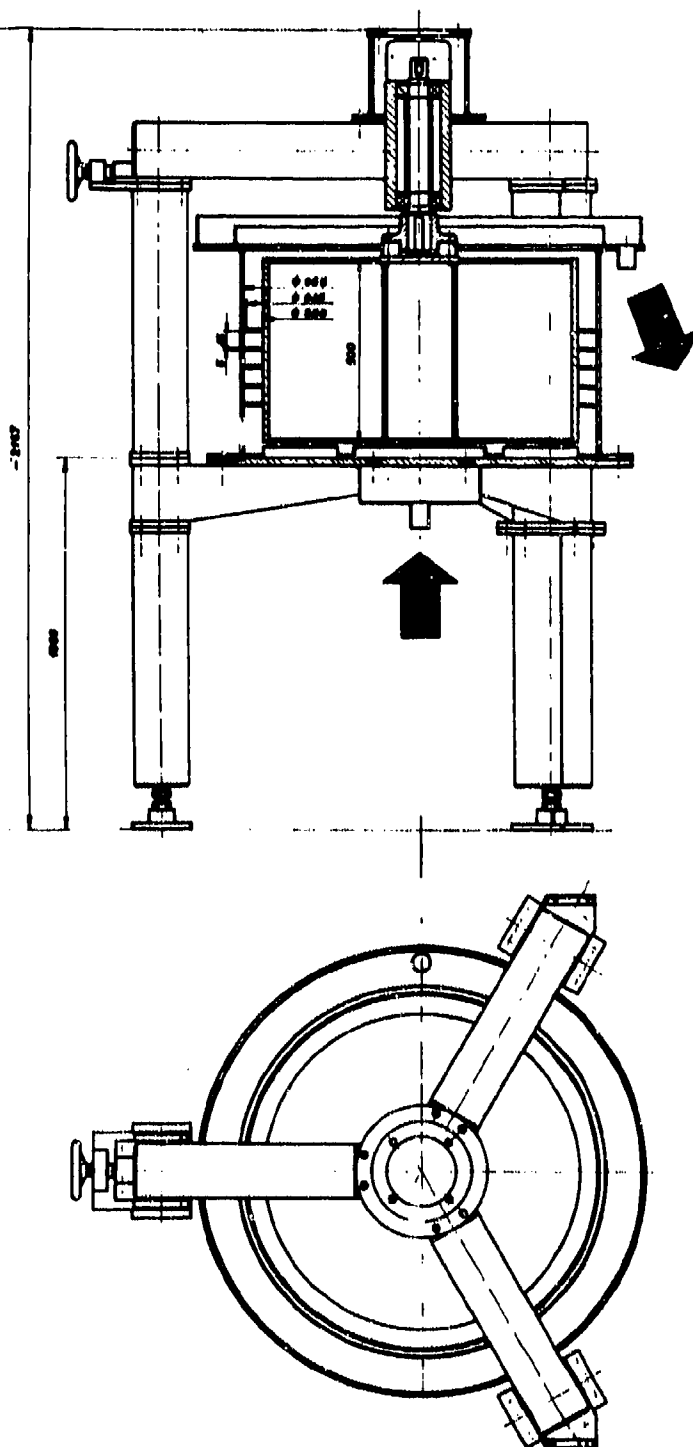
Figure 7. The large-scale-model

Figure 8.
The double-helicoidal
flow-pattern

plane of
representation

Buffering-
water $\frac{C_{t,2}}{C_{a,m}} \approx 20$ $C_{a,m} = 0$ $C_{t,2} = 0$
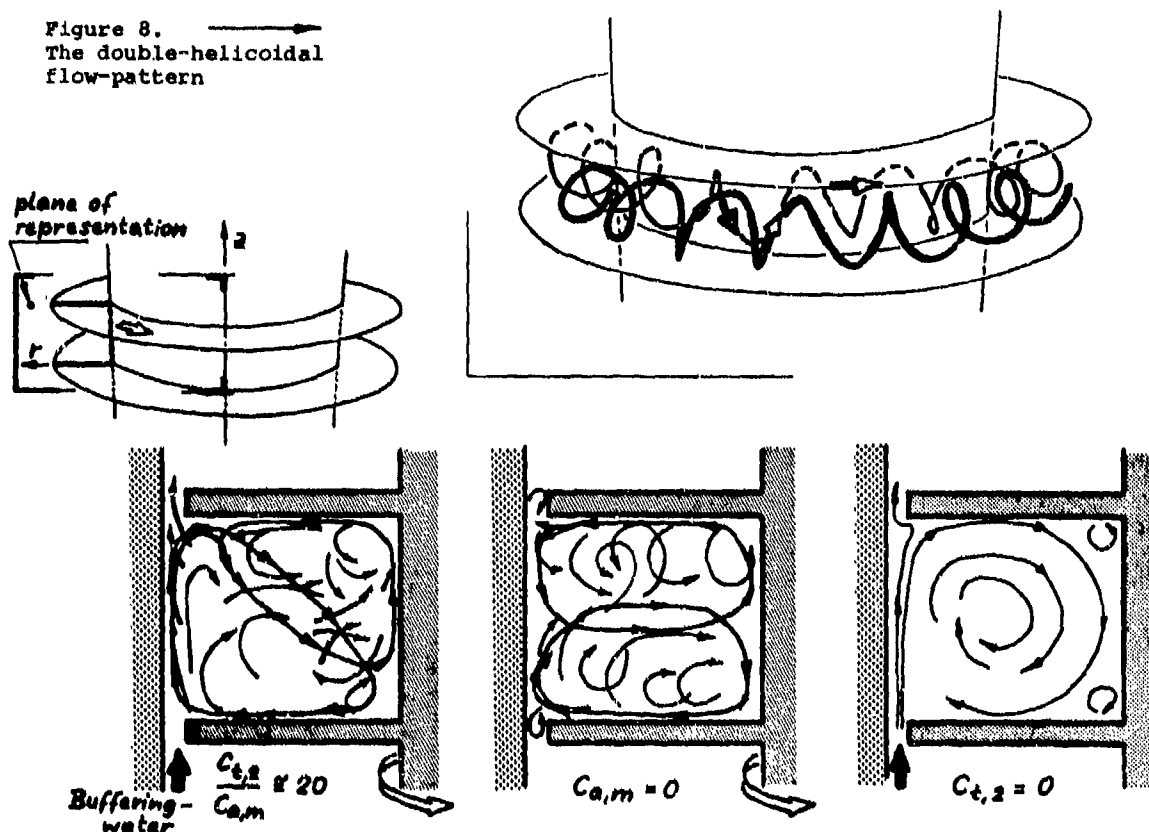
Figure 9. Flow-images obtained by dye-injection-method

4.2 Flow visualization

With the injection of colored dyes (Luconyl from BASF diluted with water) at appro-
priate injection velocities, it was possible to determine the local directions of the
flow velocities in a labyrinth-chamber for different pairs of "rotational speed - axial
velocity of buffering-water".

From the flow-images obtained with this technique and represented on figures 8 and
9 we deduce that:

• without rotation, one large helix appears,
• with rotation, but buffering-flow lacking, two similar and partially overlapping
  spirals appear,
⌣ with both rotation and buffering-flow, the two helices are distorted.

Thus, the main flow for $n \neq 0$ and $C_{a,m} \neq 0$ consists of two oppositely rotating and
partially overlapping helices.

Besides the observation of the mean flow, the flow visualization revealed also the
momentary back-flows occuring in the gap. During these experiments, the parietal injection-
point was situated approximately 5 mm on the downstream-side of the gap and in spite of
the buffering-water-flow the injected dye came momentarily back (with a random frequency)
through the gap into the labyrinth-chamber situated upstreams.

4.3 Laser-Doppler-Velocimeter (LDV) measurements

The measurements are made with a BBC-Goerz velocimeter (model LG 01) in the back-
scattering mode and a BBC-Goerz signal processor (model LSE 01). The laser source was a
5 mW Helium-Neon unit. The output-signal of the processor was sampled at the rate of 1000
samples per second and each sample was stocked in the corresponding channel of a numerical-
treatment-unit (Didac 800 from Intertechnique). The fresh tap-water did not show any diffi-
culty during the measurements, which were done through a plexiglass window presenting the
same internal curvature as the outer cylinder.

The points where the velocity measurements are performed are given on figure 10.
Except a few points close to the fins, at each point two measurements in two different
directions (namely, $\beta = \pm 30°$ relatively to the circumferential direction) have been
carried out. Here, "one measurement" means the probability density distribution of the
velocity in the concerned direction, this distribution being obtained for a total of
500'000 samples at the rate of 1000 values per second.
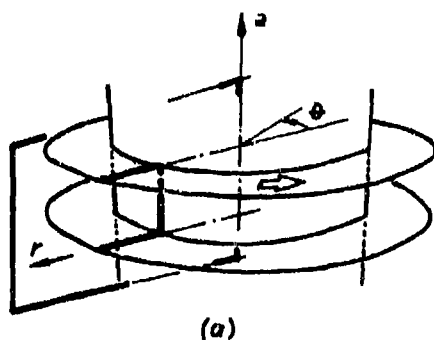
Figure 10.

a. The section of measurement

b. The disposition of the measurement-points in the labyrinth-chamber and the specifications of the LDV's optical arrangement for each measurement

	f (mm)	L (mm)	β (°)
●	57,7	30	±30
✻	57,7	30	±25
▽	57,7	30	0
□	115,3	30	±30
▲	115,3	30	0
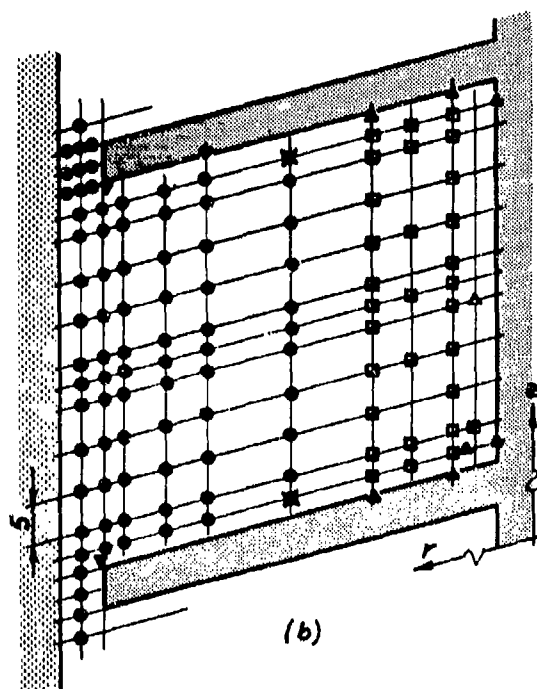
(b)
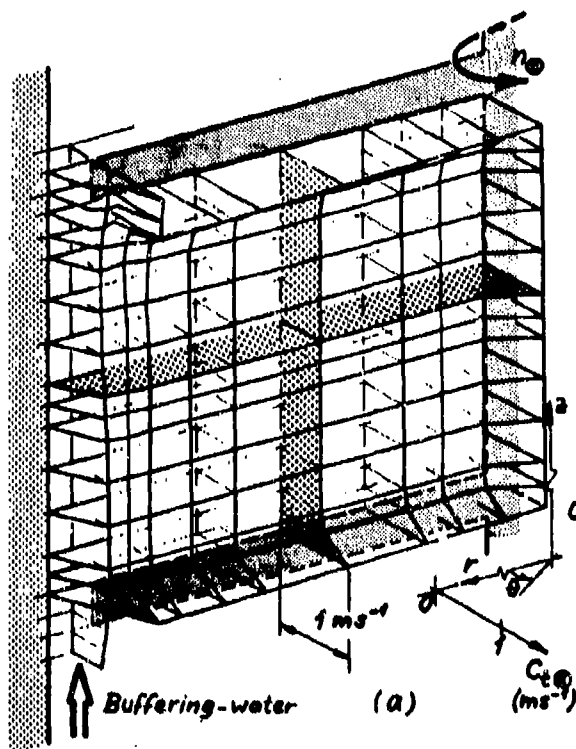
(a)
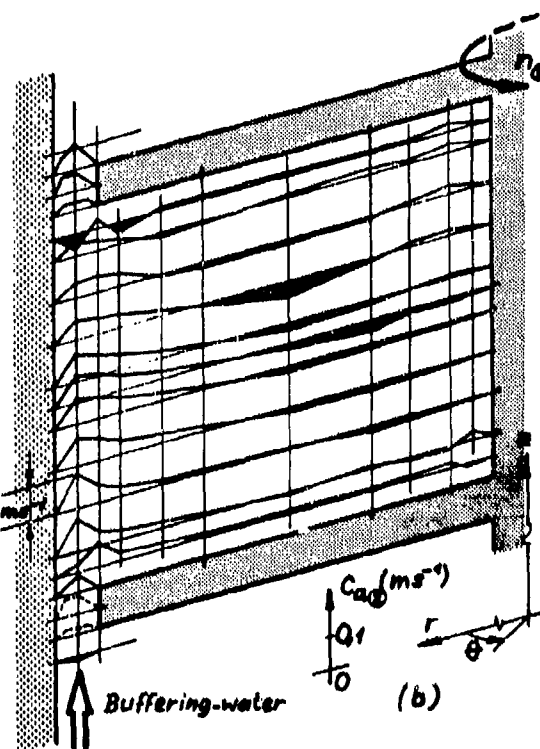
(b)

Figure 11. Tangential (a) and axial (b) velocity components deduced from LDV measurements for $n_\oplus = 21,66 min^{-1}$ and $C_{a,m\oplus} = 0,035 ms^{-1}$
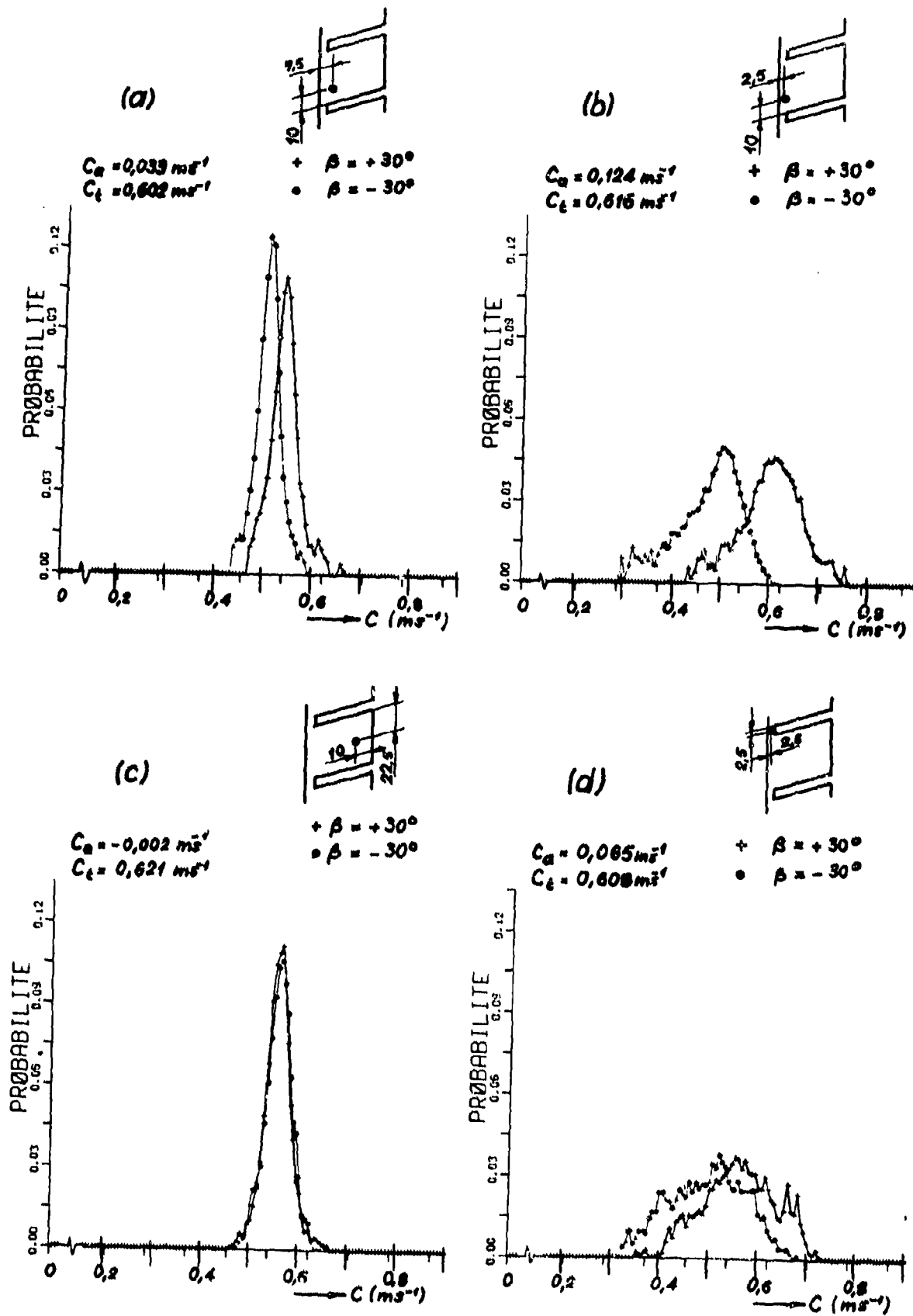
Figure 12. Probability density distributions of velocities in the directions $\beta = \pm 30°$ and deduced average values of C_a and C_t for $n_0 = 21.55 \, min^{-1}$ and $C_{a,m_0} = 0.035 \, ms^{-1}$.

From these distributions we computed the average velocities and the central moments up to the fourth moment. With two average velocities in different directions at the same point we obtained the averages of the axial and the tangential components of the velocity. The distributions of these components are given on figure 11 for $n_\bullet = 21.55\ min^{-1}$ and $C_{\theta,m\odot} = 0.035\ ms^{-1}$ (these values correspond to $n_\odot = 9000\ min^{-1}$ and $C_{\theta,m\odot} = 3\ ms^{-1}$ in the real-size model). On these representations, the inner cylinder is rotating counter-clockwise when seen from the top and the buffering-water flows from the bottom to the top. For the sake of representation of the small axial components the velocity-scales have different values for each distribution on the figure 11.

The distribution of the axial components (figure 11.b) (negative values are black) confirms the results of the visualization: we find again the two distorted vortices with a region of negative velocities across the chamber.

From the distribution of the tangential velocity components (figure 11.a) it can be seen that in the middle of the labyrinth-chamber the average tangential velocity reaches 50% of the circumferential velocity of the moving walls.

The double-helicoidal flow in the space between the fins explains the transport of droplets within a labyrinth-chamber. As to the transport from one chamber to the neighbouring one situated upstreams, the turbulent velocity fluctuations in the region of the gap may be at the origin of the momentary back-flows observed during the visualization-experiments. The variation of the fluctuations when approaching the walls and mainly in the region close to the gap can be observed on figure 12. On this figure are given the probability density distributions versus the velocity at four different points for $n_\bullet = 21.55\ min^{-1}$ and $C_{\theta,m\odot} = 0.035\ ms^{-1}$.

From figures 12.a and 12.b we see the increases of the axial component and also of the velocity fluctuations when we approach the stationary outer wall: however, there is a manifesting velocity-peak. Figure 12.c gives the situation in the middle of the chamber: the flow is practically tangential. In contrast to the distribution of the figure 12.b, the velocity distribution in the gap (figure 12.d) shows the lack of a dominant velocity and the fluctuations reach $\pm 25\%$ of the average value for $\beta = +30°$ and $\pm 33\%$ for $\beta = -30°$. Unless the fluctuations in the $\beta = +30°$ and $\beta = -30°$ directions were rigidly correlated (which is unlikely), the momentary axial velocity in the gap can well take negative values, explaining thus the transfer observed in the visualization.

The partial conclusion we can deduce from the flow-field observation is that the two helices account for the transport of a droplet within a labyrinth-chamber, and the velocity fluctuations in the region of the outer wall and, mainly, near the gaps may transport droplets from one chamber to the next one situated upstreams.

5. MOTION OF DROPLETS IN THE LABYRINTH-GLANDS

Considering the motion of discrete (non-interacting), spherical and small (Stokes-drag-law applies) droplets entrained by a gas flow (see ref. 2), we can verify:

• the centrifugation of the droplets by the predominant tangential velocity component,
• the flow tracing fidelity of particles in the fluctuating flow-field.

For tangential and radial velocity components of the droplet we have (see ref. 3):

$$C_{p,r} = \frac{D_f \cdot \omega_f^2 \cdot \rho_p \cdot D_p^2}{36 \cdot \mu_f} \qquad (at\ radius\ \tfrac{D_f}{2}) \quad (4)$$

$$C_{p,t} = \frac{D_f}{2} \cdot \omega_f \qquad (at\ radius\ \tfrac{D_f}{2}) \quad (5)$$

Thus the ratio of the two components is:

$$\frac{C_{p,r}}{C_{p,t}} = \frac{\omega_f \cdot \rho_p \cdot D_p^2}{18 \cdot \mu_f} \qquad (6)$$

Here:

$$C_{p,t} \cong C_{f,t} \qquad (7)$$

In our case, for the ratio $C_{p,r}/C_{p,t}$ we obtain the values given on table 2.

The values of the radial velocity of the particles do not exceed the order of magnitude of the radial and the axial velocity components of the afore-mentioned helices. Large droplets can not enter anyhow in the labyrinth glands-zone, being already centrifugated in the space S'. Smaller droplets will follow, to some extend, the helicoidal flow, but in any case centrifugation tends to move the droplets in the direction of the outer wall where large velocity fluctuations are present.

D_p	$1 \cdot 10^{-6}\ m$	$2 \cdot 10^{-6}\ m$	$5 \cdot 10^{-6}\ m$	$10 \cdot 10^{-6}\ m$
$\dfrac{C_{p,r}}{C_{p,t}}$	0,0025	0,010	0,0625	0,250

$$n_\odot = 9000\ min^{-1}$$
$$\rho_p = 860\ kgm^{-3}$$
$$\mu_f = 1.8 \cdot 10^{-5}\ kgm^{-1}s^{-1}$$

Table 2.

In this gland-zone close to the outer wall, the flow tracing fidelity of droplets has to be verified. Expressing the particle velocity in terms of the fluid velocity with the aid of an amplitude-ratio and a phase angle (see ref. 4), we obtain for our conditions the amplitude-ratios and the phase angles given on table 3.

These considerations show that particles of the micron-size will follow the fluctuations of the flow and can be transported in the undesired direction, in spite of a buffering-fluid-flow.

D_p	Frequency of fluctuations			
	1000 s^{-1}		5000 s^{-1}	
	Amplitude ratio	Phase angle	Amplitude ratio	Phase angle
$1.10^{-6}m$	1,000	$-1,0°$	0,996	$-5,0°$
$2.10^{-6}m$	0,998	$-4,0°$	0,944	$-19,0°$
$5.10^{-6}m$	0,917	$-23,5°$	0,417	$-65,0°$
$10.10^{-6}m$	0,497	$-60,0°$	0,114	$-83,0°$

Table 3.

6. CONCLUSIONS

- The diffusion-experiments show the possibility of an undesired transport of the oil-vapour by diffusion at reduced buffering-fluid velocities and also if only a few labyrinth-chambers are disponible.

- From the measurements with the Laser-Doppler-Velocimeter and with the aid of the visualizations we observe a double-helicoidal mean flow in the labyrinth-chamber. Turbulent velocity fluctuations are superposed to the mean flow. The intensity of the fluctuations increases when approaching the stationary wall and, mainly, the region of the gap.

- As theoretical considerations prove, droplets of the micron-size ($D_p \sim 10^{-6} m$) can accurately follow the fluctuations and move in this way in the opposite-direction to the imposed buffering-fluid-flow.

REFERENCES

1. H. L. Weissberg: "Theoretical aspects of back diffusion", ORNL Symposium on shaft seals for gas cooled reactor compressors and turbines,(16/17.12.1959)

2. J. O. Hinze: Turbulence (2nd edition), New York, McGraw Hill Book Co. ,(1975), Section 5.7-"Diffusion of discrete particles in a homogeneous turbulence"

3. J. H. Burson, E. Y. Keng and C. Orr: "Particle dynamics in centrifugal fields", Powder Technol., vol. 1, (1967), pp. 305-315

4. A. T. Hjelmfelt and L. F. Mockros: "Motion of discrete particles in a turbulent fluid", Appl. Sci. Res., vol. 16, (1966), pp. 149-161

DISCUSSION

B.Wrigley, UK

Please comment on the effect of cell proportion on oil transport.

Authors' Reply

Our tests have, up to now, been performed with only one geometry of approximately 1:1-ratio of height to breadth of the labyrinth chambers. Of course, the mass transfer coefficient k_m depends on geometrical parameters; effectively it may be expressed as a mass-transfer Stanton number St_m.

$$St_m = k_m/U = f(Re, C_a/U, geometry).$$

Our tests have resulted in the order of magnitude of $k_m = 0,007$, nearly independent on Reynolds number, slightly dependent on ratio C_a/U, but certainly influenced by geometry. We are examining this by theory and experiment. Let us remark that the mentioned value is of the same order of magnitude, as, but higher than an expected turbulent mass transfer value; the increase is due to the described flow pattern.

STUDIES ON VIBRATIONS STIMULATED BY LATERAL FORCES IN SEALING GAPS

by

H. Benckert
Research Assistant
and
J. Wachter
Professor

Institut für Thermische Strömungsmaschinen
Universität Stuttgart
Pfaffenwaldring 6
D-7000 Stuttgart 80 (Vaihingen)
Germany

SUMMARY

In high power density turbomachines vibrational problems arise. One reason is caused by exciting forces in sealing gaps. This effect can be seen in the unsymmetrical pressure distribution within the sealing. In order to get fundamental knowledge of the flow in sealing gaps a test-facility for labyrinths was installed, which allows to investigate several labyrinth configurations. The following parameters can be varied: the shaft rotation, the pressure difference on the seal, the entry-swirl, the eccentricity of the rotor and the geometry of the labyrinth.

The presented investigations show a systematic dependence of the excited lateral forces on these parameters. For a given labyrinth the corresponding force coefficient is related to the entry conditions of the flow and the pressure difference on the seal. Two examples of calculation demonstrate the application of the test results.

LIST OF SYMBOLS

c_{ao}	axial flow veloctiy before the labyrinth
c_{uo}	circumferential flow veloctiy before the labyrinth
D	rotor diameter
E_o^2	relative admission energy of the flow
e	rotor eccentricity (dimensioned)
F_B	reference force
h	height of the chamber
K_e	excitation constant
K_Q	lateral force spring coefficient
m	number of whirling chambers
p_a	static pressure after the labyrinth
p_o	static pressure before the labyrinth
$\Delta p_{st} = p_o - p_a$	differential pressure
Q	lateral force
R	restoring force
r	rotor radius
Δr	radial labyrinth clearance
t	spacing of the labyrinth
u_w	peripheral rotor speed
$= e/\Delta r$	relative eccentricity of the rotor
ρ	density of fluid
φ	peripheral angle

Subscripts:		Superscripts:	
o	refers to position before labyrinth	*	dimensionless value
i	at each chamber	¯	mean value
abs	total		
ges	summation over all chambers		
Q	lateral		
R	restoring		

INTRODUCTION

The economical requirements and the technical development led, on many technical fields, to bigger and bigger machine units. This applies especially in the case of the turbo-machine engineering due to the constantly increasing performance requirements. Self excited rotor vibrations, produced by the flow forces of the handled fluid, belong to the phenomena causing new operating problems. The origin of the exciting forces is, at the present, only partially known. Among others, the power proportional lateral forces, known under the designation "Steam Whirl Excitation", investigated by Thomas (1) belong to the causes of this occurrence which are being considered. The multiplicity of the vibrational phenomena observed on manufactured fluid machinery as well as on model tests, points to the fact that, besides the investigated clearance excitations, other exciting forces act on the rotor via the working fluid.

The search for the physical reasons of these vibrations out of rotational frequency lead to the flow occurrences in glands, sealing gaps, balance pistons and shroud bands. Even small unsymmetries in the pressure distribution on the above units give origin to forces, which are capable of lifting the weight of the rotor. The lateral force component of the resulting rotor load, caused by the uneven pressure distribution, can reach a vibration exciting extent.

Lomakin (2) shows that, in case of an eccentrical position of the shaft in the casing, variable flow resistances occur in the gap. The different flow speeds resulting from this fact cause an unsymmetrical pressure distribution with regard to the shaft center line and, therefore, lateral forces. Lomakin considers here the plain axial flow only (one-dimensional consideration). The circumferential flow and specially the influence of the shaft rotation are not taken into consideration. Domm and his collaborators (3) investigate the influence of the sealing gap at boiler feed pump impellers. The lateral forces are considered, which occur in case of smooth annular clearances and eccentrical shaft position, as well as their influence on the vibrational behaviour of the rotor. Alford (4) occupies himself with lateral forces in case of labyrinth seals. He is of the opinion that, in case of gap width variable with time, lateral forces occur, which act out-of-phase with regard to deflection. Depending on reduction or enlargement of the gap width in flow direction, exciting or damping forces appear, for which no basic explanation is given in this theory. The investigations (1, 5, 6) include, besides the sealing gap flows, also the effects of the uneven distributed blade forces, the influences of the bearings and other effects of the whole machine. The above works consider boundary conditions of the shroud band at the impeller of a turbine stage, and an incompressible flow being assumed.

It is known that the lateral forces of the shaft seal, less considered up-to-now, give much more reason for difficulties, the larger the power concentration of these machines becomes. According to manufacturers' statements, the number of operating problems with high pressure compressors due to vibrational excitations out of rotational frequency increased more and more, lately, which origin is assumed to be in the gap flow phenomena, but also with stationary gas turbines of higher power, stability problems arose for the same reason.

In order to increase the availability of the machine units, a more and more exact and complex vibrational calculation is necessary. Hereto, the speed synchronous vibrations (unbalance vibrations) as well as the self excited vibrations out of rotational frequency must also be taken into consideration. The influence of the selected bearing arrangement (spring and damping coefficients) must also be taken into consideration, since, in case of plain bearing, oil film instabilities (oil whip) may lead to self excitation (7, 8). Besides of this, the knowledge of the self exiting mechanisms caused by flow is decisive, since these modify the stability limits of the rotor (9, 1, 5, 6). Pollmann and his co-workers (10) make a comparison of the various flow effects causing vibrations out of rotational frequency.

The purpose of the labyrinth investigations shown underneath is to determine the flow induced forces appearing in the sealing gaps. The results of the investigations lead to a lateral force excitation coefficient of the shaft seal, which, comparable with the excitation coefficient at the impeller, must also be included in the vibrational calculation. In opposition to the investigations made until now, the influence of the compressible flow in seals has been investigated separately, in order to allow a separation of these effects from the other self exciting causes (10).

LABYRINTH TEST-FACILITY, TEST PROGRAMME AND EVALUATION

For the investigation of various labyrinth configurations, a new test-facility, which operation began in 1976, was conceived at the Institut für Thermische Strömungsmaschinen of the Stuttgart University. Figure 1 shows the sectional drawing of the test-facility for labyrinths. Design and installation were made together with the firms belonging to the "Forschungsvereinigung Verbrennungskraftmaschinen e.V.", Frankfurt/Main, Federal Republic of Germany. The picture shows a labyrinth sealing gap (half labyrinth) with plain shaft and seal tops mortised in the casing. Each whirling chamber of the labyrinth casing is provided in circumferential direction with twelve statical pressure measuring holes. The flow enters the test seal from above, several inflow assemblies being available, with which different entry swirls of the seal can be produced. The test medium is air which is expanded to the ambient conditions. The speed of the rotor is

continuously adjustable ($u_{w, max}$ = 150 m/s). The rotor eccentricity can be arbitrarily selected within the range of the mean gap width (Δr).

The collection of the total of 216 measuring data, pressure measuring data alone are in number of 188, is made with a measuring data collection computer. A central processing unit takes over the control of the measuring unit installed at the test facilities and processes the obtained digital measuring data for pressures, temperatures, leakage flows through the seal and rotor speed. The data output for the test evaluation at the main computer can be selected.

The labyrinths to be tested are sketched on figure 2. The following test parameters can be varied:

The entry conditions before the inlet tooth (p_o, c_{uo}).

The eccentricity of the rotor from the concentric position (ε = 0) up to the relative eccentricity ε = 0,9.

The velocity and direction of rotation of the rotor.

The number of whirling chambers (m) of each type of construction.

The geometry of the whirling chamber (Δr, t, h) of each type of construction.

The investigations on the first two labyrinth configurations (Type a and b) are completed; at the present, the test evaluation for the version b with four and two whirling chambers, respectively, is being made.

Figure 3 shows now typical dimensional pressure distributions in a labyrinth gap seal with three whirling chambers. The location of the pressure measuring planes in the chambers is sketched in the diagram. In order to determine possible pressure variations over the depth of the whirling chambers, two measurings on the peripheral line take place for each chamber (seal top slip t = 8 mm, pressure measuring holes spacing 4 mm). Over the periphery of the labyrinth, the pressures are measured in 30 degrees distances; peripheral angle φ = 0° is the position of the widest gap, φ = 180° is the location of the narrowest gap. The measuring data shown on the diagram are the mean data of each of the two measuring holes. The pressure variations of both data are less than one percent of the differential pressure acting on the seal.

Parameter of the pressure distribution presentation shown is the relative admission energy of the flow E_o^*. The full lines (point-symbol) are the result of a plain axial entry flow (E_o^* = 0), the stroke curves for a swirl entry flow (E_o^* = 0,22). The eccentricity is 0,7, the measurings take place with rotor in stand still condition. The pressure distribution for the axial entry flow has, in the first chamber, the characteristic distribution according to Lomakin (2), i. e., the highest pressure in the narrowest gap. This effect is inverse in the second chamber, in the third chamber the pressure is almost equally distributed over the periphery. For the swirl entry flow the maximal pressure is located before the narrowest gap, the pressure variations in the chamber are more evident.

The normal loads on the shaft (R and Q) shown, are the components of the loads resulting from the pressure distributions. The restoring force R acts against the rotor eccentricity, i.e., centering, the lateral force Q vertical to the eccentricity. Since the pressure distributions in the chambers ($p_i(\varphi)$) are periodic over the rotor periphery, the evaluation is made possible by means of a Fourier's development, the pressure progress being presented by a trigonometrical series. The resulting normal forces are obtained by addition over all chambers to:

Lateral force

$$Q = \sum_{i=1}^{m} r \cdot t \cdot \int_0^{2\pi} p_i(\varphi) \sin\varphi \, d\varphi$$

Restoring force

$$R = -\sum_{i=1}^{m} r \cdot t \cdot \int_0^{2\pi} p_i(\varphi) \cos\varphi \, d\varphi$$

For the pressure integration in the individual chambers, only the terms of the basic frequency are then of interest. The advantage is that small pressure measuring errors, perceptible by means of terms of higher degree, do not appear.

However, for a systematic test evaluation, a relative presentation is more recommendable. Fig. 4 shows the most important relations. The reference force for the dimensionless labyrinth mean values of the lateral and restoring forces is as follows:

$$F_b = r \cdot m \cdot t \cdot \Delta p_{st} \quad (N)$$

The pressure distributions are made dimensionless by means of the static pressure difference acting on the seal (Δp_{st}). The expansion in the labyrinth is, with this, standardized for all the pressure conditions between 1 and 0. The relative admission energy of the flow E_o^* into the labyrinth represents the relation of the flow energy in circumferential direction (+ u_w - direction of rotation of the rotor) to the flow energy in axial direction (Δp_{st}). The coefficient F_o^* is designated as dimensi .s spring constant, since it indicates the rise of the force displacement curve in dependence on the relative admission energy of the flow. The dimensional normal forces on the shaft are then obtained from the product of the specific relative spring constant with the relative rotor

eccentricity and reference force.

FORCES AND LATERAL FORCE EXCITATION CONSTANTS IN LABYRINTHS WITH SWIRL ENTRY FLOW

The relative pressure distribution is represented in Fig. 5 in dependence on the swirl entry flow for a constant axial pressure difference of a half labyrinth with 12 whirl chambers. The rotor eccentricity for the three represented tests is constant with $\varepsilon = 0,8$. The pressure variations in the individual chambers increase with rising relative admission energy of the flow. Compared with the axial flow ($E_o^w = 0$) the maximal pressure for $E_o^w > 0$ moves to a point before the narrowest gap, and the rotor load resulting from the pressure distribution gives the restoring and the exciting lateral force. The most important forces occur in the first whirl chamber, then a sudden reduction of the circumfefential flow takes place, the pressure variations after the 7th chamber are thus detectable only for large E_o^w values.

While Fig. 5 shows the parameter E_o^w, the second decisive inflow coefficient, the rotor eccentricity, is made evident in Fig. 6. For a 7-chamber labyrinth sealing gap the pressure distributions for the concentric and two eccentric rotor positions are shown. In case of concentric shaft position ($\varepsilon = 0$) the pressure on the periphery of the whirling chamber is constant. Thus, the larger the rotor eccentricity becomes, the more intensive will be the pressure variations, i.e., the resulting lateral and restoring forces on the shaft.

These force-displacement curves are graphed for the 12-chamber half labyrinth in Fig.7; the parameter is the relative admission energy of the flow. The mean relative restoring force R is slightly negative over all 12 chambers, because only the first whirling chamber has a positive restoring force. Accordingly the mean labyrinth value of the restoring force varies around zero depending on the number of chambers, and is therefore of subordinate importance compared with the lateral force under swirling entry.

The lateral forces on the shaft increase linearly with the rotor eccentricity up to deflections of $\varepsilon = 0,6 - 0,7$. As the shaft displacement increases further (though this does not happen in actual machine operation) the curve flattens out slightly. For $\varepsilon = 0$ the characteristic curves must pass through the zero. Any zero errors arising can thus be eliminated by parallel displacement. This is made clear by the curve $E_o^w = 0,083$.

The slope of the lateral force-displacement curves plotted depends only on the relative admission flow energy, i.e. on the ratio of the entry swirl energy to the total pressure gradient. This statement is valid regardless of the number of whirling chambers or the shape of a seal. Fig. 8 shows test results for the labyrinth type 'b' with six chambers. The mean gap width Δr has been halved compared with the half labyrinth. In addition a few test points have been plotted with negative rotor eccentricity, in order to show the linear zero passage of the lateral force-displacement curves.

The slopes of these characteristics, which are linear up to a rotor eccentricity $\varepsilon = 0,6$, give the dimensionless lateral force spring coefficient K_o^w (E_o^w) (relative labyrinth mean) for the particular labyrinth. The dimensioned lateral force then emerges as the product of the lateral force spring constant with the eccentricity (ε) and reference force ($\Delta p_{et} \cdot r \cdot m \cdot t$). With equal relative admission flow energy E_o^w the relative lateral force is greater with a small number of seal chambers than with more chambers, because the mean is taken over the labyrinth. It can be shown that the pattern of the lateral force across the individual chambers is influenced only by the relative admission flow energy, irrespective of the number of whirling chambers in the seal. The marked drop in the lateral forces occurs in the first chambers, as is documented also by the pressure distributions shown. The reason lies in the retardation of the circumferential flow by friction and vortex losses. At the same time, however, the axial veloctiy increases steadily, so that the chamber-specific ratio of swirl to axial component becomes progressively smaller, i.e. the flow angle to the axial direction becomes ever smaller. On the labyrinth gap seal investigated it can be observed that after the 10-12th whirling chamber there are practically no longer any lateral forces due to swirling entry flow, because the c_u component of the flow has been dissipated.

Fig. 9 summarizes the investigations for swirling flow into the labyrinth with characteristic curves for various labyrinth types having different numbers of whirling chambers in each case. The lateral force spring constant K_o^w is plotted against the relative admission energy E_o^w to double logarithmic scales. Between the spring constant K_o^w and the admission energy E_o^w there exists a parabolic relation. The influence of the number of chambers (m) is taken into account roughly reciprocally. It should be noted that the symbols entered (o, x) are not individual measuring points but the results of evaluating the associated lateral force-displacement characteristics, which in turn consist of seven different double measuring points for the various eccentricities. This evaluation route is made clear by Figs. 7 and 8.

The specimen calculation in Fig. 10 shows how the results presented previously may be used to dimension and calculate contactless seals. The numerical example relates to a labyrinth seal commonly employed in turbine engineering. As already explained, it is sufficient for the calculation to take the first 12 whirling chambers, because after these no more lateral forces appear due to swirling entry flow into the seal. The static pressure gradient on the 12 chambers is thus $p_{12} = p_o - p_{13}$. Apart form this it is important to know the admission state before the first pressure peak. From these data the relative admission energy E_o^w can be calculated. With this and the number of chambers

(m - 12 in the example) the dimensionless lateral force spring constant can then
be determined from the characteristics in Fig. 9. For an assumed shaft displacement
of e = 150 µm, i.e. ε = 0,3, the lateral force Q normal to the rotor deflection
then emerges. The dimensional exitation or spring constant figuring in the vibra-
tion calculation is the quotient of lateral force and deflection.

INFLUENCE OF SPEED ON THE LATERAL FORCE EXCITATION CONSTANTS IN
LABYRINTHS WITH AXIAL (NON-SWIRLING) ADMISSION FLOW

The foregoing remarks are confined to the lateral force excitation by the
swirling inflow into the seal. But the influence of the peripheral shaft speed cannot
be ignored either. It depends on the magnitude of the circumferential flow component,
which is determined by the shaft rotation. As a simplification it may be said that the
c_u component is a function of the ratio between the retarding surfaces (housing) and the
propelling surfaces (rotor) in the labyrinth seal.

Comparison of the labyrinth configurations (Fig. 2) shows that this ratio differs
considerably in the individual types. For labyrinth type 'b' the ratio is high, whereas
in type 'c' the c_u-propelling surfaces of the rotor predominate. In type 'c' the two
components are equal. The configurations were chosen deliberately to enable the influ-
ence of speed on the lateral forces in eccentric labyrinth seals to be defined with
general validity. Below the results with a comb groove seal having seal strips mortised
into the rotor are given.

Graphed in Fig. 11 are the lateral force-displacement characteristics of a laby-
rinth with 10 whirling chambers and axial flow admission, constant rotor peripheral
speed and variable axial pressure gradient. The sense of rotor direction has been
changed to enable the exact slope of the characteristics (K_Q^M) to be determined. Any zero
errors or errors in the seal geometry (ε = 0,1 ≙ 25 µm) are eliminated in this way. Cor-
responding to the peripheral rotor speed of u_W = ± 75 m/s illustrated as an example,
further speed tests with reversed rotation were examined for the various rotor eccen-
tricities and pressure differences on the seal.

Comparable with Fig. 9 the lateral force spring constants obtained in this way
yield characteristics for the various peripheral rotor speeds (Fig. 12). The excitation
constant is plotted against the reciprocal differential pressure at the seal to double
logarithmic scales. A parabolic relation exists. If the parallel straight-line charac-
teristics are compared, the linear speed influence of the shaft rotation on the lateral
force spring constant is revealed. Fig. 13 shows this for the six-chamber seal. Since
the mean is taken over the number of chambers in accordance with Fig. 4, approximately
the same excitation constants result for equal speed and pressure difference. The slight
increase in these values compared with the results in Fig. 12 is due to the preliminary
vortex before the first seal strip caused by rotor friction. With six whirling chambers
this has a greater impact than with ten. Also shown in Fig. 13 is the influence of the
location of the static pressure measuring holes in the whirling chambers, in order to
make it clear that no force changes of consequence occur.

In Fig. 14 the excitation constant due to speed has been estimated, as it emer-
ges from the above results under axial (non-swirling) inflow to the seal. The labyrinth
seal has strips mortised into the shaft. The number of chambers and pressure difference
correspond to the example in Fig. 10, though the mean gap width has been halved. As the
excitation constant due to rotor rotation in the dimensionless form does not depend on
the number of swirling chambers, for the reference force F_B the total number of chambers
(m = 50) and the total pressure gradient must be taken into account. Although the later-
al force is less compared with the calculation affected by swirl (u_W ≈ 0 m/s), a greater
lateral force excitation constant (low Δp_{st}) emerges in the second specimen calculation,
because the rotor displacement is only half as much with the same relative eccentricity.
However this remains true only for the above example, because for other machine para-
meters (large Δp_{st}) there is a very low K_Q^o (u_W, Δp_{st}). When determining the lateral
force spring constant, with constant peripheral speed the value $1/\Delta p_{st}$ is decisive.

CONCLUSION

In eccentric labyrinth seals, unequal pressure patterns occur over the circum-
ference of the seal due to the circumferential components of the flows in the whirling
chambers. The total force on the rotor resulting from these pressure distributions has
been determined for various labyrinth configurations. It could be proved that the com-
ponent R of the total force lying in the deflection plane of the rotor is of secondary
importance. On the other hand the lateral force component Q acting perpendicularly to
the rotor deflection constitutes a vibration-exciting factor in the rotor dynamics
which must be taken into account. As the investigations show, lateral force excitation
constants can be developed for the vibration calculation. In the presentation form
adopted, a distinction has been made between the causes of the circumferential flow.
For the swirling flow into the labyrinth the lateral force spring constant should be
represented systematically as a function of the relative admission energy E_o^M, regardless
of the labyrinth type. In comparable form the influence of the shaft rotation on the
lateral force excitation constant may be demonstrated. Future work ought to supplement
these results so that the expected lateral and restoring forces with eccentric shaft
location for labyrinth configurations to be designed can be calculated already at the

draft design stage. The resulting lateral force excitation constants will then allow
better prediction of the vibration behaviour of turbomachines.

REFERENCES

(1) Thomas, H.J.:   Unstable Oscillations of Turbine Rotors Due
                             to Steam Leakage in the Clearances of the
                             Sealing Glands and the Buckets.
                             Bulletin Scientifique, A.J.M. 71, 1958,
                             pp. 1039-1063.

(2) Lomakin, A.A.:   Bestimmen der kritischen Drehzahl des Pumpen-
                             läufers unter Berücksichtigung der Kräfte, die
                             in Dichtungen entstehen.
                             Maschgiz, Band 5, 1958.

(3) Domm, N.; Dernedde, R.   Der Einfluß von Stufenabdichtungen auf die
     and Handwerker, Th.:   kritische Drehzahl von Kesselspeisepumpen.
                             VDI-Berichte, Nr. 113, 1967.

(4) Alford, J.S.:   Protecting Turbomachinery from Self-Excited
                             Rotor Whirl.
                             Transactions ASME, J. of Eng. f. Power,
                             October 1965, pp. 333-344.

(5) Urlichs, K.:   Durch Spaltströmungen hervorgerufene Quer-
                             kräfte an den Läufern thermischer Turbo-
                             maschinen.
                             Diss. TU München, 1975.

(6) Wohlrab, R.:   Experimentelle Ermittlung spaltströmungsbe-
                             dingter Kräfte an Turbinenstufen und deren
                             Einfluß auf die Laufstabilität einfacher
                             Rotoren.
                             Diss.TU München, 1975.

(7) Kollmann, K. and   Radial-Gleitlager mit beliebiger Schmier-
     Schaffrath, G.:   spaltform.
                             Motortechnische Zeitschrift 29, 1968, 10
                             pp. 401-408.

(8) Glienicke, J.:   Experimentelle Ermittlung der statischen
                             und dynamischen Eigenschaften von Gleit-
                             lagern für schnellaufende Wellen. Einfluß
                             der Schmierspaltgeometrie und der Lagerbreite.
                             VDI-Fortschrittsberichte, Reihe 1, Nr. 22, 1970.

(9) Pollmann, E.:   Stabilität einer in Gleitlagern rotierenden
                             Welle mit Spalterregung.
                             VDI-Fortschrittsberichte, Reihe 1, Nr. 15, 1969.

(10) Pollmann, E.;   Flow Excited Vibrations in High-Pressure Turbines
     Schwerdtfeger, H.   (Steam Whirl).
     and Termühlen, H.:   Turbomachinery Developments in Steam and Gas
                             Turbines ASME, Gas Turbine Division Atlanta
                             Georgia, 1977, pp. 75-87.
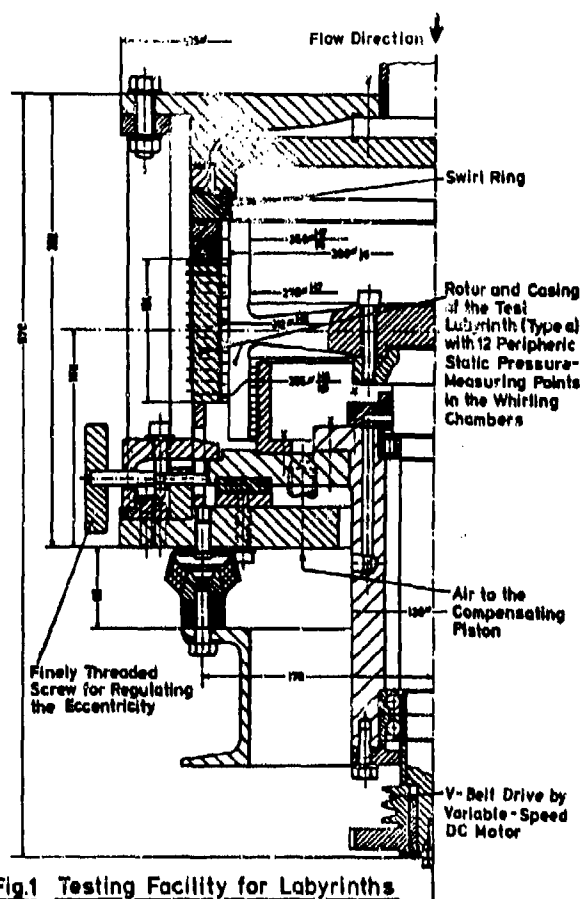
Fig.1 Testing Facility for Labyrinths

Labels in Fig.1:
- Flow Direction
- Swirl Ring
- Rotor and Casing of the Test Labyrinth (Type a) with 12 Peripheric Static Pressure-Measuring Points in the Whirling Chambers
- Air to the Compensating Piston
- Finely Threaded Screw for Regulating the Eccentricity
- V-Belt Drive by Variable-Speed DC Motor
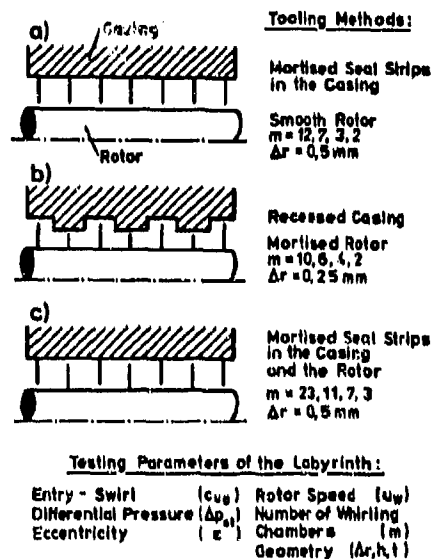
Fig.2 Tested Labyrinth Patterns

Tooling Methods:

a) Casing / Rotor — Mortised Seal Strips in the Casing, Smooth Rotor, m = 12, 7, 3, 2, $\Delta r = 0,5$ mm

b) Recessed Casing, Mortised Rotor, m = 10, 6, 4, 2, $\Delta r = 0,25$ mm

c) Mortised Seal Strips in the Casing and the Rotor, m = 23, 11, 7, 3, $\Delta r = 0,5$ mm

Testing Parameters of the Labyrinth:

Entry-Swirl (c_{u0})   Rotor Speed (u_w)
Differential Pressure (Δp_{o1})   Number of Whirling Chambers (m)
Eccentricity (ε)   Geometry ($\Delta r, h, t$)
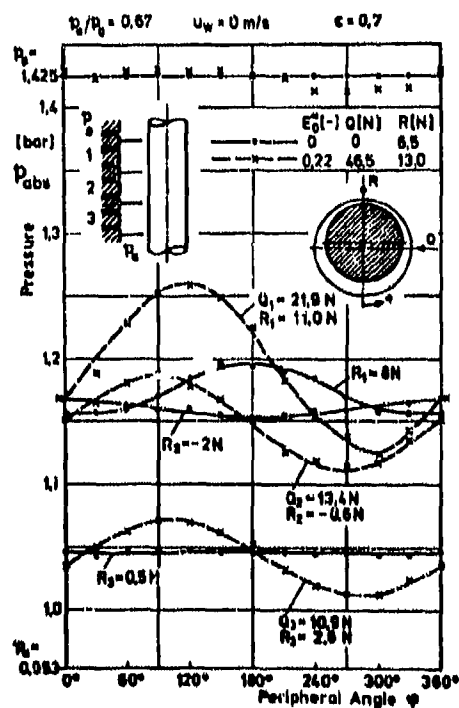
Fig.3 Pressure Distributions and Forces in a Half-Labyrinth (m = 3) with Eccentric Rotor

Relative Pressure

$$p_i^*(\varphi) = \frac{p_i(\varphi) - p_a}{\Delta p_{st}}$$

Reference Force

$$F_B = r \cdot m \cdot t \cdot \Delta p_{st}$$

Relative Admission-
Energy of the Flow

$$E_0^* = \frac{\frac{\rho_1}{2} \cdot c_{u0}^2}{\Delta p_{st} + \frac{\rho_1}{2} \cdot c_{u0}}$$

	Lateral Force	Restoring Force
(for each Chamber)	$a_i^* = \int_0^{2\pi} p_i^*(\varphi) \sin\varphi \, d\varphi$	$R_i^* = -\int_0^{2\pi} p_i^*(\varphi) \cos\varphi \, d\varphi$
Relative Load	$a_{ges}^* = \sum_{i=1}^{m} a_i^*$	$R_{ges}^* = \sum_{i=1}^{m} R_i^*$
(Mean Value)	$\bar{a}^* = a_{ges}^*/m$	$\bar{R}^* = R_{ges}^*/m$
Nondimensional Spring Coefficient	$\bar{K}_Q^*(E_0^*) = d\bar{a}^*(E_0^*)/d\varepsilon$	$\bar{K}_R^*(E_0^*) = d\bar{R}^*(E_0^*)/d\varepsilon$
Dimensioned Forces in the Seal	$Q = \bar{K}_Q^*(E_0^*) \cdot \varepsilon \cdot F_B \quad$ (N)	$R = \bar{K}_R^*(E_0^*) \cdot \varepsilon \cdot F_B \quad$ (N)

Fig.4 Calculation of the Lateral and Restoring Force

Fig.5 Pressure Distribution in an Eccentric
Half-Labyrinth (m = 12) for Different
Relative Admission-Energies of the Flow
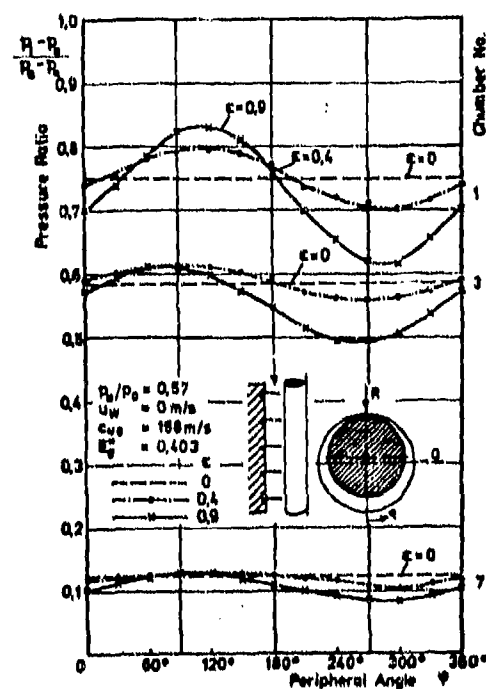
Fig.6 Relationship between the Rotor Eccentricity
and the Pressure Distribution in a
Half-Labyrinth (m = 7)
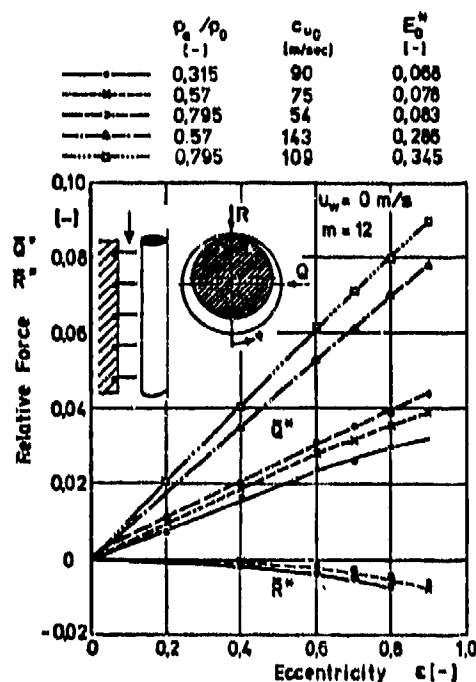
Fig. 7 Relative Lateral and Restoring Force for a Half-Labyrinth as a Function of the Rotor Eccentricity
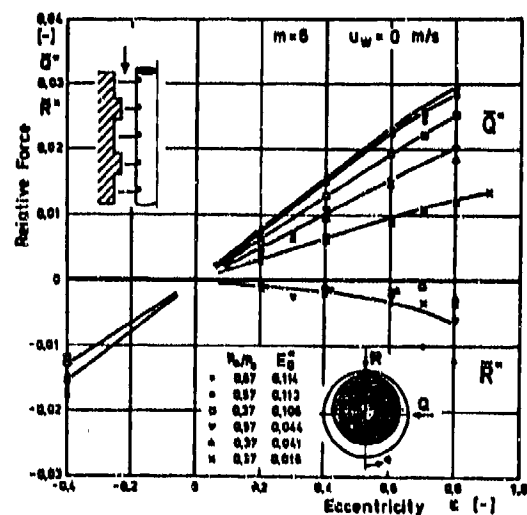
Fig. 8 Force - Eccentricity - Characteristics of a Labyrinth
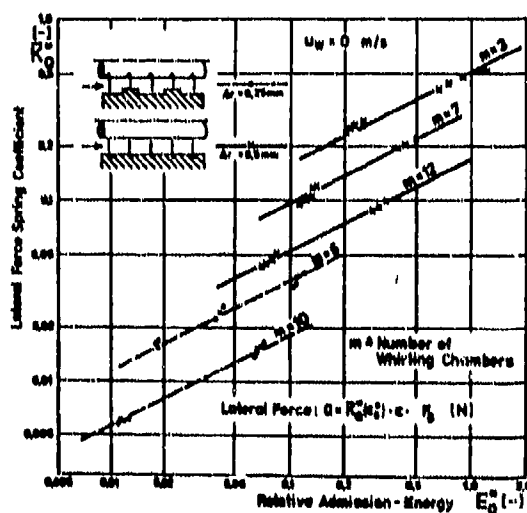
Fig. 9 Lateral Force Spring Coefficients for Different Labyrinth Patterns as Function of the Relative Admission - Energy of the Flow
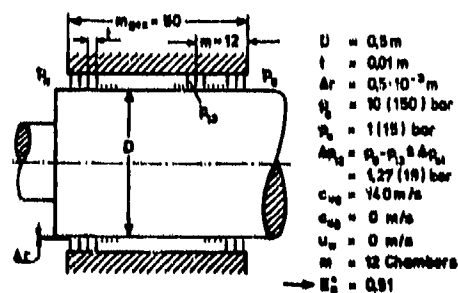
Fig. 10 Example for the Calculation of the Lateral Force due to Entry - Swirl in an Eccentric Half - Labyrinth
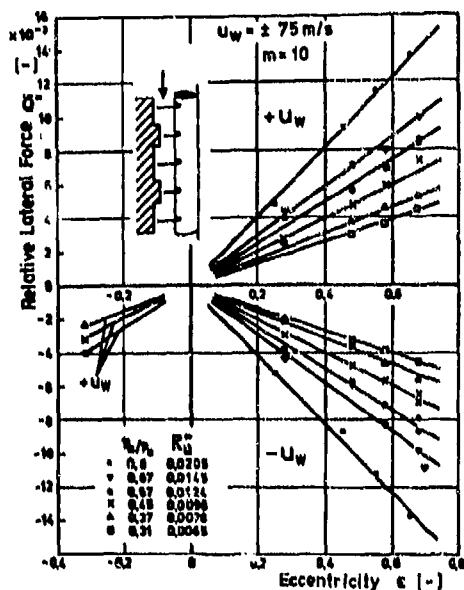
Fig.11 Lateral Force Characteristics of a
Labyrinth with Axial Flow Admission and
Reverse of the Shaft Rotation
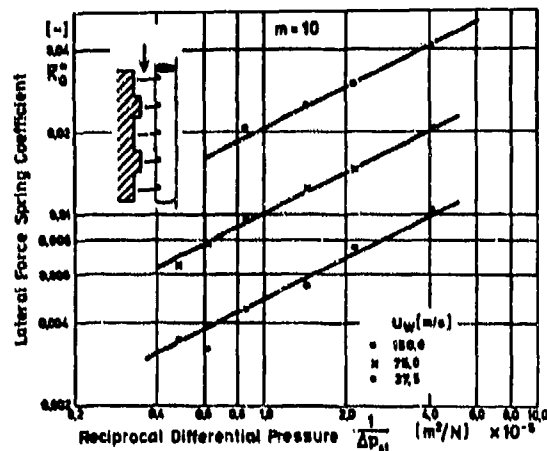
Fig.12 Lateral Force Spring Coefficients
for Different Shaft Rotations
with Axial Flow Admission in
the Labyrinth (m=10)
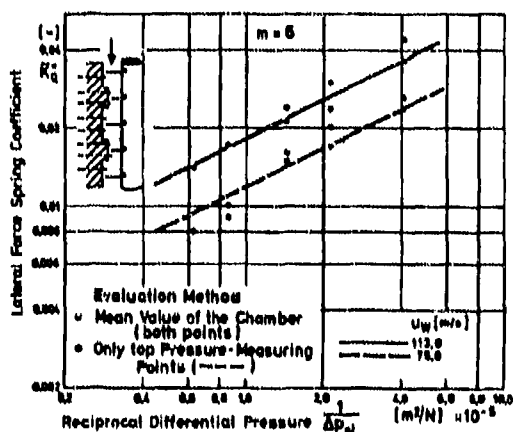
Fig.13 Lateral Force Spring Coefficients
for Different Shaft Rotations
with Axial Flow Admission in
the Labyrinth (m=6)

Fig.14 Example for the Calculation of the
Lateral Force due to Shaft Rotation
(c_ue = 0 m/s) in an Eccentric-Labyrinth

DISCUSSION

R.A.van den Braembussche, Belgium

In your paper you have studied parameters influencing the forces in a stationary (non-swirling) case. However there is also a controversial and apparently very important parameter in the case of a swirling rotor, namely the difference in clearance between the inlet and the outlet of the seal[4]. Have you done or do you intend any measurements about this parameter, or could you comment on his influence.

Authors' Reply

We have also studied the different parameters by rotation of the rotor. These results are reported in this paper, but only for the second type of labyrinth. The investigation of the labyrinth gap with a smooth rotor has shown no noticeable exciting lateral forces by axial flow admission and rotation of the rotor.

Measurements with variable clearance between the inlet and the outlet of the seal (two fins, one chamber) are not done until now. In operating turbomachines this type of seal is normally not used and therefore it is not planned to test this parameter in our next test program in the near future. The influence of the variable clearance has to be investigated due to the two reasons of the exciting forces. The lateral force, induced by the entry swirl, is increasing with the leakage stream by the same entry conditions. The effect is just opposite by the lateral force due to the rotor rotation without entry swirl. The connection of these two phenomena will give the comparison with Reference 4. In contradiction to Reference 4 the influence of the clearance variation between inlet and outlet is described by Spurk and Keiper.[*]

D.A.Campbell, UK

Referring to the Authors' Figure 2, the test configuration (a) has the sealing fins on the outer static member with a smooth rotor. This arrangement is not normally used in aero-gas turbines and it would therefore be useful to repeat the tests with the fins on the rotor and a smooth stator. This would allow comparison with configuration (b) to determine the effect of steps in the outer member.

Authors' Reply

It is planned to test these configurations too. We expect to get the same lateral forces for the investigations with entry swirl and without rotation of the rotor, when the geometry of the seal is equal to the type (a) of Figure 2. But these studies will show, that the influence of the rotor speed for this new type will be very important.

H.Zimmermann, Germany

Have you done theoretical investigations in parallel to your very elaborate measurements?

Authors' Reply

In the first step the Institute has done theoretical investigations about the numerical calculation of the flow in eccentric smooth gap seals. At the moment parallel to our experimental studies further theoretical work is done. It is possible to calculate the lateral force, but more information is needed on the coefficients for the various types of labyrinths. We want to get these values by our tests. Then a precise theoretical calculation of the exciting forces in sealing gaps can be performed.

H.Zimmermann

Do you know of any damage done to a turbomachine because of this effect?

Authors' Reply

Yes, some instability problems, due to these effects, are known. In Reference 6 a steam turbine is described with leakage flow excited vibrations. By disturbing the entry swirl in the seal and the circumferential flow in the chambers of the labyrinths, it was possible to operate the machine without vibrational problems. The same effects are observed in turbo-compressors with high power density.[†] The damping of the machinery system was going negative before reaching normal speed by exciting vibrational forces due to the lateral forces in sealing gaps.

H.L.Stocker, US

How does the shape of the seal cavity affect your results?

Authors' Reply

Until now it is not possible to determine this effect exactly. We suppose, that the height of the chamber in connection to the clearance of the sealing fins is most important. With constant clearance the exciting lateral force will increase by smaller height.

---

[*] J.H.Spurk and R.Keiper: Selbsterregte Schwingungen bei Turbomaschinen infolge der Labyrinthströmung. Ingenieur-Archiv. 43 (1974), pp.127-135.

[†] W.Aicher, P.Jenny and H.Roduner: Untersuchungen an Turbokompressoren: Rotorschwingungen, Schaufelschwingungen, Versuche mit schweren Gasen. Sulzer-Forschungsheft 1978, pp.11-18.

THE CONTRIBUTION OF DYNAMIC X-RAY TO GAS TURBINE AIR SEALING TECHNOLOGY

BY

P.A.E. Stewart and K.A. Brasnett

ADVANCED PROJECTS DEPARTMENT

ROLLS-ROYCE LIMITED

P.O. BOX 3

FILTON

BRISTOL

SUMMARY

Rolls-Royce have developed a Radiographic Technique to study the behaviour of Components particularly seals, during the full range of Gas Turbine operation. This technique has proved very powerful in its application to a wide range of engines, particularly during transient conditions.

INTRODUCTION

Historically, the measurement of air seal clearance, particularly at the tips of compressors or turbines, has been carried out using abradable probes. The data retrieved from such devices is very limited. More recently work has been carried out to determine the proximity of the rotating component by building a sensor into the fixed component. Measurements of capacitance can be calibrated to give clearance measurement. Another device is the Fenlo type probe used at Rolls-Royce which uses a motor drive to set a spark gap between a wire probe and the blade tip. An alternative is the optical type of probe using laser light which may be stroboscopically actuated to impinge on selected blades. The reflected light is collected by an electro-optic device and the data is processed to give clearance information.

All these techniques require engine modification and special engine builds, they are also difficult to install in many instances.

DEVELOPMENT OF DYNAMIC RADIOGRAPHY

The application of high energy X-radiography has been pioneered by Rolls-Royce to provide more detailed studies of component flextures and two dimensional clearances not possible with standard devices. It has also been a philosophy of our work that it should be possible to use the equipment on any engine for problem identification and study without special modification. The provision of such a capability furnishes us with an excellent front line diagnostic instrument. (Ref.1).

The development toward this capability commenced with low energy (300 KV) X-ray equipment, flash pulsed X-ray equipment of nanosecond duration and medium energy (2.3 MeV) and radioactive isotopes of medium energy up to 2 MeV and limited X-ray output (12 rads/hr). This early work showed the necessity for a higher X-ray energy level of up to 8 Megavolts (optimum for thick steel sections) and an intense continuously pulsed output of X-rays. It had earlier been supposed that nanosecond duration exposures were necessary to arrest the motion of components within turbine engines. However, the experiments with isotopes showed that the image did not substantially suffer degradation due to movements including vibration, and therefore long exposures were acceptable.

The experience thus gained led to the specification of a radiographic electron linear accelerator. This is a pulsed X-ray source with a pulse repetition frequency range between 50 and 500 pulses per second. Stroboscopic techniques may be used in which sensed engine rotational speeds trigger single pulses to build up images of specific components.

Following satisfactory trials in September, 1970, on the Olympus 593 where the movement of H.P. Compressor Labyrinth seals were clearly seen and H.P. Turbine Root Seals (Fig.1), a Radiation Dynamics Limited 'Super X' linac (Fig.2) was purchased with an X-ray output of 1500 rmm and energy level of 8 MeV. This equipment has been extensively used at Rolls-Royce on over 20 different engine projects, with about 70 installations. Specially prepared Linac Test Sites have been provided at the Main Work Centres at Nottingham, Coventry, Cheltenham and Bristol serving all Aero Engine Division Centres and the Industrial and Marine Gas Turbine Division.

As a result of this activity over 18,000 radiographs are now available for detailed analysis covering all phases of operation of the engines under study including steady states and a variety of transient engine meanoeuvres.

Radiographs can be produced with exposure times of tenths to tens of seconds, providing a time averaged image of a specific engine condition. A very large number of such radiographs would be required to cover a full engine operating envelope. It is therefore necessary 'a priori' to determine a limited number of conditions in an engine testing cycle when exposures should be made.

Thus a qualitative system was devised using X-ray television (The Delcalix) which provided a constant flow of images with an effective exposure duration of 1/25th second

(Fig.3). This capability allows the identification of the most important conditions which may then be recorded by film radiography for detailed analysis. The total Radiography system is shown schematically in Figure 4. (Ref.2).

It is our practice to first radiograph the engine when 'cold' and static, thus providing an image which serves as a reference. Any subsequent radiographs made with the engine running are compared with this cold static and the relative movements of the components are determined. This technique assumes that the radiographic parameters are maintained constant for the two exposures, therefore quality control requires considerable attention.

In the initial stages of the work, single radiographs were obtained and measurements were made using a scale and light box. It was found that there was a high degree of subjectivity and the technique was not being best served. A policy was, therefore, adopted to develop the previously little known and used techniques of X-ray photogrammetry and to centralise the analysis of the images obtained into a single calibrated group of analyst using specialised equipment.

ANALYSIS OF RADIOGRAPHIC IMAGES

To be a useful tool to the Gas Turbine Engineer, X-ray imaging must provide two levels of information. Firstly, it is required to provide a qualitative 'feel' for the problem. Such 'feel' can be easily obtained by viewing the images on light boxes, overhead viewers, comparators or video monitors. Secondly, it is necessary to obtain quantitative data on the phenomena observed, and also to look for dimensional changes that are too small for qualitative assessment.

In Rolls-Royce a number of methods are used to quantify component movements from radiographic images. The most simple method utilizes co-ordinate measuring machines, low magnification optics and skilled photogrammetrists. A 'multi-reading' technique is adopted and statistical programmes used to calculate an average result and a confidence interval. Despite the apparent subjectivity of this method it provides reliable data with a typical 95% confidence interval of 0,10 - 0,15 mm. However, many problems require greater accuracy or a less subjective approach for difficult radiographs. A custom made video microdensitometer has been developed to provide a very accurate density profile across the area of interest (Fig.5). Suitable algorithms are used to define a measurement position within the profile. A confidence interval of 0,05 mm can be obtained by this method.

Images showing very low contrast can be improved by Digital Image Processing or Optical Processing Techniques, However, care is needed to avoid converting artifacts into recognisable 'engine components.' Thus a range of methods are available to produce dimensional data from radiographic images, and a further range of computing facilities are available to assist the engineer in interpretation of this data.

APPLICATION OF RADIOGRAPHY TO SEALS

Dynamic Radiography can be used to investigate virtually all seal areas of gas turbines without modification. For this reason, the minimum of 'a priori' knowledge is required with respect to the components to be investigated. A development engine experiencing difficulty can be radiographed within days, and various areas investigated until the problem is identified. Of course, there are limitations, the technique is primarily used to investigate only one two-dimensional plane (normally a vertical centre-line), and only data on mechanical matching of components is obtained. A very necessary part of any investigation is, therefore, to correlate radiographic data with that from conventional instrumentation and engine strip information.

The main influence on mechanical behaviour of components can be broadly categorized as those that are speed dependant and those that are temperature dependant with a corresponding thermal response time. These categories can be separately investigated by suitable choice of engine conditions to be monitored. For example, short duration exposures can be used to investigate speed dependant conditions during a fast acceleration or deceleration. Longer exposure times can be used during slow handling or in the stabilisation period after a change in condition. The X-ray television system is utilized as previously described in order to define the best conditions at which to produce radiographs.

Large format radiographs are used to obtain the greatest information from one exposure. For example, a radiograph of a turbine tip seal will also yield data on all associated disc seals and guide vanes. A fixed datum is also used to allow the measurement of 'absolute' movements. For example, the diametral change of static and rotating members of seals can be calculated in addition to the change in seal clearance.

Labyrinth air and oil seals can be readily imaged in most areas of the engine (Figure 6). Good data can be obtained on axial and radial movements of both static and rotating components. This data can be used to obtain optimum build setting of the seal, and also for profiling of the static component if large axial movements occur. If the axial movement is too great then the source can be identified and a solution devised. Difficulty is only experienced when the metal path thickness is over 250 mm as can be the situation when seals are inboard of discs, large flanges or test bed structure.

Shrouded blades are radiographically similar to labyrinth seals and only on larger engines does the metal path thickness become a severe restriction (Figure 7). On air cooled blades additional information is available on seal plates, pre-swirl rings or cover plates. Guide vane and root seal movements can also be observed.

Unshrouded blades present a different problem, the metal path thickness of the blade is small relative to total thickness to be penetrated. For this reason, it is not possible to reliably image the tip clearance. However, a close approximation to tip clearance changes can be obtained by measuring blade platform to inner casing dimensions (Fig.8). The unknown dimensional change of the blade aerofoil can be calculated with reasonable accuracy.

A number of other phenomena are worthy of note in relation to seal performance. Shaft lift on squeeze film bearings and shaft whirl can both be monitored radiographically. Casing distortion can also be observed by changing the orientation of the X-ray source. Bearing loads can be estimated by measuring deflection of support structures, and seal support diaphragms can be used in a similar manner to estimate pressure loads.

A CASE HISTORY

This particular radiographic exercise is used to illustrate many of the points discussed in previous sections. The problem concerns an industrial engine that experienced seizure following an emergency shutdown from full power. The high pressure spool remained seized for between four and six hours. Initially it was thought the casing was cooling quickly and clamping the blade tips, which were not released until the discs had also cooled. However, an increase in tip clearance had no effect on the seizure characteristics, and a decision was made to use radiography to diagnose the cause.

A number of seals were identified as being potential causes of seizure, including all blade tips (Fig.9). A full programme of radiography was completed, including engine handling and a simulated emergency shutdown. The radiographs were analysed, and the results given as orbital plots. Figures 10 and 11 show the results obtained at the turbine and compressor tips, clearly indicating no contact during the six hour cooling period. Figure 12 shows the result from the H.P. Turbine front disc seal, indicating a possible light engagement for a limited period. The results from the H.P. Turbine rear stub shaft seal however indicates the main cause of seizure. Figure 13 shows a radial tightening of the seal and a large axial movement, causing heavy engagement of the seal honeycomb. Consideration of results from the radiographs of engine handling clearly showed that the honeycomb causing seizure was not contributing to seal performance. Profiling of the seal could therefore be carried out with confidence that the problem could be overcome without reducing engine performance.

From initiation of this test it took just one month to demonstrate a successfully modified engine. A bonus was also available in terms of a detailed knowledge of every seal in the H.P. spool.

CONCLUSION

Gas turbine manufacturers continually strive for higher efficiency with lower maintenance costs – the dream of every operator. This target of improved efficiency leads to higher compression ratios, higher turbine entry temperatures and a requirement for improved sealing efficiency. The task of the designers is thus becoming increasingly difficult, particularly in the prediction of transient response.

Dynamic Radiography provides an ideal empirical feedback of engine mechanical behaviour. This information can be used to refine theoretical predictions, and to 'tune' each seal during engine development. The unexpected problem can also be identified with great speed, and sufficient data collected to enable rapid solution.

REFERENCES

1. "Engine Testing using advanced techniques" - P.A.E. Stewart
   The Aeronautical Journal, August, 1975, Vol.79, No.776, Pp 331-343.

2. "High Energy X-Ray TV of Gas Turbines on Test" - P.A.E. Stewart
   Chartered Mechanical Engineer, April, 1978, Vol.25, No.4 Pp.45.

Fig.1   These sections from two radiographs show clearly that a turbine seal disengages
axially at one engine condition, although normal at another.
The shift can be measured accurately
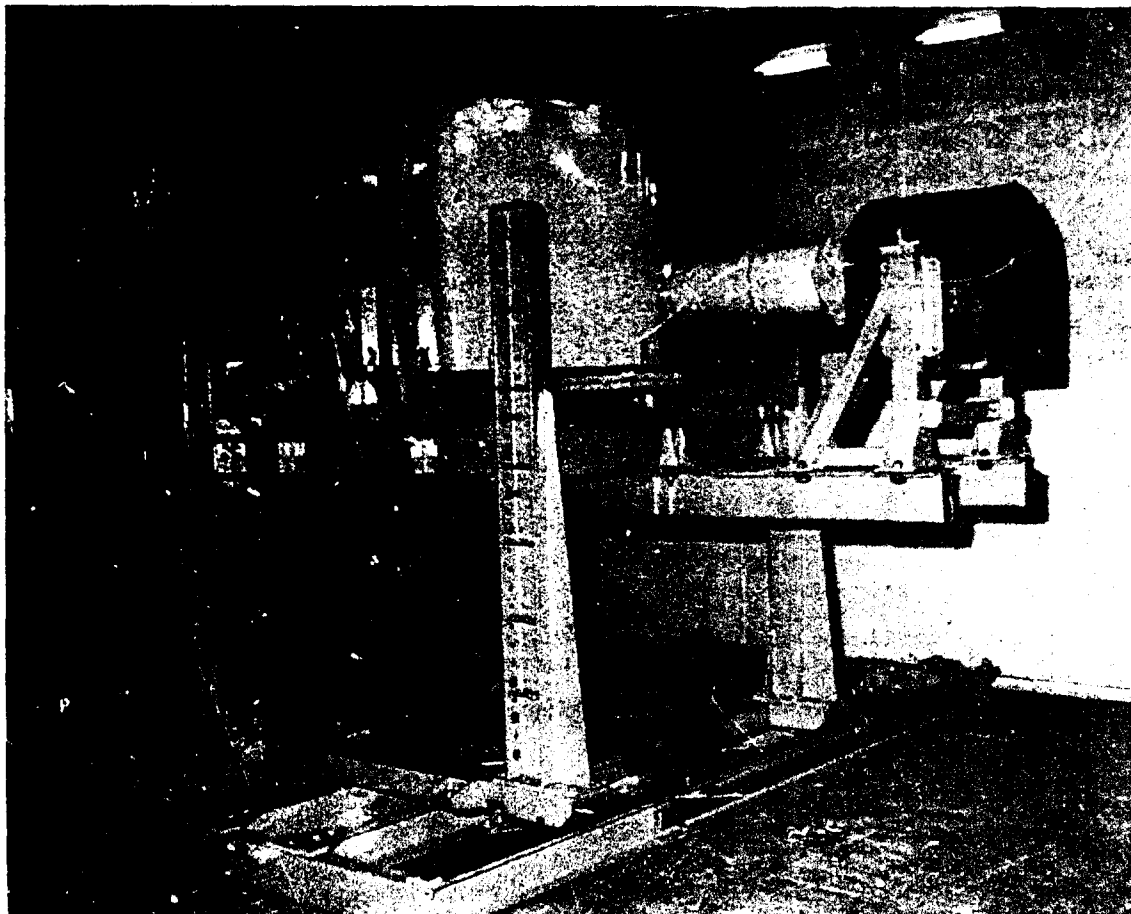
Fig.2   "Super X" mounting   4 degree of freedom mount

UPPER CASING

LEAD RADIATION SHIELD

INTERNAL ACOUSTIC BLANKET 'STILLITE' FOAM FILLED

ISOCON TV TUBE

CONTROL LOOM AND VIDEO LINE CONNECTION BOX

DETACHABLE END PANEL

COOLING AIR EXIT

FOAM RUBBER SEALING STRIP

BOWLERS E4 PRIMARY OPTIC

DOUBLE SKINNED CONSTRUCTION WITH ACOUSTIC PROTECTION FOAM FILLING

X-RAY FIREPROOF FACE-PLATE

ALUMINIUM/FOAM SANDWICH FOR ACOUSTIC PROTECTION

COOLING AIR OUTLET

COOLING AIR SUPPLY SYSTEM

LOWER CASING

'DELCALIX' X-RAY IMAGE INTENSIFIER

ELECTRONICS AND RELAY OPTICS

LIGHT INTENSIFIER

LEAD RADIATION SHIELD

FOAM ACOUSTIC PACKING

THREE POINT VIBRATION INSULATING MOUNTINGS

Fig.3   'Delcalix' X-ray image intensifier in 'RR' environmental casing
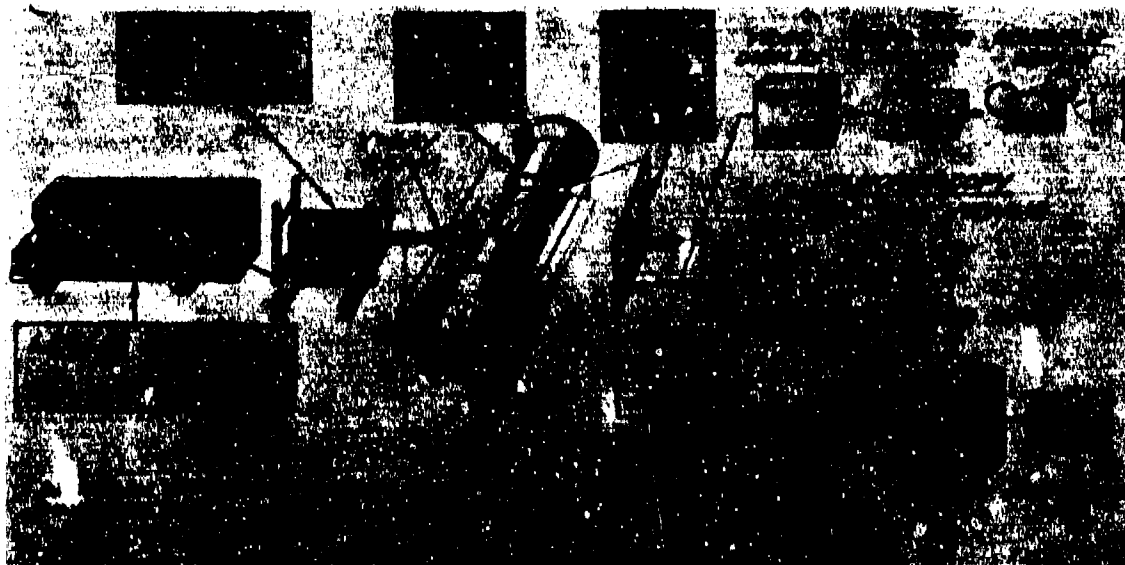
Fig.4   Rolls-Royce high-energy dynamic radiography system
for examining gas turbines on test

Fig.5   X-ray photogrammetry equipment

Fig.6   Section from a radiograph of a labyrinth air seal
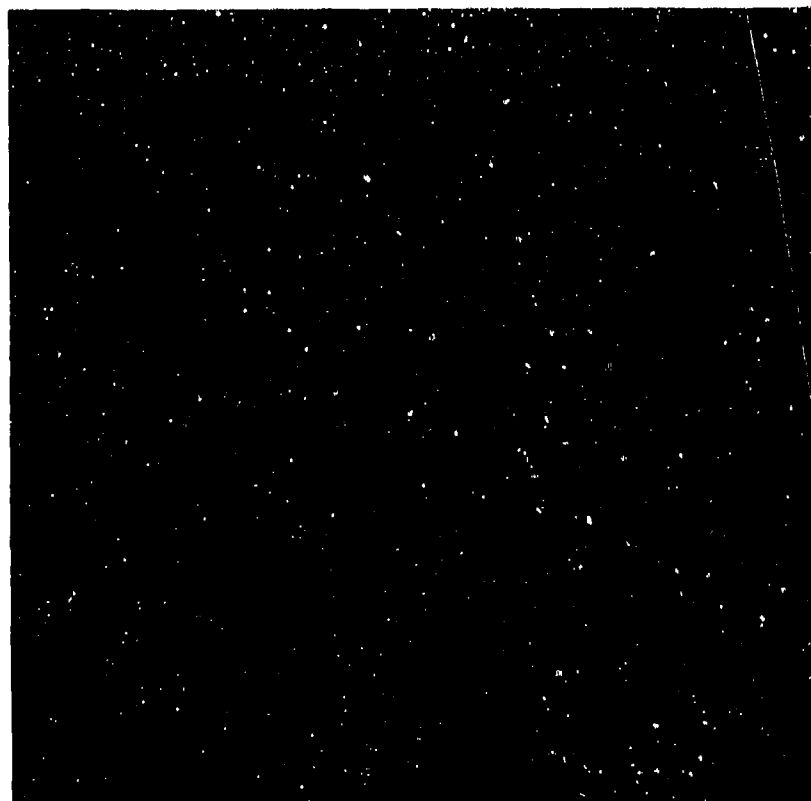
Fig.7   Section from a radiograph of a shrouded turbine tip seal

Fig.8   Section from a radiograph illustrating unshrouded blades in a compressor
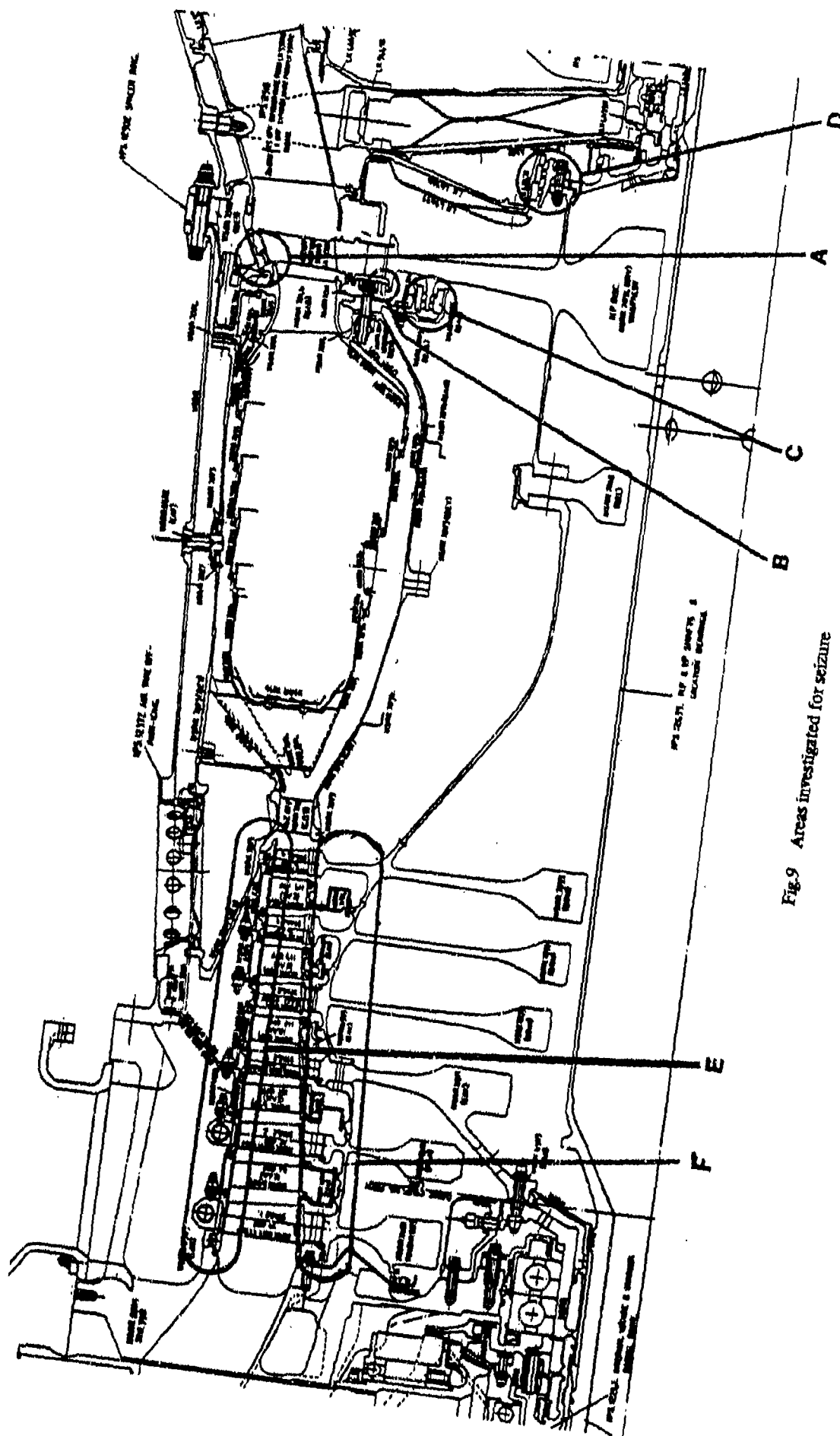
Fig.9   Areas investigated for seizure
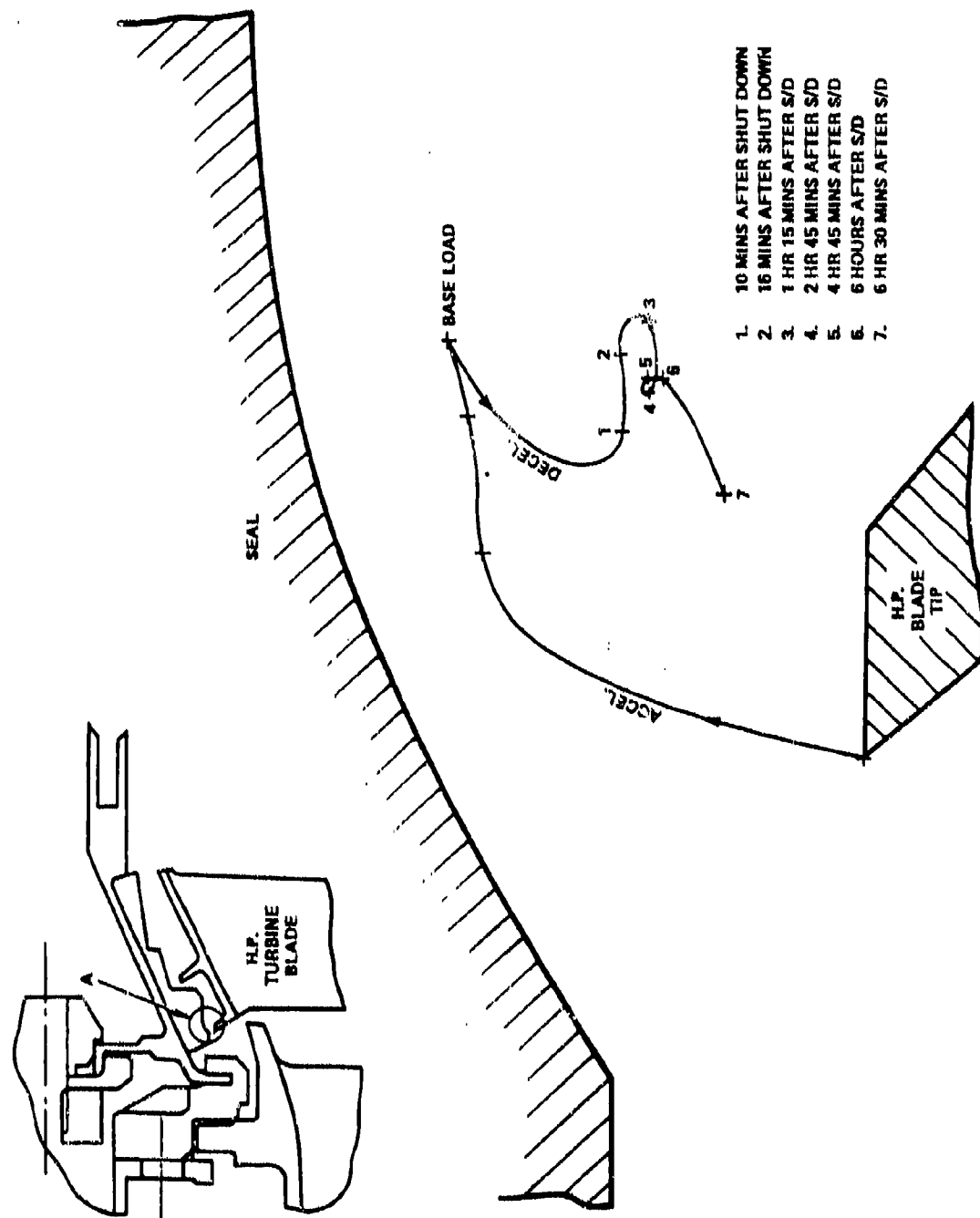
Fig. 10 Enlarged view (scale 50:1) of area A in Figure 9. Locus of H.P. turbine blade tip seal relative to static seal during accel. and full power trip conditions

1. 10 MINS AFTER SHUT DOWN
2. 16 MINS AFTER SHUT DOWN
3. 1 HR 15 MINS AFTER S/D
4. 2 HR 45 MINS AFTER S/D
5. 4 HR 45 MINS AFTER S/D
6. 6 HOURS AFTER S/D
7. 6 HR 30 MINS AFTER S/D

BASE LOAD

DECEL.

ACCEL.

SEAL

H.P. TURBINE BLADE

H.P. BLADE TIP

PART AREA E

SEAL

H.P.
COMPRESSOR
STAGE 5
ROTOR BLADE

3

2

4 5 6
7

8

+ BASE
LOAD

+ COLD STATIC

1

TIP OF BLADE

1.   10 SECS AFTER SHUTDOWN
2.   10 MINS AFTER SHUTDOWN
3.   25 MINS AFTER SHUTDOWN
4.   45 MINS AFTER SHUTDOWN
5.   1 HR 15 MINS AFTER S/D
6.   2 HR 15 MINS AFTER S/D
7.   3 HR 15 MINS AFTER S/D
8.   4 HR 15 MINS AFTER S/D

Fig.11   Enlarged view (scale 50:1) of part area E in Figure 9. Locus of H.P. compressor state 5 rotor blade relative
to static seal during full power trip condition
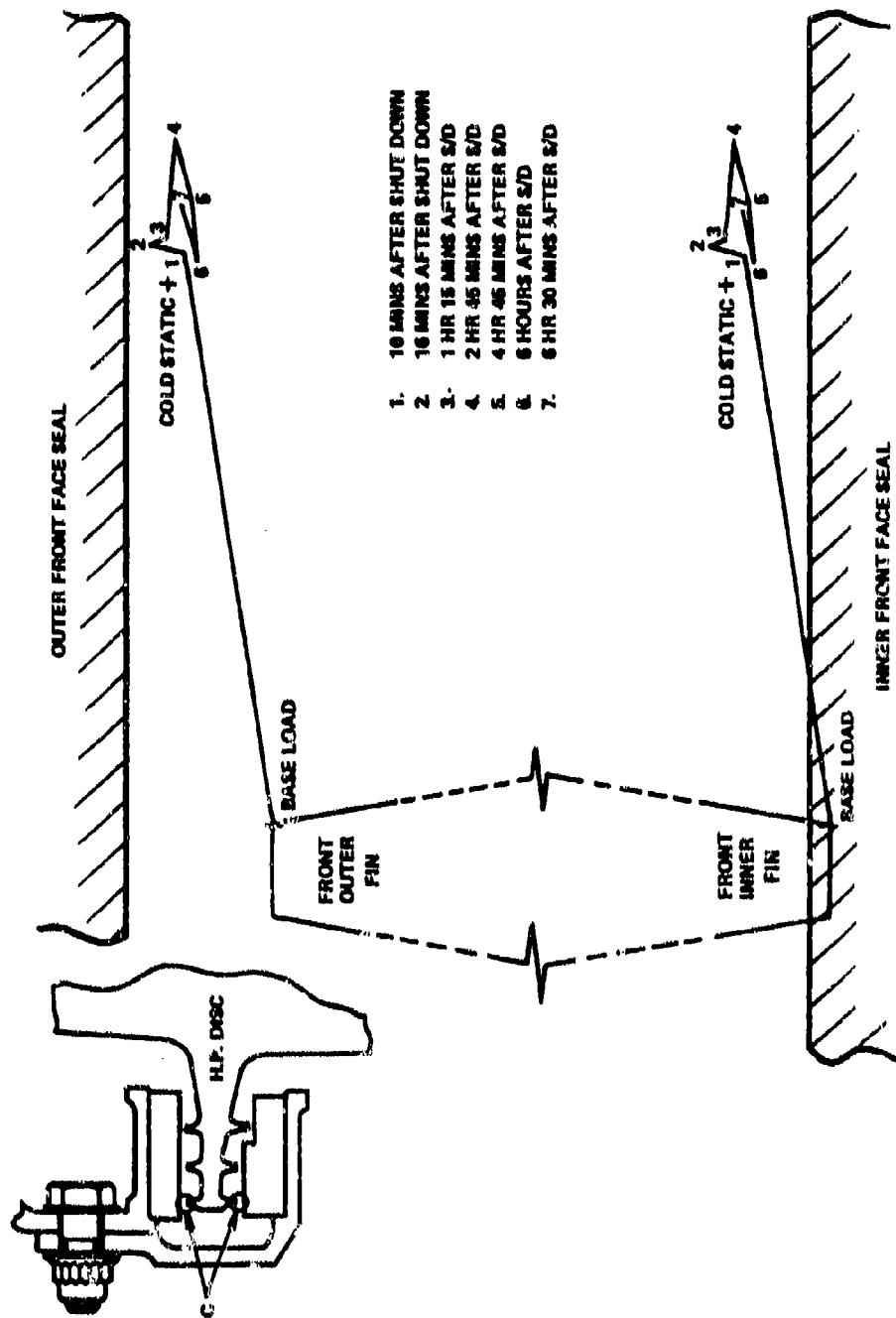
Fig12   Enlarged view (scale 50:1) of area C in Figure 9. Loads of H.P. turbine disc front face seal relative to static seal during full power trip conditions

SEAL

1. 10 MINS AFTER SHUT DOWN
2. 16 MINS AFTER SHUT DOWN
3. 1 HR 15 MINS AFTER S/D
4. 2 HR 45 MINS AFTER S/D
5. 4 HR 45 MINS AFTER S/D
6. 6 HOURS AFTER S/D
7. 6 HR 30 MINS AFTER S/D

BASE LOAD

COLD STATIC +

FRONT FIN

D
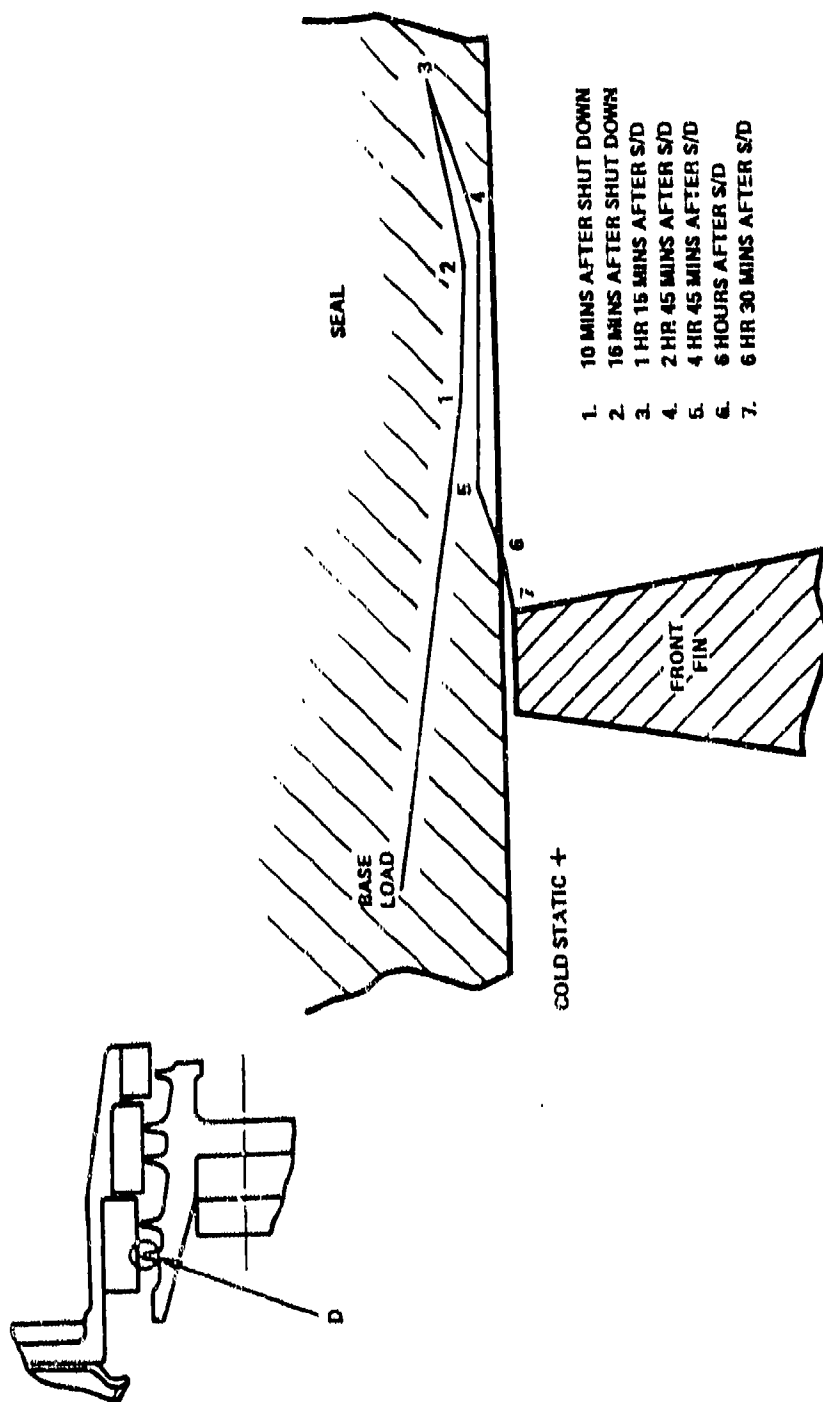
Fig.13 Enlarged view (scale 50:1) of area D in Figure 9. Locus of H.P. turbine rear rotating seal relative to static seal during full power trip conditions

DISCUSSION

H.L.Stocker, US

How do you approach the problem of circumferential variation in clearance such as case ovalization?

Author's Reply

Mounting the x-ray source at different trangential positions allows variation in circumferential clearance to be quantified. Additional information is also available from correlation of engine strip data with x-ray results.

R.A.Hartley, United Kingdom

Is it possible to investigate oil/air leakage across seals by the introduction of radioactive isotopes into the oil/air?

Author's Reply

The only possibility for investigating oil/air with x-rays is to dramatically increase the attenuation of the oil/air. This would be the equivalent of the medical barium meal. However, it is not practical to use this technique.

G.W.Fairbairn, United Kingdom

When obtaining the radiograph of a shrouded turbine tip shown in Figure 7, what was the thickness of metal penetrated?

Author's Reply

The metal path thickness was approximately 175 mm. Thicknesses of up to 300 mm of steel can be penetrated.

D.K.Hennecke, Germany

Do the x-rays penetrate the engine parallel or in a cone-like way? If the latter is true, what is the cone angle and what are the errors resulting?

Author's Reply

The x-rays are emitted as a cone of radiation having an included angle of up to 17°. This results in all radiographs having a geometric magnification, dependent on source to object and object to film distance. It is also necessary to align the beam to the subject under investigation. Areas out of alignment display obliquity effects which would result in errors of measurement.

EXPERIMENTAL RESULTS ON HIGH SPEED DOUBLE MECHANICAL SEALS

by

Enrico Bollina[1], Corrado Casci[2], Ennio Macchi[3]

Istituto di Macchine - POLITECNICO DI MILANO

Piazza Leonardo da Vinci 32 - 20133 MILANO - ITALY

[1]Research Engineer

[2]Director, Professor of Thermal and Hydraulic Machines

[3]Professor of Special Power Plants

SUMMARY

A facility for testing high speed mechanical seals is described. Its main features are:
(1) the possibility of continuosly varying the rotating speed up to 60,000 rpm; (2) the
possibility of independently selecting the flow rate, the pressure and the nature of the
sealing and cooling fluid; (3) the seal power consumption is accurately measured by means
of a force transducer.
The performance of a number of double face mechanical seals having different geometries
was investigated on this rig. Results concerning the mechanical losses and the leakage
flow rates of these seals under various operating conditions are presented and discussed.

INTRODUCTION

The adoption of face seals is undoubtely attractive in a wide range of turbomachinery ap
plications, their main advantage being the low rate of fluid which leaks through their
faces (often in the range of a few cubic centimetres per hour or less). When gases or va
pours are to be sealed, the so-called "double face seal" can be used. It comprises two
single face seals, between which a sealing and coolant liquid is injected, usually at a
pressure larger than the one of the fluid to be sealed. While face seals today are mass-
produced for low speed applications, their use in high speed turbomachinery is still li-
mited. Actually, when the rubbing speed increases, several problems appear:

1) the leakage flow rate increases; according to the Mayer correlation [1], represented
   in Fig. 1, if the sliding speed is increased from 2 to 100 m/s, the leakage rate will
   be multiplied by a factor of about 500;

2) the power consumption increases, mainly
   because of high turbolent losses occur-
   ring in the coolant; for instance, an
   example is quoted in Ref. [1] where a
   seal running at about 18,000 rpm (rub-
   bing speed 85 m/s) has a 15 kW power con
   sumption due to turbulent losses;

3) high wear rates can take place; further
   more, heat cracks can damage the seals.

The theoretical study of high speed face
seals seems unfortunately quite difficult,
because of the interrelationships occurring
between thermal and fluid dynamic phenomena.
Reliable design methods, accounting for coo
lant fluid and face materials properties,a-
re not available.
At C.N.P.M. (National Center for Research
on Propulsion and Energetics), research on
closed-cycle power plants, operating with
various working fluids,is going on since
several years. In most of the fore seen ap-
plications for these engines, the availabi-
lity of reliable high speed seals is a cru-
cial point.
Double face mechanical seals, using the fluid
working in the power cycle also as sealing
and coolant fluid, are particularly attrac-
tive for these applications. It was there-
fore decided to carry out an experimental re
search on these seals.
In this paper, the test rig built for this
investigation is described, and some results
concerning a number of double seals of va-
rious geometry are presented and discussed.

Fig. 1 - Nondimensional leakage rate
vs. the sliding speed.

DESCRIPTION OF TEST FACILITY

In designing the test rig, a number of requi

rements was taken into account:

a) the seals should be tested at various speeds of revolution, up to very high speeds;

b) the pressure, temperature and flow rate of the sealing and coolant fluid should be in dependently varied;

c) various sealing media should be tested;

d) the power consumption of the seal must be measured with good accuracy;

e) leakage rates, averaged on a proper amount of time, must be determined.

Among the various considered solutions, the one represented in Fig. 2 was chosen.
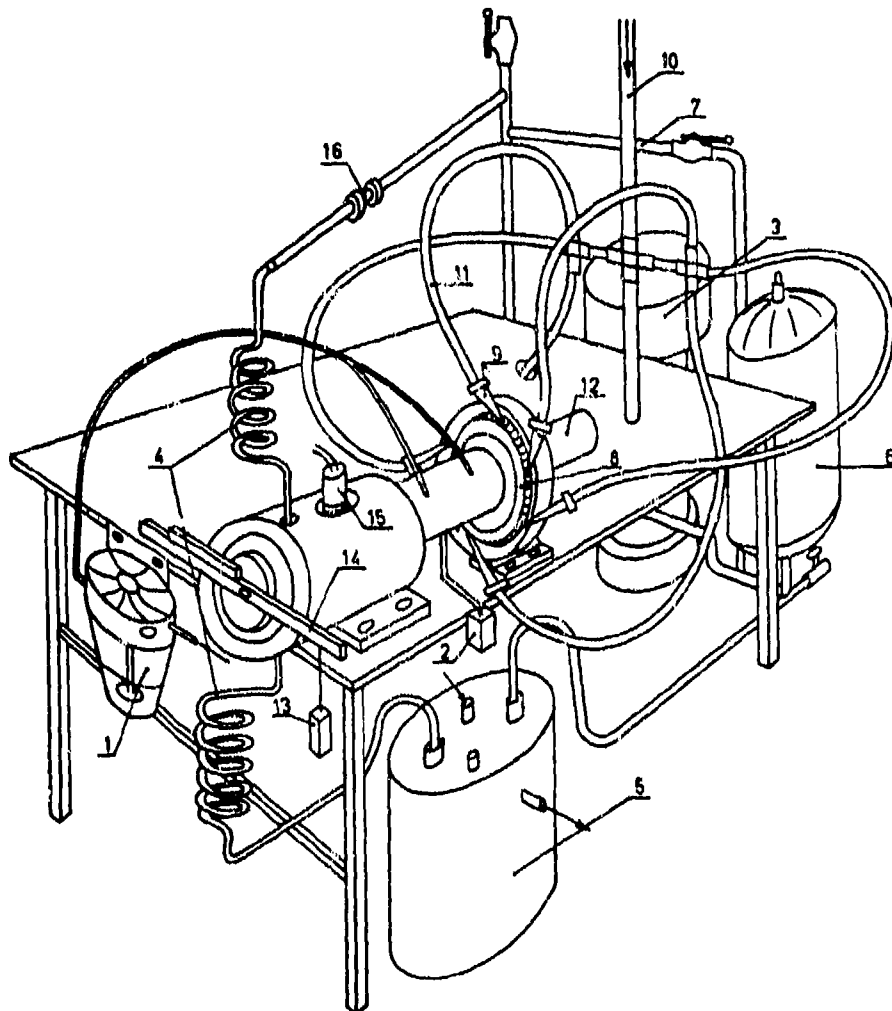
1- oil mist lubrication feeding tank
2- oil mist lubrication discharge tank
3- multistage centrifugal pump
4- sealing fluid loop flexible pipes
5- water cooled heat exchanger
6- membrane pressurizer
7- pump by-pass loop
8- compressed air impulse turbine
9- supersonic nozzles
10- compressed air main feeding
11- nozzle flexible feeding pipes
12- turbine discharge
13- calibration weight
14- calibration graduated arm
15- rpm magnetic pick-up
16- flow rate measuring diaphram

Fig. 2 - Test rig plant.

As shown in the figure, the seal to be tested is mounted overhanging a shaft supported by two couples of angular contact, spring pre loaded, oil mist lubricated, bearings; the shaft is driven by a compressed air impulse turbine, fed by six supersonic nozzles; the sealing fluid loop comprises a multistage centrifugal pump, a water-cooled heat exchanger and a membrane pressurizer; the pressure and the flow rate of the fluid circulating in the seal are controlled by means of a by-pass loop and a throttle valve. By acting on the air pressure at the turbine inlet power input variable from 0 up to 20 kW can be set, with revolution speeds up to 60,000 rpm.
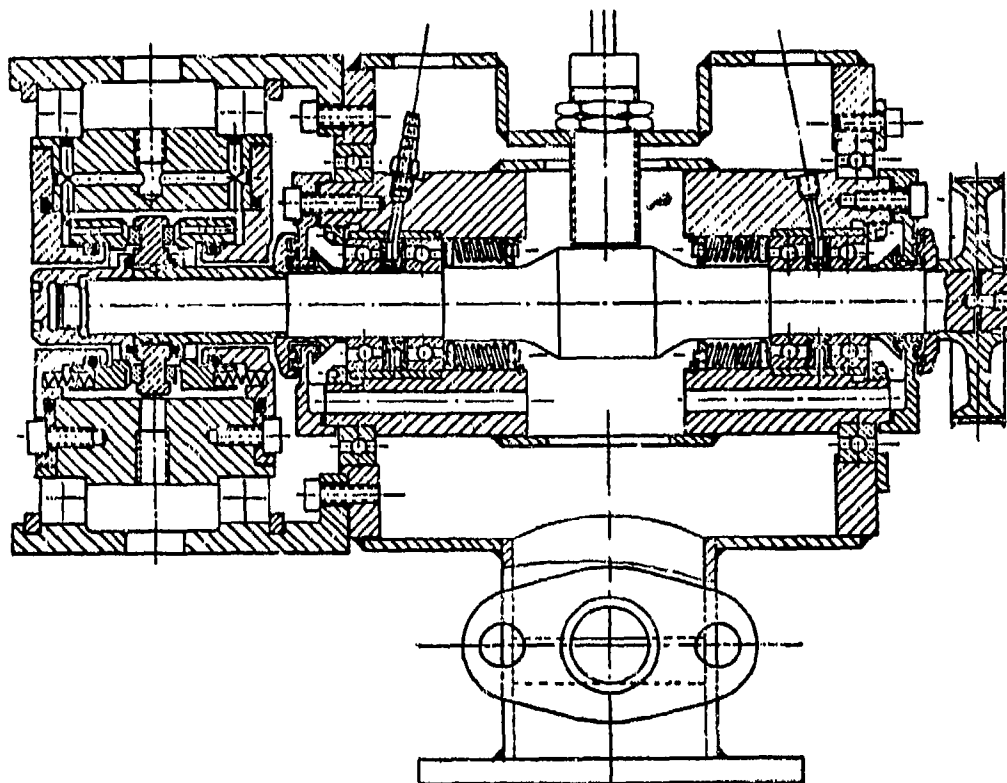
Fig. 3 - Shaft mechanical arrangement.

As shown in Fig. 3, the bearings and the seal casings are independently mounted on ball bearings; their rotation is counteracted by two force transducers, which therefore measure the reaction torques caused by the losses in bearings and seals. It is believed that this direct mechanical measurement is more precise and practical than heat balance measurements. The system can be easily calibrated under operating conditions by simply applying known weights on a graduated arm (see Fig.2).
It was found that it is necessary to repeat this calibration for every variation of the sealing pressure, which has an influence on the elastic reaction torque exerted by the pipes of the sealing loop.
The speed of revolution is measured by a magnetic pick-up, visible in Fig. 3.
Eventually, the leakage rate is measured by collecting the leaked fluid in a given amount of time in a graduated tank.
All measured data (reaction torques, rpm, sealing fluid temperature and pressure at seal inlet and outlet, sealing fluid flow rate, etc.) are sent to a data acquisition system and then computer processed. Controls of power absorption measurements are systematically performed, by comparing the mechanical power (torque x angular velocity) to the sealing fluid thermal power (flow rate x enthalpy increase across the seal).
The test rig was completed in July 1976. Since then, it has satisfactorily operated for more than one thousand hours of tests.

DESCRIPTION OF TESTED SEALS

A number of mechanical seals were designed and built, with the cooperation of an Italian firm operating in the field. The various seals arrangements are represented in the following series of figures, while the salient geometric data are given in Table 1.
All seals are double, i.e. they have two contact faces, separated by a room filled by a liquid which has the triple function of lubricating, sealing and cooling the sliding faces.
The seals A, B and C are "axial"; the sliding faces are at different axial positions and operate at the same speed. Being symmetric, they don't exert any axial thrust on the shaft.
The seals D, E and F are "radial"; the sliding faces are at the same axial position and operate at different speeds.
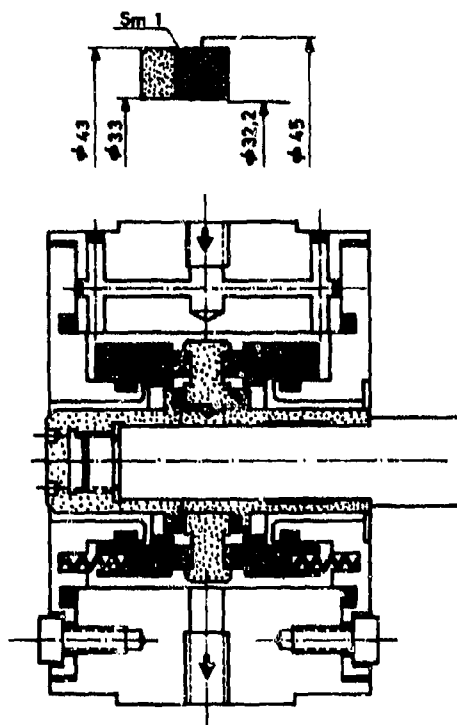
Fig. 4 - Geometry of seal A.
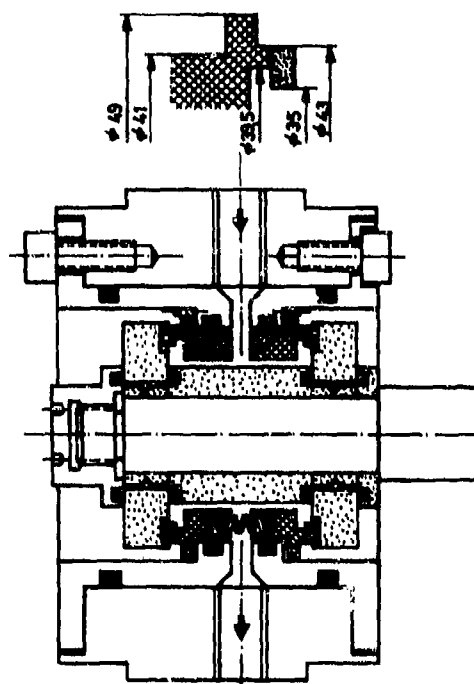
Fig. 5 - Geometry of seal B.

The seal A is made by a rotating disk, mounted floating on the shaft by means of two o-rings; the two sliding faces on the disk are of tungsten carbide; the stationary elements are made of graphite and spring loaded. The sealing liquid is brought in and out by means of the holes shown in Fig.4, and the turbulence chamber is in the outer part of the seal. Seal B is made by two rotating disks, mounted floating on the shaft; the stationary graphite elements are central and the turbulence chamber is in the inner part of the seal, at lower radii than in solution A.(See Fig. 5)
Seal C is identical to seal A, with the only exception being the holes and the radial grooves in the graphite elements, represented in Fig.6.
Seal D |2| is made of a stationary graphite disk with six holes which bring the sealing fluid in an annular groove, which substitutes the turbulence chamber of the previous seals; the rotating disk is axially floating and its contact pressure is governed by the springs load and by the hydraulic pressure of the sealing fluid, which acts on the back surface of the ring.(See Fig. 7)
Seal E is similar to D except for the outer diameter of the back surface of the rotating disk, which is larger, thus yielding a larger hydraulic load. Eventually, seal F has a floating stationary disk, spring and hydraulically loaded; the rotating disk is similar to the previous one, but doesn't have springs. (See Figs.8-9)

TABLE 1

SEAL	SPRING LOAD (N)	INTERFACE SURFACE (mm^2)	HYDRAULIC SURFACE (mm^2)	AREA RATIO	SLIDING FACES MATERIALS	MEAN ROUGHNESS (µm)
A (Fig. 4)	55	465	506	1.09	Tungsten carbide/graph.	.05
B (Fig. 5)	55	226	95	.42	Tungsten carbide/graph.	.05
C (Fig. 6)	55	369	410	1.11	Tungsten carbide/graph.	.05
D (Fig. 7)	75	471	200	.42	Ni-Resist/graphite	.1
E (Fig. 8)	75	471	471	1.0	Ni-Resist/graphite	.1
F (Fig. 9)	75	471	483+331	1.73	Ni-Resist/graphite	.1
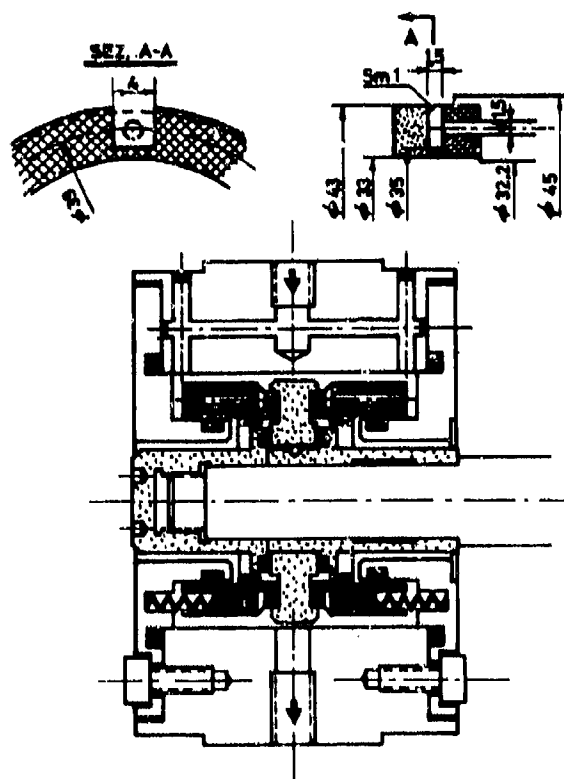
Fig. 6 - Geometry of seal C.
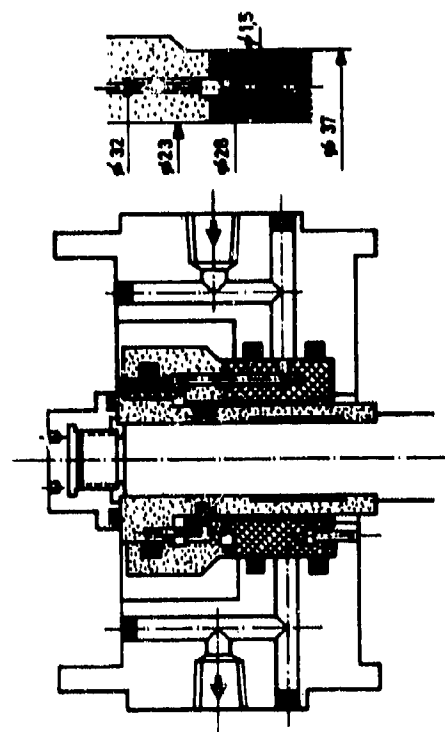
Fig. 7 - Geometry of seal D.
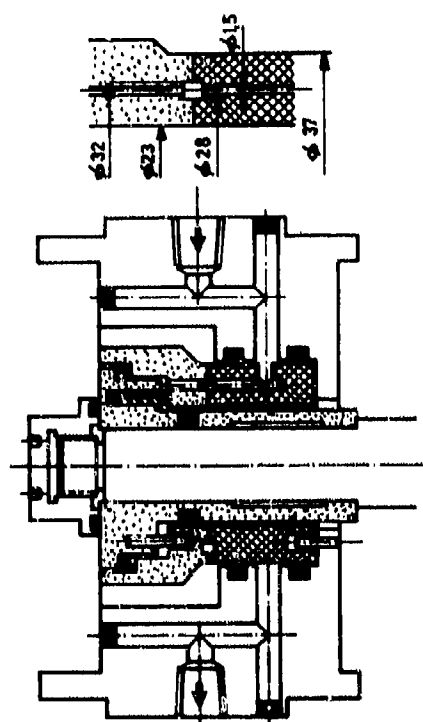
Fig. 8 - Geometry of seal E.
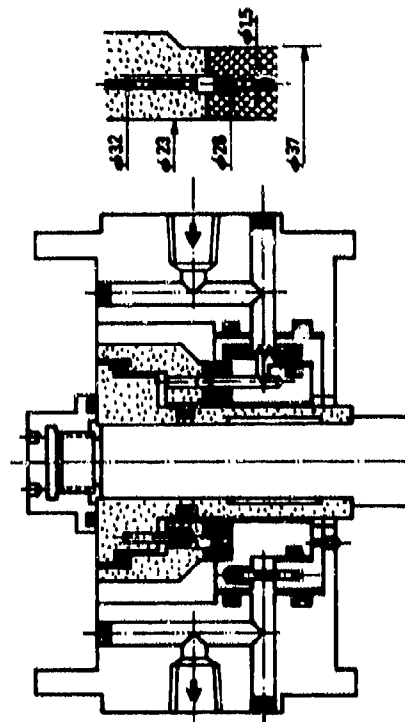
Fig. 9 - Geometry of seal F.

DISCUSSION OF RESULTS

A number of tests were performed for all the above described seals, at various operating conditions (rpm, pressure and flow rate of sealing fluid). All tests were carried out with water as sealing fluid. An investigation of the influence of the properties of the fluid is planned in a future series of tests. Just the "overall performance" of the seals was investigated, i.e. the power consumption and the leakage flow rate.

During the tests, the sealing fluid pressure was varied from 1 to 8 bars over the atmosphere; a lower sealing pressure was kept for tests on seals D, E and F in order to limit the axial thrust on the shaft. The whole range of speeds of revolution was investigated, from 0 up to the speed at which the "opening" of the sealing faces occurred. The flow rates of the sealing fluid across the seals were in a range of 50 ÷ 500 l/h; however, it was recognised that this parameter exerts only a minor influence on both losses and leakages, provided it is sufficiently high to avoid the fluid overheating.

1) Maximum speed of revolution

As said above, for all the seals the "opening" of the faces occurred at some speed of revolution; this speed varied in the 20,000 ÷ 40,000 rpm range for "axial" seals, and in the 10,000 ÷ 20,000 rpm range for "radial" seals.

This "opening" is probably caused by the large increase of the interface pressure occurring at high speeds of revolution; the sealing pressure increase delays but doesn't avoid this process. For "radial" seals, the variation of the area ratio from seal E to seal F yields just a small improvement (see Fig. 20).

It is to be said that for the "radial" seals, the axial thrust produced some shaft vibrations, which probably alter the phenomenon; modifications on the shaft arrangement to avoid this problem are already planned.

2) Power consumption

Results concerning the power consumption of the various seals are given in Figs. 10-17 in terms of total friction torque.

The obtained results suggest a number of considerations, which are given in the following:

a) influence of speed of revolution

A large increase of torques is experienced at high speed of revolution, due to turbulence losses in the sealing fluid caused by the rotation;

b) influence of sealing pressure

In general an increase of sealing pressure yields an increase of friction torque; however, the relationship between these two quantities is a rather complex function to be predicted; for example, for seal B, the increase from 6 to 8 bars produces a torque decrease (Fig. 15);

c) influence of seal geometry

- the "axial" seals have a power consumption larger than the "radial" ones; this is probably due to the better lubrication obtained by the last ones;
- the different layout of seals A and B doesn't seem to have an important influence on losses (Fig. 13); however, a lower increase of losses at high rpm can be recognized for seal B, having an inner and smaller turbulence chamber;
- the presence of grooves has a marked beneficial effect on losses, as shown in Fig. 14; this can be explained by the Mayer theory |1| ; the power consumption at low speed is similar to the one of "radial" seals;
- the area ratio influences the friction torque, as shown in Figs. 16 and 17.

3) Leakage flow rate

The obtained result are represented in Figs. 18-20.

For "axial" seals A and C the peculiar behaviour occurring at high speeds can be observed: an inversion of leakage flow occurs, and the liquid travels from the low pressure to the high pressure region.

This can be explained by the "pumping" effect of the rotating disk at high speed; when this occurs, extremely high flow rates take place.

Comparison between results of Figures 18 and 19 shows that the presence of radial grooves, which yields a far better power consumption, causes a remarkable increase of leakages, due to the large gap height consequent to the hydrodynamic action. As far as the "radial" seals are concerned, very low leakage values are found up to the "opening" of the seal.

CONCLUSION

The described seal test rig has proved to be an efficient and reliable tool for testing high speed operation of mechanical seals. None of the tested seals exhibited a completely satisfactory high speed behaviour. Very high turbulence losses were found for "axial" seals; the presence of radial grooves decreases the friction torque, but yields high leakages; the "radial" seals have a good performance, both in terms of power consumption and leakages, up to moderate speeds, but fail at high speed, due to the sudden "opening" of sealing faces. Further investigation is required for a better understanding of phenomena.

REFERENCES

1   E. Mayer - Mechanical Seals - II English Edition - London - ILIFFE Books - 1972.
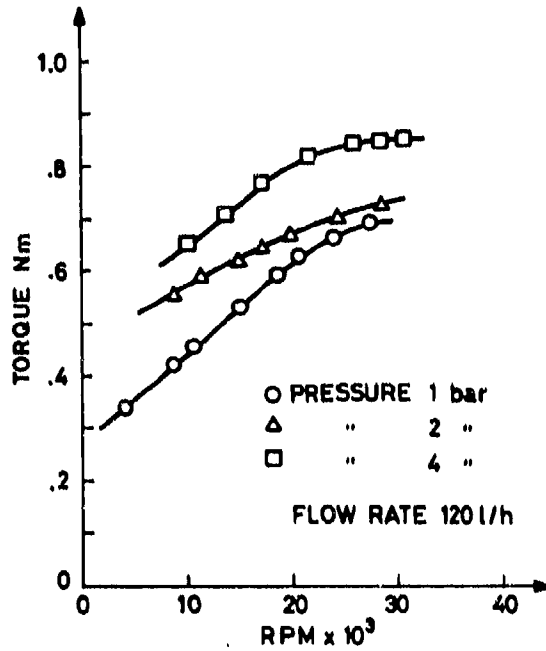
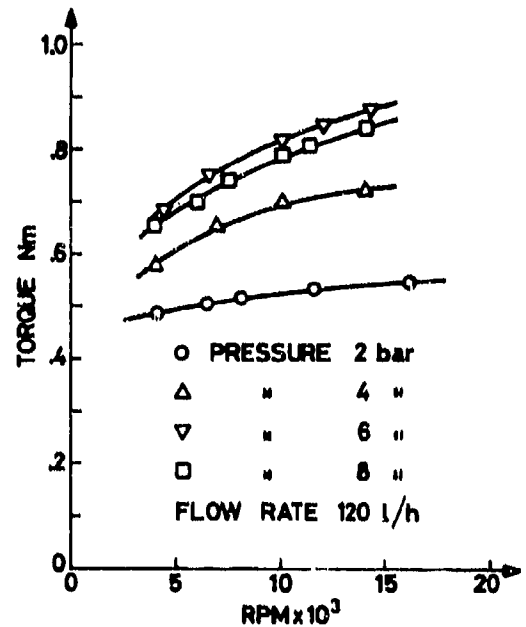2   Italian Patent n° 23089A/77.

Fig.10 - Torque consumption of
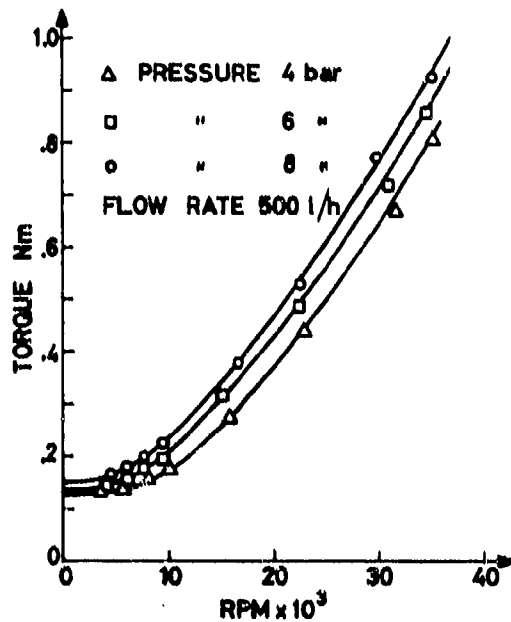seal A.

Fig.11 - Torque consumption of
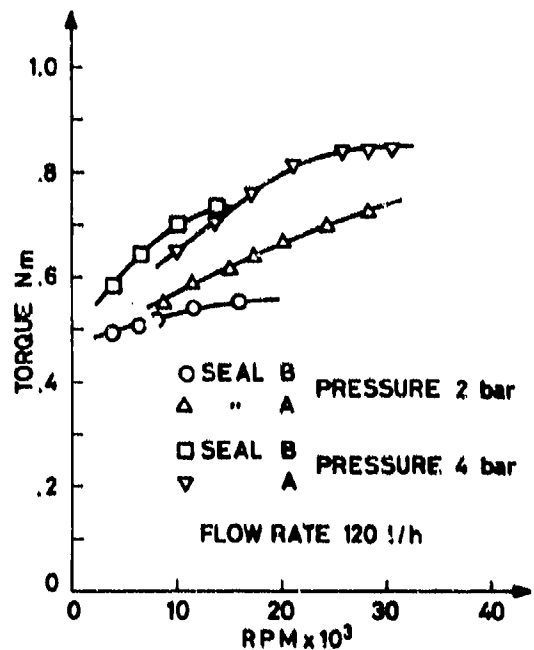seal B.

Fig.12 - Torque consumption of
seal C.

Fig.13 - Comparison of torque consump-
tion between seals A and B.
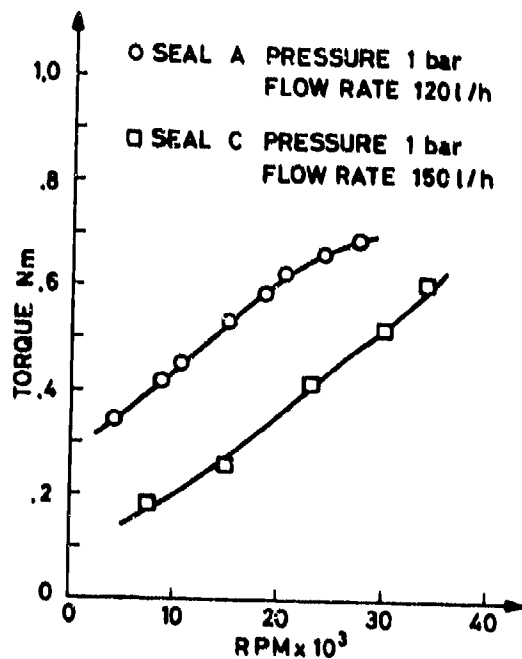
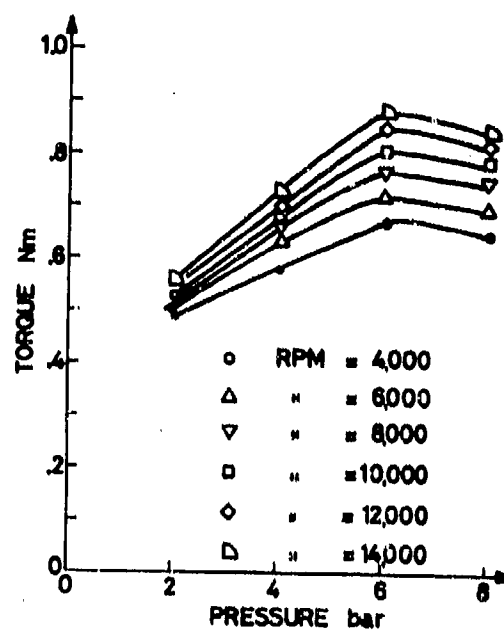Fig.14 – Comparison of torque consumption between seals A and C.
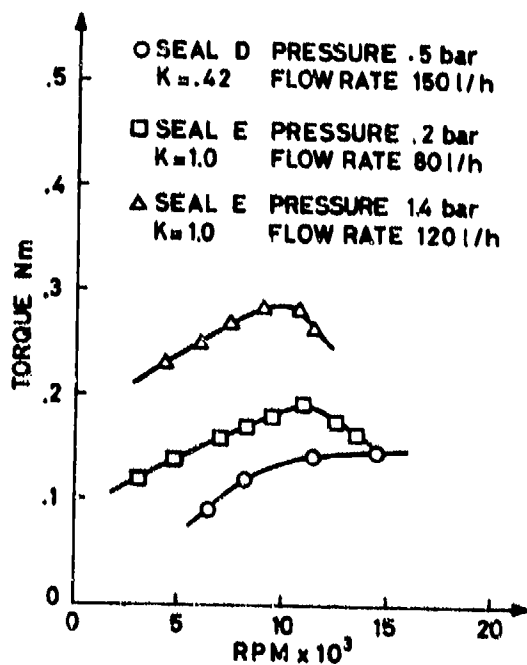

Fig.15 – Torque vs. pressure for seal B.
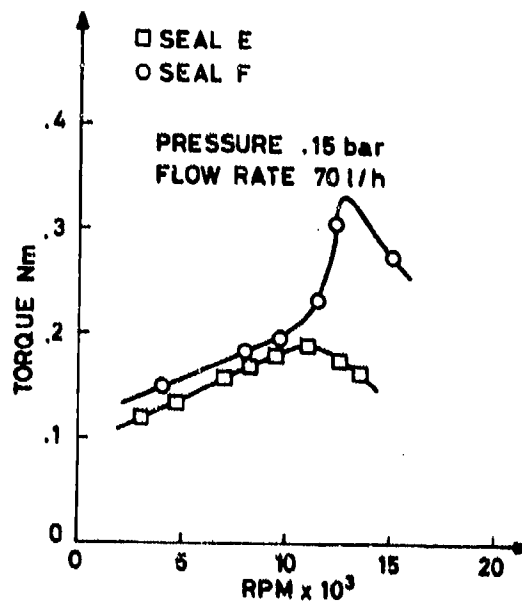

Fig.16 – Torque consumption of seals D and E.

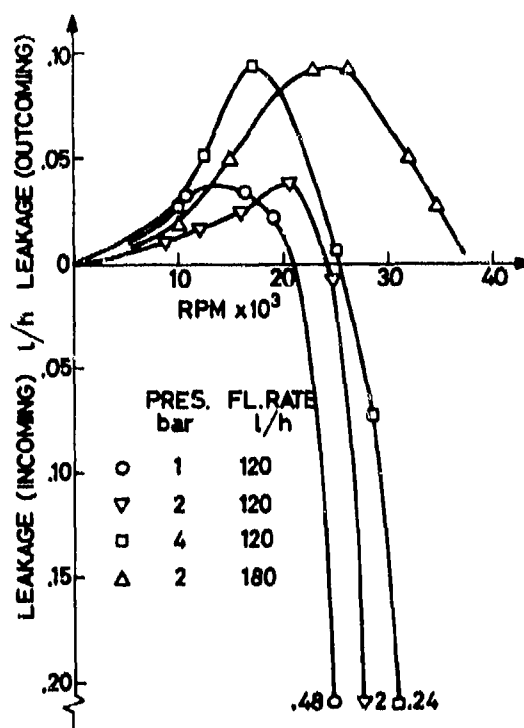Fig.17 – Comparison of torque consumption between seals E and F.
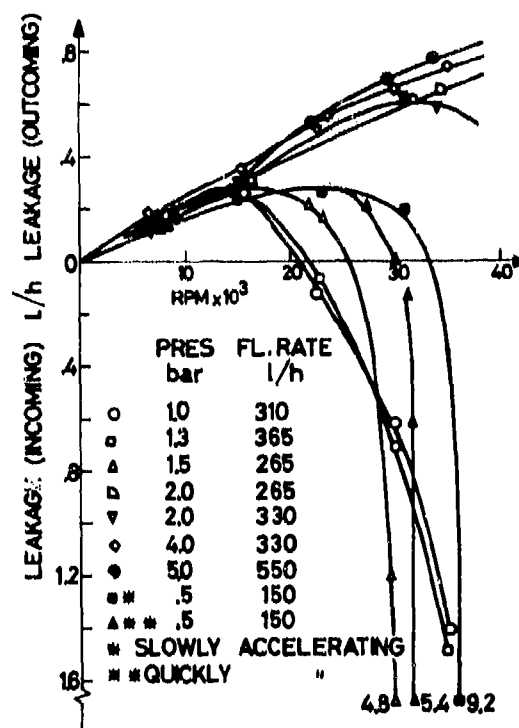
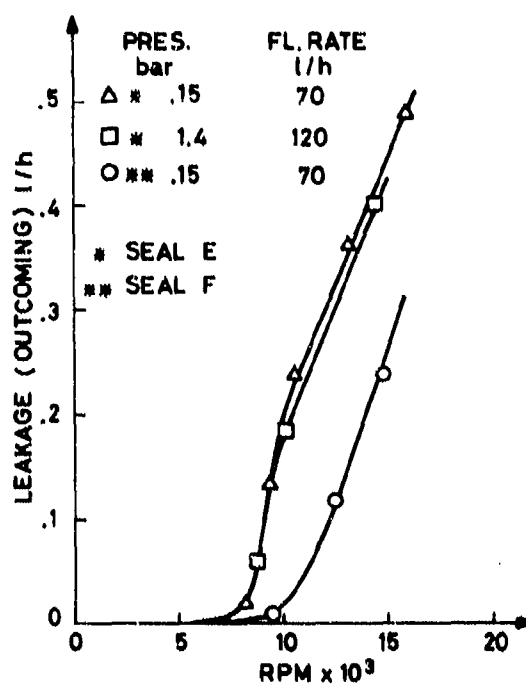Fig.18 - Leakage rate of seal A.

Fig.19 - Leakage rate of seal C.

Fig.20 - Leakage rate of seals E
and F.

DISCUSSION

J.A.Millward, UK

Were any measurement or observations of wear rate for the various seals made, i.e. is it possible to comment on the relative wear rates of the various designs?

Authors' Reply

We did not carry out any long wear test and no wear parameter was recorded; only a serial check of the seal sliding faces was made during the testing. However, no significant wear was recorded after an initial period of adjustment of the sliding faces.

Also at high speeds of revolution, no wear appeared if a proper cooling and lubricating flow rate was guaranteed.

Due to the lower power absorption of the "radial" seals, lower wear rates were noted in these types of seals.

SYSTEMS FOR THE MEASUREMENT OF ROTOR TIP CLEARANCE
AND DISPLACEMENT IN A GAS TURBINE
by

C.R. Amsbury   and   J.W.H. Chivers
Electronics and Instrumentation Research Department
ROLLS-ROYCE LIMITED
P.O. Box 31
Derby
DE2 8BJ
United Kingdom

SUMMARY

The rotor tip clearance system consists basically of a stepper motor driven insulated wire which is polarised at a high voltage and which sparks to the rotor blade tips when within a certain distance. The incidence of sparking is detected and the radial immersion of the wire is determined by electronically counting the motor drive pulses.   The displacement system is based upon a capacitance transducer specifically designed for operation within a gas turbine at temperatures of up to 600 degrees Centigrade and pressures of 300 psi.   The transducer capacitance which is a function of probe/rotating seal clearance is connected into the feedback loop of an amplifier, the output of which is proportional to the clearance.

A STEPPING MOTOR PROBE FOR MEASUREMENT OF BLADE TIP CLEARANCES

The system to be described, was developed from work done a few years ago on component profile inspection and with it a number of successful runs on test bed engines have been achieved, both in compressor and turbine environments.

The principle used is very simple and not new.   A wire probe is electrically polarised and fed towards the rotating blades until it is discharged to the blade.   The change of voltage which then occurs is used to cause the probe to retract until the voltage is re-established, when it is again fed towards the blades.   When the probe is sensing a surface it is continuously oscillating about .02mm.   The motion of the probe is continuously monitored and displayed.

By using modern techniques and components a probe has been constructed which has a fast enough response to follow engine handling conditions, with the exception of compressor surge, and the probe is small enough to fit under the cowlings of a typical engine.

The current design has a useful measuring range of 5mm and a speed of response of 1mm/sec.   The repeatability is ±.02mm and accuracy ±.05mm.   The probe does not measure tip clearance directly but the distance from a reference datum to the blade tips.   The stability and position of this datum with reference to the inside of the engine casing is obviously important.

The probe may be divided into two sections, the mechanical drive head, and the stem assembly which fits into the engine.   The latter is subject to re-design to suit different engines.

The head consists of a stainless steel body (A) which can withstand cooling air pressures up to 2700kPa (400 PSI).   This houses a modified small stepping motor (B).   The rotor of this motor is a permanent magnet and the original shaft was removed, the magnet was bored out and a new bronze shaft fitted.   This shaft is internally threaded to form a rotating nut, and externally carries two ball race bearings.

The leadscrew (C) is guided by the extended bearing housing (D) and prevented from rotating by the cross pin   (E) in a slot in the housing.   At the rear a separate spring loaded nut takes up end play in the bearings and leadscrew assembly.

The motor end plates are bored out to locate on spigots on the housing and the stator is held in place by four screws and lock nuts.   A small vent hole at the rear allows a flow of cooling air through the motor.

The front of the body houses an insulated ball and socket coupling to the probe sensing element, and the high voltage connection, including an interference suppressing resistor (H).   Mounted off the bearing housing is a backstop which the probe returns to in the retracted position.

The stem shown is designed for the lower temperature environments such as compressors, and consists of a stainless steel tube having a ceramic tubular insulator down which runs the probe sensing element, a straight stainless steel wire.

The whole probe is mounted off a boss on this tube, to be located as near the measuring zone as practical.   In this case the rear of the stem is supported in sliding seals in the engine bypass duct. The cooling air pressure prevents hot compressor air from entering the probe by travelling up the stem.

High Temperature Stem Construction

This diagram shows the type of stem construction used for tip clearance measurements in a hot turbine environment and it has operated successfully up to 1800°K.

It consists of a Nimonic tube (A) which is located from the turbine shroud ring by the bayonet fixing arrangement shown. The tube houses a ceramic insulator (B) of the cross section shown; this allows a separate feed of cooling gas, nitrogen, which travels to the tip and keeps it at a reasonable temperature. In this case the probe body is independently mounted and connected by a lockable telescopic coupling having a ball and socket joint at each end to allow for axial mis-alignment.

It will be seen that the probe sensing element in this case has a small "flag" near its out end, when the probe is retracted, this flag contacts the inner earthed surface of the probe stem and this forms a rear datum face from which measurements are made. It is located close to the gap to be measured, and thus very much reduces errors due to thermal expansion of the probe and stem. It does however pose problems with probe replacement and it is not always convenient to use this technique.

Electronic Control System

The probe is polarised at about 350V DC from a special power supply which is insulated from earth; the earth connection is made via a resistor (R) of about 2000 ohms. By this system the current passed from the probe to blade is sensed and not changes in probe voltage.

It is done because it results in much less electrical interference into the following logic circuits. Considerable precautions have to be taken when one is attempting to operate high voltage sparking circuits in close proximity to electronic logic elements.

Across Resistor (R) is developed a small voltage when the probe sparks to the blade, this is filtered to remove effects from blade passing frequencies and other short duration transients and the resultant signal is compared with an adjustable reference voltage by the comparator. The level of its output denotes whether to feed the probe in or out and it controls the motor drive logic. It also feeds the up/down line of a reversible electronic counter. A clock generator feeds both the motor logic and the counter, the frequency of this clock controls the motor speed, it is in the range 25 to 50Hz.

The output from the counter feeds a digital to analogue converter whose DC output is a measure of probe position.

This is an incremental system which may be zeroed with the probe at any position. In practice the probe is always switched on and datumed at the backstop, either the internal one or the external one shown on the high temperature stem.

Operation

The probe polarising voltage now used is 350V DC. This is not sufficient to cause any appreciable gap between the probe tip and blade tips, hence the probe rubs the blade and suffers wear.

By careful adjustment of the reference voltage in the comparator the rub is very light, and a typical wear figure is .02mm/min. The setting is made in the Laboratory by bringing the probe up to a rotating toothed wheel, it does not need frequent re-adjustment. Higher polarising voltages have been tried, up to 2KV. This results in a spark gap at lower ambient pressures, but with compressor pressures up to several MPa, totally impractical polarising voltages would be required to still maintain any spark gap. Hence one still has a rubbing probe at the engine conditions of greater interest, and an un-calibrated error gap at lower pressures; consequently, it was decided to have a known rubbing condition at all speeds and pressures.

To obtain a reasonable probe life the probe is not left in the measuring position longer than necessary to record a reading, usually about 1 to 2 seconds is sufficient. During engine accelerations and decelerations, longer measurement times are of course, required, to obtain the tip clearance profile.

To take into account probe tip wear, measurements are made at frequent intervals with the engine either stationary or rotating at a low speed, where conditions can reasonably be assumed to be stable and repeatable.

Failures in use have occured during development, the most common being conductive deposits building up across the end of the ceramic insulating tube at the inner end. This is particularly noticeable in a turbine environment. The maximum length of time achieved so far in this case is about 5 hours – this is engine running time, not actual measuring time, a typical time achieved here is a total of 20 minutes comprising some 110 spot measurements and 6 acceleration tests when the probe was measuring continuously for about 60 sec. each.

Typical Graphs

Curve 1 is a plot of compressor tip clearance against time. The engine was accelerated to max condition after 6 minutes at ground idle speed.

Curve 2 is a plot of tip clearance on a similar compressor done by X-Ray techniques.

Curve 3 is a plot of tip clearance on a turbine test rig having gas temperatures up to 1800°K.

DISPLACEMENT MEASUREMENT AT HIGH TEMPERATURE IN A GAS TURBINE

This paper describes the construction and operation of a capacitance displacement transducer which has been developed primarily to measure the clearance between rotating and stationary components in a seal. The primary reasons which led to the selection of a capacitance technique for this measurement are :-

The transducer is non-contacting. A non-contacting technique is essential as the measurement must be made between components with a rotational speed differential in the order of 300m/sec.

Very low temperature/pressure coefficient. As the transducer contains no coils or electronic components and the permittivity of air changes little with temperature and pressure a capacitance based system exhibits good stability throughout the high and transient temperatures and pressures encountered in gas turbines.

The transducer is simple and mechanically robust. These are undeniable advantages for any device required to operate reliably in close proximity to a gas turbine.

The capacitance transducer in its basic form consists of two concentric electrodes, the inner one being the sense electrode and the outer one the guard electrode. Each electrode is insulated from the other in addition to being insulated from earth. The capacitance formed between the sense electrode and an earthed conducting target which is placed in front of the transducer is used as the negative feedback element in a high gain amplifier which is driven by an oscillator. The amplifier output is demodulated and filtered, the resulting voltage being proportional to the clearance between the sense electrode and the target which in this application is a rotating seal component.

The guard system serves to completely screen the back and sides of the sense electrode, the connecting wire and the electronic components from the earthed surroundings. Thus the small capacitance (in order of 1 picofarad) between the front of the sense electrode and the earthed engine seal, which is a function of the separation of the two components, is measured in isolation and is not masked by the large fixed capacitance to earth of the transducer and cabling.

The initial system requirement was to measure a clearance of between 1 and 6mm under conditions of temperature and pressure which varied from 20 degrees Centigrade at 100kPa to 600 degrees Centigrade at 2MPa with an accuracy of ±1% full scale.

In order that the transducer should survive in an environment where the temperature can reach 600 degrees Centigrade the insulators used have to be manufactured from inorganic materials. The sense electrode is insulated from the guard electrode and the guard electrode is insulated from the earthed transducer body by means of two alumina bead insulators of different diameters. Thus the transducer body is at earth potential and can be directly attached to the engine metalwork.

The cable to the transducer is subjected to the same conditions of temperature and pressure as the transducer itself and is thus minerally insulated. It is of a double screened coaxial construction with an outside diameter of 3mm – the centre conductor connecting to the sense electrode, the inner screen connecting to the guard electrode and the outer screen being at earth potential. The cabling is changed to a single screened P.T.F.E. insulated coaxial cable when the leadout reaches the exterior of the engine where typically the temperature is less than 200 degrees Centigrade. This change of cable type helps to keep the high standing capacitance of the minerally insulated cable to a minimum and also facilitates handling as the PTFE cable is much more flexible than the stainless steel minerally insulated cable.

In practice, the transducer as described, has given very encouraging results. Initial problems were confined to difficulty of installation when using a sheet mica insulator in place of one of the ceramic insulators. However, two problems have persisted until recently in one particularly severe engine application where the transducer is subjected to an occasional cold water/kerosene mixture spray. Although clearance readings are not required whilst the transducer is wet the combination of wetting and temperature cycling severely tests the transducer sealing, any failure leading to loss of insulation resistance between electrodes due to ingress of moisture. This problem has been relieved by the use of tighter tolerance ceramic materials for the insulator and a better quality control during manufacture.

The second problem arises after several hours of operation and is caused by the formation of a conductive coating across the transducer electrodes which again has the effect of lowering the inter-electrode resistances. As the water/kerosene mixture is heated to a high temperature the kerosene tends to carbonise thus leaving a thin conductive layer. After several layers have been built up by alternately wetting and heating the transducer the insulation resistance can fall to a level which affects the system electronics. One possible solution being examined involves covering the sense and guard electrodes by a thin ceramic disc thus preventing any contamination of the transducer from affecting the inter-electrode resistances.
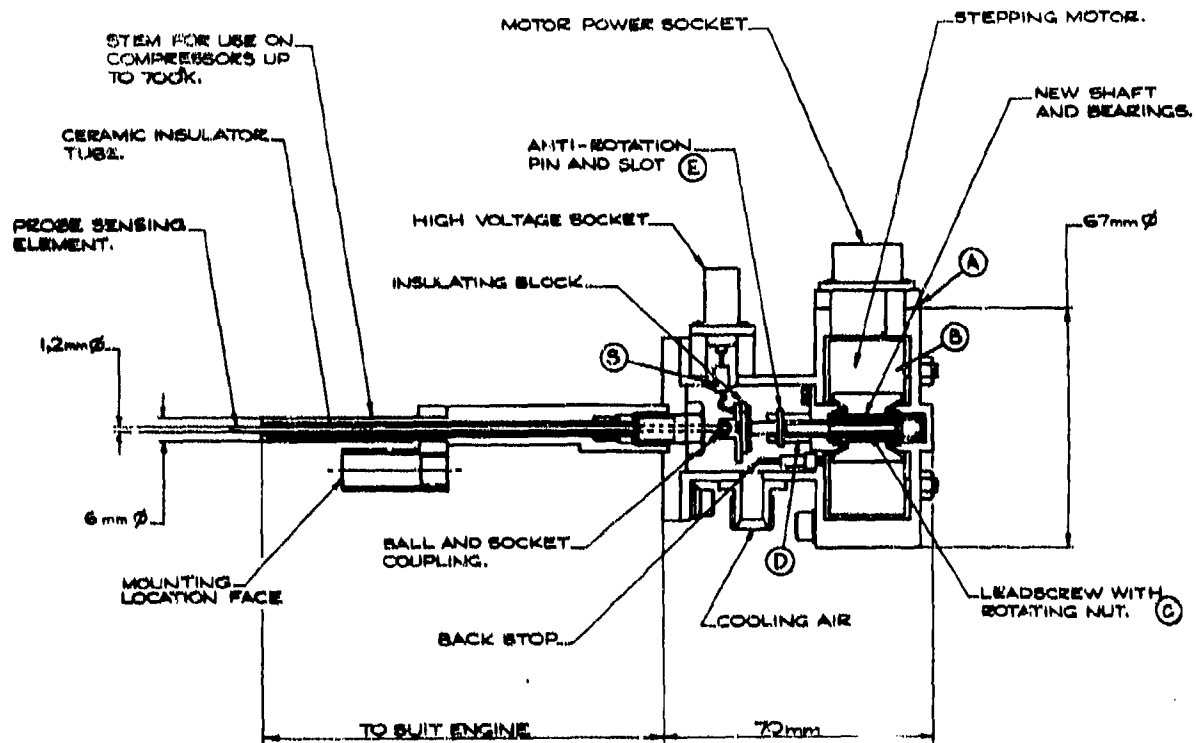
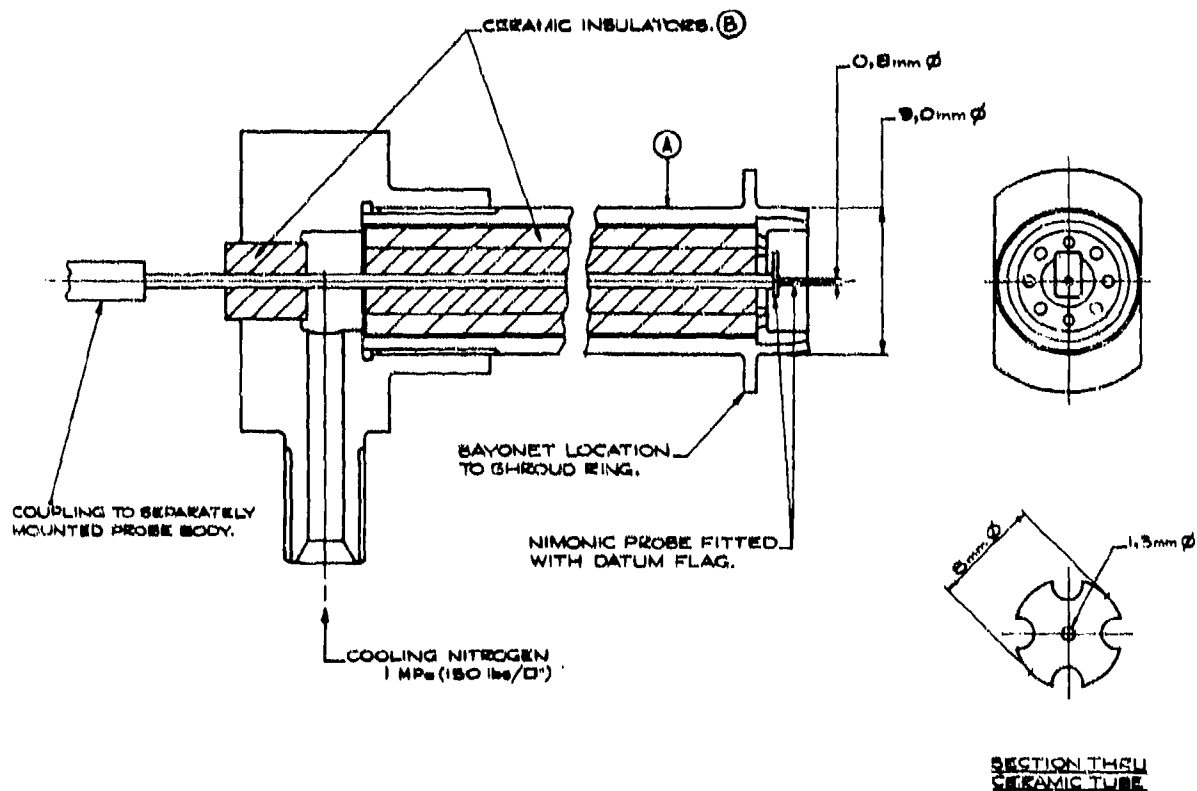Fig.1 Stepping motor tip clearance probe

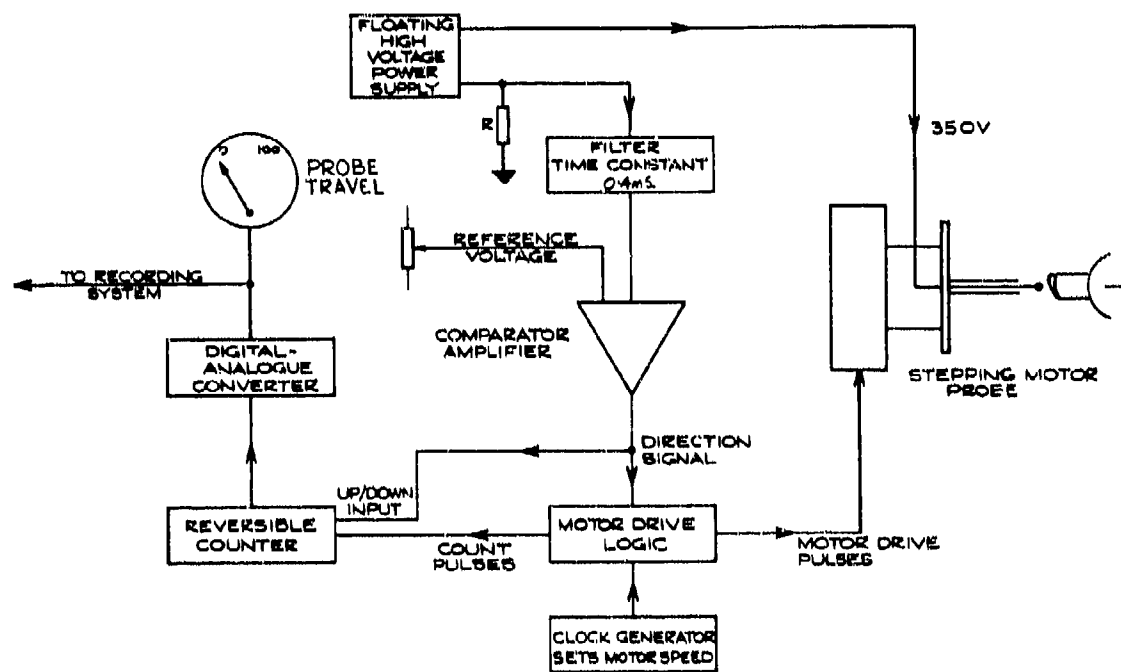Fig.2 Probe stem for use in high temperature areas

Fig.3   Block diagram of probe control circuitry

Fig.4 Turbine rig test

★ Transducer is non-contacting

★ Very low temperature and pressure coefficient

★ Transducer is simple and mechanically robust

★ Can be fabricated to withstand very high temperatures
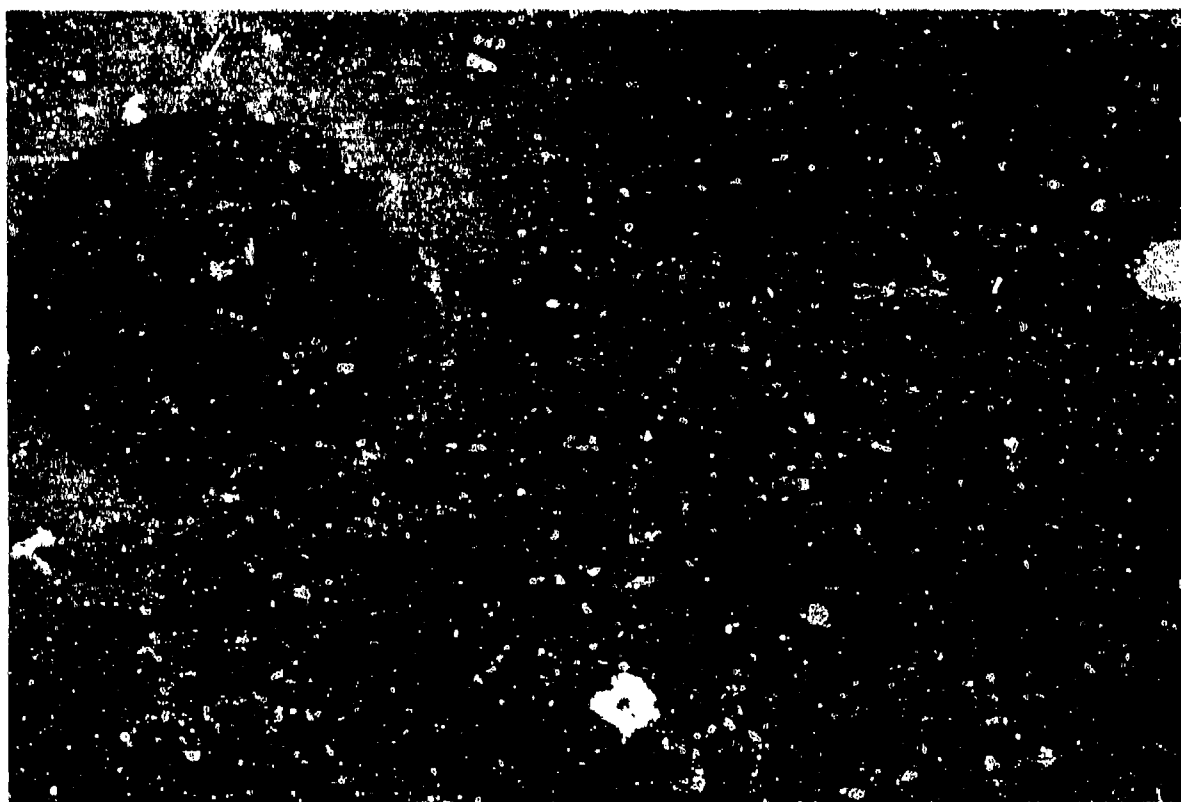
Fig. 5 Capacitive system features
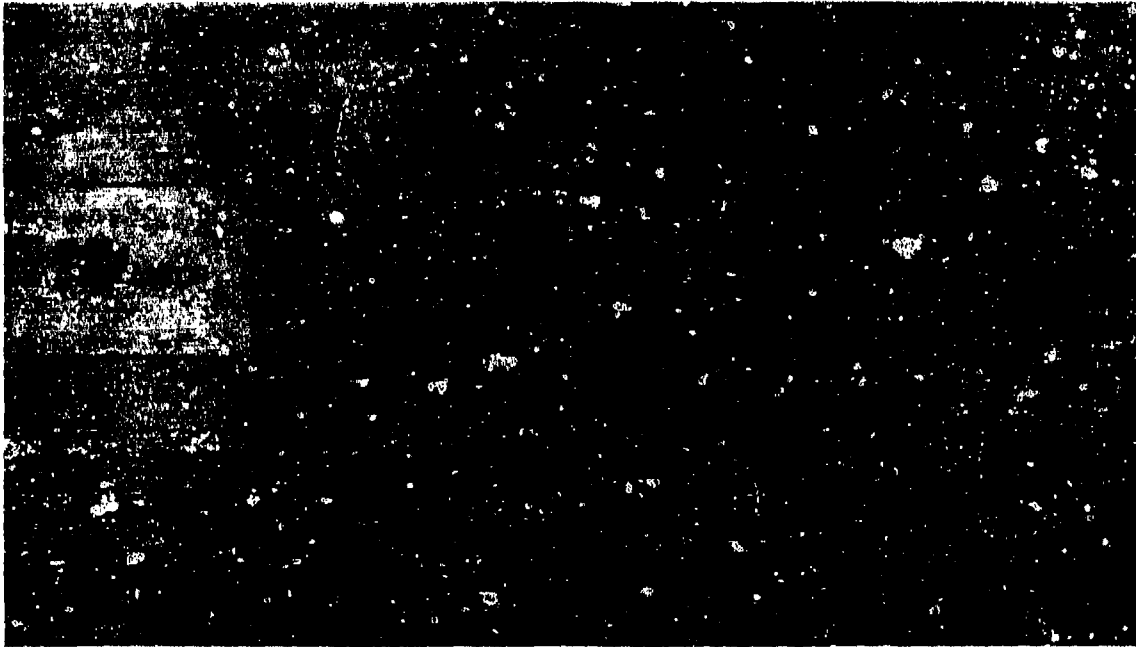

Fig.6 Transducer electrode configuration

Fig.7   Capacitance system schematic diagram

Transducer Temperature Range:-   **0-600 degrees centigrade**

　　　　Pressure Range:-   **100-2000 kPa (15-300 psia)**

System Measurement Range:-   **1-6mm**

Required System Accuracy:-   **±1% Full Scale**

Transducer must be non-contacting

Transient response requirements:-

　　　　Clearance: **0-500Hz frequency response**
　　　　Temperature: **400°C change in 10 seconds max.**
　　　　Pressure: **1600 kPa change in 5 seconds max**

Fig.8   System design criteria
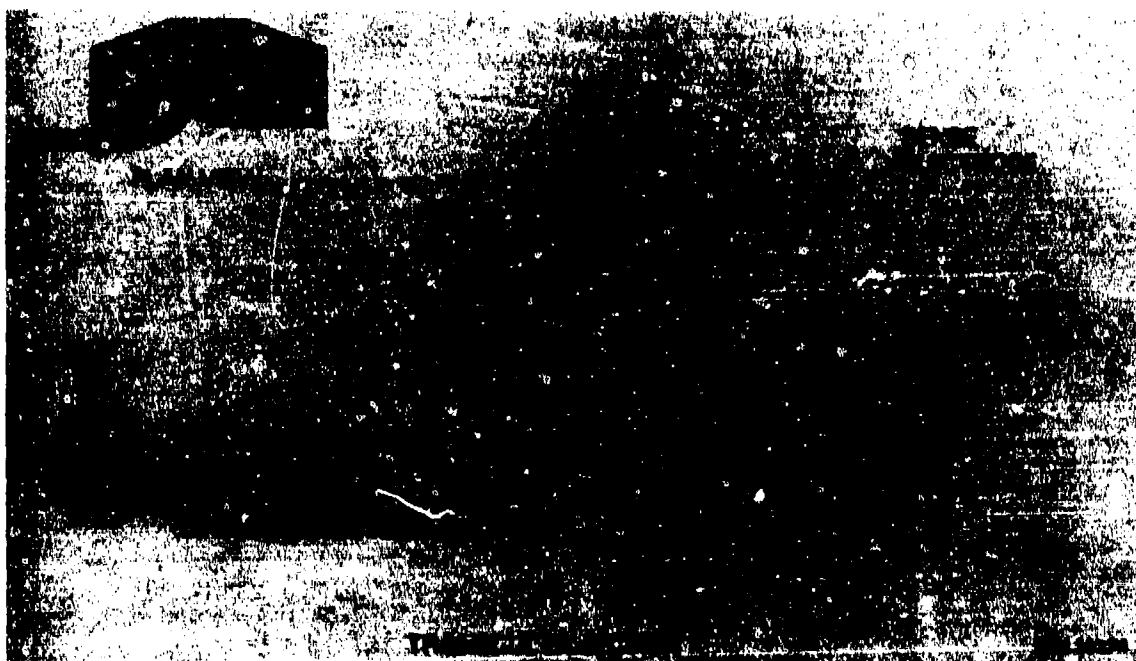
Fig.9 Redesigned transducer

Inadequate transducer sealing — unable to
cope with the combination of repeated
wetting and temperature cycling. Water
absorbed through microscopic voids in the
ceramic to metal braze caused by small
variations in concentricity of ceramic bead.

Build up of a conductive coating across the
transducer electrodes caused by repeated
wetting of the transducer with
water/kerosine
mixture followed by heating to a high
temperature. This problem unique to one
particular research gas turbine.

Fig.10   Long term operational problems
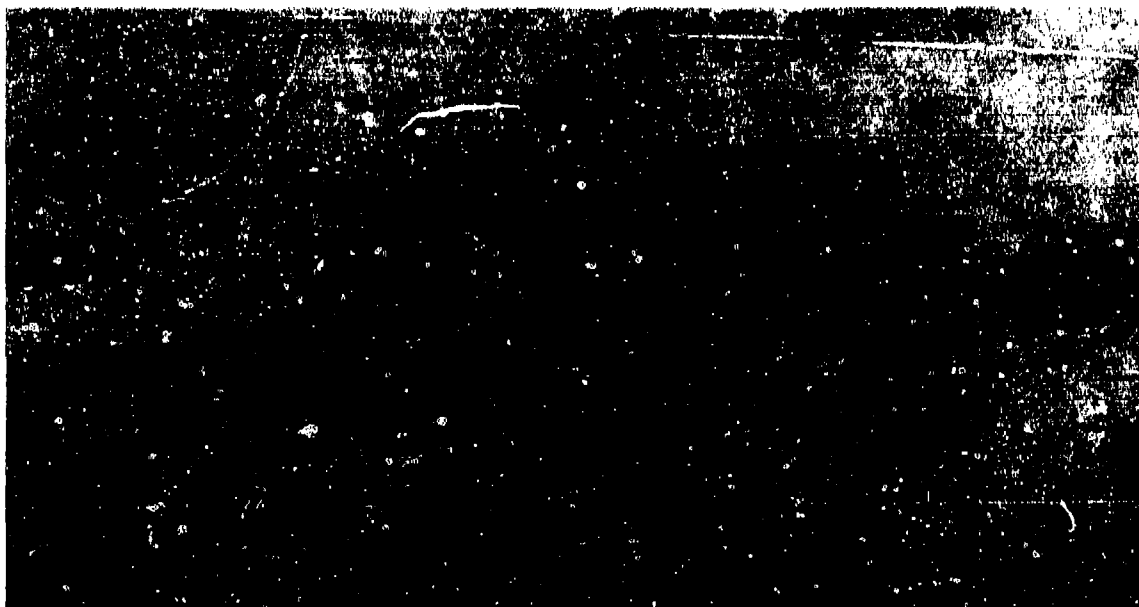
Fig.11   Future transducer development

DISCUSSION

D.A.Campbell, UK

In the stepping probe described for compressor measurements, appreciable errors due to differential thermal expansion would be expected. Would Mr Amsbury please comment on the possibilities of reducing these errors.

Author's Reply

Errors due to temperature, and hence expansion differentials between the probe wire and stem are present. To minimize these we are using low expansion alloys for these components, and are measuring the temperatures attained under engine running conditions. We can then either use calculated corrections, or choose materials to give minimal error at normal running temperatures.

J.G.Ferguson, UK

What is the measurement resolution at a probe clearance of 6 mm?

Authors' Reply

It is important to differentiate between resolution and accuracy. Although the system described has an absolute accuracy of ±1% full scale i.e. 0.06 mm for a 6 mm range probe the resolution is an order of magnitude greater than the accuracy. Thus for a 6 mm range probe the resolution is 0.006 mm (0.00024 inches).

H.L.Stocker, US

Have you correlated the rotor tip clearance system you have described with the X-ray technique presented earlier by Stewart & Brasnett?

Author's Reply

Slide 4 shows a comparison with X-ray results. This was done some 3 years ago. The X-ray techniques have improved considerably since then. We have no recent comparative results. As far as we know X-ray measurements have not been taken yet during engine handling conditions (i.e. during acceleration or deceleration tests).

B.Wrigley, UK

Could you expand further on the accuracy of the capacitance probe, please, with respect to its absolute accuracy, rather than quoting it in percentage of full scale. (*Please see answer to following question.*)

P.Suter, Switzerland

I understand that you are using different probes for the range of 1 to 6 mm gap or clearance width. Could you comment on the absolute accuracy of the different probe/gaps.

Author's Reply

I will deal with the questions from Mr Wrigley and Mr Suter together as they are closely related.

The absolute accuracy of our capacitance probes varies in proportion to the magnitude of the full-scale range. For example, a probe designed to measure a maximum clearance of 6 mm will typically have an absolute accuracy of better than ±0.06 mm in the range 0 to 6 mm. For a probe with a range of only 1 mm the absolute accuracy will be better than ±0.01 mm. In both cases changes in clearance can be measured with much greater certainty, typically to ±0.015 mm and ±0.0025 mm for the 6 mm and 1 mm range probes respectively.

DETERMINING AND IMPROVING LABYRINTH SEAL PERFORMANCE
# IN CURRENT AND ADVANCED HIGH PERFORMANCE GAS TURBINES

by

Harold L. Stocker
Supervisor, Flow Systems Group
Internal Aerodynamics
Detroit Diesel Allison
Division of General Motors Corporation
Indianapolis, Indiana   46206

SUMMARY

The leakage rate of the labyrinth seals incorporated in current and future advanced design gas turbines strongly influences the performance level of the engine. Labyrinth seal design and analysis technology, however, has not kept pace with the advances achieved in the major components of the gas turbine. Therefore, recent investigations were undertaken to (1) determine the aerodynamic performance of conventional labyrinth seals employing abradable and honeycomb lands, and (2) develop an advanced design labyrinth seal which would significantly reduce leakage.

Abradable and honeycomb lands were evaluated with a conventional straight-through seal using a static two-dimensional (rectangular flowpath) seal rig and a rotating three-dimensional seal rig. Test results show that some abradable lands leak significantly more than a solid-smooth land. However, honeycomb lands were found to reduce leakage up to 24.%.

Through aerodynamic testing, an advanced design labyrinth seal was developed which reduced leakage 54.2% compared to a conventional straight-through seal and 26.3% compared to a conventional stepped seal.

FLOW ➡

CONVENTIONAL
STRAIGHT-THROUGH
LABYRINTH SEAL

FLOW ➡

CONVENTIONAL STEPPED
LABYRINTH SEAL

FLOW ➡

ADVANCED DESIGN
LABYRINTH SEAL
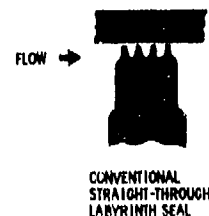
Symbols

A	Area, cm^2
CL	Radial Clearance, cm
KH	Knife Height, cm
KP	Knife Pitch, cm
KT	Knife Tip Thickness, cm
Kθ	Knife Angle, degrees
P	Pressure
SH	Step Height, cm
T	Temperature, K
V	Velocity, m/s
W	Flow, kg/s
η	Efficiency
ϕ	Flow Parameter, $W\sqrt{T}/PA$

Abbreviations

BPR	Bypass Ratio
DTC	Distance to Contact
HP	High Pressure
LTSD	Large-to-small diameter
PR	Pressure Ratio
SFC	Specific Fuel Consumption
STLD	Small-to-large-diameter
2D	Two-dimensional
3D	Three-dimensional

Subscripts

D	Downstream
S	Static Conditions
T	Total Conditions
U	Upstream

INTRODUCTION

The economic incentives imposed by future fuel conservation requirements and the continuing effort to improve performance has created increased interest in improving the efficiency of current and future gas turbine engines. Advancements in technology toward the achievement of higher thermal and propulsive efficiencies for current and advanced aircraft gas turbines have been characterized by significant increases in the operating cycle pressure ratio and turbine inlet temperature. However, these trends cause internal air seal leakage to increase because higher operating temperatures produce greater differential growth in the seal components that frequently results in larger seal clearances. The higher operating cycle pressure ratio also increases gas path and bearing compartment seal leakage, even if current clearance levels could be maintained. This problem is readily seen by considering the flow parameter characteristic, $\phi = W\sqrt{T}/PA$. The air leakage in a typical labyrinth seal (e.g., in front of the high pressure turbine disc) can be represented by $W = (PA\phi/\sqrt{T})(100./W_{engine})$ in terms of percent compressor inlet flow. Increasing the compressor pressure ratio from 15:1 to 30:1 at constant engine airflow and seal clearance would increase leakage approximately 75.%. A plot of typical seal leakage versus compressor pressure ratio is presented in Figure 1.

Compensating for the current state of seal technology by improving aerodynamic component efficiencies may result in limited payoffs relative to the time, cost, and manpower expended. Figure 2 shows an example of the improvement in compressor and turbine component efficiencies required to achieve the same increase in engine performance as a reduction in turbine seal leakage of 1.0% of engine airflow for an advanced high bypass ratio gas turbine engine. For example, reducing the high pressure turbine seal leakage 1.0% of engine airflow would produce the same improvement as a turbine efficiency increase of 0.51%. The results presented in Figure 2 show that a reduction in high pressure turbine seal leakage of 1.0% would improve engine specific fuel consumption 0.4%.

Perhaps a more meaningful presentation of the benefits of reduced seal leakage are shown in Figure 3. This figure shows the approximate total U.S. fuel savings would be 429,638,600 gallons annually if typical gas turbine seal leakage was reduced 25% throughout the engine for all current gas turbines.

An approach frequently used to reduce labyrinth seal leakage and mechanical damage has been to incorporate abradable or honeycomb lands and reduce the operating clearance. Recent investigations reported herein show that positive results may not always be achieved. In addition, to fully utilize the potential of increased cycle pressure ratio and temperature to provide higher thermal and propulsive efficiencies, sealing efficiency must be increased above present levels. Therefore, the purpose of this paper is to present the effects on the leakage of a conventional straight-through labyrinth seal using abradable and honeycomb lands and to discuss advanced labyrinth seal design concepts that significantly reduce leakage. Increased internal cavity turbulence was used to achieve reduced leakage in the advanced seal design without significantly affecting the mechanical integrity of the seal.

The results presented in this paper represent the cumulative efforts of several programs. These programs involved an aerodynamic evaluation of conventional straight-through labyrinth seals using solid-smooth, abradable, and honeycomb lands in a two-dimensional (2D) seal rig with additional tests of selected configurations conducted in a rotating (3D) seal rig. The investigations carried out on the advanced design labyrinth seals included water tunnel studies, 2D air rig tests, and dynamic air rig tests. The water tunnel provided an economical visual method of screening design concepts, while the two-dimensional air rig provided an economical and rapid means of evaluating the various seal geometric parameters. The performance of specific seal configurations under static and dynamic conditions was obtained in the three-dimensional air rig.

The seal nomenclature used throughout this paper is presented in Figure 4.

TEST RIGS AND PROCEDURES

Three labyrinth seal test rigs were used to obtain the experimental results presented in this paper:

(1) a water tunnel flow visualization seal rig

(2) a two-dimensional (2D) static air seal rig

(3) a three-dimensional (3D) or annular, rotating air seal rig

Water Tunnel Seal Rig

The water tunnel flow visualization seal rig, shown in Figure 5, was used for the pre-
liminary evaluation of the advanced labyrinth seal candidate designs. This rig was
designed to test ten-times size clear plastic models of labyrinth seals. The candidate
test seal configurations were formed using a building block concept with adjustable
seal hardware. Thus, multiple use of components was achieved. This concept provided
greater flexibility in making dimensional changes in seal pitch, clearance, and step
height as well as complete changes in seal configuration. The seal block pieces were
individually adjustable via slots machined in the seal components.

Water flow was measured with a Potter turbine-type flowmeter. The seal inlet and exit
plenum pressures were also measured. Air bubbles were introduced into the water supply
for flow visualization. A plane of light was cast through the rig to illuminate the
turbulent regions for observation and photographing. The seal configurations were
tested at pressure differentials of 7.5, 13.7, and 19.9 kPa with clearances of 0.127,
0.254, and 0.508 cm.

Two-Dimensional Seal Rig

A sketch of the two-dimensional (2D) static air seal test rig is presented in Figure 6.
This rig was used to investigate the aerodynamic effects of abradable and honeycomb
lands on conventional straight-through seal leakage. The influence of geometric varia-
tions on the performance of an advanced seal design was also evaluated and optimized in
the 2D rig.

The 2D rig seal hardware was designed on a building block concept which utilizes indi-
vidually adjustable seal components. Adjustable knife and land sections permit con-
tinuous variations in the primary geometric variables, i.e., knife pitch, knife height,
land step height, number of knives, axial clearance, and radial clearance. Figure 7
shows a photograph of the 2D rig with a stepped seal installed. The width of the test
section is 16.0 cm.

Structural deflection of the rig sidewalls under high air pressure loading was consid-
ered in determining the actual clearance tested. A micrometer dial gauge with .00005 cm
readability, shown in Figure 8, was mounted on the rig top plate to monitor the relative
movement of the seal knife with respect to the land.

The building block concept for the seal hardware tested in the water tunnel rig and the
2D rig proved to be an economical and expedient means of screening candidate seal de-
sign concepts and developing optimum performance geometry for a given design.

Three-Dimensional Seal Test Rig

A cross-sectional sketch of the three-dimensional (3D) air seal test rig is shown in
Figure 9. The rig can test a maximum seal diameter of 15.3 cm at a maximum seal knife
tip speed of 239 m/s. Static and dynamic seal leakage performance was measured with
this rig.

Description of Instrumentation

Similar pressure and temperature instrumentation was used to determine seal leakage in
both the 2D static rig and the 3D dynamic rig. The instrumentation locations for the
2D and 3D rigs are shown in Figures 6 and 9, respectively. A standard ASME square edge
orifice with pipe taps was used to measure the seal leakage flow. The inlet pressure
and temperature and the exit pressure at the orifice were obtained to determine flow.
The data acquired for each seal test also included seal inlet pressure (P_U) and temper-
ature (T_U) and exit pressure (P_D).

Test Conditions

The 2D and 3D rigs were operated with ambient inlet air temperatures (approximately
22°C). Rig discharge pressure was essentially ambient ("9.5 kPa). Rig inlet pressures
were varied up to a maximum of 8 atmospheres. Typically 15 seal pressure ratio values
were recorded for each configuration tested. The 3D rig tests were conducted statically
and at rotational speeds giving 80 m/s, 159 m/s, and 239 m/s knife tip velocities.

Seal clearances in the water tunnel and 2D air rig were set by feeler gauge. The 2D rig build-up clearances were corrected for the measured rig deflection to determine the seal leakage area. For the 3D air rig each knife on the seal rotor and each land on the stator were dimensionally inspected in the free-state. A feeler gauge was also used to check the end knife radial clearance after the hardware was assembled in the rig. The data reduction program calculates the rotor growth based on the dynamic conditions to determine the actual seal clearance.

Data Reduction and Calculation Methods

The measured pressures, temperatures, and seal leakage flow were used to calculate the air flow parameter characteristic,

$$\phi = \frac{W\sqrt{T_U}}{P_U\ A},$$

as a function of the seal pressure ratio, P_U/P_D. All the seal performance curves presented in this paper will be in the ϕ versus P_U/P_D form. Typically, seal performance comparisons will be based on the ϕ values at P_U/P_D of 2.0 for convenience.

2D Rig to 3D Rig Seal Performance Correlation

Comparison of the performance characteristics for similar seal configurations tested in the 2D and 3D rigs generally show good agreement. Figures 10 and 11 show the correlation between the two rigs obtained for a four knife straight-through seal with a solid-smooth land and a honeycomb land, respectively. The 2D rig seal performance at 2.0 pressure ratio only differs from that in the 3D $(\phi_{2D} - \phi_{3D})/\phi_{3D}$, by -1.9% for the solid-smooth land and +1.9% for the honeycomb land. Therefore, the 2D rig, except for the possible effects of rotational speed, provides reliable design data.

RESULTS AND DISCUSSION

This section is organized into (1) test results for a conventional straight-through labyrinth seal using solid-smooth, abradable, and honeycomb lands, and (2) test results for advanced design labyrinth seals. The testing of the conventional seals was primarily conducted in the 2D seal rig. Selected configurations were tested in the 3D seal rig to determine the effects of knife rotation on seal leakage. The advanced design labyrinth seals were initially evaluated in the water tunnel rig. Selected designs were fabricated for dynamic tests in the 3D seal rig. One design was developed further in the 2D seal rig to optimize the seal geometry. The optimized design was then tested in the 3D seal rig to determine the effects of rotation.

Conventional Labyrinth Seal Results

The conventional straight-through seal configuration shown in Figure 12 was used to evaluate four abradable and three honeycomb lands in the 2D rig. A photograph of the seal lands, including the solid-smooth baseline, is shown in Figure 13. The four abradable lands tested included two non-porous materials (nickel-graphite and aluminum-polyester) with material thicknesses of .076 cm, and two commercially available porous abradable materials designated abradable "A" and abradable "B", with material thicknesses of .229 cm. The cell sizes evaluated with the honeycomb lands were .079, .160, and .318 cm. The cell depth was .381 cm.

The flow parameter characteristics derived from the 2D rig aerodynamic test data (Reference 1) are presented in Figure 14 for the seals with abradable lands which were tested at .013 cm clearance. The solid-smooth land characteristic has also been included in Figure 14 as a baseline for comparison. It is evident from Figure 14 that the two porous abradable lands leak substantially more than the solid-smooth land. Similar tests were also conducted at .025 cm and .051 cm clearances. The seal performance with the abradable lands at a 2.0 pressure ratio is compared in Table I to that of the solid-smooth land for the three clearances tested. The performance comparisons summarized in Table I are also presented graphically in Figure 15. The abradable seal land results show that the porous land materials, abradable "A" and abradable "B", produced 27.4% and 60.3% leakage increase, respectively, as compared to the solid-smooth land at .013 cm clearance. At .051 cm clearance the leakage increase amounted to 9.9% and 12.6% for abradable "A" and abradable "B", respectively. The apparent leakage through the porous abradable lands diminishes as a percentage of the total flow as clearance is increased.

Another interesting result from the abradable land tests can be noted from the nickel-graphite land performance at .013 cm and .025 cm clearance. At these clearances the nickel-graphite land demonstrated lower leakages by 3.6% and 7.8%, respectively, than the solid-smooth land. The surface finish of the nickel-graphite land was rougher (880.μ cm) than the solid-smooth land (76.μ cm). The smoother aluminum-polyester land, surface roughness of 165.μ cm, however, did not experience a performance level different than the solid-smooth land at .013 cm and .025 cm clearance.

The honeycomb land seal performance measured in the 2D seal rig (Reference 1) is presented in Figure 16 for .051 cm clearance. These results show that the honeycomb lands substantially reduced leakage compared to the solid-smooth baseline land. The honeycomb lands were also evaluated at .013 cm and .025 cm clearance. A summary of the leakage performance for the honeycomb lands compared to the solid-smooth land at 2.0 pressure ratio is presented in Table II for the three clearances evaluated. Figure 17 graphically displays the results summarized in Table II. The honeycomb land results presented in Figure 17 show that honeycomb cell size can have a strong influence on seal leakage. At a small clearance (.013 cm) the large cell (.318 cm) honeycomb leakage was 96.2% higher than a solid-smooth land, but the leakage decreased as clearance increased until it became 18.4% lower at the largest clearance (.051 cm) tested. The small cell (.079 cm) honeycomb land reduced leakage, compared to the solid-smooth land, 4.9% at .013 cm clearance and 12.6% at .051 cm clearance. The intermediate cell size (.160 cm) honeycomb land shows a 24.4% leakage increase at .013 cm clearance, but a 21.1% leakage reduction at .051 cm clearance. Generally, it appears that honeycomb lands are effective for reducing leakage at large clearances, but should be selected with care for small clearance applications.

Abradable "A" material and .160 cm cell honeycomb lands were fabricated for testing in the 3D dynamic air seal test rig to determine the effect of seal knife rotation on leakage. A solid-smooth land was also tested to provide a baseline. A conventional four knife straight-through seal geometrically similar to the 2D rig seal (shown in Figure 12) was used in this evaluation. The aerodynamic leakage tests were accomplished statically and at three rotational velocity levels which resulted in knife tip speeds of 80 m/s, 159 m/s, and 239 m/s. The tests were conducted at .025 cm and .051 cm radial clearances. The reduction in clearance due to rotation was small (.002 cm at maximum speed), but it was included in the calculation of the leakage area.

The 3D rig static and dynamic test results for the solid-smooth baseline land (Reference 1) are presented in Figures 18 and 19 for .025 cm and .051 cm clearances, respectively. Similarly, the abradable and honeycomb lands performance (Reference 1) is presented in Figures 20, 21, 22, and 23. Figures 18 through 21 show that the solid-smooth land seal and the abradable land seal experienced a reduction in leakage with increasing knife rotational velocity. However, in Figures 22 and 23 the honeycomb land showed a mixed, but small effect due to knife rotation. Table III summarizes the dynamic test results and shows that the solid-smooth land experienced an 8.9% reduction in leakage at .025 cm clearance and 6.7% reduction for .051 cm clearance between static and the maximum knife tip velocity tested of 239 m/s. The air leakage past the abradable land shows a reduction of 9.9% and 10.3% from static to maximum dynamic conditions for .025 cm and .051 cm clearances, respectively. Table III also shows that the honeycomb land leakage at .025 cm clearance was increased 2.4% at 239 m/s but was reduced 2.6% at the .051 cm clearance compared with the static performance.

The 3D rig straight seal static and dynamic performance with abradable and honeycomb lands is compared to that with the baseline, solid-smooth land in Table IV at a 2.0 seal pressure ratio. The 3D rig maximum rotational velocity results show that the abradable land leakage is 2.2% higher than the solid-smooth land at .025 cm radial clearance, and 4.9% less than the solid-smooth land at .051 cm clearance. The 3D rig static results show the abradable land leakage 3.4% higher than the solid-smooth land at .025 cm clearance and 1.1% lower at .051 cm clearance. By comparison, the 2D rig results showed the abradable land leakage to be 9.8% and 9.9% higher than the solid-smooth land at .025 cm and .051 cm clearance, respectively. The difference in the abradable land leakage between the 2D rig and the static 3D rig results is attributed to the difference in porosity leakage and surface finish. Additional testing will be required to identify these individual effects on abradable land leakage.

Table IV shows that the honeycomb land leakage in the 3D rig was 4.9% less statically than the solid-smooth land, but 6.9% greater at 239 m/s for .025 cm clearance. The honeycomb land leakage at .051 cm clearance was 27.4% lower than the solid-smooth land statically and 24.2% less at 239 m/s. Therefore, the use of .160 cm cell honeycomb lands above .025 cm clearance provides a substantial reduction in leakage of conventional straight-through seals.

The approach used in this investigation to reduce labyrinth seal leakage was to improve sealing effectiveness through the use of unique geometry configurations designed to increase the internal seal cavity turbulence. Several candidate configuration concepts are shown in Figure 24 (References 2 and 3).

Numerous geometric parameters influence the level of internal seal cavity turbulence. The effects of some geometric parameters can be calculated analytically, but the interactions of the numerous geometric parameters involved in a labyrinth seal design are complex and do not lend themselves to current analytical methods. Therefore, a water tunnel flow visualization rig, with adjustable seal geometry components, was used for the preliminary evaluation of the turbulence generated by the candidate seal designs. A typical water rig photograph of an advanced seal concept is shown in Figure 25. Arrows have been added to indicate the observed flow direction. The seal pitch, knife angle, and step height were varied to obtain an optimum mix of geometry. The water rig proved to be an invaluable tool for screening seal designs since the evaluation of numerous design features of the candidate seal could be made rapidly and economically with the same hardware.

Based on the results of the water rig tests, several candidate designs and derivitive designs were fabricated and tested statically and dynamically in the 15.3 cm diameter air seal rig (shown in Figure 9.) The static results at .025 cm clearance for Designs 1, 3, 4, and 5, and a baseline conventional step seal are given in Figure 26. A performance comparison of the advanced seal configurations with the baseline seal is also presented in Table V at a 2.0 pressure ratio. This table shows that the advanced designs achieved a 12.8% to 14.0% reduction in static leakage, compared to the baseline seal. The dynamic test results at the maximum test velocity of 239 m/s show little additional effect on leakage. Table V also shows that the conventional step seal experienced a 0.8% increase in leakage, while the advanced designs ranged between a 3.2% increase to a 1.4% decrease in leakage. The net dynamic results for the advanced designs, therefore, showed a leakage reduction range from 10.7% to 15.9%.

Additional development work (Reference 1) was accomplished on the advanced seal Designs 4 and 5 shown in Figure 24. Variable geometry components similar to the water tunnel rig hardware were used in the 2D rig (Figure 6) to optimize the performance of these seal designs. The parameters investigated included knife pitch, knife height, step height, land notch, and knife angle. The Design 4 optimized configuration is shown in Figure 27. Design 5, shown in Figure 28, uses the same optimized dimensions as Design 4, but with the seal knives canted in the opposite direction. Design 4 is intended for leakage flow in the large-diameter-to-small diameter direction. Design 5 is applicable for leakage flow in the small-to-large-diameter direction. The static and dynamic performance characteristics for the optimized advanced seal derived from the 3D rig tests are presented in Figures 29 and 30 for Designs 4 and 5, respectively. A performance curve for a similar, conventional stepped seal has been included on these figures for comparison purposes. A single curve for the baseline seal has been used for simplicity since rotational effects were found to be less than 3.% of the static performance (Reference 3). The performance curves of Figures 29 and 30 apply to a .051 cm clearance.

Table VI summarizes and compares the performance of the optimized advanced seals to the baseline stepped seal. The optimized Design 4 seal reduces leakage 16.4% dynamically compared to the baseline seal. Design 5 reduced leakage 26.9% dynamically. These results show that substantial performance gains can be achieved with improved internal cavity turbulence.

Table VI also shows that the effects on leakage of seal knife rotation for the conventional stepped seal and the optimized Design 4 seal were quite small (-2.9% and -2.2%, respectively). The Design 5 seal showed slightly more sensitivity to rotation with a 5.9% reduction in leakage at the maximum test velocity of 239 m/s.

CONCLUSIONS

Advanced design labyrinth seals incorporating geometric features to increase seal cavity turbulence substantially reduce leakage. Optimized geometry for an advanced seal design with high internal cavity turbulence was developed that reduced leakage 26.9% compared to a conventional stepped seal.

Conventional straight-through labyrinth seals with honeycomb lands reduced leakage up to 24.2% at .051 cm clearance compared to a solid-smooth land. However, as clearance decreased to .013 cm, the honeycomb lands were found to increase leakage above a solid-smooth land.

Surface roughness effects of the non-porous abradable lands contributed toward reducing leakage up to 7.8% at .025 cm clearance for conventional straight-through seals. Additional studies are required to investigate this effect and to provide design guidelines and analytical methods.

Conventional straight-through seals leak substantially more with porous-abradable lands than with solid-smooth lands, as expected. The porous-abradable lands tested showed an increase in leakage over a solid-smooth land of 60.3% at .013 cm clearance and 12.6% at .051 cm clearance.

Seal knife rotational velocity had mixed effects on seal performance. Leakage for a conventional straight-through seal using a solid-smooth or an abradable land was reduced up to 10.% at 239 m/s knife tip velocity. However, the honeycomb land only experienced a ±2.5% leakage change, depending on clearance. The advanced design seal experienced a maximum leakage reduction of 5.9% at 239 m/s compared to the static results. A comparable stepped seal experienced a 2.9% leakage reduction at 239 m/s knife tip velocity.

REFERENCES

1. Stocker, H. L., Cox, D. M., and Holle, G.F., "Aerodynamic Performance of Conventional and Advanced Design Labyrinth Seals with Solid-Smooth, Abradable, and Honeycomb Lands," Detroit Diesel Allison EDR 9339, November 1977.

2. Stocker, H. L., "Exploratory Investigation for Reducing Labyrinth Seal Leakage in High Pressure Ratio Gas Turbines," Detroit Diesel Allison EDR 7968, September 1973.

3. Cox, D. M., "Advanced Labyrinth Seal Development Program," Detroit Diesel Allison EDR 8539, July 1975.

BIBLIOGRAPHY

Shapiro, A. H., The Dynamics and Thermodynamics of Compressible Fluid Flow, Vol. I, Chapter 4.

Labyrinth Seal Leakage Flow Analogy, Detroit Diesel Allison ETR 73201, March 1973.

Stocker, H. L., Advanced Labyrinth Seal Design for High Pressure Ratio Gas Turbines, ASME Paper 75-WA/GT-22, December 1975.

Meyer, C. A., and Lowrie, J. A., III, The Leakage Thru Straight and Slant Labyrinth Seals, ASME Paper 75-WA/PTC-2, August 1974.

Mahler, F., Advanced Seal Technology, AFAPL-TR-72-8, February 1972.

Mahler, F., Advanced Seal Technology, AFAPL-TR-72-7, February 1972.

Koeing, H., and Bowley, W., Labyrinth Seal Analysis, ASME, January 1972.

Ueda, T., and Jubo, T., The Leakage of Air Through Radial Labyrinth Glands, Japan Society of Mechanical Engineers, Vol. 10, No. 38, 1967.

Zabriskie, W., and Sternlicht, B., Labyrinth Seal Leakage Analysis, ASME, 1959.

Kearton, W. J., and Keh, T. H., Leakage of Air Through Labyrinth Seals, Proceedings of the Institute of Mechanical Engineers, Series A, Vol. 156.

Egli, A., Leakage of Steam Through Labyrinth Seals, ASME 1935, Vol. 57.

ACKNOWLEDGEMENTS
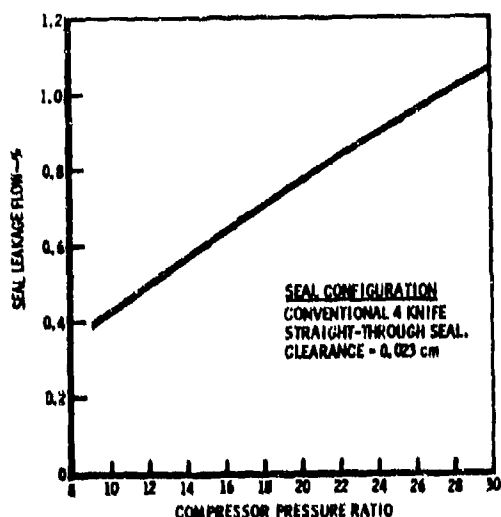
FIGURE 1. EFFECT OF COMPRESSOR PRESSURE
RATIO ON LABYRINTH SEAL LEAKAGE

The graph shows SEAL LEAKAGE FLOW—% (y-axis) versus COMPRESSOR PRESSURE RATIO (x-axis). Note on chart:

SEAL CONFIGURATION
CONVENTIONAL 4 KNIFE
STRAIGHT-THROUGH SEAL.
CLEARANCE = 0.025 cm

ADVANCED TRANSPORT ENGINE	TRADE-OFF IN COMPONENT EFFICIENCY
REDUCTION OF 1% SEAL LEAKAGE = 0.0% THRUST (WITH REMATCHING)	+0.91% η HP COMPRESSOR OR
BPR = 5.25 = -0.40% SFC	+0.51% η HP TURBINE

FIGURE 2. PERFORMANCE PAYOFFS FOR REDUCING HIGH PRESSURE
TURBINE SEAL LEAKAGE 1% OF ENGINE AIRFLOW

A 25% REDUCTION IN LEAKAGE FOR
EACH SEAL IN ENGINE TYPICALLY
YIELDS A SPECIFIC FUEL
CONSUMPTION REDUCTION OF ... 2.7%

U.S. COMMERCIAL AND MILITARY
ANNUAL JET FUEL CONSUMPTION
(PROJECTED FOR 1977)* .... 15,912,540,000 GALLONS

A 2.7% REDUCTION IN SPECIFIC
FUEL CONSUMPTION WILL SAVE
ANNUALLY .... 429,638,600 GALLONS

*PROJECTIONS OBTAINED FROM FEDERAL ENERGY ADMINISTRATION,
OFFICE OF AVIATION FUELS

FIGURE 3. EFFECT OF REDUCING ALL SEAL LEAKAGE
25% IN GAS TURBINE ENGINES
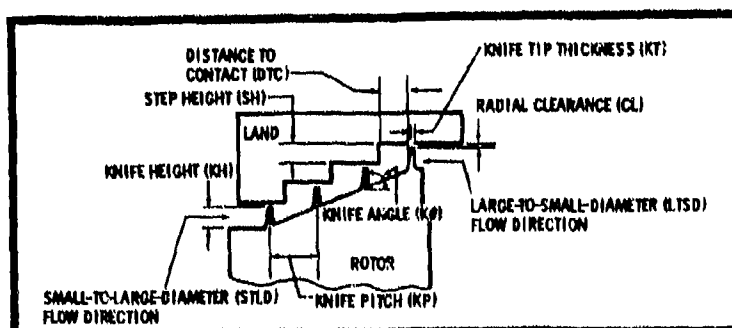
FIGURE 4. SEAL NOMENCLATURE
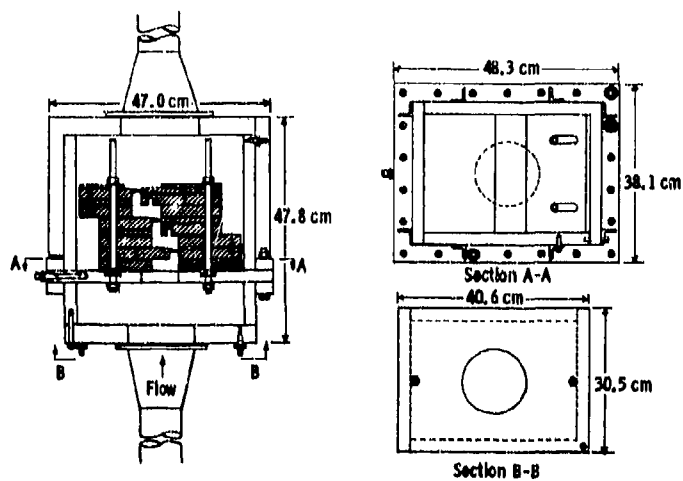
FIGURE 5. SKETCH OF WATER TUNNEL FLOW VISUALIZATION RIG
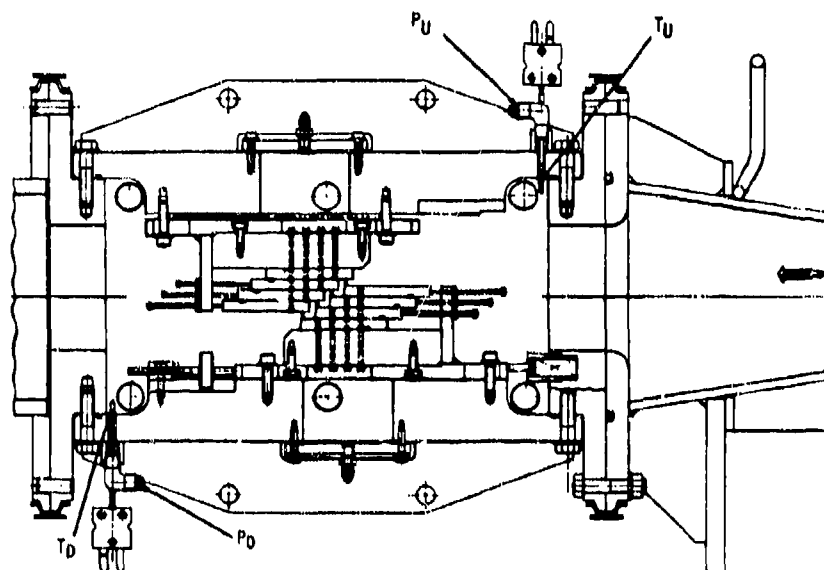
FIGURE 6. SKETCH OF TWO-DIMENSIONAL AIR SEAL TEST RIG
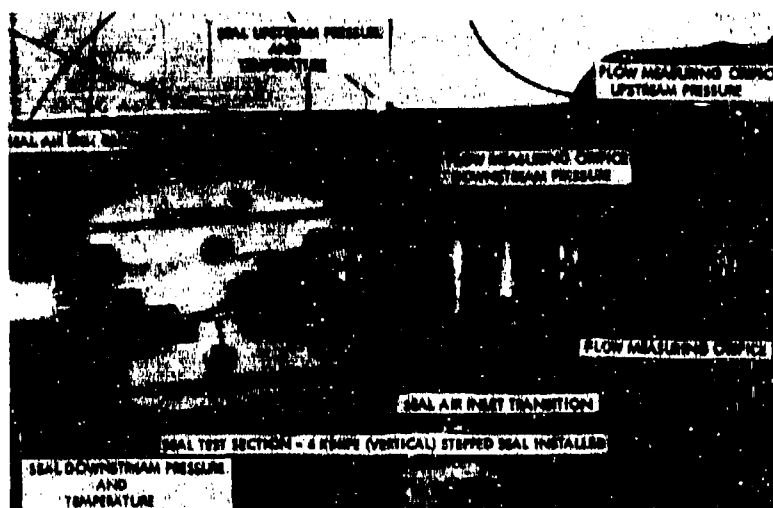
FIGURE 7. TWO-DIMENSIONAL LABYRINTH SEAL AIR TEST RIG INSTALLATION
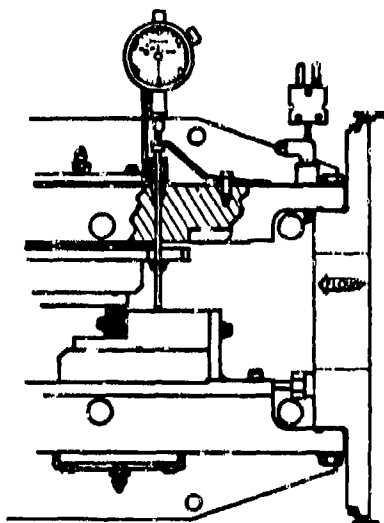
FIGURE 8. TWO-DIMENSIONAL SEAL RIG CASE DEFLECTION MEASUREMENT SYSTEM
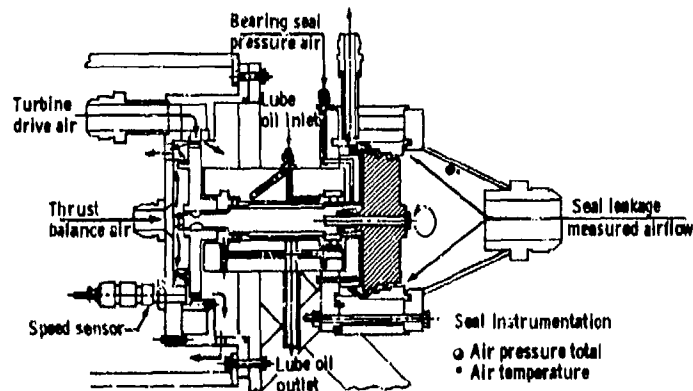
FIGURE 9. SKETCH OF THREE-DIMENSIONAL AIR SEAL TEST RIG

4 KNIFE STRAIGHT SEAL WITH SOLID SMOOTH LAND

KP = 0.279 cm   KH = 0.279 cm   CLEARANCE = 0.051 cm
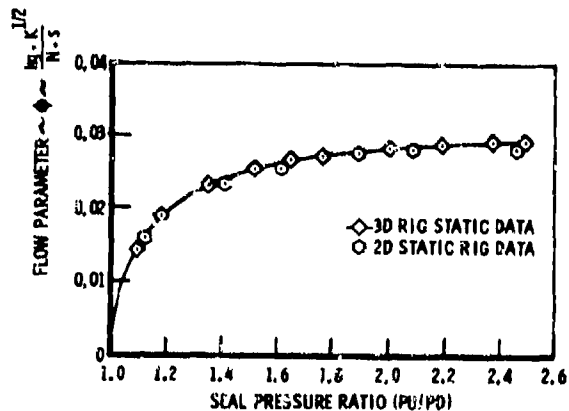
FIGURE 10. PERFORMANCE COMPARISON FOR 2D RIG AT STATIC CONDITIONS

4 KNIFE STRAIGHT SEAL WITH 0.160 cm CELL HONEYCOMB LAND

KP = 0.279 cm   KH = 0.279 cm   CLEARANCE = 0.051 cm
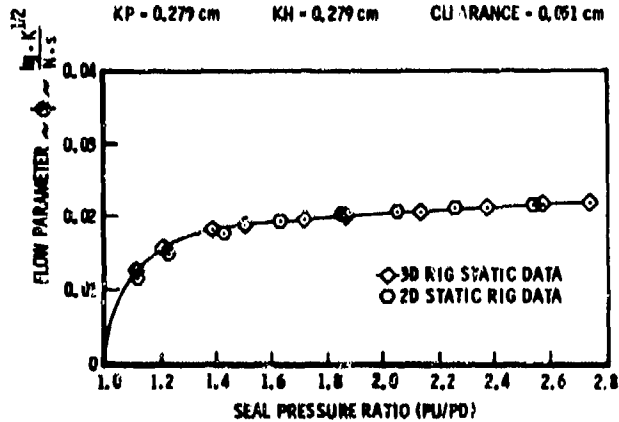
FIGURE 11. PERFORMANCE COMPARISON FOR 2D RIG AND 3D RIG AT STATIC CONDITIONS
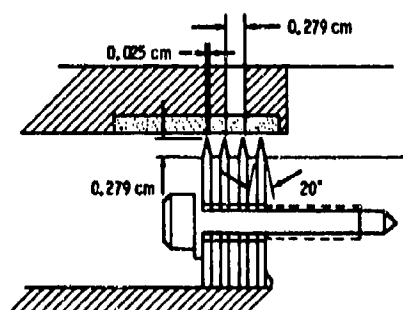
FIGURE 12. CONVENTIONAL STRAIGHT-THROUGH SEAL USED IN
2D RIG SEAL LAND PERFORMANCE EVALUATION
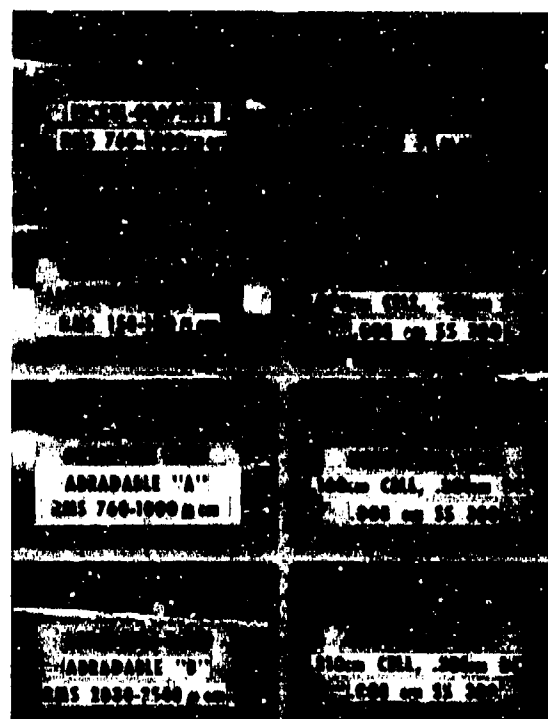
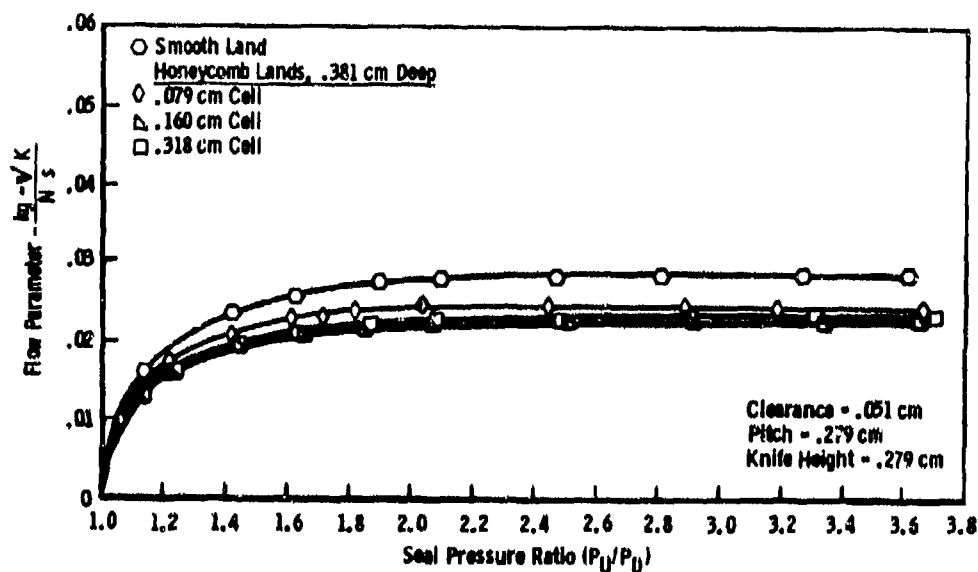FIGURE 13. 2D TEST RIG STRAIGHT SEAL LANDS
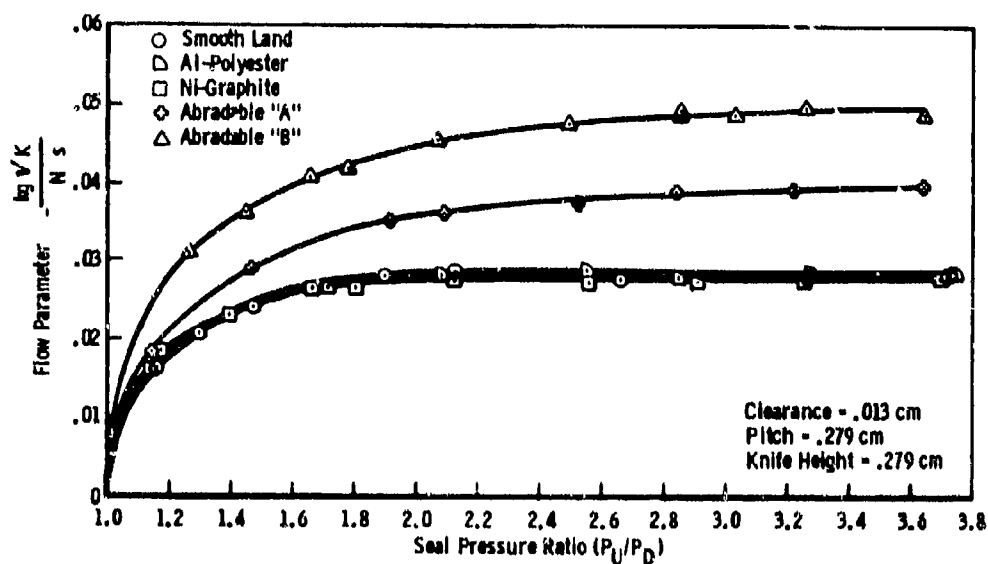
FIGURE 14. 2D RIG FOUR KNIFE STRAIGHT SEAL WITH SMOOTH AND ABRADABLE LANDS

Land Type	Clearance (cm)	$\frac{W\sqrt{T_U}}{P_U A}$	Change From Smooth Land
Smooth	.013	.0277	0.
	.025	.0272	0.
	.051	.0277	0.
Abradable "A"	.013	.0353	+27.4%
	.025	.0299	+ 9.8%
	.051	.0305	+ 9.9%
Abradable "B"	.013	.0445	+60.3%
	.025	.0344	+26.3%
	.051	.0312	+12.6%
Ni-Graphite	.013	.0268	- 3.6%
	.025	.0251	- 7.8%
	.051	.0284	+ 2.3%
Al-Polyester	.013	.0277	0.0
	.025	.0271	- 0.6%
	.051	.0298	+ 7.4%

Note: + Indicates leakage greater than smooth
     land at comparable clearance.

    - Indicates leakage less than smooth
     land at comparable clearance.

TABLE I COMPARISON OF SMOOTH AND ABRADABLE LAND
PERFORMANCE AT 2.0 PRESSURE RATIO
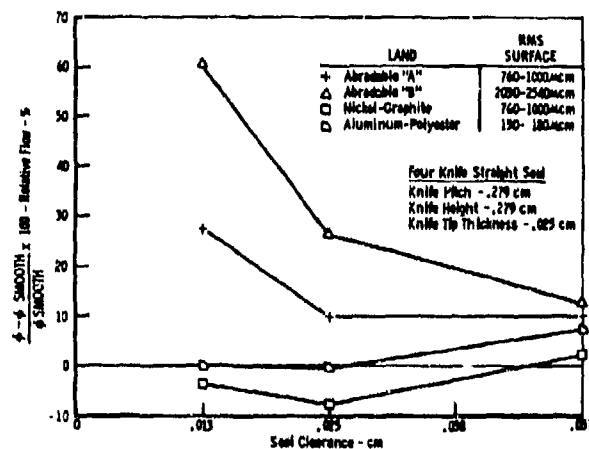
FIGURE 15. COMPARISON OF ABRADABLE LANDS PERFORMANCE
RELATIVE TO A SMOOTH LAND AT P_U/P_D = 2.0

FIGURE 16. 2D RIG FOUR KNIFE STRAIGHT SEAL WITH SMOOTH AND HONEYCOMB LANDS

Land Type	Clearance (cm)	$\frac{W\sqrt{T_U}}{P_U A}$	Change From Smooth Land
Smooth	.013	.0277	0.
	.025	.0272	0.
	.051	.0277	0.
Honeycomb Cell .079 cm	.013	.0264	- 4.9%
	.025	.0240	-11.7%
	.051	.0242	-12.6%
Honeycomb Cell .160 cm	.013	.0345	+24.4%
	.025	.0252	- 7.5%
	.051	.0219	-21.1%
Honeycomb Cell .318 cm	.013	.0544	+96.2%
	.025	.0303	+11.2%
	.051	.0226	-18.4%

Note: + indicates leakage greater than smooth land at comparable clearance.
      - indicates leakage less than smooth land at comparable clearance.

TABLE 11 COMPARISON OF SMOOTH AND HONEYCOMB LAND PERFORMANCE AT 2.0 PRESSURE RATIO
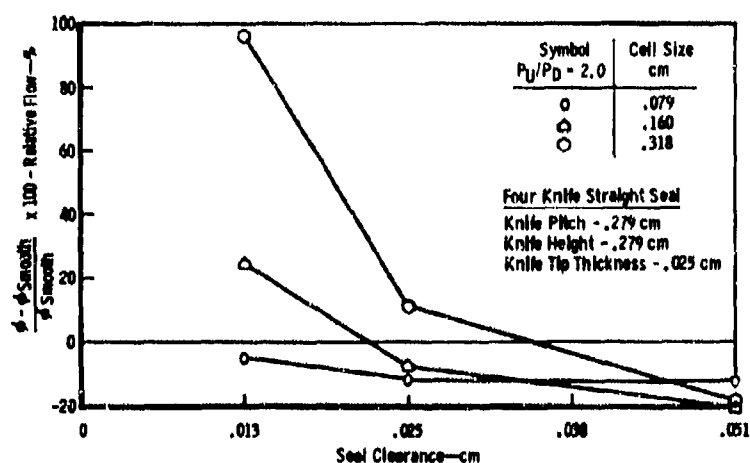
FIGURE 17. COMPARISON OF HONEYCOMB LANDS RELATIVE TO A SMOOTH LAND
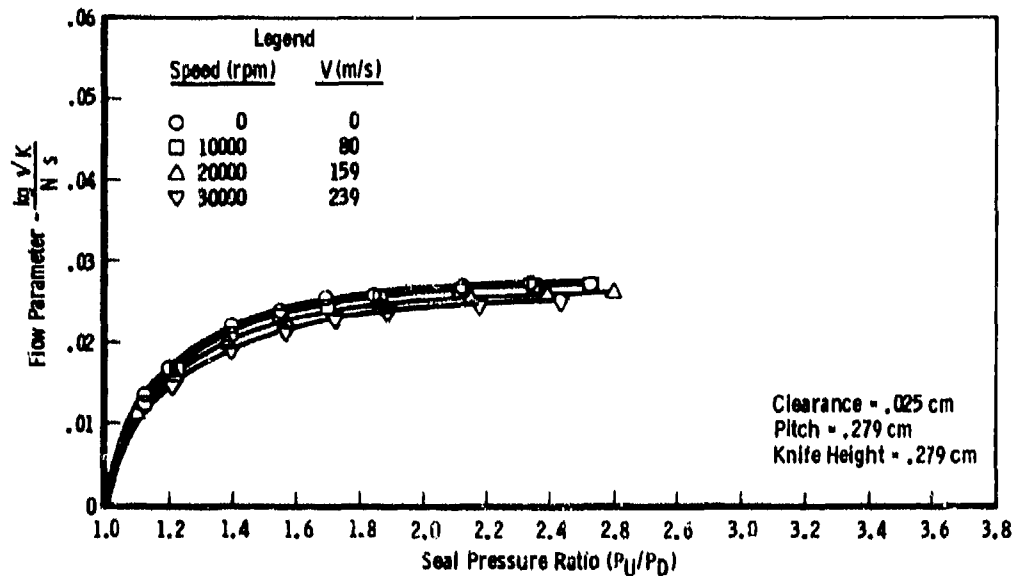
FIGURE 18. FOUR KNIFE STRAIGHT SEAL - SMOOTH LAND
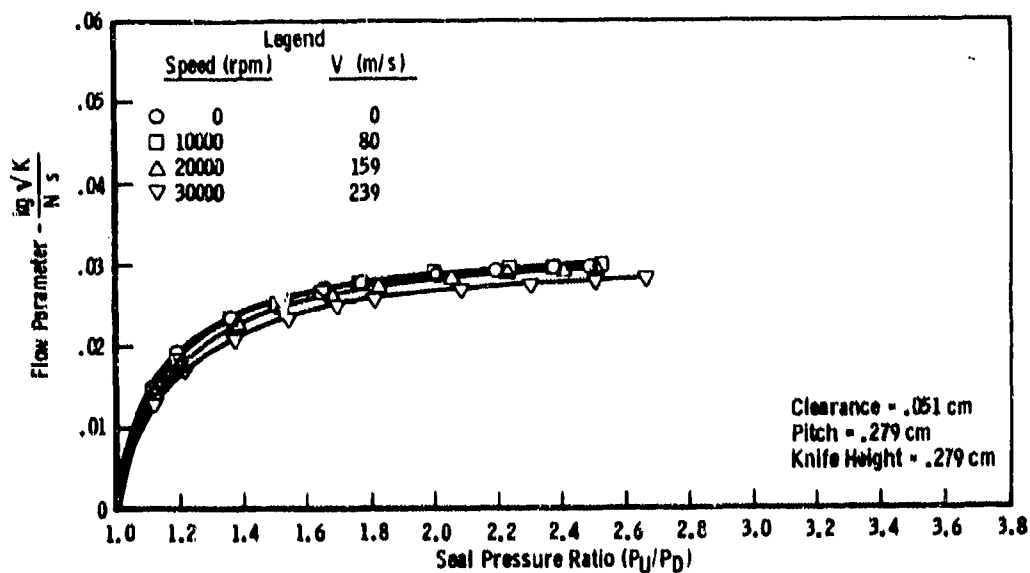
FIGURE 19. FOUR KNIFE STRAIGHT SEAL - SMOOTH LAND
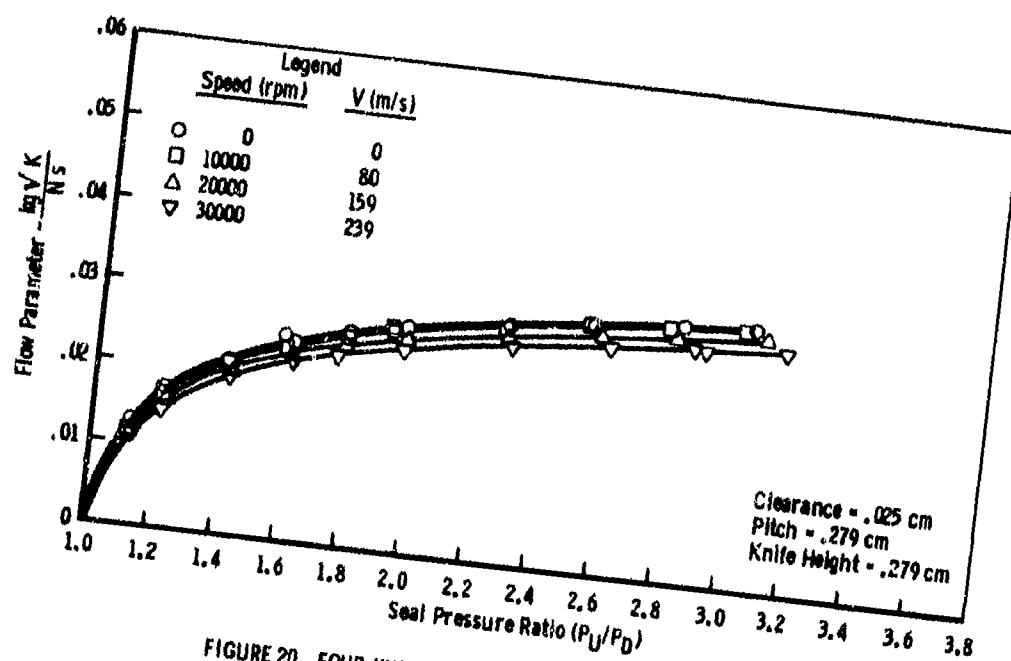
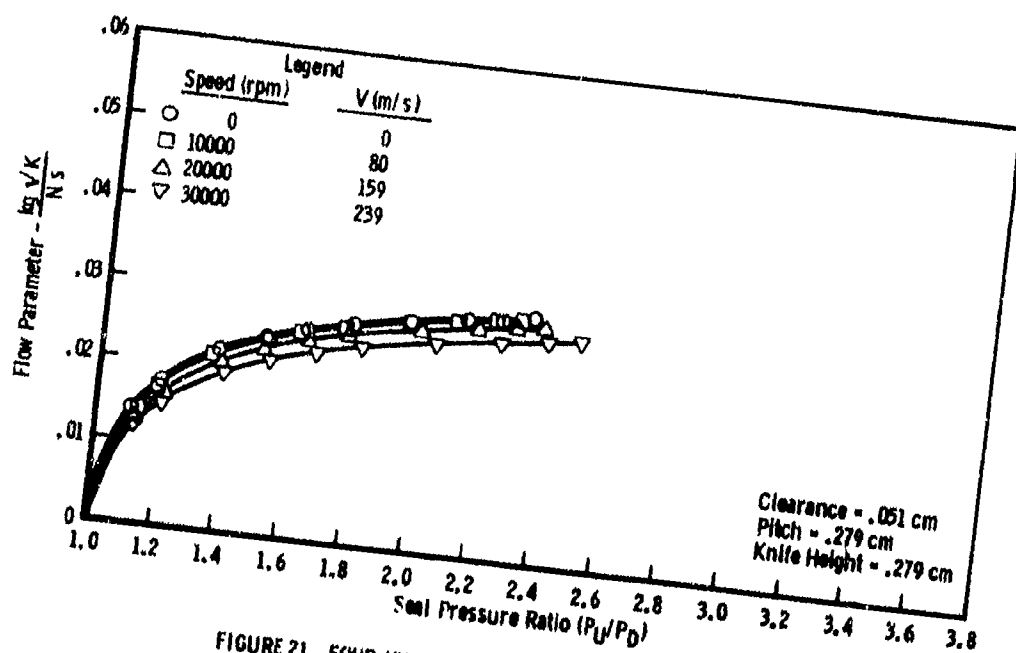FIGURE 20. FOUR KNIFE STRAIGHT SEAL – ABRADABLE "A" LAND

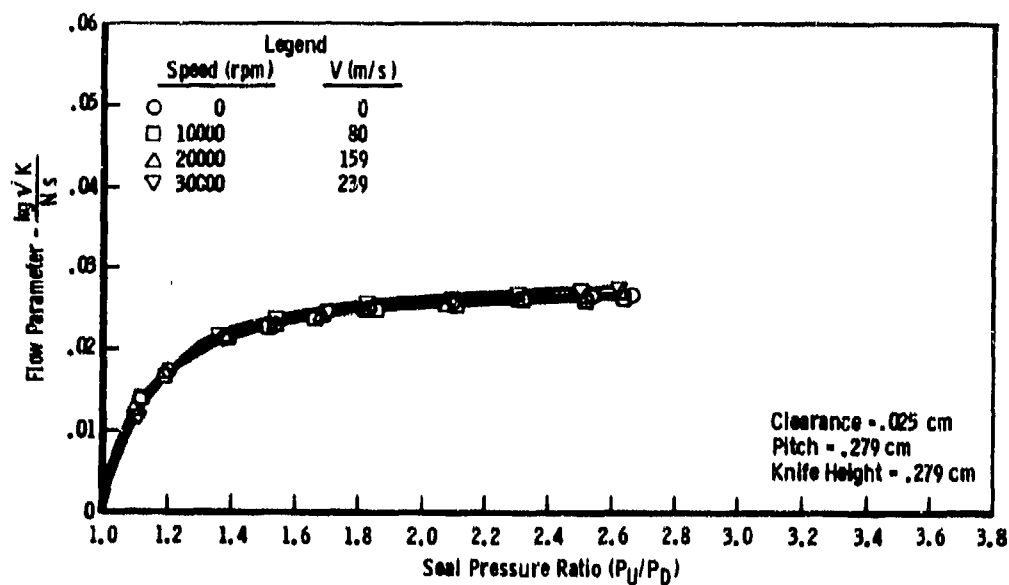FIGURE 21. FOUR KNIFE STRAIGHT SEAL – ABRADABLE "A" LAND

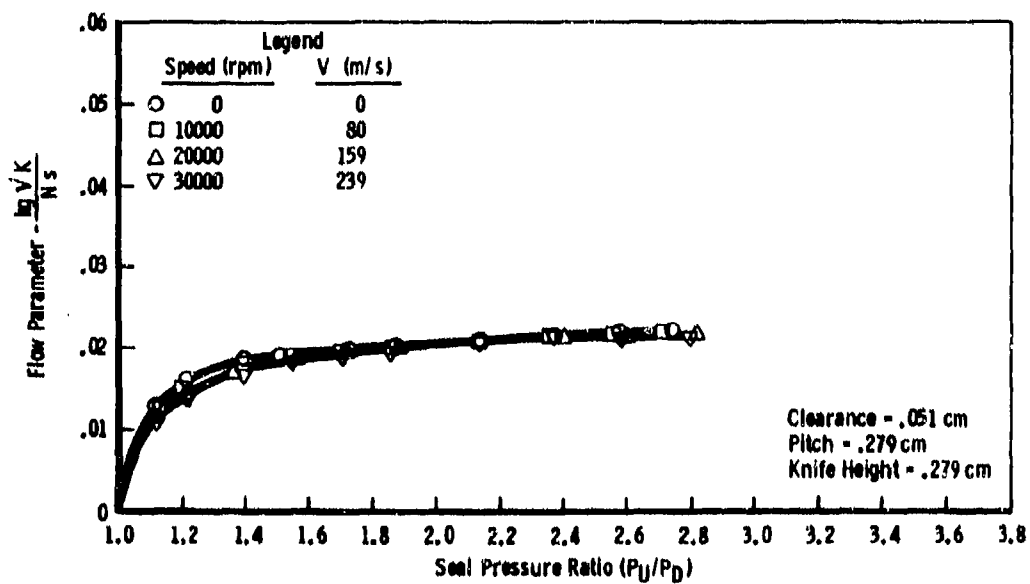FIGURE 22. FOUR KNIFE STRAIGHT SEAL - HONEYCOMB LAND

FIGURE 23. FOUR KNIFE STRAIGHT SEAL - HONEYCOMB LAND

Land	CL cm	ϕ_0 $\dfrac{W\sqrt{T}}{PA} \sim \dfrac{K_g\sqrt{K}}{Ns}$ V=0 (Static)	$\dfrac{\Delta\phi/\phi_0}{\%}$ V=80 m/s	V=159 m/s	V=239 m/s
Solid-Smooth	.025	.0266	-2.6	-6.0	-8.9
	.051	.0283	+1.3	-1.9	-6.7
Abradable "A"	.025	.0275	-1.6	-5.5	-9.9
	.051	.0280	-.8	-4.6	-10.3
Honeycomb Cell	.025	.0253	-1.2	-1.2	+2.4
.160 cm	.051	.0205	-.7	-2.2	-2.6

TABLE III EFFECT OF ROTATION ON THE PERFORMANCE OF A FOUR KNIFE STRAIGHT SEAL AT P_U/P_D = 2.0 WITH SMOOTH, ABRADABLE, AND HONEYCOMB LANDS

Land	CL cm	$\phi_{ss} - \phi/\phi_{ss} \sim \%$ V=0 m/s	V=80 m/s	V=159 m/s	V=239 m/s
Solid-Smooth	.025	Baseline	Baseline	Baseline	Baseline
Abradable "A"		+ 3.4	+ 4.4	+ 4.0	+ 2.2
*Honeycomb		- 4.9	- 3.5	0	+ 6.9
Solid-Smooth	.051	Baseline	Baseline	Baseline	Baseline
Abradable "A"		- 1.1	- 3.2	- 3.8	- 4.9
*Honeycomb		-27.4	-28.9	-27.7	-24.2

ϕ_{ss} ~ Solid-Smooth Land Flow Parameter

ϕ ~ Abradable "A" or Honeycomb Flow Parameter

*Honeycomb Cell Size - .160 cm; cell depth - .230 cm

TABLE IV COMPARISON OF ABRADABLE AND HONEYCOMB SEAL LAND PERFORMANCE WITH SOLID LAND AT 2.0 PRESSURE RATIO

Design 1   Design 2   Design 3
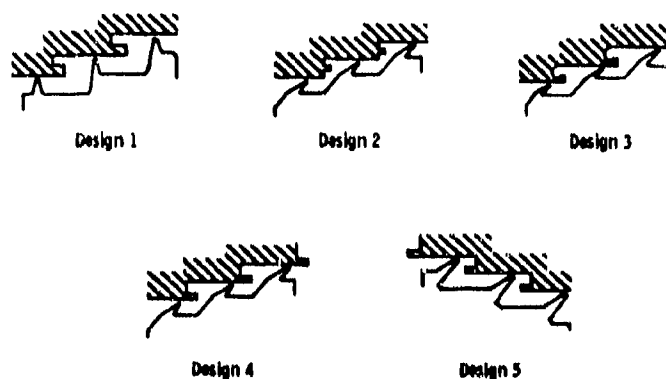
Design 4   Design 5

FIGURE 24. SKETCHES OF ADVANCED LABYRINTH SEAL CONFIGURATIONS

FIGURE 25. WATER RIG PHOTOGRAPH OF CANDIDATE SEAL 9
0.25 cm TANGENTIAL BLEED SLOT.
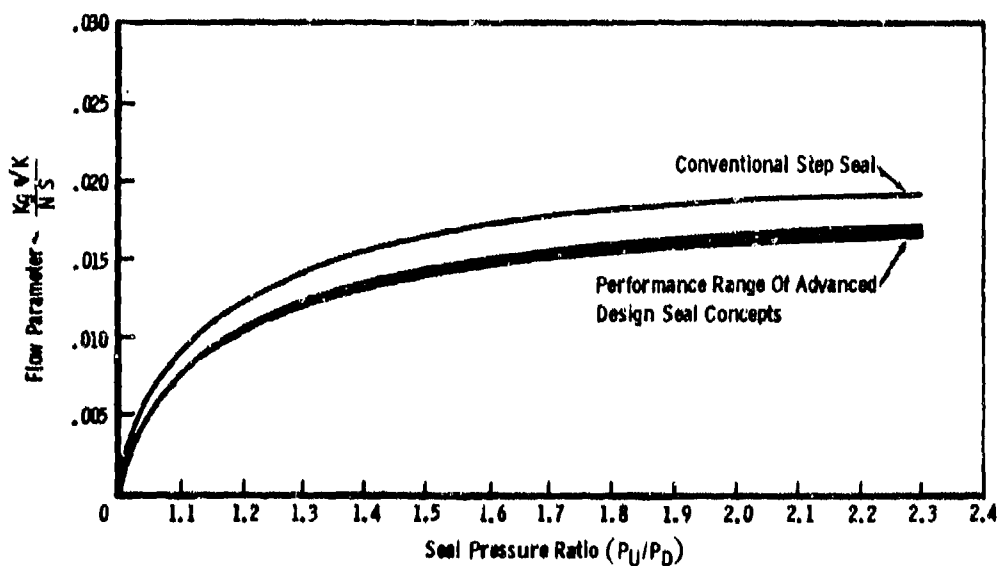(ARROWS NOTE FLOW DIRECTION.)

FIGURE 26. COMPARISON OF ADVANCED DESIGN LABYRINTH
SEAL PERFORMANCE WITH CONVENTIONAL STEP SEAL

Configuration	Percent Leakage Reduction Compared to Baseline Seal		Dynamic Test Leakage Change From Static Test
	V = 0 m/s	V = 239 m/s	
Baseline Conventional Step Seal	--	--	+0.8%
Design 1	12.8	10.7	+3.2%
Design 3	13.6	13.5	+0.9%
Design 4	13.6	13.5	+0.9%
Design 5	14.0	15.9	-1.4%
Radial Clearance = .025 cm			

TABLE V SUMMARY OF STATIC AND DYNAMIC PERFORMANCE OF ADVANCED DESIGN LABYRINTH SEALS COMPARED TO CONVENTIONAL STEP SEAL AT A 2.0 PRESSURE RATIO
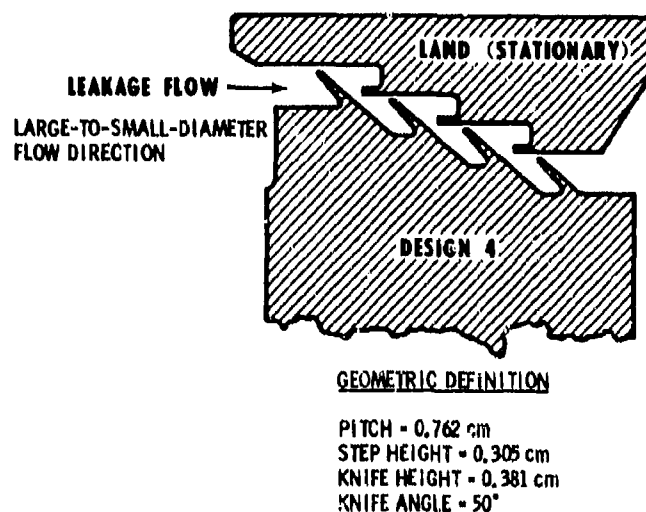

LEAKAGE FLOW →

LARGE-TO-SMALL-DIAMETER FLOW DIRECTION

DESIGN 4

GEOMETRIC DEFINITION

PITCH = 0.762 cm
STEP HEIGHT = 0.305 cm
KNIFE HEIGHT = 0.381 cm
KNIFE ANGLE = 50°

FIGURE 27. OPTIMIZED ADVANCED SEAL CONFIGURATION

LAND (STATIONARY)
0.165 cm
0.544 cm
0.038 cm RADIUS
0.0635 cm
← LEAKAGE FLOW
SMALL-TO-LARGE-DIAMETER FLOW DIRECTION

DESIGN 5

GEOMETRIC DEFINITION
PITCH = 0.762 cm
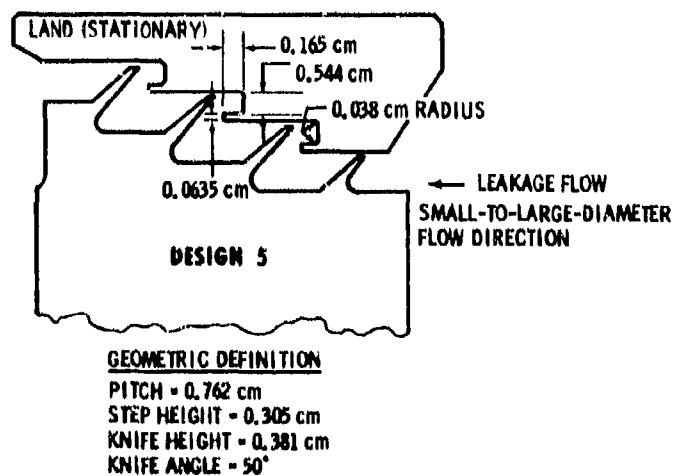STEP HEIGHT = 0.305 cm
KNIFE HEIGHT = 0.381 cm
KNIFE ANGLE = 50°

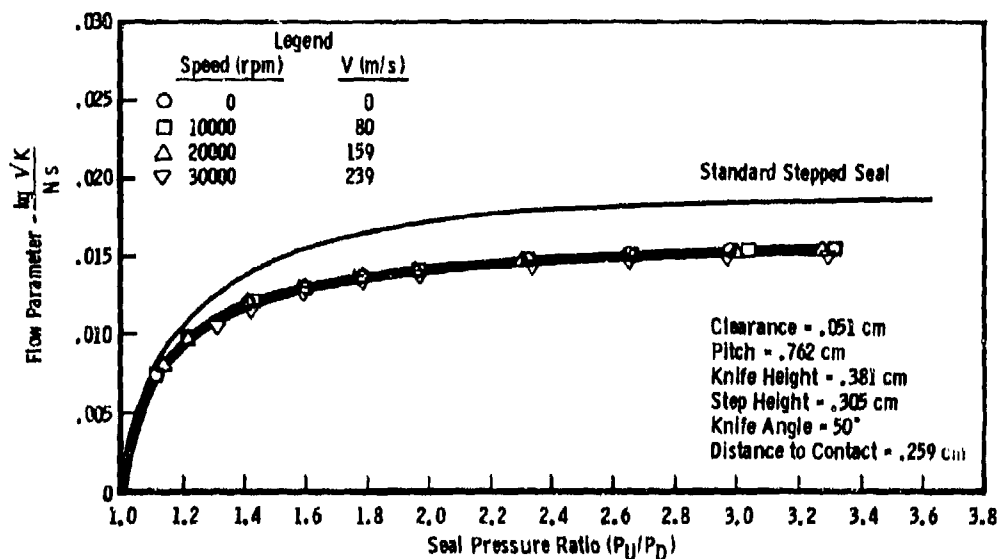FIGURE 28. OPTIMIZED ADVANCED SEAL CONFIGURATION

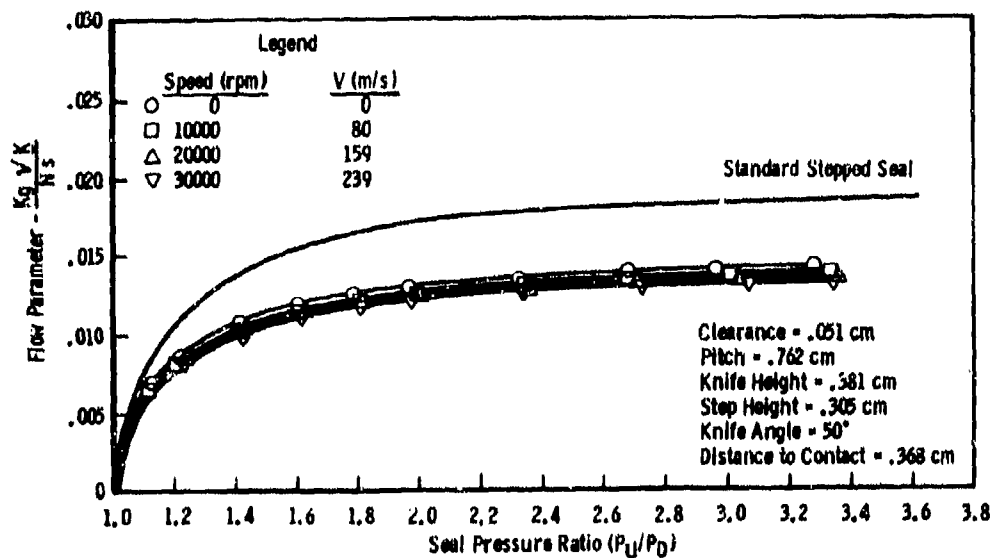FIGURE 29. FOUR KNIFE ADVANCED STEPPED SEAL – DESIGN 4

FIGURE 30. FOUR KNIFE ADVANCED STEPPED SEAL – DESIGN 5

| Configuration | Percent Leakage Reduction Compared to Baseline Seal | | Dynamic Test Leakage Change From Static Test |
	V = 0 m/s	V = 239 m/s	
Baseline Conventional Step Seal	--	--	-2.9%
Optimized Advanced Seal - Design 4	17.1	16.4	-2.2%
Optimized Advanced Seal - Design 5	23.9	26.0	-5.9%

Radial Clearance = .051 cm

TABLE VI SUMMARY OF OPTIMIZED ADVANCED DESIGN LABYRINTH
SEAL PERFORMANCE AT A 2.0 PRESSURE RATIO

DISCUSSION

A.Moore, UK

The advanced design described in your lecture uses airflows entering the seal at the smaller diameter and shows a significant improvement with rotational speed. If the airflow enters the seal at a larger diameter, i.e. if the airflow is reversed, is the effect of rotation increased?

Author's Reply

The optimized advanced seal design was developed initially for flow in the "large-to-small-diameter" direction as shown in Figure 27. Canting the knives into the flow was found to be beneficial. However, application requirements exist that require sealing in the opposite flow direction. To address this application, the advanced seal knives of Figure 27 were canted the same amount in the opposite direction as shown in Figure 28. The rotation effects were slightly different for the two configurations. Using the small-to-large-diameter seal design for flow in the opposite direction has not been tested either statically or dynamically, but I would expect the static leakage to be higher when compared to the leakage flowing in the designed direction. If the effects of rotation were greater for reverse leakage in the small-to-large-diameter seal design, it would have to offset any increase in static leakage to yield a net gain in sealing efficiency. My experience has shown that rotation has a small effect on the static leakage performance of labyrinth seals.

A.Moore, UK

Do you get the same benefits, or other benefits (more or less) with rotation when the flow is directed from a large diameter to a small diameter?

Author's Reply

The advanced seal configuration shown in Figures 27 and 28 were designed for leakage flow in a specific direction. These configurations were subsequently not tested statically or dynamically for a leakage flow direction opposite to the design direction.

However, the measured effects of rotation on leakage for the two advanced seal designs shows that the small-to-large-diameter configuration, shown in Figure 28, experienced a slightly higher reduction in leakage with rotation, 5.9%, than the large-to-small-diameter design, shown in Figure 27, which had a 2.2% reduction in leakage with rotation.

G.A.Halls, UK

Would you please comment on the accuracy and repeatability of your results, particularly on the rotating rig, bearing in mind that a small change in clearance of say 0.0025 cm can produce a 10% change in the flow of a seal of 0.025 cm gap.

How sure are you that the changes in flow which you measure are due to the configuration and do not come from a gap change which has crept in unnoticed.

Author's Reply

The dynamic rig test seals that we use are approximately 15.2 cm (6.0 in.) in diameter. Ambient temperature air is used for all testing thus eliminating the thermal growth effects. Several approaches have been used to determine seal clearance at the rotational test speeds. To begin, the seal rotor and land diameter are measured at four circumferential locations to obtain the average static condition clearance. The rotor and land are also measured to determine that the maximum and minimum diameters are within print tolerances. The assembled seal configuration in the rig is checked for radial clearance using a feeler gauge at four circumferential locations.

The running clearance is determined by applying the calculated radial growth of the rotor to the measured clearances. A check of the calculated radial growth was made by using plastic rub strips and measuring the depth of the knife groove after running at various speed levels.

It should be noted that the same straight-through seal rotor is used to evaluate the smooth, abradable, and honeycomb lands. The same radial growth increment is applied, at a given speed, for each land tested. Therefore, the test results were all obtained with the same radial clearance change and the static to dynamic percent change is consistent with each configuration. The sensitivity of seal leakage to clearance is acknowledged and I feel that the attention we have given to this influencing parameter has been adequate and accurate.

F.Mahler, US

(a) Have you any conclusions as to the sensitivity of leakage, in the advanced seal, to the axial gap between the land extension and the canted knife edge?

(b) Have you any data on the rub tolerance of the advanced seal in conjunction with the various land types with respect to either mechanical condition or leakage after rub?

Author's Reply

(a) The advanced seal has been tested for various axial gaps between the land extension and the canted knife edge. As expected, the performance of the advance seal does change with variation in the knife to land axial gap. However, a similar set of information has not been generated for the conventional step seal. Therefore, a comparison of the performance of the advanced seal design and the conventional step seal at various axial gaps has not been made. The results I have presented comparing the advanced seal to the conventional step seal have been obtained at the same axial gap.

(b) I do not have any data regarding the rub tolerance of the advanced seal design. The use of striated, abradable, and honeycomb lands with the advanced seal is being investigated. These lands provide rub tolerance for conventional labyrinth seals and may be useful for the advanced seal.

B.H.Becker, Germany

In turbomachinery there is generally a very limited axial space. Comparing the pitch values of the optimized step seal with the straight-through seal shows nearly a factor of three for the same clearance. The fact that the straight-through seal may have a much higher number of knives for a given axial length therefore should be taken into account when comparing the leakage flows.

Author's Reply

The advanced seal design is primarily directed to the same application area as the conventional step seal. This application area is high radial clearances. Granted, more knives can be gotten into a given axial distance using a straight-through seal as compared to a step seal. However, as radial operating clearances get above 0.0381 cm (0.015 in.), the efficiency of the straight-through seal is less than the step seal. Adding more knives to the straight-through seal will reduce leakage, but most designers find that for a given axial length, a stepped seal will have equal or lower leakage than the best straight-through seal when the radial clearance is 0.0381 cm (0.015 in.) or greater.

FACTORS ASSOCIATED WITH RUB TOLERANCE OF COMPRESSOR TIP SEALS

Charles W. Elrod
Aerospace Engineer
Air Force Aero Propulsion Laboratory
Components Branch (AFAPL/TBC)
Wright-Patterson AFB, Ohio

SUMMARY

This paper will examine the ineffective tolerance of compressor blade tip seals to high speed rubs. Research being conducted by the Air Force Aero-Propulsion Laboratory, at Wright-Patterson Air Force Base will be described which examine basic issues of the problem.

Two facilities used to study different facets of the problem will be described and the integration of the test data from the facilities in the overall rub tolerance program will be delineated. A Compressor Rub Test Facility (CRTF) including a single compressor stage driven by an electric motor drive is used to study rub interaction in a realistic compressor environment. The apparatus is unique in its capability to provide a full range of compressor operating conditions and rub interaction rates for a full scale tip seal configuration.

The second facility, a laser test facility, is used to examine the phenomena of self sustained combustion of titanium in a simulated compressor environment, especially the environment involved in the CRTF. Although the information being generated is applicable to various compressor environments it is of particular interest to the CRTF. The burn rate and damage criteria is being used to develop proper procedures for safe test operation. In addition, the pressure, temperature, and velocity relationships on self sustained combustion of titanium are noted to have significant relevance to many situations outside the CRTF environment.

INTRODUCTION

Performance and economy have become increasingly important to gas turbine engine technology in recent years. As a result, areas such as air flow management and in particular gas path seals are receiving concerned attention. Parameters which were considered important but not critical are now being carefully examined. One such parameter is clearance, ie., the space between a rotating and stationary part.

The effects of clearance and the desire to minimize this loss factor are known and have been reported, ref. 1. Decreasing the clearance of a turbine tip seal 0.0254 cm. can produce fuel cost savings in excess of $1,000,000 for a fleet of engines. These figures are even more striking when one considers that clearances exceeding 0.152 cm. are not uncommon.

Reducing clearances on the other hand is not accomplished without some penalty. Penalty in the form of blade wear, deleterious debris and excessive heat generation are common occurrances and are sometimes lumped into the category of rub tolerance. The concept of rub tolerance is associated with blade/case interference, vane/rotor interference and labyrinth tooth/stator interference.

The interference occurs, for example, as a result of differential thermal growth between rotating and stationary parts, as a result of sudden radial transients during landing, takeoff or hard maneuvers, or from some structural failure. The effects of these radial excursions can, in most cases, be minimized with good design and proper material selection.

In the area of tip seals, which this paper will address, the designs and material problems have been noted for a number of years, however, most solutions have been trial and error. That is not to say research is inadequate or unsystematic, but the transition from laboratory simulation to real engine environments has been difficult. Materials which look good as rub tolerant tip seals (case treatments) in laboratory rigs do not exhibit those same features in the engine.

As a result of these inconsistencies and the desire to understand the mechanism of rub tolerance, the United States Air Force, at Wright Patterson AFB has initiated study programs to examine the various features associated with wear and heat generation.

The program consists of analytical models relating to friction and wear, which will be consolidated into a generalized analysis and design tool, and experimental programs to quantify the parameters relating to rub tolerance.

It is important to note that the parameters relating to rub tolerance include not only design criteria such as the amount of energy dissipated, the heat split between rotor and stator and the wear mechanism but they also include a study of the problems arising from severe rubs. One of these problems, the ignition of titanium blades, was a catalyst in focusing attention of rub tolerance and prompted the initiation of a number of experimental programs to examine the problem. The paper will describe one program involving a full scale single stage compressor to study rub initiated titanium combustion and a complementary program defining titanium burn rates, sustained combustion criteria and extinguishment problems.

COMPRESSOR RUB TEST FACILITY

The Compressor Rub Test Facility (CRTF) was designed and built to study the ignition of titanium blades in a real engine environment during a rub situation. A number of configurations were considered

in the initial design stages but most were eliminated because of non-adaptability to the facilities that were available. One concept which appeared feasible involved a high pressure gas source, flow control valves and an exhaust system, see Figure 1. Considerable attention was given to the design, especially in the areas of system repressurization, system capacity and flow control.
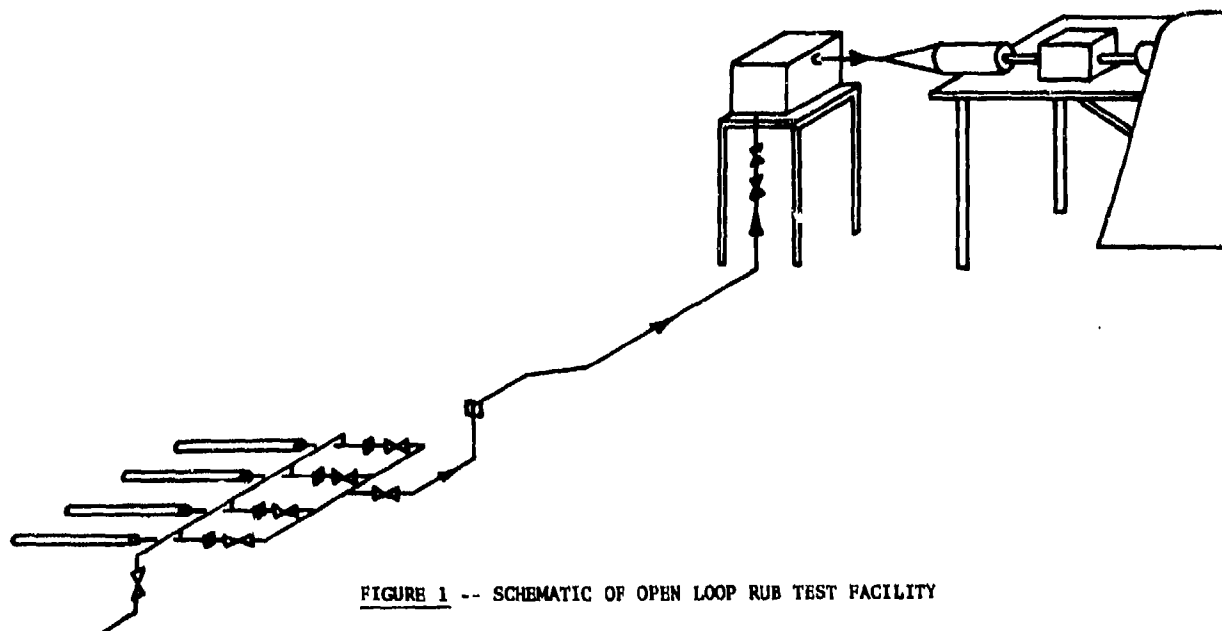
SYSTEM I

FIGURE 1 -- SCHEMATIC OF OPEN LOOP RUB TEST FACILITY

The concept was abandoned, however, in favor of the one shown in Figures 2 and 3. One of the primary reasons was air availability. If the closed loop design is successful the amount of air needed for a test sequence is only .85 m³ plus an additional .907 Kg per second for leakage control, makeup air and pneumatic valving.

Although the facility was designed to provide a full scale compressor environment for rub initiated titanium combustion, the capabilities of the apparatus far exceed these requirements. Before proceeding with a discussion of these capabilities a general physical description of the facility is in order.

Basically, the apparatus is a closed loop flow system incorporating a single compressor stage from a gas turbine engine, in the test section, driven by an electrical motor drive through a gearbox. The loop is supported by a metal structure and air is supplied from a high pressure gas source. The controls feature remote operation from beneath the test stand.

The drive system is a 1500 hp synchronous motor capable of speed variations from 0-3000 rpm. The motor is housed in a concrete structure with the output shaft 10.67 meters above ground level, since the rig was previously used to test propellers. The jack shaft of the electric motor is connected to the low speed end of an aircraft gearbox by a low speed coupling assembly.

The high speed drive from the gearbox incorporates a flexible coupling for misalignment, two bearings (one being a roller and the other a thrust absorber) and the single stage rotor assembly. The gearbox is mounted to the test loop support structure to minimize misalignment in the high speed shaft due to thermal growth differences between the metal and the concrete support structures.

The test loop includes a flow straightening or distortion section (1), a test annulus with inlet and exit guide vanes (2), a diffuser/exhaust section (3), a fill/bleed section (4), and a flow measurement section (5). Air is bled into the cavities 2a and 2b beneath the test annulus to prevent ingestion or loss of high temperature air from the test section. A hydraulic actuator is positioned on the outer surface of the case segment, included with the stator assembly, to provide controlled deflection into the rotor. The amount of interference is controlled by a Linear Velocity Differential Transducer and rub depths of .025 - .102 cm will be provided. The test loop is also insulated to prevent excessive heat loss and instrumented to obtain loop temperatures and pressures.

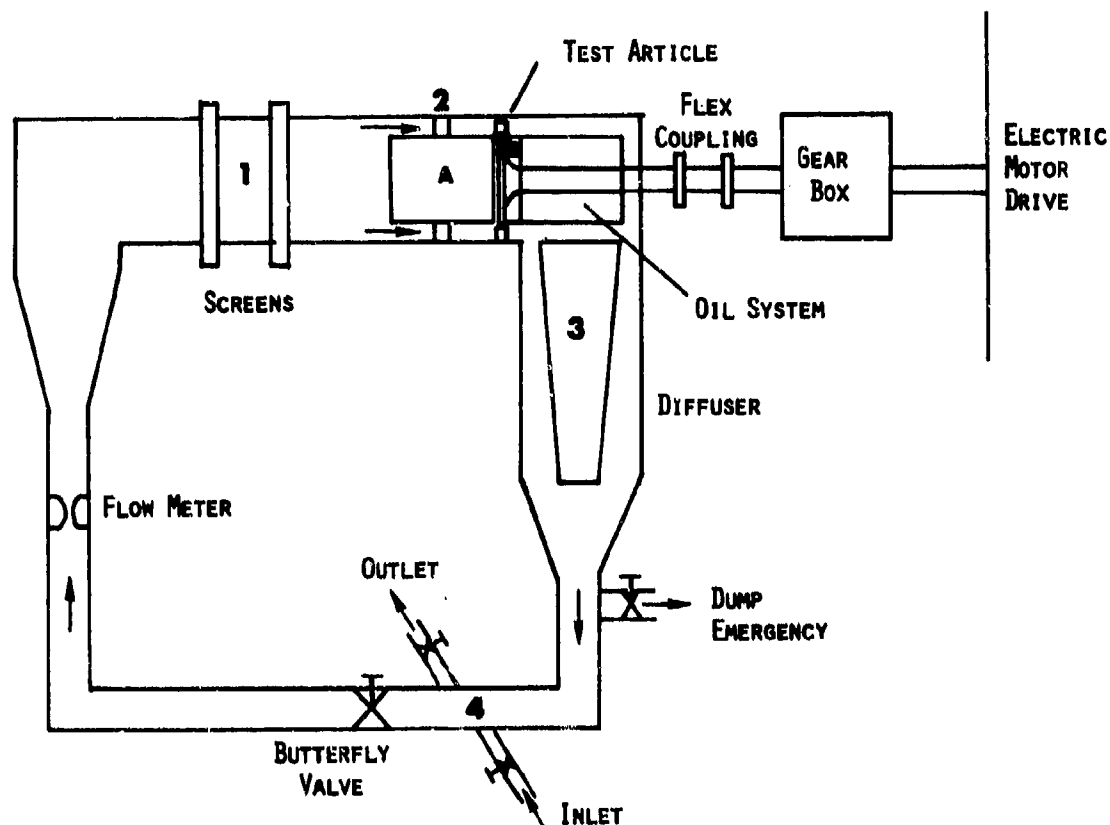# COMPRESSOR RUB TEST FACILITY

FIGURE 2 -- SCHEMATIC CLOSED LOOP

The operation of the facility involves first pressurizing the loop to the desired pressure and slowly bring the rotor up to speed. The flow through the loop is allowed to stabilize and the temperature allowed to rise until the desired conditions are reached. Once the loop is at the proper settings the inlet bleed valve is opened to introduce cold (ambient) air from the pressure source. The amount of air bled into the system (m_o) is just enough to overcome the heat input from the drive system (W_{in}) less the heat loss through the insulation (Q_L), the hot air lost through leakage (m_L) and the hot air removed by the pressure relief system (m_R).

$$mC_pT = W_{in} - Q_L - m_L C_p T - m_R C_p T$$

At this point the apparatus is ready to initiate testing.

The facility in its current configuration is capable of performing tests on the installed compressor stage within the limits shown below:

> Speed -- 9000-14,000 rpm
> Temperature -- 150°C - 480°C
> Pressure -- 345 kPa - 830 kPa
> Incursion Rates -- .0025 - .025 cm/sec

These limitations are primarily a function of the stage being tested. The first series of tests will be run at the upper ranges of speed, temperature and pressure while the rub depth will be .076 cm and the incursion rate .013 cm/sec. The blades in the test stage are, of course, titanium and the rub strip material is a plasma sprayed Ni Cg. The rub strip material will be varied to determine the effect of rub tolerance on titanium combustion. Initial screening of the rub strip materials to determine their relative abradability is accomplished with a mini rub rig incorporating a 12.7 cm test disk rotating at 2000 rpm.

The facility is currently in the final stages of checkout prior to the initiation of the first test sequence. Prior to the initiation of testing in the CRTF, however, a complementary program was required to obtain some basic information on titanium combustion and extinguishment. The extinguishment portion of the program was required to provide a means of protecting the rub test facility in the event of a
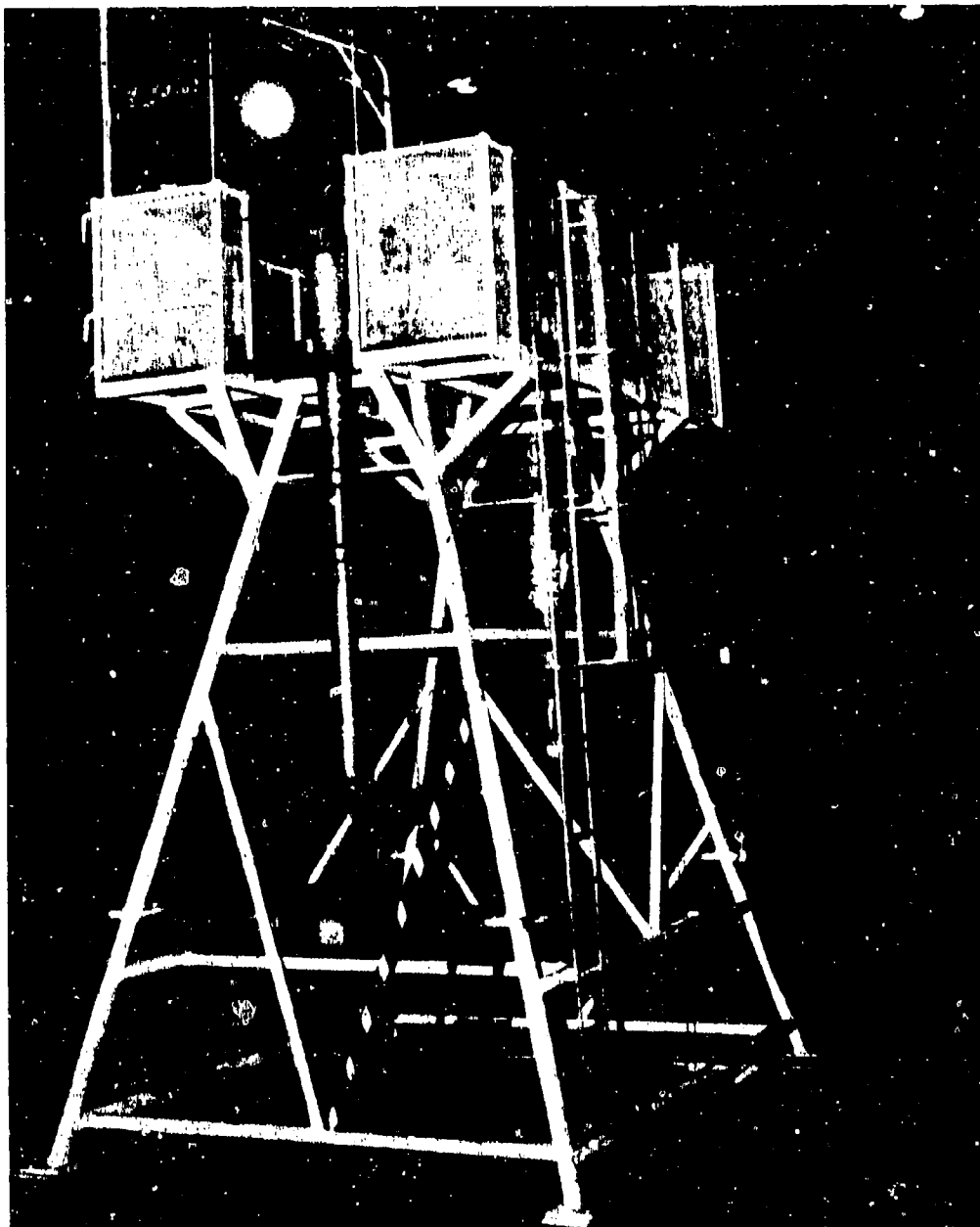
FIGURE 3 -- COMPRESSOR RUB TEST FACILITY

massive fire and the self sustained combustion data provides information on the burn rate (reaction time for extinguishment) and probability for massive metal combustion. Although these programs were initially established to provide information for the CRTF they have been expanded to form the basis of a very complete study on titanium combustion.

TITANIUM COMBUSTION PROGRAM

The basic titanium combustion data was obtained in two programs: a Melt Ignition Test (Ref 2) and a Laser Ignition Test (Ref 3). The former program provided an insight into the phenomena of self-sustained combustion and the effects of pressure, temperature and flow on the burn process but was abandoned in favor of the laser test. This shift from melt ignition to laser ignition was necessary to effectively evaluate the burn rate and self-sustained combustion process in greater depth. Laser ignition is a more controlled and reliable energy source with respect to the site of ignition and the area affected by the energy input. The results of both programs will, however, be reported since some information from each program will be used in the CRTF.

The melt ignition program was performed in the apparatus shown in Figure 4. Air at a specified temperature, pressure and velocity is directed at a sample (2.54 cm X 7.62 cm X .016 cm) of titanium 6A1-4V canted 40° to the flow. Once the flow is established, a wire (7.62 cm X 6.3 mm X 1.6 mm) across an arc
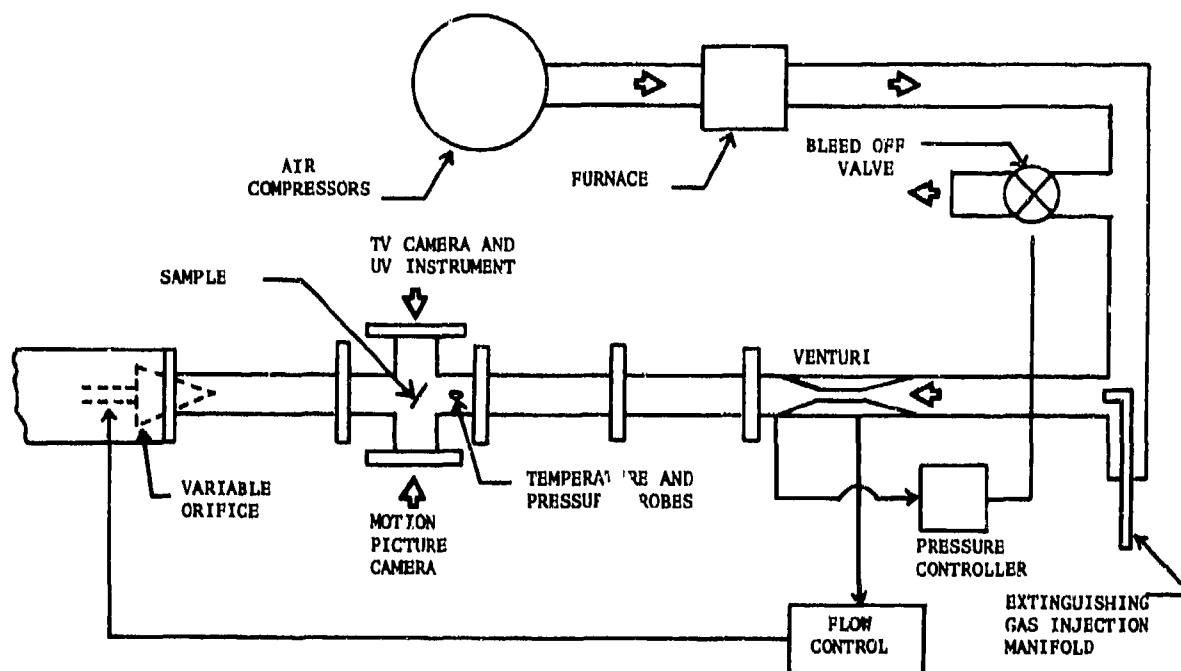
FIGURE 4 -- TITANIUM TEST FACILITY SCHEMATIC

welder is melted by current flow and the melt impinges on the test sample. The energy contained in the melt is sufficient for ignition to occur, however, the dispersal of the burning droplets is difficult to control and the ignition site varied depending on where the melt impinged on the sample. Once the fire went out, the flow was shut off and the test terminated.

The primary data from the tests were in the form of movies. Each run was recorded by a 16mm Miliken camera operating at 250 frames/sec and observed by closed circuit TV with a video tape capability. The films were processed and projected on a grid and drawings made of the luminous boundaries at selected times to obtain burn progression.

The data was plotted as boundary lines between the regions of sustained and non-sustained burning for velocity versus temperature and velocity versus pressure. The velocity versus temperature graph, Figure 5, indicates a relationship between velocity and temperature where an increase in velocity is required to blowout or prevent sustained combustion as the air temperature for each isobar plotted increases. The relationship seems more pronounced at low pressure than at higher pressures. There does not appear to be as much of a relationship between velocity and pressure, see Figure 6, as observed in the previous plot.

Two additional features of the study which should be mentioned are the effects of sample thickness and extinguishers. Figures 5 and 6 both illustrate the larger sustained burning region for the thin .06 cm sample than the .016 cm sample. This phenomenon is significant when related to an actual compressor blade with an airfoil shape, i.e., thin leading and trailing edges, thick mid-sections. The thin sections would be expected to burn first and faster than the thicker middle section which was observed when real blades were tested.

The extinguishment tests confirmed previous expectations relating to the difficulty of extinguishing a titanium fire. Argon was found to be an acceptable extinguishing agent but only in concentrations exceeding 50% by volume. With argon concentrations of 90% the flame suppression was, in effect, immediate. Nitrogen and CO_2, as expected, encouraged the combustion process rather than suppressed it.

As previously mentioned, the indepth investigation of titanium combustion fundamentals was conducted in the laser ignition facility because of the reproducible nature of the ignition process. Both the site of ignition and the amount of material ignited can be precisely controlled.

The procedure was similar to the previous test with the major differences being the substitution of the laser source for the melted wire and the orientation of the sample, parallel to the flow rather than canted 40° to the flow. High speed cinematography was employed and the film analyzed in a manner similar but more extensive than in the previous test program.
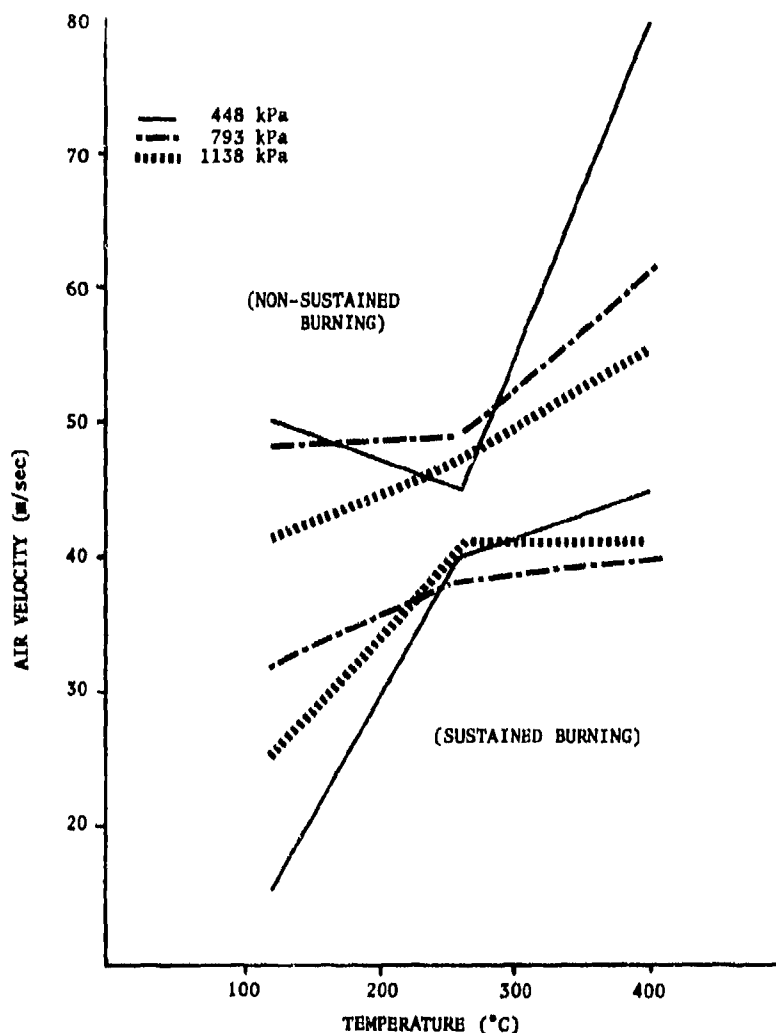
FIGURE 5 -- SUSTAINED, NON-SUSTAINED BURNING
DATA FOR SAMPLES .016cm & .06cm

The data was plotted in a variety of parameter relationships with the most meaningful being the pressure versus temperature for various velocity ranges, Figures 7, 8, 9, 10, and 11. Furthermore, the individual data points were identified in terms of the damage (% mass loss) each sample sustained and segregated in regions of similar damage.

The figures illustrate a strong pressure dependence but less of a temperature dependence which appears to be a direct contradiction to the previous results. The data is being examined in further detail to understand the possible anomalies but one must remember the ignition process was considerably different and the sample orientation was changed. Once the original melt data is examined in more depth some of the initial differences may disappear or a significant difference relating to melt ignition phenomena may develop.

Some of these answers may surface during a planned extension of the laser ignition work involving cascade or multiple blade tests. Ignition of one blade by the laser and subsequent ignition of downstream blades by melt impingement could clear up the current discrepancies.

The burn rate of the titanium samples was analyzed and the data plotted as shown in Figure 12. The lines represent a best fit of the data to the equation:

$$y = A_1 \ Exp \ (-A_2 x1) + A_3 \ Exp \ (-A_4 x) + A_5$$

The dependence of burn rate on pressure and velocity is quite evident from this figure. Although a precise quantification of burn rate is not available at this time, the data does indicate the ranges of allowable reaction times.
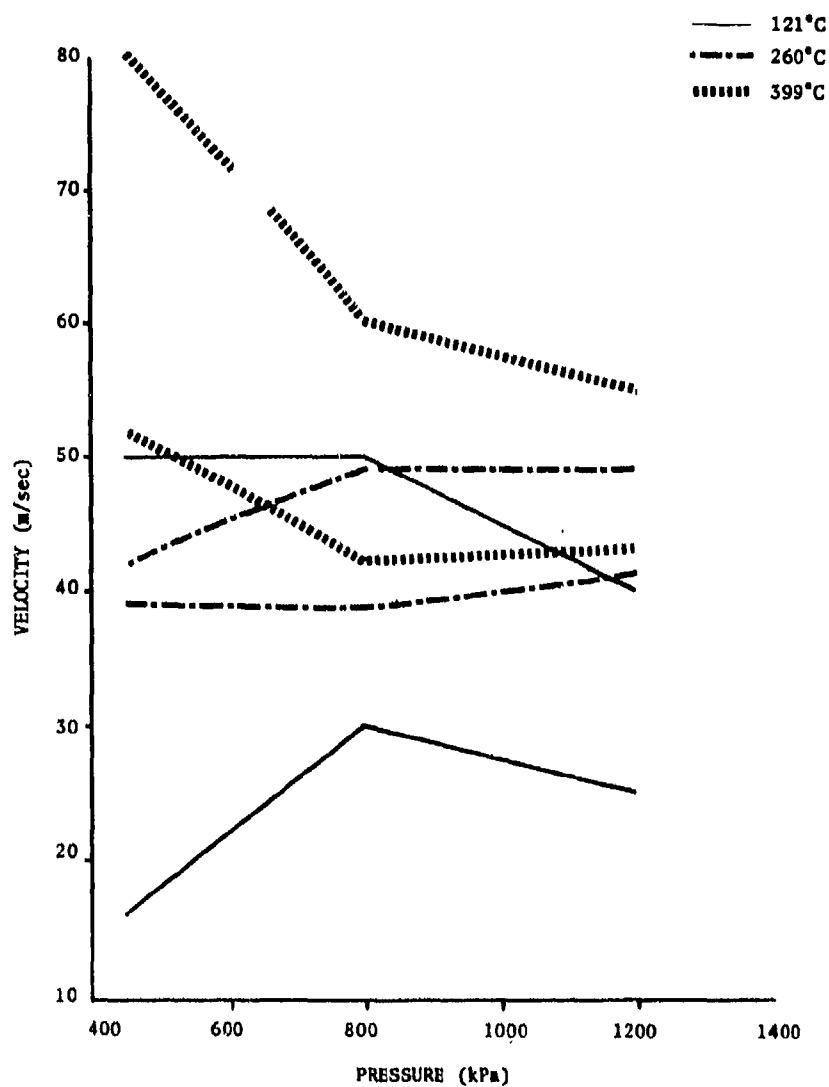
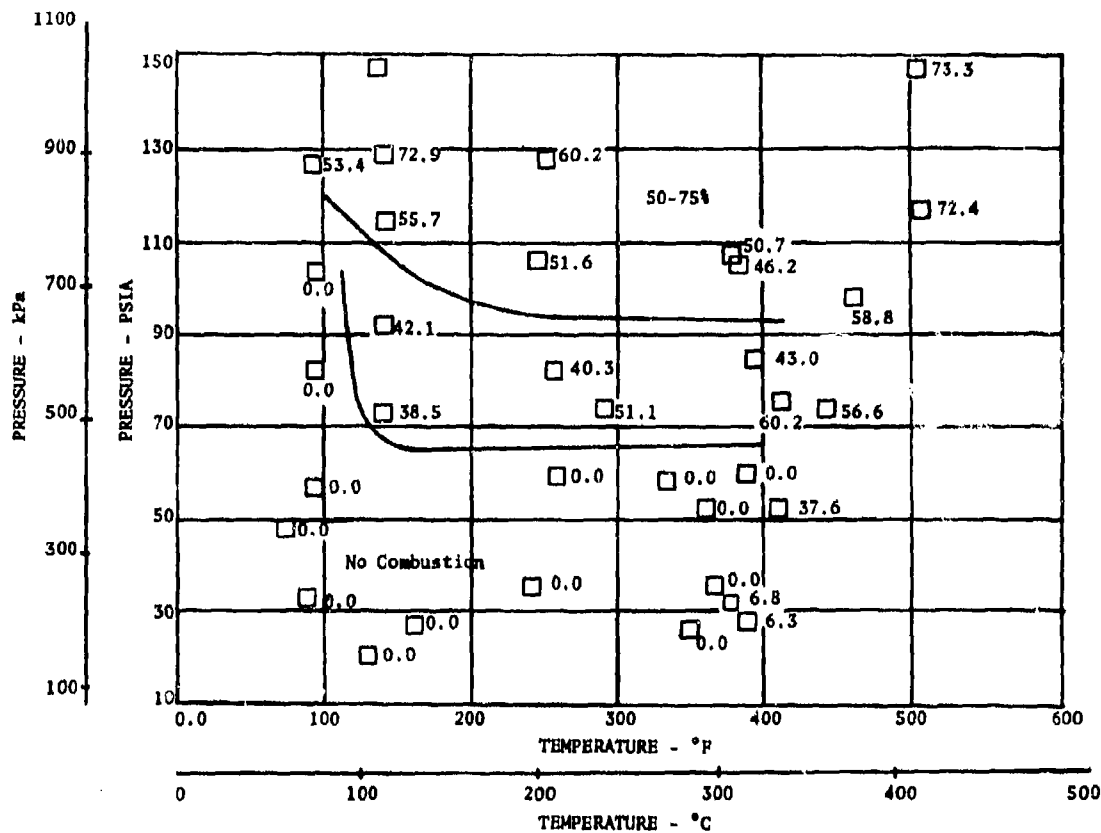FIGURE 6 -- SUSTAINED, NON-SUSTAINED BURNING DATA FOR
SAMPLES .016cm & .06cm

FIGURE 7 — MATERIAL LOSS FOR THE VELOCITY RANGE 0-49 m/SEC
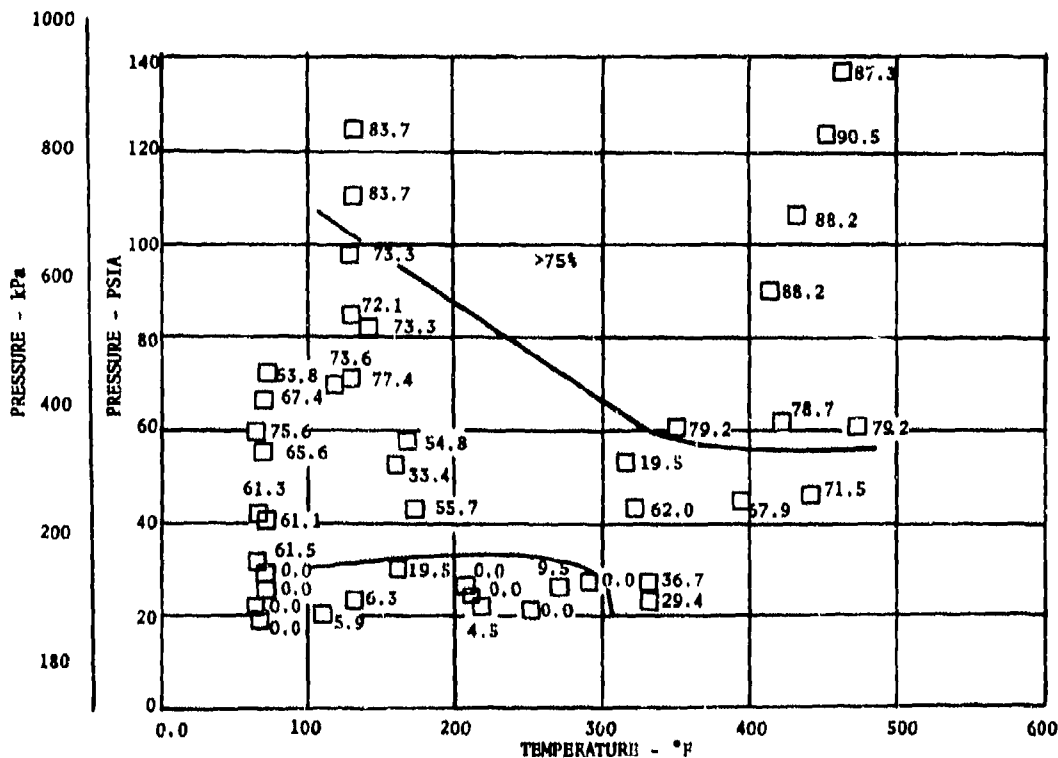**NUMBERS BESIDE THE DATA POINTS REFER TO DAMAGE (% LOSS)**

Figure 7 (top): Axes — PRESSURE - kPa (100, 300, 500, 700, 900, 1100) and PRESSURE - PSIA (10, 30, 50, 70, 90, 110, 130, 150); TEMPERATURE - °F (0.0, 100, 200, 300, 400, 500, 600) and TEMPERATURE - °C (0, 100, 200, 300, 400, 500).

Data labels: 73.3; 53.4; 72.9; 60.2; 50-75%; 72.4; 55.7; 51.6; 50.7; 46.2; 58.8; 0.0; 42.1; 40.3; 43.0; 0.0; 38.5; 51.1; 60.2; 56.6; 0.0; 0.0; 0.0; 0.0; 0.0; 0.0; 37.6; No Combustion; 0.0; 0.0; 6.8; 0.0; 0.0; 6.3; 0.0; 0.0

FIGURE 8 — MATERIAL LOSS FOR THE VELOCITY RANGE 50-100 m/SEC
NUMBERS BESIDE THE DATA POINTS REFER TO DAMAGE (% LOSS)

Figure 8 (bottom): Axes — PRESSURE - kPa (180, 200, 400, 600, 800, 1000) and PRESSURE - PSIA (0, 20, 40, 60, 80, 100, 120, 140); TEMPERATURE - °F (0.0, 100, 200, 300, 400, 500, 600).

Data labels: 87.3; 83.7; 90.5; 83.7; 88.2; 73.3; >75%; 88.2; 72.1; 73.3; 73.6; 53.8; 77.4; 67.4; 78.7; 79.2; 75.6; 79.2; 65.6; 54.8; 19.5; 33.4; 61.3; 71.5; 61.1; 55.7; 62.0; 57.9; 61.5; 0.0; 19.5; 0.0; 9.5; 0.0; 36.7; 0.0; 29.4; 0.0; 6.3; 0.0; 0.0; 0.0; 5.9; 4.5
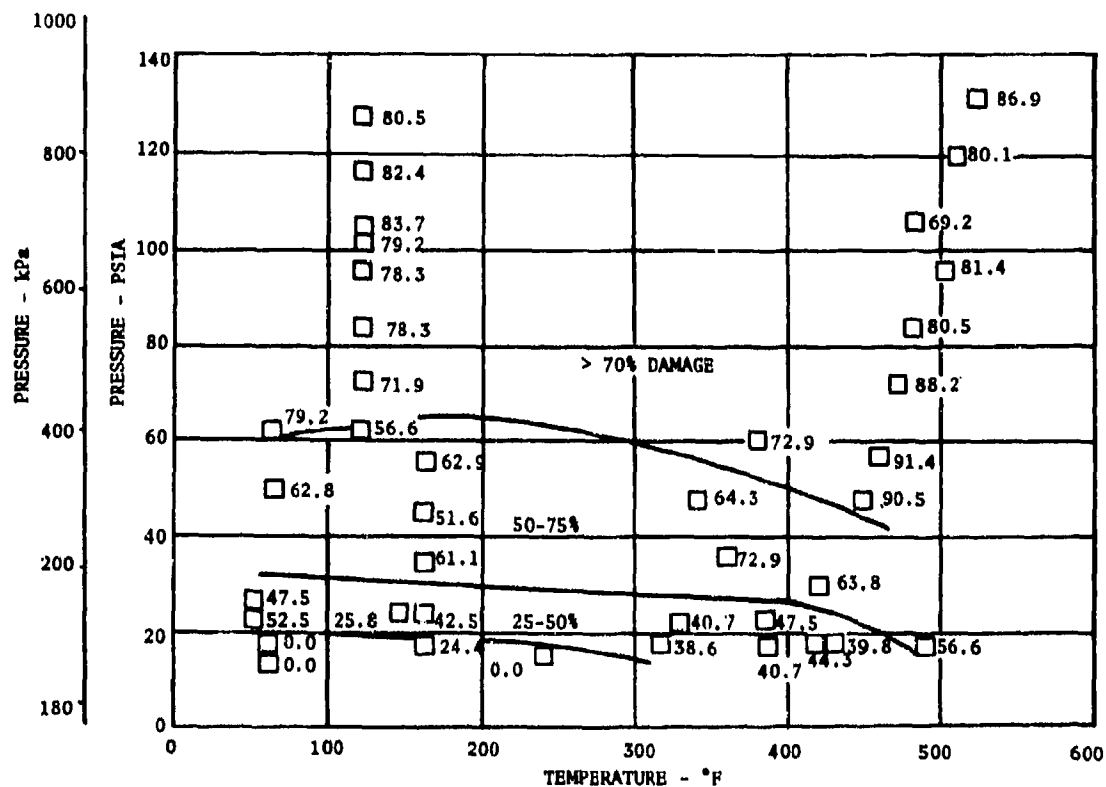
FIGURE 9 -- MATERIAL LOSS FOR THE VELOCITY RANGE 110-183 m/SEC
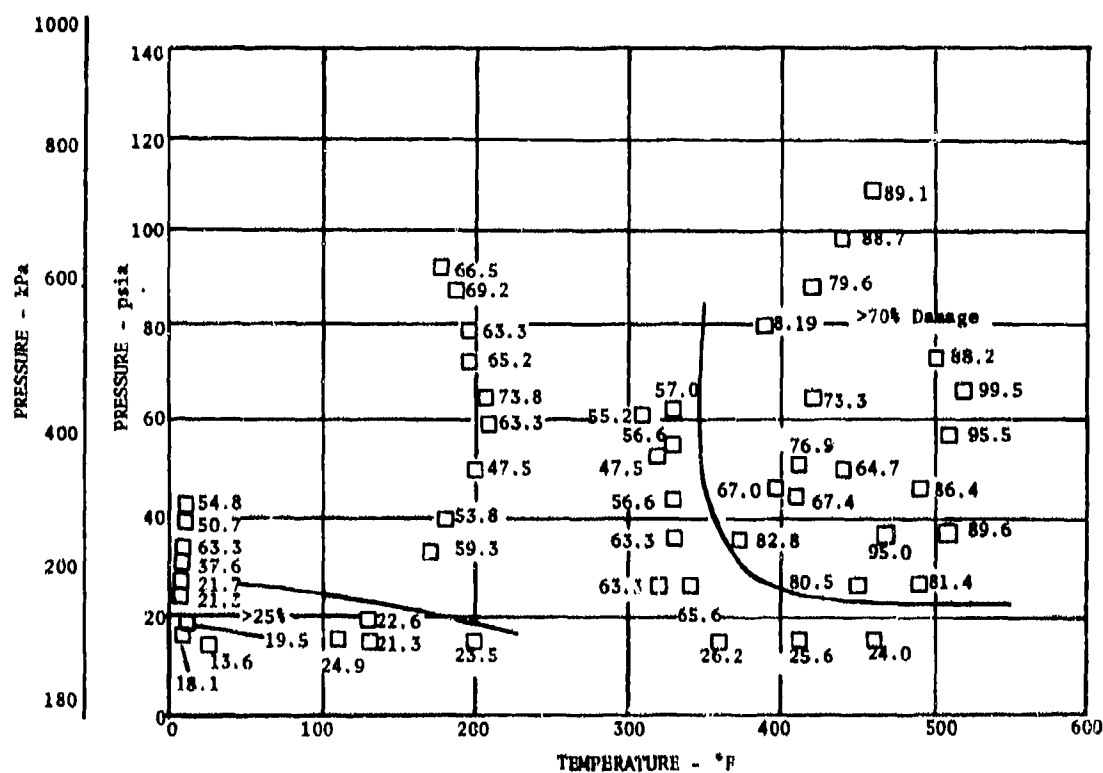NUMBERS BESIDE DATA POINTS REFER TO DAMAGE (% LOSS)

FIGURE 10 -- MATERIAL LOSS FOR THE VELOCITY RANGE 183-274.5 m/SEC
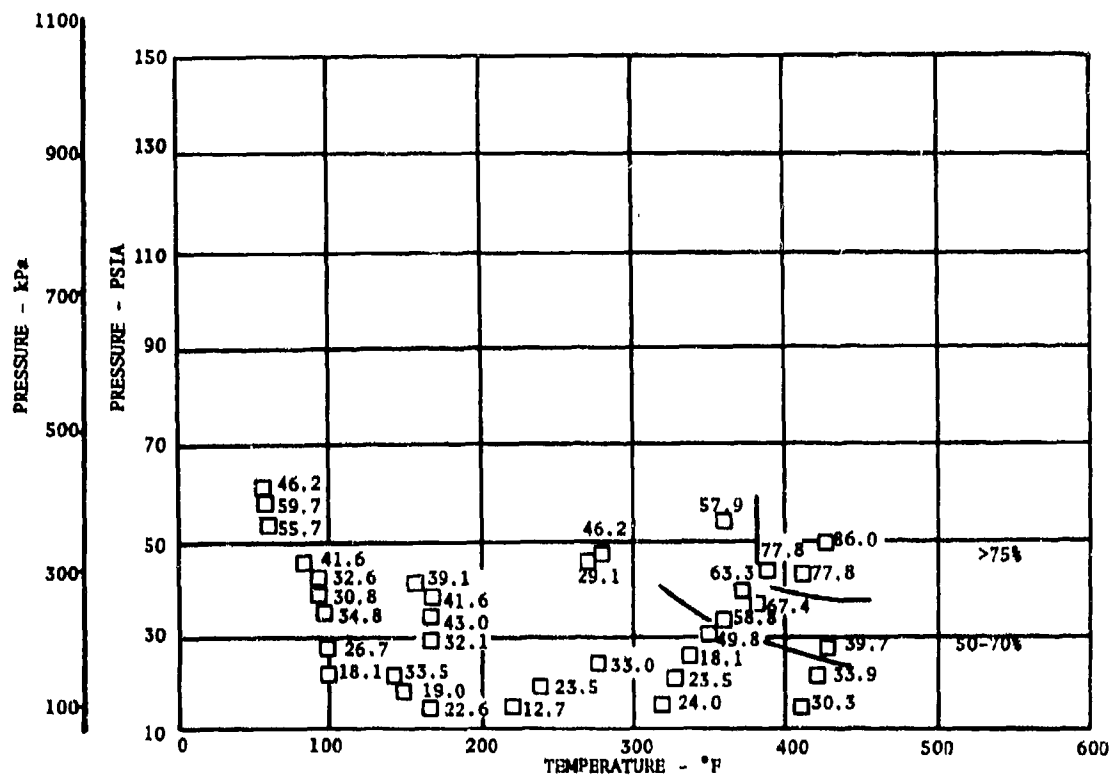NUMBERS BESIDE THE DATA POINTS REFER TO DAMAGE (% LOSS)

FIGURE 11 -- MATERIAL LOSS FOR THE VELOCITY RANGE 274.5 - 296.5 m/SEC
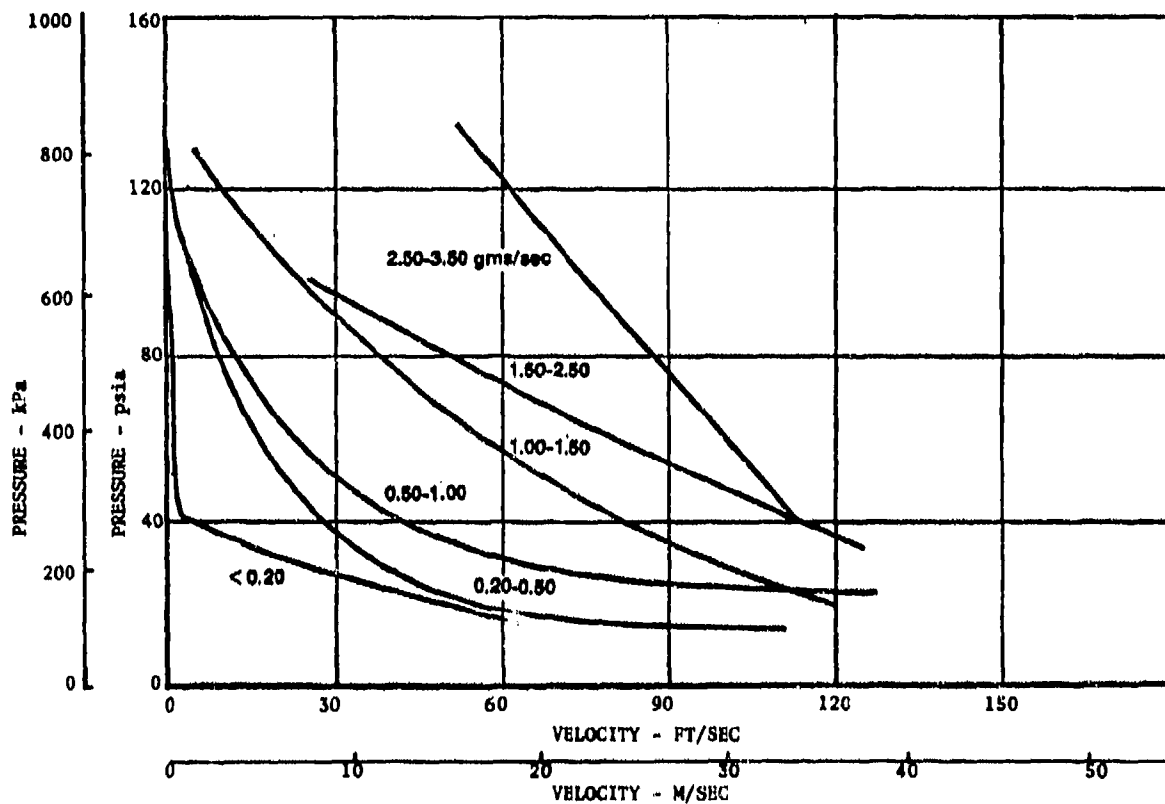NUMBERS BESIDE THE DATA POINTS REFER TO DAMAGE (% LOSS)

FIGURE 12 -- COMBUSTION RATE DEPENDENCE ON VELOCITY AND TOTAL PRESSURE --
CURVES REPRESENT AN ARBITRARY CHOICE OF RANGES

CONCLUSIONS

The programs described will provide valuable insights into one of the important problem areas relating to rub tolerance but more importantly two unique facilities have evolved. One with enormous potential for testing compressor related problems over a wide range of environmental conditions and a second facility for the study of titanium combustion in a flowing airstream are now an important part of the United States Air Force research and development capabilities. Future programs are currently being formulated for both experimental rigs.

The CRTF will become a source for testing new seal materials, blade coatings or blade tip treatment and possibly a prerequisite before the final engine verification or engine demonstration phase in a new product development cycle. In addition, programs relating to blade flutter, disc stress, or similar technologies can be included in the test program planning for the CRTF.

The laser ignition test program results include, in addition to the Ti 6-4 parallel flow tests, a series of Ti 6-4 canted blade tests (where the blades are angled at 10° to the air flow), a series of titanium alloy tests (currently 26 alloys have been ignited) and a select number of coated titanium blade ignition tests. Future programs include multiple blade (cascade) tests, locus of ignition tests (where the ignition site will be moved to the trailing edge and the leading edge at the midspan of the blade) and ignition energy tests (where the minimum ignition energy as a function of airstream temperature, pressure and velocity will be determined).

An important feature of the laser ignition tests is the applicability of the data not only to the CRTF operation but also to the actual engine problem. A detailed knowledge of titanium combustion behavior in an aerodynamic environment if of invaluable assistance to the engine designer. Furthermore, the tests on titanium alloys, coatings and tip treatment will offer the engine manufacturer reassurance in the practical use of titanium in current and future gas turbine engines.

REFERENCES

(1) Mahler, F.H., Advanced Seal Technology, Technical Report AFAPL-TR-72-8, February 1972.

(2) Fox, Duane G., Investigation of Titanium Combustion Characteristics and Suppression Techniques, Technical Report AFAPL-TR-75-63, February 1976.

(3) Glickstein, M.R., Manty, B.A., Lyon, S.R., Elrod, C.W., Ignition and Self-Sustained Combustion of Titanium Alloys; Proceedings of the 5th DOD Laser Effects/Hardening Conference, San Diego, California.

DISCUSSION

I.Glassman, US

How did you choose the alloys?

Author's Reply

We have gone through a list of commercially available alloys. Those which are normally used not only in the aircraft industry but also in other industries to see if — if we look at a large cross section, a large specimen of alloys — there are any alloying trends which tend to show up an incombustible trend.

I.Glassman

There is a lot of knowledge in the combustion of metals which would simply say that you want to pick a metal which basically would perform an oxide which has a self-healing effect. The trouble with titanium is that at certain temperature titanium oxides. Perhaps the best with which you can make an alloy would be simply aluminium. Have you tried that and does it still burn?

Author's Reply

Yes we have tried that. We tried Ti 3Al and TiAl and both burned. We could not ignite the last alloy under our test conditions, if the weight percentage of Aluminium was between 24 and 36%. When we dropped the Aluminium below 24% we were able to ignite the alloy. We are going to continue the testing a little more to get a more indepth analysis of that burning process with Aluminium.

The problem with Titanium-Aluminium is because it is very brittle. Now, if you can get some ductility back into Titanium-Aluminium, it is very possible that we could use this in some isolated incidents, e.g. a casing or a vane.

E.E.Covert, US

In combustion of liquid droplets in gas turbine combustors, there is a correlating parameter which is the product of pressure and temperature and the reciprocal of the velocity of the air flow. Have you looked for a similar type of correlating parameter for your data?

Author's Reply

That's a distinct possibility. We had not actually considered putting it into that form. I think we may go back and try to see if we can get some correlations.

SELF-ACTING SHAFT SEALS

Lawrence P. Ludwig
National Aeronautics and Space Administration
Lewis Research Center
Cleveland, Ohio 44135

SUMMARY

Self-acting seals are described in detail. The mathematical models for obtaining a seal force balance and the equilibrium operating film thickness are outlined. Particular attention is given to primary ring response (seal vibration) to rotating seat face runout. This response analysis reveals three different vibration modes with secondary seal friction being an important parameter. Leakage flow inlet pressure drop and affects of axisymmetric and nonaxisymmetric sealing face deformations are discussed. Experimental data on self-acting face seals operating under simulated gas turbine conditions are given; these data show the feasibility of operating the seal at conditions of 345 N/cm^2 (500 psi) and 152 m/sec (500 ft/sec) sliding speed. Also a spiral groove seal design operated to 244 m/sec (800 ft/sec) is described.

SYMBOLS

B constant $= h_m - \dfrac{\alpha(r_o - r_i)}{2}$

F sealing dam force, N; lbf

h film thickness, cm; in.

h_{char} characteristic film thickness $= (h_1^2 h_2^2 / h_m)^{1/3}$, cm; in.

ℓ primary seal radial length

L sealing dam circumferential length, cm; in.

M Mach number

P pressure, N/m^2 or N/cm^2; psi

ΔP pressure difference, N/m^2 or N/cm^2; psi

Q net leakage (volume) flow rate, scmm; scfm

R radius, cm; in.

ΔR sealing dam radial width, $R_o - R_i$, cm; in.

R gas constant, universal gas constant/molecular weight

Re Reynolds number

r radial direction coordinate

T temperature, K; ^{o}F

V velocity, m/sec; ft/sec

x coordinate in pressure gradient direction (radial direction)

y coordinate across film thickness

z shear flow coordinate in Cartesian system

α relative inclination angle of primary seal faces, rad

β axisymmetric relative inclination of primary seal faces, rad

γ nonaxisymmetric relative inclination of primary seal faces, rad

μ absolute or dynamic viscosity, N-sec/m^2; (lbf-sec)/ft^2

ρ density, kg/m^3; (lbf)(sec^2)/ft^4

Subscripts:

av average

char based on characteristic film thickness

h based on film thickness

i inner cavity

m mean

o outer cavity

r based on radius

s spring

1 sealed pressure, upstream reservoir pressure

2 pressure at and within sealing gap inlet

3   pressure at and within sealing gap exit

4   downstream reservoir pressure

INTRODUCTION

The continuing increases in gas pressure and temperature which accompany the evolution of the gas turbine, industrial compressor, and other rotating machinery places burdens on a shaft seal technology, which seems to some to be barely adequate for current needs. In addition, the emphasis on efficiency caused by the impending fuel shortage causes an additional need for seals with reduced leakage rates. In the gas turbine shaft seals are used to restrict leakage from a region of a gas at high pressure to a region of gas at a lower pressure and to restrict gas leakage into the bearing sumps. (Bearing sumps contain an oil-gas mixture at near ambient pressure, and gas leakage through the seal helps prevent oil leakage out and maintains a minimum sump pressure necessary for proper scavenging.) Bearing sumps in the high pressure turbine area are usually the most difficult to seal because the pressures and temperatures surrounding the sump can be near compressor discharge conditions.

Labyrinth seals are commonly used for shaft sealing in gas turbine engines (a simplified model of one system is shown in Fig. 1). The advantage of labyrinth seals is that the speed and pressure capability is limited only by the structural design; one disadvantage is a relatively high leakage rate.   Is leakage can be a significant performance penalty, and will provide easier passage of air-borne wat . and dirt into the sump. In this regard high leakage rates of hot gas into the bearing compartment tend t. carry oil overboard and add significantly to the heat dissipation burden of the oil cooling system. An added complication in small engines is the limited space available for seals and bearing sumps, here the multiple labyrinth seal with associated bleed and venting passages is difficult to accommodate.

Conventional rubbing contact seals, shaft riding and radial face types, are also used for sealing bearing sumps. Because of wear rate, shaft riding and circumferential seals (see Fig. 2 for one version), have been limited to pressure less than 69 N/cm^2 (100 psi); and successful operation has been reported at a sealed pressure of 58 N/cm^2 (85 psi), a gas temperature of 644 K (700° F), and a sliding velocity of 73 m/sec (240 ft/sec)(Ref. 1). On the other hand, the conventional rubbing contact face seal (Fig. 3) is limited to approximately 90 N/cm^2 (130 psi) and 122 m/sec (400 ft/sec) for long operational life. Rubbing contact seals are attractive because they have lower leakage rates than labyrinth seals. Associated with this lower gas leakage rate is less entrained debris, lower heat dissipation requirement for the oil cooling system, and lower efficiency penalty.

By incorporating thrust bearing geometry into a conventional face seal, nonrubbing operation can be achieved. This seal concept has been termed the "self-acting" seal, since the mechanism is similar to a self-acting thrust bearing in that the mating faces lift out of contact because of the pressure developed by relative motion between the seal faces. Studies (Refs. 2 and 3) demonstrated that the self-acting seals can operate at advanced aircraft engine conditions, that they have lower leakage rates than labyrinth seals, and hence that they are attractive from an efficiency standpoint.

The objectives of this paper are to (a) review the operating principle and design of the self-acting seal, (b) point out effects of adverse operating conditons, and (c) present some experimental data. The data are for two seal sizes, a 16.76-cm (6.60-in.) nominal diameter seal suitable for large gas turbines and a 6.44-cm (2.54-in.) diameter seal for small engines. The experimental portion of the program was run in rigs which simulated the bearing compartments of gas turbines, this placed the sealed pressure at the seal inside diameter; thus the bearing oil/air mixture was at the seal outside diameter and centrifugal force acted against oil leakage.

DISCUSSION AND ANALYSIS

Self-Acting Face Seal Terminology

The terms "hydrodynamic" and "hydrostatic" are often applied to describe seals for compressible fluids as well as for incompressible fluids. But following the bearing terminology, the terms "self-acting" and "pneumostatic" will be used when the sealed fluid is compressible, and the terms "hydrodynamic" and "hydrostatic" will be reserved for sealing incompressible fluids.

It should be noted that conventional "contact" seals often operate with separation of the sealing surfaces because of forces produced by self-acting, pneumostatic, hydrodynamic, or hydrostatic effects. This is particulary true in conventional radial face seals for liquids (such as pump seals), the hydrodynamic forces being produced by miniscule misalignments and surface waviness (which are largely unplanned and occur by happenstance) caused by such effects as local thermal expansions, friction, and wear. In contrast, in the seals which are the subject of this paper, the self-acting or hydrodynamic action is produced by a "machined in" bearing geometry and not by uncontrolled effects. Figure 4 shows this type of self-acting seal. (Since a hydrodynamic seal assembly would be the same in principle, the discussion can be limited to the self-acting seal.)

As previously mentioned, a self-acting face seal is similar to a conventional face seal except for the added feature of a self-acting geometry (gas lubricated thrust bearing). As with a conventional face seal, it consists of a rotating seat which is attached to the shaft and a nonrotating primary ring assembly which is free to move in an axial direction; thus the seal can accommodate axial motion such as is due to engine thermal expansion. The secondary seal (piston ring) is subjected only to the axial motion (no rotation) of the primary ring assembly. Several springs provide mechanical force to maintain contact at start and stop. In operation, the sealing faces are separated a slight amount (in the range of 2.5 to 1.27 μm (0.0001 to 0.0005 in.)) by action of the self-acting lift geometry. This positive separation results from the balance of seal forces and the gas film stiffness of the self-acting geometry. The self-acting geometry can be any of the various types used in gas thrust bearings; the Rayleigh step bearing is illustrated in Figs. 4 and 5.

Within the seal industry there is a wide variety of terms used to describe similar seal parts. The ASLE seal glossary (Ref. 4) has provided some guidance in seal nomenclature, and the self-acting nomenclature which follows is mainly an extension of this ASLE work. The nomenclature applying to an assembly of parts (Fig. 4) is

1. Primary seal - Seal formed by the sealing faces of the seat and primary ring. Relative rotation occurs between these sealing faces.

2. Secondary seal - Seal formed by the sealing surfaces of the secondary ring. In the case of a bellows seal the secondary seal is the bellows itself.

3. Static seal - Seal formed by the mating surfaces of the primary ring and its carrier (in some designs the static seal is an interference fit).

4. Self-acting geometry - Lift-pad geometry (Rayleigh step bearing) and mating face which together produce the thrust bearing action to separate the sealing surfaces.

5. Film thickness (h) - Distance between primary sealing faces or between surfaces forming the self-acting geometry. For parallel surfaces the film thickness at the primary seal is the same as at the self-acting geometry. (Note that h may vary with radial and circumferential position and with time.)

6. Seal head - Assembly that is axially movable and consisting of primary ring, its retainer (if any), and its carrier. (The retainer and the carrier are combined into one part in some designs.)

The nomenclature applying to single parts (Fig. 4) is

1. Seat - Part having a primary sealing face and mechanically constrained with respect to axial motion.

2. Primary ring - Part having a primary sealing face and not constrained with respect to axial motion.

3. Secondary ring - Part having secondary sealing surfaces which mate to the secondary sealing surfaces of the carriers.

Force Balance

General description. - To determine film thicknesses and leakage in a self-acting seal, the axial forces acting on the seal head (assembly of the primary ring and its carrier) must be determined over the range of operating conditions. These forces comprise the self-acting lift force, the spring force, and the pneumatic force due to the sealed pressure. Essentially, the analysis requires finding the film thickness for which the opening forces balance the closing forces. When this equilibrium film thickness is known, the leakage rate can be calculated. This force balance analysis is readily obtained for the steady-state case in which the seat face has zero runout. (A seat with face runout causes dynamic changes in film thickness; this is a complicating factor which is discussed in a later section.) For most seal design purposes the steady-state solution is sufficient.

The following sections outline the analysis used to obtain seal performance predictions over the operating range; for aircraft gas turbines this range is spanned by the idle and takeoff seal pressures, temperatures, and sliding speeds. To provide an example, the 16.76-cm (6.60-in.) diameter seal was selected for illustrating the performance prediction analysis. Also, for comparison purposes, the performance maps are given for a 6.44-cm (2.54-in.) diameter seal.

Primary Seal Pressure Gradient

To establish the axial force balance of the primary ring, the pressure gradient in the primary seal must be determined. (See Fig. 4 for primary seal location.) The mathematical models described in Refs. 5 to 7 were used for these calculations. From a gas leakage flow standpoint the primary seal is a long passage. For example, a typical operating film thickness of a self-acting seal is in the range of 10.2 μm (0.0004 in.), and a typical radial length of the primary seal is 0.127 μm (0.050 in.). Thus, the length to height (ℓ/h) ratio of the flow channel is in the range of 125/1. Data from Refs. 6 and 7 show that this leakage passage has the following qualitative features:

1. Laminar leakage flow prevails over much of the range of interest in seals for gas turbines (pressure range of 345 N/cm^2 abs (500 psia)).

2. Sonic velocity (choking) can exist at the passage exit for some of the larger pressure ratios and film thicknesses which occur in seal operation.

3. Pressure profiles across the primary seal for choked and nonchoked flow can be very different.

4. Since the primary seal radial width is small compared with its diameters, the area expansion effect on flow can be ignored.

5. The leakage flow and pressure profile are significantly different if the surfaces of the primary seal are not parallel. (See Ref. 8 for a discussion of the effects of converging and diverging sealing surfaces.)

The primary seal mathematical model used in the one-dimensional analysis of Refs. 5 and 7 is shown in Fig. 6. As mentioned, the area expansion effects are ignored, and the model is a passage of height h and length ℓ.

From stagnation source conditions of P_1 and V_1 (see Fig. 6) an isentropic expansion is considered to occur ahead of the entrance to the primary seal gap. Thus, the entrance pressure, P_2, is less than the stagnation pressure P_1, and the entrance velocity, V_2, is a finite value. To account for entrance loss and viscous friction, it was found necessary to use an entrance loss coefficient. Thus, the entrance velocity, V_2, is less than that calculated by isentropic expansion. In a later section the entrance effects are discussed in more detail.

Flow in the sealing gap is assumed one-dimensional and a friction factor is introduced to account for viscous losses. At the exit, three conditions are considered in the analysis: First, exit velocity, V_3, is subsonic and exit pressure, P_3, is equal to reservoir pressure, P_4. Second, exit velocity, V_3, is sonic and exit pressure, P_3, is equal to reservoir pressure, P_4. And third, exit velocity, V_3, is sonic, the flow is choked, and exit pressure, P_3, is greater than the reservoir pressure, P_4.

If the flow is subsonic throughout, the analysis reduces to the following equations:

a. Leakage flow rate

$$Q = \begin{Bmatrix} 2.726 \\ 0.001287 \end{Bmatrix} \frac{h_{char}^3 L(P_1^2 - P_4^2)}{\mu R T (R_o - R_1)} \begin{Bmatrix} scfm \\ scms \end{Bmatrix} \qquad (1)$$

b. Pressure distribution

Parallel film case

$$P = P_4 \left[1 - \left(1 - \frac{P_1^2}{P_4^2} \right) \left(\frac{R_o - r}{R_o - R_1} \right) \right]^{1/2} \qquad (2)$$

Small deformation case

$$P = P_1 \left(1 + \frac{\left[\left(\frac{P_4}{P_1} \right)^2 - 1 \right] h_o^2 x (2B + \alpha x)}{2(R_o - R_1) h_m (B + \alpha x)^2} \right)^{1/2} \qquad (3)$$

c. Sealing dam force

Parallel film case

$$F = \frac{2 P_1 L (R_o - R_1) \left[1 - \left(\frac{P_4}{P_1} \right)^3 \right]}{3 \left[1 - \left(\frac{P_4}{P_1} \right)^2 \right]} \qquad (4)$$

Small deformation case

$$F = L \int_0^{R_o - R_1} (P - P_{min}) dx \qquad \text{(Evaluated numerically)} \qquad (5)$$

Typical pressure gradients across the primary seal for two design points (idle and take-off) for the 16.76 cm (6.60 in.) diameter seal are shown in Fig. 7; these data were developed by the analytical procedures of Ref. 5 and is given in more detail in Ref. 9. The important point is that choked and nonchoked flows can have pressure gradients with very different shapes thus affecting the opening force, which is the integrated force under the pressure-gradient curves.

Self-Acting Geometry

The self-acting geometry (lift pads) consist of a series of shallow recesses, typically about 25 μm (0.001 in.) deep, arranged circumferentially around the seal under the primary seal face as shown in Figs. 4 and 5. An important point is that the lift pads are bounded at the inside diameter and the outside diameter by the sealed pressure P_1. (This is accomplished by feed slots connecting the annular groove directly under the primary seal.) Therefore, the pressure gradient, due to gas leakage, occurs only across the primary seal and not across the self-acting geometry.

The self-acting geometry is approximated by the mathematical model (shown in Fig. 8) in which the curvature effects have been neglected. This mathematical model and associated analysis are described in detail in Ref. 10; the following restrictions apply:
1. The fluid is Newtonian and viscous.
2. A laminar flow regime is assumed.
3. Body forces are negligible.

Figure 9 shows the calculated lift force (see Ref. 10 for details) produced by the self-acting geometry for idle and take-off seal conditions. Inspection of Fig. 9 reveals that at film thicknesses of 2.7 μm (0.0005 in.) and greater the lift force is small. However, at film thicknesses less than 2.7 μm (0.0005 in.) the lift force increases as the film thickness decreases, and as a result the self-acting geometry has a high film stiffness which enables the seal head to track the face runout motions of the rotating seat face. As mentioned previously, the self-acting lift force tends to open the seal, and is added to the primary seal opening force to obtain the total opening force.

Closing Forces

The closing forces acting on the primary ring are a spring force and a pneumatic force. Since the full sealed pressure acts to the inside diameter of the primary seal, the net pneumatic closing force acts only on the annular area between the primary-seal inside diameter and the secondary-seal outside diameter. For the 16.76-cm (6.60-in.) diameter seal this annular area (see Fig. 10) is 4.66 cm² (0.722 in.²), and the resulting closing forces due to the sealed pressure are listed in Tab. I, for idle and take-off sealed pressures. It should be noted that these closing forces are for average dimensions at room temperature. At operating temperature a thermal growth difference may cause a change in the relation between the secondary-seal outside diameter and the inside diameter of the primary seal. Thus, the closing force could be a function of temperature.

Equilibrium Film Thickness

In a rubbing contact seal the closing force is resisted by solid-surface rubbing contact; thus, a total force balance is achieved. But in self-acting seals the force balance is achieved without rubbing contact. Therefore, for a given design point the seal will operate at a film thickness such that the

total opening force exactly balances the total closing force, and, as illustrated in Fig. 11 from Ref. 9, the intersection of these force curves gives the steady-state equilibrium film thickness. (This film thickness determination does not take into account dynamic running factors such as seat face runout and piston ring damping.)

Each operating point should be checked for equilibrium film thickness. If these film thicknesses are not satisfactory, it may be possible to adjust the closing force such that all operating points fall within a satisfactory limit. Experience has shown that the satisfactory film thickness regime is about 2.5 μm (0.0001 in.) on the low end (some tolerance to thermal deformation must be maintained) and 0.0013 μm (0.0005 in.) on the high end. These limits are only approximate and depend to a large extent on the dynamic and thermal condition to which the seal is subjected. The high limit of practical film thickness is established by seal dynamics and leakage considerations. In particular, the primary ring response to the seat face runout becomes excessive as the mean film thickness increases (Ref. 11); this is because the stiffness of the gas film decreases as the film thickness increases.

Performance Maps

Once the equilibrium film thickness is found, the predicted leakage can be determined by using the one-dimensional method outlined in Ref. 5. By cross-plotting the equilibrium film thickness over the leakage curves, a performance map can be generated; and typical data for the 16.76-cm (6.60-in.) diameter seal is given in Fig. 12 (from Ref. 12). Inspection of Fig. 12, which covers a range of sealed pressure differential from 34 to 276 N/cm^2 (50 to 400 psi), reveals that air leakage increases as speed is increased; this is due to more effective Rayleigh step bearing performance. Also for any given speed, as pressure is increased, the equilibrium film thickness increases slightly. This suggests that the net pneumostatic force (pressure gradient across the sealing dam minus the closing force due to the sealed pressure) is decreasing slightly.

Performance maps (Fig. 13) for a smaller seal (6.44 cm (2.54 in.) nominal diameter) are similar except that the design selection of the pneumostatic force balance led to a decreasing film thickness with increasing pressure. Figure 14 shows the construction details of a small diameter seal design.

Care is taken to insure flatness of the sealing surfaces after assembly. The seal seat is keyed to the shaft spacer and is axially clamped by a machined bellows which exerts a predetermined clamping force, thus minimizing distortion of the seal seat. The bellows also acts as a static seal between the seat and the shaft spacer. Cooling oil is passed through the seat to reduce thermal gradients, and the oil dam disc also serves as a heat shield. Windbacks are used to prevent oil from approaching the sealing surfaces.

Inlet Effects

As mentioned previously, shaft seals for gases have very small sealing gap heights h (direction perpendicular to the leakage flow), and these are in the range of 2.5 to 12.5 μm (0.0001 to 0.0005 in.). In the direction of flow the gap length ℓ is relatively long, in the range of 1270 μm (0.05 in.). In other words the leakage channel is long and narrow with ℓ/h ratios of over 100. The mathematical modeling of this leakage channel is critical, in that the validity of the equilibrium film thickness prediction depends to a large part on the accuracy of predicting the pneumostatic opening forces on the primary seal; this is the pressure gradient which accompanies the leakage flow. The fully developed portion of the flow is readily obtained (Ref. 5), but the entrance region loss data for seal configurations and operation is generally not available.

Data with some applicability has been developed for gas lubricated bearings. But the flow in the cavity region just before the inlet of gas thrust bearings is generally different from that before seal configurations because the flow to the inlet of thrust bearings is often a strong function of radius and not so for seals. For this reason the inlet condition in bearings can be sonic or even supersonic. In this regard sonic, or supersonic, inlet flow is not predicted by the seal mathematical model (Ref. 5); and subsonic inlet flows are thought to prevail.

As an illustration of inlet effects the mathematical model of Ref. 5 was used to calculate the pressure gradient for the small diameter seal depicted in Fig. 14. Assumed gap thicknesses were from 2.54 to 12.7 μm (0.0001 to 0.0005 in.) and the operating conditions assumed were

Sliding speed	198 m/sec	(650 ft/sec)
Sealed gas temperature	677 K	(750° F)
Sealed gas pressure (P_1)	148 N/cm^2 abs	(214.7 psia)
Bearing cavity pressure (P_4)	25.6 N/cm^2 abs	(37.1 psia)

A constant inlet coefficient of 0.6 was assumed for the range of gap heights, and the pressure gradient curves are as shown in Fig. 15, in which the areas under the curves represent an opening force. An important point is the inlet pressure loss: the mathematical model predicts that the smaller leakage gaps have less inlet loss than the larger gaps (assuming the inlet coefficient is constant). The other point to note is that the larger gaps are operating under choked flow conditions at the exit, while the smaller gaps are not choked. The choked flow condition tends to increase the area under the curve, but the inlet loss tends to decrease the area (decrease closing force). The net result is a smaller closing force exists under the curves for the larger gaps. This is beneficial since it introduces positive axial film stiffness; that is, if the leakage gap closes, the opening force increases, and this tends to hinder further closing. This is a desirable feature since it is a positive stabilizing force from a dynamic operating standpoint.

In order to check the inlet loss coefficient magnitude which applies to seals, experiments were made using a scaled-up simulated primary seal with a fixed clearance of 25.4 μm (0.001 in.). A schematic of the test rig is shown in Fig. 16, and an example of the data obtained is shown in Fig. 17 for a pressure ratio of 10 with an upstream reservoir pressure of 62.1 N/cm^2 (90 psia). In addition to the inlet loss the pres-

sure gradient across the primary seal was measured by means of a set of small diameter pressure taps.

Analysis of the data shows the inlet coefficient to be 0.66. In addition the data provides a convenient check on the accuracy of the primary seal pressure gradient model of Ref. 5. Figure 17 shows some deviation between the measured data and the calculated profile but the agreement is good. It should be noted that a slight convergent deformation, if it actually exists in the rig, will produce the deviation shown. And, in fact, analysis revealed that theory and experiment will agree exactly if a convergent deformation of 0.0004 radian is assumed; and for this case the coefficient drops to 0.61. It is apparent from theoretical data (Fig. 15) and measured data (Fig. 17) that neglect of inlet effect in the mathematical model for the pressure gradient will result in a predicted opening force which is too large. This is the significant point of the data.

Adverse Operating Conditions

Effect of nonparallel sealing faces. - Figure 18 shows, in an exaggerated manner, the axisymmetric coning displacement of the seal seat. (The primary ring could also be coned.) This type of coning displacement, which can be caused by thermal gradients, results in nonparallel faces within the primary seal and the self-acting geometry. These nonparallel faces have a significant effect on load capacity of the self-acting geometry; also the primary seal opening force is affected. Thus, in design, the equilibrium operating film thickness should also be calculated for anticipated coning displacements.

As an example of the effect of this coning, cruise condition operation was checked (using the methods of Ref. 9) for equilibrium film thickness for a distortion of 13 μm (0.0005 in.) across the self-acting pad. This is a distortion of 2 milliradians and is typical of some seal operation (Ref. 12).

Figure 19 shows the self-acting lift force for the 2-milliradian distortion of the seat face. Note that the force is plotted as a function of the mean film thickness of the self-acting pad. Also plotted is force generated for a parallel film, and comparison shows a significant reduction in lift force due to the axisymmetric coning, especially at the lower film thicknesses.

As noted previously, the primary seal opening force is also affected by nonparallel faces; and this was calculated by using an analysis similar to Ref. 7 for the 2-milliradian distortion. The results are given in Fig. 20. For the divergent deformation shown in Fig. 18, there is a marked reduction in opening force as the film thickness decreases (negative film stiffness). In contrast, for convergent deformation the opening force increases as film thickness decreases (positive film stiffness). However, in aircraft mainshaft seals, the divergent deformation is a natural tendency due to thermal gradients.

Finally, in Fig. 21 the equilibrium film thickness for a 2 milliradian distortion is found by finding the intersection between the total closing force and total opening force. The mean film thickness is about 1.69 μm (0.00066 in.). Thus the minimum film thickness is 10.4 μm (0.00041 in.).

With the equilibrium film thickness values for the axisymmetric distortion, the gas leakage was calculated by using the method previously outlined. The results revealed that the leakage rate for the 2-milliradian deformation was nearly twice that of the parallel-face case.

Effect of seat face runout. - The preceding analyses were for operating film thicknesses that did not vary with time. This would be the situation if the rotating seat face had zero runout. However, the seat face will, in general, have some runout (misaligned with respect to axis of rotation); and in particular, the maximum runout used in practice is of interest since it will induce the maximum time-dependent film thickness changes.

Of interest, then, is how the primary ring responds to the runout motions of the seat face. This response determines the film thicknesses at any instant. Experimental data reported in Ref. 13 reveal that the primary ring can follow (dynamically track) the seat face motion over a considerable range of face runouts. These data were obtained by mounting two proximity probes (90° apart) on the ring retainer and recording the change in film thickness as a function of time. A schematic showing the probe location is given in Fig. 22. Some results from Ref. 13 are given in Fig. 23 which shows that for a seat face runout of 20 μm (0.00085 in.) full-indicator reading (F.I.R.), the ring response is in phase and the total change in film thickness is 17 μm (0.00067 in.) and that the film thickness varies circumferentially; that is, the film thickness is not axisymmetric and is similar to that depicted in Fig. 24.

This nonsymmetric angular misalignment is an inherent tendency because of secondary seal friction and seal head inertia, which are introduced by the tracking response to the seat face axial runout. As the high point of the seat face runout (see Fig. 24) rotates, the seal head must move back, and this is resisted by the secondary seal friction and head inertia; thus the film thickness tends to be smaller opposite the high point of face runout. In contrast, the friction and inertia are acting in opposite directions at the low point (180° away). Therefore, a rotating force couple exists which is synchronous with the face runout (if the seal head is properly tracking the seat motion); this causes the sealing faces to have an inherent angular misalignment.

As previously indicated, nonparallel faces cause changes in the pressure gradient across the primary seal and, therefore, affect the contribution of the primary seal to seal stability; this contribution can either have a positive (converging faces) or negative (diverging faces) effect. Table II (from Ref. 14) outlines some of the possible primary seal distortions, axisymmetric and nonaxisymmetric; and the resultant contribution for seal stability is indicated. Table II was constructed for incompressible fluid but these stability models, in general, also apply when sealing a compressible gas. For gas turbine mainshaft seals, model X, with the sealed pressure at the inside diameter, is probably the most prevalent with the nonaxisymmetric displacement (angular misalignment) being produced by the response of the seal head to the face runout motions of the seat. The axisymmetric portion of the nonparallel displacement will be due to thermal gradient which arises because of two effects: (a) the temperature gradient between the sealed gas and the bearing sump, and (b) the shearing of the fluid film in the primary seal. Analysis suggests that

the thermal coning can readily predominate, therefore, with reference to model E of Tabl II, β will be greater than γ, and the seal force will be divergent over the full 360°; this is a destabilizing condition, and overall seal stability must be provided by the self-acting geometry if rubbing contact is to be avoided.

An analytical program has been developed for the purpose of predicting primary seal ring response to seat face runout (Ref. 11). Analysis of the 16.67-cm (6.60-in.) diameter seal depicted in Fig. 4 revealed that the primary ring response is markedly affected by secondary seal friction and by inertia of the primary ring assembly. The friction effect is illustrated in Fig. 25; as runout increases, there is a friction level that, if exceeded, will retard the primary ring motion to such an extent that rubbing contact will occur (line (1)); also for the higher face runouts there is a friction level below which the inertial forces are so high that the primary ring cannot follow the runout (line (2)). Therefore, some friction is probably desirable for most applications because of the practical limits on control of face runouts. Further, the data suggest that the primary ring assembly inertia should be kept as small as practical in order to maintain good response (avoid unstable operation).

In a detailed analysis (Ref. 11) three different types of nosepiece responses were revealed by a parametric study using different magnitudes of seat face runout and secondary seal friction. These three cases are

Case 1 – Primary ring motion duplicates seat face runout motion and can be described by rotation (rocking) about two orthogonal axes. However, because of primary ring inertia and/or friction, the face of the ring has an angular misalignment with respect to the face of the seat. Therefore, the film thickness between the faces is not uniform (see Tab. II, model D).

Case 2 – Same as case 1 plus an additional axial vibration component.

Case 3 – Seal failure (film thickness reaches zero). This case can occur when the frictional forces are either two low (when inertia forces are high) or too high for the available load capacity of the self-acting pads.

An analysis was made of the seal head dynamic response of the 6.44-cm (2.54 in.) diameter seal with a seat face runout of 13 μm (0.000512 in.) and with secondary seal friction considered. The mathematical model described in Ref. 11 was used, and the data are given in Fig. 26, in which the minimum film thickness is given as a function of time for a seal sliding speed of 244 m/sec (800 ft/sec). The plot in Fig. 26 shows stable operation with a minimum film thickness of 5.6 μm (0.000219 in.) was achieved within a very short time span; stable operation of the case 1 type (tracking without axial vibration) was predicted.

EXPERIMENTAL DATA

16.76-Centimeter (6.60-In.) Nominal Diameter Seal

Table III (from Ref. 12) shows typical experimental data on the large diameter seal. The maximum combined conditions attempted in the rig test were a sliding speed of 175 m/sec (575 ft/sec), a sealed gas temperature of 811 K (1000° F), and a sealed pressure of 207 N/cm² gage (300 psig). This set of data and resulting posttest inspection of the parts confirmed the analytical predictions that the seal would function without rubbing contact at operating conditions expected in advanced engines.

Figure 27 (from Ref. 12) shows some experimentally obtained leakage results compared with the predicted total leakage (combined primary and secondary seal leakage). The correlation is reasonable, and the experimental data show the scatter typical of leakage values obtained throughout the test. This scatter in results is due to the strong dependence of leakage on sealing clearance (A very small change in clearance will produce a significant change in leakage. See formula (1).)

In addition to the performance evaluation at various operating conditions, the seal was subjected to a 320-hour endurance test (Ref. 15) at the following test conditions:

	120-hr segment	200-hr segment
Sealed air temperature	775 K (1000° F)	775 K (1000° F)
Sealed pressure differential	138 N/cm² (200 psi)	138 N/cm² (200 psi)
Seal velocity	122 m/sec (400 ft/sec)	122 m/sec (400 ft/sec)
Spring load	68.5 N (15.4 lb)	68.5 N (15.4 lb)

During the first segment of testing, seal leakage averaged approximately 0.33 scmm (11.7 scfm) as shown in Fig. 28. During the second segment, leakage averaged 0.40 scmm (14 scfm) for the first 100 hours, and increased at the rate of approximately 0.03 scmm (1 scfm) every 20 hours for the second 100 hours.

Inspection of the seal after the 320 hours suggested that the gradual increase in leakage was due to air-entrained debris erosion of the sealing dam. (Erosion due to debris is discussed in the following section.) A profile trace of the carbon primary seal face taken after 120 hours of endurance is shown in Fig. 29(a). The deepest scratch (air entrained debris) in the sealing dam was approximately 5.08 μm (0.0002 in.). The average Rayleigh pad wear for the 120-hour test was less than 1.27 μm (0.00005 in.).

After the second segment of testing the carbon primary seal and seal seat were still in good condition. A profile trace (Fig. 29(b)) taken at the same location as the traces in Fig. 29(a) shows more shallow scratches 2.54 μm (0.0001 in.) deep. The average wear on the Rayleigh pads for the second segment of 200 hours was less than 1.27 μm (0.00005 in.).

The effects produced by air entrained debris were checked by the introduction of abrasive particles

(Arizona road dust) into the test rig at the rate of 3.5 g/hr over a 14.5-hour test run. Data indicated a gradual increase in seal leakage due to wear of the sealing dam by the air entrained dirt. No significant wear occurred to the Rayleigh step pad portion. The erosion wear pattern of the primary seal is shown in Fig. 30, which is a surface profile trace taken radially across the primary seal. It is thought that the sealing dam wear may proceed until the leakage gap height becomes large enough to pass the entrained debris.

6.44-Centimeter (2.54-In.) Nominal Diameter Seal

Table IV contains gas leakage data for relatively small diameter self-acting seals (see Fig. 14) operating in a test rig over a pressure differential range from 23 to 111 N/cm² (34 to 161 psi) and a sliding speed range from 91 to 183 m/sec (300 to 600 ft/sec). (This is a rotative speed range of 27 300 to 54 600 rpm.)

The test setup contained two seals, one fore and one aft of the rig bearing. This simulated a bearing compartment in a small gas turbine. Neither the forward nor the aft carbon nose or seal seat showed any wear during this evaluation (Tab. IV, from Ref. 16). Thus the sealing surfaces were separated by a gas film over the entire matrix of operating variables. This suggests that the gas bearing film stiffness was sufficient to prevent rubbing contact under the high inertia forces which are associated with high rotative speeds (inertia forces increase as the square of the rotating speed).

Data in Tab. IV indicate a seal leakage increase with a sliding speed increase (for any given pressure differential). This leakage increase is due to a slight increase of the sealing gap.

To further explore the operating limits of the small diameter self-acting seals, 500 hours of endurance operation at ambient temperature (~381 K (225° F)) was conducted as follows (Ref. 16):

Hours	Speed			Air pressure differential (max)	
	m/s	ft/sec	rpm	N/cm² abs	psia
1 - 100	145	475	43 000	125	181
100 - 200	152	500	45 500	129	186.5
200 - 300	160	525	47 700	130	189
300 - 400	168	550	50 000	129	187
400 - 467	175	575	52 300	128	186
467 - 500	183	600	54 600	128	186

The same aft seal carbon and seat were used throughout the test, and a forward carbon ring was used that had previously operated for 150 hours.

Table V from Ref. 16 outlines test results for the 500-hour run. The last run was typical of the airflow that can be expected through two seals at an air pressure differential of 127 N/cm² (184 psi); approximately 0.007 kg/sec (12 scfm or 0.015 lb/sec).

The depth of the self-acting geometry was checked by surface profile measurements for the purpose of monitoring the wear process. The average total wear of the carbon rings during the 500-hour test was 51 μm (0.0002 in.) (Ref. 16). In addition to endurance runs, the effect of seat face runout was evaluated in a 10-hour test run by using seats which had been machined such that in the assembled state a full indicated runout of 50.8 μm (0.002 in.) existed; this magnitude is twice the usual practice for conventional seals of this size range. Baseline tests were also conducted on seal assemblies which had runouts of 15 μm (0.0006 in.). A comparison of leakage rates is shown in Fig. 36. Maximum speed was 43 000 rpm or 145 m/sec (475 ft/sec). The data of Fig. 31 reveal a significant axial runout effect on leakage rate, the seals with 50.8-μm (0.002-in.) seat face runout - having about three times the leakage of the seals with normal runout values (15 μm (0.0006 in.)). Inspections after the two tests, 10 hours of baseline testing and 10 hours of testing with 40.8-μm (0.0020-in.) runout, revealed that wear was insignificant; therefore, noncontact operation was maintained in both 10-hour tests. The increase in leakage over the baseline test is due to a greater average film thickness induced by response of the primary ring to the seat face runout (see previous discussion on effects of seat face runout).

Spiral Groove Self-Acting Seal

The Rayleigh step bearings of the small diameter seal depicted in Fig. 14 were replaced with a set of spiral grooves (see Fig. 32), and the seal was run at simulated engine conditions. Typical seal leakage data are shown in Fig. 33 (from Ref. 17) for sliding speeds of 182.9 m/sec (600 ft/sec). Data at other sliding speeds confirmed that the general trend for self-acting seals was a leakage increase as speed increased. The leakage, however, was relatively low and considered within the usable range for application in small gas turbine engines.

A 54-hour endurance run was made at 148.1 N/cm² abs (215 psia) sealed pressure and the data are given in Tab. VI. The sliding speeds ranged from 122 to 243.8 m/sec (400 to 800 ft/sec), with the majority of the time being at 213 m/sec (700 ft/sec). The maximum sliding speed of 243.8 m/sec (800 ft/sec) corresponds to a maximum rotating speed of 72 500 rpm.

The measured wear in the spiral groove region after the 54 hours of operation was (Ref. 17):

Forward seal. . . . . No measurable wear
Aft seal. . . . . 1.0 μm (0.000040 in.)

Leakage Rate Comparison to Conventional Seal

Leakage tests were made on various conventional seals of a size comparable to the 6.44-cm (2.54-in.) diameter Rayleigh step pad seal (Fig. 14); the comparison is shown in Fig. 34. In general, the plot shows that the self-acting face seal has the potential of significantly reducing leakage as compared with the conventional seals.

Of the conventional configurations, face seals allowed the least air flow at high pressure differentials. Circumferential segmented seals are as tight as face seals at moderate operating conditions; however, experience and the subject test program results have shown that at pressure differentials above 41.4 N/cm^2 (60 psi) and speeds above 107 m/sec (350 ft/sec), these (unbalanced) circumferential segmented seals rapidly wear out and finally operate as labyrinths. In that case there is little to choose between circumferential, rotating ring, and labyrinth seals in terms of air flows.

To gain some perspective of the magnitude of air flow under discussion, engine experience has shown that excessive air flow into a bearing package incorporating seals of the size used in the test program would be in the order of 0.012 kg/sec (0.029 lb/sec). Taking midpoint values of the range of pressure differentials in Fig. 34, the face seal could not meet this criterion at pressure differentials above approximately 85 N/cm^2 (123 psi), and the limiting pressure differential for circumferential segmented seals (which wear rapidly), rotating ring seals, and simple labyrinths would be approximately 40 N/cm^2 (58 psi). The self-acting seal, however, did not reach the limiting leakage rate and had a leakage of 0.0046 kg/sec (0.0102 lb/sec) at a pressure differential of 107.6 N/cm^2 (156.0 psi). In general the self-acting seal had about one third the leakage of the conventional face seal.

CONCLUDING REMARKS

Self-acting seals are described, and their potential for meeting operational requirements of gas turbine engines is explored by means of predictive analysis of their operation at sealing speed, pressure, and temperature conditions which would be imposed by the engine. In particular, the analytical procedure is given for predicting the leakage and operating film thicknesses. Performance maps for two seal sizes are given; these are a 16.76-cm (6.60-in.) nominal diameter seal suitable for large engines and a 6.44-cm (2.54-in.) diameter seal for small engines. The analysis and subsequent operation of these seals under simulated gas turbine conditions revealed the following:

1. Analysis

a. Noncontact operation with acceptable leakage is predicted over the range of engine operation conditions (idle, takeoff, climb, and cruise) for both seal sizes.

b. The predicted operating film thickness of the 16.76-cm (6.60-in.) diameter seal ranged between 4.6 and 11.9 μm (0.00018 and 0.00047 in.) for idle, takeoff, climb, and cruise.

c. The calculated seal leakage rates of the 16.76-cm (6.60-in.) diameter seal ranged between 0.01 and 0.40 scmm (0.4 and 14.0 scfm) for idle, takeoff, climb, and cruise.

d. For a typical operating condition noncontact operation was predicted under the assumption of a 2-milliradian face deformation. Gas leakage was about twice that for parallel-face operation.

e. Analysis reveals that the pressure drop in the inlet to the primary seal gives rise to a positive film stiffness and has a significant effect on seal opening force magnitude.

f. Proper tracking of the seat face runout by the carbon ring is predicted for practical levels of face runout magnitudes.

2. Experiment, Simulated Engine Operation

a. In general the self-acting seals operate, as predicted, without rubbing contact over the range of simulated engine operating conditions. Of particular interest was: (a) the noncontact operation of the 16.76-cm (6.60-in.) diameter seal at the advanced engine conditions of a 152-m/sec (500-ft/sec) sliding speed, a 345-N/cm^2 (500-psi) sealed pressure differential, and a 811 K (1000° F) sealed air temperature and (b) the noncontact operation of the 6.44-cm (2.54-in.) diameter seal at a 243.8-m/sec (800-ft/sec) sliding speed and a 148.1-N/cm^2 (215 psi) sealed pressure level.

b. The self-acting face seal leakage was significantly lower than that of conventional seal types.

REFERENCES

1. Schweiger, F. A., "The Performance of Jet Engine Contact Seals," Lubr. Eng., vol. 19, no. 6, June 1963, pp. 232-238.
2. Parks, A. J., McKibbin, R. H., Ng, C. C. W., and Slayton, R. M., Pratt & Whitney Aircraft, "Development of Main-Shaft Seals for Advanced Air Breathing Propulsion Systems," 1967, PWA-3161, NASA CR-72338.
3. Povinelli, V. P., and McKibbin, A. H., Pratt & Whitney Aircraft, "Development of Mainshaft Seals for Advanced Air Breathing Propulsion Systems," 1967, PWA-3161, NASA CR-72737.
4. Brown, P. F., Jr., "A Glossary of Seals Terms," Special Publication SP-1, American Society of Lubrication Engineers, 1969.

5. Zuk, J., Ludwig, L. P., and Johnson, R. L., Lewis Research Center, "Quasi-One-Dimensional Compressible Flow Across Face Seals and Narrow Slots. I - Analysis," 1972, NASA TN D-6668.

6. Zuk, J., and Ludwig, L. P., Lewis Research Center, "Investigation of Isothermal, Compressible Flow Across a Rotating Sealing Dam. I - Analysis," 1969, NASA TN D-5344.

7. Zuk, J., and Smith, P. J., Lewis Research Center, "Computer Program for Viscous Isothermal Compressible Flow Across a Sealing Dam with Small Tilt Angle," 1969, NASA TN D-5373.

8. Johnson, R. L., and Ludwig, L. P., Lewis Research Center, "Shaft Face Seal with Self-Acting Lift Augmentation for Advanced Gas Turbine Engines, 1969, NASA TN D-5170.

9. Ludwig, L. P., Zuk, J., and Johnson, R. L., Lewis Research Center, "Design Study of Shaft Face Seal with Self-Acting Lift Augmentation. IV - Force Balance," 1972, NASA TN D-6368.

10. Zuk, J., Ludwig, L. P., and Johnson, R. L., Lewis Research Center, "Design Study of Shaft Face Seal with Self-Acting Lift Augmentation. I - Self-Acting Pad Geometry," 1970, NASA TN D-5744.

11. Colsher, R., and Shapiro, W., Franklin Research Institute, "Steady State and Dynamic Performance of Gas-Lubricated Seals, 1972, F-C3452-1, NASA CR-121093.

12. Dobek, L. J., Pratt & Whitney Aircraft, "Development of Mainshaft Seals for Advanced Air Breathing Propulsion Systems," 1973, PWA-TM-4683, NASA CR-121177.

13. Hady, W. F., and Ludwig, L. P., Lewis Research Center, "Experimental Investigation of Self-Acting-Lift-Pad Characteristics for Main Shaft Seal Applications," 1971, NASA TN D-6384.

14. Ludwig, L. P., Lewis Research Center, and Greiner, H. F., Sealol Inc., "Design Considerations in Mechanical Face Seals for Improved Performance - II Lubrication," NASA TM X-73736, 1977.

15. Povinelli, V. P., and McKibbin, A. H., Pratt & Whitney Aircraft, "Development of Mainshaft Seals for Advanced Air Breathing Propulsion Systems, Phase II," 1970, PWA-3933, NASA CR-72737.

16. Lynwander, P., Avco Lycoming Division, "Development of Self-Acting Seals for Helicopter Engines," 1974, LYC-74-55, NASA CR-134739.

17. O'Brien, M., Avco, "Development of Spiral Groove Self-Acting Face Seals," 1977, LYC-77-41, NASA CR-135303.

TABLE I

Closing Force

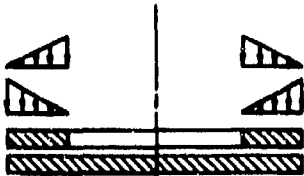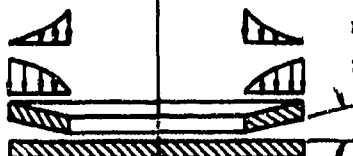|	Design point	
	Idle	Takeoff
Sealed gas temperature.	311 K (100° F)	977 K (1300° F)
Seal sliding speed.	122 m/sec (200 ft/sec)	137 m/sec (450 ft/sec)
Sealed pressure, P_1	45 N/cm^2 a (65 psia)	217 N/cm^2 a (316 psia)
Pressure change, ΔP	34.5 N/cm^2 (50 psi)	207 N/cm^2 (300 psi)
Sealed-pressure closing force, F_p	160.6 N (36.1 lbf)	963.4 N (216.6 lbf)
Spring force, F_s	71.2 N (16 lbf)	71.2 N (16 lbf)
Total closing force, $F_t = F_p + F_s$	231.7 N (52.1 lbf)	1034.6 N (232.6 lbf)

TABLE II

Seal Stability Models
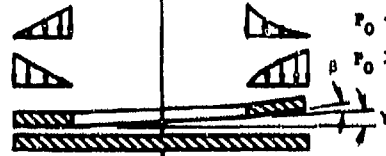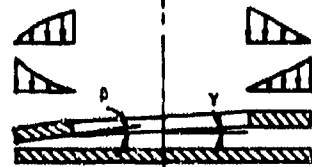
	Pressure pattern	Axial stiffness	Restoring moment
A. Parallel			
$P_0 < P_i$	Axisymmetric	Zero	Zero
$P_0 > P_i$	Axisymmetric	Zero	Zero
B. Coned			
$P_0 < P_i$	Axisymmetric	Negative	Negative
$P_0 > P_i$	Axisymmetric	Positive	Positive
C. Coned			
$P_0 < P_i$	Axisymmetric	Positive	Positive
$P_0 > P_i$	Axisymmetric	Negative	Negative
D. Misaligned			
$P_0 < P_i$	Nonaxisymmetric	Positive	Positive
$P_0 > P_i$	Nonaxisymmetric	Negative	Negative
E. Coned and misaligned			
$P_0 < P_i$	Nonaxisymmetric	Negative	Negative
$P_0 > P_i$	Nonaxisymmetric	Positive	Positive
F. Coned and misaligned			
$P_0 < P_i$	Nonaxisymmetric	Positive	Positive
$P_0 > P_i$	Nonaxisymmetric	Negative	Negative

TABLE III

Typical Test Data for 16.76-centimeter (6.60.-in.) Nominal Diameter Seal[a]

Time, hr	Sliding speed		Seal pressure		Air temperature		Oil-in temperature		Actual total air leakage	
	m/sec	ft/sec	N/cm²	psi	K	°F	K	°F	scms×10³	scfm
2.0	111	365	207	300	700	800	394	250	15.0	31.9
2.0			224	325					16.5	34.9
2.0			241	350					17.8	37.8
2.0			259	375					18.8	39.9
2.0			275	400					19.6	41.5
2.0	122	400	275	400					26.6	56.4
8.0	122	400	293	425					27.8	59.0
1.0	137	450	207	300	811	1000			17.2	36.5
.5	152	500							17.5	37.0
.5	160	525							16.5	35.0
.75	168	550							16.5	35.0
.25	175	575							17.9	38.0

[a]Ref. 12.

TABLE IV

Self-Acting Face Seal Evaluation
[6.44-cm (2.54-in.) nominal diameter seal.]

Rpm	Speed		Air pressure differential		Airflow (two seals)		Seal temperature	
	m/sec	ft/sec	N/cm²	psi	kg/sec	lb/sec	K	°F
27 300	91	300	23.4	34.0	<0.0006	<0.0013	333	140
36 400	122	400	23.1	33.5	<.0006	<.0013	352	174
45 500	152	500	23.1	33.5	<.0006	<.0013	371	210
54 500	183	600	22.1	32.0	.0011	.0024	392	246
27 300	91	300	111.4	161.5	.0023	.0050	364	196
36 400	122	400	110.7	160.5	.0032	.0070	373	212
45 500	152	500	109.6	159.0	.0036	.0079	386	236
54 600	183	600	107.6	156.0	.0046	.0102	402	263

TABLE V

500-Hour Endurance Test Results[a]
[Sealed pressure, 148 N/cm² abs (215 psia).]

Hours	Maximum airflow (two seals)			Maximum cavity pressure		Maximum seal temperature				Number of stops
						Forward		Aft		
	kg/s	scfm	lb/sec	N/cm² abs	psia	K	°F	K	°F	
b1 - 100	0.011	18.5	0.024	25.3	36.7	407	272	380	225	8
b100 - 200	.008	13.5	.017	21.8	31.7	417	290	385	234	9
b200 - 300	.007	12.5	.016	21.5	31.2	421	298	390	242	21
b300 - 400	.008	14.5	.018	22.5	32.7	420	296	395	251	9
400 - 467	.007	12.5	.016	21.2	30.7	420	296	399	258	8
467 - 500	.007	12.0	.015	21.2	30.7	426	306	407	272	3

[a]Ref. 16.

[b]Air leakage results includes leakage through scavenge fittings.

TABLE VI

Endurance Test for 6.44-Centimeter (2.54-in.) Diameter Spiral Self-Acting Seal
[Sealed air pressure, 148 N/cm² abs (215 psia).]

[Sealed air pressure, 148 N/cm² abs (215 psia).]

| Accumulated time, hr	Speed			Cavity pressure		Airflow			Seal temperature			
	m/sec	ft/sec	rpm	N/cm² abs	psia	kg/sec	scfm	lb/sec	Forward		Aft	
									K	°F	K	°F
4	122.0	400	35 900	28.7	41.7	0.0116	20.0	0.0255	359	185	360	189
9	152.0	500	45 100	32.0	46.7	.0119	20.5	.0261	377	220	386	235
19	183.0	600	54 100	28.9	40.7	.0093	16.9	.0204	402	263	407	273
24	213.0	700	62 900	28.1	40.7	.0079	13.5	.0172	454	358	469	385
45	213.0	700	62 900	26.7	38.7	.0070	12.0	.0153	480	405	504	448
52	215.5	707	63 800	32.2	46.7	.0104	18.0	.0229	527	490	544	520
53.7	230.7	757	68 300	34.2	49.7	.0115	20.0	.0255	547	524	559	547
54	236.4	777	70 100	34.9	50.7	.0115	20.0	.0255	550	530	562	554
54.1	243.8	800	72 500	34.2	49.7	.0115	20.0	.0255	555	540	562	553
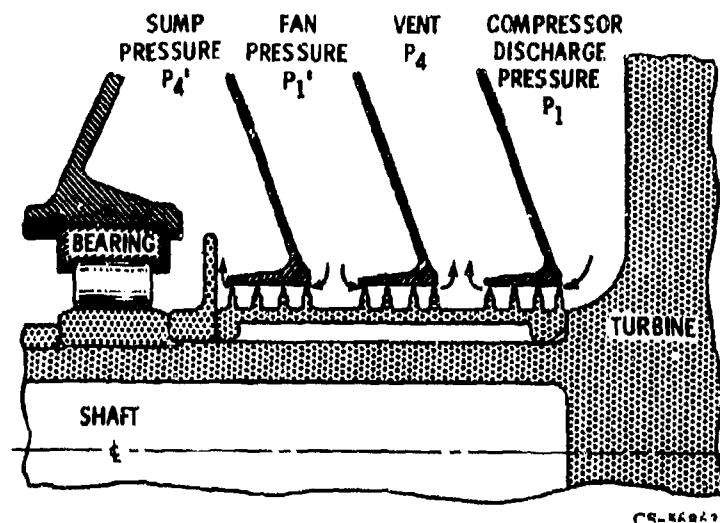
Fig.1   Labyrinth seal system schematic
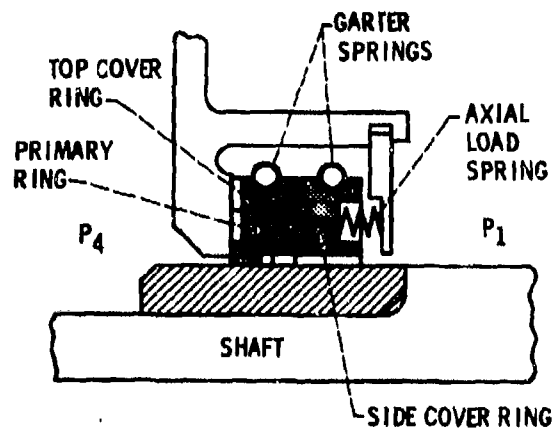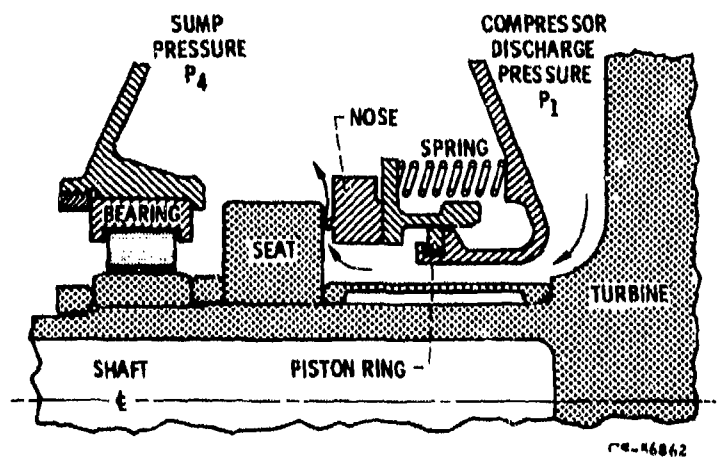

Fig.2   Shaft riding or circumferential seal

Fig.3   Schematic of a conventional radial face seal

(a) NOMENCLATURE

(b) SELF-ACTING GEOMETRY

DIMENSIONS IN CM (IN.)
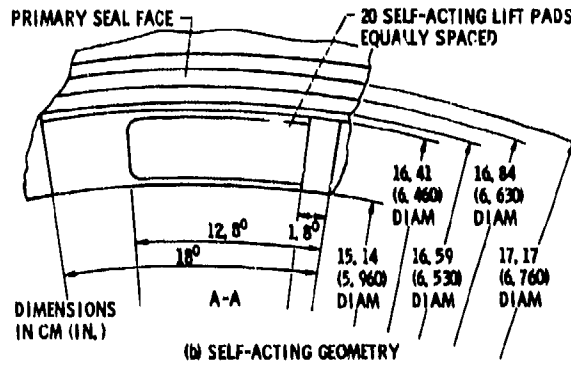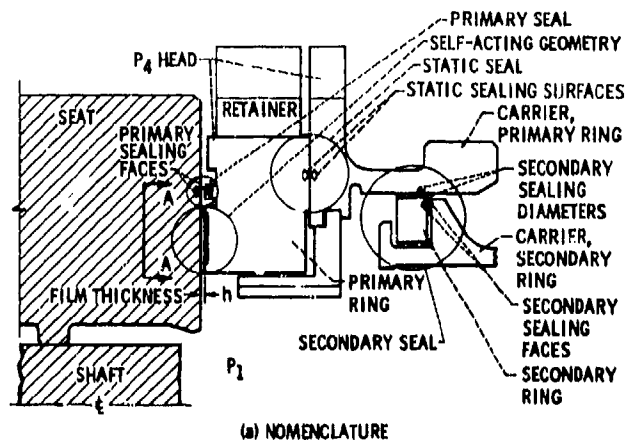
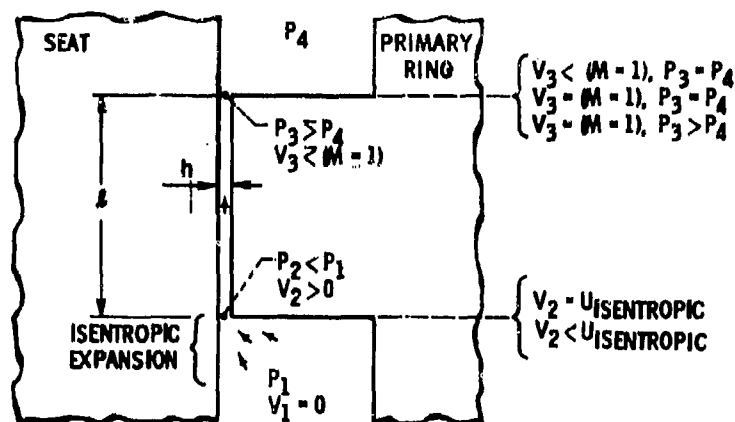Fig.4   Self-acting face seal

Fig.5   Primary ring assembly
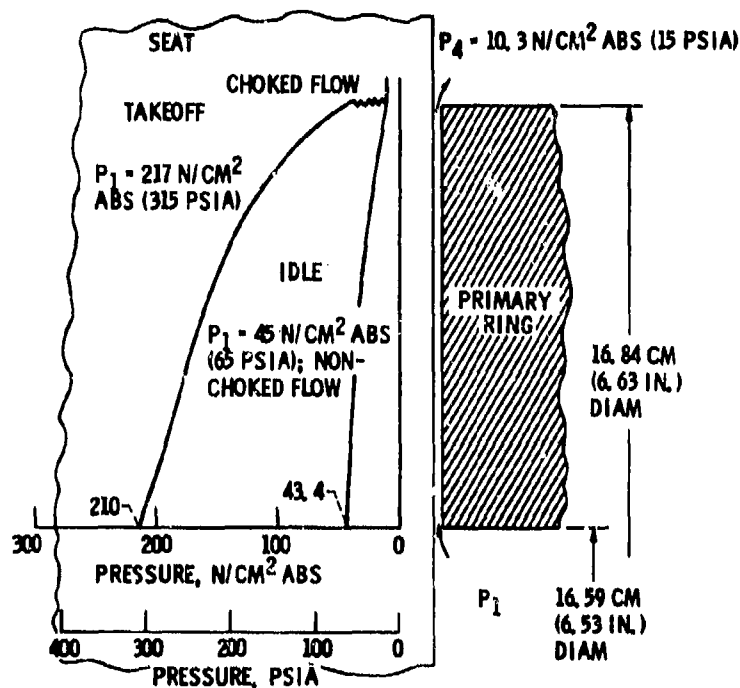
Fig.6 Mathematical model of primary seal

Fig.7 Pressure gradient in primary seal, illustrating choked and nonchoked flow. Parallel faces; mean film thickness h_m, 0.0010 centimeter (0.0004 in.). (From Ref.9)
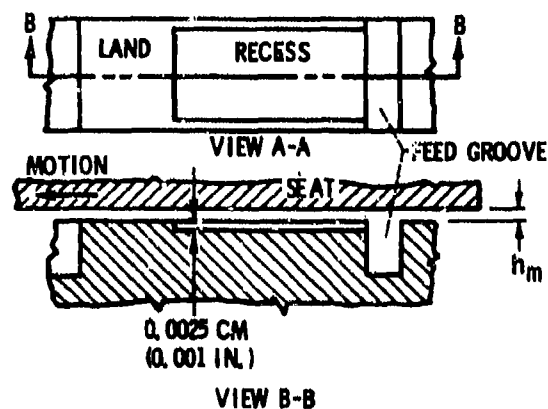

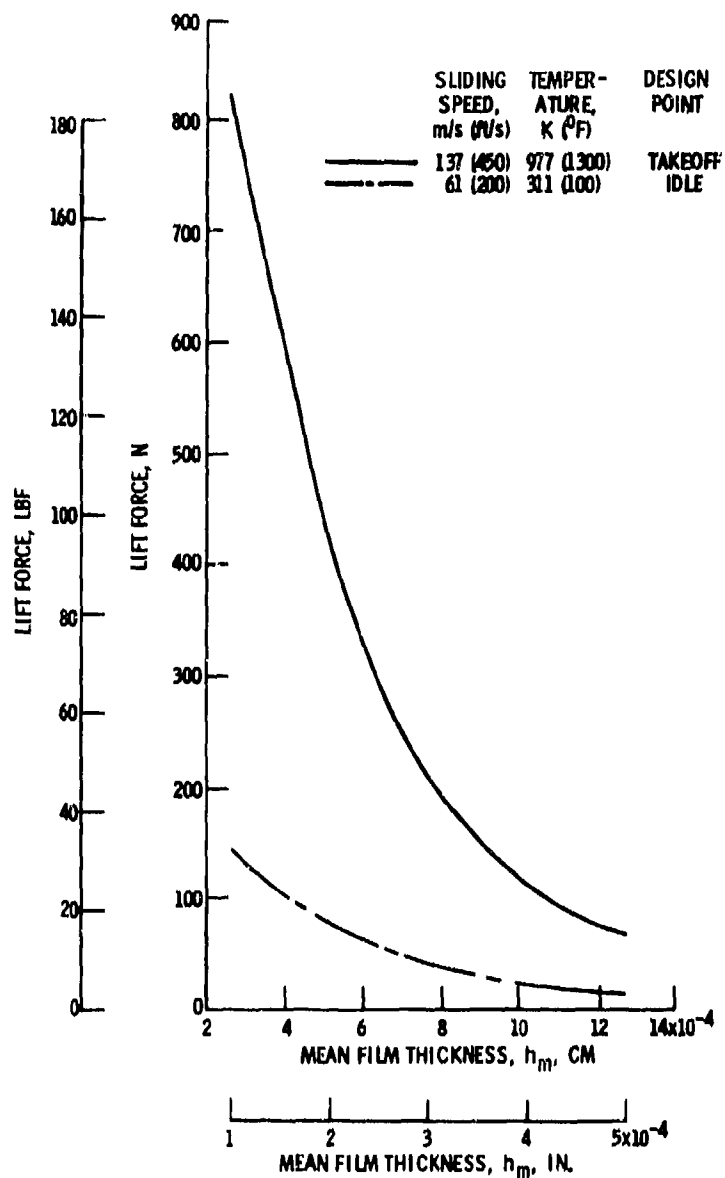Fig.8 Mathematical model of self-acting pad with curvature effects neglected

Fig.9 Lift force of self-acting geometry, Number of pads, 20; recess depth, 0.0025 centimeter (0.001 in.); fluid, air; parallel faces. (From Ref.9)
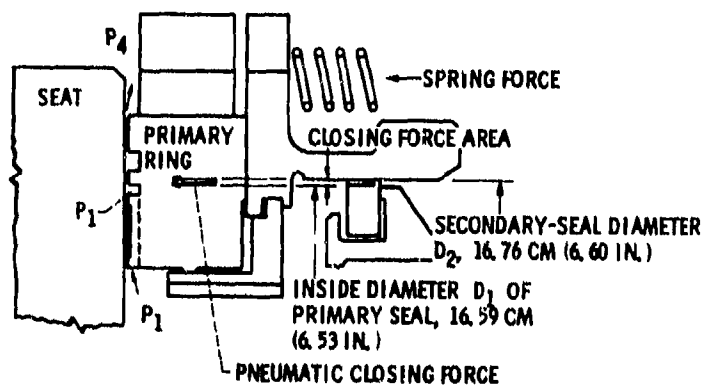

Fig.10 Closing forces — spring force and net closing force due to sealed pressure
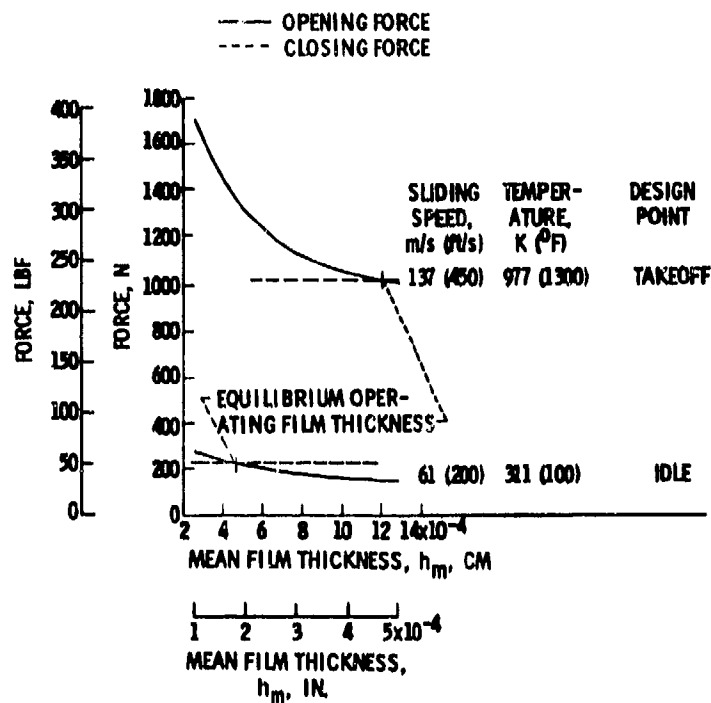
Fig.11 Equilibrium gas film thickness as determined by total seal opening and closing forces. Parallel faces (from Ref.9)
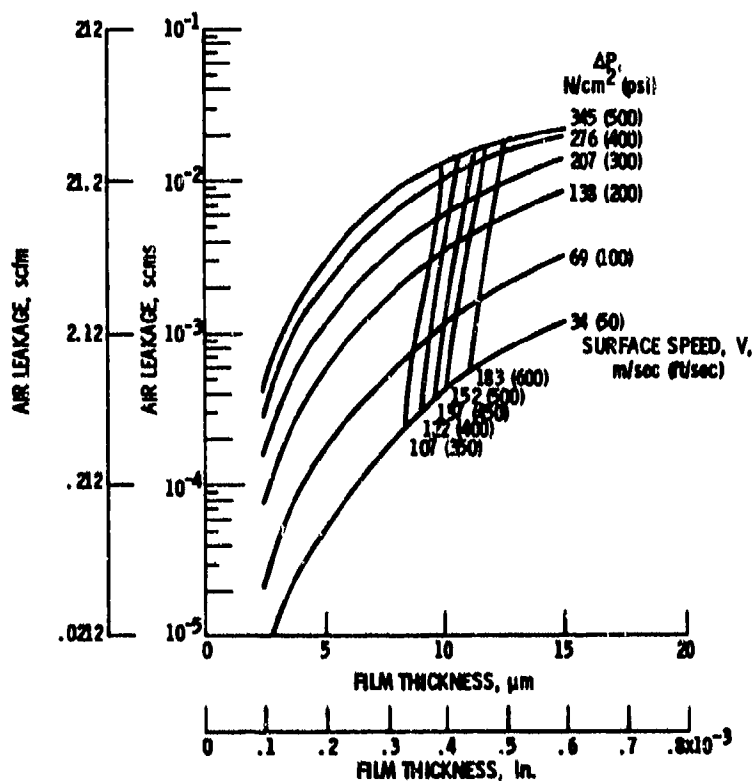

Fig.12 Primary seal leakage as function of film thickness. Nominal diameter seal (from Ref.12), 16.76 cm (6.60 in.); seal air temperature, 700 K (800° F); spring force, 75 N (17 lbі)
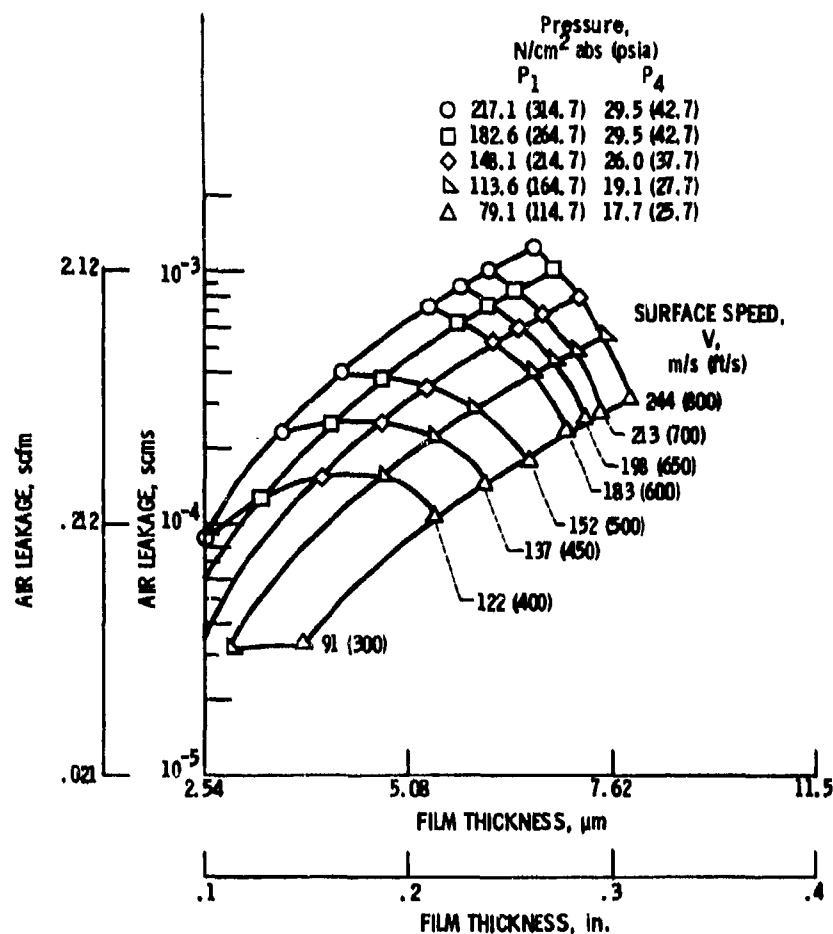
Fig.13 Performance map for 6.44 cm (2.5 in.) nominal diameter seal. Sealed air temperature, 644 K (700° F); spring force, 31.1 N (7 lbf); inlet loss coefficient, 1.0.

1. SPRING PLATE
2. COMPRESSION SPRING
3. SPRING PIN
4. HOUSING
5. CARRIER

6. PISTON RING (SECONDARY SEAL)
7. BELLOWS SPACER
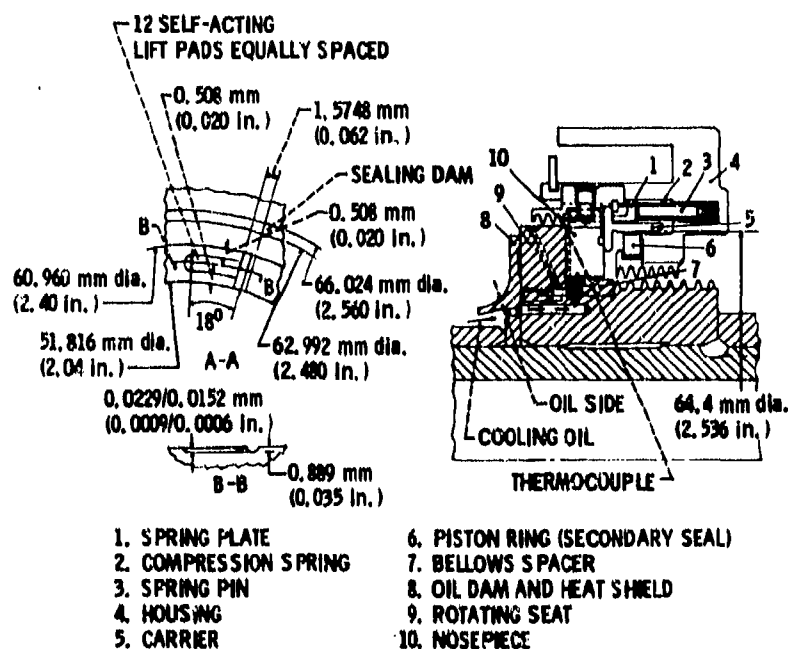8. OIL DAM AND HEAT SHIELD
9. ROTATING SEAT
10. NOSEPIECE

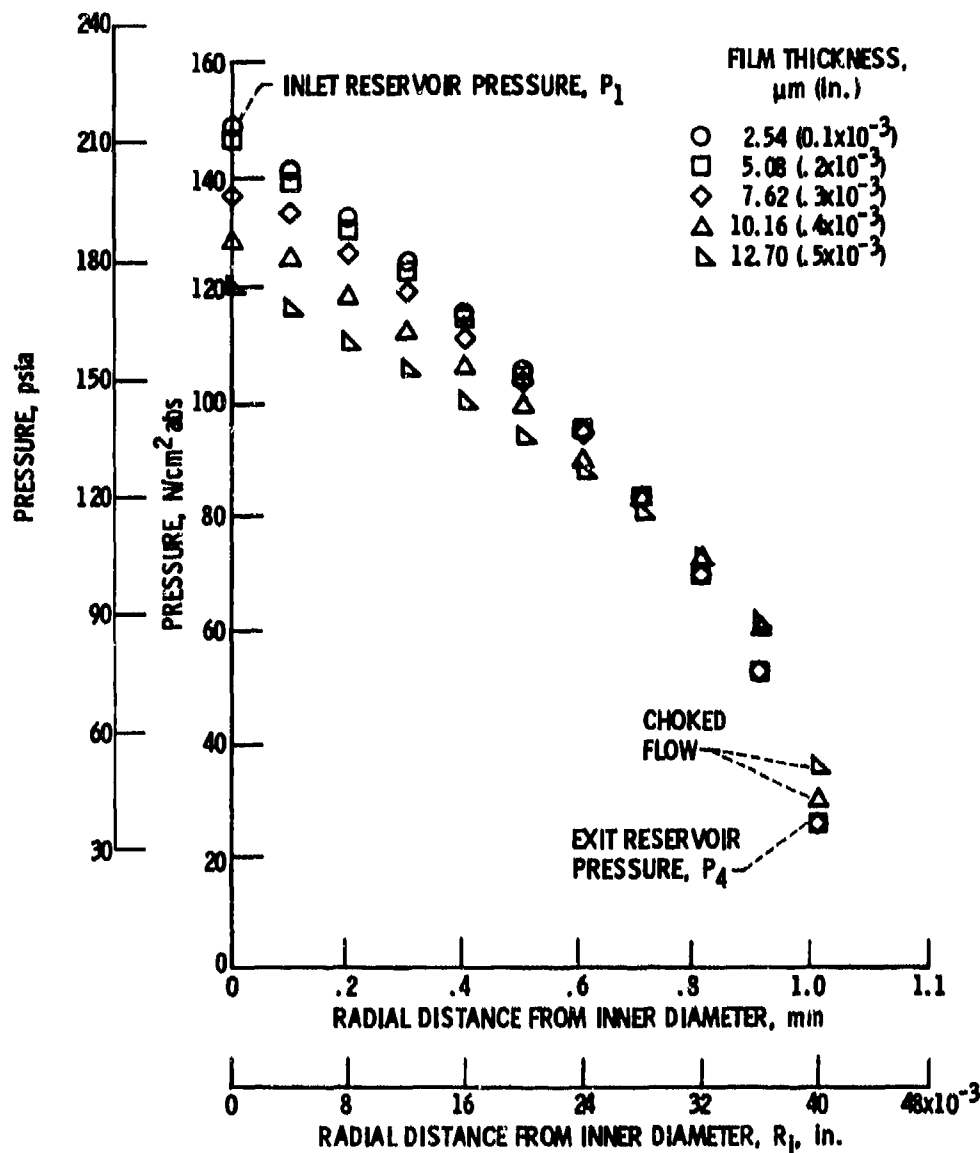Fig.14 Self-acting face seal design, 6.44 cm (2.54 in.) nominal diameter

Fig.15   Calculated radial pressure gradient across primary seal. Seal diameter, 6.44 cm (2.5 in.);
sealed gas temperature, 672 K (750° F); spring force, 31.1 N (7.0 lbf); sliding speed,
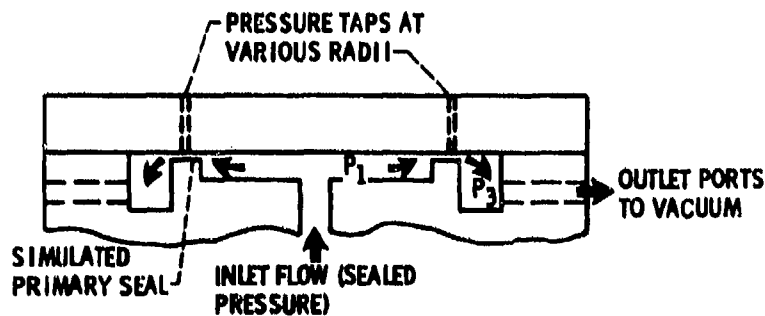192 m/s (650 ft/s); assumed inlet coefficient, 0.6

Fig.16   Schematic of test rig for measurement . ···· .ffect and
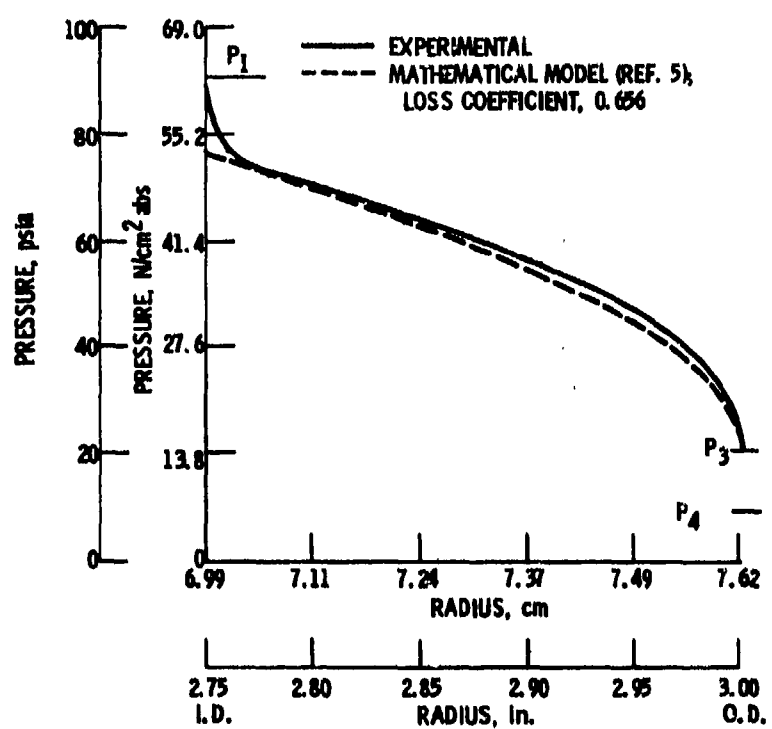pressure gradient across the primary seal

Fig. 17   Primary seal inlet pressure drop and pressure gradient. Sealed pressure, 62.3 N/cm² abs (90.4 psia); pressure ratio, ~ 10; sealing gap, h , 0.0028 cm (0.0011 in.); parallel seal faces
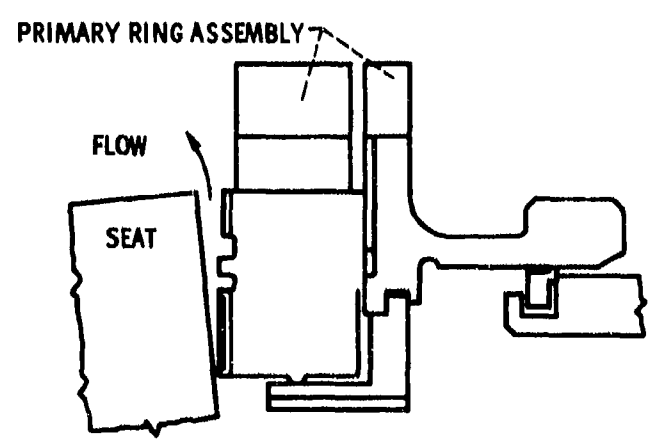

Fig. 18   Axisymmetric coning displacement of seat, causing nonparallel faces in primary seal and in self-acting geometry
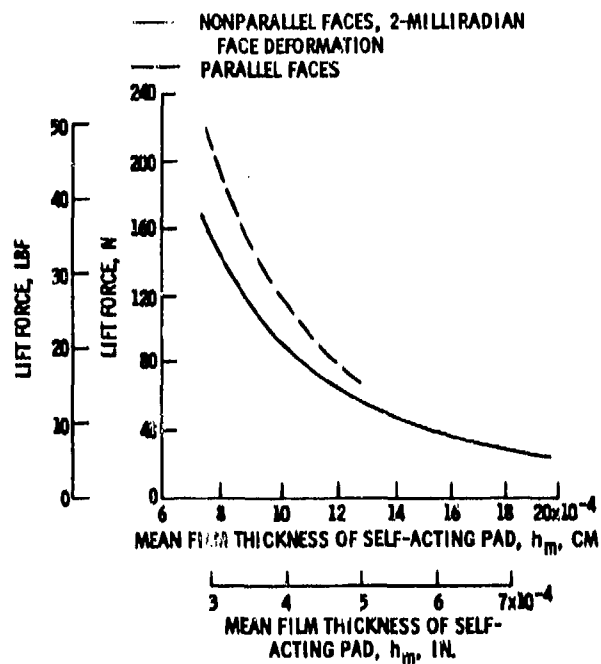
Fig.19 Lift force of self-acting geometry. Number of pads, 20; pad depth, 0.0025 centimeter (0.001 in.); fluid, air. Sealed pressure, 148 N/cm² abs (215 psia); sliding speed, 153 meters per second (500 ft/sec); fluid temperature, 700 K (800° F)

Fig.20 Opening force acting on primary ring assembly, sealed fluid, air. Sealed pressure, 148 N/cm² (215 psia); fluid temperature, 700 K (800° F). (From Ref.9)
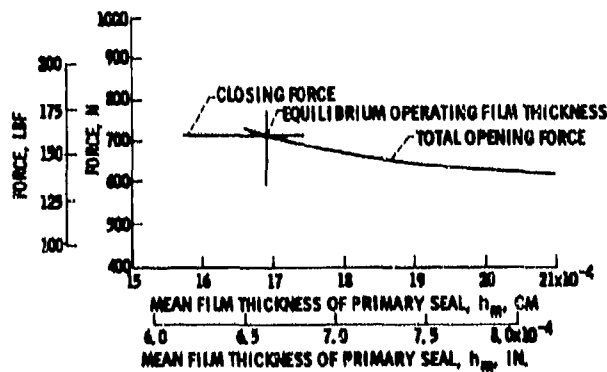
Fig.21 Equilibrium gas film thickness as determined by total opening and closing forces for 2-milliradian face deformation. Sliding speed, 153 meters per second (500 ft/sec); sealed pressure, 148 N/cm² abs (215 psia); sealed gas temperature, 700 k (800° F)
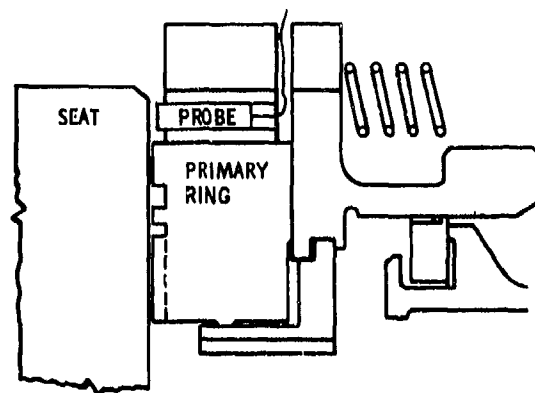
Fig.22 Schematic showing proximity probe location

PROBE ON SEAL RING
0.0017 CM (0.00067 IN.)

SEAT FACE MOUNT F. I. R.
0.0020 CM (0.00085 IN.)

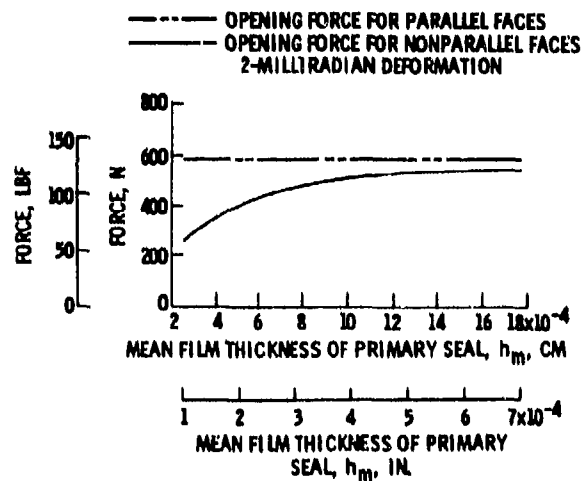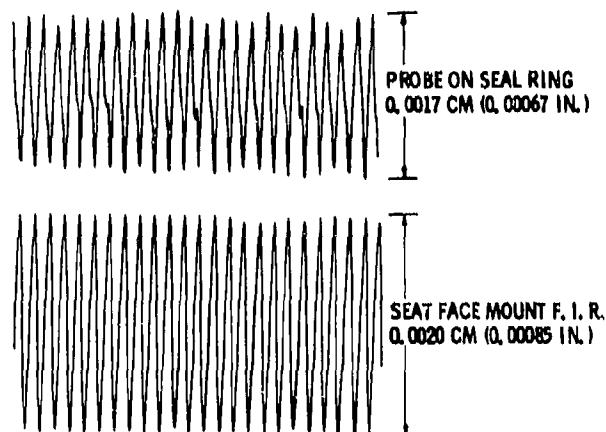Fig.23 Oscillograph traces showing response of ring to seat face runout. Recess-pad length to land-length ratio, 2:1; recess-pad depth, 0.0013 centimeter (0.0005 in.); sliding velocity, 61 meters per second (200 ft/sec); ambient pressure, 10 newtons per square centimeter (14.7 lb/in.^{2}); room temperature, 300 K (80° F); spring load, 1.13 kilograms (2.50 lb). (From Ref.13)

PRIMARY
RING

SEAT

FRICTION
FORCE

℄ OF SEAT
ROTATION

FRICTION
FORCE

MAXIMUM
GAP
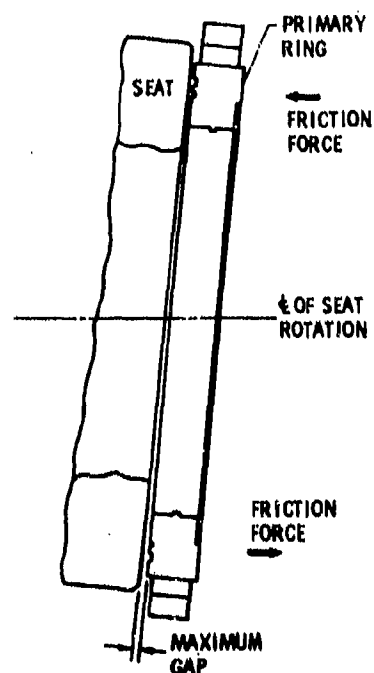
Fig.24 Angular misalignment of sealing faces, nonaxisymmetric sealing gap
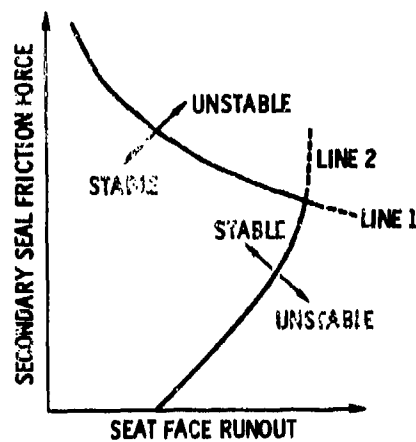
Fig.25   Typical stability map of primary ring response to seat face runout
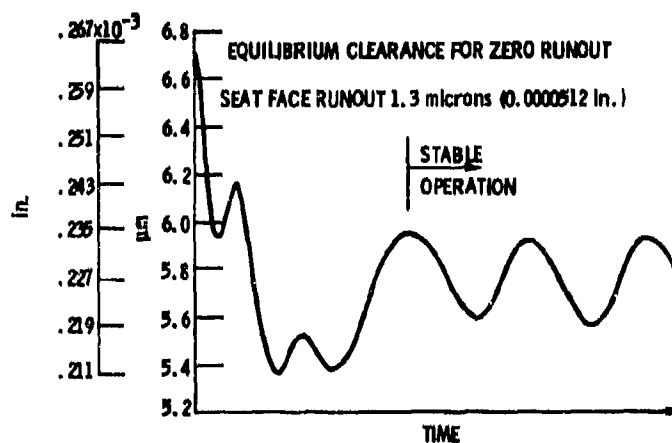
Fig.26   Minimum clearance from start-up (time = 0) for 6.44 cm (2.5 in.) nominal diameter seal; sliding speed, 244 m/sec (800 ft/sec)
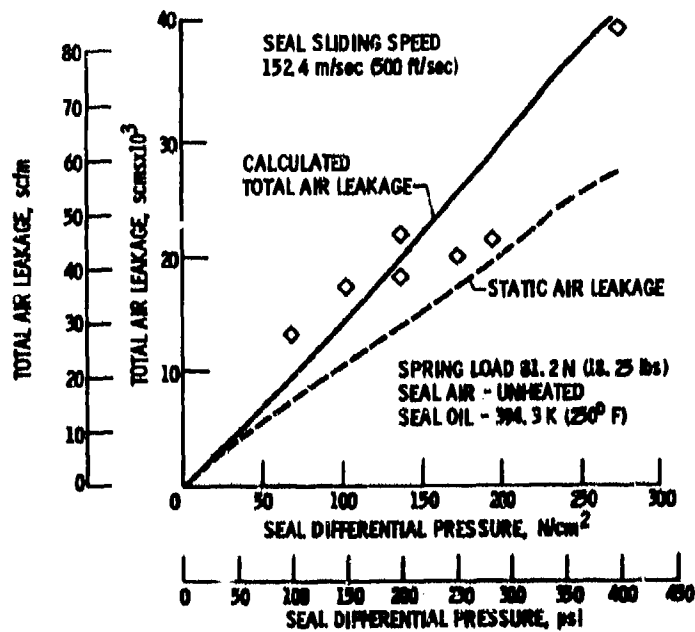
Fig.27   Seal leakage; 16.76 cm (6.6 in.) nominal diameter seal. (Ref.15)

30% INCREASE   100% INCREASE
REAR BEARING   REAR BEARING
FAILURE INDICATOR   FAILURE INDICATOR
READING   READING (CAUSED
INCREASE IN SEAL
LEAKAGE)

AIR TEMPERATURE   775 K (1000° F)
SEAL VELOCITY   122 m/sec (400 ft/sec)
DIFFERENTIAL PRESSURE   138 N/cm² (200 psi)
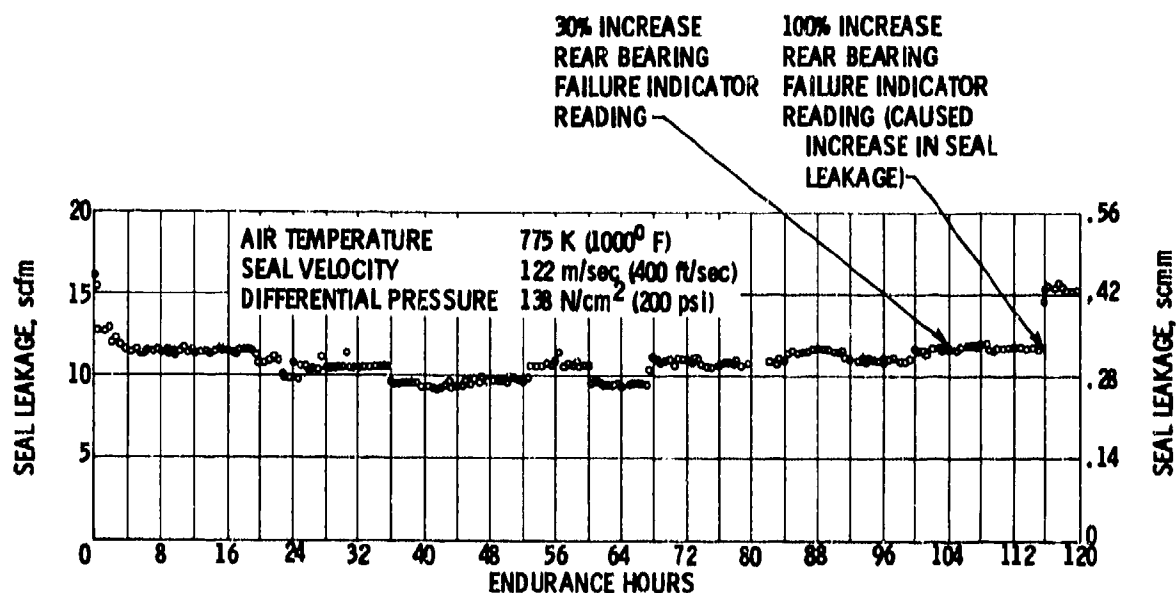
Fig.28   Air leakage for 120-hour endurance test of 16.76 cm (6.6 in.) nominal dia seal (Ref.15)

(a) AFTER 120 hr OF ENDURANCE.

(b) AFTER 200 hr OF ENDURANCE; TOTAL TIME n SEAL 338.5 hr.
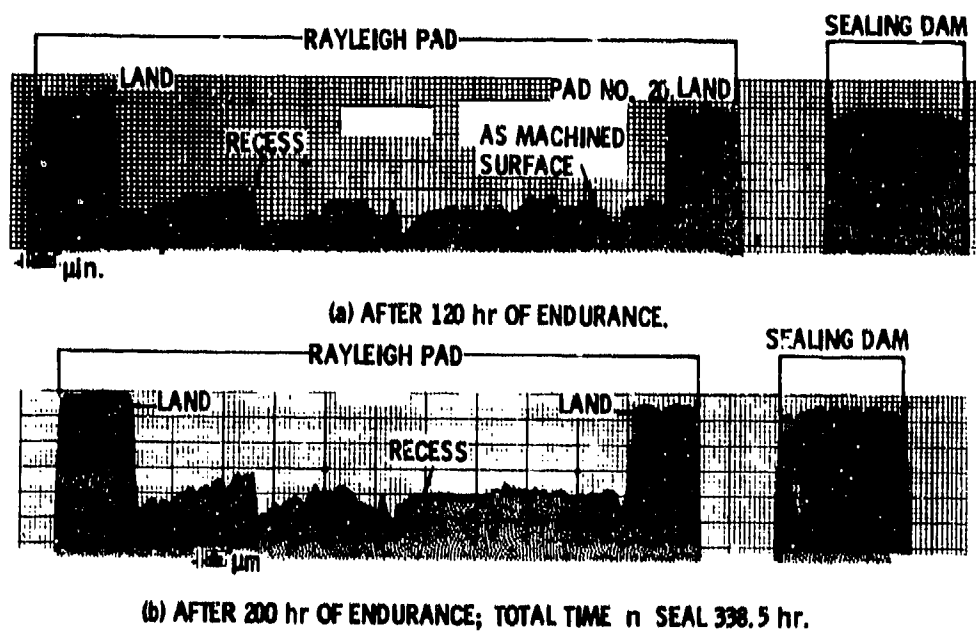
Fig.29   Representative profile trace radially across a Rayleigh pad and primary seal after 200 hours of endurance.
Total time on seal 338.5 hours. (From Ref.15)
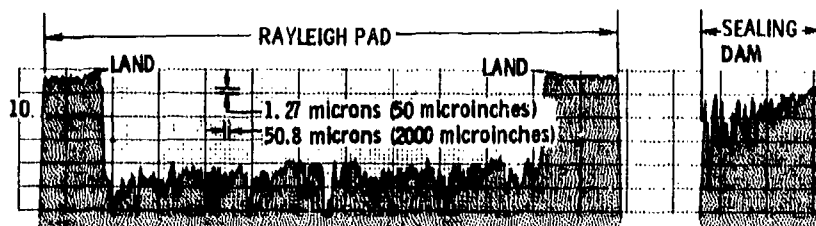
Fig.30 Representative profile trace taken radially across the face of the carbon ring at completion of air entrained dirt test. Total test time, 14.5 hours
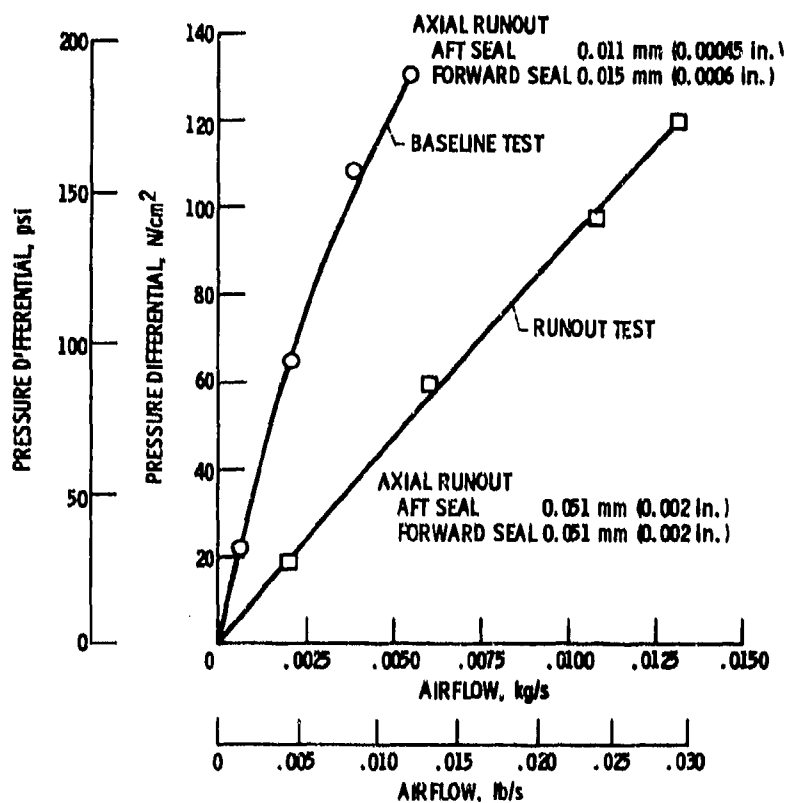
Fig.31 Airflow through two seals as function of pressure differential at 145 m/s (475 ft/s) for seat face axial runout testing (Ref.16)
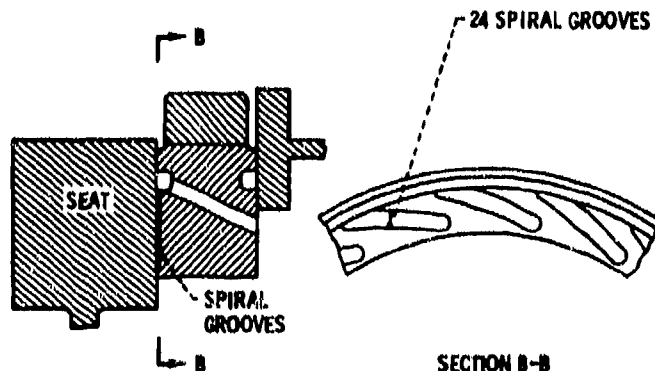
Fig.32 Spiral groove self-acting seal
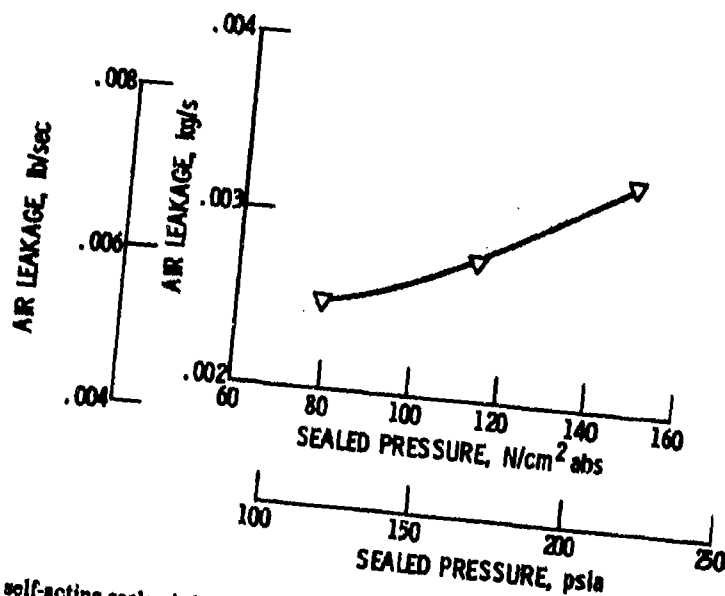
Fig.33   Spiral groove self-acting seal; air leakage versus sealed pressure; sliding speed 182.9 m/s (600 ft/sec); 2 seals
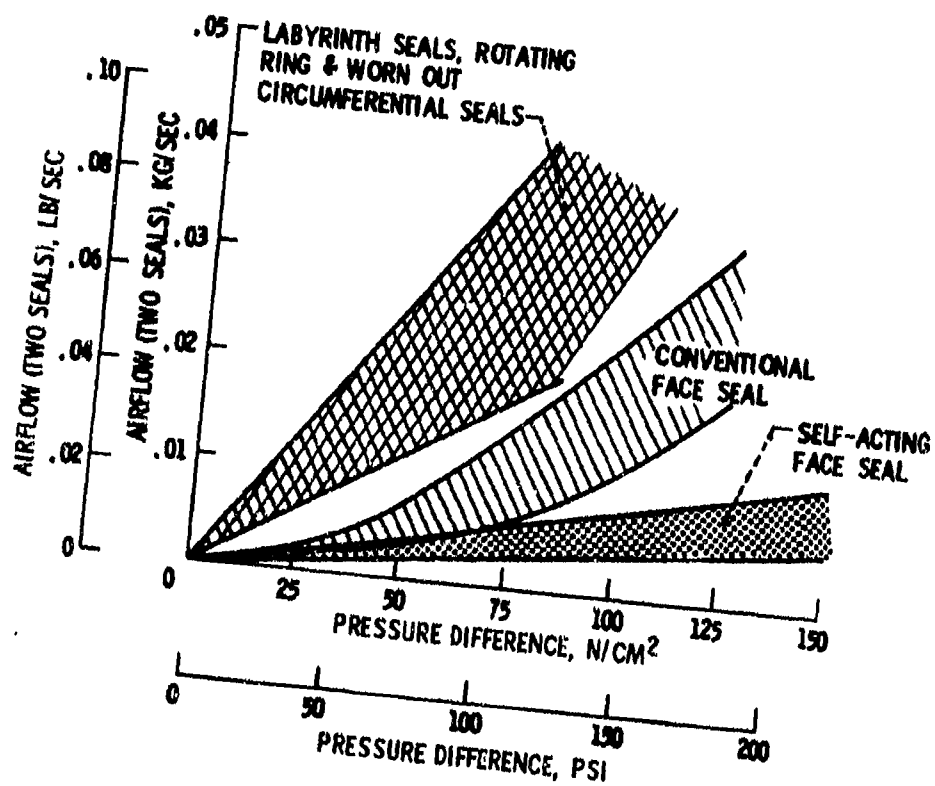
Fig.34   Comparison of seal configurations

DISCUSSION

J.G.Ferguson, UK

Have you had any problems in your secondary seals especially in the case where you have got run-out?

Author's Reply

In answer to the question by J.G.Ferguson on secondary seal problems in the self-acting seal, problems generally start to show up when attempting to seal high pressures (over 275 N/cm^2) and high temperatures (over 677 K). In general, there have been no problems with the secondary seals (carbon material) in the 6.44 cm diameter seal tests. However, secondary seal problems (carbon rings and metal rings) have been noted in the 16.76 cm seal diameter when operating at high pressures and temperatures. Test runs have been made under high levels of runout axial motion in both the 6.44 cm and 16.76 cm seal and no secondary seal problems that were attributable to the axial motion were noted.

B.Wrigley, UK

The paper states that film stiffness at idle is satisfactory but have high altitude conditions at high engine speed been examined?

Author's Reply

At high altitude conditions, no problems in film stiffness are anticipated since the sliding speed is adequate and the pressure is such that the fluid viscosity is also adequate. From a sliding speed standpoint, tests have shown that lift-off occurs at relatively low sliding speeds; also numerous tests which have been run at the relatively low sliding speed of 61 m/sec (200 ft/sec) with both the 16.7 cm and 6.44 cm seals, demonstrated that operation occurred without rubbing contact. From a fluid viscosity standpoint, a significant decrease in the self-acting force will not occur until the pressure reaches very low values (probably less than 3.5 N/cm^{2}a (5 psia)).

D.C.Whitlock, UK

How does the heat generation (particularly heat into the oil system) for the self-acting seal compare with that for conventional carbon face seals operating under similar conditions?

Author's Reply

Your question raises an important point. When the three seal systems, labyrinth, conventional rubbing, and the self-acting seals are analyzed for heat load into the lubrication system, we find that the labyrinth seal adds considerable heat because of the relatively high leakage of hot air into the bearing compartment. On the other hand, the rubbing seal has relatively low leakage, but adds considerable heat into the lubrication system by virtue of the high speed rubbing contact. In contrast, the self-acting seal has both low leakage and low sliding heat generation, and there is a considerable reduction of heat to the lubrication system. This consideration becomes important for those systems (such as some supersonic operation) in which there is competition for the heat sink capacity of the fuel.

J.G.Ferguson, UK

Does this seal you have described cater for gross-axial movement which can sometimes occur?

In other words: due to the thermal differential expansion you encounter an axial shift of the rotor and the seal has to follow this. Have you had problems when this occurred?

Author's Reply

Following the gross-axial movement, either due to differential thermal expansion or surge motion, should present no problem since adequate axial motion length can be designed into the seal, and the stiffness of the self-acting gas bearing is sufficient to prevent rubbing contact. There is some test experience that relates to this question of operation under axial motion and this was obtained when the rig thrust bearing failed in two tests. In both cases, the seals survived the bearing failure and associated axial motion without excessive wear.

G.A.Halls, UK

Both this paper and the one delivered by Professor Dini deal with very similar solutions to almost identical problems. That is self-adjusting seals to control bearing chamber seal leakage. Would both authors comment on the differences and similarities in their approaches to this problem.

Author's Reply

Both papers cover the same self-acting seal concept. However, Dr Dini shows in detail how the seals may be applied to a particular gas turbine engine. I particularly like Dr Dini's application approach since it provides a fail-safe test of the concept. That is, if the self-acting geometry is eroded away by air entrained dirt, then the seal acts as a

conventional rubbing contact seal; and at the pressure and temperature of his application the conventional rubbing seal will not fail catastrophically.

In regard to the potential erosion wear problem, our current approach is to place the self-acting geometry (spiral grooves) into the hard surface rather than in the carbon ring, and this, we feel, will provide improvement in erosion resistance.

SELF ACTIVE PAD SEAL APPLICATION
FOR HIGH PRESSURE ENGINES

by

Dino Dini
Istituto di Macchine, Università di Pisa, Italy

SUMMARY

A more effective and improved engine sealing system is analyzed and discussed for application to an advanced high pressure engine.

Very high leakage results in labyrinth seal applied at high pressure and temperature locations of high-performance engines. A solution to this shortcoming is offered by a self-acting lift pad seal added to the primary sealing surface, enabling a very thin gas film separation of the surfaces during shaft rotation.

Details of construction and design to operate at a clearance less than 1/10th that associated with labyrinth seals are given in the paper. Operation was obtained at a rotating speed of 600 ft/sec and a sealed air temperature of 600 °F.

The maximum speed and pressure capability is at present tested for use in high-pressure engine applications.

INTRODUCTION

The operation of shaft seals in high pressure turbo-engines is not yet fully understood.

A large gas turbine engine can have hundreds of major and minor seals for restricting gas leakage, providing thrust balancing, metering cooling gas flow, and protecting bearings and other mechanical components.

In addition to being used for cooling purposes, air from the compressors is used to seal the bearing housings, so preventing the leakage of oil into the engine main casings or into the compressor inlet. This is achieved by directing the air across the bearing oil seals, the flow being inward towards the bearing or oil supply, thus preventing the escape of any oil. An oil seal reduces the working clearance between the rotating and static members to a minimum value. Oil and air seals may be of various forms.

The air that enters the oil system from the various pressurized oil seal creates a small positive pressure to assist the oil return system. The air is finally separated from the oil by a de-aerator system, which sometimes incorporates a centrifugal breather, from which is vented outboard.

For example, in the two spool gas turbine engine T53 AVCO-Lycoming of figure 1, three compartment seals are located adjacent to the engine main shaft bearings, and are the compressor bearing compartment seal and the turbine compartment seals. The turbine bearing compartment shaft seals present critical problems to minimize high-pressure air leakage into the compartment. This seal is face pressurized by compressor discharge air, used to isolate the bearing compartment from the hot environment.

The internal cooling system provides cooling air to the internal engine components and pressurizes the No. 1 and 2 main bearing seals and the intershaft oil seal. Internal cooling and pressurization air is obtained from five different pressure and temperature supplies: from the fourth stage compressor spacer; from the tip of the centrifugal compressor impeller; from the edge of the combustion chamber deflector; from the area surrounding the gas producer and power turbine assemblies; and from external air through the hollow struts of the exhaust diffuser. Compressed air, bled from the tip of the centrifugal compressor impeller, cools the forward face of the diffuser housing and pressurizes the No. 2 bearing forward seal, continuing rearward through transfer tubes in the bearing housing to pressurize the No. 2 aft oil seal. It also passes through a series of holes in the rear compressor shaft into the space between the rotor assembly and the power shaft. At this point it separates into three separate flow paths, one of which flows forward into an area between the carbon elements of the No. 1 bearing seal and continues on the aft face of the intershaft seal, located forward of the No. 1 bearing. The No. 1 bearing seal is an internally pressurized seal. The radial labyrinths on the forward face of the seal body are designed to work in conjunction with labyrinths on the paddle pump to reduce the flow of oil to the positive contact portion of the seal. The positive contact portion contains carbon elements.

The No. 2 bearing package contains positive contacts of seals and a controlled gap air seal.

As the feed oil is distributed to all the necessary parts of the engine, a substantial amount of sealing air mixes with it and increases its volume. Therefore, to prevent the flooding of the bearing housings, it is necessary to use more than one pump to return or scavenge it to the oil tank. This is achieved by using a pack of pumps, each of which returns the oil from a particular section of the engine. To protect the pump gears, each return pipe is provided with a strainer that, during inspection, can reveal the failure or impending failure of a component.

However, Ref. 2 and 3, main shaft sealing is becoming increasingly critical in advanced gas turbine for hel
icopters. As shaft speeds, air temperatures, and air pressures increase; engine size has decreased, leav-
ing less envelope to accomplish the sealing function. Because of their non-contacting feature, labyrinth
seals offer infinite life; however, at high pressures and temperatures, simple labyrinths will not suffice,
and complicated multistage labyrinths must be used.

Labyrinth seals comprise more stages of rotating knife edges that act as flow restrictors against rigid
stationary surfaces. The gap between the knife edge and the stationary surface must be large enough to
accomodate large dynamic motions, distortions of the shaft, and high leakage in high-performance engines.
Oil is entrained as the leakage vents out of the engine. Venting and pressurization passages are costly
to produce.

In order to overcome these higher airflows, which must be absorbed by the lubrication system, face contact
seals are sometimes used. In this application, a seal ring assembly, with a carbon sealing surface, is
held against a rotating seal seat that is attached to the shaft. The non-rotating seal ring assembly can
move axially to adapt motions of the seal seat. However, the face contact seal is pressure and speed lim-
ited by the high heat generation and subsequent susceptibility to wear or to determine other surface failures
that can result from the rubbing contact.

The self-acting lift pad seal has much greater pressure and speed capability than face contact seals, and
gives lower leakage than either labyrinth and face contact seals. A self acting lift pad geometry, added
to the primary sealing surface, permits positive separation of the sealing surfaces during rotation by a
very thin gas film, in the range of 0.0001 to 0.0005 in. Stability and performance of this self acting
seal are of particular interest at rotative speeds to 50,000 rpm, where high inertia forces are induced on
the high pressure and temperature gas.

SELF-ACTING LIFT PAD SEAL

This type of sealing, figure 2, a finite width pad sealing with side step to limit leakage, offers the sig
nificant advantage of large tolerance to wear, no moving parts and the capacity to be used as both a hy-
drostatic and hydrodynamic sealing. The desired operating gap between rotating and stationary members of
the seal is generated by a properly designed hydrodynamic pattern on the seal ring surfaces. Circumfer-
ential steps and recessed pads (pockets) are typical seal ring patterns used to establish hydrodynamic
face separation, such as shrouded Rayleigh step bearings. During shutdown or period of non-rotation, the
primary seal ring is held in contact with the seat (rotating ring) by compression spring. Thus, positive
sealing is maintained.

Like in a shrouded step thrust bearing, the side steps have the purpose of limiting the side leakage from
the pockets (recessed pad areas), and this shrouding action (lifting force) gives the seal its name. The
pads are arranged on the annular thrust surface with a radial feed groove (drain passage) between each
pad and its neighbors. The recessed pad area is depressed an amount, approximately 0.001 inch deep, be-
low the otherwise uniform lifting surface (side step). As the seal clearance between face may so small as
0.0002 inch (less than 1/10th to 1/100th that relative to labyrinth seals), a significant amount of atten-
tion has been paid to potential thermal and mechanical distortion of these seal systems, Ref. 4. The
sealed pressure p_o is imposed by the gas supply. Ambient sump pressure p_3 surrounds the sealing dam, Seat
rotation is anti-clockwise.

During hydrostatic operation, gas under pressure is supplied to the recessed pad area via the radial feed
groove. During hydrodynamic operation (rotation of the seat), the high pressure gas is dragged into the
pad and compressed as it passes over the step. The resulting lifting action separates the primary seal
ring and the rotating ring. The stiffness of the gas film between faces results in a stable equilibrium
configuration for a properly designed seal at operating conditions.

These mechanical face seals, operating without rubbing contact, have the obvious advantages of longer life
and reliability and lower power requirements. From the other hand, there is a maximum frequency at which
a typical non-contacting face seal may be run in the presence of axial runout. As a result of axial
runout, contact will occur between rotor and stator when the stator is no longer able to dynamically track
the wobble motion of the rotor. This will happen when a rotor angular velocity is reached where the gas
film wedge between stator and rotor is not able to generate the torque required to enable the stator to
track the rotor.

Conventional face contact seals, presently used in gas turbine engines, are generally limited to sealing
pressure less than 200 psi, at sliding velocities below 400 ft/sec, and gas temperature of 200°F.
Surface speeds to 500 ft/sec, differential pressure to 500 psi, and sealed air temperature to 1,300°F,
have been demostrated with self-acting lift pad seals for advanced aircraft engines.

Gas film seal performance and analysis are considered in Ref. 2 to 11, where solution of compressible flu
id flow across shaft face seals with deformation are obtained from an approximate integral analysis, pre-
dicting gas film seal behavior operating at subsonic or choked flow conditions. Laminar or turbulent
flow regimes, entrance losses, fluid inertia effects, sealing face deformation and lip motion, heat trans
fer and subsequent stresses, pressure balancing of gas film, designs and experiments, have been object of
detailed development for application on aircraft advanced gas turbine engines.

Much significant analytical work has been done, as indicated by the References at the end of this paper,
to provide the engineer with rational fundations for the design of gas film bearings. To remove the restric
tions of incompressibility we must derive a more general form of the Reynolds equation, Ref. 12.

DESIGN STUDY FOR MAINSHAFT SEALS APPLICATION

Because of high reliability, low leakage and stable gas interface on the rotating parts (to speeds as high as 20,000 rpm or more), requirements in the design of mainshaft seals; conventional rubbing contact types are abandoned in favor of non-contacting type seals.

Leakage is minimized primarily by the introduction of external forces on the leakage gas; axial forces (self-acting lift force, spring force, and pneumatic forces due to the sealed pressure) in the case of the shrouded step seal, centrifugal forces in the slinger seal, and viscous shear forces in the case of the screw seal.

These kinds of non-contacting seals, and new seal concepts of labyrinth stages, are under test in our laboratory.

The test rig, figure 3, permits simultaneous operation of two seal samples at the sides of a split inner race ball bearing. During normal operation, desired air pressure is maintained into the cavities comprised between the ball bearing and the refrigerant sides of the seals, and the air that leaks is passed into the sump. I.e., a pressure differential is available to derive refrigerant gas into the sump. It is required that the sump pressure be maintained close to the pressure in chamber B during normal operation. Therefore, the seal leakage must be vented from the sump back to the refrigerant loop as shown in figure 3. It is required to pass the vented refrigerant through a fine mesh filter to trap the oil particles. The test rig simulates the effects on the seals with a simple open loop configuration.

The important measurements pertinent to evaluating seals performance are seal leakage rate, which is measured with calibrated flow meters, and seals temperature which is measured with thermocouples embedded in the carbon graphite stators. The ball bearing and each seal face are, respectively, fed and cooled by oil jets. The bearing compartment drains by gravity into a static air-oil separator. To separate air from the oil returning to the oil accumulator, a de-aerating device and a centrifugal breather are incorporated. The return air-oil mixture is fed on the de-aerator where partial separation occurs, the remaining air-oil mist then passes into the centrifugal breather for final separation. The rotating vanes of the breather centrifuge the oil from the mist and the air is vented overboard. A variation in temperature of the cooling air will give some indication of seal distress through a thermocouple system to a temperature gauge. The test rig is suitable for different seal sizes, and supply air temperatures and pressures, to simulate many operating conditions of bearing oil seal internal pressurization in high pressure gas turbine engines. For that, the air supply is derived from a large reservoir, in which air is contained at the pressure desired for each test; the temperature level being established on the delivered flow by a variable heater. In such a way, air may be delivered in the appropriate condition simulating bleeding extraction from a stage compressor spacer.

The gas bearing, like the shrouded step seal in figure 2, is offering a more difficult analytical challenge than the oil bearing in the governing Reynolds partial differential equations. As shown in figure 4, the streamlines are of such a nature that neither the fluid velocity along the z axis nor the first derivative of the velocity along the x axis can be neglected at certain locations. Fortunately, the effect of dropping the velocity terms may be checked approximately by using the two-dimensional model. The theory may be developed for the infinite pad, on the assumption that the inapplicability of film theory in the neighborhood of the step will not result in serious error. Establishing that the pressure within each of the two uniform-thickness film portions must satisfy Laplace's equation, the pressure at the common boundary is determined by flow continuity, according the pressure distribution in figure 4. For that, the step pad pad bearing operating load capacity, for a given minimum film thickness is high, and a seal is introduced between hot gas discharging from one pad and relatively cool gas supplied to the pad directly downstream from it.

To provide acceptable numerical values of sealing performance on which to base the seal design, the pads are assumed to be linearized and to form a continous strip, referring for computation at the mean diameter with corrections to account for curvature and for flows across the corners of the pad. In addition to this approximation; all inertia, entrance and body, effects may be neglected; all flows are considered one-dimensional; the recessed pad pressure is dependent on the length dimension only; and steady-state operation may be applied.

The gas bearing analysis may be carried out starting from the Navier-Stokes equations, applied to a cartesian element of space, the continuity and energy conservation equations, combined with the equation of state for compressible fluid. A simplification is deriving from the fact that the gas viscosity is comparatively insensitive to both pressure and temperature (dry air at atmospheric temperature increases in absolute viscosity of about 12% of its atmospheric pressure value as the pressure is increased to 1,000 psia). If inertia and body forces are considered to have small effects on pressure compared with viscous forces, and additional assumption of an isothermal film eliminates temperature as a dependent variable, absolute viscosity may be treated as constant over space and time. A further simplification permits the problem to be treated with the Reynolds equations, in which the space between the solid surface is so small to consider the flow as laminar.

If we assume an incompressible fluid in place of the perfect gas law, making density constant, the set of equations of the usual theory of hydrodynamic gas films are semplified to solve the problem of the evaluation of the pressure at every point in a lubricant thin laminar film, neglecting inertia and body forces and assuming viscosity to be invariant over space.

In such a way, the solution for film pressure, as a function of x for the infinite (along y direction) pad, is resulting in the pressure distribution of figure 4, where p_{im}, p_a and p_m are, respectively, the

pressure at the inlet, at the outlet and at the step location.
As an adequate approximation for design purposes of oil thrust bearings, we get, Ref. 13

$$p_m - p_a = 0.718 \ (p_{in} - p_a) + (0.413 \ \mu \ u \ B)/h_2^2 \qquad (1)$$

and, for the pad load capacity

$$W = 0.718 \ (p_{in} - p_a) \ B \ L + (0.206 \ \mu \ u \ B^2 \ L)/h_2^2 \qquad (2)$$

where B and L are the pad dimensions along x and y axes, and μ is the absolute viscosity.
Considering the large influence on the real result of side leakage, film thickness, and step height $(h_2 - h_1)$, and the difficulty to take into account all the flow parameters, it is convenient to give an empirical form at the expression (2) to compute the necessary spring load for the high pressure self-acting lift seal ring, with a given number of pads as represented on figure 2. In this sense, the incompressible fluid analysis may be acceptable.

For evaluating the radial flow between two coaxial parallel disks, the seal ring and the seat in figure 2, the quasy fully developed flow model is widely used.
As in Ref. 4, the balance between the pressure and viscous friction force in a control volume, figure 5, is, neglecting entrance effects,

$$A \cdot d_p = - \tau_w \cdot d \ A_w \qquad (3)$$

with A and τ, respectively, the cross-sectional area and the viscous friction force per unit wetted (w) area. And, introducing the hydraulic diameter $D = 4 A/d \ A_w/d \ x$, the mean friction factor $f = \tau_w/\rho \ v^2/2$, and the mass flow $\dot{M} = \rho \cdot v \cdot A$ (being v the radial velocity), Eq. 3 is becoming (with the perfect gas law $p = \rho RT$)

$$p \cdot dp = - \ 2 \ f \ R \ T \dot{M}^2 \cdot dx/D \ A^2 \qquad (4)$$

Integrating Eq. 4, with laminar radial stream, we obtain, Ref. 4, respectively for leakage mass flow, radial pressure distribution, entrance distribution

$$\dot{M} = 2 \ \pi \ h^3 \ (p_1^2 - p_2^2)/24 \ \mu \ R \ T \ \ln R_1/R_2 \qquad (5)$$

$$p = p_1 \ \{1 + |(p_2/p_1)^2 - 1| \ x \ /(R_2 - R_1)\}^{0.5} \qquad (6)$$

$$p_1 = p_0/|1 + (\gamma - 1) \ M_1^2/2 \ C_L^2|^{\gamma/C_\gamma - 1)} \qquad (7)$$

where h, γ, M_1 and C_L, are, respectively, film thickness, constant pressure and volume specific heat ratio, Mach number of the entrance flow conditions, and lift coefficient.
In this simplified analysis, influence of seal face deformations due to the centrifugal force, shaft thermal coning, other kinds of distortions, and turbulent flow are of course not considered. For application purposes, empirical forms of Eqs. 5, 6 and 7 may be used.

As shown on figures 6 to 10, labyrinth seals normally precede the shrouded step thrust sealing, to reduce as possible leakage in between stationary and rotating knives separating different pressure spaces. Lamination occurs, without any surface contact, in the gas going from a space to the other through a long and winding path. A pressure drop for each lamination develops a gas velocity running down in the following free space, which is relatively large in comparison to the gas amount passed through the restricted clearance. To continue its path to the labyrinth outlet, the gas is undergoing another pressure drop for passing through the successive flow restriction. By means of an adequate number of laminations, the overpressure in respect to the receiving ambient, as well as the gas leakage, will be sufficiently reduced. The intent is to produce a pressure in the annular groove which is only slightly greater than that existing on the low pressure side of the seal, maintaining the desired pressure difference with the other seal side.
In order for this concept to work, each labyrinth stage must have several times the gas flow resistance of the internal vent passage. Therefore, the seal is constructed so that the clearance between the rotor and the stator parts is minimized. To achieve this, the inside diameter of the seal stator is constructed from a carbon graphite composition and the seal assembled with zero to 0.002 inch diametral clearance. To retain a low leakage characteristic throughout the life of the machine, it is essential that the sharp

tips of the labyrinth teeth not be worn.
A first approximation numerical solution, for many stages of equal pressure drop $p_n - p_{n+1}$ and restriction cross area labyrinth laminations, give a leakage mass flow

$$\dot{M} = s \ \sqrt{\rho_1 \ (p_1^2 - p_2^2)/p_1 \ n} \qquad (8)$$

where s, n, p_1 and p_2, are, respectively, the restricted cross sectional area, the number of stages, and the pressures on the two sides of the labyrinth seal.
Espression 8 is derived by combination of the restriction velocity $v = \sqrt{2 \ (p_n - p_{n+1})/\rho}$, the average pressure $p = (p_n + p_{n+1})/2$ in a small pressure drop, and the mass flow $\dot{M} = s v \rho$ after n stages with a known total pressure drop $(p_1 - p_2)$.

As shown on figure 9, an oil slinger seal is following the No. 1 bearing of figure 8, in between the under race lubricating ball bearing and the screw labyrinth seal oil return. This type of non-contacting dynamic seal has shown leakage rate comparable to mechanical contact face seals, and demonstrated the possibility of extremely long seal life because of the absence of rubbing parts. The configuration on figure 9 is applied for pressure oil lubricated ball bearing, particularly the ones operating at speeds up to 3 million DN (DN is a speed parameter equal to the bearing bore diameter in millimeters multiplied by the shaft speed in rpm). For example, a 120 - millimeter -bore bearing running at 25,000 rpm would be operating at 3 million DN. Mainshaft bearings on current engines operate at DN value as high as 2.4 million. Jet lubrication, used to cope with the more difficult lubrication and cooling requirements at high speeds, is not effective at speeds above 2 to 2.5 million DN, since the lubricant is centrifugally thrown away from the inner-race-ball contacts, these areas resulting rapidly deteriorated. Introducing the lubricant under the race, figure 9, the centrifugal effects are supplying lubricant directly to the inner-race contact areas; for increased cooling effect, some lubricant may be directed through axial slots under the race. To maintain the desired temperature equilibrium between the inner and outer races, outer-race cooling may also be employed.
With a slinger seal downstream the under race lubricated ball bearing, it is possible to maintain a stable liquid-to-vapor interface on the rotating parts, and thus the only leakage is the evaporative loss from liquid-to-vapor interface. In the configuration at the left of figure 9, relative to bearing No. 1 in figure 8, the axial clearance between the rotating disk and stationary wall of the plane slinger is maintained at the relatively large value of 0.020 to 0.025 inches and the labyrinth screw return at the inner diameter of the stationary wall is relied upon to return any leakage down to the stationary wall to seal interface. A jet lubrication system is utilized both by the plane slinger and housing disk.
Design of the plane slinger with screw return is carried out on Ref. 19, where, with a given slinger diameter, an axial clearance is chosen to allow for differential expansion between the rotor and stator. The turbulent mode of operation with merged boundary layers is depending upon the Reynolds number relative to the chosen lubricant and its temperature. The pressure generating capability of the slinger and the total power loss in the bearing is deduced.
Regarding the labyrinth screw return on figure 9, analysis and test experience are presented on Ref. 20. The purpose of the screw return is to stop the drops of fluid coming from the interface due to instability. As the screw will not normally run flooded, a simple thread form is used.

In figures 6 and 7, representing self active pad seal applications for the bearing No. 1 and No. 2 of figure 1, the seals are face pressurized by high pressure air directly bled from the centrifugal compressor outlet and passed through labyrinth sets of carbon elements.

In figure 9 and 10, a combination of self active pad seal, labyrinth seal, and slinger bearing is shown for the No. 1 and No. 2 bearings on figure 8. The slinger seal in the No. 1 bearing acts as a centrifugal separator, and its main function is to form a stable interface between the vapor and the liquid, and to pump the liquid up to the return line pressure. For the No. 1 bearing, is also shown a solution of the slinger seal, Ref. 21, which not only restricts the leakage from the interface but provides a method for the return of any leakage to the interface. It consists of a hollow slinger, the outer portion of which operates as an ordinary slinger and serves to scavenge the bearing cavity.
As shown in figure 8, 9 and 10, the compressor rotor bears the serrated parts of three labyrinth-type seals: the balance chamber seal, the first stage air seal, which prevents the inlet air from becoming trapped and losing energy between the first stage compressor disk assembly and the front compressor rotor disk assembly; and the tenth stage air seal, which permits compressor air leakage for cooling the gas generator first stage turbine nozzle. The No. 2 bearing transmits both the radial and axial loads imposed by the dynamically balanced rotor assembly, and mounts an oil deflector on each side. Both the forward and rear double labyrinth seals are pressurized by the tenth stage compressor seal leakage air.

Seal design study, however, may be only limited to deriving empirical numerical solutions adequately correcting theoretical results obtainable from approximated and simplified assumptions. It is in fact obviously impossible, as above mentioned, to carry out an analytical solution, taking into account: all the hydrostatic effects, as axisymmetric radial taper due to distortion, surface tension effects, and molecular adhesion; and the most important hydrodynamic effects, as non-Newtonian fluid effects, thermal and pressure wedge effects, surface waviness, viscous shearing of surface waves, vibration, misalignment and eccentricity.

However, the sealing problem has had an appreciable contribute from analytical studies, referring about theoretical results, often obtained with computer programs, and experiments simulating the real operating conditions.

As conclusion of this paper, whose intent concept is the one to discuss practical seal applications suitable for the more and more stringent requirements of high speed gas turbine engines operating with gas at very high temperature and pressure values, some results are presented from our empirical and experimental investigations.

SEALS UNDER TEST

Essentials of the used seal test rig are shown schematically in figure 3, and details of the seals under test shown in figures 6, 7, 9 and 10. Both seals are for compressors, figures 1 and 8, of turboshafts, whose gas generators speed, compression ratio and free turbine maximum power, are in the range, respectively, of 25,000 rpm, 10 to 1 and 1,250 Hp. Sealing air is supplied from the reservoir to the test rig at a temperature of the order of 550°F, through a heater. But, higher temperatures and pressures are obtainable, because of the variable power heater and the changeable pressure level in the storage reservoir.
Running time may be very large, because of the capacity of the 20 cylindrical containers used, 63.5 cubic feet each as volume, in comparison to the low required air mass flow supplying the test rig for compensating the exhaust seal air leakage from the test rig. The containers may be charged with air at the maximum pressure level of 3,000 psia.
To check the practical validity of such test rig, in regard to the high temperature and pressure levels of advanced gas turbine engines, some results have been obtained at peripheral seal rotating speed of 600ft/s with supplying air at temperature higher than 600°F.
Leakage mass flow are resulting quite in agreement with approximated computations.
The seal behavior at very high speed and pressure is at present tested for use in high-pressure engine applications.

Because of the inadequate tecnology of the inexpensive construction of our self active pad seals, it is not possible at present compare the first results obtained to the actual performances of existing sealing systems. From the other hand, advantages in sealing leakage capacity have been evident in comparing labyrinth seals and self acting seals, both realized inexpensively in our laboratory.

Starting, in our experiments, with labyrinth seals, a pitched serrated bushing (stationary) closely encircling a rotating cylindrical piece was realized. Nine serrations were formed by one continuous groove. The diametral clearance between the seal rotor and stator was 0.002 to 0.006 inches, depending upon the tolerance stackup. The seal stator was held in place by two spiral-wound retaining rings and was locked against rotation by a pin. This seal was very reliable and inexpensive. However, it was felt that the leakage rate could be reduced, improving performance of the unit. A reliable low leakage seal was required at no overall increased cost. No commercial seal was found to fit both the technical and economical constraints of the application. A new labyrinth seal concept, with lower leakage characteristic, was therefore under development with the rotor constructed from a carbon steel, heat treated to a Brinell hardeness of 200.
The seal stator was a base carbon grade impregnated with a filler to make it more impervious to air flow. The carbon was shrunk fit into a steel retaining ring in order to minimize thermal differential expression between the rotor and the stator.

Now, our first experience on combined labyrinth and self acting seals is proceeding with the choice of suitable composite material, with adequate thermal expansion coefficient to hold a constant cleatance and a self acting face separation on the range of 0.0005 inches. A successful self acting face seal design requires a detailed accounting of all thermal as well as mechanical distortions with corresponding design features to maintain parallelism between the primary sealing faces.
Our air leakage experienced with the face seal design appear to be abnormally high. The erratic leakages observed suggest either coning of the primary sealing faces, insufficient force balance, or excessive secondary seal leakage.

REFERENCES

1. D.F. Wilcock and E.K. Booser, " Bearing Design and Application", McGraw - Hill Book Co. Inc., 1st Ed., 1967.

2. L.P. Ludwig and P. Lynwander, "Mainshaft Seals for Small Gas Turbine Engines", ASLE Transactions, Volume 19, 1, 33-47.

3. J. Zuk, "Engine Sealing and Lubrication Systems", The Proceedings of a Conference held at Lewis Research Center in Cleveland, Ohio, on May 13 and 14, 1975.

4. J. Zuk, "Analysis of Face Deformation Effects on Gas Film Seal Performance", 27th Annual ASLE Meeting, Houston, Texas, May 1972.

5. D.S. Kupperman, "Dynamic Tracking of Non-contacting Face Seals", ASLE/ASME Lubrication Conference, Montreal, Canada, October 1974.

6. L.P. Ludwig and W.F. Hady, "New Circumferential Seal Design Concept Using Self-Acting Lift Geometries",

NASA TN D-6805, 1972.

7. L.P. Ludwig and R.L. Johnson, "Design Study of Shaft Face Seal with Self-Acting Lift Augmentation. III - Mechanical Components", NASA TN D-6164, 1971.

8. L.P. Ludwig, J. Zuk and R.L. Johnson, "Design Study of Shaft Face Seal with Self-Acting Lift Augmentation. IV - Force Balance", NASA TN D-6568, 1972.

9. J. Zuk, L.P. Ludwig and R.L. Johnson, "Design Study of Shaft Face Seal with Self-Acting Lift Augmentation. I - Self-Acting Pad Geometry", NASA TN D-5744, 1970.

10. J. Zuk, L.P. Ludwig and R.L. Johnson, "Design Study of Shaft Face with Self-Acting Lift Augmentation. II - Sealing Dam", NASA TN D-7008, 1970.

11. L.P. Ludwig and R.L. Johnson, "Sealing Technology for Aircraft Gas Turbine Engines", AIAA Paper 74-1188, Oct. 1974.

12. O. Reynolds, "Papers on Mechanical and Physical Subjects", Vol. 2, The MacMillan Company, New York, 1901.

13. P.R. Trumpler, "Design Film Bearings", The Company, New York, 1966.

14. M.L. Adams and A.A. Raimondi, "A Centrifugal Compressor Seal", ASLE/ASME Lubrication Conference, Boston, Massachusetts, October 5-7, 1976.

15. H.S. Stephens and C. Richardson, "Proceedings of the Sixth International Conference on Fluid Sealing", The British Hydromechanics Research Association, Cranfield, Bedford, England, Munich 1973.

16. R.A. Burton, "Bearing and Seal Design in Nuclear Power Machinery", The American Society of Mechanical Engineer, New York, 1967.

17. R.J. Parker, "Bearings and Gears for Advanced Turbine Engines and Transmissions", Aeronautical Propulsion Conference, Lewis Research Center, Cleveland, Ohio, 1975.

18. D. Dini, "Macchine" Vol. I and II, Editrice Tecnico Scientifica, Pisa, 1976.

19. H.N. Ketola and J.M. McGrew, "Theory of the Partially Wetted Rotating Disk", British Hydromechanics Research Association, Proc. of 3rd International Conference on Fluid Sealing, April 1967.

20. J.M. McGrew and J.D. McHugh, "Analysis and Test of the Screw Seal in Laminar Turbulent Operation", Trans. ASME Journal of Basic Engineering, Series D, Vol. 87, 1965.

21. J.M. McGrew and A.J. Orsino, "Non-Contacting Dynamic Seals for Space Power Alternator", Bearing and Lubrication Unit, Research and Development Center of General Electric Company, Schenectady, New York, 1967.

22. V.P. Povinelli and A.H. McKibbin, "Development of Mainshaft Seals for Advanced Air Breathing Propulsion Systems, Phase II", Pratt & Witney Aircraft, Rep. PWA-3953, June 1970.

23. V.P. Povinelli and A.H. McKibbin, "Development of Mainshaft Seals for Advanced Air Breathing Propulsion Systems, Phase III, Pratt & Witney Aircraft, Rep. PWA-4263, July 1971.

24. H.J. Wilkerson, C.J. Bliem, T.W. Blalock and C.R. Brooks, "Basic Research in Dynamic Sealing, Tennessee University, Knoxville, December 1974.

25. J. Hofman, "Preliminary Investigation of a Magnetic Seal for a Hydrodynamic Bearing", Holldse Signaal apparaten N.V. Hengelo, Netherlands, April 1975.

26. L.P. Ludwig and W.F. Hody, "High Speed, Self-Acting Shaft Seals", NASA Lewis Research Center, Cleveland, Ohio, April 1975.

27. T.N. Strom and L.P. Ludwig, "Development of Circumferential Seal for Helicopter Transmissions: Result of Bench and Flight Test, NASA Lewis Research Center, Cleveland, Ohio, September 1975.

28. W.W. Buchanan and L.E. Wicks, "High Pressure Quasi-Static Seals Configuration", Naval Surface Weapons Center, Dahlgren, Va, September 1975.

29. C.A. Turner, "Result of Helicopter Flight Tests of a Circumferential Carbon Oil Seal", Bell Helicopter Co., Fort Worth, Texas, June 1975.

30. L.T. Shiembob, " Continue Development of Abradable Gas Path Seals", Pratt & Whitney Aircraft, East Hartford, Conn., November 1975.

31. J. Zuk, "Gas-Path Seal Technology", NASA Lewis Research Center, Cleveland, Ohio, 1976.

32. L.E.C. Ruskell, "Metal Seals. Results of a Theoretical and Experimental Study of their Elastohydrodynamic Lubrication", Royal Aircraft Establishment, Farnborough, June 1976.

33. W. Wagner, "Experimental Investigation on Clearance Seals with Radial Outward Flow", British Library Lending Div. Boston S.p.A. England, May 1976.

34. C.M. Taylor, "Thermal Stress Analysis of a Graded Zirconia/metal Gas Path Seal System for Aircraft Gas Turbine Engines", NASA Lewis Research Center, Cleveland, Ohio, April 1977.

35. T.J. Podgorski, "Method of Forming Shrink-Fit Compression Seal", NASA Langley Research Center, Langley Station, Va., April 1977.

36. R.C. Bill and L.P. Ludwig, "Gas Path Seals", NASA Lewis Research Center, Cleveland, Ohio, May 1977.

37. M. Birchak and W.F. Huges, "Simplified Computer Programs for the Analysis of Phase Change in Liquid Face Seals", Final Report, Carnegie-Mellon University, Pittsburgh, May 1977.

38. W.F. Hady and Ludwig, "Shaft Seal Assembly for High Speed and High Pressure Applications", NASA Lewis Research Center, Cleveland, Ohio, July 1977.

39. L.P. Ludwig and H.F Greiner, "Design Considerations in Mechanical Face Seals for Improved Performance. II: Lubrication", ASME Meeting, Atlanta, 1977.

DISCUSSION

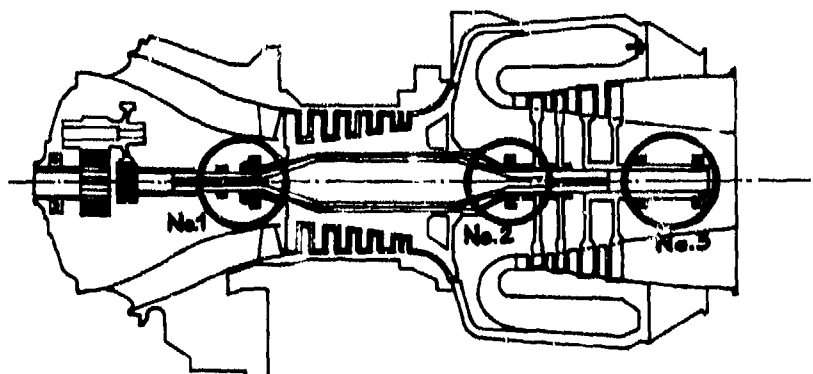Refer to the last question of the Discussion following Paper 16.
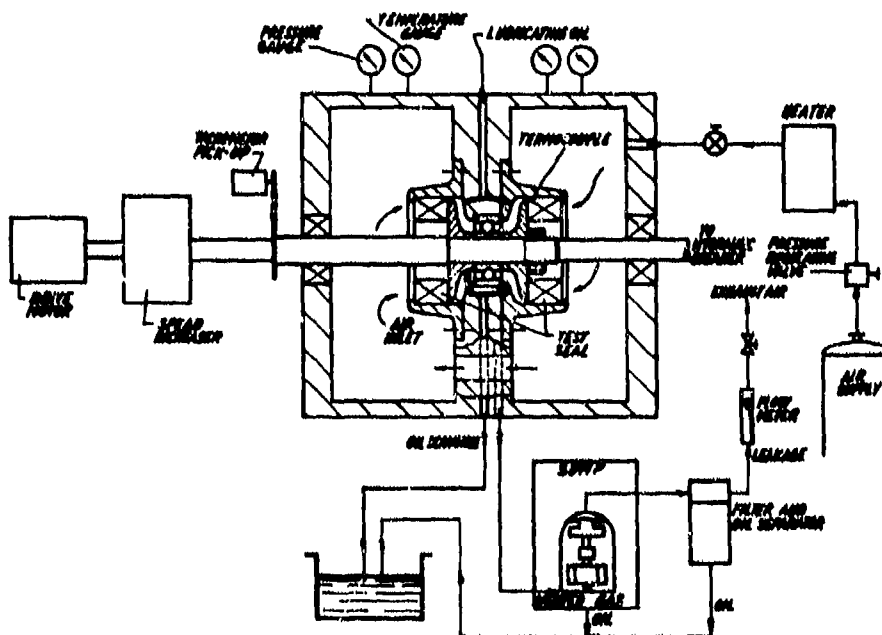

Fig. 1 - Two-spool gas turbine engine

Fig. 3 - Schematic of seal test rig.

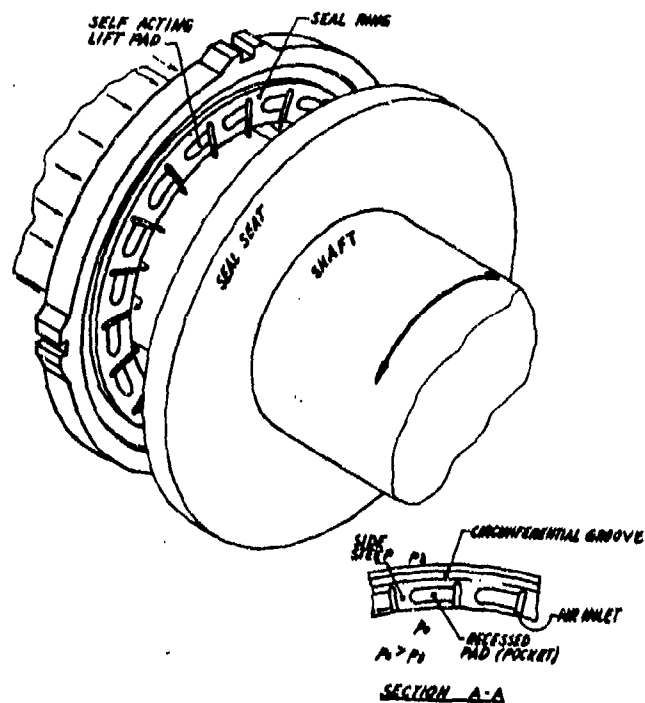Fig. 2 - Self-acting lift pad seal.

SECTION A-A
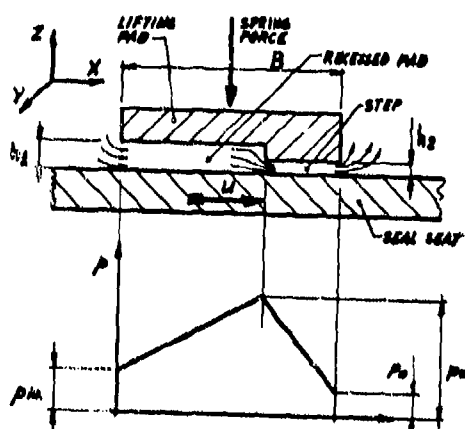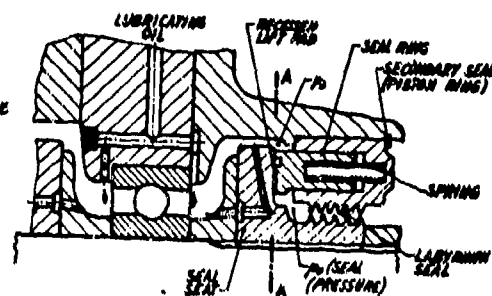
Fig. 4 - Schematic of shrouded step seal, and peripheral pressure distribution.
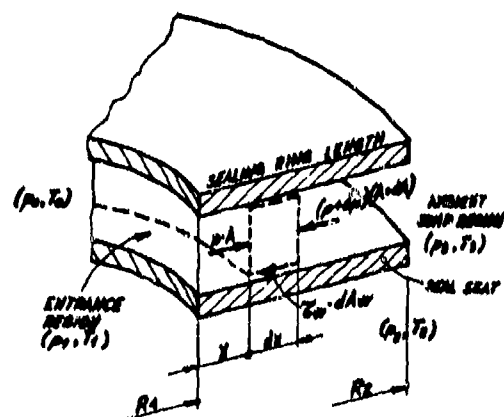
Fig. 5 - Model of ideal radial flow with area change.

Fig. 8 - Compressor for two-spool helicopter turboshaft.
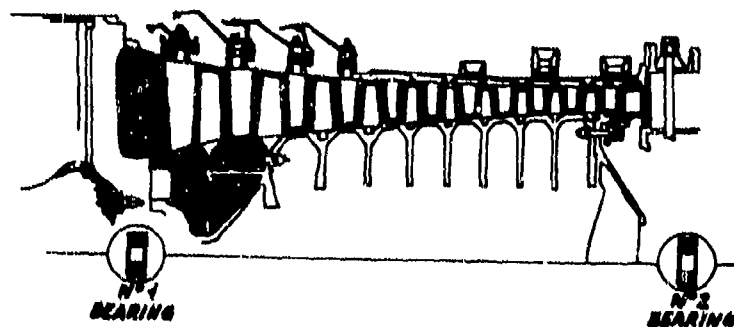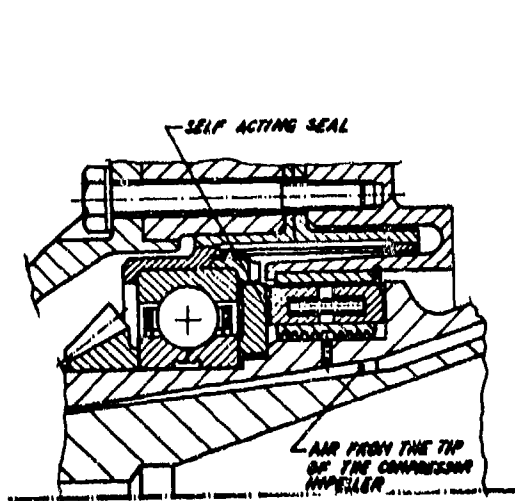
Fig. 6 - Possible oil seal pressurization with air, by a combination of labyrinths and self acting lift seal, of No.1 bearing in figure 1.
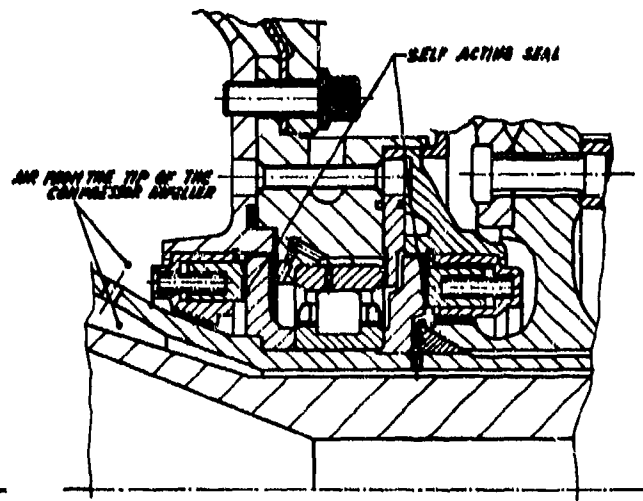
Fig. 7 - Possible oil seal pressurization with air of No. 2 bearing in figure 1.
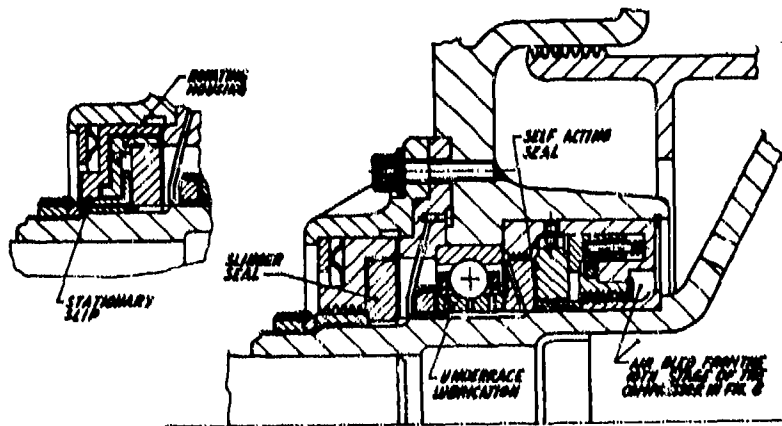
Fig. 9 - Possible oil seal pressurization with air of No. 1 bearing in figure 8.
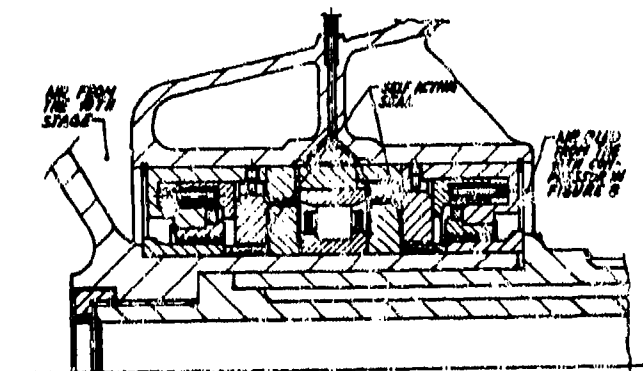
Fig. 10 - Possible oil seal pressurization with air of No. 2 bearing in figure 8.

GAS TURBINE DISC SEALING SYSTEM DESIGN

D A CAMPBELL
Technical Design Group (PTr)
Rolls-Royce Limited
PO Box 31
Derby DE2 8BJ, U K

SUMMARY

This Paper reviews the design of Gas Turbine Disc Sealing and Cooling Air Systems.

The turbine sealing system must seal the disc spaces against ingress of hot turbine gases, and absorb windage and conducted heat with limited air temperature rises. Air leakage in the system must be controlled to minimise engine performance losses, to avoid loss of blade cooling effectiveness and to maintain the integrity of associated shaft and bearing cooling systems.

The effect of the required bleed flow on engine performance is considered and found to be fairly small provided that an accurate assessment of this offtake is made at the beginning of the design process. Subsequent increases of the air bleed during the development phase can bring substantial penalties in turbine entry temperature.

The various factors to be considered when determining the sealing and cooling flows are briefly reviewed and the areas where further research would be useful are indicated.

1.0 INTRODUCTION

1.1 Secondary Flow Systems

The secondary flow system of a gas turbine engine has four main features.

a) Turbine Aerofoil and Working Annulus Wall Cooling.

This includes blades, nozzle guide vanes, rotating and static blade shrouds and nozzle guide vane platforms.

b) Disc Sealing and Cooling Systems.

These systems protect turbine discs and blade roots from excessive temperatures and are used to control the rotor thrust bearing end loading.

c) Bearing Sealing Systems.

These systems interact with the disc sealing systems to maintain a satisfactory environment for the engine bearing chambers.

d) Parasitic Leakage.

This is unwanted leakage between parts without relative motion such as blade and nozzle guide vane platform gaps, shroud segment gaps etc.

1.2 Disc Sealing and Cooling Systems - General Considerations

The purpose of this paper is to discuss the problems of Disc Sealing and Cooling Systems and the design solutions to these problems. Such systems depend very much on the good performance and reliability of labyrinth-type seals.

1.3 System Objectives

Disc air systems have four main functions.

a) Minimising unwanted leakage between rotating and static parts.

b) Protection from the hot gases in the working annulus. Items to be

protected are :

> Blade cooling air supply
> Blade fixings
> Disc Rims
> Disc Bores

c) Protection of blade cooling systems from leakage. This is particularly important for systems using a pre-swirled cooling air supply.

d) Balancing of rotor end loading to obtain satisfactory thrust bearing loads.

e) Interface with the bearing sealing systems.

2.0 QUANTITY OF AIR USED - EFFECTS ON ENGINE PERFORMANCE

By using large quantities of air bled from the engine compressor the above objectives could be met fairly easily. However, increase air bleed causes corresponding increases in turbine entry temperature (TET) and specific fuel consumption (sfc), and so we must reduce the bleed to the minimum required to obtain satisfactory design conditions for the engine parts affected. When designing such systems it is important to know the effects of air bleeds in detail, using data from engine cycle performance calculation.

Figs. 2.1 to 2.4 show the effects of disc sealing and cooling air bleeds on engine performance. For a typical transport engine cycle the performance was calculated at a constant cruise thrust per unit intake flow giving a by-pass ratio of about 4.5. The TET, jet velocity ratio and component efficiencies were kept constant at the cruise design point for the range of assumed bleed. The assumed disc flows were distributed through the turbine stages in typical proportions. Two types of system have been considered :

a) All bleed from HP compressor delivery.

b) Bleeds taken from four different compressor stages to minimise cycle losses caused by secondary flow throttling.

In the RB 211 Engine, for example, bleeds for disc air systems are taken from

> IP compressor 4th stage   5th stage overall
> IP compressor delivery   8th stage overall
> HP compressor 3rd stage   11th stage overall
> HP compressor delivery   14th stage overall

Fig. 2.1 shows the effect of these bleeds on sfc.

The beneficial effect of multistage bleed is clear. The normal range of total disc air bleed is 2 to 4% and at 3% an sfc penalty of 2.1% for a single HP compressor delivery bleed point system is reduced to 0.9% for a system with four bleed stages.

Fig. 2.2 shows the effect on take-off TET. This is quite small, as with increasing bleed level the core engine size was increased to obtain constant cruise TET. This effect on core engine size is shown in Fig. 2.3.

There is a further advantage of multistage bleed in that bleed air from lower stages is cooler; this allows either smaller flows or lighter, more economical turbine disc designs. The bleed stage must be chosen so that there is a minimum but adequate pressure drop between the bleed point and the highest pressure in the turbine to which the bleed must flow. The design conditions for the air system must be chosen carefully to avoid unforeseen deficiencies at some flight conditions.

Fig. 2.4 shows similar data for a military reheated turbofan engine with a by-pass ratio less than 1. TET and dry thrust per unit intake flow were kept constant by reducing the by-pass ratio and fan pressure ratio as the bleed was increased. In this case the bleed was all from HP delivery and the effect on sfc is somewhat less than that for the transport engine.

Figs. 2.1 to 2.4 assume constant turbine efficiency.

In fact turbine efficiencies are reduced by sealing flows entering the annulus

immediately in front of the rotor. With care in design of the Blade and Nozzle platforms this loss can be kept to less than 0.3% of efficiency for a sealing flow of 1% of the turbine flow. The sealing flow is, however, not included in the turbine flow for performance calculation purposes.

When the core size of a projected engine is fixed the effect of bleed on TET increases, as any deterioration of core engine performance cannot be compensated by an increase in size. For the transport engine the effects on sfc are about the same as before, but the effect on TET is now about 10^6K per 1% of bleed. This emphasises the importance of making realistic rather than hopeful initial estimates of sealing air requirements and the necessity of ensuring that these flows are not exceeded in the production engine.

3.0 FACTORS DETERMINING QUANTITY OF AIR REQUIRED FOR DISC SEALING

3.1 Flow required to prevent hot annulus gas ingestion at the blade-nozzle gap. This is determined by

  a) Circumferential variation of static pressure.

  b) Radial flow produced by the pumping action of friction between the air and the disc face.

3.2 Flow required to absorb windage heat with a suitably limited temperature rise.

3.3 Flow required to supply the relevant labyrinth seal.

4.0 DESIGN CONSIDERATIONS FOR GAS INGESTION

4.1 Circumferential Static Pressure Variation

  a) The Problem

  It is clear that appreciable static pressure variation around the annulus exists. This has been long apparent from turbine blade vibration problems associated with variations of pressure upstream of a nozzle guide vane row. There are also fluctuations of pressure caused by variations of Blade and Nozzle throat area and by flow curvature effects near blade and nozzle trailing edges. Where the static pressure drop across the annulus seal is less than the range of pressure variation at the seal exit, some ingestion of turbine gas is to be expected.

  The objective of the designer must be to minimise the flow required to prevent gas ingestion with a given static pressure variation. Fig. 4.1 shows a typical turbine nozzle-rotor gap. What features are desirable?

  b) Reduction of Pressure Variation

  Clearly large values of 1_r and 1_n will reduce the static pressure variation at the sealing air exit and are therefore desirable. Circumferential variations of Nozzle and Blade throat area should also be minimised.

  c) Design of the Clearance at the Annulus

  A small clearance c will reduce the flow required for a given pressure drop across the gap. The overlap h and the shingle height s tend to reduce the flow of annulus gas caused by a local increase of the annulus static pressure However, these features also tend to increase the discharge of sealing air for a given pressure drop, thus reducing the pressure drop available from a given sealing flow. The overlap and a slight shingle allow the sealing air to enter the turbine with minimal disturbance to its efficiency; this arrangement is therefore preferred.

  d) Two Stage Sealing

  It is difficult to have a sufficiently small clearance c, owing to manufacturing limitations. In any case, a small clearance would be subject to relatively large variations due to manufacturing tolerances, working deflections and thermal expansions, and in some cases this would cause difficulties

with rotor thrust balance. It is therefore often desirable to design the
blade root region for a temperature allowing for some turbine gas ingestion
and to incorporate an additional seal as shown in Fig. 4.1. The Space A
allows equalisation of the static pressure and eliminates the possibility
of inwards flow through the inner seal. Thus the disc rim is completely
protected from annulus gas by a very small sealing flow through the inner
seal.

e) Data

This is an area where few data are available and research is therefore
desirable.

4.2 Disc Pumping

a) Theory and Test Data

The frictional drag of the disc on the air in the disc space generates an
outwards flow near the disc. If this flow is allowed unobstructed access
to the working annulus as in Fig. 4.2 then a sealing flow of about the same
level must be supplied to avoid the ingestion of annulus gas. The approxi-
mate magnitude of these flows can be determined. The conventional non-
dimensional functions used are

$$C_w = \frac{w}{\mu r} \qquad \text{Flow Coefficient} \quad \cdots \quad \cdots \quad (4.1)$$

$$Re = \frac{\rho \omega r^2}{\mu} \qquad \text{Reynolds Number} \quad \cdots \quad \cdots \quad (4.2)$$

Using Von Kàrmàns 1/7 power law analysis we have

$$C_w = 0.22 \, Re^{0.8} \qquad \qquad \cdots \quad \cdots \quad (4.3)$$

This applies to a free disc without any influence from static parts.

The case of a disc with shrouded stator as in Fig. 4.2 has been investiga-
ted by Bayley and Owen (Ref.1) who propose the correlation

$$C_w = 0.61 \, Re \, g/r \qquad \qquad \cdots \quad \cdots \quad (4.4)$$

Here, the flow is that just sufficient to prevent ingestion of fluid from
the outer space. The experimental data used cover the ranges

$$Re \quad \text{up to } 4.10^6$$

$$g/r \quad \text{from 0.0033 to approximately 0.06}$$

b) Application

The most important gas turbine sealing situations involve Reynolds numbers
around 10^7 which are beyond Owen's experimental data. There are two further
considerations which make it difficult to accept Owen's flow criterion in
gas turbines.

i) High Axial velocity of the annulus flow.

This makes it much more difficult for external fluid to penetrate the
disc space.

ii) Projections on the rotor.

These are assumed to deflect the pumped flow from the direct path to
the annulus and thus reduce the gas ingestion caused by the pumping
effect.

Further experimental work is therefore needed to clarify the situation
with more realistic conditions.

c) Design Features

The effects of disc pumping will be reduced by the sealing arrangement shown in Fig. 4.1. The use of swirl nozzles to introduce the sealing air tends to suppress the pumping action and also to reduce windage and is therefore beneficial.

4.3 Windage

a) Discs

The frictional heating of sealing air by the adjacent rotor is an important factor in system design. Enough air flow must be provided to limit the temperature rise due to this effect to an acceptable value. For normal clearances between the disc and the adjacent static parts the windage drag is not more than the value for a free disc rotating in a large space, and data for this case may be used for design purposes.

Projections such as nuts and bolt heads greatly increase the windage heating and should be avoided or covered by a fairing unless the tangential speed is relatively small.

Windage can be appreciably reduced by admitting the sealing air through pre-swirl nozzles.

In estimating windage we use a moment coefficient defined by

$$C_m = \frac{M}{\frac{1}{2}\rho\omega^2 r^5} \qquad \qquad \text{.. .. (4.5)}$$

This can be correlated with Reynolds number by the equation

$$C_m = 0.982 \, (\log_{10}\text{Re})^{-2.58} \qquad \qquad \text{.. .. (4.6)}$$

This is taken from Ref.2 and agrees with test data for Reynolds numbers up to 7×10^6. Engine Reynolds numbers run up to about 3×10^7 so some extrapolation is required.

b) Shafts

For cylindrical rotor parts a correlation from Ref.3 can be used :

Define a friction coefficient $C_f = \tau/\frac{1}{2}\rho r^2 \omega^2$ .. (4.7)

External surface windage drag is given by

$$\frac{1}{C_f} = 4.07 \, \log_{10} \, (\text{Re}\sqrt{C_f}) - 0.6 \qquad \qquad \text{.. .. (4.8)}$$

$$C_m = C_f \cdot 2\pi l/r \qquad \qquad \text{.. .. (4.9)}$$

c) Pre-Swirled Cooling Air

Some test data for the effects of pre-swirl are available from Ref.4 but have not been entirely successfully correlated. Fig. 4.3 shows test data for a disc and shaft plotted as E_m/E_c vs. V_s/U. The data used have been published in Ref. 4.

E_m is the measured windage power

E_c is the windage power calculated from equations 4.6 and 4.8

V_s is the swirl nozzle exit tangential velocity

U is the disc tangential speed at the swirl nozzle radius.

d) Conclusion

Design calculations using these data are generally satisfactory. However,

further research into the effects of cooling throughflow, cooling air pre-swirl and discrete projections in the rotor would allow significant improvement.

4.4 Seal Leakage

a) Effect of Seal Leak

Each disc space has one or more flows controlled by labyrinth seals, and unless the seals are of very small diameter, they have a very important effect on the system design.

A seal may either supply flow or take flow out of the disc space. In Fig. 4.4 for example the seal A is removing flow from space 1 and supplying it to space 2.

The pressures in spaces 1 and 2 are determined primarily by the nozzle guide vane inlet and outlet pressures, since the pressure drops at the annulus seals are relatively small.

Seals B and C are removing some of this flow from space 2 and leaking it into the turbine bearing chamber sealing system which is part of a lower pressure system which also supplies sealing air to the back of the second turbine. Sealing air is supplied to the space 1 through slots at C.

b) Seal Failure

Any increase of clearance of seal A, increasing the flow through it, will reduce the flow available for sealing at the annulus. Deterioration of such a seal can therefore lead to overheating due to gas ingestion. The leakage flow itself will then be hotter than normal and the overheating problem will spread to other parts of the system; this effect is particularly likely to be troublesome in systems where there is maximum utilisation of seal leakage air for sealing subsequent turbine stages. It is a requirement of the British Civil Aviation Authority that the system should withstand a degree of seal failure. This requirement is normally met by supplying sufficient flow to feed a failed seal with zero annulus sealing flow. The failed seal is usually taken to have about twice the normal running clearance.

This criterion establishes the basic design flow requirement.

Additional flow is then provided if the basic flow is insufficient to deal with windage and annulus gas ingestion.

Note that with the type of system shown in Fig. 4.4 the bleed flow for sealing is controlled by fixed metering orifices (eg slots X) and seal deterioration in service will not increase the total bleed. The associated engine performance deterioration is therefore restricted to the effect of changes in the turbine stages to which the same total bleeds are exhausted. Both orifice controlled and seal controlled types of system suffer from increased disc space temperatures if the seals deteriorate. This can lead to reduced turbine disc life and the possibility of failure hazard.

c) Seal Design

It should be noted that the seal design objective here is not always minimum flow, since the leakage is often required for sealing subsequent stages. However, reliability of flow control is always extremely important and the highest possible standard of thermal and mechanical design is required. This will only be achieved if the seal rotor and stator design is considered as a single problem.

d) Seal Leakage Data

The correlation of seal leakage data is difficult and complex. Many experimental data are available but not all have been adequately correlated. Detailed consideration of this problem is, however, beyond the scope of this paper.

More comprehensive correlations of existing data would be useful, particularly for seals with textured liners and for stepped seals.

Inaccuracies in the estimation of running clearance are often greater than data correlation errors. Greater technical effort is required here, particularly in the prediction of transient thermal behaviour of static seal assemblies.

5.0 BLADE COOLING AIR SUPPLY SEALING

The objective is to pass pre-swirled cooling air to the blade with the minimum addition of leakage air. Leakage air mixing with the pre-swirled air adds windage heat and reduces the cooling air whirl velocity. Both effects increase the cooling air temperature relative to the rotor and it is desirable to avoid them.

Leakage that would otherwise mix with the pre-swirled cooling air can be diverted through a by-pass passage as shown in Fig. 5.1. Three problems must be overcome when using this method.

1) Pressure Drop

Sufficient pressure drop must be made available both to drive the leak flow through the passage and to overcome the vortex pressure rise between the inner and outer radii of the swirl chamber. This tends to give an increase of leakage flow.

2) Space

It is often difficult to find space for these passages in the region of the heavily loaded HP turbine nozzle location features.

3) Increased Flow Requirement

As the leakage flow no longer enters the turbine blade, additional flow is required, causing a performance penalty. It is therefore important to find a use for this air and thus avoid losses. The following methods may be used.

a) Split Feed Turbine Blade.

This type of blade uses cooling air at two pressure levels, the lower pressure air being supplied from leakage.

b) The leakage air can be bled away for use in disc sealing systems.

c) The leakage air can be used for turbine nozzle guide vane platform and trailing edge cooling.

Disc pumping can also reduce pre-swirl system performance, and it is therefore good practice to have a seal at the inner boundary of the swirl chamber to prevent the pumped flow circulating into it. See Fig. 5.2.

6.0 ROTOR THRUST BALANCE

Turbine and Compressor end loads combine to give a net rotor thrust much less than the individual component loads. The residual thrust can however be large enough to give thrust bearing problems. This particularly applies to HP thrust bearings in multi-shaft high by-pass ratio engines, which have a very high centrifugal loading on the bearing balls, giving a reduced thrust capacity.

It is therefore necessary to adjust the end loads by altering seal radii, and this will usually give increased leakage flows. Larger capacity thrust bearings can therefore give engine performance improvements.

Rotor thrust balance should be investigated as early as possible in the engine design process so that this factor can be considered when deciding the compressor and turbine design parameters.

7.0 CONCLUSIONS

Research and Development in Gas Turbine Sealing is mostly directed towards reduction

of Leakage Flows.   In the design of Turbine Disc Sealing and Cooling systems, obtaining the lowest possible design leakage flow through individual seals is, however, not always the most important objective.

In the high pressure turbine stages, annulus static pressure variation and disc windage often determine the required disc sealing and cooling flows.   At the initial design stage the disc sealing and cooling air bleeds have a relatively small effect on engine performance.   If we reduce a transport engine's disc sealing air require- ment from a typical 3% of core engine flow to half this amount the sfc saving is about ½% (See Fig. 2.1).   The effects on TET can be virtually eliminated by choice of by-pass ratio.

However, once the engine cycle parameters are fixed, the effect on TET of bleed changes is quite large.   To increase that 3% bleed by 50% would cost a TET increase of around $15^{\circ}K$, reducing the HP turbine blade creep life by roughly 30%.

This indicates the importance of making realistic and accurate estimates of disc sealing and cooling air requirements at the earliest stage of design.   These flow levels must be carefully monitored and adhered to during the engine development process.   In-service deterioration of seals can contribute to worsening of engine TET and sfc, and may cause increased turbine disc rim temperatures.   This empha- sises the importance of seal durability and long term reliability as well as design performance.

8.0   NOMENCLATURE

c	Radial Clearance (see Fig. 4.1)
C_f	Friction Coefficient : $C_f = \tau/(\tfrac{1}{2}\rho\omega^2 r^2)$ for a Rotating Cylinder
C_m	Moment Coefficient : $C_m = M/\tfrac{1}{2}\rho\omega^2 r^5)$ for a Rotor
C_w	Flow Coefficient : $C_w = w/\mu r$
E_m	Measured Windage Power
E_c	Calculated Windage Power
g	Axial Gap (see Fig. 4.2)
h	Turbine Platform Axial Overlap (see Fig. 4.1)
l	Length of Rotating Cylinder
l_n) l_r)	See Fig. 4.1
M	Windage Drag Moment from both sides of a Disc or the outer surface of a Cylinder
m_{CE}	Core Engine Flow at Cruise
r	Outer Radius of a Disc or Cylinder
Re	Reynolds Number : $Re = \rho\omega r^2/\mu$
S	Turbine Shingle Height (see Fig. 4.1)
sfc	Specific fuel consumption
TET	Turbine Entry Temperature
U	Disc tangential velocity at the pre-swirl nozzle radius
V_s	Pre-swirl Nozzle Exit Tangential Velocity
w	Air Mass flow
μ	Dynamic Viscosity
ρ	Density
τ	Surface Shear Stress
ω	Angular velocity

9.0 REFERENCES

1) Bayley and Owen.   The Fluid Dynamics of a Shrouded Disc System with Radial
    Outflow of Coolant.   ASME 70-GT-6.   Journal of Engineering for Power.

2) L A Dorfman.   Hydrodynamic Resistance and the Heat Loss of Rotating Solids.
    Book Translated from Russian, Published by Oliver and Boyd London.

3) Theodorsen and Regier.   Experiments on Drag of Rotating Discs, Cylinders and
    Streamline Rods at High Speeds.   NACA TR 793 1944.

4) A Moore.   Gas Turbine Internal Air Systems: A Review of the Requirements and
    the Problems.

    ASME 75-WA/GT-1.

10.0 ACKNOWLEDGEMENTS

TRANSPORT ENGINE: EFFECTS OF DISC SEALING FLOW ON S.F.C. AT CRUISE

MOTEUR DE TRANSPORT:EFFETS DU DEBIT D'AIR D'ÉTANCHÉITÉ DU DISQUE SUR CONSOMMATION SPECIFIQUE EN CROISIÈRE

Figure 2.1

TRANSPORT ENGINE: EFFECTS OF DISC SEALING FLOW ON T.E.T. AT TAKE-OFF

(CONSTANT CRUISE T.E.T.)

MOTEUR DE TRANSPORT:EFFETS DU DÉBIT D'AIR D'ÉTANCHÉITÉ DU DISQUE SUR TEMPERATURE D'ENTRÉE TURBINE AU DÉCOLLAGE(T.E.T. CONSTANT EN CROISIÈRE)
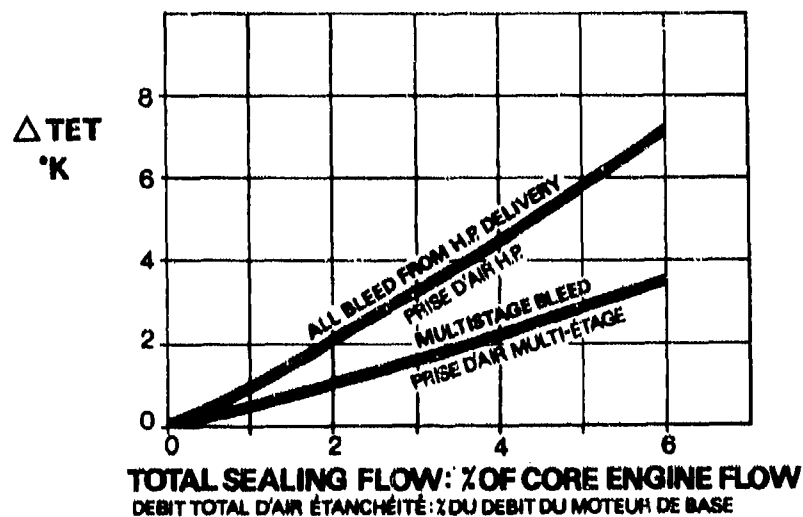
Figure 2.2

TRANSPORT ENGINE: EFFECTS OF DISC SEALING FLOW ON CORE ENGINE FLOW M_{CE}
MOTEUR DE TRANSPORT:EFFETS DU DÉBIT D'AIR D'ÉTANCHÉITÉ DU DISQUE SUR LE DÉBIT DU MOTEUR DE BASE
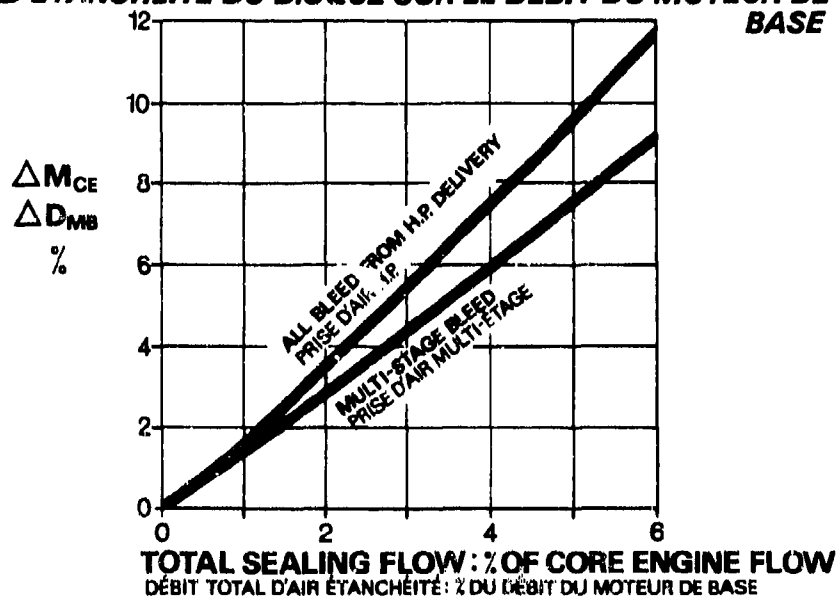
Figure 2.3

MILITARY REHEATED TURBOFAN ENGINE EFFECT OF DISC SEALING FLOW ON S.F.C. AT S.L.S. ALL H.P. BLEED
TURBOSOUFFLANTE MILITAIRE AVEC POST COMBUSTION EFFETS DU DEBIT D'AIR D'ÉTANCHÉITÉ DU DISQUE SUR CONSOMMATION SPECIFIQUE S.L.S. PRISE D'AIR H.P.
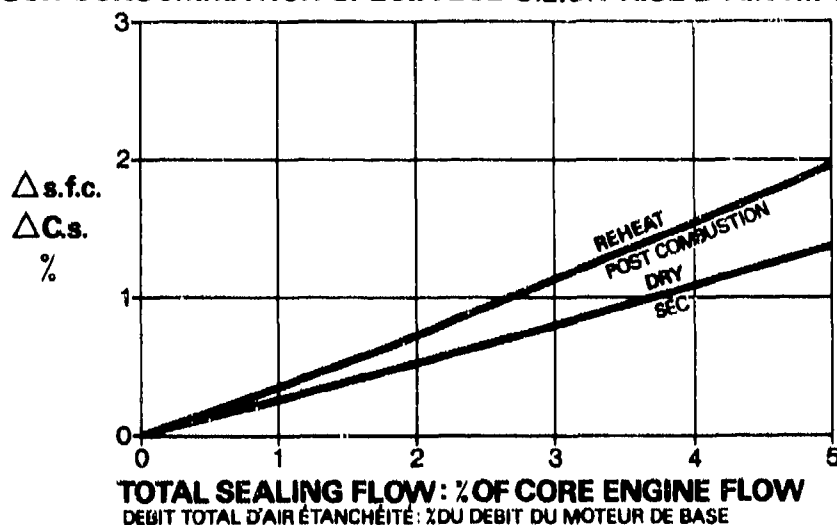
Figure 2.4

TURBINE NOZZLE—ROTOR GAP
JEU ENTRE TUYÈRE ET ROTOR DE TURBINE
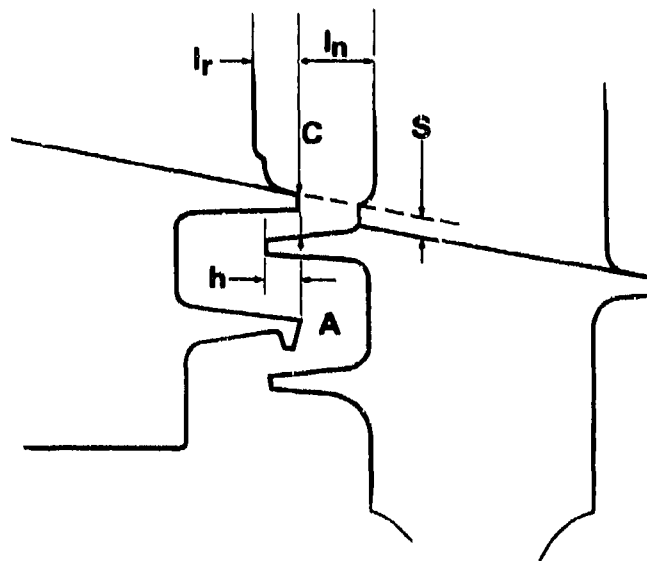
Figure 4.1

DISC PUMPING: RESEARCH MODEL
POMPAGE DU DISQUE: MAQUETTE DE RECHERCHE
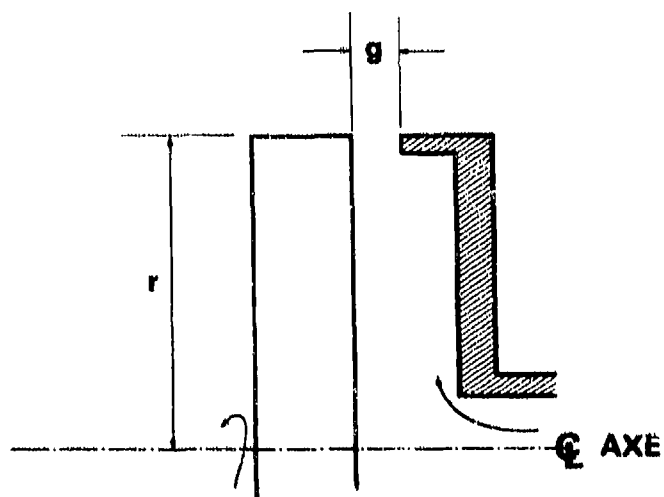
Figure 4.2

DISC AND SHAFT WINDAGE: EFFECT OF PRE-SWIRLED COOLING AIR

PERTES DE POMPAGE DU DISQUE AVEC ARBRE: EFFET DE L'AIR DE REFROIDISSEMENT PRÉ-TOURBILLONNÉ

$$\frac{Ec}{Em}$$

$$\frac{Vs}{U}$$
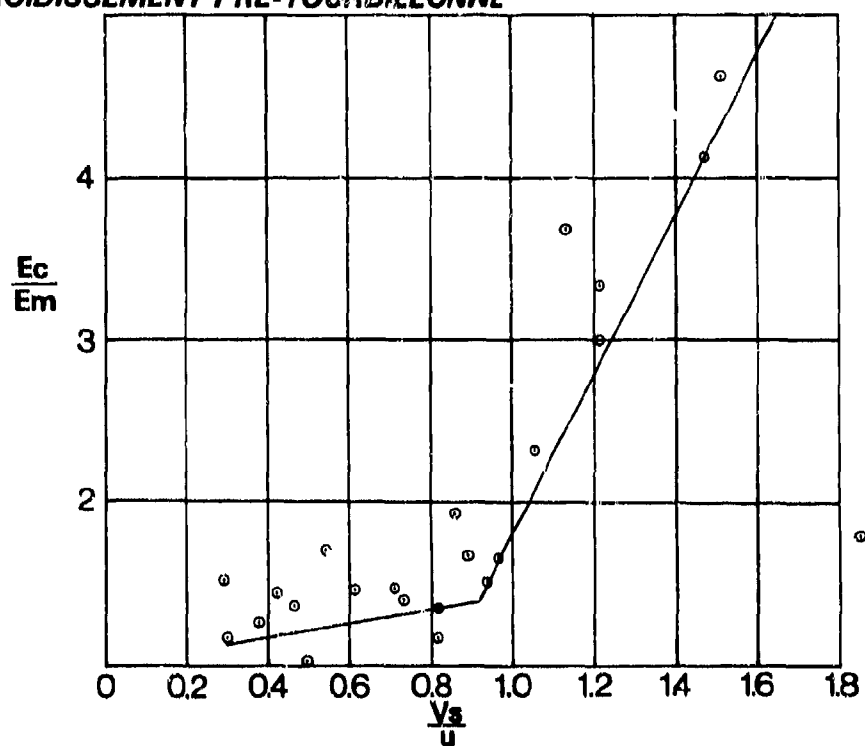
Figure 4.3

SEAL
LEAKAGE
EFFECTS

*EFFETS DE FUITE
AU NIVEAU
DU JOINT*
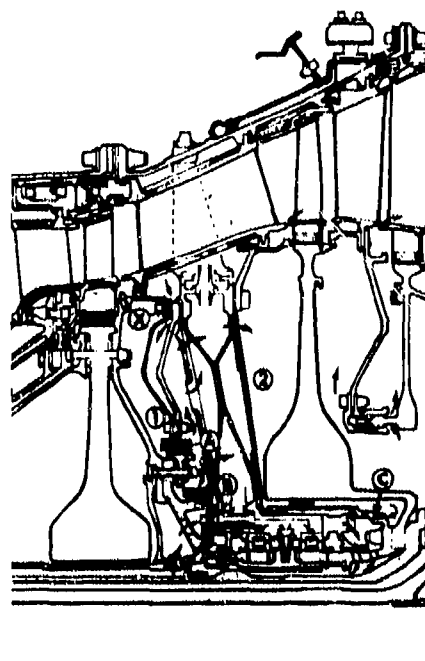
Figure 4.4

PRE-SWIRLED TURBINE BLADE COOLING AIR BY-PASS
BY-PASS DE L'AIR DE REFROIDISSEMENT DE PALE TURBINE PRE-TOURBILLONNÉ
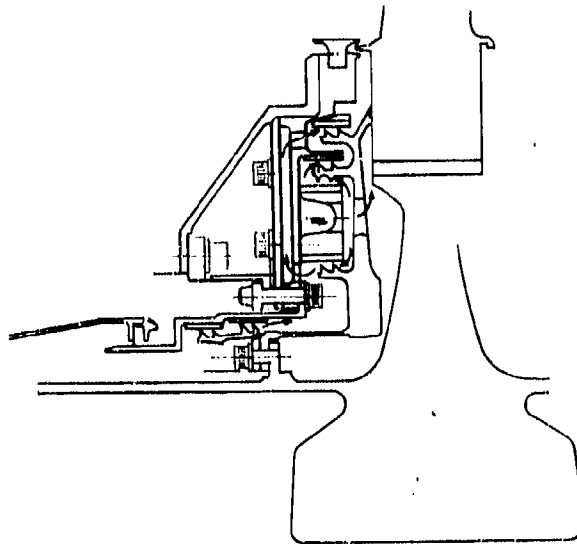
Figure 5.1

ISOLATION OF DISC PUMPED FLOW FROM PRE-SWIRLED TURBINE BLADE COOLING AIR
DÉBIT POMPÉ DU DISQUE ISOLÉ DE L'AIR DE REFROIDISSEMENT DE PALE TURBINE PRÉ-TOURBILLONNÉ
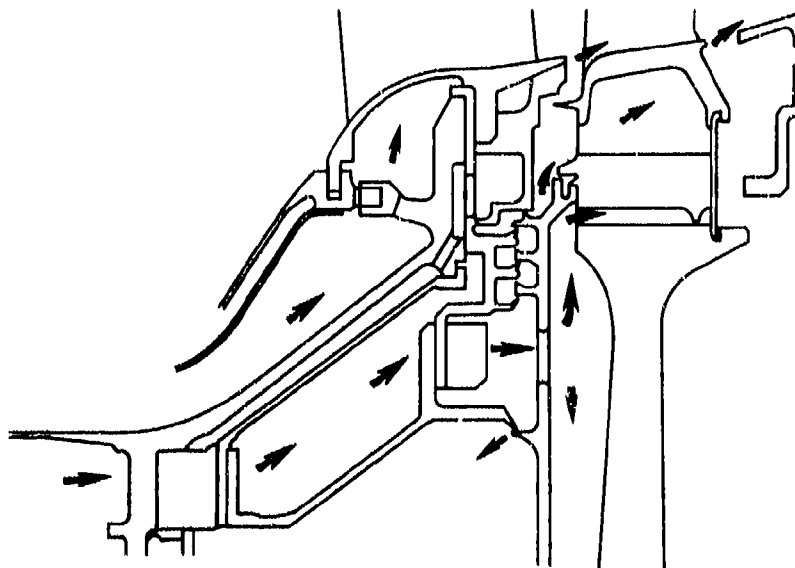
Figure 5.2

ROTOR THRUST BALANCE
EQUILIBRAGE DE LA POUSSÉE DU ROTOR
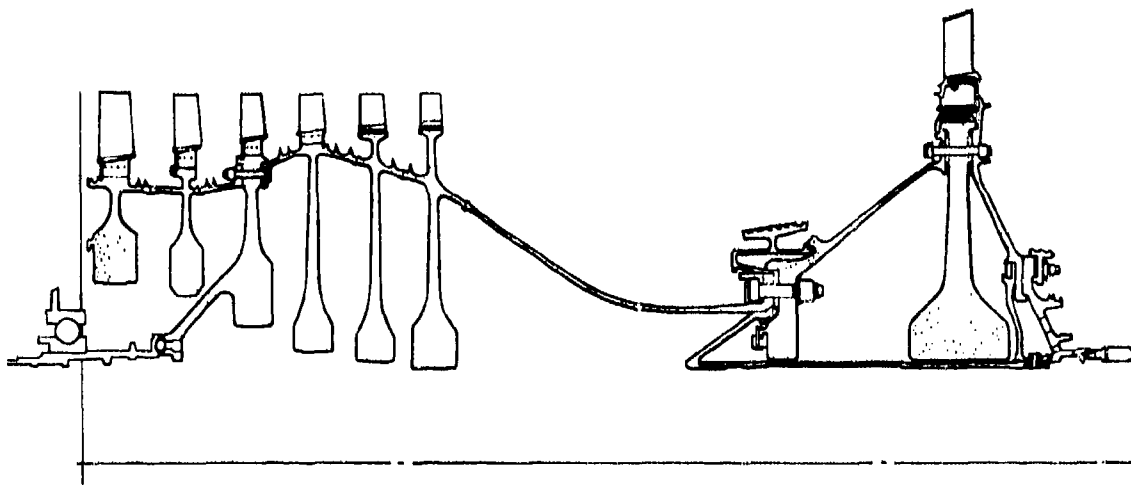
Figure 6.1

DISCUSSION

H.L.Stocker, US

I would like to reinforce Mr Campbell's comment regarding the need for improved data correlation relative to the calculation of seal leakage performance.

What information do you have that shows there is a circumferential static pressure gradient in the turbine — nozzle rotor gap of sufficient magnitude as to cause hot gas in-flow locally?

Author's Reply

Measurements in cold flow turbine rigs show considerable circumferential variation of static pressure immediately downstream of the nozzle. Variation upstream of turbine nozzles is apparent from vibration problems associated with excitation of the rotor blades by these variations. Considerable further work needs to be done before we can predict the effects on disc space temperature of these variations in any particular case.

A.Moore, UK

So far this meeting has considered the sealing between rotating and static members only. There are flow losses in gas turbines caused by leakage between two nominally static parts. Attempts to seal these leakage paths are not, in general, satisfactory. Would you like to comment on this problem please.

Author's Reply

This is certainly an important problem, particularly in the high pressure regions of engines. Leakage between parts in rotor assemblies can also be considered in this category. Sealing devices using small wires and strips are used in modern engines to minimize this sort of leakage and are thought to be reasonably effective, but more investigation should be done to verify their effectiveness under running conditions of load and temperature. Heavily loaded multiple flanges and nozzle guide vane locating features remain a problem. The potential for this kind of leakage should always be remembered when deciding the method of engine construction at the initial design stage.

H.Zimmermann, Germany

Could I extend this question? What experience have you got with piston rings? Do you use them or do you generally try to avoid them?

Author's Reply

Sealing rings of various types can be used, including piston rings. These can be designed to accommodate a considerable amount of relative movement using multiple rings with overlapping gaps. However there is concern over the possibility of these more complex rings sticking in the compressed position and thus leaving a large gap. Generally, it is felt to be preferable to replace or supplement sealing rings with a positively clamped joint where possible.

G.W.Fairbairn, UK

You refer to the difficulties experienced in estimating the transient running clearances in labyrinth glands. Do you find that predicting the transient behaviour of the disc space to annulus seal is also a critical problem?

What success have you achieved in predicting running seal clearances?

Author's Reply

The disc space to annulus seal clearance is normally rather larger than labyrinth seal clearances and so can potentially be estimated with better proportional accuracy. It is felt, however that we do not know enough about pressure variation and pumping effects to make much use of this information except to predict the mean pressure drop across the annulus seal. This pressure drop is usually small but often has a significant effect on rotor thrust balance.

The prediction of disc labyrinth seal clearances has not so far been very satisfactory owing to the difficulty of estimating the transient thermal behaviour of static assemblies with complicating features such as bolted joints.

"A COMPUTATIONAL TOOL FOR MECHANICAL SEAL DESIGN"

Dr. B.S. Nau, Group Head,
Mr. R.T. Rowles, Research Engineer,
BHRA Fluid Engineering,
Cranfield, Bedford, MK43 0AJ
England.

Summary

Rotary mechanical seals are used for many rotary sealing duties, gas turbine engine fuel pumps for instance. The factors affecting performance of such seals have been intensively studied in recent years, so that it is now feasible to incorporate this knowledge into a computer program as a design tool. The paper describes how this has been done at BHRA in a program which takes account of: surface topography; interfacial film dynamics, with cavitation allowed for; self-generated heat; thermal distortion; and distortion due to the sealed pressure. The significance and treatment of the various factors are discussed and the program structure outlined.

1. FACTORS AFFECTING MECHANICAL SEAL PERFORMANCE

A typical mechanical seal is illustrated in Fig. 1. The factors affecting design and performance of mechanical seals have been discussed in detail in Ref. 1, the physical (and chemical) processes influencing seal performance can be summarised as:-

- lubrication of the sliding interface
- heat transfer of frictional heat
- structural distortion of the sealing faces
- compatability of the seal components with the sealed fluid.

Several lubrication modes occur under different operating conditions but under the steady running conditions with which this paper is concerned the hydrodynamic lubrication mode, combined with some hydrostatic support, is generally believed to be predominant. Questions of material compatibility are outside the scope of the present paper.

Early experimental work (Ref. 2) established that hydrodynamic films are generated in the sliding interface of the seal and this has been confirmed by several subsequent workers. The film thickness is typically about 0.001 mm and is generated by viscous shear interacting with residual waviness of the nominally flat faces. Any structural stresses causing seal face displacements of this order of magnitude produce significant changes in the hydrodynamic situation, and hence in seal performance. Any design procedure must take this into account, particularly strains resulting from the sealed pressure on the one hand and thermal stresses on the other. Thermal stresses arise particularly from the temperature variation through the seal resulting from the generation of heat in the sliding interface – typically a few hundred watts for a 50 mm diameter seal. The effective heat sink is usually the sealed liquid although heat is also lost to the shaft and housing and hence to the outside environment.

2. SEAL DESIGN CONSIDERATIONS

In the present work attention is concentrated on the main design parameter which cannot be readily determined by simple means, this is the interface loading. In general this load derives partly from hydraulic pressure acting on the rear of the floating seal ring and partly from the spring(s) acting on this member. It is required that the load should minimise the interface film thickness whilst avoiding physical contact between the sliding faces. Part of the applied load is carried by the hydrostatic pressure field in the interface film and the balance by the hydrodynamic pressure field, and both components are modified by any change in the profile of the interface film due to the causes already mentioned. Clearly it is not a simple matter to evaluate the optimum load. In practice the load is evaluated by some combination of experience and more-or-less approximate estimates of the load component carried hydrostatically. The present work was undertaken to eliminate some of the uncertainties inherent in current design procedures, the approach followed being to apply the results of earlier experimental studies to the generation of a computer program which would predict the seal loading required for individual applications.

3. COMPUTER PROGRAM DESIGN CONSIDERATIONS

3.1 General

Technical considerations apart, certain general considerations were given particular emphasis in the design of the computer program : it should be reasonably economic in terms of computer processing time and computer store demands; the input data presentation and information output should be in a form facilitating use by the designer as

opposed to the lubrication scientist or computer specialist.

To meet these requirements the approach adopted was one in which general purpose programs for stress analysis or thermal analysis were avoided in favour of purpose-written routines tailored to the particular requirements of the mechanical seal geometry. The policy has also been to aim for simplification rather than generalisation. Thus, for example, axisymmetric distortion modes are known to be very important (Ref. 3) and are included whereas asymmetric modes, though possibly of significance in some circumstances, are regarded as second-order effects and neglected with useful simplification of the analysis (reducing stress and thermal analysis to two dimensions). The use of a modified ring theory (Ref. 7) provides further simplification at the expense of limiting validity to seals with radial thickness small relative to the mean radius, a not unreasonable assumption for most seals.

3.2 Discretisation

For the purpose of the numerical analysis a computational grid has to be imposed over the seal cross-section. In the present case, a two level grid system is used. Typical seal rings can be visualised as comprising a series of rectangular-section rings which, in reality, are joined to form a continuous body. These rectangular "parts" form the high-level grid for the analysis, and each part is permitted different physical properties. Each rectangular "part" is next subdivided by a finer rectangular mesh, at the nodes of which temperatures will be evaluated. This low-level mesh can vary from part to part, provided there is continuity across part-boundaries, this is a useful facility for dealing with regions of rapidly changing temperature. The high-level grid is used both in the stress analysis and to simplify the computer input data presentation. An example of a seal with the two-level grid is shown in Fig. 2.

3.3 Temperatures and thermal moments

It will be noted that the grids in Fig. 2 extend over both seal rings and also the interface film, the latter being treated as a heat source in the thermal analysis. Another feature of Fig. 2 is the presence of additional external "parts" on wetted surfaces. These external parts facilitate the treatment of the heat transfer boundary conditions. The internal nodes in these parts have a specified temperature which is that of the bulk liquid, which being in a turbulent state is assumed to be effectively of uniform temperature. The half-thickness of the part is taken to represent the laminar sub-layer of liquid attached to the seal ring, heat transfer from seal to bulk liquid being controlled by conduction through this laminar sub-layer. In general, the thermal analysis permits two boundary condition types : specified temperature and specified flux.

A temperature map is computed from Poisson's equation using the appropriate interface flux and external boundary conditions. From these temperature values thermal moments about the centroid of the floating seal ring are evaluated to be added to the hydraulic moments calculated elsewhere in the program. The total moment is then used to evaluate the axisymmetric ring distortion which modifies the seal face geometry. An iterative procedure (Fig. 3) is used to take account of the interactions of distortion, heat flux and film pressures.

3.4 Face Distortion

The axisymmetric moment (M) producing face distortion includes the above thermal moments plus an hydraulic moment due to the fluid pressures acting on the various wetted surfaces of the seal. The hydraulic moments are straightforwardly calculated in the program once the coordinates of the overall centroid of the floating ring have been determined from the geometrical input data. The thermal moments are evaluated by regarding thermal stresses as equivalent to distributed body forces (Ref. 8).

The stiffness of the floating seal ring in its axisymmetric ring distortion mode is dependent on the second moment of area (I) about a radial axis through the centroid. This quantity, like the centroid coordinates, is quite simply evaluated by summing the contributions of the individual "parts". Given the values of M, I, elastic modulus E, and mean radius r_m, the angular distortion is given by:-

$$\phi = \frac{M r_m^a}{E I}$$

3.5 Interface film pressure

The appropriate equation for evaluating the film pressures , and hence the load-capacity of the film, is Reynolds lubrication equation in polar coordinates (Ref. 9).

$$r \frac{\partial}{\partial r}\left(r h^3 \frac{\partial p}{\partial r}\right) + \frac{\partial}{\partial \theta}\left(h^3 \frac{\partial p}{\partial \theta}\right) = \frac{\partial h}{\partial \theta}$$

where all variables have been non-dimensionalised. The quantity $h = h(r,\theta)$ is the dimensionless film thickness and is obtained by combining the initial seal face profile with any modification due to the distortions described above.

The solution of the Reynolds equation is not simple since account must be taken of 'cavitation' in regions where film pressure falls below the pressure at which the liquid is saturated with gas. Effectively the cavitation region has an initially undetermined boundary which is one of the boundaries of the region in which Reynolds equation is to be

solved.

The procedure employed to overcome this difficulty involves a finite difference procedure in which the film is scanned radially for each incremental θ-value in turn, solving for p along the radial row of computational nodes, until the cavitation region is reached (indicated by p ≤ p_cav). The procedure around the cavitation region is similar except that the radial scan is only between the cavity boundaries and the seal edges. Assumption of a tentative radial co-ordinate for the cavity boundary location permits calculation of the liquid film pressures for the current value of θ and hence the net flow into a control volume, Fig. 4. If the net flow is not effectively zero the tentative position of the cavity radial coordinate at θ is adjusted and the process repeated. This procedure is employed separately for the radially external and internal cavity boundaries at the current θ. By this means the cavity boundary is generated automatically as the computation proceeds circumferentially.

The efficiency of this solution procedure for Reynolds equation is such that adequate convergence is usually obtained within a few circumferential sweeps of the seal.

The importance of an effective treatment of the cavitation region is illustrated by Fig. 5. This shows the extent of the cavitation regions for the two extremes of cavitation pressure (zero absolute, and ambient) and in both cases a large proportion of the film is cavitating, this is due to the high rotational speed combining with the surface waveform to produce very intense hydrodynamic pressures. Fortunately, since the value is not easy to define, the value of the cavity pressure has only a minor effect on the total load capacity and, therefore, on the required closing force.

4. EXAMPLES OF INPUT AND OUTPUT

Typical input data lists are illustrated in Fig. 6. Input Tables 1-5 relate to the thermal and deflection computations with the size of the problem defined in Input Table 1 and the mesh and dimensions for each "part" in Input Table 2. Physical properties of the seal are tabulated in Input Table 3. The topology is defined by Input Table 4, which lists for each part the neighbouring part and boundary condition (type and value) to left and right, and above and below the part in question. For example, part 1 has neighbours 53, 2, 4 and 52 with temperature boundary values of 60 C on two (wetted) sides and a value "zero" on the remaining sides, indicating internal interfaces. The next input table sets the initial guess for the part temperatures.

Information required by the lubrication equation is set out in Input Table 6. Items of particular interest in this list are the minimum film thickness, surface wave amplitude and number of waves which together define the film profile.

Examples of output are shown in Fig. 7 and 8, part of the thermal map, and the final design and performance parameters respectively. The section of the thermal map shown in Fig. 7 relates to two "parts" forming the interface film, this is useful as an indication of the risk of vaporisation due to elevated film temperature. The key item of information in the output is, of course, the seal closing load required to operate at the specified minimum film thickness.

5. DISCUSSION AND CONCLUSIONS

The program described is in the final stage of testing, although much running has already been achieved for major segments such as the thermal and lubrication elements. These also exist independently as self-contained programs.

The validity of a program such as this is not easily established but in the present case a parallel project involving an experimental program on high-speed fuel pump seals is in progress and will be used for validation purposes. Once confidence has been established in the program it can be expected to be of great value in speeding up the design of mechanical seals.

6. REFERENCES

1. Fern, A.G. and Nau, B.S.   "Seals". Oxford : Oxford University Press. 36 pp (1976).

2. Denny, D.F.   "Some measurements of fluid pressures between plane parallel thrust surfaces with special reference to the balancing of radial-face seals" BHRA report RR613, 27 pp (January, 1959).

3. Nau, B.S. and Turnbull, D.E.   "Some effects of elastic deformation on the characteristics of balanced radial-face seals". Proc. 1st International Conference of Fluid Sealing, Harlow, BHRA. Paper no. D3 (17th - 19th April, 1961).

4. Fisher, M.J.   "An analysis of the deformation of the balancing ring in high pressure radial-face seals". Proc. 1st International Conference on Fluid Sealing, Harlow, BHRA. Paper no. D4 (17th - 19th April, 1961).

5. Watson, P.D.   "Effect of seal ring deflection on the characteristics of face-type mechanical shaft seals in high pressure water". Atomic Energy of Canada Ltd, AECL - 2242, 18 pp (October, 1963).

6. Cheng, H.S. Castelli, V and   "Performance characteristics of spiral – groove and shrouded Rayleigh
    Chow, C.Y.   step profiles for high – speed non-contacting gas seals". ASME Paper
                                        68 – LUBS – 38 (1968).

7. Gill, S.S.   "The stress analysis of pressure vessels and pressure vessel compon-
                                        ents" section 6.4.1 : "Stress analysis of taper hub flanges : cylindrical
                                        vessel" Oxford : Pergamon Press. pp 290-297 (1970).

8. Boley, B.A. and Weiner, J.H.   "Theory of thermal stresses", Chapter 3 : "Alternate formulations of
                                        thermoelastic problems". New York : John Wiley & Sons pp. 75 – 100
                                        (1960, 1966 reprint).

9. Nau, B.S.   "Review of the mechanism of hydrodynamic lubrication in face seals".
                                        Proc. 3rd International Conference on Fluid Sealing, Cranfield, BHRA
                                        Fluid Engineering. Paper E5 (1967).

7. ACKNOWLEDGEMENT
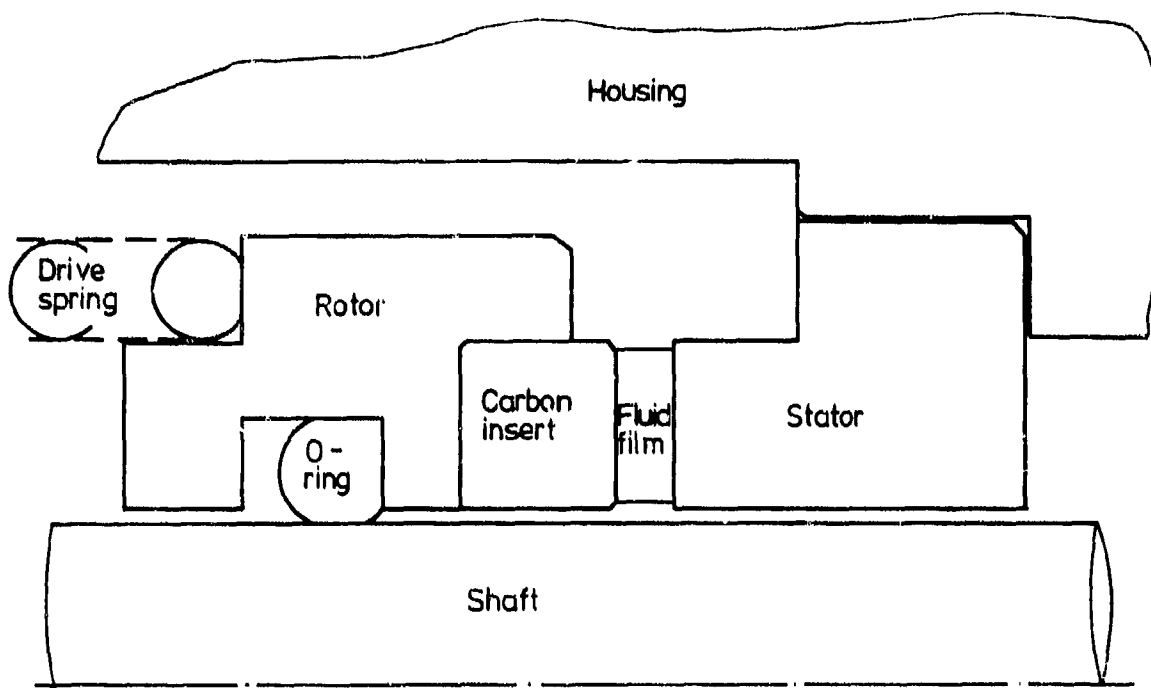
Fig. 1   A typical mechanical seal (diagrammatic).
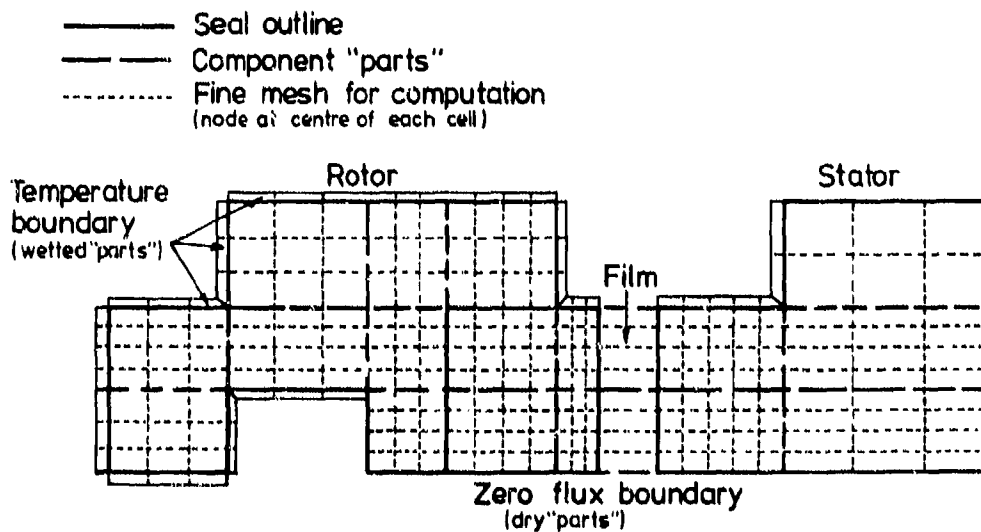
Fig. 2   The two-level computational grid
applied to a mechanical seal.
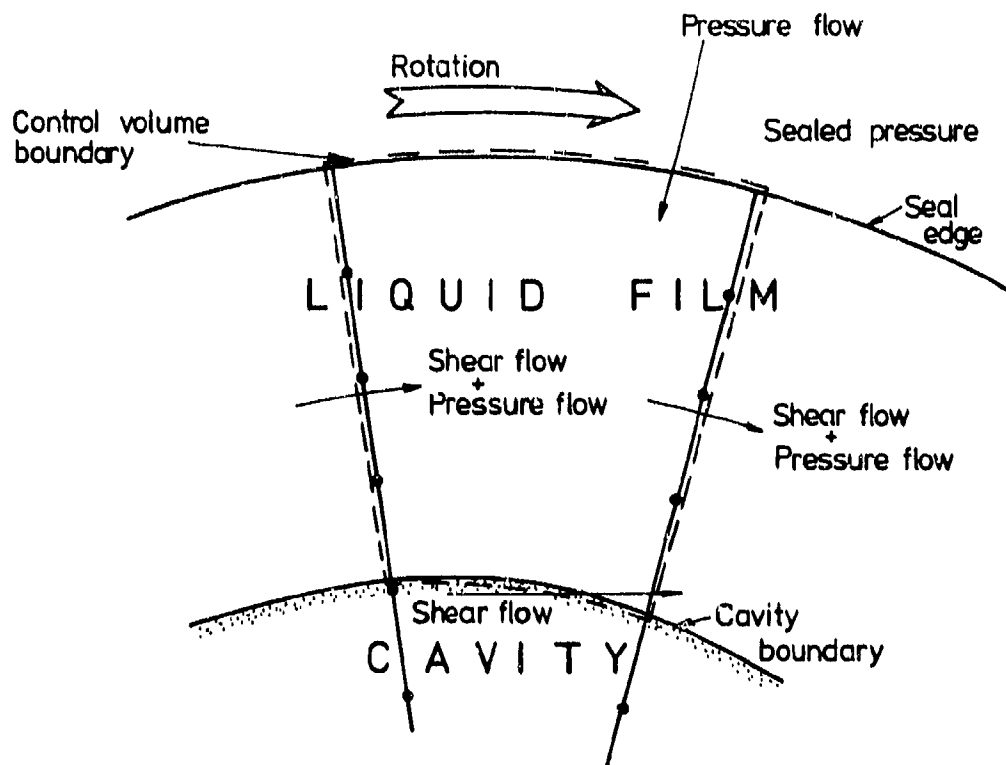
Fig. 3 Flow chart showing iterative procedure.

CALCULATE VISCOSITY AND FLUX

CALCULATE TEMPERATURE DISTRIBUTION

CALCULATE CENTROIDS & 2nd MOMENT OF AREA

CALCULATE PRESSURE MOMENT

CALCULATE THERMAL MOMENT

CALCULATE DISTORTION

CALCULATE PRESSURE FIELD

OUTPUT RESULTS

Fig. 4 Control volume used in the determination of the boundary of the cavitation region.

Fig. 5 Computed cavitation boundaries with cavity
pressure (a) zero MPa abs. (b) 0.1 MPa abs.
PI = 0.1, PO = 0.415 MPa

INPUT DATA TABLE 1 - NUMBERS OF PARTS

THERE ARE   42   INTERNAL PARTS

THERE ARE   61   PARTS INCLUDING BOUNDARIES

THE FILM CONSISTS OF   3   PARTS

INPUT DATA TABLE 2 - PART DIMENSIONS

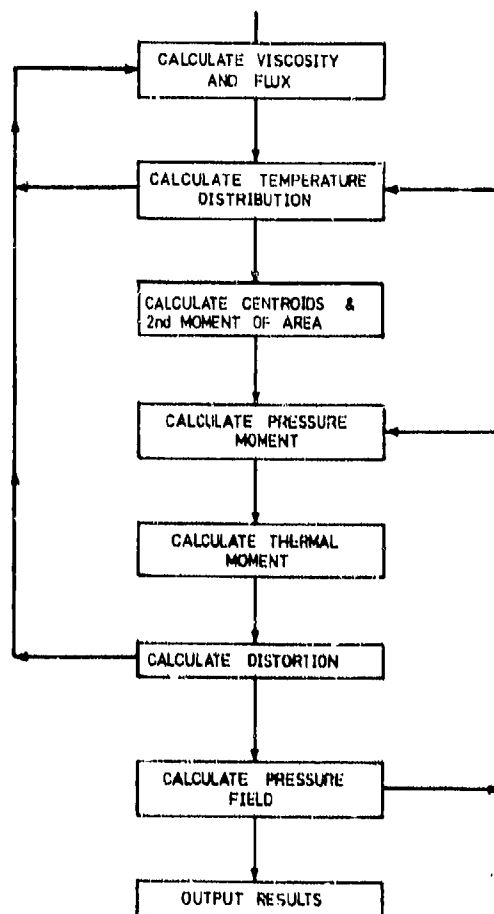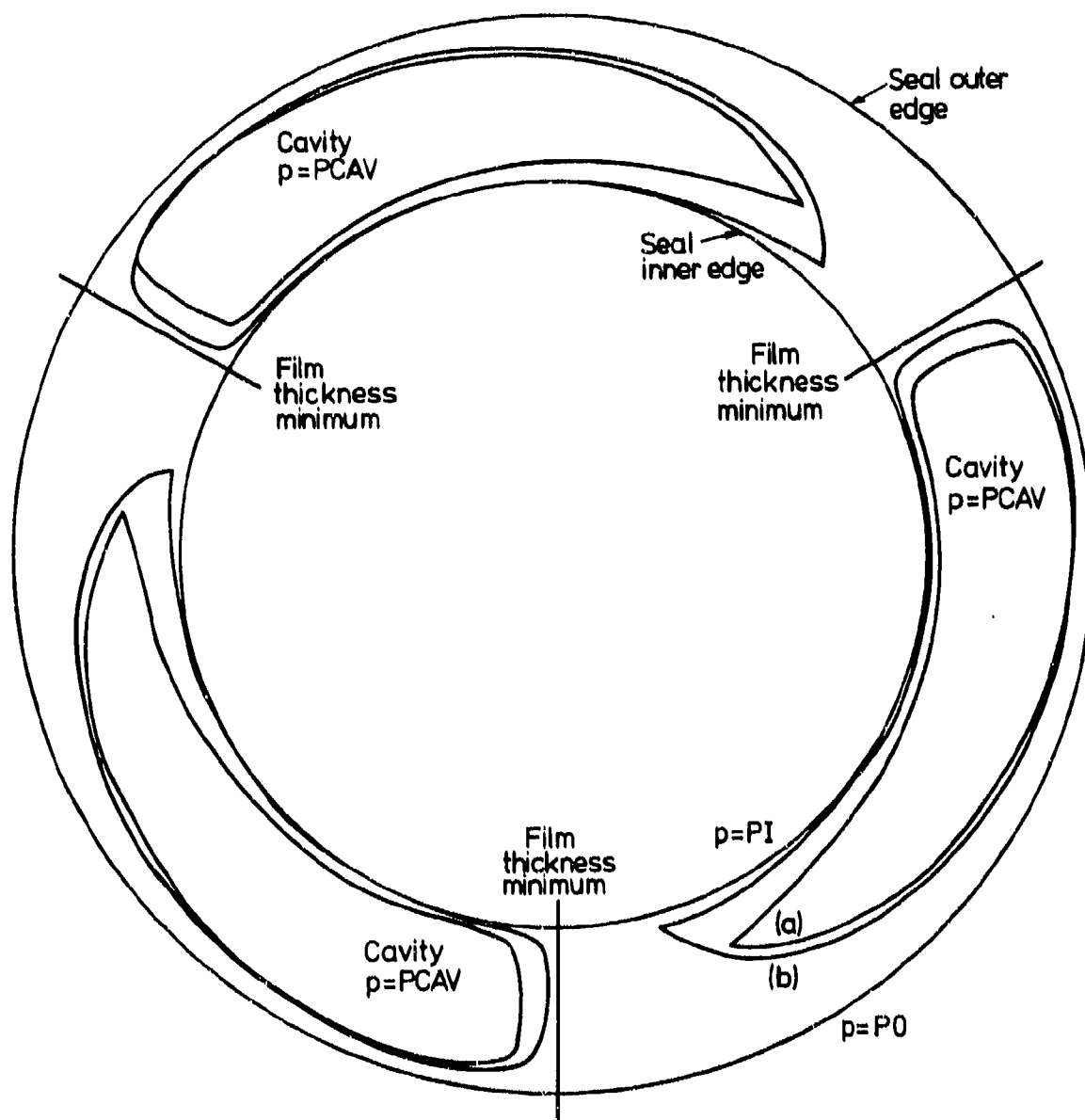| PART NUMBER	MESH IN PART AXIAL	RADIAL	LENGTH OF SIDES AXIAL	RADIAL	PART NUMBER	MESH IN PART AXIAL	RADIAL	LENGTH OF SIDES AXIAL	RADIAL
1	3	2	3.175	1.588	2	3	2	3.175	1.780
3	3	1	3.175	3.251	4	4	2	4.763	1.588
5	4	2	4.763	1.780	6	3	4	3.175	1.588
7	3	2	3.175	1.780	8	3	4	3.175	3.251
9	4	2	3.175	1.588	10	4	2	3.175	1.780

INPUT DATA TABLE 3 - PROPERTIES

PART NUMBER	THERMAL CONDUCTIVITY W/MM,K	YOUNGS MODULUS N/SQ MM	THERMAL EXPANSION COEFFICIENT /K	PART NUMBER	THERMAL CONDUCTIVITY W/MM,K	YOUNGS MODULUS N/SQ MM	THERMAL EXPANSION COEFFICIENT /K
1	0.013570	0.1931E 06	0.1600E-04	2	0.013570	0.1931E 06	0.1600E-04
3	0.013570	0.1931E 06	0.1600E-04	4	0.013570	0.1931E 06	0.1600E-04
5	0.013570	0.1931E 06	0.1600E-04	6	0.013570	0.1931E 06	0.1600E-04
7	0.013570	0.1931E 06	0.1600E-04	8	0.013570	0.1931E 06	0.1600E-04
9	0.013570	0.1931E 06	0.1600E-04	10	0.013570	0.1931E 06	0.1600E-04

INPUT DATA TABLE 4 - BOUNDARIES (BOUNDARY VALUES IN C OR W/SQ MM)

							NEIGHBOUR							
PART NUMBER	PART	LHS TYPE	BOUNDARY VALUE	PART	TOP TYPE	BOUNDARY VALUE	PART	RHS TYPE	BOUNDARY VALUE	PART	BOTTOM TYPE	BOUNDARY VALUE
1	53	2	60.000	2	2	0.000	4	2	0.000	52	2	60.000
2	54	2	60.000	3	2	0.000	5	2	0.000	1	2	0.000
3	55	2	60.000	56	2	60.000	57	2	60.000	2	2	0.000
4	1	2	0.000	5	2	0.000	6	2	0.000	51	2	60.000
5	2	2	0.000	58	2	60.000	7	2	0.000	4	2	0.000
6	4	2	0.000	7	2	0.000	9	2	0.000	50	2	60.000
7	5	2	0.000	8	2	0.000	10	2	0.000	6	2	0.000
8	0	1	0.000	0	1	0.000	11	2	0.000	7	2	0.000
9	6	2	0.000	10	2	0.000	14	2	0.000	49	2	60.000
10	7	2	0.000	11	2	0.000	15	2	0.000	9	2	0.000

INPUT DATA TABLE 5 - ESTIMATED PART TEMPERATURES AND CONTROL DATA

PART NUMBER	ESTIMATED TEMPERATURE	PART NUMBER	ESTIMATED TEMPERATURE	PART NUMBER	ESTIMATED TEMPERATURE	PART NUMBER	ESTIMATED TEMPERATURE
1	65.000	2	65.000	3	65.000	4	70.000
5	70.000	6	75.000	7	80.000	8	80.000

THE MAXIMUM NUMBER OF ITERATIONS TO BE CARRIED OUT IS   900
INTERMEDIATE RESULTS WILL BE PRINTED OUT EVERY   100   ITERATIONS

THE SOLUTION IS CONSIDERED TO BE CONVERGED WHEN THE LARGEST TEMPERATURE
DIFFERENCE BETWEEN ITERATIONS IN ANY PART IS   0.001   DEGREES CENTIGRADE

THE FILM CONSISTS OF PARTS   27   28   29

THE SEALED FLUID IS ON THE INSIDE OF THE SEAL, PRESSURE =   0.690E 00 N/SQ.MM

INPUT DATA TABLE 6 - SLIDING INTERFACE PARAMETERS

SEAL FACE OD =   .02720 M
SEAL FACE WIDTH =   .00160 M
DIAMETER RATIO,R =   .897

MINIMUM FILM THICKNESS,HMIN =   .8800-06 M
WAVE AMPLITUDE,HAMP =   .8800-06 M
TILT RATIO,E =   .333

MAXIMUM FILM AT ANGLE,PHI =   .0000   RADIANS
FACE DISTORTION,PSI =   .0000   RADIANS
VISCOSITY =   .1200-02 N.S/M
SHAFT SPEED =   .2300+05 RPM

NO. OF WAVES,IW =   3
MESH DIMENSIONS,M=N =   21=60

PRESSURES: INTERNAL,PI =   .00000   N/SQ M
           EXTERNAL,PO =   .31400+06 N/SQ M
           CAVITATION,PCAV = -.10000+05 N/SQ M

Fig. 8   Input data for computer program
(sample only).

OUTPUT TABLE 1 - TEMPERATURE FIELD:DEGREES CENTIGRADE

CONVERGENCY CRITERION IS   0.001 DEGREES CENTIGRADE
MAXIMUM TEMPERATURE DIFFERENCE BETWEEN ITERATIONS IN ANY ONE PART

TEMPERATURES IN PART 27 - FILM

HEAT SOURCE 0.8475E 02 WATTS/UNIT VOLUME

132.07
129.98

TEMPERATURES IN PART 28 - FILM

HEAT SOURCE 0.9916E 02 WATTS/UNIT VOLUME

135.03
133.76

TEMPERATURES IN PART 29 - FILM

HEAT SOURCE 9.1981E 03 WATTS/UNIT VOLUME

134.97
133.79
136.14
135.92

OUTPUT TABLE 2 - CENTROIDS AND SECOND MOMENT OF ELASTICITY

PART NUMBER	CENTROID AXIAL	CENTROID RADIAL	PART NUMBER	CENTROID AXIAL	CENTROID RADIAL	PART NUMBER	CENTROID AXIAL	CENTROID RADIAL
1	1.587	0.794	2	1.587	2.478	3	1.587	4.993
4	5.556	0.794	5	5.556	2.478	6	9.525	0.794
7	9.525	2.478	8	9.525	4.993	9	12.700	0.794

GLOBAL CENTROID RING 1 - AXIAL 14.051 - RADIAL 0.901

GLOBAL CENTROID RING 2 - AXIAL 30.082 - RADIAL 5.566

SMOE1 = 0.1230E 10 SMOE2 = 0.3312E 09

OUTPUT TABLE 3 - MOMENTS AND DISTORTIONS

TEMPERATURE AT THE GLOBAL CENTROID, RING 1   73.9,   RING 2   99.4

THERMAL MOMENT: RING 1 =-0.2054E 03N.MM/MM CIRC.   RING 2 = 0.1538E 03N.MM/MM CIRC.

PRESSURE MOMENT: RING 1 =-0.1884E 02N.MM/MM CIRC.   RING 2 = 0.3267E 02N.MM/MM CIRC.

THE DISTORTION IN RING 1 IS -0.7215E-03 RADIANS
THE DISTORTION IN RING 2 IS   0.1998E-02 RADIANS

POSITIVE MOMENTS AND DEFLECTIONS ARE CLOCKWISE

Fig. 7   Output from computer program : seal temperatures
(sample only) and various intermediate parameters.

RESULTS OF ANALYSIS

R	E	n	H
.897	.333	21	20

AVERAGE FILM PRESSURE = .33096+06 N/SQ.M   CLOSING FORCE REQUIRED = .38463+02 N

FRICTION FORCE = .37706+01 N   OVERALL LEAKAGE = .11998+02 ML/HR   POWER = .12377+03 WATTS

Fig. 8   Output from computer program : seal
design and performance parameters.

DISCUSSION

A.J.B.Jackson, UK

What are the limitations of the technique you describe in respect of film thickness? You describe a minimum thickness — is there a maximum thickness?

Authors' Reply

The upper limit on our analysis is determined by the assumption of negligible fluid velocities normal to the plane of the film, one would imagine this to be valid to the upper limit of typical bearing films, say 1.0 mm. The lower limit is fixed by the transition from hydrodynamic to boundary lubrication and, hence, by surface roughness. For a face seal the latter might be about 0.0002 mm.

A.Pautot, France

Quelle est l'influence de la rugosité des surfaces sur l'établissement du film d'huile. Spécialement dans le cas d'une rugosité très faible on observe un échauffement des faces. Avez vous vérifié ce fait?

Authors' Reply

We believe that waviness is normally more important than roughness in mechanical seals, since it provides an efficient hydrodynamic mechanism for separating the two surfaces and so keeps apart the roughness asperities. Most of our test work has been with seal faces polished to permit examination under an optical flat, we have not observed overheating with such seals.

L.P.Ludwig, US

Would you comment on the existence of liquid to vapor interface developing because of high speed shear of the liquid film?

Authors' Reply

A vapour interface is predicted by our computer model of the film hydrodynamics but this has certain limitations since it is assumed to be at a pressure P_{cav} which has a single value input as data. In practice there would be a range of values corresponding to different liquid temperatures and since, of course, the temperature varies radially over the sealing gap this too must be taken into account. Our total flow conservation method of handling the prediction of the cavity boundaries could in fact be adopted to treat this more general situation.

ROUND TABLE DISCUSSION

Mr A.J.B.Jackson, as the moderator of the Round Table Discussion, opened the Session and introduced the Round Table Panel Members:

Mr A.J.B.JACKSON, (Moderator)	UK
Prof. J.CHAUVIN	Belgium
Ing.Gén.A.JOURNEAU	France
Prof. F.WAZELT	Germany
Mr B.WRIGLEY	UK

A.Journeau: Je préfère que l'on n'emploie pas le terme d'expert à mon sujet étant donné que je ne suis pas du tout spécialiste des joints et que j'en ai surtout entendu parler au cours de cette session qui a été très instructive pour moi, car elle m'a fait prendre conscience de l'importance de poursuivre des recherches dans ce domaine. Je me contenterai donc de faire quelques remarques générales.

Si je ne me trompe, c'est le premier meeting organisé par le PEP sur ce sujet et si l'on compare cette situation aux nombreux meetings qui ont été consacrés aux écoulements principaux dans les compresseurs et dans les turbines, on peut dire que le rapport du nombre de communication est peut-être proportionnel au rapport des débits de fluide dans les deux cas. Alors qu'on arrive à étudier ce qui se passe dans les écoulements secondaires des turbomachines, c'est-à-dire dans les coins, dans les bords de l'écoulement principal, là où interviennent les phénomènes de couche limite, tridimensionnels, et ceci surtout en vue d'accroître les performances des étages d'aubages, il me semble qu'on a encore peu étudié les écoulements dans les joints à passage de fluide. Ce sujet a heureusement été abordé au cours de ce meeting, en particulier au cours de la session IV d'hier où nous avons eu deux études scientifiques très intéressantes.

Si on considère l'importance des joints dans les coûts d'exploitation, les économies d'énergie, la sécurité d'emploi des turbomachines, comme cela a été mis en évidence par les exposés des utilisateurs opérationnels, en particulier par Mr Smith, il me semble que l'effort de recherche devrait être accru. Des recherches de base devraient être menées tant en ce qui concerne les systèmes avec contact solide (problèmes de matériaux, recherche sur le frottement) que les systèmes à joints gazeux, à labyrinthes avec une étude approfondie de ces écoulements entièrement tridimensionnels, ainsi que des études sur les phénomènes vibratoires et les transferts thermiques.

Je n'en dirai pas plus; je pense seulement, qu'au cours de cette table ronde, il serait bon qu'un échange de vue entre chercheurs d'une part et utilisateurs d'autre part permette de mieux dégager les objectifs de recherche et de définir des priorités parmi ceux-ci.

L.P.Ludwig: As we got into the meeting it became apparent that we had a very complex subject and our research efforts should be stepped up. I certainly was impressed with these papers and this AGARD meeting. In general, it was gratifying to see the number in attendance and the interest shown by the people present.

As has been pointed out by a number of comments, we did not get into all the subjects, e.g., static seals (we only skimmed over them); and we also did not get into the very important subject of wear. We need to know more about wear mechanisms because we have been talking about running very close clearances which lead to rubbing contact. The subject of wear theory and experiments would take another whole meeting. I might just mention that we are doing some work on the theoretical and experimental aspects of wear. A number of new theories have surfaced within the last couple of years that are interesting and suggest that we might now be in a position to put together a better wear model. This wear model would involve the surface instability mechanism which I mentioned was first investigated by Barber (Reference 50 of Paper No.1) and is now being studied by Burton (Reference 51 of paper No.1). Also the wear model would probably need to take into account some of the aspects of machining theory, both cutting and grinding. For example, in the compressor there are high speed blades cutting into abradable materials; and there are some aspects of grinding when abrasive blade tips rub against ceramic materials in the high pressure turbine, or when vanes rub against the abrasive coating on drum rotors. Some of these machining mechanisms are currently being investigated at Ohio State University in the USA under a NASA grant.

In addition, there have been some theories developed involving the thermally affected surface layer, some call it the "frictional energy affected layer". (R.Bill of NASA Lewis Research Center and L.Roseanu of Technion, Israel have published work on these surface layers.) We suspect that this thermally affected surface layer may be responsible for the sometimes very destructive blade metal transfer (to the shroud) in a high pressure turbine. In a turbine the blade passing frequencies are greater than ten thousand blades a second and if transfer starts on the shroud we can quickly machine a very large gap. With ten thousand blades per second even if each blade contributes a very thin layer, the transfer would quickly build up.

Also when we talk about friction and wear, we have to be concerned with the dynamics of the whole system. There is a possibility of inducing backward whirl, which is part of the rotor dynamics problem mentioned in the first paper, and I was pleased to see the paper by Benckert and Wachter on the effects of non-uniform clearances and its relation to shaft dynamics; this is a very important subject especially in the very high pressure machines.

As far as the labyrinth seals are concerned, we will always have a large number of labyrinth seals in engines. And certainly the systematic study which Allison presented will go a long way towards clarifying some of the questions regarding effects of mating materials, such as honeycomb and porous materials; and the labyrinth transport phenomena which was the subject of the paper by Boyman and Suter was very interesting and informative.

In relation to the wear study, there are some other comments which relate to some other questions asked yesterday on labyrinth thermal stability. This is related to the thermal transfer and heat split into the shrouds and down into the rotor. This is a very complex situation and some very odd things may happen. Sometimes the contact on a labyrinth seal will only be a small arc -- maybe 5 degrees. I think there is a picture in the first paper showing what can occur when the shroud rubs into the rotor. The first point on the labyrinth knife-edge which happens to contact grows thermally -- it forms a macroscopic tooth on the knife-edge outside diameter (or hot spot) and this eventually wears down and some other point makes contact. So we get a whole series of small contact events. Thus the heat transfer down into the rotor is very different in this case as compared to its rubbing all the way around the knife-edge. And certainly more research should be made into this question of heat split and thermal transfer.

The paper we had this afternoon by Campbell, brought up a subject which we have somewhat ignored for quite a while, and that is the secondary flow system design, and in particular sealing to prevent the ingestion of hot gas down into the turbine cavities. As engine design advances to higher temperatures and pressures, the secondary flow system will assume even more importance, and more attention should be given to this subject, particularly in the turbine where hot part life and thermal cycling are critical factors.

F.Wazelt: Now comes the view of a non-expert again and it will be a view from some distance. I am not actively involved in the development of seals and if this is a handicap or an advantage we will all know in a couple of minutes.

First, let me give some of my personal observations and impressions on the current status.

Air Path Seals

Deformations between rotor support and rotor under mechanical and thermal loads are observed resulting in transient relative movements between those two components and leading to occasional contacts, rubs. These contacts seem to me to be currently accepted. Much of the effort and work we have heard about tries to minimize the damage done during such contacts and to absolutely prevent catastrophic failures. The measures which are used are design and material selection for the seal surfaces. In essence, it looks to me at this stage that we allow our machines to adjust the required clearances themselves by working at it.

During engine operation we observe performance deterioration -- a portion of it is identified as being due to seals. I had the impression that it is not entirely clear if under different loads different rubs cut deeper grooves, what part erosion plays in this change of clearance and which part is due to distortion of the stationary seal supports.

One thing impressed me very much: that these seals cannot very easily be repaired and I believe further work on suitable repair techniques is being required.

Shaft Seals

Primarily they serve to retain oil in bearing packages. It seems to me that an additional objective is to avoid contamination of engine parts. Preventing oil leaks into the gas paths reduces accumulation of dirt on profiles and channel walls and helps to reduce corresponding performance deteriorations. Oil contamination of cavities inside rotating components could lead to serious unbalances. I got the impression that the deterioration of such shaft seals in actual operation seems to be less than that of gas path seals. They seem to live longer, however their repair is always a costly undertaking.

Progress seems to be in the offing by incorporating self-action seals. I also welcome the efforts of increasing the tolerance of such shaft seals against radial excursions. Interesting phenomena like the migration of small oil droplets against the blockage airflow and the possible problem of creating periodic lateral excitation forces in eccentric seals might receive further attention.

We have heard about clearance measuring techniques, and I believe those techniques are of extreme importance. And we have heard about two ways of measuring running clearances in operation with instrumented engines and in particular with non-instrumented engines. These techniques will be of extreme importance for a while to come. Especially since they allow us to measure clearance during the steady state at various power levels, but also at extreme transients.

Now some general remarks regarding the current status.

I was glad to hear that the sealing of cooling air supplied to turbine rotors was not reported to be a serious problem area. And maybe this is due to the very systematic studies which apparently have been done and are in progress about which we have heard this afternoon.

I was somewhat surprised that -- aside from the subject of balancing axial loads -- bearings in connection with providing the concentricity for seals did not receive much attention during the meeting and if I have to speculate then I would guess that bearing effects and wear of bearings could be completely shadowed by the displacement of the bearing support structures which may be predominant in this aspect.

We have heard about problems with stationary and rotating seals. I always wondered why ordinary flanges are not a problem, especially if I think that through flanges compressor discharge air can leave the cycle completely and these flanges also distort; now in most applications probably this problem is well in hand. I am myself somewhat plagued by the memory of problems we have had with the regenerative engine where turbine components are very small compared to the flanges surrounding the heat-exchanger due to the dimensions of the heat-exchanger casing. I would like to point out that in such situations compressor discharge air can leak inside the engine directly to the

exhaust and not participate in the cycle. And I think with regenerative engines that type of sealing problem with distortions under different loads and thermal expansions may also be an interesting problem and not an easy one.

That much to the current status. If you permit me, I would like to give my personal outlook on future work. And I am not thinking of near-term development but of some long-term research subjects.

First, some remarks to the system aspects. I believe we need further refinement of all clearance measurement techniques suitable for application in actual operation. And I would like to see those applied while actually putting the engine under external mechanical loads.

Second, I believe parallel to this we should make every effort of computing and measuring the deflections under mechanical and thermal loads of the stationary structure and of the rotating structure separately and then join them to get a feeling about the influences on relative distances between those parts, the required clearances. I think the objective of this type of effort should be to derive reliable development tools and prediction methods for those deflections under various thermal and mechanical loads. And third, it would help if one could clear up the question: Are bearings and bearing wear really unimportant for the location of the rotor in relation to the stationary supports?

From the result of such activities, I hope that we receive quantitative information on the required clearances.

Now some seals aspects. I would like to call one aspect a clearance control. By that, I mean to maintain a more or less constant gap between the two parts under all loads and operating conditions.

We have heard about self-acting seals -- one could think of displacible elastic or pneumatic supports of the stationary seal surfaces. I think a confirmation and extension of the work which is already initiated should prove to be helpful. Such approaches seem to me quite promising for shaft seals.

Now I would like to propose a second activity which is still surely in the category of the preliminary brainstorming -- I would like to call that a leakage control. By that I understand to maintain flow rates at a constant level through gaps of varying size. I think in that sense the beginnings of the flow studies (we have heard about them) could lead further and we could even consider to take active counteractions against the leakage flows. I am thinking of using bleed flows to suppress and control the leakage. I would as a layman really hope that such approaches could also be applicable to gas path seals.

Now in concluding my remarks I would like to address myself to the engine design. Eliminate seals whenever it is possible. A seal which is not there, does not cost anything, does not weigh anything, does not wear nor fail.

B.Wrigley: I would like to take one of Professor Wazelt's points first of all, and that is the question of flanges and leakages between static parts. It is one of the points I was going to bring up anyway. I don't think I'll be overestimating the significance of the point if I point out here that it was a crucial factor in failing to achieve the performance of the RB 211 in the early stages of its development, i.e. prior to 1971, and I am sure we all recall the consequences of that. In particular it is important to pay attention to sealing in the vicinity of nozzle guide vane locations, and one of the features that was eventually introduced into the RB 211 was a concept called chordal sealing, where the circumferential flange was in fact produced as a series of chords rather than a complete circumference. Any rotation that took place then was about a straight line which did not open up the flange.

During the conference I have seen considerable emphasis placed on sealing in the main flow path of the engine, particularly compressor and turbine blade tips. It does raise the question whether the unshrouded HP turbine blade is the best solution, and perhaps, coming from Rolls-Royce (Derby), I am a little bit prejudiced (in favour of the shrouded blade). Nevertheless, we have convinced ourselves I think, at Derby, that there are very good points in favour of the unshrouded turbine. The lower stress levels reduce the requirement for cooling air for example. Those good points are worth striving for, and we must develop solutions to reduce overtip leakage.

I think designers must also distill the best features of our current engines, and I refer mainly to the high bypass engines. I think it is important to have short rigid rotor systems with strong casings. This may cause weight penalties. There is no doubt that the three spool concept adds some weight to the engine, but we have demonstrated that short rotor systems minimise carcase deflections. We must also have strong casings which stay round. Engines of this sort, I am sure, can be demonstrated to have less in-service deterioration than the figures that we have seen during the last two days. I would draw your attention at this point, to the graphs that were shown as part of the X-ray lecture yesterday, which were for the industrial version of the RB 211, but which showed quite small relative excursions of the rotating to the static part.

A theme of the conference has been performance deterioration in service and the impression has been given, unwittingly, that all of the current generation of high bypass ratio turbofans suffer to the same extent. This is not so. Firstly analysis of RB 211 flight certification engine performance shows that performance is not lost over the first few flights whereas other engines suffer about 1% irreversible specific fuel consumption deterioration. Factors contributing are:

(a) Small relative deflections of rotor to casing in the HP compressor. In circumstances which cause the engine carcase to bend, e.g. manoeuvres, thrust modulation and heavy landings. The short axial length between bearings which the 3 spool concept provides and isolation of casings from structural carcase are beneficial in reducing these deflections.

(b) Strong bearing support structures, which by proximity and by remaining circular under carcase deflection, provide a higher degree of roundness in critical casings of the engine.

Secondly, the situation with higher in-service hours can be analysed from the annual in-flight fleet audits conducted by one of the major operators of the engine. These data show that after 4 years of service the fleet average deterioration of the RB 211 is about 1% specific fuel consumption and although the time between overhauls of the HP module containing the hot section of the engine, has been quite short, sufficient data are available to demonstrate that the rate of deterioration of this module is slight.

Factors contributing in addition to (a) and (b) above are:

(c) Careful attention to matching the axial and radial thermal growths, particularly of the HP compressor and the turbines. This was achieved partly by design calculation, supported by extensive transient measurements of disc and casing temperatures and partly by development action, using X-rays and other techniques. A particular example was additional mass of metal in the vicinity of HP turbine casing flanges, which has allowed very accurate matching of radial growths throughout the engine operation.

(d) Axial positioning of bearing and support structure to minimise relative radial clearance excursions, from deflection and tolerance build-up.

(e) Shrouded HP turbine blade, which by providing seal knives and perhaps easing the design problems of the overtip shroud, has reduced the variation of clearance and the sensitivity to clearance simultaneously.

These RB 211 data provide in my opinion an approach to minimise performance deterioration in the design of future energy efficient engines, at least as far as sealing in the main gas path is concerned.

If I could be provocative for a moment, I think that I might suggest that from RB 211 and RB 401 experience (the RB 401 is a small business jet-engine), I don't see a strong case for active clearance control.

Still staying with the main flow path, a possibility for improving the effect of over-tip clearance is to change the hub-tip ratio at the back of the HP compressor. It is interesting to speculate on this — that if hub-tip ratio is changed from 0.92 to 0.9, we would estimate that it might be worth about 1% efficiency for a given level of clearance. But such a change can react adversely. In changing the hub-tip ratio by that amount, the rotational speed rises by nearly 30% and as the turbine bore is constrained by shafting within that bore, the tangential speed rises, and it has less capability for supporting the blade and other parasitic loads that are applied at the rim. If there is freedom in the turbine region, change of compressor hub-tip ratio could be helpful. If there isn't, there may be as much lost HP turbine efficiency as the gain on the compressor.

David Campbell showed us that in the design of secondary flow systems, the flows are quite often determined by fixed orifices and the consequence of a seal failure is not necessarily a deterioration of SFC, but one of loss of integrity or reduction in integrity margin.

Nevertheless air is discahrged at a different point into the flow path as he has pointed out. That raises a question which has hardly been touched on during the conference, that is the effect of air leaking into the main engine flow path, and the effect that it has on component efficiency. This I think, is a subject that needs much more attention. In fact I would like to ask Harold Stocker and David Campbell, who presented information on the effect of leakage on SFC, whether they have made any allowance for the effect of the flow on the component efficiency, or whether it was a straight-forward thermodynamic calculation.

We have had tremendous emphasis put on cost of ownership. Not only are the airlines of the world pressing in this direction, but we know that the Air Forces are as well. Designers might well give attention to commonisation of bearings throughout an engine, and this might help to commonise seals too, which would allow smaller spares holding to be maintained.

I agree with Professor Wazelt with respect to the emphasis he put on better measurement tools. There is a complementary role for the two systems that have been discussed during this conference. I think that the probe system has some advantages in cases where one may be doubtful about roundness of the static component. It is probably easier to place several probes at different points around the periphery.

Finally, a plea to the compressor specialists to agree on the sensitivity factor due to tip clearance over annulus height ratio. We have seen the values presented by Mr Ludwig yesterday with reference to a paper by Mr Mahler which were quite different in shape from the ones that Rolls-Royce normally see, and I think that the compressor specialists might take this up for discussion. It would be very helpful for us to know really how significant this particular point is.

A.J.B.Jackson: Thank you Mr Wrigley.

The Round Table is now open to the floor and perhaps I would like to start the ball rolling with a question: do we think that seal technology is keeping up; is it keeping pace with the work that goes on in other parts of the engine?

Has anybody any comments or questions?

D.C.Whitlock: I cannot answer the question directly but I would like to make this comment with regard to oil sealing.

Rolls-Royce's approach to oil path sealing is different to that of our American competitors. I suspect that this difference is maintained because none of us like to divert significantly from our previous experience.

We have, however, heard from Mr Ludwig and also Professor Dini about rig test work on advanced oil seals; work that has been proceeding for several years. Before such advances can be incorporated in production engines, the engine

manufacturers must accept the risk of extending the rig work into engine research. They must weigh the time and financial risks on research engine programmes against the possible improvements to be gained.

Perhaps Mr Ludwig could comment on proposed engine test work?

L.P.Ludwig: I would like to add the comment that self-acting seals are being put into prototype engines, and these are small diameter types (6.44 cm dia). I believe that there is a size effect, in small sizes it is easier to keep the faces flat. But as you go up in size, the flexibility of the rings starts to give you trouble. The largest size on which we have some operation is 25 centimeters, beyond that, keeping ring flatness within a reasonable weight is becoming very difficult. And I should emphasize that keeping the sealing faces flat is the secret to success in self-acting seals.

F.H.Mahler: I think the question you have posed is central because in addition to improving seals, per se, we are endeavoring to effectively apply new sealing techniques in engines now being developed and in the design of advanced engines for higher performance. To do this, we will have to work hand-in-hand with the aerodynamicist to achieve improved component efficiencies. Optimistic predictions of better performance based on advanced aerodynamics may prove illusory without the benefit of an equally efficient sealing system. We are in a period of transition that in a way is similar to that we went through when axial flow machinery was first adapted for flight, focusing on clearances as one of the major losses in the overall system.

Seal technology is advancing rapidly, as the material presented at this meeting illustrates, attempting to match the pace of engine development toward fuel economy. To meet reduced fuel consumption goals, the planners and managers of engine development programs are learning to approach sealing in a fundamental sense comparable to compressor and turbine aerodynamics. Seal specialists are becoming more involved in the development process and in preliminary design so that the proper seal philosophy is in the engine at the start rather than as a band-aid. To judge whether seal technology is sufficiently mature and whether the process of system integration can be successfully implemented, is, I think, very difficult at this time.

A.J.B.Jackson: I would like to endorse your remarks very much. An obvious link between the compressor aerodynamicists' work and the work of the seal engineer is in the simple matter of choice of the reaction in the compressor and turbine. This choice of reaction can alter the end load very substantially and therefore the seal diameters and therefore the difficulty in the seal. That is just one example. Can I quote another one perhaps: the shrouded and unshrouded turbine tip seal is another obvious case. And I certainly feel, as perhaps a man brought up more in the aerodynamic side than in the seal side, that the aerodynamics of seals is still incredibly old-fashioned and in its early stages, as we say, relative to the state-of-the-art in rotating machinery. This is really why I asked the question. I feel the answer is that there is much further to go in the art of seal design. We are still at an early stage compared with rotating machinery and I think that the objective that we can go at — a figure of 4% of specific fuel consumption has been mentioned — is very well worth pursuing, and it is there to be achieved at a much lower capital investment than getting the same improvement by attention to the details of the rotating machinery.

L.P.Ludwig: I want to add just a comment about the probes which were mentioned by Professor Wazelt. I think here is something that might be the key element. We need, of course, to find out what the transient clearance changes are; there we suffer because of the lack of small probes. And we probably have only several people here in the UK and maybe several in the USA trying to develop probes. In general, probes are very large and capacitance probes suffer because of thermal drift. So I think maybe here is an area which we should really concentrate on. We need a strong effort to develop transient clearance measurement devices which are small and easily put into an engine. And preferably an engine which is flying and not one run just on a test stand.

H.Stocker: I will try to combine Mr Jackson's inquiry regarding "has seal technology kept up with the rest of the components" somewhat with Brian Wrigley's comment about losses associated with seal leakage. I approach this subject from the standpoint that over the years there has been a lot of money spent on improving and pushing up the level of demonstrated compressor and turbine efficiency. The performance gains that may be possible, beyond the levels demonstrated in advanced gas turbine engines, will be more difficult to achieve since the gap between demonstrated and ideal efficiencies has been substantially reduced with improved aerodynamics. The performance gains are also becoming much more expensive in dollar per point of efficiency gain. And I just wonder if the aerodynamicists have gotten to the point that they are going to have to turn their attention quite strongly to the question of how does seal leakage keep them from achieving higher component efficiencies. There must be potential turbine blading efficiency improvements to be gained when I look at the amount of flow that enters the turbine either coming in through a cooling circuit mechanism or through labyrinth seal leakage. There are certainly thermodynamic losses and momentum losses depending on how the flow is brought back into the turbine flow path. And there are probably windage losses of a magnitude we have yet to verify. I believe similar effects in a reverse fashion are present in the compressor. You are certainly having an effect on the downstream aerodynamic performance when you have leakage around the tip and hub of the airfoils and create a profile distortion for the next compressor stage to handle. In discussions with compressor specialists on the subject of leakage, I believe that I could supplement Brian Wrigley's comment about the shape of the sensitivity curve for the compressor and add a third curve, representative of Allison experience, to the two mentioned.

In the turbine regions, I believe the magnitude of the identified loss mechanisms have yet to be completely qualified as to what the amount and method of bringing flow back into the turbine flow path really does to

performance. I do not believe that engine cycle accountability is giving complete credit or blame to seal leakage effects on performance deterioration within the gas turbine. There is, in the amount of flow by-passing the combustor, a certain amount of work that is lost depending on where and how the flow is returned to the gas path. And certainly there have been studies done – I know – by Rolls-Royce and also by Allison, on the loss effects when you bring the flow back in to the turbine flow path. I believe this is why you see some of the treatment in the hub region of the flow path. There has been an effort by designers to get the flow back into the main gas path with as little cost to the energy of the main gas path as possible. However, I am not convinced, since I am seeing some conflicting magnitudes of results, that sufficient knowledge is available on the penalty of seal leakage or cooling flow re-entering the turbine region.

In my opinion, the area of sealing technology covers a broad spectrum of difficulties that still exist in the gas turbine engine and they certainly have not been adequately addressed. If you were to take a survey of gas turbine related technical publications for the past ten years and compare the amount of work done on compressors, turbines, combustors, heat transfer, etc., to the number of reports published on improved gas turbine sealing technology, I believe that you will get a reasonably clear picture of the lack of technology development in the gas turbine sealing area. Just a casual glance at any annual technical publication summary will also give you an indication as to whether seal technology has or has not kept up with the rest of the gas turbine component technology efforts.

D.A.Campbell: I would like to complement H.Stocker's remarks by first answering a direct question from the top table about my assumptions in my paper on disc sealing, about the effects on engine performance. The answer is that in fact the effect on turbine efficiency of the flow re-entering the turbine was neglected. This could have been worked out but in fact I did not do so because of the lack of time. But I have remarked in the full version of the paper that this effect can be kept fairly small by appropriate design of the interface with the annulus. And I suggest a quantity of about 0.3% of turbine efficiency for each 1% of cooling air.

Now I do have to admit that this is based on very few data and there is certainly scope for obtaining more data of this sort from turbine rig testing.

In Professor Wazelt's summing up I think I detected an implication that I have given the impression that everything was under control in the disc sealing design area. I did not mean to do this. And in fact I did outline several areas where we need more research and more data in order to do good design work.

Now the question has also been asked: Do we think that seal technology is as advanced as the other technological aspects? My feeling is that the amount of money spent on testing and research in the seal technology area is disproportionally small compared with the resources allocated to the testing of major aerodynamic components. And that if we are to improve the performance standard of engines we must spend much more on seal technology and this will still be a small amount compared with what is spent on conventional main component technology.

This also applies to the preparation of such things as computer applications programmes, where I feel that we in systems design are starved of resources compared with those allocated to main turbomachinery applications.

I was impressed in an earlier paper by a diagram showing the effects on direct operating costs of various parameters related to engines and I was very impressed by the smallness of the effects on engine weight. I think we have an attitude to engine weight which comes from a time of much lower fuel costs. I think it is time now for us to reappraise our attitude to engine weight and to see where we can add features to engines that will improve sealing performance and the reliability and durability of that performance, perhaps at the expense of some weight, with only a small offsetting penalty on operating cost due to that weight increase itself.

D.K.Hennecke: I would also like to point out an area where seal technology has not kept pace with the rest of technology and that is the area of heat transfer in seals. The knowledge of heat transfer to compressor or turbine casing above the rotating blades is still very limited. Also, the heat transfer to the rotating and static members of labyrinth seals has not been investigated thoroughly. Yet this has to be understood quite well if one wants to achieve a good thermal match between the rotating and stationary parts which is important as we have heard many times during this meeting. So, I would plead that future research is also directed to the seal heat transfer problem and that people who study the flow in seals also ask themselves whether they could extend their research by studying the heat transfer too.

A.J.B.Jackson: I think that we have in fact covered in the discussion all of the major points that have come out of the meeting. And so if you think that there are no other comments to make I would like very briefly to sum up as I see the situation.

First of all, I think this has been a good conference and it is really just the next step in the historical evolution of the importance of seals which was referred to by Mr Ainley in his opening address. We have had papers on a number of subjects and I do feel that having heard them that the general state-of-the-art is not as advanced as in other areas in the engine particularly the turbomachinery. However, I think there is one encouraging aspect of the work shown at this conference which is that very clearly at all times has the relevance of the work to an engine been kept in mind. I feel that in some of the more esoteric research areas that we have had conferences on that it has not been always quite so clear what the relevance of the work to the engine is. But in the case of seals we have had at least three papers and many other comments about the gains to be obtained from improved seal design. I refer once again to the incentive of 4% of SFC. Four percent perhaps does not sound much to somebody not used to dealing with specific fuel consumption and direct operating cost; but it is an enormous amount, particularly in view of the developing fuel situation which has been referred to, again, during the conference. I think the comments also at the end by Mr Campbell regarding the relative importance of fuel and weight should be borne in mind.

It may also be argued that this could be described as a rather mundane subject for a scientific conference. The fact that you are all here and the quality of the papers has shown that this is clearly not the case and that this conference has been very well worthwhile having.

The key items out of each of the sessions are — in my view — as follows:

In the field of materials much has been done but there is still a great deal to do. The fact that one paper on ceramics was cancelled is surely a good indication where we might go in some areas.

The question of the users; they the users said that there ought to be more communication. And I appreciate that from first hand experience of talking to Service Engineers (Field Engineers).

They are extremely vociferous in their views of the designs of the engines which they have to maintain in the field, and I would recommend that each of you does talk to a Service Engineer for about 10 minutes in the near future and get that input; it will be very firm. I ask the users however, whether there is anything they can do in the way they use the engines to maintain the performance of seals. We have seen latterly the use of flexible ratings and generally rather more care of the engine being taken by the Pilot than has been, perhaps, sometimes the case in the past and I feel that this line could be developed further.

Regarding measurement techniques, there can be no doubt whatever that this limits the basic standards of data, and so anything that can be done to improve measurement techniques is bound to have a fundamental effect on the rate at which the technology advances.

Regarding laboratory experiments, I was very encouraged to see that there was a whole session of six papers (out of the total of 17 papers actually presented) on this subject, and it is only an indication of what is going on. There is clearly other work going on and I feel here that the function of a Conference such as this is to bring this kind of work out into the open and to help the communications problem between seals engineers which has also been referred to many times at this Conference.

Regarding design aids, these papers merely emphasised the need for more data and this is where the work on experimental tests is so important.

The work shown therefore at this Conference is only a small part of everything that is going on. The need for more communications is obvious on the subject of seals; there has in fact been noted (just as a result of this Conference) some duplication of work due to lack of communication. Conferences on this kind of subject are all too rare.

So in concluding I would say please continue the good work, which is very important in view of the developing fuel situation.

Thank you all very much indeed.

REPORT DOCUMENTATION PAGE

1. Recipient's Reference	2. Originator's Reference	3. Further Reference	4. Security Classification of Document
	AGARD-CP-237	ISBN 92-835-0218-3	UNCLASSIFIED

5. Originator

Advisory Group for Aerospace Research and Development
North Atlantic Treaty Organization
7 rue Ancelle, 92200 Neuilly sur Seine, France

6. Title

SEAL TECHNOLOGY IN GAS TURBINE ENGINES

7. Presented at

the Propulsion and Energetics Panel's 51st (B) Specialists' Meeting
in London, United Kingdom 6–7 April 1978.

8. Author(s)	9. Date
Various	August 1978

10. Author's Address	11. Pages
Various	286

12. Distribution Statement This document is distributed in accordance with AGARD policies and regulations, which are outlined on the Outside Back Covers of all AGARD publications.

13. Keywords/Descriptors

Seals (stoppers)	Gas turbine engines	Gaskets
Gas seals	Maintenance	Test facilities
Oil seals	Design criteria	

14. Abstract

These Conference Proceedings contain 17 papers presented at the 51st (B) Specialists' Meeting of the AGARD Propulsion and Energetics Panel, held at Church House, Westminster, London, UK on 6 and 7 April 1978.

The papers were grouped into six sessions: Survey, Material Technology, User's View of Seal Technology, Measurements of Seal Behaviour, Laboratory Experiments, and Design Aids. The meeting was concluded with a Round Table Discussion. This discussion as well as those after each presentation, and the Technical Evaluation Report are included in the Conference Proceedings.

The purpose of the meeting was to provide a forum to discuss technology of gas turbine engine seals. The discussion was limited to cases where relative motion exists between parts of seals. Both gas path and oil path seals were covered. Due to relevant and timely contributions an overview on the present status and the shortcomings of seal technology is reached as well as on the current developments. Various aspects were taken into account like engine operating and maintenance costs, and the engine design procedure. Within the Round Table Discussion and even more extensively in the Technical Evaluation Report conclusions are drawn and recommendations are given whereto future interest should be directed.

AGARD Conference Proceedings No.237 Advisory Group for Aerospace Research and Development, NATO SEAL TECHNOLOGY IN GAS TURBINE ENGINES Published August 1978 286 pages These Conference Proceedings contain 17 papers presented at the 51st (B) Specialists' Meeting of the AGARD Propulsion and Energetics Panel, held at Church House, Westminster, London, UK on 6 and 7 April 1978. The papers were grouped into six sessions: Survey, Material Technology, User's View of Seal Technology, Measurements of Seal Behaviour, Laboratory P.T.O.	AGARD-CP-237 Seals (stoppers) Gas seals Oil seals Gas turbine engines Maintenance Design criteria Gaskets Test facilities
AGARD Conference Proceedings No.237 Advisory Group for Aerospace Research and Development, NATO SEAL TECHNOLOGY IN GAS TURBINE ENGINES Published August 1978 286 pages These Conference Proceedings contain 17 papers presented at the 51st (B) Specialists' Meeting of the AGARD Propulsion and Energetics Panel, held at Church House, Westminster, London, UK on 6 and 7 April 1978. The papers were grouped into six sessions: Survey, Material Technology, User's View of Seal Technology, Measurements of Seal Behaviour, Laboratory P.T.O.	AGARD-CP-237 Seals (stoppers) Gas seals Oil seals Gas turbine engines Maintenance Design criteria Gaskets Test facilities

Experiments, and Design Aids. The meeting was concluded with a Round Table Discussion. This discussion as well as those after each presentation, and the Technical Evaluation Report are included in the Conference Proceedings. The purpose of the meeting was to provide a forum to discuss technology of gas turbine engine seals. The discussion was limited to cases where relative motion exists between parts of seals. Both gas path and oil path seals were covered. Due to relevant and timely contributions an overview on the present status and the shortcomings of seal technology is reached as well as on the current developments. Various aspects were taken into account like engine operating and maintenance costs, and the engine design procedure. Within the Round Table Discussion and even more extensively in the Technical Evaluation Report conclusions are drawn and recommendations are given whereto future interest should be directed.	Experiments, and Design Aids. The meeting was concluded with a Round Table Discussion. This discussion as well as those after each presentation, and the Technical Evaluation Report are included in the Conference Proceedings. The purpose of the meeting was to provide a forum to discuss technology of gas turbine engine seals. The discussion was limited to cases where relative motion exists between parts of seals. Both gas path and oil path seals were covered. Due to relevant and timely contributions an overview on the present status and the shortcomings of seal technology is reached as well as on the current developments. Various aspects were taken into account like engine operating and maintenance costs, and the engine design procedure. Within the Round Table Discussion and even more extensively in the Technical Evaluation Report conclusions are drawn and recommendations are given whereto future interest should be directed.
ISBN 92-835-0218-3	ISBN 92-835-0218-3
Experiments, and Design Aids. The meeting was concluded with a Round Table Discussion. This discussion as well as those after each presentation, and the Technical Evaluation Report are included in the Conference Proceedings. The purpose of the meeting was to provide a forum to discuss technology of gas turbine engine seals. The discussion was limited to cases where relative motion exists between parts of seals. Both gas path and oil path seals were covered. Due to relevant and timely contributions an overview on the present status and the shortcomings of seal technology is reached as well as on the current developments. Various aspects were taken into account like engine operating and maintenance costs, and the engine design procedure. Within the Round Table Discussion and even more extensively in the Technical Evaluation Report conclusions are drawn and recommendations are given whereto future interest should be directed.	Experiments, and Design Aids. The meeting was concluded with a Round Table Discussion. This discussion as well as those after each presentation, and the Technical Evaluation Report are included in the Conference Proceedings. The purpose of the meeting was to provide a forum to discuss technology of gas turbine engine seals. The discussion was limited to cases where relative motion exists between parts of seals. Both gas path and oil path seals were covered. Due to relevant and timely contributions an overview on the present status and the shortcomings of seal technology is reached as well as on the current developments. Various aspects were taken into account like engine operating and maintenance costs, and the engine design procedure. Within the Round Table Discussion and even more extensively in the Technical Evaluation Report conclusions are drawn and recommendations are given whereto future interest should be directed.
ISBN 92-835-0218-3	ISBN 92-835-0218-3